Technische Universität München

Fakultät für Medizin

Multi-directional genome-wide CRISPR/Cas9 screens to uncover resistance mechanisms and co-dependencies in the context of PI3K pathway inhibition in PDAC

Katia Sleiman

Vollständiger Abdruck der von der Fakultät für Medizin der Technischen Universität München zur Erlangung des akademischen Grades eines

Doctor of Philosophy (Ph.D.)

genehmigten Dissertation.

Vorsitzender: Prof. Dr. Stefan Lichtenthaler

Betreuer: Prof. Dr. Dieter Saur

Prüfer der Dissertation:

1. Prof. Dr. Manuel Kaulich
2. Prof. Dr. Radu Roland Rad

Die Dissertation wurde am 19.09.2022 bei der Fakultät für Medizin der Technischen Universität München eingereicht und durch die Fakultät für Medizin am 21.09.2022 angenommen.

Table of Contents

List of Figures *3*

List of Tables: *3*

List of Abbreviations *6*

1. Introduction *8*

1.1 Etiology of Pancreatic Ductal Adenocarcinoma *8*

1.1.1 Genetics of PDAC 8

1.2 KRAS at the core of oncogenic signaling in PDAC **11**

1.2.1 Biology of KRAS: GTPase activity and regulation 11

1.2.2 Downstream effectors of KRAS in PDAC 12

1.3 Targeting KRAS Signaling **18**

1.3.1 Direct RAS targeting 18

1.3.2 Targeting Upstream RAS regulators and interactors 19

1.3.3 Targeting RAS vulnerabilities 20

1.3.4 Targeting RAS effector pathways 21

3.4.2 Targeting the PI3K/AKT pathway 23

1.4 CRISPR-Cas system as a revolutionary Genome Engineering technology **23**

1.4.1 Targeted nucleases as Genome editing tools 24

1.4.2 CRISPR-Cas as a bacterial adaptive Immune system 25

1.4.2 CRISPR-Cas as a genome engineering system 26

2. Materials *33*

2.1 Equipment **33**

2.2 Disposables **35**

2.3 Reagents **37**

2.4 Kits for Molecular Biology **39**

2.5 Competent cell strains and Plasmids **40**

3. Methods *41*

3.1 Mouse experiments **41**

3.1.1 Mouse strains 41

3.1.2 Genotyping of genetically engineered animals 43

3.1.3 Mouse dissection 43

3.1.3 Orthotopic transplantation of PDAC cells into the pancreas 43

3.1.4 Tamoxifen Treatment for Mice 44

3.2 Cell culture **44**

3.2.1 Culture of primary mouse PDAC cell lines 44

3.2.2 Treatment of cells with 4-hydroxytamoxifen (4-OHT) 44

3.2.3 CellTiter Glo® assay 45

3.2.4 Clonogenic assay 45

3.2.5 Cell Cycle analysis 45

3.2.6 Caspase-Glo® 3/7 Assay 45

3.2.7 Lentivirus production 45

3.2.5 Lentiviral transduction 46

3.2.6 Titer determination of the Lentivirus for Screening 46

3.2.7 Lentiviral transduction for Genome-wide Screens 47
3.2.7 Fluorescence-activated cell sorting (FACS) and flow cytometry analysis 47
3.2.8 Multicolor competition assays 47
3.2.9 Drug Screen 48

3.3 Molecular biology 48
3.3.1 Isolation of genomic DNA 48
3.3.2 Isolation of genomic DNA from CRISPR Screens 49
3.3.3 Isolation of RNA from primary cell cultures 49
3.3.4 RNA Sequencing and analysis 49
3.3.5 Polymerase chain reaction (PCR) 50
3.3.6 Separation of DNA by agarose gel electrophoresis 51
3.3.7 Amplification of pooled sgRNA libraries 51
3.3.8 Next Generation Sequencing of the amplified sgRNA library 51
3.3.9 Golden gate Cloning 53
3.3.11 Akt1 mutagenesis 55
3.3.10 Transformation of bacteria 55
3.3.11 Plasmid DNA isolation from glycerol stocks 56

3.4 Protein biochemistry 56
3.4.1 Protein extraction 57
3.4.2 Protein concentration estimation 57
3.4.3 SDS polyacrylamide gel electrophoresis (SDS-PAGE) 57
5.4.4 Immunoblot 58
5.4.5 Phospho Explorer Antibody Microarray 60

3.6 Statistical analysis 60

4. Aim Of The Work 61

5. Results 62

5.1 *Pdk1* deletion impairs the growth of PDAC cells *in vitro* by blocking PI3K/AKT signaling 62

5.2 A subset of PDAC clones shows proliferation independent of *Pdk1* deletion 68

5.3 Murine PDAC cell lines recapitulate human PDAC biology 71

5.3 Unbiased CRISPR screens to identify PI3K/AKT/PDK1 collateral dependencies in PDAC 74

5.4 Global view of the screens 79

5.5 Pathway- and Gene-Level View of the screens 84
5.5.1 Role of the MAPK Signaling Pathway in PDAC survival Parallel to PI3K Signaling 85
5.5.2 Role of other Signaling Pathways in PDAC survival Parallel to PI3K Signaling 92

5.6 Informed Drug screening identifies potential drugs for combinatorial therapies 92

5.7 CRISPR screens identify resistance mechanism to the growth arrest induced by *Pdk1* deletion 99

5.8 CRISPR screens identify resistance mechanism to the growth arrest induced by *Pdk1* deletion induced by *Pten* loss 101

6. Discussion and Outlook 111

6.1 The role of PI3K signaling in *Kras*-driven PDAC maintenance 111

6.2 Genome-wide genetic and drug screens identify therapeutic vulnerabilities in *Pdk1*-independent clones 111

6.3 Genome-wide genetic and drug screens identify resistance mechanism to *Pdk1* loss induced growth arrest mediated by *Pten* loss 113

6.4 Pten loss confers resistance to *Pdk1* deletion induced growth arrest **114**

7. Conclusion ***118***

Acknowledgements ***119***

References ***120***

Appendix ***140***

List of Figures

Figure 1: MAPK-ERK1/2 Signaling Pathway 15
Figure 2: PI3K-AKT Signaling Pathway 17
Figure 3: Mechanism of CRISPR Immunity (Van der Oost et al., 2014 [236]) 27
Figure 4: Scheme of sgRNA-Cas9 complex 28
Figure 5: DSB repair mechanisms promote CRISPR-Cas9 genome editing 29
Figure 6: Deletion of *Pdk1* in PDAC cell lines derived from a dual recombinase mouse model impairs growth 63
Figure 7: *Pdk1* deletion inhibits the PI3K/AKT signaling pathway 65
Figure 8: Exploratory RNASeq analysis of the effect of Pdk1 deletion on the transcriptional level 66
Figure 9: Functional enrichment analysis of the differentially regulated genes upon *Pdk1* deletion 68
Figure 10: A subset of PDAC clones show a persistent proliferative capacity independent of *Pdk1* 69
Figure 11: The persistent clones show inhibition of the PI3K/AKT signaling pathway 71
Figure 12: CRISPR-Cas9 Fitness screens in murine primary PDAC cell lines identify core fitness genes comparable to human PDAC 72
Figure 13: Metascape enrichment analysis of genes identified as essential in murine PDAC 73
Figure 14: Overview of CRISPR screens performed to identify collateral signaling pathways that sustain PDAC growth independent of the Pdk1 and the PI3K/AKT pathway 75
Figure 15: Validation of efficient Cas9 activity in the cell lines used for the genome-wide CRISPR screens 77
Figure 16: Flow Cytometry Charts of the Cas9 activity assay 79
Figure 17: Quality control of the CRISPR screens in *Pdk1*^{lox} bulk cell line with acute *Pdk1* deletion 79
Figure 18: Quality control of the CRISPR screens in *Pdk1*^{lox} and *Pdk1*$^{\Delta}$ clones 80
Figure 19: Global View of the CRISPR screens in *Pdk1*$^{\Delta}$ and *Pdk1*^{lox} clones 82
Figure 20: The Enrichment Network, including gene names 83
Figure 21: The Dropout Network, including gene names 84
Figure 22: CRISPR activation screens corroborate LOF screen findings 85
Figure 23: Fingerprint plot of putative genes involved in the MAPK pathway. 86
Figure 24: Schematic representation of the genes of the ERK 1/2 module of the MAPK signaling pathway. 87
Figure 25: Genetic ablation of *Raf1 and Braf* in combination with *Pdk1* results in complete regression in a syngeneic implantation model of PDAC 90

Figure 26: Western blot analysis of key effectors in the MAPK pathway suggests activation of the MAPK pathway in *Pdk1*$^{\Delta}$ and *Pdk1*^{lox} clones 91
Figure 27: Role of the mTOR Signaling Pathway in PDAC survival along PI3K Signaling 93
Figure 28: Role of the Hippo Signaling Pathway in PDAC survival along PI3K Signaling 94
Figure 29: Role of the Ral Signaling Pathway in PDAC survival along PI3K Signaling 95
Figure 30: Informed drug screens identify new combination therapies for PDAC 97
Figure 32: Global view of the resistance mechanisms to *Pdk1* deletion-induced growth arrest identified by CRISPR screens 100
Figure 33: Loss of Pten confers resistance to the growth arrest phenotype induced by *Pdk1* deletion 103
Figure 34: Validation of the Pten KO resistance phenotype in clones. 105
Figure 35: Loss of *Pten* reverses the tumor inititation inhibitory phenotype induced by *Pdk1* deletion *in vivo* 105
Figure 36: Signaling analysis identifies the resistance mechanism conferred by *Pten* loss.. 106
Figure 37: Genome-wide CRISPR screens and drug screens identify vulnerability to AKT1 inhibition in 4-OHT treated cells with Pten knockout 108
Figure 38: Genome-wide CRISPR screens and drug screens identify resistance to MAPK inhibition in 4-OHT treated cells with Pten knockout 109
Figure 39: Graphical summary of Signaling downstream of KRAS in PDAC and the variation in vulnerabilities based on the driver oncogene status and the mutational landscape 117

List of Tables

Table 1: Laboratory equipment 33
Table 2: Disposables 35
Table 3: Reagents 37
Table 4: Kits for molecular biology 39
Table 5: Competent bacterial strains 40
Table 6: Plasmids 40
Table 7: Transfection Mix for HEK293T cells for Lentivirus Production 46
Table 8: Composition of Soriano Lysis Buffer 48
Table 9: Composition of pre-mix for PCR 50
Table 10: Reaction conditions for standard PCRs 50
Table 11: Annealing temperatures and PCR products of genotyping and recombination PCRs 50
Table 12: Composition of the KAPA HiFi PCR for plasmid library amplification 52
Table 13: Cycling conditions for the KAPA HiFi PCR for plasmid library amplification 52
Table 14: Design of the Forward and Reverse primers used for Plasmid Library Amplification and Sequencing 52
Table 15: Sequence of the Forward and Reverse primers used for Plasmid Library Amplification and Sequencing 53
Table 16: Sequence of the primers used in Illumina Sequencing 53
Table 17: Composition of the Golden gate Cloning reaction 54
Table 18: Reaction conditions for golden gate Cloning 54
Table 19: Sequence of the used sgRNAs 54

3.3.10 Cloning AKT cDNA into Lentiviral vectors 55
Table 20: Primers used for Amplification of *Akt1* cDNA 55
Table 21: Primers used for Myr-*Akt1* Mutagenesis 55
Table 19: The composition of all Buffers used in the protein biochemistry assays 56
Table 20: Components of the separating SDS-PAGE gels 58
Table 21: Components of the stacking SDS-PAGE gels 58
Table 22: List of Primary Antibodies used in Western Blots 58
Table 22: List of Secondary Antibodies 60
Appendix Table 1: Phospho arrays fold changes in Clone 7G9 vs Clone 5E2 140
Appendix Table 2: Genes specifically depleted in *Pdk1*$^{\Delta}$ clones 172
Appendix Table 3: Genes enriched in *Pdk1*$^{\Delta}$ clones (Chronic Setting) 175
Appendix Table 4: Genes enriched in 4-OHT treated bulk CV7250 cell lines 184
Appendix Table 5: Table showing the classic GRmetrics measures of drug sensitivity in the acute *Pdk1* deletion setting in CV7250 cell line 194
Appendix Table 6: Table showing the classic GRmetrics measures of drug sensitivity in the chronic *Pdk1* deletion setting in CV7250 cell line 262
Appendix Table 7: Phospho arrays fold changes in 4-OHT treated CV7250 cells transduced with *Pten* sgRNA 1 relative to a non-targeting sgRNA 329

List of Abbreviations

CRISPR	clustered regularly interspaced short palindromic repeats
Cas	CRISPR associated
crRNA	CRISPR RNA
bp	base pair
crRNP	CRISPR ribonucleoprotein complex
pre-crRNA	precursor CRISPR RNA
tracrRNA	trans-activating crRNA
PAM	protospacer adjacent motif
HR	homologous recombination
DSB	double-strand breaks
NHEJ	nonhomologous end-joining
indels	insertions or deletion mutations
ZFP	Zinc Finger protein
ZFN	Zing Finger nuclease
TALEN	transcription activator-like effector nucleases
TALE	transcription activator-like effector
SpCas9	Streptococcus pyogenes Cas9
sgRNA	single guide RNA
nt	nucleotide
HDR	homology-directed repair
KO	knockout
ChIP- Seq	chromatin immunoprecipitation and high throughput sequencing
NGS	Next generation sequencing
nCas9	nickase Cas9
CRISPR GUARD	CRISPR Guide RNA Assisted Reduction of Damage
dCas9	dead Cas9
CRISPRi	CRISPR interference
KRAB	Kruppel- associated Box)
CRISPRa	CRISPR activation
SAM	synergistic activation mediator
AID	activation-induced adenosine deaminase
RNAi	RNA interference
ORF	open reading frame
Myr	myristoylated
PDAC	Pancreatic ductal adenocarcinoma
GEMMs	genetically engineered mouse models
PanIN	pancreatic intraepithelial neoplasia
IPMN	intraductal papillary mucinous neoplasia
AFLs	atypical flat lesions
SNV	Single Nucleotide Variation
RB	Retinoblastoma Protein
LOH	Loss of heterozygosity
TSG	Tumor Suppressor Gene
TGFβ	transforming growth factor-beta
TGFBR1/2	TGFβ receptors I or II

R-SMAD	Receptor SMAD protein
ACVR1B	activin A receptor type 1B
SWI/SNF	Switch/Sucrose-Nonfermentable
GEF	nucleotide exchange factor
GAP	GTPase-activating protein
GPCR	G-protein coupled receptors
RTK	receptor tyrosine kinases
EGFR	Epidermal growth factor receptor
GRB2	growth factor receptor bound protein 2
NF1	neurofibromin 1
RalGDS	Ral guanine nucleotide dissociation stimulator
PI3K	Phosphatidyl inositol 3-kiase
PLC-ε	Phospholipase Cε
RASSF	RAS association domain family
MAPK	mitogen-activated protein kinase
NF-kB	nuclear factor kappa B
IkB	inhibitor of nuclear factor kappa B
DDR	DNA damage response
PLK1	Polo-like kinase 1
AURKA	Aurora kinase A
P90-RSK	Ribosomal S6 kinase
TF	transcription factors
MAPKKK	MAPK kinase kinases
MAPKK	MAPK kinase
MAPK	mitogen-activated protein kinase
JNK	Jun amino-terminal kinases
PI3K	phosphoinositide 3-kinase
mTOR	mechanistic target of rapamycin
mTORC	mechanistic target of rapamycin complex
PtdIns	phosphatidylinositides
PIP_2	PtdIns 4,5-bisphosphate
PIP_3	PtdIns(3,4,5)P_3
PDPK1 or PDK1	phosphoinositide-dependent protein kinase 1
VPS34	vacuolar protein sorting 34
GSK3	glycogen synthase Kinase 3
RHEB	Ras homologue enriched in brain
PTEN	phosphatase and tensin homolog deleted on chromosome ten
NSLC	non-small lung cancer
WT	Wild type
ASO	anti-sense oligonucleotides (ASO
PDEδ	phosphodiesterase-δ (PDEδ)
PROTAC	proteolysis targeting chimera
PIKK	phosphatidylinositol 3-kinase-related kinase
DDR	*DNA damage response*
LOF	Loss of function
Ras	Rat sarcoma virus
FDA	Food and Drug Administration

1. Introduction

1.1 Etiology of Pancreatic Ductal Adenocarcinoma

To date, pancreatic cancer remains one of the most dismal prognoses in medicine with a mortality rate of 94% [1]. Pancreatic cancers are the seventh leading cause of global cancer deaths in industrialized countries, accounting for 432,242 deaths in 2018. [1] The incidence and mortality of pancreatic cancer are projected to increase with 356,358 new cases and 345,181 deaths from 2018 to 2040 [1]. Despite advancements in pancreatic cancer care, the 5-year survival rate of pancreatic cancer increased modestly from 6% to 9% from 2014 to 2018 [1]. Pancreatic ductal adenocarcinoma (PDAC) is by far the most abundant form of pancreatic cancer accounting for 85% of the cases [1]. The high mortality of PDAC can be attributed to several factors such as the late detection associated with insidious symptoms of the disease, infrequent amenability to surgical resection, limited therapeutic options, and complex biology such as the pronounced desmoplastic stromal reaction that limits drug delivery and early metastasis [2]. Half of PDAC patients are diagnosed with metastasis and have an average survival of less than one year [2]. Current treatment strategies are still based on cytotoxic therapy using Gemcitabine, alone or in combination with nab-paclitaxel (nanoparticle albumin-bound paclitaxel) or FOLFORINOX (combination therapy of folinic acid, 5-fluorouracil, irinotecan, and oxaliplatin) [3, 4]. These therapies are highly toxic to patients and the physiological effects of PDAC, mainly cachexia or muscle-wasting, further aggravate patient intolerance to these therapies [2].

1.1.1 Genetics of PDAC

Histopathological analysis revealed that PDAC develops via acinar-ductal metaplasia (ADM) from neoplastic precursor lesions, such as pancreatic intraepithelial neoplasia (PanIN), intraductal papillary mucinous neoplasia (IPMN), mucinous cystic neoplasia and atypical flat lesions (AFLs), into invasive carcinomas [5]. PDAC is thought to progress through a stepwise accumulation of somatic aberrations that include *KRAS*, *CDKN2a*, *TP53,* and *SMAD4* [6].

KRAS activating mutations are the most common oncogenic alteration in PDAC, occurring in 90% of the cases [7]. *KRAS* mutations are also the first and most frequent genetic alteration detected in low-grade PanIN lesions[8]. These observations implicated *KRAS* activation as an early initiating event for pancreatic transformation. The role of oncogenic Kras in PDAC initiation was corroborated by genetically engineered mouse models (GEMMs,) where the targeting of mutant *Kras* specifically to the pancreas was sufficient to initiate pancreatic cancer in mice. All *KRAS* mutations in PDAC are single-nucleotide variants (SNVs) and occur exclusively in codons 12 (91%), 13 (2%) and 61 (7%) [9]. Following *KRAS* activation, allelic imbalance in association with whole-genome duplication might occur, further increasing the dosage of the mutant *KRAS* allele [10]. More than one mechanism of *KRAS* allelic imbalance was observed within different metastatic sites of PDAC. Collectively, these mechanisms

converge on a net activation of MAPK-ERK signaling and PI3K-AKT signaling, the central effector pathways of *KRAS* [10, 11]. Similar findings were observed in mouse models of PDAC, where *Kras* allelic imbalance was shown to occur in the setting of *Cdkn2a* homozygous deletion, whereas heterozygous loss of *Cdkn2a* was associated with alternative oncogenic events, suggesting that PDACs undergo distinct evolutionary routes to increase *Kras* dosage depending on the status of *Cdkn2a* [12].

Activating mutations in *KRAS* are typically followed by inactivation of the *CDKN2A* locus during PDAC progression. Loss of function of *CDKN2A* occurs early in low-grade PanIN lesions and is detected in more than 90% of PDAC cases [6, 13]. *CDKN2A* inactivation occurs via multiple mechanisms, that include homozygous deletion, mutation coupled with loss of heterozygosity (LOH), or hypermethylation[8, 14-16]. The *CDKN2A locus* encodes two physically linked tumor suppressor proteins, the *INK4* family member *p16 or* $p16^{INK4a}$ and $p14^{ARF}$ ($p19^{Arf}$ in the mouse). p16 is a cyclin-dependent kinase inhibitor that arrests the cell cycle in the G1 phase by inhibiting the binding of CDK4 or CDK6 with cyclin D1 resulting in hypo-phosphorylation and inactivation of Retinoblastoma protein (RB) [17, 18]. p14, on the other hand, sequesters MDM2, an E3 ubiquitin ligase that regulates TP53 protein stability and degradation, and initiates p53-dependent cell cycle arrest, senescence, or apoptosis in addition to other p53-independent functions [18-20]. The unusual genomic relationship of these two proteins raised speculation about whether both genes were bona fide tumor suppressors or only one was a tumor suppressor, and the loss of the other was coincidental. Systematic analysis of the mutational profile of *CDKN2A* underpins a key role for p16 as a tumor suppressor. Mutations exclusively inactivating $p16^{INK4a}$ but sparing the $p14^{ARF}$ gene have been described in human PDAC [21]. In addition, $p16^{INK4a}$-specific germline mutations, but not $p14^{ARF}$, are associated with PDAC predisposition [22]. Underpinning a role for $p14^{ARF}$ as a tumor suppressor has been more challenging as $p14^{ARF}$-specific mutations sparing $p16^{INK4A}$ have not been reported in human PDAC [21]. Mouse models with targeted inactivation of $p16^{Ink4a}$ with $p19^{Arf}$ or heterozygous *Trp53* showed rapid PDAC progression compared to mice with heterozygous *Trp53* suggesting that the inactivation of $p16^{Ink4a}$ and $p19^{ARF}$-p53 pathway play a cooperative role in PDAC [21].

Unlike *KRAS* and *CDKN2A*, the inactivation of *TP53* and *SMAD4* occurs in more advanced PanIN stages [6, 23, 24]. *TP53* alterations occur in 80% of PDAC cases and consist predominantly of missense mutations that alter the DNA binding domain and result in the functional inactivation of *TP53* [25]. *TP53* is a tumor suppressor gene (TSG) that encodes a protein that serves as a major guardian of the genome [26]. TP53 senses aberrant growth signals or oncogenic signaling via ARF, and DNA damage via ATM/ATR proteins. These result in phosphorylation of MDM2 and stabilization of TP53 that results in reversible cell cycle arrest to enable DNA damage repair or senescence and apoptosis in case of unresolved or extensive DNA damage [27]. In addition, TP53 was shown to mediate tumor suppression by additional functions that include transcription, regulation of metabolism and autophagy,

modulation of the tumor environment, and metastasis [28]. *SMAD4*, also a TSG, is inactivated in around 50% of PDAC cases [29] via homozygous deletion or somatic mutations followed by LOH [29]. *SMAD4* encodes a transcription factor that mediates canonical transforming growth factor-beta (TGFβ) signaling that regulates tissue homeostasis. Canonical TGFβ signaling is activated by binding of TGFβ to type I and type II TGFβ receptors (TGFBR1and TGFBR2) dimers. Following ligand binding, type II receptors phosphorylate the type I, which then propagate the signal by phosphorylating SMAD proteins [30, 31]. Receptor SMAD proteins (R-SMADs) are directly phosphorylated by TFGBR1. This phosphorylation results in exposure of the nuclear localization signal and translocation of R-SMADs into the nucleus, where they form dimeric or trimeric transcriptional complexes with the co-SMAD, SMAD4, to regulate a broad set of target genes [30, 31]. Loss of *SMAD4* was shown to occur in invasive PDAC organoids and to induce a metastatic switch *in vivo* in PDAC mouse models [32, 33]. Alternative aberrations in the TGFβ signaling pathway are reported in PDAC cases with intact *SMAD4* including inactivating mutations or deletions in *TGFBR2*, in addition to inactivating mutations in *ACVR1B* (activin A receptor type 1B), a type I TGFβ receptor or *SMAD3* [15, 34-38].

In addition to these recurrent alterations in PDAC, other genes are altered at frequencies lower than 10%. The detection of these alterations was possible by several large-scale sequencing studies of PDAC exomes and genomes that revealed the extensive heterogeneity of PDAC [15, 37, 38]. These alterations were detected in chromatin modifier genes such as members of the Switch/Sucrose-Nonfermentable (SWI/SNF) complex (including *ARID1a, ARID1b, ARID2, PBRM1, SMARCA2,* and *SMARCA4*) and members of the COMPASS complex (including the histone methylases *KMT2C* and *KMT2D*, and the histone demethylase *KDM6A*) [15, 16, 37-39]. Alterations in chromatin modifier genes were found to be mutually exclusive within genes of each complex and between the two complex [15, 40, 41], suggesting a convergence for attenuation of enhancer function that has been linked to basal-like transcriptional features [9, 40, 42-45]. Alterations in DNA damage repair, such as *BRCA1, BRAC2, PALB2, FANCC, FANCG,* and *ATM* were also detected in PDAC, these mutations were linked to genetic instability in PDAC and PDAC predisposition when occurring as germline mutations [15, 46-49]. Mutations in genes involved in axon guidance such as ROBO/SLIT family members and their regulators and the RNA splicing machinery such as *SF3B1* and *RBM10* were detected, however their functional relevance remains less understood [15, 38]. Activating point mutations in *GNAS*, that encodes the α subunit of G protein complex (G protein α_s), are detected in up to 10% of PDAC cases. GEMMs showed that $Gnas^{R201C}$ cooperates with $Kras^{G12D}$ to promote initiation and maintenance of PDAC via lipid remodeling and fatty acid oxidation [16, 50]. In addition, alterations in known oncogenes such as *MYC* amplifications have also been identified in PDAC [15].

1.2 KRAS at the core of oncogenic signaling in PDAC

The prevalence of *KRAS* mutations in 90% of PDAC cases signifies an essential role for *KRAS* in PDAC tumorigenesis. KRAS serves as a transducer that couples cell surface receptors to intracellular effector pathways, regulating oncogenic transcription, proliferation, cell cycle progression, cell survival, cell growth, metabolism, cell motility and migration, microenvironment remodeling, and immune evasion in PDAC [51, 52].

1.2.1 Biology of KRAS: GTPase activity and regulation

In humans, three *RAS* genes encode four distinct but highly homologous RAS family members: HRAS, NRAS, and two forms of KRAS; KRAS4A and KRAS4B, that are generated by alternative splicing of the fourth coding exon of *KRAS* gene [52, 53]. Ras (Rat sarcoma virus) proteins are members of the guanine nucleotide binding protein superfamily that cycle between active, GTP-bound, and inactive, GDP-bound, conformation. Under physiological conditions, the intrinsic rate of GDP dissociation and GTP hydrolysis and the transition between the two states is regulated by guanine nucleotide exchange factors (GEFs), which promote the activation of RAS proteins by stimulating GDP for GTP exchange, and by GTPase-activating proteins (GAPs), which catalyze GTP hydrolysis [51, 53]. RAS signaling can be activated via a number of cell surface receptors including receptor tyrosine kinases (RTKs), G-protein coupled receptors (GPCRs), and integrin family members [52]. These receptors initiate RAS activation via the assembly of several scaffolding proteins that mediate the conversion of RAS from an inactive to an active state [52]. Upon dimerization of RTKs such as Epidermal growth factor receptor (EGFR), in response to growth factors, scaffolding proteins such as growth factor receptor bound protein 2 (GRB2) and SHC that can recruit further docking proteins or RAS-GEFs such as SOS1 which activates the RAS protein through a conformational switch [52, 54]. In addition, several GPCRs and integrins can activate RAS signaling [52, 55]. Additional RAS-GEFs, such as RAS-GRPs and RAS-GRFs, and RAS-GAPs, such as neurofibromin 1 (NF1), can regulate Ras signaling in response to RTK signals or additional less understood signals [52, 56]. Association with the plasma membrane is critical for RAS signaling. This is achieved by the addition of an isoprenyl group by farnesyl transferase (farnesylation) to the C-terminal end of the RAS proteins. NRAS and HRAS further require palmitoylation to ensure they are selectively localized to the Golgi or plasma membrane. KRAS does not require palmitoylation and can localize to the plasma via a poly-lysine region in its C-terminal end that fastens KRAS to the plasma membrane through electrostatic interaction within the anionic phospholipids of the membrane [52, 53, 56]. Most oncogenic *RAS* mutations occur at codons 12, 13, or 61 and interfere with KRAS inactivation by GTP hydrolysis. Oncogenic mutations at Q61 directly impair the GTP hydrolysis mechanism destroying both intrinsic and GAP-mediated GTP hydrolysis. Oncogenic substitutions in residues G12 and G13 prevent the interaction of RAS and its GAP through steric hindrance, which results in a strong decrease in GTP hydrolysis. Hence, all these mutations lock KRAS in a constitutively active GTP-bound state [51, 56, 57]

1.2.2 Downstream effectors of KRAS in PDAC

KRAS signaling is highly complex and dynamic involving a multitude of downstream effectors that bind to GTP-KRAS via putative RAS binding domains (RBD) [58]. Among known KRAS effectors are RAF kinases, Ral guanine nucleotide dissociation stimulator (RalGDS), Phosphatidyl inositol 3-kinase (PI3K), Phospholipase Cε (PLC-ε), RAS association domain family (RASSF) proteins, GAPs including p120GAP and NF1 and others [58, 59]. Oncogenic KRAS signaling in PDAC is believed to flow via three main cascades, the mitogen-activated protein kinase (MAPK) pathway, phosphoinositide 3-kinase (PI3K)-AKT pathway, and Ral guanine nucleotide exchange factor pathway.

1.2.2.1 MAPK Signaling in PDAC

The RAS-MAPK pathway plays a central role in human PDAC. RAF1 was the first RAS effector to be discovered and the canonical RAS-MEK-ERK pathway has been extensively studied since (Figure 1) [60]. RAF1, also known as CRAF, along with its related family members BRAF and ARAF, play a critical role in transducing signals from membrane-bound, GTP-RAS proteins to MEK and ERK kinases [61]. The binding of RAF to active KRAS stimulates RAF activation that in turn activates the dual-specificity kinases MEK1/2, which subsequently phosphorylate and activate the ERK family of kinases, ERK1/2 [62-64]. This results in ERK translocation to the nucleus where they phosphorylate a large spectrum of substrates the majority of which are transcription factors (TFs) [61, 65]. Unlike the restricted substrate specificity of RAF and MEK, hundreds of putative ERK substrates have been identified [65]. The ERK compendium database (http://sys-bio.net/erk_targets) includes around 2500 putative direct and indirect ERK substrates that have been identified via various large scale proteomics approaches [65], among those more than 400 are validated substrates based on the PhosphoSitePlus resource (http://www.phosphosite.org) and comprehensive analysis by Yang *et al.,* 2019 [66, 67]. Among the most notorious ERK nuclear substrates is MYC. MYC protein overexpression is reported in more than 40% of PDAC cases [68]. Phosphorylation of MYC and its subsequent stabilization was shown to be mediated by ERK in PDAC and was shown to play an essential role in *KRAS*-driven PDAC maintenance [69, 70]. In addition, ERK phosphorylates a number of cytoplasmic substrates such as Ribosomal S6 kinases (p90-RSKs) [71]. In addition, MAPK-activation of ERK was shown to activate the transcription factors FOS, JUN, ELK1, and ETS and the cytoplasmic MAPKAPK family members, including RSKs, MSKs, and MNK, among few to mention [72, 73]. Systematic analysis of the various ERK substrates is required to delineate their contribution to *KRAS*-driven PDAC and other cancers.

Extensive genetic studies allowed the dissection of the requirements for each of the MAPK pathway components in *KRAS*-driven tumors including PDAC [61]. Individual ablation of *Erk1/2* has no effect on the initiation of *Kras*-driven lung adenocarcinomas, yet their combined elimination completely blocks lung tumor formation. Similar results were observed with the individual or combined ablation of *Mek1/2* [74]. Similarly in PDAC, individual ablation

of *Mek1* does not block PDAC tumor formation and the combined deletion of *Mek1/2* was shown to inhibit the growth of *Kras* driven primary PDAC cells *in vitro* [75]. Interestingly, genetic investigation of the role of individual RAF isoforms revealed distinct requirements in various *KRAS*-driven cancers. Although targeting oncogenic *Braf* mutant to the murine pancreas was shown to induce PDAC development [76], it was shown to be completely dispensable for the induction of KRAS-driven lung tumors [74]. On the contrary, *Raf1* was shown to be essential for *Kras*-driven lung tumor initiation, progression and maintenance and skin cancer formation [74, 77, 78], but dispensable for PDAC tumorigenesis [79]. However, combined ablation of *Raf1* and *Egfr* is sufficient to block PDAC tumor initiation [80] and induce complete tumor regression in a subset of PDAC mice [81]. The cooperation of *Egfr* ablation *Raf1* loss was shown to be independent of MAPK and PI3K signaling, and to induce activation of pro-apoptotic pathways, however, the exact mechanism remains to be elucidated [78, 81]. The exact mechanism for the selective requirement for the RAF isoforms in *Kras*-driven tumors has not been established, a plausible explanation can be derived from the known differences among the three RAF. These observations set an exemplar for tissue-, context- and isoform-specificity that characterize oncogenic MAPK signaling in Ras-driven cancers. Although the three isoforms can phosphorylate MEK, RAF1 was shown to exhibit a variety of other functions that may contribute to its role in cancer independent of MAPK signaling [61]. RAF1 was shown to phosphorylate RB1 inhibiting its repression of E2F1 transcription and cell proliferation [82, 83]. RAF1 was also shown to promote nuclear factor (NF)-kB signaling via phosphorylation of MEKK1 and inhibitor of nuclear factor kappa B (IkB) [84]. In addition, RAF1 was shown to have an anti-apoptotic function; BCL2 was also shown to target RAF1 to the mitochondria where it can phosphorylate BAD and inhibit apoptosis [85]. RAF1 was shown to exhibit additional kinase-independent functions. For instance, RAF1 was shown to modulate Rho signaling by inhibiting ROCK2 kinase which contributes to its anti-apoptotic functions [86, 87]. Similarly, RAF1 interaction with ASK1 and MST2 was shown to mediate RAF1 anti-apoptotic functions [88, 89]. In addition, RAF1 was shown to contribute to the DNA damage response (DDR) via interaction with CHK2, and to mitosis by biding with Polo-like kinase 1 (PLK1) and Aurora kinase A (AURKA) at the mitotic spindles [90, 91].

Other MAPK signaling modules have also been implicated in PDAC tumorigenesis including the MEK5-ERK5 and p38 modules. All MAPK modules, similar to the ERK1/2 module follow a three-tiered structure; MAPK kinase kinases (MAPKKK) are typically activated by GTPases or RTK-activated and in turn activate MAPK kinases (MAPKK), that subsequently activate MAPKs that can be grouped into three families, ERK, Jun amino-terminal kinases (JNKs), and p38 kinases [92]. In the ERK5 module, MEK5 is the MAPKK that phosphorylates ERK5 in response to growth factors, serum, oxidative stress, and hyperosmolarity [93, 94]. MEK5 is activated by MEKK2 and MEKK3 which can also activate the JNK and p38 modules. Once activated, ERK5 is translocated to the nucleus where its transcriptional activation domain is exposed allowing it to exert direct transcriptional activation, a unique property of ERK5 compared to other ERKs [95]. ERK5 substrates include MEF2 transcription factor, c-MYC, SGK, RSKs, and cyclin D1 thus

allowing it to regulate survival and proliferation [95]. In PDAC, MEK5-ERK5 was shown to compensate for ERK1/2 inhibition by phosphorylating and stabilizing MYC [70]. The JNK and p38 modules respond to various environmental stresses and inflammatory cytokines, including oxidative stress, UV irradiation, hypoxia, ischemia, interleukin-1 (IL-1), and tumor necrosis factor alpha (TNF-α). Various MAPKKKs, GPCRs, and Rho family GTPases such as RAC and CDC42 can activate the p38 MAPK cascade. The MAPKs, MKK3, and MKK6 are thought to be the major protein kinases responsible for p38 activation. Activated p38 phosphorylates a large number of substrates, including the cytoplasmic substrates cPLA2, MNK1/2, MK2/3, HuR, BAX, and Tau, and the nuclear substrates ATF1/2/6, MEF2, Elk-1, GADD153, Ets1, p53, and MSK1/2[72]. P38 levels were found to be elevated in human PDAC and p38 was shown to play an essential role in proliferation and metabolism in PDAC by stimulating GLUT2-dependent aerobic glycolysis [96]. Paradoxically, other studies suggested a tumor suppressor function for p38 in PDAC; p38 was identified as a good prognostic marker correlated with improved survival and was shown to mediate this function via inhibiting JNK signaling [97].

1.2.2.2 PI3K-AKT Signaling in PDAC

The PI3K-AKT pathway is the most commonly activated pathway in human cancers [98]. PI3K-AKT signaling is activated downstream of RTKs, cytokine receptors, integrins, and GPCRs and plays a central role in promoting cell survival and growth [98]. PI3Ks are heterodimeric lipid kinases that are divided into three classes based on their structures and substrate specificities [99]. Class I PI3Ks are heterodimers that contain a p110 catalytic subunit, and a p85 regulatory subunit. Three highly homologous class IA catalytic subunits, encoded by *PIK3CA*, *PIK3CB* and *PIK3CD,* associate with one of the five p85-type regulatory isoforms, p85α, p55α, p50α, p85β and p55γ encoded by *PIK3R1* (encoding the three splice variants p85α, p55α, p50α), *PIK3R2* and *PIK3R3* respectively [99]. Class IB PI3Ks are heterodimers of a p110γ catalytic subunit, encoded by *PIK3CG*, coupled with the regulatory isoforms p101 or p87, encoded by *PIK3R5* or *PIK3R [99]*. The p110α and p110β catalytic subunits are ubiquitously expressed, whereas the p110δ and p110γ subunits are strictly expressed in leukocytes [99]. In absence of stimulation, the p85 regulatory subunit interacts with and inhibits the p110 catalytic subunit. Following stimulation, class I PI3Ks are recruited to the plasma membrane, where p85 inhibition of p110 is relieved and p110 phosphorylates the 3'-hydroxyl group of PtdIns 4,5-bisphosphate (PIP_2) converting it into PtdIns(3,4,5)P_3 (PIP_3). Class II PI3Ks are monomeric lipid kinases, however their biological functions are less well understood [99]. Class III PI3Ks compromise a single member vacuolar protein sorting 34, VPS34, encoded by the *PIK3C3,* that dimerizes with myristoylated, membrane associated VPS15, encoded by *PIK3R4*, and also phosphorylates phosphatidylinositides (PtdIns) to PIP_3. The VPS34–VPS15 dimer was shown to play important roles in intracellular trafficking and autophagy [99].

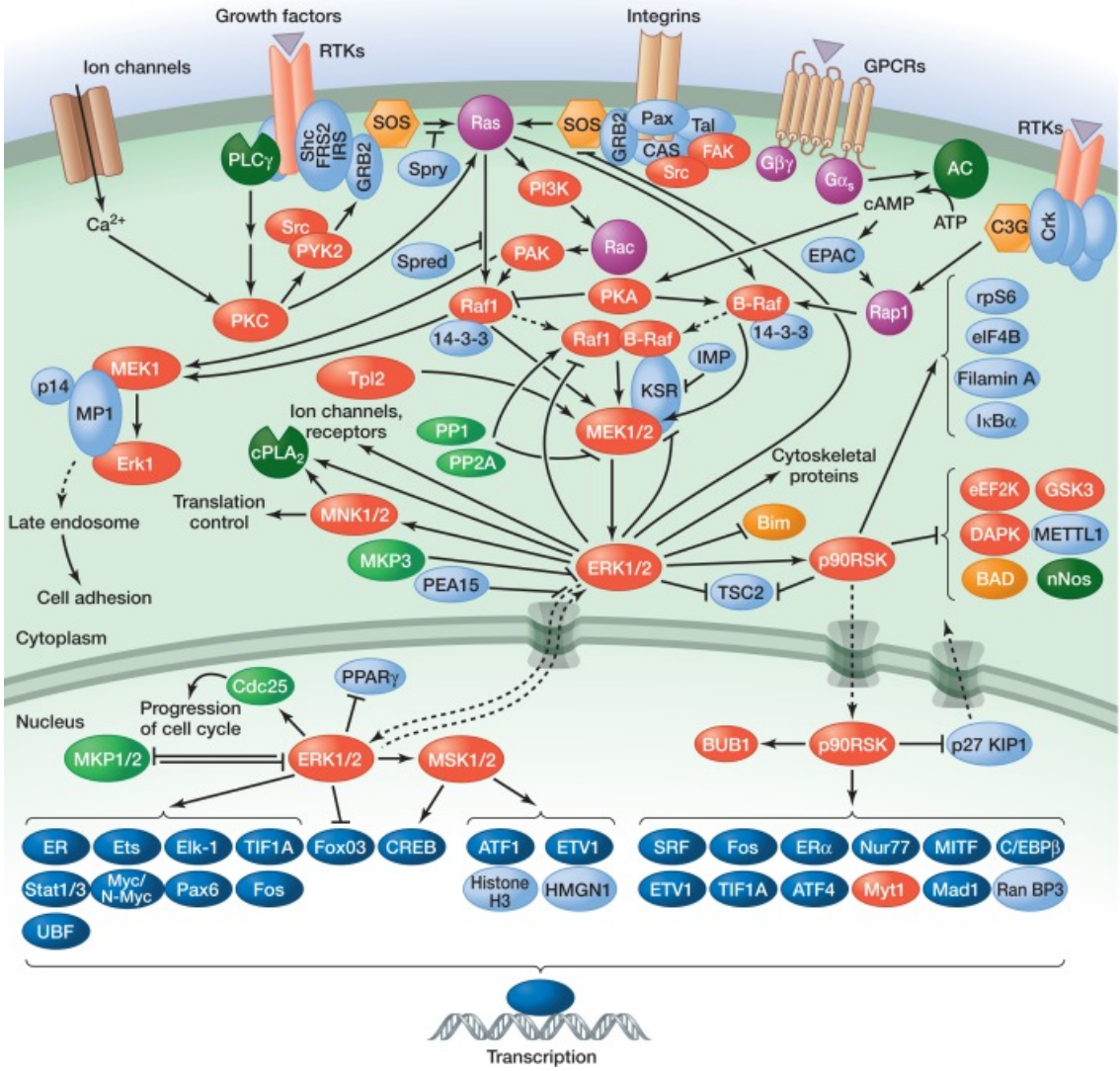

Figure 1: MAPK-ERK1/2 Signaling Pathway
(Morrison 2012 [92])

As mentioned above, Class I PI3Ks, referred to as PI3Ks forth on for simplicity, are activated in response to various signals. PI3K activation by RTKs can occur via different modes. The p85 subunit can bind directly to a specific phospho-motif within the RTK, or via the adaptor and scaffolding proteins, Grb2 and Gab, that bridge the RTKs and p85 subunit that activates the p110 catalytic subunit. Alternatively, PI3K activation can occur independently of the p85 subunit where Grb2 binds to the RTK, activating SOS that activates RAS. RAS can directly interact with and activate the p110 subunit that contains an RBD [100-102]. Upon activation, PI3K phosphorylates PIP_2 to generate PIP_3 which acts as a second messenger. PIP_3 creates docking sites at the membrane to recruit downstream effector proteins that contain a pleckstrin homology (PH) domain. Among these major effectors are the serine-threonine kinase AKT, previously known as protein kinase B or PKB, and phosphoinositide-dependent protein kinase 1, PDPK1 also known as PDK1. Upon its membrane recruitment, AKT is

phosphorylated by PDK1 at T308 residue in the activation loop resulting in its partial activation, and the mechanistic target of rapamycin (mTOR) complex 2 (mTORC2) or DNA-PK at S473 that stimulate its full activity [103-107]. Mammalian cells express three highly similar AKT isoforms (AKT1, AKT2, and AKT3), which are all activated in this manner. AKT1 and AKT2 are ubiquitously expressed, while AKT3 exhibits a restricted tissue distribution, being highest in the brain [98]. Activated AKT phosphorylates a broad array of downstream targets that regulate a variety of cell biological functions, including cell growth, proliferation, survival, translation, and metabolism [103-106]. Glycogen synthase kinase 3 (GSK3) was the first identified AKT substrate. Under basal conditions, GSK3 blocks glycogen synthesis by phosphorylating glycogen synthase in addition to several transcription factors that regulate metabolism and thus marking them for proteasomal degradation. This function of GSK3 is inhibited by AKT phosphorylation in response to growth factors [98, 108-110]. In addition, AKT can activate mTORC1 via phosphorylation of the tuberous sclerosis complex 2 (TSC2) protein. The TSC protein complex, consisting of TSC1 and TSC2, acts as a GAP to inhibit the small G protein Ras homologue enriched in brain (RHEB). AKT-mediated phosphorylation of TSC2 disrupts colocalization of the TSC complex with RHEB. The subsequent accumulation of active RHEB-GTP activates mTORC1 which plays an essential role in cell growth and metabolism [98]. Among AKT substrates are the FOXO family of transcription factors (FOXO1, FOXO3A, FOXO4). FOXO transcription factors induce the expression of numerous suppressors of growth, proliferation, and survival. AKT-mediated phosphorylation of FOXOs results in their sequestering in the cytoplasm and thus shutting off their expression program [111-114]. Negative regulation of PI3K is primarily mediated via the phosphatase and tensin homolog deleted on chromosome ten (PTEN). PTEN encodes a lipid and protein phosphatase that opposes the PI3K signaling primarily by converting PIP_3 to PIP_2. The physiological relevance of PTEN protein phosphatase function is less established [115]. Genetic aberrations leading to growth factor-independent activation of the PI3K–AKT pathway are among the most common drivers of human cancer [98]. In PDAC, in addition to RAS activation of the PI3K-AKT pathway, *PIK3CA* activating mutations or amplification is present in up to 3% of PDAC cases (cBioportal Database [116, 117]). In addition, mutations in *PIK3R1* and amplifications of PI3K downstream effector (*AKT2*), and decreased expression of PTEN have been reported in PDAC [118-122]. Collectively, these aberrations occur in more than one-third of PDAC cases. In a *Ptf1a*$^{Cre/+}$-based mouse model, pancreas-specific overexpression of *Pik3ca*^{H1047R} phenocopied *Kras*^{G12D}-driven PDAC initiation and progression [79, 123]. In addition, genetic ablation of *Pdk1* in a *Kras*^{G12D}-driven PDAC mouse model completely blocked PDAC initiation corroborating an essential role for PI3K-AKT signaling downstream of KRAS in PDAC [79]. In addition, ablation of *Pten* in a *Kras*^{G12D}-driven PDAC mouse model was shown to promote metastatic PDAC development and dramatically reduce survival through upregulation of PI3K-AKT signaling resulting in activation of the NF-κB pathway [119, 122]. In addition to activating AKT, PI3K signaling can activate the Rho family GTPase RAC1 via PIP_3 docking [124]. Pancreas-specific ablation of *Rac1* in a *Kras*^{G12D}-driven PDAC mouse model showed that *Rac1* is required for metaplastic changes and neoplasia-associated actin rearrangements in early PDAC

development [125, 126]. However, expression of constitutively active *Rac1* (*Rac1*^{G12V}) in the pancreas without concomitant oncogenic *Kras* was insufficient to initiate PDAC [79]

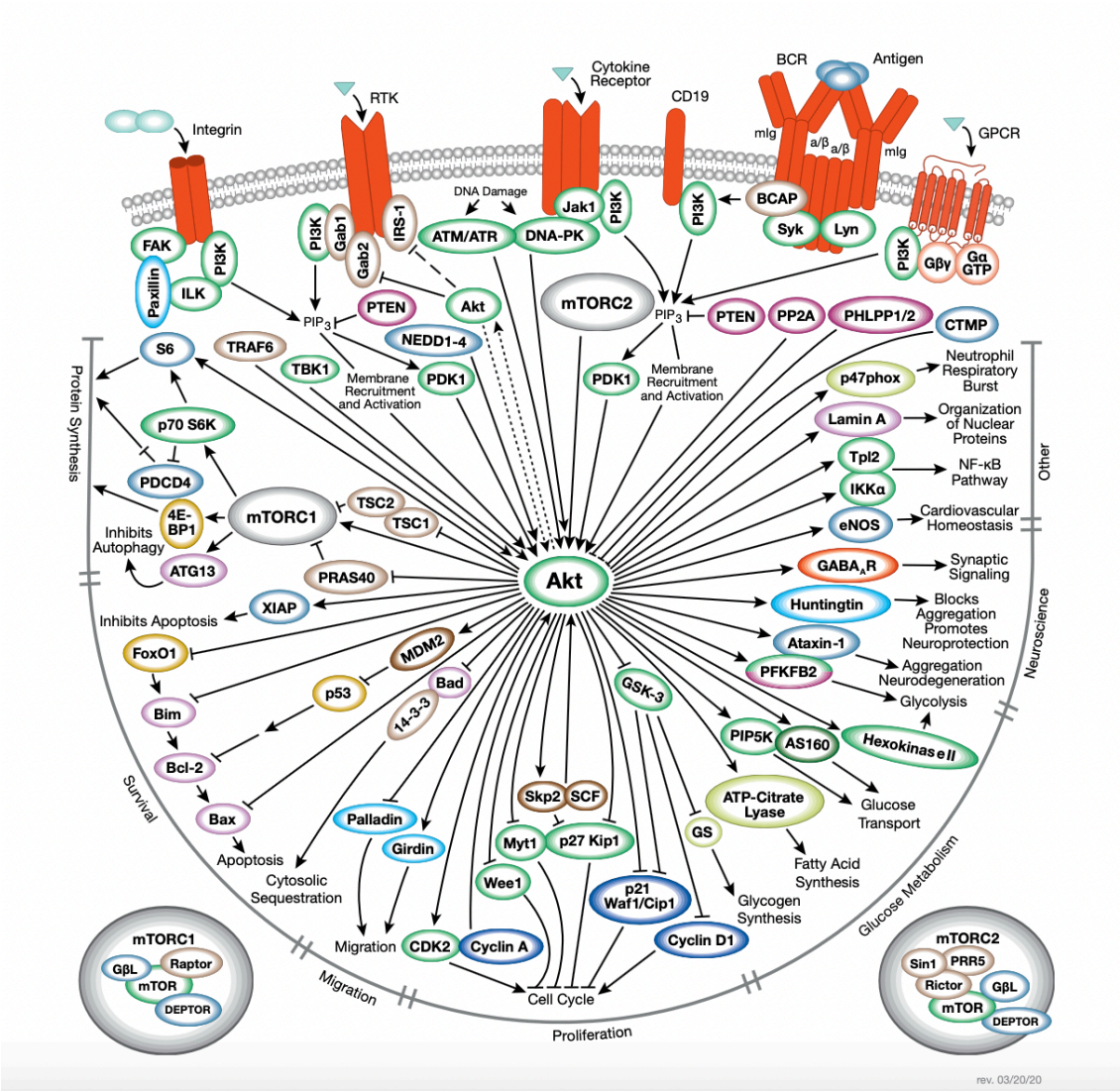

Figure 2: PI3K-AKT Signaling Pathway (Courtesy of Cell Signaling Technology©)

1.2.2.3 RalGEF Signaling in PDAC

RAL (RAS-like) GTPases were initially identified based on homology with Ras sequences [127]. In humans, two Ral genes, RALA and RALB, are ubiquitously expressed. RalGEFs, compromising RalGDS, RGL, RGL2, and RGL3, are RAS effectors that serve as a link between Ras and Ral GTPases [58]. Activated Ral-GTP interacts with multiple, functionally divergent downstream effectors. RalBP1 (Ral binding protein 1) also known as RLIP76 (76-kDa Ral-interacting protein 1) and RIP (Ral-interacting protein) was the first Ral effector to be discovered. RalBP1 was shown to be involved in the regulation of coated-pit endocytosis via interaction with clathrin adaptor proteins and receptor-mediated endocytosis [128]. Another

well-characterized role of Ral is the regulation of the SEC6-8 complex, also known as the exocyst. The exocyst is a large hetero-octameric complex responsible for the targeting and tethering of a subset of secretory vesicles to specific plasma membrane domains. Ral proteins regulate the exocyst by direct interaction with EXO84 and SEC5 subunits, promoting the assembly and function of the exocyst complex. [127]. RalGEF was shown to play a crucial role in RAS-induced transformation *in vitro* via activation of RalA [129]. Chronic depletion of *RALA* in a large panel of human pancreatic cancer cell lines, through stable integration of shRNA expression constructs, impaired or eliminated the capacity of these cells to form tumors following subcutaneous inoculation of nude mice, and both *RALA* and *RALB* were shown to play a critical role in metastatic tumor growth in PDAC, suggesting that RalA is required for the early stages of Ras-driven pancreatic tumorigenesis, whereas RalB is required for later stages of malignant growth. In addition, high levels of active RalA and RalB were detected in a panel of human PDAC samples[130].

1.3 Targeting KRAS Signaling

After decades of intensive research, clinically proven therapies for RAS-driven cancers are still absent, highlighting an urgent need for RAS-targeted therapeutics. The main challenges for developing efficient RAS targeted therapeutics can be attributed to multiple causes [131]. First, the RAS structure does not display a druggable topology which led to the long-held belief that RAS itself is undruggable. Second, inhibitors targeted at disrupting RAS membrane association, farnesyltransferase inhibitors, proved ineffective due to unexpected compensatory mechanisms in the cells. In addition, targeted therapies aimed at RAS effector pathways, mainly MAPK and PI3K signaling, were often associated with resistance due to complex feedback mechanisms and dynamic rewiring in the RAS signaling network. Last, the search for synthetic lethal partners of mutant RAS was hindered by the used technologies, mainly the high rate of off-target activity of RNA interference (RNAi) used in genetic screening for RAS synthetic-lethal interactors. Below, I discuss the various efforts aimed at drugging Kras-driven tumors, with focus on PDAC.

1.3.1 Direct RAS targeting

The concept that RAS is undruggable has been recently challenged by the development of RAS inhibitors that directly target the G12C mutant KRAS. *KRAS*^{G12C} is prevalent in smoking-associated non-small lung cancer (NSLC) which is the leading cause of cancer deaths in both genders in the United States [131]. Using a fragment-based screening approach called tethering aimed at the cysteine residue to distinguish the mutant KRAS from the Wild type (WT) KRAS, a new allosteric pocket, S-IIP, located beneath the dynamic SWII region of KRAS-GDP was identified. The binding of targeted molecules to this pocket leads to the stabilization of KRAS in the inactive GDP-bound state [132]. This work culminated in first-in-class KRAS^{G12C} inhibitors entering clinical trials for solid tumors with promising results [133-136]. Unfortunately, this strategy to target KRAS^{G12C} exploits a unique property of this mutant, and

is not readily applicable to other KRAS mutants. Although the identified pocket is present in all GDP-bound RAS proteins, compounds targeting $KRAS^{G12C}$ rely on the unique nucleophilicity of cysteine thiols in this substitution [131, 132]. In addition, $KRAS^{G12C}$ inhibitors rely on the continuous dependency of this mutant on GEF activity for full activation. As discussed previously, KRAS mutations function by primarily blocking RAS interactions with its corresponding GAP hindering GTP hydrolysis, however, the $KRAS^{G12C}$ mutant retains its intrinsic GTP hydrolysis and thus cycles between the GDP-bound and GTP-bound states more frequently compared to other KRAS mutants that are locked in the GTP-bound state. The existence of $KRAS^{G12C}$ in the GDP-bound status provides a therapeutic window in which the targeted inhibitors can bind to GDP-$KRAS^{G12C}$ and lock it in this inactive state [131, 137]. In addition, pan-RAS inhibitors were designed based on computational docking, synthesis, and testing on candidate molecules that can potentially reduce KRAS interaction with its effectors. RAS-IN-3144 was shown to have a selective affinity to mutant *$KRAS^{G12D}$* compared to WT RAS isoforms and was shown to block KRAS effector pathways *in vitro*. RAS-IN-3144 was also tested in a *$Kras^{LSL.G12D/+}$Tp53$^{fl/fl}$Pdx1-Cre* (KPC) mouse model of PDAC where it was shown to inhibit KRAS signaling with modest induction of apoptosis. Overall efficacy of the compound could not be evaluated due to toxicity that was attributed to the presence of only one functional *Kras* allele, making the model more sensitive to pan-RAS inhibition [138]. Alternatively, genetic depletion of mutant *KRAS* with antisense oligonucleotides (ASO) was shown successful in preclinical models [139] and was tested in a phase I clinical trial in patients with *KRAS*-mutant solid tumors (NCT03101839), however these trials were recently discontinued in favor for alternative strategies to target KRAS.

Regardless, several key issues in attempts to directly inhibit RAS can be foreseen. First is the concept of RAS independency [140]. In PDAC for instance, although initial studies showed oncogenic KRAS addiction in established Kras-driven PDAC mouse models [141, 142], other studies showed that KRAS addiction can be bypassed both *in vivo* in mouse models and *in vitro* in a panel of human and mouse PDAC cell lines via several mechanisms including YAP1 activation and PI3K-induced MAPK signaling activation [143, 144]. In addition, as expected by most targeted therapies, acquired resistance is anticipated to reduce the long-term efficacy of RAS inhibitors. Using genome-wide CRISPR interference, Lou et al., identified collateral dependencies that once targeted enhance response to $KRAS^{G12C}$ inhibitors and delay resistance onset [145]. These included upstream components of RTK signaling such as RTKs, adaptor proteins, and RAS GEFs in addition to components of the PI3K-AKT pathway and cell cycle regulators among others [145].

1.3.2 Targeting Upstream RAS regulators and interactors

Early efforts in developing RAS targeted therapeutics, focused on blocking RAS membrane association. Several potent farnesyl transferase inhibitors were identified and tested. These inhibitors effectively blocked the farnesyltransferase-dependent association of HRAS, but not

NRAS or KRAS, with the cell membrane, rendering them ineffective for patients with *NRAS* or *KRAS*-driven cancers [146, 147]. This selective efficacy was attributed to isoform-specific differences in post-translational processing where alternative prenylation of NRAS and KRAS by geranylgeranyl transferases was sufficient to compensate for farnesyltransferase inhibition [146, 148]. Dual targeting of farnesyl transferase geranylgeranyl transferases was proposed as an effective alternative for targeting KRAS-driven cancers but was hindered by the toxicity of these compounds that do not distinguish between mutant and WT RAS proteins [149]. More recently, inhibitors of phosphodiesterase-δ (PDEδ) were evaluated for their potential to block KRAS membrane localization. PDEδ is a guanine nucleotide dissociation inhibitor (GDI)-like solubilization factor that sequesters KRAS from the cytosol by binding the farnesyl moiety, preventing KRAS translocation from the Golgi apparatus and endomembranes to the plasma membrane. These compounds inhibited the growth of a panel of human pancreatic cancer cell lines *in vitro* [150]. In an alternative strategy, inhibitors of the RAS-GEF, SOS1 were identified using high-throughput fragment screening. These inhibitors blocked downstream RAS signaling by disrupting the RAS-SOS1 interaction [151].

1.3.3 Targeting RAS vulnerabilities

An alternative approach to direct targeting of oncogenic cancer drivers is to exploit the concept of synthetic lethality or induced essentiality. Synthetic lethality is a type of genetic interaction where the co-occurrence of two genetic events results in organismal or cellular death, in this case, mutant *KRAS* with chemical inhibition of a synthetic lethal partner [152, 153]. Targeting synthetic lethal vulnerabilities in cancer also provides the advantage of reducing potential side effects, as normal cells lacking oncogenic *KRAS* should be, in principle, less susceptible to the inhibition of the synthetic lethal partner.

Several synthetic lethal short hairpin RNA screens in *KRAS*-mutant cancers have been performed. In an early screening attempt by Lou et al., 2009, using an isogenic $KRAS^{G13D}$ and WT colorectal cancer cell lines, genes involved in the regulation of mitosis including subunits of the anaphase-promoting complex/cyclosome (APC/C), the proteasome and the mitotic kinase polo-like kinase (PLK1) were identified as candidate *KRAS* synthetic lethal interactors. These results were corroborated by using PLK1 inhibitor that supported the mitotic machinery as an "Achilles' heel" for *KRAS* mutant colorectal cancer [154]. In another high throughput loss-of-function RNAi screen in eight human cancer cell lines, representing five cancer entities including pancreatic cancer, *STK33* was identified as an essential gene for in the context of mutant *KRAS* [155]. Subsequent studies using STK33 dominant mutants and STK33 inhibitors contradicted the initial finding that could be likely the result of off-target effects of RNAi [156-158]. In yet another RNAi screen by Barbie et al., 2009 in a panel of 19 *KRAS* mutant cancer cell lines, TBK1 inhibition was identified as a synthetic lethal partner of oncogenic *KRAS* [159]. Further investigation showed that TBK1 might have a role in RAS function in cells with additional genetic alterations but not in all *KRAS*-mutant tumors [160]. Notably, the various studies lacked overlap in genes identified as candidate *KRAS* synthetic lethal partners. In

addition to the difference in the experimental settings in these studies, this inconsistency mainly stemmed from the off-target effects of RNAi. Advances in genetic screening, mainly the implementation of CRISPR-Cas technologies as an alternative means of genetic perturbation have enabled the refinement of this approach [161]. Loss of function CRISPR-Cas9 screens performed in AML cancer cell lines with mutant or WT *KRAS* identified PREX1, a GEF for Rac GTPases, as an AML-specific activator of MAPK signaling in the context of mutant *KRAS* [162]. Another CRISPR-Cas9 screen performed in colorectal cancer identified metabolic enzymes and the chromatin remodeling protein INO80C as novel targets for mutant *KRAS* colorectal tumors [163].

1.3.4 Targeting RAS effector pathways

The failure of the aforementioned approaches led to intensified efforts in targeting downstream KRAS effectors in an attempt to combat *KRAS*-driven tumors. These efforts were fueled by the development and advancement of a multitude of compounds targeting various nodes in the MAPK and PI3K pathways that were shown to be the main effectors of KRAS signaling.

1.3.4.1 Targeting the MAPK pathway

As discussed earlier, genetic evidence implicated components of the MAPK pathway as oncogenes in PDAC. This resulted in enormous efforts to target KRAS-mutant tumors by inhibiting downstream MAPK signaling. Sorafenib was among the first drugs aimed at blocking the MAPK signaling pathway [61, 164]. Sorafenib was developed as an ATP-competitive CRAF inhibitor, however, its clinical efficacy was attributed to its unspecific multi-kinase inhibitory effects [71, 164]. Phase II Clinical trials for Sorafenib in lung cancer showed limited efficacy independent of *KRAS* mutational status that didn't warrant Food and Drug Administration (FDA) approval [165]. The detection of activating *BRAF* mutations in human cancer prompted the development of the second generation of RAF inhibitors with higher specificity toward BRAF mutant proteins such as vemurafenib, dabrafenib, and encorafenib [61, 71, 140]. Although these inhibitors showed significant therapeutic efficacy in $BRAF^{V600E}$-driven tumors, this response was short-lived due to acquired resistance via various mechanisms that lead to the re-activation of MAPK signaling [140]. When tested in other *RAS*-mutant tumors with WT *BRAF*, these inhibitors showed paradoxical activation of MAPK signaling, due to drug-mediated transactivation of RAF dimers [166, 167]. This unexpected activation of MAPK signaling was evident by accelerated tumor growth observed in patients with Chronic Myeloid Leukemia and the development of cutaneous squamous cell tumours in patients treated with these RAF inhibitors [168, 169]. This lead to the development of the third generation of RAF inhibitors that can be classified into two main classes [170]. The first group includes the so-called paradox breakers. These inhibitors, such as PLX7904 and PLX8394, inhibit the paradoxical activation of ERK signaling by disrupting BRAF-containing dimers (BRAF

homodimers and BRAF-CRAF heterodimers) [171, 172]. These inhibitors however show no effect on CRAF dimers and thus are expected to have less robust effects in *KRAS*-driven tumors [172]. The other class includes pan-RAF inhibitors such as LY3009120, TAK-632, MLN2480, and LXH254 [61, 170]. LY3009120 inhibits all RAF isoforms including BRAF, CRAF, and ARAF [173]. Despite, showing efficacy in pre-clinical testing [174] [173], Phase I clinical trials of LY3009120 revealed high toxicity and insufficient efficacy (NCT02014116) [175]. TAK-632 and MLN2480 (TAK-580) [176, 177] show similar characteristics with promising results in preclinical testing [177, 178]. MLN2480 (TAK-580), also known more recently as DAY101 is currently in Phase II clinical testing for patients with known BRAF alterations (NCT01425008, NCT03429803, and NCT04775485). However, Yen *et al.* showed that these pan-RAF inhibitors showed little efficacy as monotherapies in a large panel of *KRAS*-mutant tumors [179]. RAS mimetics that block RAF interaction with KRAS have also been described, such as rigosertib [180] and MCP110 [181]. LXH254, a novel RAF inhibitor, targeting CRAF and BRAF while sparing ARAF [182], is currently in phase II testing for Melanoma (NCT04417621). LXH254-centric combinations are also being tested in NSCLC or Melanoma (NCT02974725). A number of allosteric MEK inhibitors have also been developed and investigated for their anti-cancer efficacy such as the FDA-approved drug, Trametinib. Inhibitors of MEK, have been approved for melanoma treatment in combination with $BRAF^{V600E}$ inhibitors [183-185]. Despite their efficacy in BRAF-mutant cancers, these MEK inhibitors failed to achieve significant benefits in *KRAS*-driven cancers, including lung cancer and pancreatic cancer, as monotherapies or in combination with chemotherapy [61, 186-189]. The failure of MEK inhibitors is generally a consequence of dose-limiting toxicities that prevents reaching the necessary doses to achieve the anti-tumor response, in addition to the rapid development of resistance through various mechanisms including the feedback activation of the PI3K pathway and reactivation of the MAPK pathway [61, 140, 190, 191]. More recently, direct ERK inhibition has shown promise in overcoming some limitations of RAF and MEK inhibition [140]. Clinical trials showed that an average of 80% inhibition of ERK is required in patients to achieve an objective clinical response, indicating that broad target inhibition of the MAPK pathway is required to modulate the cascade [140, 192]. Direct ERK inhibitors were proposed as an alternative approach to circumvent the persistence of ERK signaling observed with RAF and MEK inhibitors [192]. Indeed, when tested in pre-clinical models, ERK inhibitors were able to overcome resistance in BRAF or MEK inhibitor-resistant models [193, 194], and suppress the growth of *KRAS*-mutant cancers specifically pancreatic cancer [69]. When tested in patient-derived colorectal cancer organoids, sensitivity to ERK inhibitor was correlated with the *BRAF* mutation but was not completely consistent with the *KRAS* status [195]. Several ERK inhibitors entered clinical trials. The ERK inhibitor MK-8353 was tested in melanoma patients (NCT01358331) showing promise in *BRAF*-mutant melanomas [196]. MK-8353 centric combination are also currently being tested in advanced cancers (NCT02972034 and NCT03745989). Another ERK inhibitor, ulixertinib (BVD-523) is also in clinical testing as single agent as well as in combinations with Phase I trials showing early evidence of clinical activity in *RAS* and *RAF*-mutant cancers as monotherapy (NCT02296242) [197]. As expected with

targeted therapies, acquired resistance was reported with ERK inhibitors that arise via various mechanisms that include ERK mutations [198-200].

3.4.2 Targeting the PI3K/AKT pathway

Increased activation of PI3K signaling has been observed in PDAC patients [79] and has been linked to poor overall survival in PDAC [201]. The use of GEM models identified components of the PI3K pathway as the major mediators of *Kras* transformation in PDAC [79, 202], hence rationalizing the targeting of this pathway to combat *Kras*-driven PDAC. The class I PI3K inhibitor (GDC0941) was shown to stabilize tumor growth in KPC mice and human-derived xenografts [79]. A general limitation of systematic administration of PI3K inhibitors was the inherent resistance caused by induction of insulin feedback that results in reactivation of PI3K-mTOR signaling [203]. AKT inhibitors were also tested in PDAC patients. Among these MK2206 was tested as monotherapy and showed a minor anti-tumor response in patients [204]. Another node in the PI3K pathway that was extensively targeted is mTOR. The first-generation mTOR inhibitors, Rapalogs (rapamycin-based compounds) that bind to the intracellular rapamycin binding domain (FKBP-12) failed the clinical trials as monotherapies [205, 206]. This has been mainly attributed to upstream feedback loops that result in AKT reactivation [207, 208]. This led to increased interest in dual vertical inhibition of the PI3K pathway by targeting both mTOR complexes or mTOR and other components in the pathway [209]. Unfortunately, resistance to second-generation inhibitors such as AZD2014, that target both mTORC1 and mTORC2, has also been detected due to adaptive rewiring via various mechanisms that lead to reactivation of AKT [210, 211]. In addition, Phase II clinical trials of AZD2014 have been withdrawn due to lack of efficacy (NCT03166176). Dual PI3K/mTOR Inhibitors have also been developed and tested in PDAC. Similar, to other dual inhibitors, resistance due to overactivation of the MAPK pathway has been reported [212]. Interestingly, Rapalogs showed a unique response in *KRAS* tumors with *PTEN* loss when tested in a GEM model [213]. In addition, mTOR inhibition showed partial response in patients with *LKB1* mutations. This emphasizes the importance of genetic stratification in clinical trials that remains mainly absent [209].

1.4 CRISPR-Cas system as a revolutionary Genome Engineering technology

The development of recombinant DNA technology in the 1970s, marked by the discovery of restriction enzymes [214-216], revolutionized molecular biology, granting scientists for the first time the ability to manipulate DNA and driving a number of discoveries in molecular biology and genetics [217, 218]. A few decades later, genome engineering technologies, brought about a new era in molecular biology, this time allowing scientists to manipulate DNA in its endogenous locus in living eukaryotic cells including mammalian cells. Zheng and colleagues defined genome engineering as ‘the process of making targeted modifications to the genome, its contexts (e.g, epigenetic marks), or its outputs (e.g., transcripts)’ [217]. A

breakthrough that enabled initial genome manipulation was the development of gene targeting by homologous recombination (HR), which allows cells to incorporate exogenous DNA into their genome, from a repair template that contains sequence homology to the donor site [219-222]. Despite enabling the functional characterization of many genes in model organisms, HR has several limitations. Mainly, the rate of spontaneous integration by HR is extremely low (1 in 10^6-10^9 cells), making the approach far from being scalable [217, 218, 222]. These limitations powered an active search for new tools to enable genome engineering.

1.4.1 Targeted nucleases as Genome editing tools

A major advancement in genome editing came from studies that led to the realization that targeted DNA double-strand breaks (DSBs) can greatly enhance HR-mediated recombination events [223, 224], and that these DSBs can be also corrected by the nonhomologous end-joining (NHEJ) repair pathway that induces insertions or deletion mutations (indels), in the absence of a homology template [225]. Hence, establishing DSB-induced HR and NHEJ as pathways that could be exploited for genome engineering [217]. This led scientists to exploit various endonucleases and program them into genome engineering tools. Among those, meganucleases were among the initial nucleases that were used to induce DSBs and enhance HR [223]. Despite the availability of hundreds of naturally-occurring meganucleases, the probability to find a meganuclease that targets the desired locus was still low due to their unique recognition sites [218]. Efforts to re-engineer these meganucleases and alter their DNA-targeting specificities were limited by the absence of a clear relation between meganuclease protein residues and their target DNA sequence specificity [217, 226]. The discovery of Zinc Finger proteins (ZFPs) with modules that bind DNA based on a specific 3-bp sequence made them an attractive tool for biologists. Zing Finger nucleases (ZFNs) were engineered by fusing these Zing Finger proteins to the DNA cleavage domain of the Fok I endonuclease[227]. The DNA binding specificity of these ZFNs could be manipulated by assembling multiple zinc finger modules, that in turn direct the nuclease to specific genomic loci. Thus, by combining of up to 7 Zinc fingers out of the unique 64 naturally occurring zinc finger modules, unique genomic sequences of up to 21bp could be targeted specifically [218, 228]. Similarly, transcription activator-like effector nucleases (TALENs) were generated by the chimeric fusion of transcription activator-like effector (TALE) proteins, that can specifically recognize one single base instead of three bases, to Fok I DNA cleavage domain [229-232]. Despite the great advantage these programmable nucleases offered, they suffered from major limitations. When assembled into large arrays, ZFPs exhibit context-dependent binding preference due to crosstalk between the adjacent modules, which makes the assembly of ZFNs with a desired DNA binding specificity a laborious process that requires extensive screening [217, 233]. In addition, the engineering of both ZFNs and TALENs proved to be a labor-intensive, time-consuming, and costly task [217, 218]. More recently, programmable nucleases based on the CRISPR system revolutionized the genome engineering field by

offering robust editing of nearly any location in the genome with a simple design and hence allowing complex applications from basic biology to medicine.

1.4.2 CRISPR-Cas as a bacterial adaptive Immune system

The CRISPR-Cas system (clustered regularly interspaced short palindromic repeats-CRISPR associated) is a naturally occurring system that functions as an adaptive immune system in Bacteria and Archaea that fends off infecting bacteriophages and viruses [234, 235]. The CRISPR-Cas systems are highly diverse due to an arms-race rapid evolution between Bacteria and their invaders [236]. CRISPR immunity functions in 3 different stages that include Adaptation (or spacer acquisition), CRISPR RNA (crRNA) biogenesis, and interference that allow Bacteria to store records of past infections and elicit fast and robust responses upon reinfection, analogous to vertebrate adaptive immunity [237-239].

1.4.2.1 Discovery of CRISPR-Cas

CRISPR-Cas systems are generally defined as genomic loci consisting of a clustered set of CRISPR-associated (Cas) genes and a signature CRISPR array, a series of 20-50 base pair (bp) direct repeats separated by variable sequences (spacers) that correspond to sequences within foreign genetic elements (protospacers) [217, 237, 240]. The CRISPR loci were initially reported as early as the late 1980s when several groups reported these loci in model organisms and pathogenic bacteria. [217, 234, 241-246]. The acronym CRISPR referring to these loci was later coined in 2002 with the frequent observation of these loci that was possible by the increased availability of Bacterial and Archaeal genome sequences [234, 240]. The function of the CRISPR-Cas system remained elusive until 2005 when systematic analysis of bacterial genomes and their infecting phages suggested a phage-associated origin of the spacer sequences, and that the presence of a specific spacer was correlated with resistance to the corresponding virus. This led to hypothesizing that CRISPR may function as an immune memory and defense mechanism against foreign invaders [247-249]. Further experimental proof showing that the removal or addition of particular spacers modified the phage-resistance phenotype supported the role of the CRISPR-Cas system in Bacterial adaptive immunity [217, 250].

1.4.2.2 Mechanism of CRISPR-Cas Immunity

CRISPR immunity (Figure 3) begins with adaptation, also known as spacer acquisition, where foreign DNA is identified, processed, and integrated into the CRISPR locus as a new spacer [236, 237]. The selection of protospacer sequences is non-random and depends on the presence of a protospacer adjacent motif (PAM) sequence [236, 237, 251, 252]. This is followed by the processing of the foreign DNA into spacer precursors of a defined size [236]. Cas 1 and Cas2, which are conserved among all CRISPR-Cas systems, mediate the integration of these spacers into the CRISPR locus [236, 237, 253]. CRISPR immunity further requires the

assembly of CRISPR ribonucleoprotein (crRNP) complexes to mediate inference. Assembly of these complexes begins with transcription of the CRISPR locus to generate a long, precursor transcript (pre-crRNA). This transcript is processed into mature crRNA guides, which each contains a single spacer, via endoribonucleolytic cleavage within the repeat sequences, mediated either by Cas6 homologs or by RNase III [236, 237, 254, 255]. In the interference stage, an effector complex (crRNP complex) is assembled and uses the crRNA to find and destroy phages with sequence complementarity to the spacer sequence of the crRNA via DNA cleavage [237]. Based on the nature of the effector nucleases that mediate this targeting, the CRISPR-Cas system is classified into 2 classes, class 1, which uses a multiprotein effector complex (cascades), and Class 2, which employs a single protein. These classes are further divided into six types (I-VI) based on the encoded Cas proteins. In a canonical type II CRISPR–Cas system (class 2), the most commonly used system for genomic engineering, Cas9 endonuclease is the only enzyme within the *cas* gene cluster that mediates target DNA cleavage [256]. A noncoding *trans*-activating crRNA (tracrRNA) that hybridizes with crRNA was shown to be crucial for effective RNA-guided targeting of Cas9 [257]. In addition, CRISPR interference relies on PAM sequences to initiate target recognition and subsequent cleavage[236].

1.4.2 CRISPR-Cas as a genome engineering system

The elucidation of the mechanism of CRISPR-Cas9 immunity was followed by several studies that demonstrated that CRISPR can be adapted for *in vivo* genome editing in eukaryotic cells. First, it was shown that the CRISPR system is transferrable; and that the CRISPR locus can be transplanted heterologously, generating functional CRISPR interference in the host bacterial strain [258]. In addition, it was shown that purified Cas9 nuclease, guided by crRNAs, can cleave target DNA in vitro [259, 260]. Eventually, it was shown that this CRISPR-Cas9 system can be used for efficient genome editing in mammalian cells [261-263]. This CRISPR-Cas9 system was used to achieve genome editing in various cells and model organisms ranging from bacteria to human cells, mice, rats, and monkeys [264-267].

1.4.2.1 Mechanism of CRISPR-Cas9 Genome Editing

Streptococcus pyogenes Cas9 (SpCas9) is the prototype CRISPR-Cas system most commonly used for genome editing. Efficient interference by the CRISPR-Cas9 system requires 3 main components: Cas9 protein, tracrRNA, and crRNA (Figure 2). S*p*Cas9 is a large multidomain and multifunctional DNA endonuclease [268]. It consists of two major lobes, the recognition (REC) lobe and the nuclease (NUC) lobe that are connected through two linking segments, an arginine-rich bridge helix and another disordered linker. The REC lobe contains three alpha-helical domains (Hel-I, Hel-II, and Hel-III). The nuclease (NUC) lobe contains the conserved HNH nuclease domain, split RuvC nuclease domain, and a variable C-terminal domain (CTD) that contains PAM-interacting sites required for PAM interrogation [268-271]. Endogenously,

DNA recognition and cleavage by Cas9 requires the loading of a guide RNA (a native crRNA–tracrRNA), where the 20 nucleotides (nt) crRNA confers DNA target specificity, and the tracrRNA plays a crucial role in Cas9 recruitment [260, 268, 269]. Chimeric single guide RNAs (sgRNAs), engineered by fusing the crRNA, to up to 72 bp of the tracrRNA, were shown to be

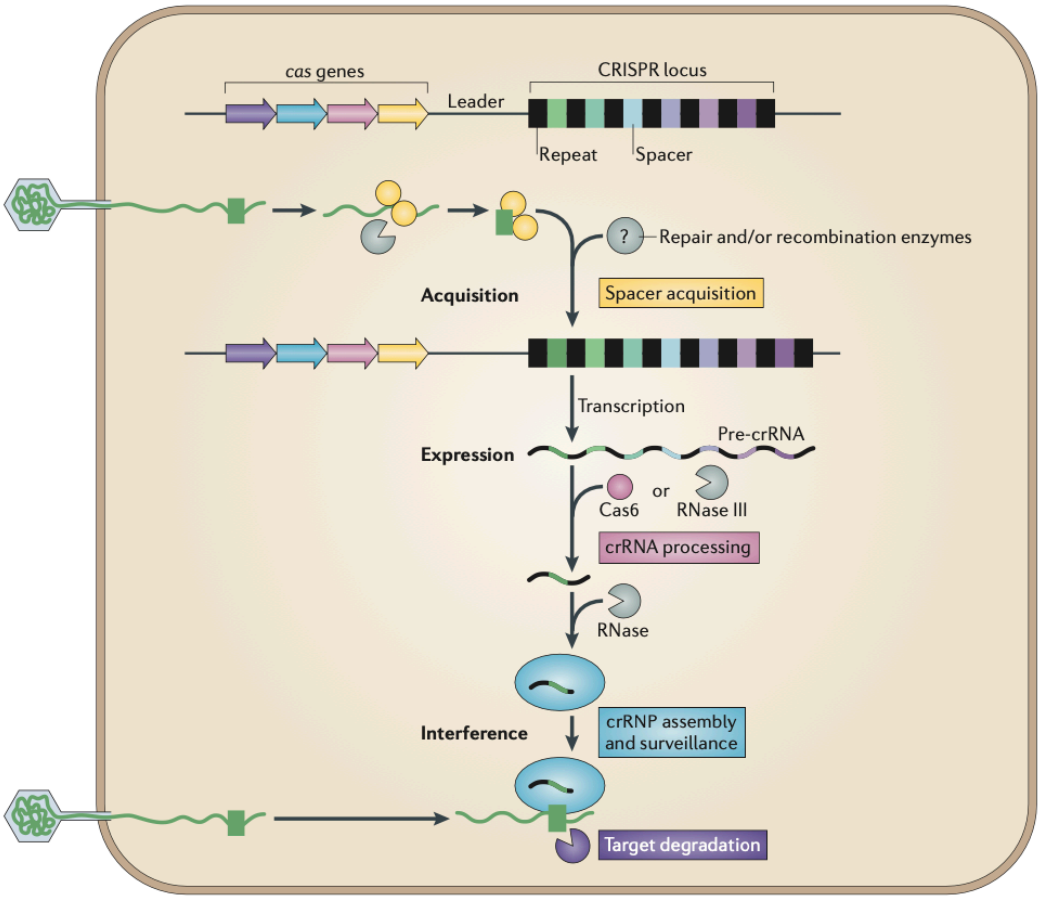

Figure 3: Mechanism of CRISPR Immunity (Van der Oost et al., 2014 [236])

sufficient for proper Cas9-sgRNA-DNA ternary complex formation and effective genome editing [217, 260, 263, 271, 272]. SgRNA loading results in extensive structural rearrangements in Cas9 [270], the preordering of the seed sequence required for initial DNA interrogation, and the pre-positioning of the PAM-interacting sites, enabling Cas9 to form a DNA recognition-competent structure [268, 273-277]. This assembled complex is now capable of searching for target DNA sites, based on complementary base pairing between the 20-nt sgRNA sequence and the target DNA, in addition to the presence of the PAM sequence (5′-NGG-3′ for spCas9) adjacent to the target site [259, 260, 268, 277]. Single-molecule imaging studies showed that the assembled Cas9 complex first probes for PAM sequences throughout the genome, before interrogating the flanking DNA for potential guide RNA complementarity [268, 278]. This occurs through three-dimensional collisions, in which Cas9 rapidly dissociates

from DNA that does not contain the appropriate PAM sequences. Once a PAM sequence is found, the binding time of Cas9 to DNA depends on the complementarity between the guide RNA and the DNA sequence adjacent to the PAM [268, 278-280]. After finding a target site, Cas9 triggers local DNA melting followed by RNA strand invasion to form an RNA–DNA heteroduplex and a displaced DNA strand (termed R-loop) from PAM-proximal to PAM-distal end. Cas9 enzyme is then activated for DNA cleavage using both of its nuclease domains, the HNH domain and the split RuvC domain [268, 278, 281]. Each domain specifically cleaves one strand of the target dsDNA 3bp upstream from the PAM sequence generating a blunt-ended DSB. [259, 260, 268].

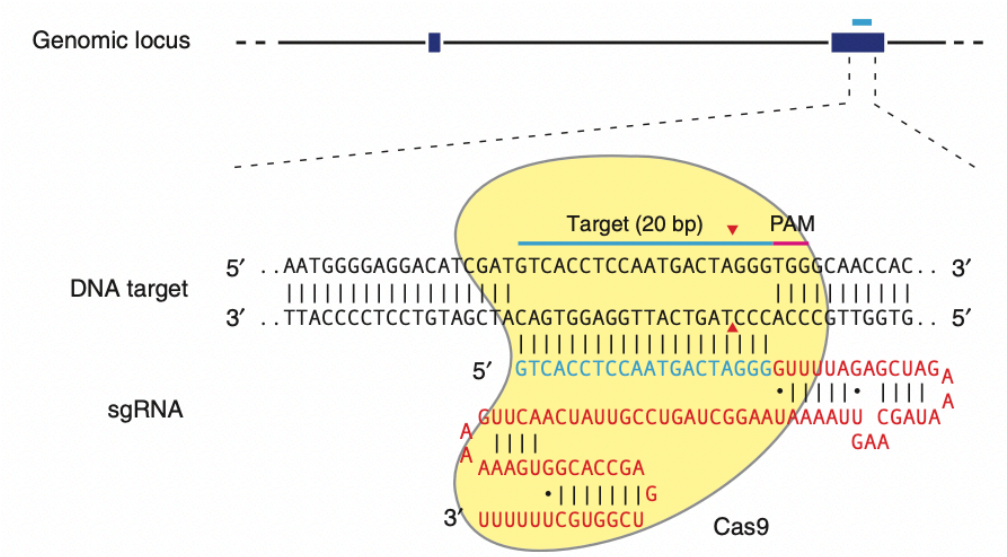

Figure 4: Scheme of sgRNA-Cas9 complex (Ran et al., 2013 [282])

These DSBs can be repaired by the cell using two main pathways: nonhomologous end-joining (NHEJ) and homology-directed repair (HDR) (Figure 3) [282]. NHEJ is error-prone and leads to the introduction of insertion/deletion mutations (indels) of various lengths, which results in frameshift mutations and often premature stop codons, resulting in a knockout (KO). HDR-mediated repair occurs in the presence of a donor template with homology ends to the target site and allows the insertion of specific sequences or mutations via HR [282].

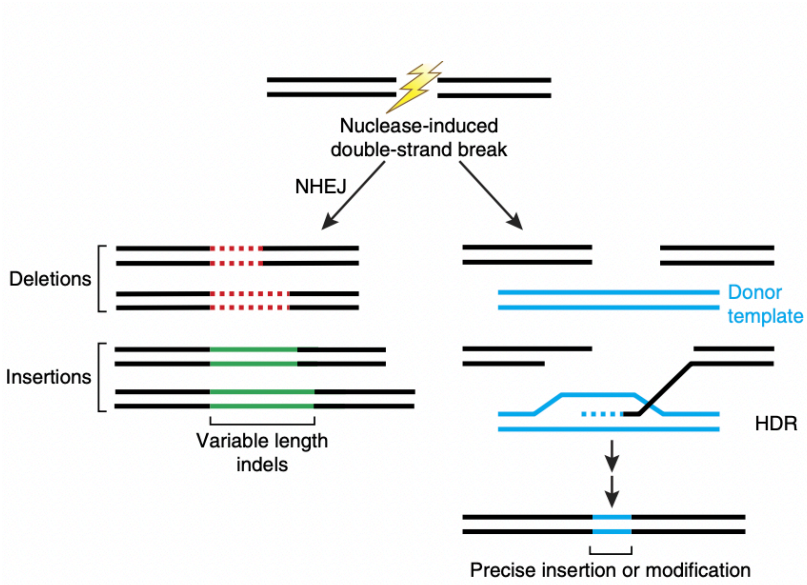

Figure 5: DSB repair mechanisms promote CRISPR-Cas9 genome editing (Ran et al., 2013 [282])

1.4.2.2 Specificity of Cas9 Targeting

CRISPR-Cas9 adaptation as a genome-editing tool brought great hope for its use for clinical applications and gene therapy. A major concern was the specificity of Cas9 targeting. Various approaches have been utilized to assess Cas9 targeting specificity. Several groups used sgRNA mutagenesis combined with reporter assays to assess Cas9 specificity. [263, 272, 283, 284]. These studies showed that multiple mismatches are less tolerated at the 'seed' sequence (8-12 bp at the 3' end of the guide sequence) compared to the 5' end of the guide sequence, consistent with previous *in vitro* and bacterial work [285, 286], however, they also showed that all positions within the guide contribute to the overall specificity and the effect of single or double mismatches cannot be always predicted based on location within the guide sequence [263, 272, 283, 284]. It was also shown that Cas9 tolerance to mismatches was concentration-dependent, with mismatches being better tolerated with higher Cas9 concentrations, and that decreasing Cas9 concentration significantly improves the on- to off-target cleavage ratio [272, 284]. In addition, other genome-wide tools were used to understand CRISPR-Cas9 targeting specificity, such as chromatin immunoprecipitation and high throughput sequencing (ChIP- Seq) [287, 288]. These studies showed that the rate of Cas9 off-target binding was much higher than that of Cas9 off-target cleavage and that Cas9 DNA binding is decoupled from Cas9 cleavage activity. [287, 288] Whole Genome deep sequencing was also used to assess Cas9 off-targets. [289, 290] This method however is very costly, and thus alternative NGS (Next Generation Sequencing) approaches that specifically enrich for DSB sites were developed such as BLESS [291], GUIDE-Seq [292], Digenome-Seq [293], SITE-Seq [294], CIRCLE-Seq [295] and others that combine NGS with prediction

methods [296]. In addition, several studies focused on increasing Cas9 fidelity using various approaches. Re-engineering Cas9 by introducing specific point mutations was shown to significantly increase the specificity of SpCas9 (Cas9-HF1) [297]. In addition, structure-guided protein engineering was also employed to generate Cas9 variants with increased specificity [298]. Directed evolution methods also allowed the identification of SpCas9 variants with higher specificities such as HIFI-Cas9 and Sniper-Cas9 [299, 300]. Other approaches focused on the delivery method of the Cas9-sgRNA complex, direct delivery of Cas9-sgRNA as a ribonucleotide protein (RNP) complex was shown to result in more transient Cas9 activity and less off-target effects [301, 302]. A double-nicking approach based on tandem targeting of a locus with two separate sgRNAs and a mutant Cas9 with one catalytically inactivated nuclease domain that functions as a nickase (nCas9) or a catalytically inactive Cas9 (dCas9) fused to the DNA cleavage domain of the Fok I, was shown to improve specificity up to thousand folds relative to WT-type Cas9 [282, 303-305]. Another approach termed CRISPR Guide RNA Assisted Reduction of Damage (CRISPR GUARD) protects off-target sites by co-delivery of short guide RNAs directed against the off-target loci and that compete with the on-target guide RNA reducing off-target cleavage without affecting the on-target editing efficiency [306]. On the other hand, several studies tried to alter the PAM specificity of Cas9 in an attempt to expand its genome targetability [307, 308]. This culminated with the generation of a near-PAMless Cas9 (SpRY) promising unconstrained editing of any region of the genome [309]. In addition, orthogonal Cas9 nucleases from various systems with different PAM requirements were investigated for use in genome editing [261, 310-315].

1.4.2.3 Second-generation CRISPR-Cas9 genome editors

A second-generation of CRISPR editing tools, capable of precisely editing single nucleotides, was developed. These single-base editing tools utilize Cas9 nickase, for specific targeting without generating DSBs, fused to adenine or cytidine deaminases for base conversion [316-318]. These CRISPR base editors were used to introduce early STOP codons in genes (CRISPR-STOP) as a less deleterious alternative to WT Cas9-mediated gene KO [319-322]. Additionally, the activation-induced adenosine deaminase (AID) enzyme has also been fused to the dCas9 enzyme and was used as a powerful local mutagenesis tool for gain of function screening [323-325].

1.4.2.4 Repurposing CRISPR-Cas9 beyond Genome Editing

Due to its robustness and flexibility, The CRISPR-Cas system was repurposed in various ways to allow additional genome and chromatin manipulations. A major example is the adoption of Cas9 as a transcription regulation tool. This is achieved by engineering Cas9 into a DNA recognition complex rather than a targeted nuclease. Cas9 nuclease activity can be abolished by mutating both the NHN and RucV domains, without compromising its RNA-guided DNA-targeting capacity [260, 326]. This dead Cas9 (dCas9) can then be fused to various effectors enabling a broad range of applications [218, 327]. By fusing dCas9 to transcription repressors

and activators, it can function as a transcription regulation tool allowing scientists to manipulate the expression of genes from their endogenous locus. Interestingly, the binding of dCas9 to DNA can repress transcription by sterically hindering the RNA polymerase machinery [326]. Although this CRISPR-based interference, or CRISPRi, works efficiently in Prokaryotes, it was shown to be less efficient in eukaryotic cells [328, 329]. To enhance this repressive function of CRISPRi, dCas9 was fused to transcriptional repressor domains such as the Kruppel- associated Box (KRAB), which promotes epigenetic silencing by heterochromatin formation [329]. However, these dCas9-mediated transcriptional repressors suffered from incomplete silencing of target genes.[329]. Several efforts focused on improving these CRISPRi tools. One study reported an improved Cas9 repressor based on the rational design of a bipartite repressor domain, of methyl-CpG binding protein 2 (MeCP2) fused to KOX1 KRAB, that can be fused to dCa9 [330]. Another systematic study assayed 57 out of the 350 KRAB domains encoded in the human genome, in search of a more potent KRAB repressor. Indeed, they identified ZIM3 KRAB domain, that once fused to dCas9 outperformed the previous CRISPR repressors [331]. Similarly, Cas9 can be converted into a transcriptional activator by fusing it to transcription activation domains. CRISPR activation (CRISPRa) was achieved using various approaches. Initial studies fused dCas9 to VP64 which is composed of four tandem copies of the viral transactivation domain (VP16) [303, 332, 333]. This strategy results in only a modest transcriptional upregulation (generally less than 2-fold) and was further improved. dCas9 was fused to a tripartite transactivation complex, which is composed of VP64, P65, the transcription activation domain of the mammalian NF-κB transcription factor, and Rta, the R transactivator of Epstein-Bar virus (VPR) proteins [334]. A parallel, approach was to recruit effector domains through the sgRNA scaffold. The sgRNA scaffold was engineered to contain RNA modules such as MS2 hairpin aptamers, that can bind to specific RNA binding proteins such as bacteriophage MS2-coat protein (MCP), and in turn recruit MCP-fused VP64 or the P65-HSF1 transactivation complex [335, 336]. The two approaches were combined to generate a synergistic activation mediator (SAM) complex, where the dCas9-VP64 fusion complex was used in combination with an engineered sgRNA scaffold that recruited MCP-fused P65-HSF1 transactivation domains. This approach was termed synergistic activation mediator (SAM) [336]. In another approach, dCas9 was fused to a protein scaffold that contains a repeating peptide array termed SunTag, which can recruit multiple copies of an antibody fused VP64 domains [337]. Comparative analysis of the various Cas9 activator systems across multiple species demonstrated that the 3 approaches, VPR, SAM, and Suntag, had comparable efficiencies, with the SAM approach exhibiting a trend of higher potency, and were consistently superior to the standard VP64 standard [338]. This study also showed gene-to-gene variability in activation efficiency that was negatively correlated with basal gene expression [338]. dCas was also fused to various other effectors to achieve various functions such as live cell imaging and epigenetic editing [218, 327].

1.4.2.5 Harnessing CRISPR-Cas for large-scale functional Screens

Traditionally, functional genetic studies are divided into forward or reverse screens. In forward genetic screening, genes are mutated at random to generate a phenotype of interest, and then mutations are mapped, and the phenotype is attributed to the mutated genes. Conversely, reverse genetic approaches involve the disruption of a known gene of interest to assign its function [339]. The availability of the genome sequence of model organisms and humans in addition to the evolution of tools for targeted perturbation of genes of interest allowed extensive reverse genetic screening to be possible. These functional genetic screens proved to be powerful tools to interrogate gene function and phenotype-to-genotype interactions in a high-throughput setting [340]. Genetic screens can be designed in an arrayed (plate, single well) format, where single genes are perturbed separately in distinct single wells. Alternatively, pooled screens (barcode format) allow the simultaneous targeting of a large number of genes in a pooled, single batch manner, with one gene perturbation per cell. This pooled format is advantageous as it ensures lower costs and less intensive labor and eliminates the requirement for high-throughput robotics [340]. Gene perturbation can be achieved by direct gene KO using CRISPR or knockdown using RNA interference (RNAi), or CRISPRi for loss-of-function screening. Gain-of-function screens, traditionally achieved by exogenous gene overexpression of open reading frames (ORFs), nowadays rely mostly on CRISPRa [340]. The advancement of CRISPR/Cas9 technology circumvented many of the limitations of the previously used RNAi technology, mainly the partial knockdown and extensive off-target effects, and was massively adapted for large-scale loss of function (LOF) genetic screening. Swiftly following the adaptation of the CRISPR/Cas9 system for mammalian applications, prove of principle papers demonstrating the ability to adapt the CRISPR/Cas9 technology for robust negative and positive selection genetic screening in human cells, that actually outperformed the methodologies used at that time (shRNA screens) [341, 342]. The ongoing massive efforts to identify cancer vulnerabilities led by the Broad Broad Institute of MIT and Harvard and the Wellcome Sanger Institute to shift from shRNA screens to CRISPR screens and generated a plethora of CRISPR data [343-345]. The availability of all this data was paralleled with the major development of computational tools to analyze the large data sets generated from those CRISPR screens such as MAGeCKFlute and Bagel to name a few [346-348]. This made genome-wide CRISPR screens a highly accessible and powerful tool to use.

2. Materials

2.1 Equipment

Table 1: Laboratory equipment

Device	Source
Analytical balance A 120 S	Sartorius AG, Göttingen, DE
Analytical balance BP 610	Sartorius AG, Göttingen, DE
Autoclave 2540 EL	Tuttnauer Europe B.V., Breda, The Netherlands
AxioCam HRc	Carl Zeiss AG, Oberkochen, DE
AxioCam MRc	Carl Zeiss AG, Oberkochen, DE
Centrifuge Avanti® J25	Beckman Coulter GmbH, Krefeld, DE
Centrifuge Rotina 46R	Andreas Hettich GmbH & Co. KG, Tuttlingen, DE
ClarioStar MARS microplate reader	BMG Labtech, Ortenberg, DE
CO_2 incubator HERAcell®	Heraeus Holding GmbH, Hanau, DE
CO_2 incubator MCO-5AC 17AI	Sanyo Sales & Marketing Europe GmbH, Munich, DE
Dewar carrying flask, type B	KGW-Isotherm, Karlsruhe, DE
Electrophoresis power supply Power Pac 200	Bio-Rad Laboratories GmbH, Munich, DE
Electroporation System, Gene Pulser®II	Bio-Rad Laboratories GmbH, Munich, DE
FACSAriaTM III Cell Sorter	BD Medical Device company, Franklin Lakes, NJ, USA
Flu-O-Blu blue light table	Biozym Scientific GmbH, Hessisch Oldenburg, Germany
Fluorescence microscope HG 100 APO HC	Leica Microsystems GmbH, Wetzlar, Germany
Glass ware, Schott Duran®	Schott AG, Mainz, DE
Heated paraffin embedding module EG1150 H	Leica Microsystems GmbH, Wetzlar, DE
Heidolph Rotamax 120 Orbital Shaker	Heidolph Instruments GmbH & Co. KG, Schwabach, Germany
HERAsafe® biological safety cabinet	Thermo Fisher Scientific, Inc., Waltham, MA, USA
HERAfreezeTM HFU T Series -86°C Upright Ultra-Low Temperature Freezers	Thermo Fisher Scientific, Inc., Waltham, MA, USA
HiSeq 2500 Sequencing System	Illumina, Inc., San Diego, CA, USA
Horizontal gel electrophoresis system	Biozym Scientific GmbH, Hessisch Oldenburg, DE
Horizontal shaker	Titertek Instruments, Inc., Huntsville, AL, USA
Incubator shaker Thermoshake	C. Gerhardt GmbH & Co. KG, Königswinter, DE

Infors Ecotron Incubator shaker	Infors GmbH, Sulzemoos, Germany
Laminar flow HERAsafe	Heraeus Holding GmbH, Hanau, DE
Leica Microscope DM E	Leica Microsystems GmbH, Wetzlar, Germany
Magnetic stirrer, Ikamag® RCT	IKA® Werke GmbH & Co. KG, Staufen, DE
Microcentrifuge 5425	Eppendorf AG, Hamburg, DE
Microcentrifuge 5427 R	Eppendorf AG, Hamburg, DE
Mini centrifuge MCF-2360	LMS Consult GmbH & Co. KG, Brigachtal, Germany
Microscope Axio Imager A1	Carl Zeiss AG, Oberkochen, DE
Microscope Axiovert 25	Carl Zeiss AG, Oberkochen, DE
Microscope DM LB	Leica Microsystems GmbH, Wetzlar, DE
Microwave	Siemens AG, Munich, DE
Mini centrifuge MCF-2360	LMS Consult GmbH & Co. KG, Brigachtal, DE
Mini-PROTEAN® Tetra Cell	Bio-Rad Laboratories GmbH, Munich, DE
Miseq platform	Illumina, San Diego, CA, USA
Multipette® stream	Eppendorf AG, Hamburg, DE
NALGENE® Cryo 1°C Freezing Container	Thermo Fisher Scientific, Inc., Waltham, MA, USA
Neubauer hemocytometer, improved	LO-Laboroptik GmbH, Bad Homburg, DE
Odyssey® Fc Imaging System	Li-Cor Biosciences, Lincoln, NE, USA
pH meter 521	WTW Wissenschaftlich-Technische Werkstätten GmbH, Weilheim, DE
Pipettes Eppendorf Research Plus	Eppendorf AG, Hamburg
Pipetus Hirschmann	Hirschmann Laborgeräte GmbH & Co. KG, Eberstadt
Power supplies E844, E822, EV243	Peqlab Biotechnologie GmbH, Erlangen, DE
Qubit® 2.0 Fluorometer	Invitrogen GmbH, Karlsruhe, DE
ROTINA 380 R Centrifuge	Andreas Hettich GmbH & Co. KG, Tuttlingen
Shaking Water Bath SB-12	Biozym Scientific GmbH, Hessisch Oldendorf
Spectrophotometer NanoDrop 1000	Peqlab Biotechnologie GmbH, Erlangen, DE
StripettorTM Plus pipetting controller	Corning Inc., Corning, NY, USA
StripettorTM Ultra pipetting controller	Corning Inc., Corning, NY, USA
StepOnePlus™ real time PCR system	Applied Biosystems, Inc., Carlsbad, CA, USA
Stereomicroscope Stemi SV 11	Carl Zeiss AG, Oberkochen, DE
Surgical instruments	Thermo Fisher Scientific, Inc., Waltham, MA, USA
Thermocycler Tone	Biometra GmbH, Göttingen, DE

Thermocycler Tgradient	Biometra GmbH, Göttingen, DE
Thermocycler Tprofessional Basic	Biometra GmbH, Göttingen, DE
Thermocycler Tadvanced	Biometra GmbH, Göttingen, DE
Thermomixer compact	Eppendorf AG, Hamburg, DE
Thermoshake incubator shaker	Gerhardt GmbH & Co. KG, Königswinter
Tumbling Table WT 17	Biometra GmbH, Göttingen, DE
Vortex Genius 3	IKA® Werke GmbH & Co. KG, Staufen, DE
Water bath 1003	GFL Gesellschaft für Labortechnik mbH, Burgwedel, DE
Western Blotting Electrophoresis Chambers	Bio-Rad Laboratories GmbH, Munich, Germany
Western Blotting Criterion Blotter Chambers	Bio-Rad Laboratories GmbH, Munich, Germany

2.2 Disposables

Table 2: Disposables

Disposable	**Source**
BioPur® Safe-lock reaction tubes	Eppendorf AG, Hamburg, Germany
CELLSTAR® Cell culture multiwell plate (6, 12, 24, 48, 96 well)	Greiner Bio-One GmbH, Kremsmünster, Austria
Costar® Multiple Well Cell Culture Plates (6, 12, 24, 48, 96 well)	Corning Inc., Corning, NY, USA
Cell scrapers	TPP Techno Plastic Products AG, Trasadingen, Switzerland
Cell strainer, 100 µm, yellow	BD Biosciences, Franklin Lakes, NJ, USA
Chromatography paper, 3 mm	GE Healthcare Europe GmbH, Munich, DE
Combitips BioPur®	Eppendorf AG, Hamburg, DE
Corning® Centrifuge Tubes (15ml, 50ml)	Corning Inc., Corning, NY, USA
Cover slips	Gerhard Menzel, Glasbearbeitungswerk GmbH & Co. KG, Braunschweig, DE
CryoPure tubes	Sarstedt AG & Co., Nümbrecht, DE
Cuvette	Greiner Bio-One GmbH, Kremsmünster, Austria
Disposable scalpels	Feather Safety Razor Co., Ltd., Osaka, Japan
Feather® disposable scalpels	Socorex Isba SA, Écublens, Switzerland

Gene Pulser®/MicroPulser™ cuvettes, 0.2 cm gap	Bio-Rad Laboratories GmbH, Munich, DE
Filtropur S 0.2	Sarstedt AG & Co., Nümbrecht, DE
Filtropur S 0.45	Sarstedt AG & Co., Nümbrecht, DE
Glass slides Superfrost® Plus	Gerhard Menzel, Glasbearbeitungswerk GmbH & Co. KG, Braunschweig, DE
MicroAmp® optical 96-well reaction plate	Applied Biosystems, Inc., Carlsbad, CA, USA
Mr. Frosty™ freezing container	Thermo Fisher Scientific, Inc., Waltham, MA, USA
Multichannel Reagent Reservoirs	INTEGRA Biosciences AG, Zizers, Switzerland
Nitrocellulose Membrane 0.45 µm	Bio-Rad Laboratories GmbH, Munich, Germany
NuncTM EasYFlaskTM Cell Culture Flasks (T25, T75, T175)	Thermo Fisher Scientific, Inc., Waltham, MA, USA
Pasteur pipettes	Hirschmann Laborgeräte GmbH & Co. KG, Eberstadt, DE
PCR reaction tubes	Brand GmbH + Co. KG, Wertheim; Eppendorf AG, Hamburg, DE
PCR Plates	Eppendorf AG, Hamburg, Germany
Petri dishes	Sarstedt AG & Co., Nümbrecht, DE; nerbe plus GmbH & Co. KG, Winsen, Germany
Pipette tips	Sarstedt AG & Co., Nümbrecht, DE
Reaction tubes, 0.5 mL, 1.5 mL and 2 mL	Eppendorf AG, Hamburg, DE
Precision wipes	Kimberly-Clark Worldwide Inc., Irving, TX, USA
Serological pipettes (2ml, 5ml, 10ml, 25ml, 50ml)	Sarstedt AG & Co., Nümbrecht, DE; Greiner Bio-One GmbH, Kremsmünster, Austria
Single use needles Sterican® 27 gauge	B. Braun Melsungen AG, Melsungen, DE
Single use syringes Filtropur	Sarstedt AG & Co., Nümbrecht, Germany
Tissue Culture Dish (6cm, 10cm, 15cm)	TPP AG, Trasadingen, Switzerland
Western Blotting Filter Paper	Bio-Rad Laboratories GmbH, Munich, Germany

2.3 Reagents

Table 3: Reagents

Reagent	**Source**
1 kb DNA extension ladder	Invitrogen GmbH, Karlsruhe, DE
1,4-Dithiothreitol (DTT)	Carl Roth GmbH + Co. KG, Karlsruhe, DE
2-Log DNA ladder (0.1–10.0 kb)	New England Biolabs GmbH, Frankfurt am Main
2-Mercaptoethanol, 98%	Sigma-Aldrich Chemie GmbH, Munich, DE
2-Propanol (isopropanol)	Carl Roth GmbH + Co. KG, Karlsruhe, DE
2x Taq PCR Master Mix	Thermo Fisher Scientific, Inc., Waltham, MA, USA
4-hydroxytamoxifen (4-OHT)	Sigma-Aldrich Chemie GmbH, Taufkirchen, Germany
Agarose	Carl Roth GmbH & Co. KG, Karlsruhe, Germany
Agencourt AMPure XP Beads	Beckman Coulter GmbH, Krefeld, DE
Ammonium persulfate	Sigma-Aldrich Chemie GmbH, Munich, DE
Ampicillin sodium salt	Carl Roth GmbH + Co. KG, Karlsruhe, DE
Blotting grade blocker non-fat dry milk	Bio-Rad Laboratories GmbH, Munich, DE
Bovine serum albumin, fraction V	Sigma-Aldrich Chemie GmbH, Munich, DE
Bradford reagent	Serva Electrophoresis GmbH, Heidelberg, DE
CellTiter Glo® assay	Promega, Walldorf, DE
Chloramphenicol	AppliChem GmbH, Darmstadt, DE
Collagenase Type II	Gibco, Life Technologies GmbH, Darmstadt, Germany
Complete, EDTA-free, protease inhibitor cocktail Tablets	Roche Deutschland Holding GmbH, Grenzach-Wyhlen, DE
CreActive TAM400	LASvendi, Soest, DE
Dimethylsulfoxide (DMSO)	Carl Roth GmbH + Co. KG, Karlsruhe, DE
dNTP mix, 10mM each	Sigma-Aldrich Chemie GmbH, Taufkirchen, Germany
Dodecylsulfate Na-salt in pellets (SDS)	Serva Electrophoresis GmbH, Heidelberg, DE
Dulbecco's phosphate buffered saline, powder	Thermo Fisher Scientific, Inc., Waltham, MA, USA
Ethanol (100%)	Merck KGaA, Darmstadt, DE

Ethidium bromide	Sigma-Aldrich Chemie GmbH, Munich, DE
Ethylenediaminetetraacetic acid (EDTA)	Invitrogen GmbH, Karlsruhe, DE
Gel loading dye, blue	New England Biolabs GmbH, Frankfurt am Main, DE
GeneRuler™ 100bp DNA ladder	Fermentas GmbH, St. Leon-Rot, DE
Glycerol	Sigma-Aldrich Chemie GmbH, Munich, DE
HotStarTaq DNA polymerase	Qiagen GmbH, Hilden, DE
Hydrochloric acid (HCl)	Merck KGaA, Darmstadt, DE
Isotonic sodium chloride solution	Braun Melsungen AG, Melsungen, DE
KAPA HiFi HotStart ReadyMix	Roche Deutschland Holding GmbH, Grenzach-Wyhlen, DE
Kanamycin	Carl Roth GmbH & Co. KG, Karlsruhe, Germany
LB agar (Luria/Miller)	Carl Roth GmbH + Co. KG, Karlsruhe, DE
LB broth (Luria/Miller)	Carl Roth GmbH + Co. KG, Karlsruhe, DE
Magnesium chloride	Carl Roth GmbH + Co. KG, Karlsruhe, DE
Methanol	Merck KGaA, Darmstadt, DE
N, N-dimethylformamide	Sigma-Aldrich Chemie GmbH, Munich, DE
Phosphatase inhibitors mix I	Serva Electrophoresis GmbH, Heidelberg, DE
Polyethylene glycol 4000	Merck KGaA, Darmstadt, DE
Precision Plus Protein™ all blue standard	Bio-Rad Laboratories GmbH, Munich, DE
Proteinase K, recombinant, PCR grade	Roche Deutschland Holding GmbH, Grenzach-Wyhlen, DE
REDTaq® ReadyMix™ PCR reaction mix	Sigma-Aldrich Chemie GmbH, Steinheim, DE
Restriction endonucleases	New England Biolabs GmbH, Frankfurt am Main, DE
RNase-free DNase set	Qiagen GmbH, Hilden, DE
RnaseA	Fermentas GmbH, St. Leon-Rot, DE
Rotiphorese® gel 30	Carl Roth GmbH + Co. KG, Karlsruhe, DE
S.O.C. medium	Invitrogen GmbH, Karlsruhe, DE
Sodium acetate buffer solution	Sigma-Aldrich Chemie GmbH, Munich, DE
Sodium chloride (NaCl)	Merck KGaA, Darmstadt, DE
Sodium hydroxide solution (NaOH)	Merck KGaA, Darmstadt, DE
TE buffer, pH 8.0	AppliChem GmbH, Darmstadt, DE

TEMED	Carl Roth GmbH + Co. KG, Karlsruhe, DE
TransIT-LT1	Mirus Bio LLC, Madison, USA
Tris hydrochloride	J.T. Baker® Chemicals, Phillipsburg, NJ, USA
Tris Pufferan®	Carl Roth GmbH + Co. KG, Karlsruhe, DE
Triton® X-100	Merck KGaA, Darmstadt, DE
Tween® 20	Carl Roth GmbH + Co. KG, Karlsruhe, DE

2.4 Kits for Molecular Biology

Table 4: Kits for molecular biology

Kit	**Source**
Antibody Array Assay Kit (KAS02)	Full Moon Biosystems, California, USA
GenEluteTM Mammalian Genomic DNA Miniprep Kit	Sigma-Aldrich Chemie GmbH, Taufkirchen, Germany
Monarch® DNA Clean-up Kit	New England Biolabs GmbH, Frankfurt am Main, Germany
Monarch® DNA Gel Extraction Kit	New England Biolabs GmbH, Frankfurt am Main, Germany
NucleoSpin Plasmid EasyPure DNA purification Mini kit	MACHEREY-NAGEL GmbH & Co. KG, Düren , Germany
NucleoBond Xtra Midi kit for transfection-grade plasmid DNA kit	MACHEREY-NAGEL GmbH & Co. KG, Düren , Germany
NucleoBond Xtra Maxi EF Kit	MACHEREY-NAGEL GmbH & Co. KG, Düren , Germany
Phospho Explorer Antibody Array (PEX100)	Full Moon Biosystems
QIAprep® Spin Miniprep Kit	QIAGEN GmbH, Hilden, Germany
QIAGEN Blood&CellCulture DNA MaxiKit	QIAGEN GmbH, Hilden, Germany
RNeasy Protect Mini Kit (250)	QIAGEN GmbH, Hilden, Germany
TruSeq® Stranded mRNA Sample Preparation Kit	Illumina Biotechnology company, San Diego, CA, USA
Q5® Site-Directed Mutagenesis Kit	New England Biolabs GmbH, Frankfurt am Main, Germany
Q5® High-Fidelity DNA Polymerase	New England Biolabs GmbH, Frankfurt am Main, Germany

2.5 Competent cell strains and Plasmids

Table 5: Competent bacterial strains

Competent Bacteria	**Source**
Endura Electro Competent cells (60240)	Lucigen
One shot® Stbl3TM chemically competent E. coli	Invitrogen GmbH, Karlsruhe, Germany
One shot® TOP10 TM chemically competent E. coli	Invitrogen GmbH, Karlsruhe, Germany

Table 6: Plasmids

Plasmid	**Source**	**RRID**
LentiCas9-Blast (#52962)	Addgene, Watertown, MA, USA	Addgene_52962
LentiCRISPRv2 puro (#98290)	Addgene, Watertown, MA, USA	Addgene_98290
The mouse CRISPR Knockout Brie pooled Library (#73632)	Addgene, Watertown, MA, USA	n/a
The mouse CRISPR/Cas9 Synergistic Activation Mediator (SAM) pooled library (#1000000075)	Addgene, Watertown, MA, USA	n/a
lentiMPH v2 #89308	Addgene, Watertown, MA, USA	Addgene_89308
lenti dCaS-VP64_Blast # 61425	Addgene, Watertown, MA, USA	Addgene_61425
psPAX2 #12260	Addgene, Watertown, MA, USA	Addgene_12260
pMD2.G (#12259)	Addgene, Watertown, MA, USA	Addgene_12259
pUSE WT AKT1 (# 17-251)	Upstate Biotechnology, NY, USA	n/a
pUSE DN-AKT; K179M mutant (# 21-152)	Upstate Biotechnology, NY, USA	n/a
pUSE Myr-AKT (# 21-151)	Upstate Biotechnology, NY, USA	n/a
pKLV2-U6gRNA5(Empty)-PGKmCherry2ABFP-W	Addgene, Watertown, MA, USA	Addgene_67985
pKLV2-U6gRNA5(gBFP)-PGKmCherry2ABFP-W	Addgene, Watertown, MA, USA	Addgene_67986

3. Methods

Disclosure: Standard procedures followed in the research group of Prof. Saur has been used in this thesis and hence the description of the methods can bare resemblance to previous work published by members of Prof. Saur research group, including the PhD thesis of Christian Veltkmap that characterized the Dual recombinase mouse model with the floxed *Pdk1* allele and established the PCRs and some of the other methods. (https://mediatum.ub.tum.de/1308250).

3.1 Mouse experiments

All animal studies were performed in compliance with the European guidelines for the care and use of laboratory animals and by the Institutional Animal Care and Use Committees (IACUC) of the local authorities of Technical University of Munich and the Regierung von Oberbayern (the District Government of Upper Bavaria).

3.1.1 Mouse strains

Mouse models with conditional Cre/loxP and Flp/frt recombinase systems were used in this study. Mice expressing transgenes flanked by *loxP* or *frt* sites or silenced by an loxP-stop-loxP (LSL) or frt-stop-frt (*FSF)* cassette were bred with mice expressing Cre or Flp recombinase under the control of a pancreas-specific promoter to allow conditional inactivation of flanked genes or deletion of the *LSL or FSF* cassette to activate tissue specific expression of the target genes. For time specific inactivation of genes an inducible dual-recombination Flp/frt;Cre^{ERT2}/loxP system was used [349]. All animals were on a mixed *C57BL/6;129S6/SvEv* genetic background. All mouse models have been described previously in the indicated references.

Ptf1a$^{Cre/+}$ [350]
The *Ptf1a$^{Cre/+}$* knock-in mouse strain was kindly provided by Dr. Hassan Nakhai (Klinikum rechts der Isar, Technical University Munich). The Ptf1a gene expresses a subunit of the pancreas transcription factor (Ptf) and plays a fundamental role in pancreas development in mice. This strain ensures Cre expression specifically in pancreatic precursor cells.

LSL-Kras$^{G12D/+}$ (RRID:IMSR_JAX:008179) [351, 352]
This knock-in mouse strain was kindly provided by Prof. Tyler Jacks (Massachusetts Institute of Technology, Cambridge, MA, USA). *LSL-Kras$^{G12D/+}$* mice carry a point mutation in codon 12 that leads to a glycine to aspartate amino acid substitution, mimicking the alteration frequently detected in human PDAC. Cre-mediated deletion of the *LSL* cassette, constitutively active KRAS is expressed in the targeted tissue.

Pdk1$^{lox/+}$ [353]
In this knock-in mouse strain, exons 3 and 4 of the *Pdk1 endogenous* locus are flanked by *loxP* sites. Cre recombination induces conditional deletion of *Pdk1*.

Pdx1-Flp [349]
This transgenic mouse strain was generated in the laboratory of Prof. Dieter Saur. Codon-optimized FLPo recombinase is expressed under the control of the *Pdx1* (Pancreatic and Duodenal Homeobox 1) promotor, which is active in pancreatic progenitor cells and in adult pancreatic acini, ducts and islets.

FSF-Kras$^{G12D/+}$ [349]
This knock-in mouse strain was generated in the laboratory of Prof. Dieter Saur. oncogenic *Kras^{G12D}* allele is silenced by and FSF cassette in the endogenous locus and can be activated by FLP recombinase.

FSF-R26$^{CAG\text{-}CreERT2/+}$ [349]
This mouse strain was generated in the laboratory of Prof. Dieter Saur. FSF-R26^{CreER} is a knock in transgene at the Rosa26 locus. Cre^{ERT2} allele encodes a latent tamoxifen-inducible CRE recombinase silenced by the FSF cassette. Flp recombinase resuts in FSF cassette deletion, and expression of the Cre^{ERT2} allele under the strong CAG promoter induction, the system allows spatial or temporal manipulation by Cre. Tamoxifen induction allows spatial and temporal regulation of the Cre function.

Trp53$^{frt/+}$ (RRID:IMSR_JAX:017767) [354]
This mouse strain was kindly provided by Dr. David Kirsch (Duke University School of Medicine, Durham, NC, USA). Exons 2 to 6 of the pro-apoptotic transformation related protein 53 gene*Trp53* gene are flanked by *frt* sites and p53 can be inactivated by Flp expression.

Pten$^{lox/lox}$ (RRID:IMSR_JAX:006440) [355]
This mouse strain was kindly provided by Dr. Hong (UCLA School of medicine, Los Angeles, CA, USA). Exon 5 of the PTEN gene is flanked by LoxP sites. Cre-mediated recombination results in excision of exon 5 that codes the phosphatase domain resulting in PTEN inactivation.

Braf$^{lox/lox}$ (RRID:IMSR_JAX:006373) [356]
This mouse strain was kindly provided by Dr. Alcino J. Silva (University of California, Los Angeles, CA, USA). Exon 12 of the *Braf* gene is flanked by LoxP sites. Cre-mediated recombination by Tamoxifen induced Cre^{ERT2} results in excision of exon 12 which is the first exon that encodes the kinase domain resulting in BRAF inactivation.

cRaf$^{lox/lox}$ **[357]**

This mouse strain was kindly provided by Manuela Baccarini. Exon 3 of *c-Raf* gene were flanked by *loxP* sites. Cre-mediated recombination by Tamoxifen induced Cre^{ERT2} results in excision of exon 3 resulting in CRAF inactivation.

3.1.2 Genotyping of genetically engineered animals

Mice were genotyped 2-3 weeks after birth. Ear clipping was used to identify individual mice. Clipped ear tissues were used as biopsies for genotyping. DNA was isolated from the biopsies and the isolated DNA was subjected to PCR amplification and gel electrophoresis as described below.

3.1.3 Mouse dissection

Prior to dissection, the mice were anesthetized with medetomidine-midazolam-fentanyl (MMF) administered by intraperitoneal injection followed by cervical dislocation and bleeding to euthanize the mice. The mice were then fixed and disinfected with 70% ethanol and dissected. Pancreatic tissue samples were taken for DNA, RNA and protein isolation as well as cell line generation. The DNA samples were directly snap frozen. Samples for RNA were homogenized using SilentCrusher M in 600 µL RLT buffer supplemented with 1% β-mercaptoethanol. similarly, samples for protein isolation were homogenized in 500 µL IP buffer containing 1% phosphatase and 4% proteinase inhibitors. All samples were stored at -80 °C until further analysis. For histological analysis, remaining part of the pancreas, spleen, liver, lung, heart, and kidneys were fixed overnight in 4% Roti® Histofix. For primary murine cancer cell line isolation, pancreatic tissue were transferred to sterile PBS and then cut into small pieces with sterile scalpels and digested in 5 ml cell culture medium containing 200 U/ml collagenase type II at 37°C overnight. After digestion, the cells were centrifuged and the pelleted cells were resuspended in fresh media and cultured in a T25 cell culture flask. Typically, two different pieces of tumor tissue were used to isolate primary murine tumor cells from the same tumor. For ascites isolation, ascites was taken from the peritoneal cavity and directly cultured in medium. Cell culture procedures are described below.

3.1.3 Orthotopic transplantation of PDAC cells into the pancreas

PDAC cells were trypsinized and diluted to a final concentration of 125 cells/ µl in 1 ml DMEM without FCS. Next, mice were anesthetized using 50 µl MMF (150 µg/ kg Medetomidine, 4.0 mg /kg Midazolam and 50 µg/ kg Fentanyl) via intraperitoneal injection. Eye cream was applied to the mouse eyes to prevent dryness, The mouse was shaved around the site of implantation using an electric razor. An approximate 5 mm skin wound was cut with sterile scissors above the pancreas position, the peritoneum around the skin wound was separated with scissors. The peritoneum was cut opened with inner scissors and forceps at the same position under the skin wound, and the tail of pancreas was pulled out with blunt forceps.

Subsequently, 2500 cells in 20 µl DMEM were injected into the pancreas by clean glass syringe. The peritoneum wound was closed with around 3 stitches by sewing. The skin wound was clipped with around 3-4 metal clips. The mouse was injected with 200 µl of AFN and 150 µl of Metacam.

3.1.4 Tamoxifen Treatment for Mice

For the orthotopic implantation experiments, Tamoxifen was dissolved in the corn oil at the concentration of 20 mg/ml, and the mice were injected by intraperitoneal injection of tamoxifen solution with a dose of 4 mg Tamoxifen/30g body weight twice per week after 1 week of implantation, followed by a tamoxifen-containing diet (400 mg tamoxifen citrate per kg diet).

3.2 Cell culture

Isolated primary murine pancreatic cancer cell lines (see above) were propagated in cell culture medium (DMEM supplemented with 10% FCS and 1% penicillin/streptomycin) at 37 °C, 5% CO_2 and 100% humidity.

3.2.1 Culture of primary mouse PDAC cell lines

All the cell culture procedures were carried out under a cell culture laminar flow hood used exclusively for primary cell culture. For passaging of cells the medium was aspirated, and the adherent cells were washed with PBS and detached from the culture dish by incubation with trypsin/EDTA at 37 °C for an appropriate time period. To stop trypsinization, fresh medium was added the cell suspension was seeded in an appropriate culture vessel depending on the experimental procedure. A Neubauer hemacytometer was used to determine cell number in a given suspension.

For cryopreservation, trypsinized cells were resuspended in fresh medium and centrifuged at 1200 rpm for 5 min. The pellet was dissolved in ice-cold freezing medium (DMEM supplemented with 20% FCS and 10% DMSO), dispensed in CryoPure tubes and transferred to -80 °C in cell freezing containers. After freezing for a minimum of 24h, the frozen cells were transferred to liquid nitrogen tanks for long-term storage. To thaw frozen cell lines for subsequent analysis, the cryopreserved cells were thawed in a 37 °C water bath. Cells were then resuspended in fresh medium and centrifuged at 1000 rpm for 5 min. The supernatant was aspirated, and cells were cultured in culture medium in a new flask.

3.2.2 Treatment of cells with 4-hydroxytamoxifen (4-OHT)

To activate $CreER^{T2}$ in cell culture experiments, pancreatic cancer cells were treated with vehicle (ethanol) or 600nM 4-hydroxytamoxifen (4-OHT), the active metabolite of Tamoxifen,

for 7 days to delete the *loxP*-flanked sequences. Subsequently, treated cells were seeded for a variety of assays as elaborated in results section.

3.2.3 CellTiter Glo® assay

The CellTiter Glo® assay was used to measure cell viability by indirectly measuring ATP levels via luminescence. Cells were seeded at a density of 500 cells per well in 96-well plates. 25 µl of CellTiter Glo® reagent was added to each well and incubated on an orbital shaker for 10 minutes at 100 rpm before measuring luminescence with a luminometer.

3.2.4 Clonogenic assay

Cells were seeded at density of 2000 cells per well in a 6-well plate. At end point, after 10 or 15 days of culture unless otherwise stated, culture medium was aspirated and cells were fixed and stained with 750 µl of a 0.2% crystal violet solution and incubated on an orbital shaker for 10 min at room temperature. Afterwards the staining solution was aspirated, and the plates were washed with water and air dried overnight. Images of the plates were documented. For quantification, the staining was solubilized with 1% SDS solution and absorbance was measured at 570 nm using a spectrophotometer.

3.2.5 Cell Cycle analysis

For cell cycle analysis, the cells at a confluency of ~70% were trypsinized and washed in PBS. The cells were resuspended in 70% EtOH for fixation. Also, the supernatant cell culture medium was aspirated, centrifuged (1000 rpm, 5 min), and washed with PBS to collect any detached apoptotic cells. Before the measurement, 25 µl/ml of propidium iodide as well as RNAse, at a final concentration of 0.5 µg/ml, were added to the fixed cells and incubated for 30 min.

3.2.6 Caspase-Glo® 3/7 Assay

To assess apoptosis, cells were seeded at a density of 1000 cells per well in a 96-well plate. After 48 hours, caspase 3/7 activity was determined by measuring luminescence using Caspase-Glo® 3/7 Assay from Promega according to the manufacturer's instruction.

3.2.7 Lentivirus production

HEK293T cells were transfected with the expression plasmid of interest along with plasmids for lentiviral packaging (PMD2.G, PsPAX) using TransIT-LT1 based on the manufacturer's recommendation. Shortly, HEK293T cells were seeded at a density of 2×10^6 cells in a 10-cm dish. Around 24 h later, plasmid DNA was diluted with OptiMEM and incubated with TransIT-LT1 for 30min at RT. The lipid-DNA complexes were added dropwise to HEK293T cells at ~70%

confluency and incubated for additional 24hrs before changing media. 48hrs post-transfection, media containing lentivirus was harvested and filtered using a 0.45 µm filter. The viral supernatant was used directly for target cell transduction or stored at -80 °C.

Table 7: Transfection Mix for HEK293T cells for Lentivirus Production

Component	Per plate
Opti-MEM	1500 µl
psPAX	6.3 µg
pMD2	4.1 µg
POI	8.2 µg
TransIT-LT1	55 µl

3.2.5 Lentiviral transduction

Target cells for lentiviral transduction were seeded in 6-well plates at a density of 150 000 cells per well. After 24 h, an appropriate volume filtered of the viral supernatant was added with polybrene at a final concentration of 8 µg/ml. Spin-infection was performed by spinning the plates at 1000 x g for 30 min at 30 °C in a plate centrifuge. The cells were further incubated with the virus overnight. Selection of the transduced cells with an appropriate concentration of a mammalian selection antibiotic was performed 48hrs post infection.

3.2.6 Titer determination of the Lentivirus for Screening

For each lentivirus batch, 7 wells of a 12-well plate were seeded with the target cells at a density of 3×10^6 cells in 2 ml medium per well with 8 g ml^{-1} polybrene. In each well, 0, 10. 25, 50,100, 200 0r 400ul of lentivirus was added. The cells were spin-infected by centrifugation of the plates at 1,000*g* for 2 h at 33 °C. 24hrs after the spin infection, the cells were trypsinized and seeded in a 96-well clear-bottom opaque tissue culture plate. 6 wells were seeded per concentration. 48hrs post infection, 100ul media was added to each well with or without the selection antibiotic. When the antibiotic selection is completed in the no-virus conditions and the no-antibiotic selection conditions reach 80–90% confluency, cell viability was cell viability for each condition using CellTiter Glo according to the manufacturer's protocol. For each virus condition, the MOI was calculated as the average viability, of the 3 wells in the condition with antibiotic selection divided by the average luminescence of the 3wells in the condition without antibiotic selection. A linear relationship between lentivirus supernatant volume and MOI was observed.

3.2.7 Lentiviral transduction for Genome-wide Screens

For the generation of a cell line with stably expressed Cas9 components, the corresponding Cas9 components were titrated and transduced at an MOI of ≤ 0.5 and selected with the corresponding antibiotic. Clones with stable expression of the Cas9 component were generated and tested by western blots and functional assays to confirm the expression. For the knockout screens, Cas9 was expressed from the pLentiCas9-Blast plasmid and selection with 9 μg/ml Blasticidin was performed for 7 days. For the CRISPRa screens, SAM components (dCas9-VP64 and MS2-p65-HSF1) were expressed from lenti dCaS-VP64-Blast and lentiMPH v2 that were sequentially transduced into the target cell line and and selection with 9 μg/ml Blasticidin and 1 mg/ml Hygromycin was performed for 7 days.
For the screening, these cell lines were then transduced with the sgRNA library. The cells were seeded at a density of 3×10^6 cells in 2ml media in 12-well plates together with the appropriate amount of viral supernatant based on the titer and centrifuged at 1,000*g* for 2 h at 33 °C. To ensure that most cells harbor a single genetic perturbation, the sgRNA library was transduced at an MOI of 0.3. The transduction was scaled up such that the sgRNA library has coverage of > 500x i.e. each unique sgRNA is expressed in at least 500 cells. 16hrs post infection, the cells were trypsinized and seeded into 175cm flasks at an appropriate density. 48hrs post infection, antibiotic selection with puromycin was started. A no-virus control was included to confirm the complete selection. A minimum of 50 million cells was maintained throughout the culture to maintain the library representation. Cell pellets for gDNA were collected throughout various time points of the screening including the final timepoint. In screening settings where 4-hydroxytamoxifen treatment was performed, the transduced cells were divided into two groups (EtOH control and 4-OHT treatment) post-selection. The treatment was performed for 7 days and then the cells were cultured in normal media till the final timepoint.

3.2.7 Fluorescence-activated cell sorting (FACS) and flow cytometry analysis

Cells were sorted and analyzed by BD FACSAria III Cell Sorter after transduction. Cells were trypsinized and centrifuged first, cells pellets were resuspended with 400µl sorting medium (2% FCS in PBS). The cells were then filtered through a 70 µm cell strainer and collected in Flow Cytometry tubes. The cells were then analyzed, and fluorescence positive cells were collected in a sterile falcon tube with 2ml fresh cell culture medium when needed.

3.2.8 Multicolor competition assays

For *in vitro* competition assays, lentiviral vectors expressing a target sgRNA together with GFP or RFP were used. sgRNAs targeting *Pten* or control sgRNAs were cloned into the BsmBI-digested vectors, using the protocol described below. Cas9-expressing cells were infected

with these vectors expressing each sgRNA and sorted for the full infected population. The cells were mixed in equal ratios and the percentage of Green/RFP-positive cells was quantified over time using a BD FACSAria III Cell Sorter as described above. For each sgRNA, the percentage of Green/RFP-positive cells was normalized to respective values at Day zero post mixing.

3.2.9 Drug Screen

The compounds were purchased from SelleckChem and MedChemExpress either in DMSO or water. 500-2000 cells were seeded in 96-well plates in culture medium. The optimal cell number for each cell line was determined to ensure that each cell line was in growth phase at the end of the assay. After overnight incubation, the cells were treated with 7 concentrations of each compound (3-fold dilutions series) and a solvent control, using a pin tool. 72hrs post-incubation, viability was measured using CellTiter-Glo® Luminescent Assay (Promega) as described above. Each cell line was treated with a library of 200 compounds. Dose-response curves were generated using the R package *GRmetrics* to derive both growth rate adjusted and traditional measures of drug sensitivity (IC50, AUC, Emax) [358, 359]. Only drugs for which a sigmoid curve could be fitted (coefficient of determination, r^2>0.9) were considered for further analysis.

3.3 Molecular biology

3.3.1 Isolation of genomic DNA

Genomic DNA for subsequent genotyping and recombination PCR analysis was isolated by adding an adequate volume of Soriano lysis buffer (Table 8). The tissue or cell pellet was then lysed at 55 °C for 90 min in the presence of Proteinase K. The samples were then heated to 95°C t´for 15 min to ensure heat-inactivation of Proteinase K. The debris were removed by centrifugation at 14000 rpm and 4 °C for 10 min. The supernatant was then transferred into a new tube and stored at 4 °C or -20 °C for short or long term storage.

For NGS applications, genomic DNA was isolated using the DNeasy Blood & Tissue Kit (Qiagen) from murine primary cell cultures. Around 5 x10^6 cells were used for DNA isolation according to the manufacturer's instructions of the DNeasy Blood & Tissue Kit.

Table 8: Composition of Soriano Lysis Buffer

Buffer	Component
10x Gitschier's buffer	670 mM Tris, pH 8.8 166 mM (NH4)2SO4 67 mM MgCl2

Soriano lysis buffer	0.5% Triton® X-100 1% 2-Mercaptoethanol 1x Gitschier's buffer 400 µg/mL Proteinase K (add prior to use)

3.3.2 Isolation of genomic DNA from CRISPR Screens

Genomic DNA was extracted from frozen cell pellets using the QIAGEN Blood&CellCulture DNA MaxiKit (cat. No. 13362) according to the manufacturer's instructions. Shortly, the pellets were thawed and resuspended in PBS and lysed in Buffer C. The supernatant was discarded, and the nuclei were resuspended and lysed in Buffer G2 and QIAGEN Protease. The lysed nuclei were applied to an equilibrated QIAGEN Genomic-tip, followed by 2 washing steps to eliminate contaminants in the gDNA preparation. The DNA was the eluted from the column and precipitated in Isopropanol. The gDNA was spooled into TE buffer and incubated at RT overnight to allow complete resuspension. The final DNA concentration was determined using a Nanodrop.

3.3.3 Isolation of RNA from primary cell cultures

For RNA isolation, primary cell lines were grown on a 10 cm dish in DMEM supplemented with 10% FCS but not containing P/S, to 60-80% confluency. The adhered cells were washed twice with ice-cold PBS. 500 µl of RLT buffer supplemented with 1:100 ß-mercaptoethanol was used to lyse and collect the cells using a cell scraper. The collected solution was then transferred to a QiaShredder column and centrifuged for 2min at maximum speed. The homogenized cells were snap-frozen and stored at -80°C. RNA was isolated with the RNeasy Mini kit (Qiagen) according to the manufacturer's instructions.

3.3.4 RNA Sequencing and analysis

Bulk 3' transcript end RNA-seq (SCRB-seq) was performed by Prof. Roland Rad's lab (TranslaTUM, Technical University of Munich). RNA was extracted as described above and cDNA was synthesized using oligo-dT primers with sample barcodes, unique molecular identifiers, and adapters. The cDNA samples were pooled, and unincorporated primers were digested with Exonuclease I. The cDNA pool was amplified with KAPA HiFi ReadyMix and tagmented using the Nextera XT kit and the 3' ends were further using a specific primer for the adaptor on the 3' ends. The library was sequenced by paired-end sequencing on a HiSeq1500 with 16 cycles for Read 1 to decode sample barcodes and unique molecular identifiers, and 51 cycles on Read 2 into the cDNA fragment. Data were processed using the Drop- seq pipeline [166] to generate sample- and gene-wise unique molecular identifier tables. Reference genome (GRCm38) was used for alignment. Further analysis was performed

with R using DEseq2 [360]. Gene set enrichment analysis (GSEA) was performed with gProfiler [361] or GSEA software from the 'Molecular Signature Database' (MSigDB) [362, 363].

3.3.5 Polymerase chain reaction (PCR)

For standard genotyping or recombination PCR, a PCR pre-mix containing buffer, polymerase, and dNTPs was used. Standard PCR reaction setup and conditions are shown below. PCR conditions were optimized depending on the PCR product. The annealing temperatures for each PCR are shown below. PCR products were stored at 4 °C until further analysis by gel electrophoresis.

Table 9: Composition of pre-mix for PCR

Ingredient	**Volume for one reaction**
distilled water	4.375 µL
10x buffer S	2.5 µL
30% sucrose	2.5 µL
SucRot	2.5 µL
PeqTaq	0.125 µL
dNTPs (10 µM each)	0.5 µL

Table 10: Reaction conditions for standard PCRs

Temperature	**Time**	**Cycles**
95 °C	3'	1x
95 °C	45''	40x
X °C	1'	40x
72 °C	1'30''	40x
72 °C	5''	1x
72 °C	hold	---

Table 11: Annealing temperatures and PCR products of genotyping and recombination PCRs

PCR	**Annealing temperature**	**PCR products (bp)**
Pdx1-Flp	55 °C	620 (mut) / 300 (internal control)
FSF-Kras^{G12D}	55 °C	350 (mut) / 270 (WT)
FSF-Kras^{G12D} recombination	60 °C	196 (rec)
FSF	60 °C	600 (mut)
CreER^{T2}	55 °C	190 (mut)

R26-CAG	62 °C	450 (mut) / 650 (WT)
FSF recombination	60 °C	490 (rec)
Pdk1^{lox}	63 °C	280 (mut) / 200 (WT)
Pdk1^{lox} recombination	63 °C	250 (rec) / 380 (mut) / 350 (WT)
Trp53^{frt}	57 °C	292 (mut)/ 258 (WT)
Ptf1a^{Cre}	60 °C	400 (mut) / 600 (WT)
LSL-Kras^{G12D}	55 °C	170 (mut) / 270 (WT)
Pten^{lox}	60 °C	328 (mut) /156 bp (WT)
Pten^{lox} recombination	62 °C	250 (rec) / 380 (mut)

mut = mutated allele; WT = wild type allele; rec = mutated allele without translational stop element after recombination

3.3.6 Separation of DNA by agarose gel electrophoresis

Nucleic acids were separated by gel electrophoresis using 2% agarose gels. Appropriate amount of agarose was dissolved in 1x TAE buffer by heating in a microwave. Ethidium bromide was then added to the melted agarose and casted. DNA samples were then applied to the solidified gel and separated at 120 V. For documentation, a system allowing UV light excitation and imaging was used.

3.3.7 Amplification of pooled sgRNA libraries

The mouse CRISPR Knockout Pooled Library (BRIE) [364] (#73632) and the mouse CRISPR/Cas9 Synergistic Activation Mediator (SAM) pooled library [365] (#1000000075) were purchased from Addgene. The libraries were amplified by electroporation into Endura ElectroCompetent cells according to the manufacture's recommendation. One electroporation per 10'000 sgRNAs in the library was performed. The Bacteria was then plated on 245-mm square bioassay dishes at a convenient density to avoid inter-colony competition and biases in sgRNA distribution and incubated at 30°C for 16-18h. Post incubation, the electroporation efficiency was calculated and confirmed to be greater than 100 colonies per sgRNA in the library. MaxPreps were performed to isolate the plasmids using the Macherey-Nagel NucleoBond Xtra Maxi EF Kit according to the manufacturer's directions. One column was used for 0.45g of wet bacterial pellet.

3.3.8 Next Generation Sequencing of the amplified sgRNA library

To determine sgrna distribution in the amplified Libray, 10 ng of the plasmid library was amplified using KAPA HiFi HotStart ReadyMix (KK2602) as shown in Table and using primers containing overhangs with adapters compatible with Illumina sequencing (Table). The

amplified PCR product was purified using the Qiagen PCR purification Kit. 2ug of the purified PCR product was then separated using agarose gel electrophoresis and the band corresponding to the correct size amplified PCR product was cut and purified using the Qiagen Gel purification Kit. Amplicons were sequenced by Prof. Roland Rad's lab (TranslaTUM, Technical University of Munich)on a MiSeq (Illumina) with a single-end 50 bp run sequenced using the Illumina sequencing and indexing primers (Table). The design of the primers used for the amplification and barcoding of the BRIE and SAM library samples is shown in Table and were adapted from the sequencing strategy by [341].

Table 12: Composition of the KAPA HiFi PCR for plasmid library amplification

Component	Volume	Final Concentration
KAPA HiFi Master Mix (2x)	25 ul	1x
Forward Primer	2 ul	0.5 uM
Reverse Primer	2 ul	0.5 uM
Template (Plasmid)	10 ng	
Water	Up to 50ul	

Table 13: Cycling conditions for the KAPA HiFi PCR for plasmid library amplification

Step	Temp.	Duration	Cycles
Initial Denaturation	95 °C	3 min	1
Denaturation	98 °C	15 sec	20
Annealing	62 °C	30 sec	
Extension	72 °C	30 sec	
Final Extension	72 °C	1min	1
HOLD	4 °C	∞	1

Table 14: Design of the Forward and Reverse primers used for Plasmid Library Amplification and Sequencing

Primer	Library	Flow cell binding region	6/8bp barcode	vector binding site
P5/MS2 primer	SAM CRISPRa Library	AATGATACGGCGACCACCGAGATCTACAC	NNNNNNNN	GCCAAGTTGATAACGGACTA
(P5/sgRNA scaffold)	BRIE Library	AATGATACGGCGACCACCGAGATCTACAC	NNNNNN/NN	CACCGACTCGGTGCCACTTTT

(P7/U6 primer)	SAM CRISPRa and BRIE Library	CAAGCAGAAGACGGCATACGAGAT	NNNNNN/NN	TTTCTTGGGTAGTTTGCAGTTT T

Table 15: Sequence of the Forward and Reverse primers used for Plasmid Library Amplification and Sequencing

Primer	Sequence
sgRNA_NGS-P502	AATGATACGGCGACCACCGAGATCTACACctctctCACCGACTCGGTGCCACTTTT
sgRNA_NGS-P503	AATGATACGGCGACCACCGAGATCTACACtatcctCACCGACTCGGTGCCACTTTT
sgRNA_NGS-P504	AATGATACGGCGACCACCGAGATCTACACagagtaCACCGACTCGGTGCCACTTTT
sgRNA_NGS-P505	AATGATACGGCGACCACCGAGATCTACACgtaaggCACCGACTCGGTGCCACTTTT
sgRNA_NGS-P506	AATGATACGGCGACCACCGAGATCTACACactgcaCACCGACTCGGTGCCACTTTT
sgRNA_NGS-P701	CAAGCAGAAGACGGCATACGAGATgccttaTTTCTTGGGTAGTTTGCAGTTTT
sgRNA_NGS-P702	CAAGCAGAAGACGGCATACGAGATagtacgTTTCTTGGGTAGTTTGCAGTTTT
sgRNA_NGS-P703	CAAGCAGAAGACGGCATACGAGATctgcctTTTCTTGGGTAGTTTGCAGTTTT
sgRNA_NGS-P704	CAAGCAGAAGACGGCATACGAGATtcaggaTTTCTTGGGTAGTTTGCAGTTTT
sgRNA_NGS-P705	CAAGCAGAAGACGGCATACGAGATgagtccTTTCTTGGGTAGTTTGCAGTTTT
sgRNA_NGS-P706	CAAGCAGAAGACGGCATACGAGATtgcctaTTTCTTGGGTAGTTTGCAGTTTT

Table 16: Sequence of the primers used in Illumina Sequencing

Primer	Sequence
Illumina Sequencing primer	CGGTGCCACTTTTTCAAGTTGATAACGGACTAGCCTTATTTTAACTTG CTATTTCTAGCTCTAAAAC
Illumina Indexing primer	TTTCAAGTTACGGTAAGCATATGATAGTCCATTTTAAAACATAATTTTAAAACTGCAAACT ACCCAAGAAA

3.3.9 Golden gate Cloning

To clone sgRNAs into expression backbones with U6 promoters, complementary DNA oligonucleotides corresponding to the sgRNA sequence with BsmBI overhangs were annealed and incubated with the backbone. Ten cycles of digestion and ligation using T4 DNA Ligase (NEB) were performed using the program below. This mix was then used to transform competent bacteria. The sequence of the sgRNAs used is shown in Table 19.

Table 17: Composition of the Golden gate Cloning reaction

Ingredient	**Volume for one reaction**
Plamsid backbone (90µg/µl)	1 µl
Annealed and diluted oligos	1 µl
T4 DNA Ligase Buffer (10x)	2 µl
T4 DNA Ligase	1 µl
BsmBI restriction enzyme (10 000 units/mL)	1 µl
H_2O	14 µl

Table 18: Reaction conditions for golden gate Cloning

Temperature	**Time**	**Cycles**
37°C	5 min	10x
16°C	10 min	
55°C	5 min	1x
80°C	5 min	1x
10°C	Pause	---

Table 19: Sequence of the used sgRNAs

sgRNA	Sequence
PTEN_sgRNA1	CCTCCAATTCAGGACCCACG
PTEN_sgRNA4	GGTTTGATAAGTTCTAGCTG
Vgll4_sgRNA1	CAGCCCGTTCAATGGGACTG
Vgll4_sgRNA2	GATGCACAGGTAATCACAGA
mNTC_sgRNA	GGAGTGTTATACGCACCGTT
LacZ_sgRNA	TGCGAATACGCCCACGCGAT
FOXO1 sgRNA 1	GGAGAGTGAGGACTTCGCGC
FOXO1 sgRNA 3	GGCGGTGCAAACGAATAGCA
TSC2 sgRNA 1	TGAACCACATGGCTATGACG
TSC2 sgRNA 4	CTGATCCTAGCACACATGTG
NF2 sgRNA1	GACCCCTCTGTGCACAAGCG
NF sgRNA2	GTCGCCTCATAAATAGGTCA
Cdkn2b sgRNA1	GTGCACGACGCAGCTCGGGA

Cdkn2b sgRNA2	GTCGTGCACAGGTCTGGTAA

3.3.10 Cloning AKT cDNA into Lentiviral vectors

WT, DN (K179M mutant) and Myr-AKT1 cDNA were cloned from pUSE plasmid into pLenti-Cas9 Blast template. Cas9 was excised from pLenti-Cas9 Blast plasmid using XbaI and BamHI or AfeI. The AKT cDNA was amplified and XbaI and BamHI OR AfeI restrictions sites were added during the PCR amplification using the primers in Table 20. Q5 enzyme was used to amplify the cDNA according to the manufacturer's instructions. The PCR product was digested using the corresponding Restriction enzymes and then were ligated to the digested backbone using NEB Ligase according to the manufacturer's instructions

Table 20: Primers used for Amplification of *Akt1* cDNA

cDNA	Forward Primer	Reverse Primer
WT and DN *Akt1*	GCTCTAGAATGAACGACGTAGCC ATTGTG	CGCGGATCCGGCTGTGCCACTGGCTGA
Myr-*Akt1*	GCATGCAGCGCTATGGGGAGCAG CAAGAGCA	CGCGGATCCGGCTGTGCCACTGGCTGA

3.3.11 Akt1 mutagenesis

The Q5 Site-Directed Mutagenesis Kit was used to generate the Myr-Akt1 S473A and T308A mutants. The clones pLenti-Myr AKT plamid was used as a template and the kit was used according to the manufacturer’s instructions. The primers used for mutagenesis are shown in Table 21.

Table 21: Primers used for Myr-*Akt1* Mutagenesis

Mutant	Forward Primer	Reverse Primer
T308A	CACTATGAAGgCATTCTGCGC	GCACCATCCTTGATCCCC
S473A	CCCCCAGTTCgCCTACTCAGCC	AAGTGCGGCCTCCGCTCA

3.3.10 Transformation of bacteria

Chemically competent bacteria (Endura^{TM}) were transformed using KCM transformation. The assembled mix from the cloning procedure was added to 1x KCM solution. This transformation mix was added to 100 µl competent Endura^{TM}. The bacteria were incubated for 10 min on ice and for 10 min at room temperature afterwards. Then, 1 mL of Rescue (SOS)

medium was added to the bacteria and incubated for 1 h at 37°C in the thermomixer at 1000 rpm to allow expression of ampicillin resistance. The transformed bacteria were streaked on LB agar plates containing an appropriate bacterial selection antibiotic and incubated overnight at 37°C to select transformed clones. Then, single bacterial clones were picked and cultured for subsequent Plasmid isolation.

3.3.11 Plasmid DNA isolation from glycerol stocks

Glycerol stocks were obtained by mixing glycerol and freshly shaken bacterial culture 1:1 and stored at -80 °C. Bacteria from glycerol stocks were plated on LB-agar and incubated at 37°C overnight. Single bacterial clones were then picked and cultured in LB media by shaking in the bacterial incubator at 200 rpm and 37 °C overnight. DNA was isolated from the culture using the QIAprep® spin miniprep kit according to the manufacturer's instructions.
For the isolation of plasmids for mammalian cell culture applications, endo-free preparation was used. Starter cultures propagated from single clones were used to inoculate larger cultures based on needs in LB media with the appropriate selection antibiotic. For endo-free plasmid isolation and purification, NucleoBond® Xtra Midi or Maxi kits were used according to the manufacturer's instructions. Shortly, bacterial pellets were collected, lysed, and then loaded onto an equilibrated NucleoBond® Xtra Column filter. The column was emptied by gravity flow, allowing simultaneous filtration and plasmid DNA binding to the column. Following washing steps, DNA was eluted and precipitated using Isopropanol. The plasmid DNA pellet was washed with 70 % ethanol and dissolved in TE buffer or sterile H_2O.

3.4 Protein biochemistry

Table 19: The composition of all Buffers used in the protein biochemistry assays

IP buffer pH7.9	50 mM HEPES 150 mM NaCl 1 mM EDTA 0.5% Nonidet P40 10% Glycerol Phosphatase inhibitor (supplemented before lysis) Protease inhibitor (supplemented before lysis)
Separating gel buffer	Tris-HCl 1.5 M , pH 8.8
Stacking gel buffer	Tris-HCl 0.5 M , pH 6.8
Running buffer (10x)	35 mM SDS 250 mM Tris 1.92 M Glycine
Transfer buffer (10x) pH8.3	250mM Tris

	1.92 M Glycine
Transfer buffer (1x)	700mL ddH_2O 200mL methanol 100mL transfer buffer 10x
Washing Buffer	PBS 0.1% Tween
5% blocking BSA	5g BSA per 100mL TBS
5% blocking milk	5g milk powder per 100mL TBS
5x Protein loading buffer (Laemmli), pH 6.8	10% SDS 50% Glycerol 228 mM Tris hydrochloride 0.75 nM Bromphenol blue 5% 2-Mercaptoethanol

3.4.1 Protein extraction

For protein extraction, primary cell cultures were seeded in a 10-cm dish. At 70% confluency, medium was removed from cultured cells and cells were washed twice with ice-cold PBS. Excess PBS was removed and 150 µL µl of RLT buffer supplemented with protease and phosphatase inhibitors was used to lyse the collect the cells using a cell scraper. The suspension was incubated on ice for 3omin to allow complete lysis followed by centrifugation at 13200 rpm for 30 min at 4°C and the supernatant was transferred into a new reaction tube. The protein lysates were snap frozen and stored at -80°C.

3.4.2 Protein concentration estimation

The protein concentration of cell lysates was determined by using standard Bradford assay (Bradford, 1976) and measuring absorbance at 600 nm with the microplate reade. Protein concentration was estimated in comparison to a reference generated using a BSA dilution series with known concentrations. Each sample was measured in triplicates.

3.4.3 SDS polyacrylamide gel electrophoresis (SDS-PAGE)

SDS-PAGE (Laemmli, 1970) was performed to separate the proteins based on heir molecular size. 7%, 10% or 15% separating gels were used depending on the size of the protein of interest. The components of the separating gel were mixed, as shown in Table 20. After casting the gels between in a glass chamber, the gel was covered with a layer of 2-propanol and allowed to polymerize. After the stacking gel mixture was poured and polymerized. 60–100 µg of the protein per sample was loaded on the SDS polyacrylamide gel. Prior to that, the protein concentrations of all samples were adjusted to the same amount by adding loading buffer (Laemmli, 1970) and IP buffer. Protein samples were subsequently denatured at 95 °C for 5 min and loaded on the SDS-PAGE gel. Electrophoresis was carried out at 120 V.

Table 20: Components of the separating SDS-PAGE gels

Reagents	7.5% separating gel	10% separating gel	15% separating gel
H2O	1660µl	1500 µl	1175µl
Separating gel buffer	490µl	650µl	975µl
30% acrylamide		375µl	
10% SDS	25µl	25µl	25µl
10% APS	12.5µl	12.5µl	12.5µl
TEMED	5µl	5µl	5µl

Table 21: Components of the stacking SDS-PAGE gels

Reagents	7.5% separating gel
H2O	2050 µl
Separating gel buffer	1300 µl
30% acrylamide	1650 µl
10% SDS	25µl
10% APS	12.5µl
TEMED	5µl

5.4.4 Immunoblot

After separation on a SDS-PAGE gel, the proteins were blotted onto a Nitrocellulose membrane which was activated equilibrated in transfer buffer. A typical sandwhich set-up using spongs and filter paper. The protein transfer was performed at 300mA, 4 C for 2 hours 20 minutes in the cold room using 1x transfer buffer in the transfer chamber. After protein transfer the membrane was blocked by incubation in 5% BSA or 5% milk blocking buffer at room temperature for one hour. Subsequently, the membrane was incubated with specific primary antibody solution (Table 21) diluted in 5% BSA or milk and incubated at 4 °C over night. After three washing steps with PBS-Tween, 15 min each, the membrane was incubated with the secondary antibody (Table 22) diluted in 5% BSA or milk for 1 h at room temperature. The membranes were again washed three times and scanned at 700 nm or 800 nm wavelength using Odyssey® infrared imaging system.

Table 22: List of Primary Antibodies used in Western Blots

Antibody	Catalog Number	RRID
β-Actin	Cell Signaling 4970	AB_2223172
AKT	Cell Signaling 9272	AB_329827
pAkt (S473)	Cell Signaling 9271	AB_329825
pAkt (T308)	Cell Signaling 2965	AB_2255933
pS6 (S235/236)	Cell Signaling 4858	AB_916156
pS6 (S240/244)	Cell Signaling 5364	AB_10694233
S6	Cell Signaling 2217	AB_331355
p4E-BP1	Cell Signaling 2855	AB_560835
Caspase 3	Cell Signaling 9662	AB_331439
p-p38	Cell Signaling 9211	AB_331641
pSGK1 S422	Abcam ab55281	AB_882529
pGSK3-ß S9	Cell Signaling 9323	AB_2115201
GSK3ß	Cell Signaling 9315	AB_490890
PTEN	Cell Signaling 9188	AB_2253290
PDK1	Cell Signaling 3062	AB_2236832
pYAP	Cell Signaling 53749	AB_2799445
Raf	Cell Signaling 9422	AB_390808
peIF4B Ser422	Cell Signaling 3591	AB_2097522
pFoxO1 S319	Cell Signaling 2487	AB_561444
pFoxO1 1 T24	Cell Signaling 9464	AB_329842
FoxO1	Cell Signaling 2880	AB_2106495
Hsp90 alpha/beta	Santa Cruz sc-13119	AB_675659
pRSK2 S227	Cell Signaling 3556	AB_2181465
RSK2	Cell Signaling 5528	AB_10860075
pFAK Y397	Cell Signaling 8556	AB_10891442
pEpHA2 S897	Cell Signaling 6347	AB_11220420
pEGFR Y845	Cell Signaling 2231	AB_1264155
pEGFR Tyr1068	Cell Signaling 3777	AB_2096270
p-mTOR	Cell Signaling 5536	AB_10691552
p-mTOR S2481	Cell Signaling 2974	AB_2262884
mTOR	Cell Signaling 2983	AB_2105622
Cyclin D1	Cell Signaling 55506	AB_2827374
pRictor (T1135)	Cell Signaling 3806	AB_10557237

Rictor	Cell Signaling 2140	AB_2179961
Cas9	Cell Signaling 14697	AB_2750916

Table 22: List of Secondary Antibodies

Antibody	**Catalog Number**	**RRID**
Goat anti-Rabbit IgG (H+L), DyLight 800	Thermo Scientific SA5-35571	AB_2556775
Goat anti-Mouse IgG (H+L), DyLight 800	Thermo Scientific SA5-35521	AB_2556774

5.4.5 Phospho Explorer Antibody Microarray

The Phospho Explorer Antibody microarrays (PEX100) and the assay kits (KAS02) from Full Moon Biosystems were used to phosphorylation profiling between different conditions based on manufacturer instructions. Shortly, the cell lines were treated as indicated in the results section per experiment. Cells were collected using a scraper and lysed using the extraction buffer and lysis beads. The lysis buffer was exchanged to labelling buffer using a spin column. The proteins were labelled with Biotin using a 10 ug/ul Biotin/ *N,N*-Dimethylformamide solution for 2 hours. The labelled proteins were then added to the blocked microarrays and incubated for 2 hours to allow coupling. Detection buffer with Cy3-streptavidin (0.5 mg/mL) was used for detection. The slides scanned using a microarray scanner.

3.6 Statistical analysis

All the graphic analyses, statistical analyses, and data correlation were done using GraphPad Prism version 8.0 and R studio. Experimental data were presented as Mean ± Standard error of the mean. For the caspase-3/7 assay and cell viability assay, all experiments were conducted in the number of indicated replicates, and the one-way analysis of variance (ANOVA) multiple comparison test was used for comparisons between experimental and control groups. Kaplan-Meier and Log-rank tests were used for statistical analysis of animal survival curves. For RNA sequencing analysis, the false discovery rate (FDR) cutoff of 30% (FDR q-value < 0.3) was set for the enrichment analysis. For the CRISPR screens, the MAGeCKFlute pipeline was used and NTC-normalized or cell-cycle normalized β-scores were generated with corresponding p values and FDRs. For the drug screens, dose-response curves were generated using the Prism and the R package *GRmetrics* to derive both growth rate adjusted and traditional measures of drug sensitivity (IC50, AUC, Emax) [358, 359]. In this thesis, statistical significance was considered in all analyses only when the p-value is less than 0.05, or lower as indicated throughout the results section.

4. Aim Of The Work

The genetics of PDAC has been extensively characterized in the last decade, however, the exact mechanisms that govern PDAC survival and resistance to most therapeutic approaches remain less understood. KRAS constitutes a major driver for PDAC with *KRAS* mutations occurring in 90% of the patients. KRAS contributes to PDAC tumorigenesis via mediating signals to various downstream effectors, with the MAPK pathway and PI3K-AKT signaling being the major effector pathways. The complex and dynamic signaling pathways downstream of KRAS, or independent of KRAS can constitute collateral mechanisms that contribute to PDAC maintenance and resistance to various therapies by compensating the targeted functions. In this work, we inhibit a major effector pathway in PDAC, the PI3K-AKT pathway, by genetically deleting *Pdk1* in GEMM-derived primary PDAC cell lines. Inhibiting this major pathway allows the potentiation of the collateral signaling pathways that we aim to identify by performing genome-wide CRISPR-Cas9 Knockout and activation screens in various sensitization and resistance settings. In addition, we evaluate the effect of introducing a single additional aberration (*Pten* loss) on the rewiring of the whole signaling network in order to understand the extent of the effect of the heterogeneity of a patient's mutational landscape on the signaling networks when the main driver oncogene is conserved. This knowledge of the complex signaling in PDAC can provide us with informed strategies for combinatorial treatments to eradicate PDAC.

5. Results

5.1 *Pdk1* deletion impairs the growth of PDAC cells *in vitro* by blocking PI3K/AKT signaling

To investigate the role of *Pdk1* in pancreatic cancer maintenance, GEMM-derived PDAC cell lines employing a dual recombinase system were used to allow for the conditional inactivation of *Pdk1*, which is sufficient to block PI3K effector signaling [79] (Figure 6a). A Flp recombinase expressed under the control of *Pdx1* promoter allows for the activation of oncogenic *Kras* in the pancreas. The derived PDAC cell lines express an inducible $CreER^{T2}$ and *Pdk1* gene flanked by loxP sites. The treatment of these cell lines with the active tamoxifen derivative (4-hydroxy tamoxifen, 4-OHT) results in the activation of $CreER^{T2}$ and the recombination of *Pdk1* alleles (Figure 6b), and this results in complete loss of PDK1 protein (Figure 6c). Our data show that deletion of Pdk1 results in severe growth arrest as assessed in short- and long-term growth assays (Figure 6d, 6e, and 6f). This growth defect is mediated by an arrest in the G1 phase of the cell cycle and delayed progression to the G2/M phase (Figure 6g and 6h). Pdk1 deletion growth arrest is not accompanied with apoptosis as detected by the Caspase3/7 activity assay (Figure 6i).

The effect of *Pdk1* deletion on PI3K signaling was assessed by western blot (Figure 7a). Western blots showed efficient PDK1 deletion on the protein level following 4-OHT treatment. Main effectors in the PI3K signaling pathway showed a substantial reduction in phosphorylation following *Pdk1* deletion. Direct phosphorylation substrates of PDK1, including RSK2 S227, was blocked entirely, in addition to RSK2 phosphorylation targets such as S6 and eIF4B. The levels of pAKT S308, a direct PDK1 phosphorylation target, were below detection. However, direct phosphorylation targets of AKT were blocked or massively reduced, including the phosphorylation of FOXO1, GSK3β , and EPHA2. These results collectively indicate that loss of PDK1 results in the blocking of PI3K signaling, a major effector pathway of KRAS. In addition, 4-OHT treated cells with *Pdk1* deletion showed resistance to PDK1 and AKT inhibitors compared to isogenic cells with intact *Pdk1* (ETOH control), further confirming PDK1 loss and inactivation of the PI3K/AKT signaling cascade (Figure 7b, c, d & e).

To further investigate the effect of *Pdk1* deletion, transcriptional changes were analyzed using RNA sequencing. RNA isolated from primary PDAC cell lines with floxed Pdk1 treated with ETOH or 4-OHT was sequenced and analyzed to identify differentially expressed genes in *Pdk1* deleted cells. Principle component analysis and unsupervised hierarchical clustering showed that the 4-OHT samples clustered together and were distinct from the control ETOH cells (Figure 8a &b). The top differentially expressed genes between the two conditions are represented in a Volcano plot (Figure 8c) and heat map format (Figure 8d). Gene Set

Enrichment Analysis (GSEA) showed downregulation of PI3K_AKT_MTOR Signaling and MTORC1 signaling hallmarks in accordance with signaling data obtained from western blot

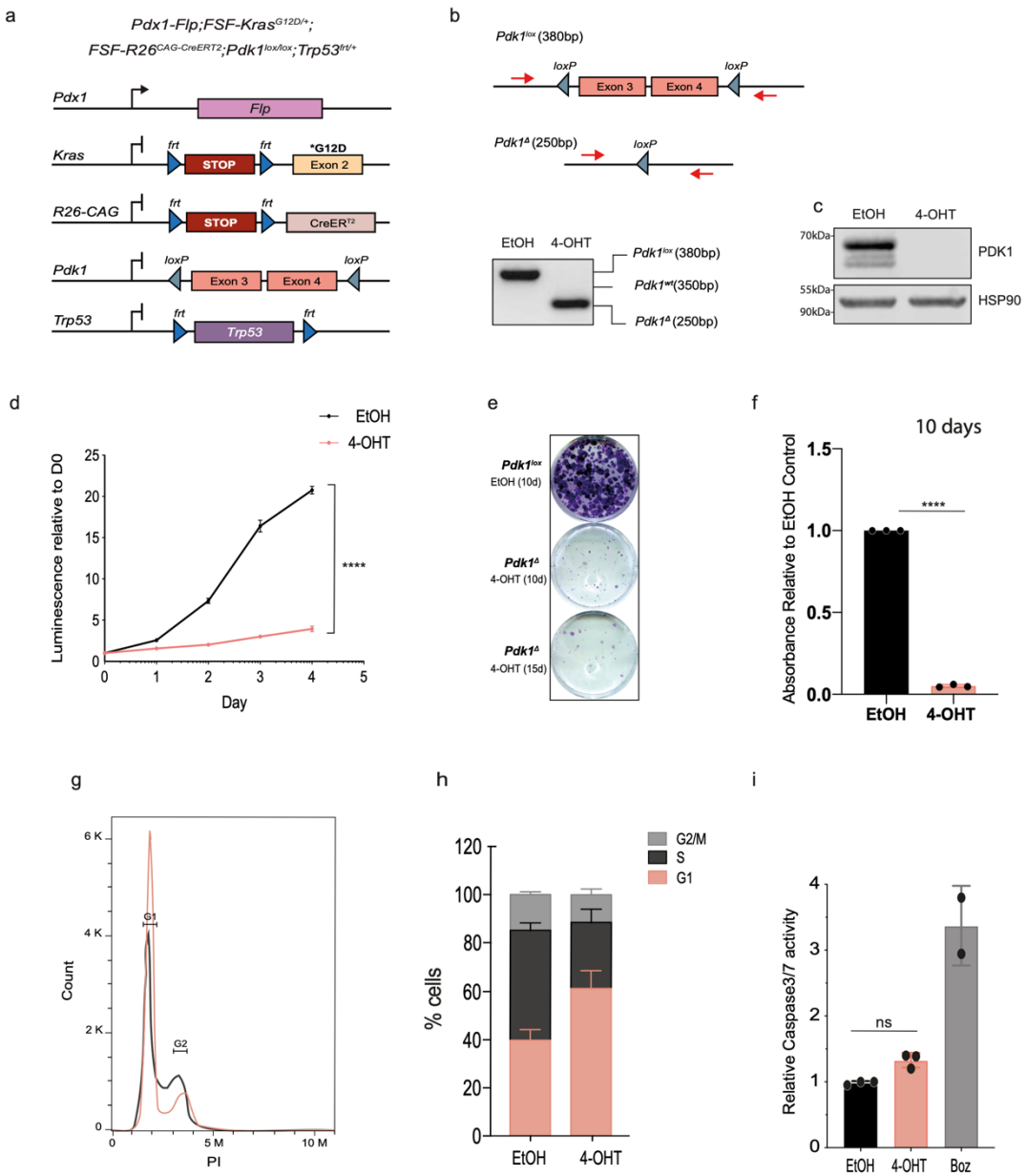

Figure 6: Deletion of *Pdk1* in PDAC cell lines derived from a dual recombinase mouse model impairs growth
(a) Schematic representation of the dual recombinase GEM model that allows inducible deletion of *Pdk1*. (The cell lines from this model were generated by Christian Veltkamp)
(b) Schematic representation of the PCR used to detect recombination of the *Pdk1* allele flanked by loxP sites and the results of the recombination PCR after seven days of EtOH or 600nM 4-OHT treatment of the CV7250 cell line
(c) Western blot results showing PDK1 protein levels in CV7250 cell line treated with ETOH (vehicle) or 600nM 4-OHT for 7 days
(d) Growth curve of PDAC cell lines (CV7250) treated with EtOH or 600nM 4-0HT for 7 days as measured by CTG. Data are shown as mean ± SD; n = 3 independent experiments, **** p <0.001, Two-Way ANOVA test

(e, f) Long-term growth colony formation assay of PDAC cell lines (CV7250) treated with EtOH or 600nM 4-0HT and corresponding quantification. Data are shown as mean ± SD; n = 3 independent experiments, **** p <0.001, two-tailed student's t-test.
(g,h) Cell cycle analysis of EtOH or 4-0HT treated cells (CV7250) showing the effect of Pdk1 deletion. Data are shown as mean ± SD; n = 7 independent experiments. PDAC cells (CV7250) were treated with 600nM of 4-OHT or a corresponding volume of EtOH for seven days. The cells at a confluency of ~70% were fixed in 70% EtOH and stained with 25 µl/ml of propidium iodide and analyzed by flow cytometry. This experiment was performed together with Lukas Neudegger and is part of his thesis. (LN performed the cell culture experiment, KS planned the experiment together with LN, and KS performed the flow cytometry acquisition)
(i) Caspase3/7 activity assay in EtOH or 4-0HT treated cells showing the effect of Pdk1 deletion on apoptosis. PDAC cells (CV7250) were treated with 600nM of 4-OHT or a corresponding volume of EtOH for 7 days. The cells were then seeded at a density of 1000 cells per well in a 96-well plate. After 48 hours, caspase 3/7 activity was determined by measuring luminescence using Caspase-Glo® 3/7assay. The graph represents the induction of caspase 3/7 activity relative to the untreated control. Data are shown as mean ± SD; n = 3 independent experiments, ns p = 0.3452, One-way ANOVA multiple comparisons test (This experiment was performed together with Mingsong Wang and will be part of his thesis).

analysis (Figure 7a). In addition, E2F targets and G2M_Checkpoint hallmarks were also enriched in the downregulated gene sets between the 4-OHT and ETOH samples, which complement our cell cycle analysis data that show the effect of Pdk1 deletion that results in cell cycle arrest in the G1 phase and delayed progression through the G2/M phase (Figure 6g). In addition, MYC_Targets V1&V2 hallmarks are both enriched in the downregulated gene set, implicating a link between KRAS signaling via the PI3K/AKT pathway and MYC activation.
Moreover, several metabolic hallmarks were enriched in the downregulated gene set, including glycolysis. PDK1 is a central component of the PI3K pathway and regulates AKT, PKC, S6K, and SGK, which are tightly associated with the glycolytic metabolism [98, 366]. On the other hand, the most enriched hallmark in the downregulated gene set is the Epithelial-Mesenchymal Transition (EMT) hallmark. However, it is worth noting that no microscopic transition to a more mesenchymal phenotype was not observed upon Pdk1 deletion (data not shown). Functional enrichment analysis using gProfiler (Figure 9b) showed similar enrichment of the cell cycle and metabolic KEGG pathways in the downregulated gene set. On the hand, in the upregulated gene set FoxO signaling was detected which indicates inhibition of the PI3K/AKT pathway in accordance with the aforementioned data (Figure 7 a, c, e, and 4a). Also, the top enriched KEGG term is autophagy. Inhibition of the PI3K pathway has been shown previously to induce autophagy [367]. In addition, similar to the GSEA analysis, TNF and TGF-Beta signaling was enriched in the upregulated genes, Interesting, the KEGG enriched terms included MAPK signaling, Hippo signaling, and Proteoglycans in Cancer. In both GSEA and gProfiler analysis, apoptosis signatures were enriched in the 4-OHT treated samples compared to the ETOH controls although no apoptosis was detected in the Caspase 3/7 assay (Figure 6i).

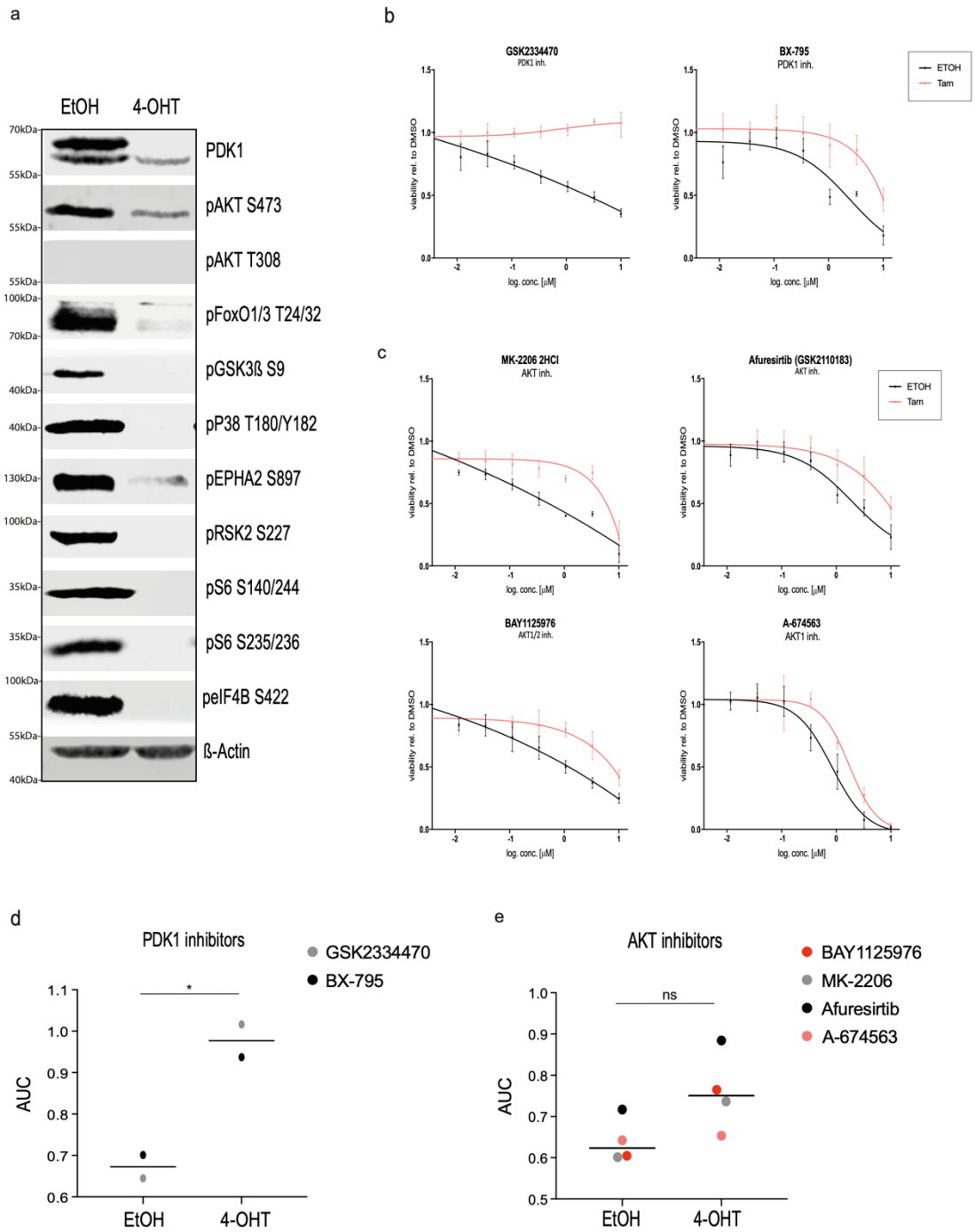

Figure 7: *Pdk1* deletion inhibits the PI3K/AKT signaling pathway

a) Western blot analysis showing inhibition of the PI3K/AKT signaling following Pdk1 deletion in 4-OHT treated cells compared to the ETOH control. PDAC cells (CV7250) were treated with 600nM of 4-OHT or a corresponding volume of EtOH for 7 days. Protein samples were then collected, and the protein lysates were then quantified and separated on an SDS-PAGE gel and then probed with the indicated antibodies. Tim Klaubert performed part of the experiment (KS planned the experiment, and did the cell culture transduction, treatment, and protein sample collection, and trained TK. TK performed the Western Blots).

b, c) Dose-response curve showing the response of ETOH or 4-OHT treated cells to PDK1 and AKT inhibitors. The cells were treated with increasing concentrations of the respective inhibitor, as indicated in the graphs. The lines represent the fitted curves, where each dot indicates the mean

value of four independent replicates. CV7250 cells were treated with 600nM of 4-OHT or a corresponding volume of EtOH for 7 days. ETOH and 4-OHT treated cells were seeded at a density of 500 and 2000 cells per well respectively in a 96-well plate. After overnight incubation, the cells were treated with 7 concentrations of each oft he indicated compounds (3-fold dilutions series) and a solvent control, using a pin tool. 72hrs post-incubation, viability was measured using CellTiter-Glo® Luminescent Assay. The experiment was repeated twice, each with 2 technical replicates.
d,e) Dot plot comparing the AUC of the response of EtOH or 4-OHT treated CV7250 cells to the respective PDK1 and AKT inhibitors. Each dot represents the mean AUC of four independent replicates. The mean AUCs of all drugs of the EtOH and 4-OHT groups were compared using the two-tailed student's t-test. ns $p > 0.05$, * $p=0.0246$

Figure 8: Exploratory RNASeq analysis of the effect of Pdk1 deletion on the transcriptional level
a) PCA plot of gene expression data for six independent replicates corresponding to the ETOH or 4-OHT treated CV7250 samples. CV7250 cells (untransduced, or trasduced with nontargeting LacZ sgRNA or mNTC sgRNA) were treated with 600nM of 4-OHT or a corresponding volume of EtOH for 7 days and then RNA samples were collected and sequenced using bulk 3' transcript end RNA-seq (SCRB-seq).
b) Heat map showing the hierarchical clustering of the ETOH and 4-OHT treated samples. The Top 500 differentially expressed genes between the samples were used. Each column represents the expression profile of an individual experimental replicate. The color scale represents the z-score.
c) Volcano plot representation of the differential expression analysis of genes in the ETOH and 4-OHT treated samples. Red points mark the genes with significantly increased or decreased expression in 4-OHT treated cells compared to the ETOH controls with pValue Cutoff = 0.0001 and FCcutoff = 1.2. The x-axis shows log2fold-changes in expression, and the y-axis shows the log odds of a gene being differentially expressed. FC stands for log2fold-change.
d) Heat Map showing the top 100 differentially expressed genes between the ETOH or 4-OHT treated samples. Each column represents the expression profile of an individual biological replicate. The color scale represents z-score.

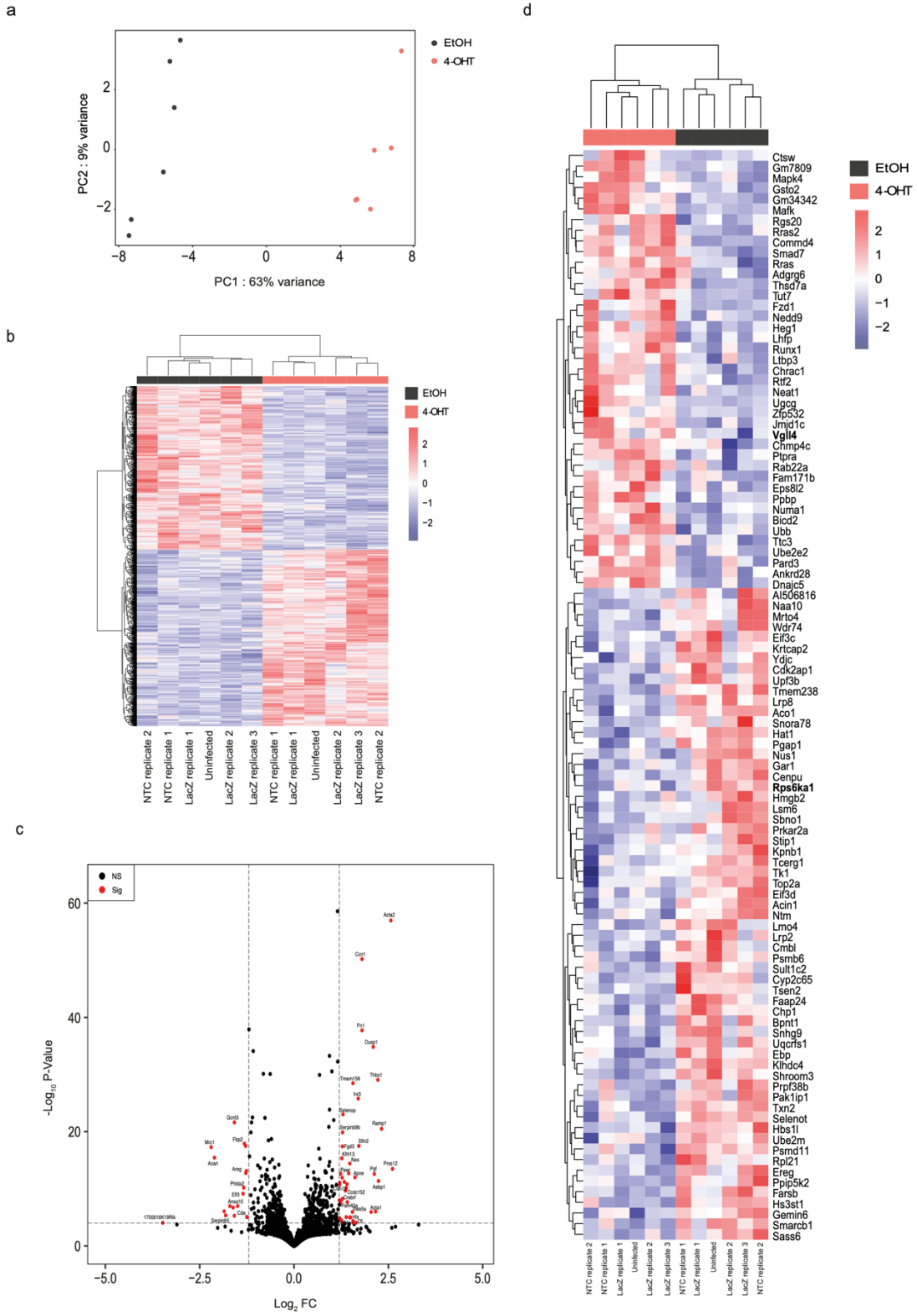
a
EtOH
4-OHT
PC2 : 9% variance
PC1 : 63% variance
b
EtOH
4-OHT
NTC replicate 2
NTC replicate 1
LacZ replicate 1
Uninfected
LacZ replicate 2
LacZ replicate 3
NTC replicate 1
LacZ replicate 1
Uninfected
LacZ replicate 2
LacZ replicate 3
NTC replicate 2
c
NS
Sig
-Log10 P-Value
Log2 FC
d
EtOH
4-OHT
Ctsw
Gm7809
Mapk4
Gsto2
Gm34342
Mafk
Rgs20
Rras2
Commd4
Smad7
Rras
Adgrg6
Thsd7a
Tut7
Fzd1
Nedd9
Heg1
Lhfp
Runx1
Ltbp3
Chrac1
Rtf2
Neat1
Ugcg
Zfp532
Jmjd1c
Vgll4
Chmp4c
Ptpra
Rab22a
Fam171b
Eps8l2
Ppbp
Numa1
Bicd2
Ubb
Ttc3
Ube2e2
Pard3
Ankrd28
Dnajc5
Al506816
Naa10
Mrto4
Wdr74
Eif3c
Krtcap2
Ydjc
Cdk2ap1
Upf3b
Tmem238
Lrp8
Aco1
Snora78
Hat1
Pgap1
Nus1
Gar1
Cenpu
Rps6ka1
Hmgb2
Lsm6
Sbno1
Prkar2a
Stip1
Kpnb1
Tcerg1
Tk1
Top2a
Eif3d
Acin1
Ntm
Lmo4
Lrp2
Cmbl
Psmb6
Sult1c2
Cyp2c65
Tsen2
Faap24
Chp1
Bpnt1
Snhg9
Uqcrfs1
Ebp
Klhdc4
Shroom3
Prpf38b
Pak1ip1
Txn2
Selenot
Hbs1l
Ube2m
Psmd11
Rpl21
Ereg
Ppip5k2
Farsb
Hs3st1
Gemin6
Smarcb1
Sass6
NTC replicate 2
NTC replicate 1
LacZ replicate 1
Uninfected
LacZ replicate 2
LacZ replicate 3
NTC replicate 1
LacZ replicate 1
Uninfected
LacZ replicate 2
LacZ replicate 3
NTC replicate 2

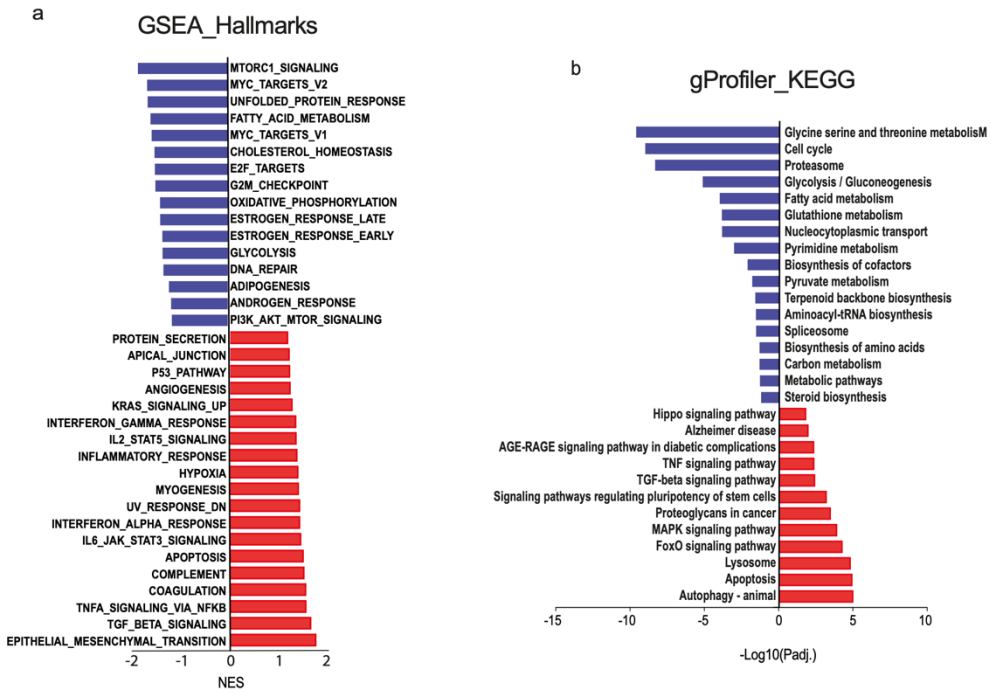

Figure 9: Functional enrichment analysis of the differentially regulated genes upon *Pdk1* deletion
a) Gene set enrichment analysis (GSEA) with the hallmarks gene set from MSigDB showing the main hallmarks upregulated or downregulated in the 4-OHT treated samples compared to the ETOH control with (with FDR < 0.3). The x-axis represents the normalized enrichment score (NES)
b) gProfiler KEGG enriched terms for the top upregulated (log_2(FC) > 0.2; Padj. < 0.1) or downregulated (log_2(FC) < -0.2; Padj. < 0.1) genes between the 4-OHT treated cells and the control ETOH cells with p-Value threshold of 0.05. The x-axis represents the -Log10 (Padj.).

5.2 A subset of PDAC clones shows proliferation independent of *Pdk1* deletion

Although the deletion of Pdk1 showed a strong growth arrest in PDAC, clonogenic assays showed a subset of cells that retain a proliferative capacity despite Pdk1 deletion (Figure 10a). We isolated these colonies from the 4-OHT treated cell lines, along with control clones. Recombination PCRs confirmed that *Pdk1* in indeed deleted and that these clones are capable of proliferating independent of PDK1 (Figure 10b). These clones termed 'persistent clones' show an intermediate proliferation rate compared to an isogenic clone with intact *Pdk1* (*Pdk1*^{lox}) as well as following chronic *Pdk1* deletion (*Pdk1*$^{\Delta}$) (Figure 10c). Western blot analysis confirmed loss of PDK1 and inhibition of the PI3K/AKT pathway as assessed by pS6 levels in the persistent *Pdk1*$^{\Delta}$ clones (Figure 11a). In addition, the persistent *Pdk1*$^{\Delta}$ clones showed a resistance tendency to PDK1 and AKT inhibitors when compared to isogenic clones with intact *Pdk1* (*Pdk1*^{lox} clones), further confirming PDK1 loss and inactivation of the PI3K/AKT signaling cascade and that these persistent clones are able to proliferate independently of PI3K/AKT signaling (Figure 11b & 11c). In order to detect major signaling pathways that may be

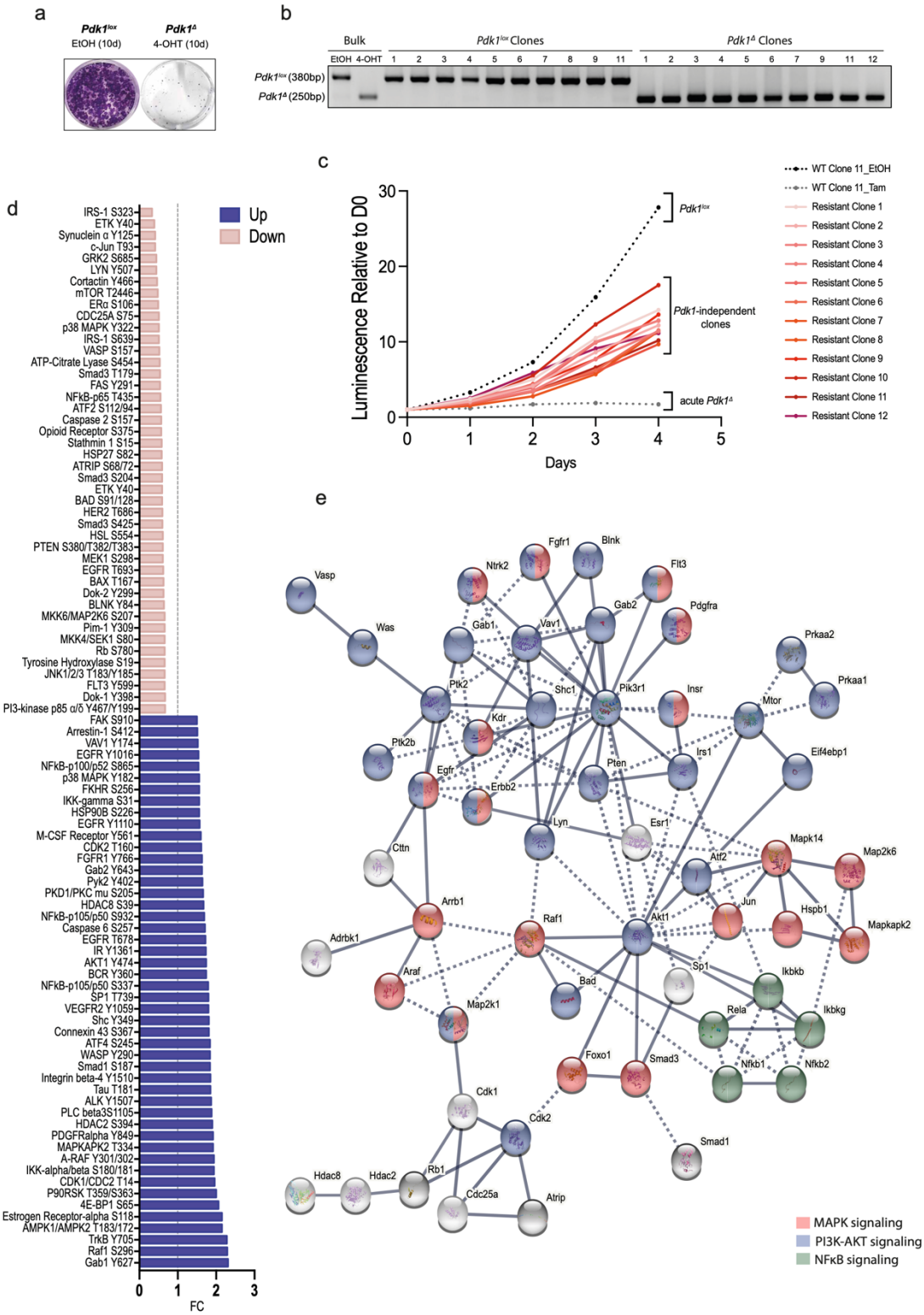

Figure 10: A subset of PDAC clones show a persistent proliferative capacity independent of *Pdk1*

a) Clonogenic assay showing growth of a subset of PDAC clones following *Pdk1* deletion by 4-OHT. CV7250 cell line was treated with 600nM 4-OHT or an equivalent volume of ETOH for 7 days. The

cells were then seeded at a density of 2000 cells per well in a 6-well plate and cultured for 10 days. This is a representative image of at least three independent experiments.
b) PCR showing Pdk1 recombination status in the picked persistent clones (*Pdk1*$^{\Delta}$ clones) compared to control clones (*Pdk1*^{lox} clones) from the CV7250 cell line. Katarina Ondrejkova participated in this experiment (KS planned the experiment, isolated, and characterized the clones and trained KO. KO performed the recombination PCR and ran the gel).
(c) Growth curves of the CV7250 persistent clones compared to a pre-picked clone treated with EtOH and 4-OHT for 7 days to induce acute deletion of *Pdk1* as measured by cell titer glow viability assay (CTG). Data are shown as mean ± SD; n = 3 replicates. Katarina Ondrejkova and Kevin Fink participated in this experiment (KS planned the experiment, isolated, and characterized the clones, generated part of the growth curves and trained KO and KF. KO and KF performed some of the growth curves.)
(d) Phospho explorer array results of the fold change in phosphorylation levels of proteins in a set of signaling pathways as compared between a sensitive and resistant clone treated with 4-OHT. A sensitive and a resistant V592 clone (5E2 and 7G9) were isolated and characterized by Christian Veltkamp. V592 clones (5E2 and 7G9) were treated with 600nM 4-OHT for 7 days. Protein samples were collected and analyzed using Phospho explorer array. The average signal for each phospho antibody is then normalized to the average signal of the corresponding non-phospho antibody. Then the ratio of the resistant clone is divided by that of the sensitive clone to calculate the Fold change (FC) for phosphosite as shown in Appendix Table 1. FC cutoff of 1.4 was used. The array was done once, each antibody had 3 replicate spots.
(e) String analysis of the major proteins showing altered phosphorylation status based on the phospho explorer array. FC cutoff of 1.4 was used. The protein-protein interaction (PPI) enrichment p-value: < 1.0e-16. The pathways were assigned based on functional enrichment by String version 11.0 and manual curation based on literature (String analysis was performed in July 2021).

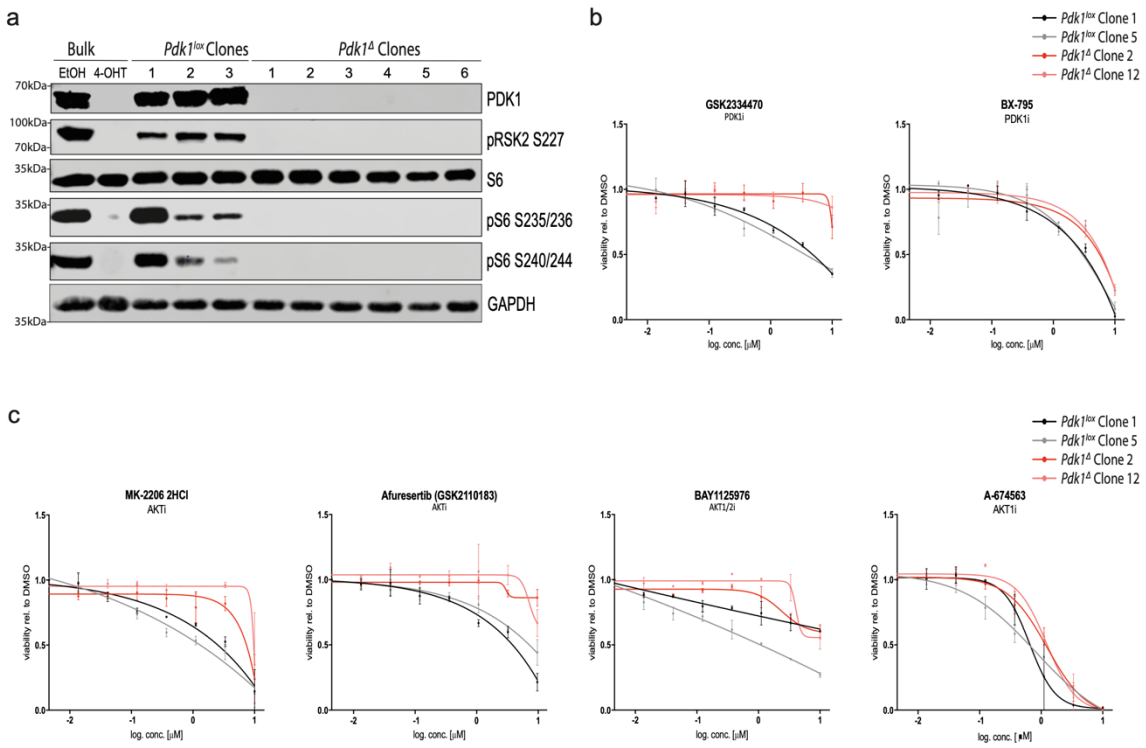

Figure 11: The persistent clones show inhibition of the PI3K/AKT signaling pathway
a) Western blot analysis confirms PDK1 loss in the persistent clones and shows inactivation of the PI3K/AKT pathway. The samples are shown in this order: CV7250 Bulk (EtOH treated), CV7250 Bulk (4-OHT treated), CV7250 WT (*Pdk1*^{lox}) clones 1, 2 and 3 followed by CV7250 persistent (*Pdk1*$^{\Delta}$) clones 1,2,3,4,5, and 6. Michael Otabil collected the protein samples and Christian Biedinger ran the western blots. Katia Sleiman generated the clones and planned the experiments and trained MO and CB.
b,c) Dose-response curve showing the response of CV7250 WT (*Pdk1*^{lox} clones) clones 1 and 5 or persistent clones (*Pdk1*$^{\Delta}$ clones) 2 and 12 to PDK1 and AKT inhibitors. The cells were treated with increasing concentrations of the respective inhibitor, as indicated in the graphs. The lines represent the fitted curves, where each dot indicates the mean ± SD of two independent replicates.

contributing to resistance to *Pdk1*-loss induced growth arrest, we performed phospho explorer antibody microarray analysis that allows the simultaneous analysis of multiple signaling pathways using a preprinted array with 1318 antibodies. The fold change in phosphorylation signal was blotted between a sensitive and a resistant clone derived from the same cell line after 4-OHT treatment (Figure 10d). Enrichment analysis was done using String to identify signaling pathways or processes altered in the resistant clones compared to the sensitive ones. Based on this analysis, differential phosphorylation in the PI3K-AKT and MAPK kinases was detected between the resistant and sensitive clones. In addition to changes in the NFκB Pathway and cell cycle regulators (Figure 10e). Note that this enrichment analysis is insensitive to the phosphosites and is based on only PPI interactions of the detected proteins.

5.3 Murine PDAC cell lines recapitulate human PDAC biology

To systematically investigate the signaling pathways and biological processes that act in parallel to PI3K-AKT-PDK1 signaling in PDAC downstream of KRAS, and that might compensate for the inhibition of the PI3K/AKT pathway and confer proliferative capacities in the persistent clones independent of PDK1, we sought to perform unbiased genome-wide CRISPR screens in various contexts to identify the mechanisms that sustain the persistent clones Pdk1-independent growth and how these can be targeted to eradicate these clones. As a first step, we aimed to establish the reliability of primary murine PDAC cell lines for use in genetic screening to model human disease. Toward that end, we performed genome-wide CRISPR-Cas9 fitness screens in murine PDAC and compared the results to available screening results from public databases to identify the overlap in essentiality determinants in human and mouse PDAC cell lines (Figure 6c). In a great effort by the Sanger Institute termed Project

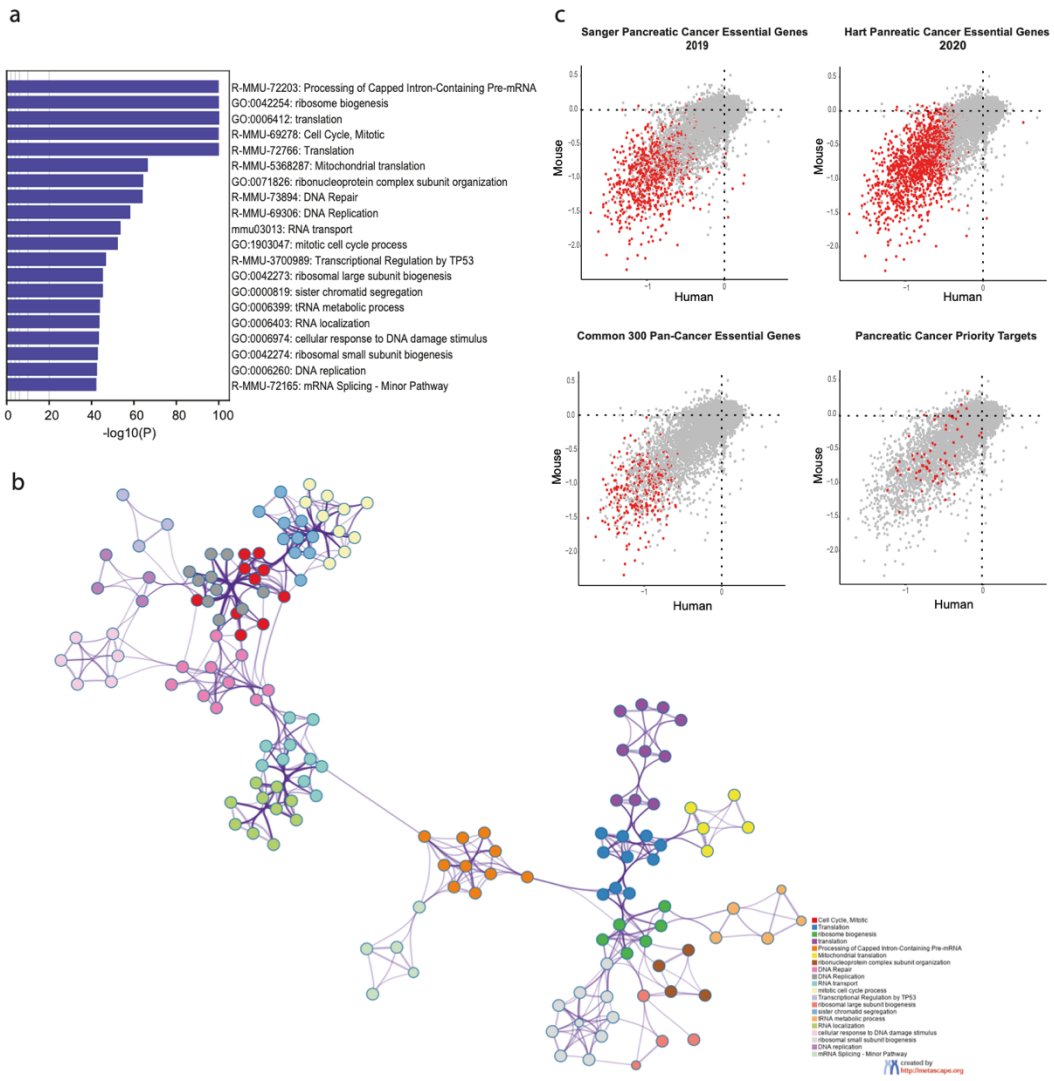

Figure 12: CRISPR-Cas9 Fitness screens in murine primary PDAC cell lines identify core fitness genes comparable to human PDAC

a, b) Metascape enrichment analysis genes identified as essential in murine PDAC cell lines showing the top essential biological processes in PDAC. Dropout Essentiality screens were performed in PDAC cell lines (CV7250 WT clone 1 and 5), and the top 3000 genes with negative CRISPR scores (p <0.0035) were chosen for Metascape analysis.

c) Comparison of CRISPR scores of corresponding genes in human and murine PDAC cell lines. The CRISPR scores from dropout screens performed in humans (obtained from the DepMap project [343]) and murine PDAC cell lines were compared. Genes identified as pan-cancer core fitness genes based on the DepMap [343] and Sanger human CRISPR screens [368] and the 300 common essential genes are highlighted in red. The coefficient of determination (R^2) is equal to 0.601. Fengchong Wang participated in the analysis (KS planned the experiments and performed all the screens. FW established the MAGeCKFlute pipeline in the lab, performed the bioinformatic QCs, and ran the analysis. Further data mining, analysis, and visualization were performed by KS)

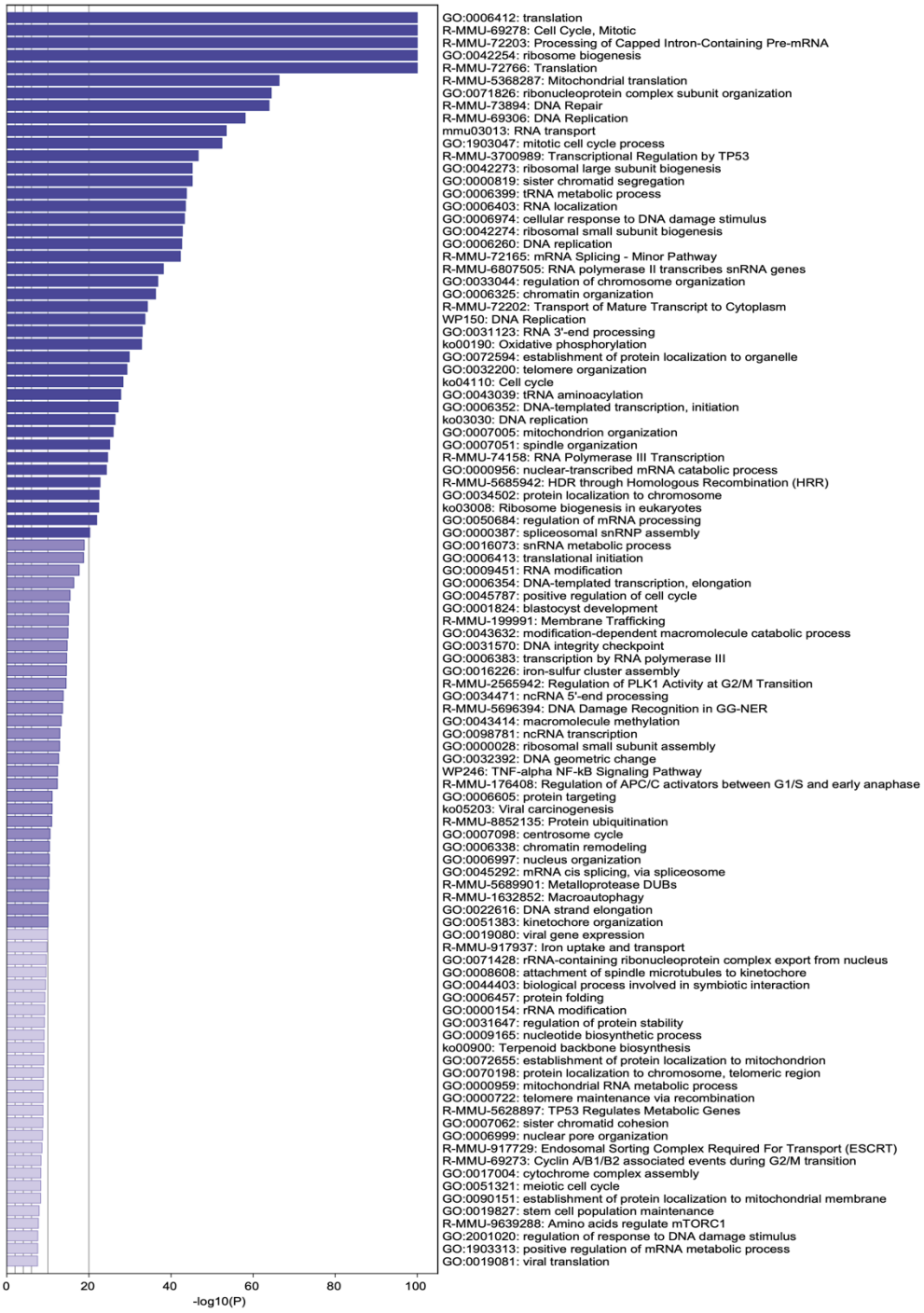

Figure 13: Metascape enrichment analysis of genes identified as essential in murine PDAC
Extended view of Metascape enrichment analysis on genes identified as essential in murine PDAC cell lines showing the top essential biological processes in PDAC. Dropout essentiality screens were performed in PDAC CV7250 cell line (WT clone 1 and 5), and the top 3000 genes with negative CRISPR scores ($p < 0.0035$) were chosen for Metascape analysis.

score, systematic CRISPR-Cas9 fitness screens were performed in 339 human cancer cell lines, including 23 pancreatic cancer cell lines [343]. Using this data set, Behan *et al.,* 2019 identified a set of 553 pan-cancer core fitness genes that displayed common essentiality in the screened human cancer cells. Similarly, Dede *et al.,* 2020 [368] used the Avana data set of CRISPR-Cas9 fitness screens performed in 769 human cancer cell lines by the Broad Institute under the DepMap Project [344]. Dede *et al*., 2020 *identified* 954 high-confidence pan-cancer essential genes, with 300 common genes overlapping with the Sanger pan-cancer core fitness gene set. To compare the fitness scores of genes between mouse and human PDAC, we analyzed the raw data from the DepMap human PDAC cell lines along with the raw data from our murine PDAC screens and calculated a CRISPR score for each gene (Figure 12c), and we used the Sanger and Hart pan-cancer core fitness genes as the gold standard for essentiality (highlighted in red). Our data show a high correlation between gene essentiality in human PDAC, and primary PDAC cell lines derived from our GEM model with a coefficient of determination (R^2) above 0.6. In addition, we performed enrichment analysis on the essential genes identified in the mouse fitness screens using the Metascape analysis [369] and identified key biological processes corresponding to essentiality in mouse PDAC. This analysis allowed us to identify critical essential biological processes such as cell cycle regulation, ribosome biogenesis, DNA maintenance, and translation and transcription regulation (Figure 12 and 13).

5.3 Unbiased CRISPR screens to identify PI3K/AKT/PDK1 collateral dependencies in PDAC

To systematically investigate the signaling pathways and biological processes that act in parallel to PI3K-AKT-PDK1 signaling in PDAC downstream of KRAS, and that might compensate for the inhibition of the PI3K/AKT pathway and confer proliferative capacities in the persistent clones independent of PDK1, we sought to perform unbiased genome-wide CRISPR screens in various contexts to identify the mechanisms that sustain the persistent clones *Pdk1*-independent growth and how these can be targeted to eradicate these clones (Figure 14a). The screens were performed in the context of acute or chronic Pdk1 deletion. In the context of acute Pdk1 deletion (Figure 14b), pooled genome-scale genetic screens were performed by transducing the primary murine PDAC cell lines with floxed Pdk1 alleles and stably expressing the corresponding Cas9 system components with the mouse CRISPR Knockout Pooled Library (BRIE) [364] or the mouse CRISPR/Cas9 Synergistic Activation Mediator (SAM) pooled library [365]. The transduced cells were then treated with ETOH or 4-OHT for seven days and cultured further for several doubling times. The abundance of each sgRNA in the evolving cell populations was monitored by deep sequencing to determine how the knockdown or activation of the corresponding gene contributes to cell growth or death in the context of *Pdk1* deletion compared to the ETOH control. For the screens in the context of chronic Pdk1 deletion, forward knockout genetic screens were performed (Figure 14c) by

transducing *Pdk1*^{lox} clones and *Pdk1*$^{\Delta}$ clones, expressing stable Cas9, with the BRIE library and following the evolution of the sgRNA abundance in both population over several doublings. Growth phenotypes specifically associated with acute or chronic Pdk1 deletion were quantitatively defined by the differences in sgRNA enrichment or depletion between the 4-OHT and ETOH treated cells or *Pdk1*$^{\Delta}$ clones and *Pdk1*^{lox} clones, respectively.

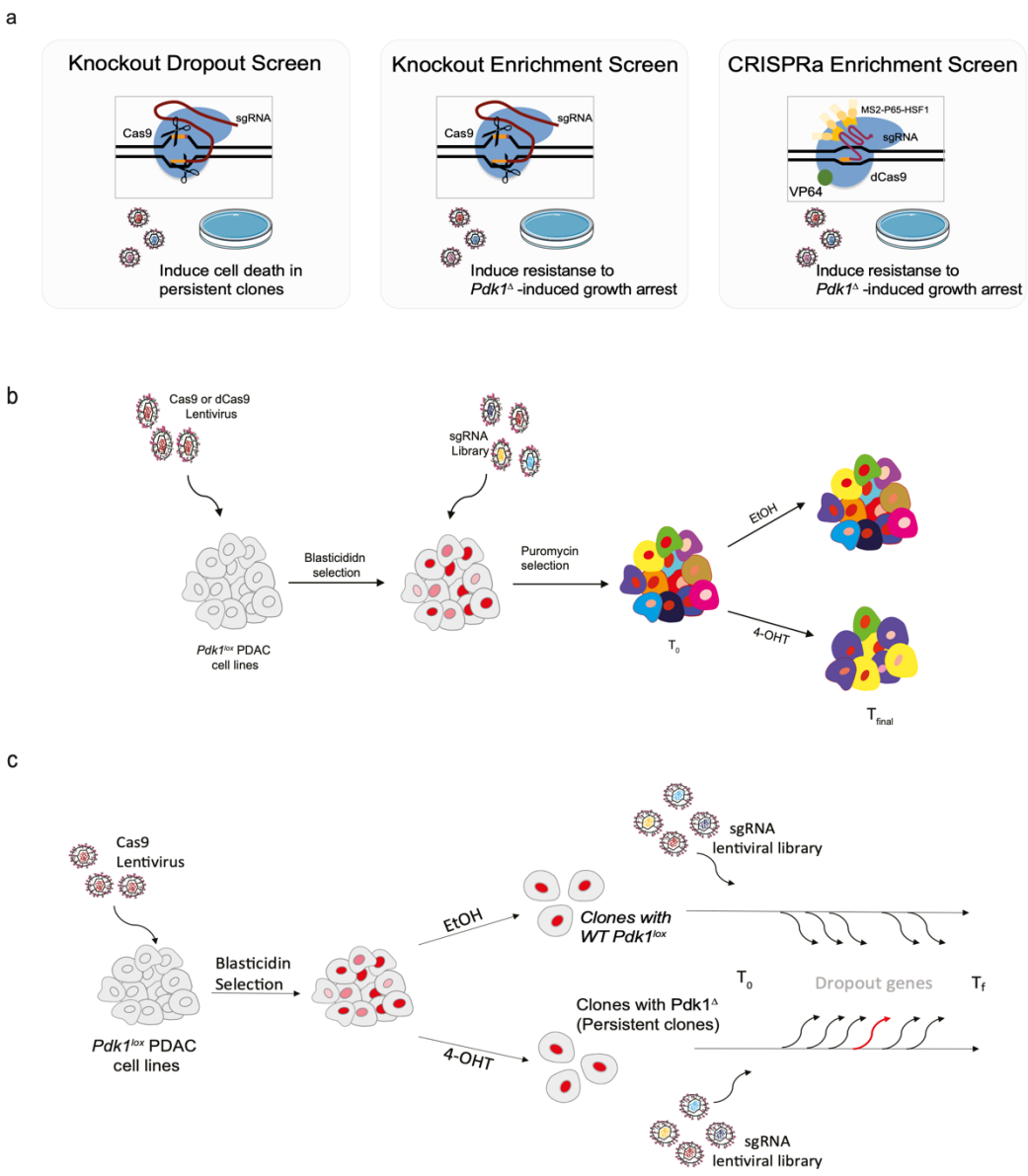

Figure 14: Overview of CRISPR screens performed to identify collateral signaling pathways that sustain PDAC growth independent of the Pdk1 and the PI3K/AKT pathway

a) Overview of CRISPR knockout and activation screens performed to identify mechanisms that potentiate or counteract the persistent proliferation phenotype in the context of *Pdk1* deletion

b) Schematic of the CRISPR screens in the context of acute *Pdk1* deletion in the CV7250 cell line (each treatment condition, EtOH and 4-0HT, was done in 2 independent replicates). For the generation of a cell line with stably expressed Cas9 components, the corresponding Cas9

components were titrated and transduced at an MOI of ≤ 0.5 and selected with the corresponding antibiotic. For the knockout screens, Cas9 was expressed from the pLentiCas9-Blast plasmid and selection with 9 μg/ml Blasticidin was performed for 7 days. For the CRISPRa screens, SAM components (dCas9-VP64 and MS2-p65-HSF1) were expressed from lenti dCaS-VP64-Blast and lentiMPH v2 that were sequentially transduced into the target cell line and selection with 9 μg/ml Blasticidin and 1 mg/ml Hygromycin was performed for 7 days. For the screening, these cell lines were then transduced with the sgRNA library an MOI of 0.3. The transduction was scaled up such that the sgRNA library has coverage of > 500x. 16hrs post infection, the cells were trypsynized and seeded into 175cm flasks. 48hrs post infection, antibiotic selection with puromycin (2,5 μg/ml) was started and carried out for 7 days. The transduced cells were divided into two groups (EtOH control and 4-OHT treatment) post-selection. The treatment was performed for 7 days and then the cells were cultured in normal media till the final timepoint. A minimum of 50 million cells was maintained throughout the culture to maintain the library representation. Cell pellets for gDNA were collected throughout various time points of the screening, with 3-day intervals, including the final timepoint. The final time point was collected 27 days post selection and 20 days post EtOH and 4-OHT treatment.
c) Schematic of the CRISPR screens in the context of chronic *Pdk1* deletion in CV7250 WT clones 1 and 5 and persistent clones 2 and 12, each done in two independent replicates. For the generation of a cell line with stably expressed Cas9 components, CV7250 cells were transduced with Cas9 Lentivrus at an MOI of ≤ 0.5 and selected with 9 μg/ml Blasticidin for 7 days. Cas9 was expressed from the pLentiCas9-Blast plasmid. The Cas9-expressing CV7250 was then treated with EtOH or 600nM 4-OHT for 7 days. Clones were then selected from the control cells (*Pdk1*^{lox} clones) as well as persistent cells from the 4-OHT cells (*Pdk1*$^{\Delta}$ clones) and propagated in culture. WT clones 1 and 5 and persistent clones 2 and 12 were used for the screening. These were then transduced with the sgRNA library an MOI of 0.3. The transduction was scaled up such that the sgRNA library has coverage of > 500x. 16hrs post infection, the cells were trypsynized and seeded into 175cm flasks. 48hrs post infection, antibiotic selection with puromycin (2,5 μg/ml) was started and carried out for 7 days. A minimum of 50 million cells was maintained throughout the culture to maintain the library representation. Cell pellets for gDNA were collected throughout various time points of the screening, with 3-day intervals, including the final timepoint. The final time point was collected 30 days post selection.

Before the screening, Cas9 editing efficiency was assessed in the bulk population and clones to be used. Western blot analysis confirmed adequate expression of Cas9 (Figure 15a). To verify Cas9 functionality, a Cas9 activity reporter was used [370]. The lentiviral vector expresses a gRNA against BFP and a mCherry-2A-BFP protein (Figure 15b). The same vector with no sgRNA was used as a control (empty). Cas9 cutting efficiency was assessed as the ratio of mCherry-expressing cells (with no BFP expression) to the double-positive cells (expressing both mCherry and BFP) (Figure 15c). The bulk population (Figure 16a) showed a considerably high cutting efficiency of 83.9%. This efficiency was even higher in the individual clones (Figure 16b-e), confirming the suitability of these for screening.

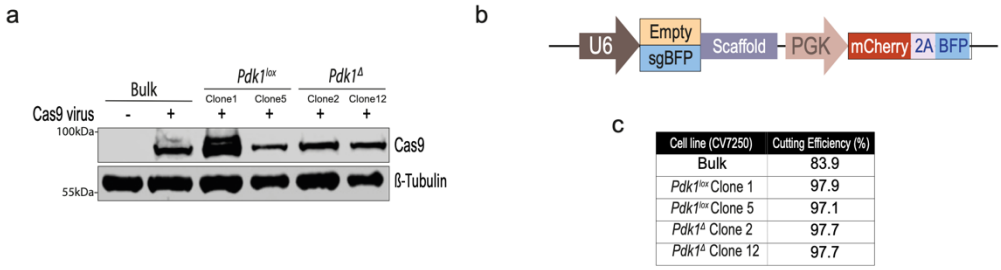

Cell line (CV7250)	Cutting Efficiency (%)
Bulk	83.9
Pdk1^{lox} Clone 1	97.9
Pdk1^{lox} Clone 5	97.1
Pdk1$^{\Delta}$ Clone 2	97.7
Pdk1$^{\Delta}$ Clone 12	97.7

Figure 15: Validation of efficient Cas9 activity in the cell lines used for the genome-wide CRISPR screens
a) Western blot showing the levels of Cas9 in the cell lines used. The order of the samples is the following CV7250 bulk, WT clones 1 and 5 and persistent Clones 2 and 12.
b) Scheme of the reporter pKLV2-U6gRNA5(Empty)-PGKmCherry2ABFP-W (Addgene #67986) and pKLV2-U6gRNA5(gBFP)-PGKmCherry2ABFP-W (Addgene #67985) [370] used to assess cas9 functionality in the cell lines to be screened. The reporter expresses a mCherry-2a-BFP protein and a sgRNA against BFP.
c) Table summarizing Cas9 cutting efficiency in the various lines used in the screens as assessed by the reporter assay and flow cytometry. The cells were transduced with the reporter described above. Seven days post transduction, the cells were analyzed by flow cytometry to determine the proportion of mCherry and/or BFP-positive cells. Cas9 efficiency was estimated from the ratio of mCherry-positive cells to the double-positive cells. Daniel Rossmeisl contributed to these experiments by running the western blot and transducing the bulk population with the reporter.

Cas9 efficiency was also assessed bioinformatically from the screen results by comparing essential genes' scores to those of nonessential ones (Figure17a and 18a). The premise of this comparison is that those essential genes are expected to be depleted and hence should show negative β-scores compared to non-essential genes that are expected to have a more neutral distribution of β-scores. The essential genes here were defined by MAGeCKFlute [348] based on Zuber *et al.,* 2011 criteria [371]. As an additional Quality control (QC) step, the diversity of sgRNAs in each sample was assessed by the Gini index, which measures read depth evenness within samples. A low Gini index indicates the evenness of the sgRNAs and thus a good representation of genes in the samples. As expected, the Gini index is low, and it increases with the timepoints, indicating increased unevenness in the sgRNAs as guides are enriched or depleted in the screen (Figure17b and 18b). Another QC measure of the screen was visualization of the sgRNAs sequences of the various samples on a PCA plot (Figure 18c). The PCA plots show a very high clustering of the replicates at each time. Also, T0 looks more similar to the original BRIE library, and this distribution evolves differently in the different

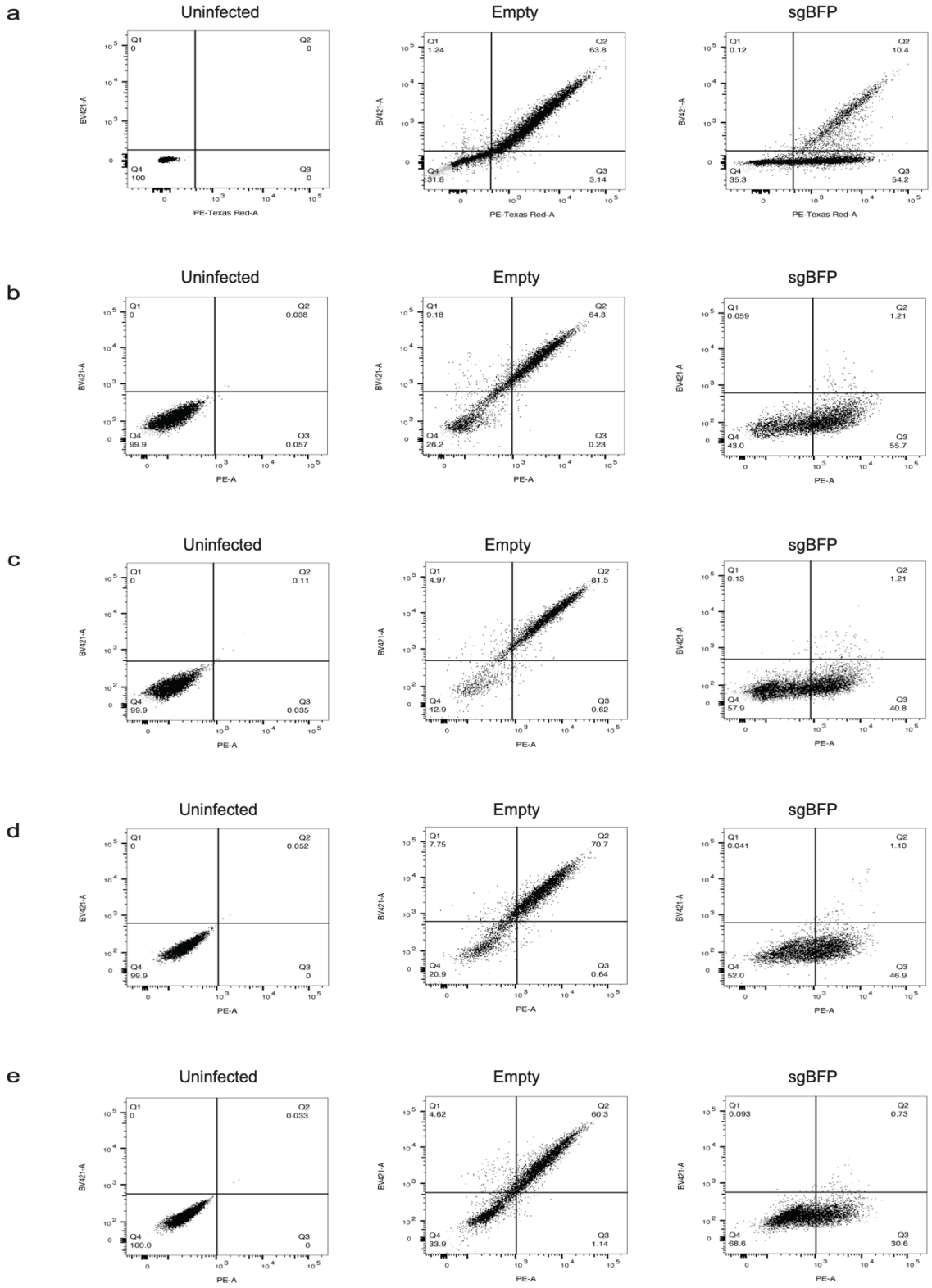
a
Uninfected
Q1 0
Q2 0
Q4 100
Q3 0
Empty
Q1 1.24
Q2 63.8
Q4 31.8
Q3 3.14
sgBFP
Q1 0.12
Q2 10.4
Q4 35.3
Q3 54.2
BV421-A
PE-Texas Red-A
b
Uninfected
Q1 0
Q2 0.038
Q4 99.9
Q3 0.057
Empty
Q1 9.18
Q2 64.3
Q4 26.2
Q3 0.23
sgBFP
Q1 0.059
Q2 1.21
Q4 43.0
Q3 55.7
BV421-A
PE-A
c
Uninfected
Q1 0
Q2 0.11
Q4 99.9
Q3 0.035
Empty
Q1 4.97
Q2 81.5
Q4 12.9
Q3 0.62
sgBFP
Q1 0.13
Q2 1.21
Q4 57.9
Q3 40.8
BV421-A
PE-A
d
Uninfected
Q1 0
Q2 0.052
Q4 99.9
Q3 0
Empty
Q1 7.75
Q2 70.7
Q4 20.9
Q3 0.64
sgBFP
Q1 0.041
Q2 1.10
Q4 52.0
Q3 46.9
BV421-A
PE-A
e
Uninfected
Q1 0
Q2 0.033
Q4 100.0
Q3 0
Empty
Q1 4.62
Q2 60.3
Q4 33.9
Q3 1.14
sgBFP
Q1 0.093
Q2 0.73
Q4 68.6
Q3 30.6
BV421-A
PE-A

Figure 16: Flow Cytometry Charts of the Cas9 activity assay
a) in CV7250 bulk population b) in CV7250 WT *Pdk1*^{lox} clone 1 c) in CV7250 WT *Pdk1*^{lox} clone 5 d) in CV7250 *Pdk1*$^{\Delta}$ clone 2 e) in CV7250 *Pdk1*$^{\Delta}$ clone 12. The cells were transduced with the reporter described in Figure 15b. Seven days post transduction, the cells were analyzed by flow cytometry to determine the proportion of mCherry and/or BFP-positive cells. Cas9 efficiency was estimated from the ratio of mCherry-positive cells to the double-positive cells as shown in Figure 15c.

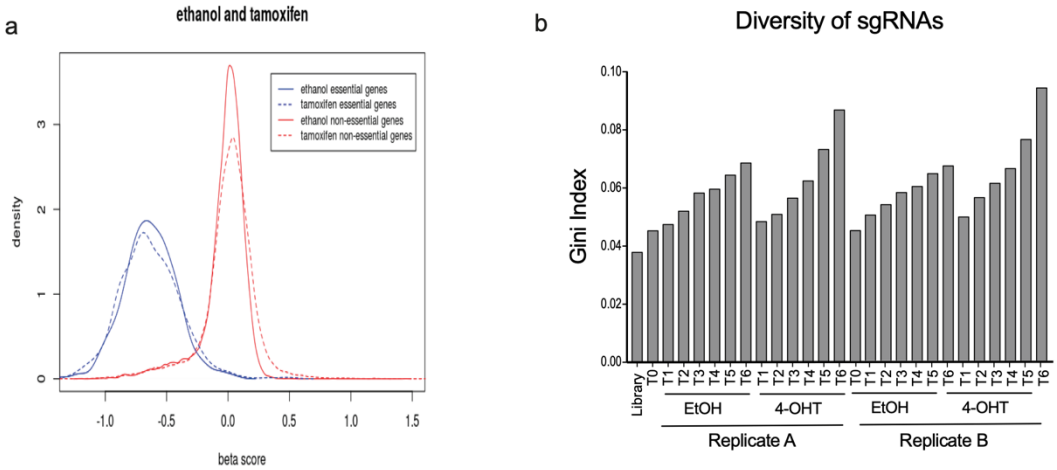

Figure 17: Quality control of the CRISPR screens in *Pdk1*^{lox} bulk cell line with acute *Pdk1* deletion
a) Density plot of the Beta scores calculated based on MAGeCKFlute analysis of essential and non-essential genes for the screens performed as described in Figure 14b. The essential genes are based on the classification by Zuber *et al.,* 2011.
b) Evolution of sgRNA Diversity across various time points in the screened clones and the BRIE library as shown by the Gini index. The Gini index is an economic measure used to reflect income inequality in a population. The Gini index, as calculated by the MAGeCKFlute pipeline, represents the variation in representation between the different sgRNAs. The lower the Gini index the more uniform the sgRNA representation is. KS planned the experiments and performed all the screens. Fengchong Wang performed the QC analysis. Further analysis and visualizations were performed by KS.

conditions indicating selective dependencies or enrichment in the *Pdk1*^{lox} and *Pdk1*$^{\Delta}$ clones. Also, the distance on the PCA between the final time points of the same condition is reduced, indicating stabilization of the system (T6 and T7). T7 was used as the final time point for further analysis.

5.4 Global view of the screens

To gain a global overview of the screen results, we first identified the enriched and depleted hits in the screens in *Pdk1*$^{\Delta}$ clones compared to *Pdk1*^{lox} clones (figure 14c). The criteria to

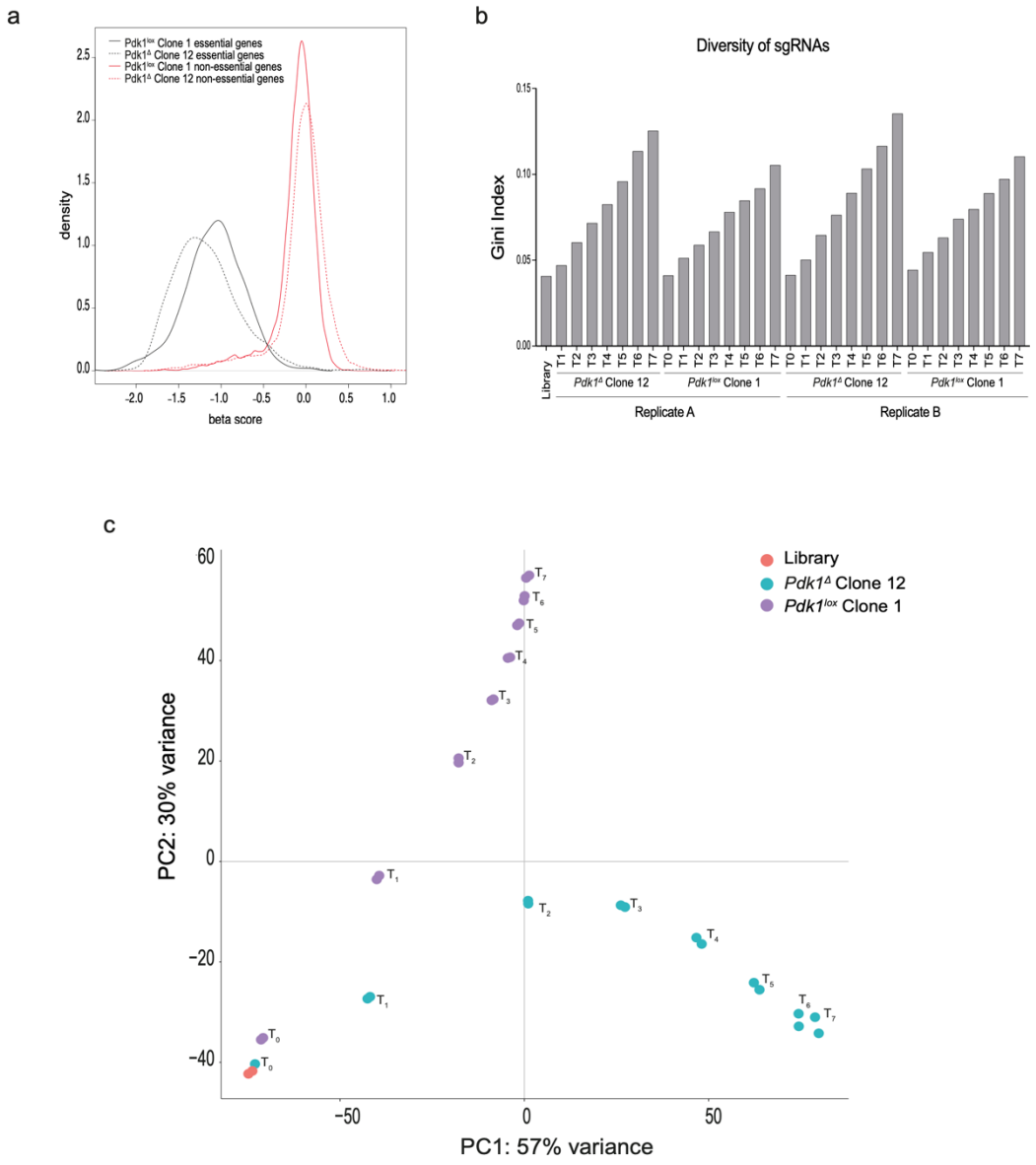

Figure 18: Quality control of the CRISPR screens in *Pdk1^{lox}* and *Pdk1$^{\Delta}$* clones

a) Density plot of the Beta scores calculated based on MAGeCKFlute analysis of essential and non-essential genes for the screens performed as described in Figure 14c. The essential genes are based on the classification by Zuber *et al.,* 2011.

b) Evolution of sgRNA Diversity across various time points in the screened clones and the BRIE library in *Pdk1^{lox}* clone 1 and *Pdk1$^{\Delta}$* clone 12

c) PCA plot of sgRNA sequencing data across various time points. Each dot represents a replicate at the indicated time point. The pink, violet, and blue dots correspond to the BRIE library, CV7250 *Pdk1^{lox}* clone 1, and CV7250 *Pdk1$^{\Delta}$* clone 12 respectively. Fengchong Wang and Niklas de Andrade Krätzig performed the QC analysis (KS planned the experiments and performed all the screens and data visualization. FW ran the MAGeCKFlute pipeline. NK generated the PCA plot).

identify hits in these screens were as follows: For the enriched genes; more specifically genes whose knockout caused resistance to *Pdk1*-deletion induced growth arrest, we selected genes with a cell-cycle normalized β-score of > 0.3 and pValue < 0.01. For the depleted genes, or genes whose knockout caused sensitization or death in combination with *Pdk1* deletion, we selected genes with a cell-cycle normalized β-score below -0.5, which showed at least a -0.2 difference in β-score from the corresponding *Pdk1*^{lox} clones. Essential genes, as defined by Zuber *et al.,* 2011 criteria, were excluded prior to this selection. These filters identified around 400 genes whose loss led to resistance and around 200 genes whose loss led to selective depletion in the context of *Pdk1* deletion.

In order to better understand the role of these genes in the resistance or depletion phenotype, we built a network based on known and predicted protein-protein interactions of the proteins encoded by the identified genes using String Database [372-374]. To visualize structure within this network, we employed a high confidence interaction score of > 0.7 and excluded disconnected nodes. The resulting networks are composed of highly connected core subnetworks and defined clusters. In both the enrichment and depletion network (Figure 19a-b, Figure 20, and Figure 21), we detect common pathways like mTOR signaling, PI3K and MAPK signaling, and the Hippo pathway, where positive and negative regulators of the pathway were enriched in the depletion and enrichment network respectively. In addition, various chromatin regulators were enriched in both networks. The enrichment network was also enriched in negative cell cycle regulators, autophagy genes, genes involved in Ubiquitinylation, and components of the SAGA and Mediator complexes (Figure 19a). Interestingly, the most connected nodes in this network were *Hras, Pten,* and *Ep300* with 56, 50, and 43 edges respectively, based on Cytoscape analysis [375] (data not shown). Extended Figures 3 and 4 depict the networks with gene names included.

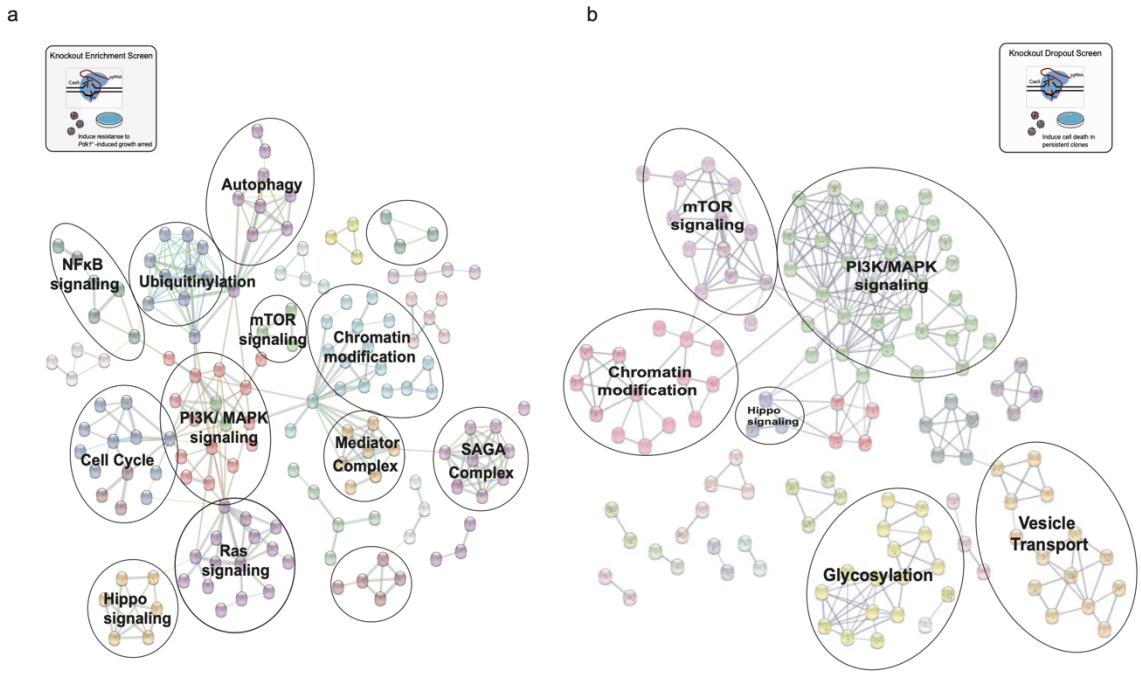

Figure 19: Global View of the CRISPR screens in *Pdk1*$^{\Delta}$ and *Pdk1*^{lox} clones
a) Network of genes enriched in *Pdk1*$^{\Delta}$ clones and displaying at least one connection with another gene a minimum required interaction score of high confidence (> 0.7) and with PPI enrichment p-value < 1.0e-16. The color of the nodes is based on the clusters. The clusters are assigned based on functional clustering by String version 11 and manual curation. The screens were performed as described in Figure 14c in two CV7250 persistent clones (2 and 12), each in two replicates. The average β-score were calculated for the four replicates (2 biological replicates each performed in 2 technical replicates). The enriched genes were selected as genes whose cell-cycle normalized β-score is > 0.3 and with a pValue < 0.01 in the *Pdk1*$^{\Delta}$ clones. (The string analysis was performed in July 2021). The genes are shown in Appendix Table 2.
b) Network of genes depleted in *Pdk1*$^{\Delta}$ clones compared to *Pdk1*^{lox} clones and displaying at least one connection with another gene with a minimum required interaction score of high confidence (> 0.7) with PPI enrichment p-value < 1.0e-16. The color of the nodes is based on the clusters. The clusters are assigned based on functional clustering by String version 11 and manual curation. The screens were performed as described in Figure 14c in two CV7250 WT clones (1 and 5) and two CV7250 persistent clones (2 and 12), each in two replicates. The average β-score were calculated for the four replicates of each the *Pdk1*$^{\Delta}$ and *Pdk1*^{lox} clones (2 biological replicates each performed in 2 technical replicates for each state). The depleted genes were selected as genes whose cell-cycle normalized β-score is below -0.5, and that showed at least a -0.2 difference in β-score from the corresponding *Pdk1*^{lox} clones. (The string analysis was performed in July 2021). The genes are shown in Appendix Table 3.

It is noteworthy that a similar enrichment analysis was performed on the genes enriched after acute *Pdk1* deletion in the screens described in Figure 14c and will be shown later in Figure 28. On the other hand, we decided to not focus on the depleted hits from these screens as they were done in a bulk Cas9 positive population, which results in heterogenous Cas9 expression and hence reduced editing efficiency (~84% in the bulk population as compared to ~ 97-98% in the selected single clones as shown in Figure 15b). This heterogenous Cas9 expression within cells of a bulk population that we observed by western blotting (data not shown) was similarly reported by other groups such as Yusa's group [370]. Similar differences in editing efficiency to ours were also reported by the Elling group, where Cas9 positive mouse embryonic stem cell lines revealed very diverse knockout efficiencies from 0 to 100%, with the bulk population showing ~84% knockout efficiency and only a few clones with editing efficiency above 95% [376]. Although this is not a limitation for the enrichment phenotype, this reduced editing efficiency results in less pronounced negative -scores, as observed with the essential genes when compared in the bulk population versus the clones (Figure 17a and 18a) can dilute the depletion phenotype. Similar observations were reported by the Boutros group, where they directly compared performance of pooled CRISPR viability screening in clonal and bulk Cas9 cell lines and showed that screening in single-cell clones increased the depletion phenotype of essential genes compared to a Cas9 bulk population [377]. We also performed CRISPR activation screens using the SAM system, which consists of using a dCas9 and the recruitment of various transcriptional activators to activate targeted gene expression (Figure 22a-c). The analysis of these CRISPRa screens showed that the system has limited efficiency and high noise that make them less optimal than the LOF screens. However, we were able to cross-reference the data with our findings from the LOF screens by focusing on

particular genes of interest (Figure 22d). Interestingly, *Cdk4, Akt1, Mtor*, and *Yap1* were shown to be enriched in the 4-OHT treated samples confirming that their activation counteracts the *Pdk1* loss phenotype. *Myc* activation led to a strong growth advantage regardless of *Pdk1* status, confirming its role in PDAC tumorigenesis. Consistently, *Myc* gene was among the strongest depleted genes in both samples in the LOF screens. The activation of negative cell cycle regulators such as *Rb1, Cdkn2a, Cdkn1b*, and *Foxo1* led to increased growth arrest or cell death. Similarly, activation of *Ep300* and *Lats2* led to a growth disadvantage, consistent with the resistance phenotype of their knockout.

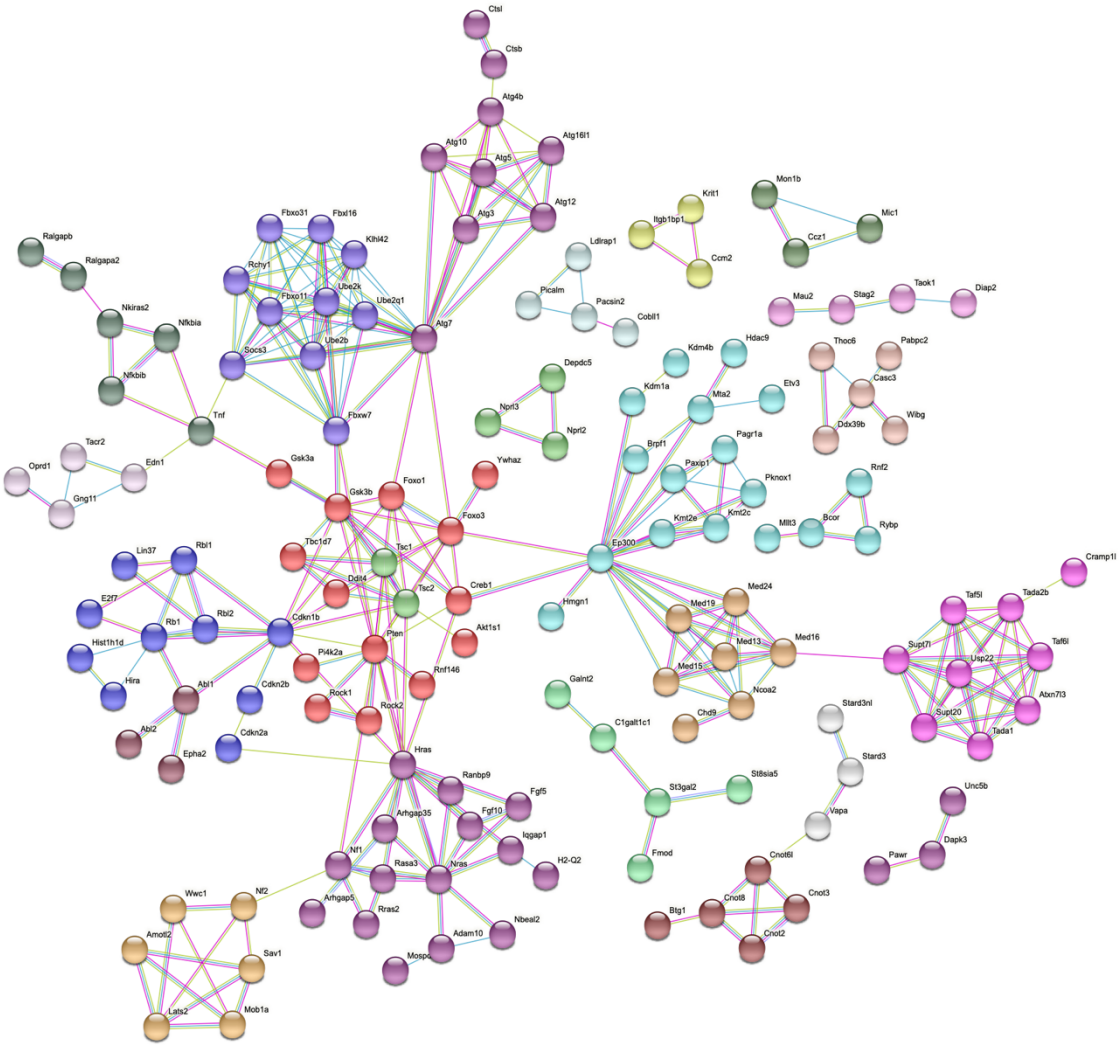

Figure 20: The Enrichment Network, including gene names
Same network from Figure 19a including gene labels

5.5 Pathway- and Gene-Level View of the screens

The network analysis of the hits of the screens in both enrichment and dropout context, generated a tight network with defined modules and we expect that exploration of this network will reveal valuable insights about a wide range of pathways and biological processes that impinge on survival in PDAC and that might constitute targetable collateral dependencies in the context of PI3K pathway inhibition. Toward that purpose, we initially focused on the pathways that were enriched in both the enrichment and dropout networks, and we mined them at a gene level. These include the MAPK signaling pathway, mTOR signaling, Hippo-Yap Pathway, and the Ral pathway.

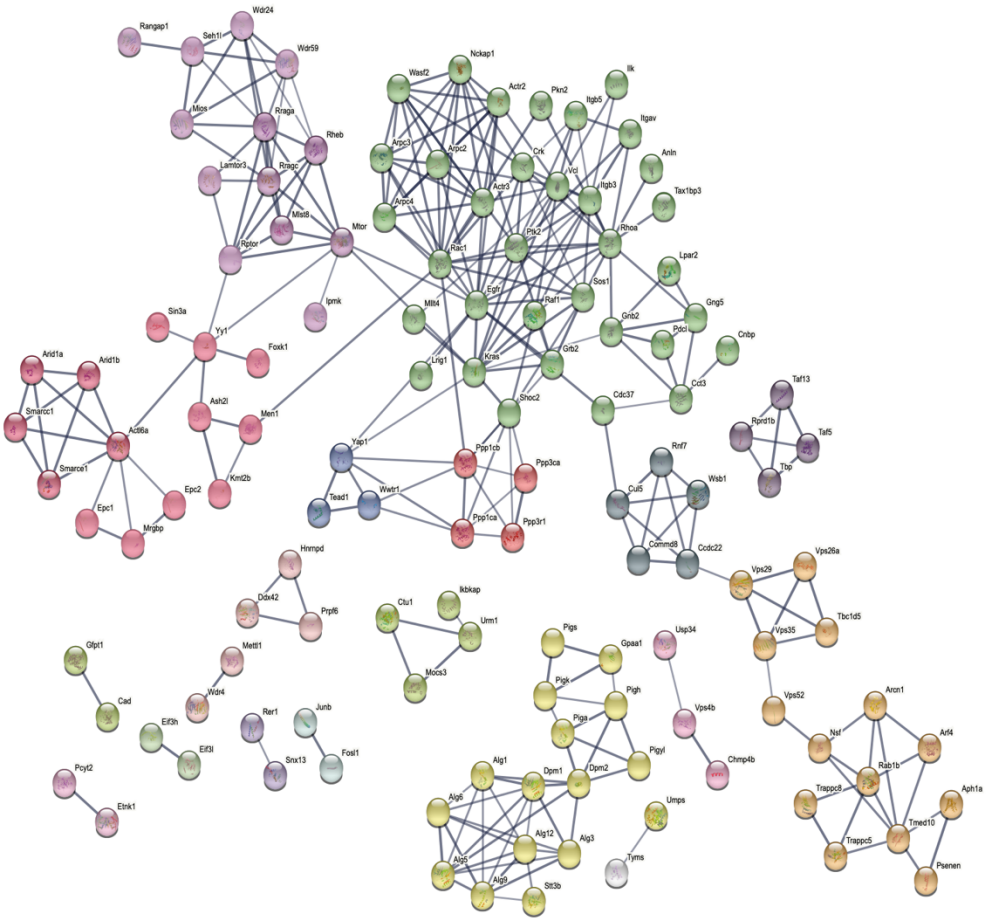

Figure 21: The Dropout Network, including gene names
Same network from Figure 19b including gene labels

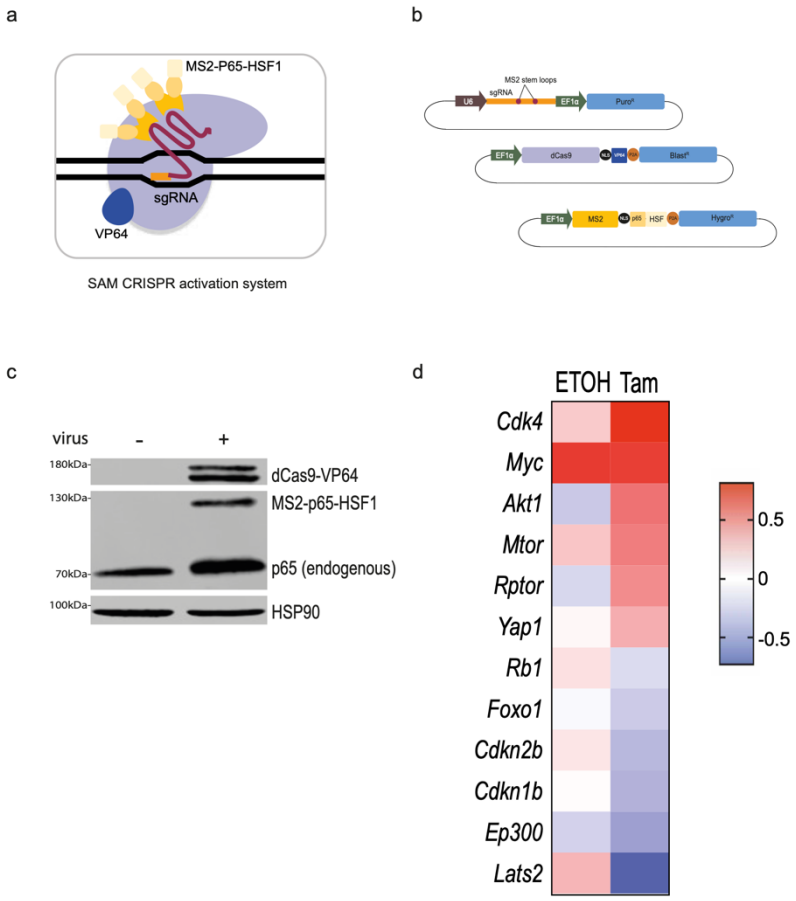

Figure 22: CRISPR activation screens corroborate LOF screen findings
a) Schematic representation of the SAM CRISPR activation system used in our genome-wide activation screens
b) Schematic representation of the constructs used to express the SAM CRISPR activation system.
c) Western blot analysis showing efficient expression of the components of the SAM CRISPR activation system. Kevin Fink performed the western blots.
d) Heat map showing the β-scores of the CRISPRa screen of genes of interest in the ETOH and 4-OHT treated cells. The genes were selected based on overlap with pathways detected in the enrichment and depleted screens and that showed a phenotype in the activation screen. CV7250 cell lines expressing components of the SAM CRISPR activation system were screened as described in Figure 14b, with each treatment condition, EtOH and 4-OHT, performed in two independent replicates. Kevin Fink performed the CRISPRa screen together with KS and it will be part of his thesis. The bioinformatics analysis was done by FW. The shown heatmap analysis was done by KS.

5.5.1 Role of the MAPK Signaling Pathway in PDAC survival Parallel to PI3K Signaling

Components of the MAPK Signaling pathway were identified in the network analysis pinpointing the selective essentiality of this pathway in the context of *Pdk1* deletion and PI3K pathway inhibition. We further mined the data and focused on the hits in the MAPK pathway

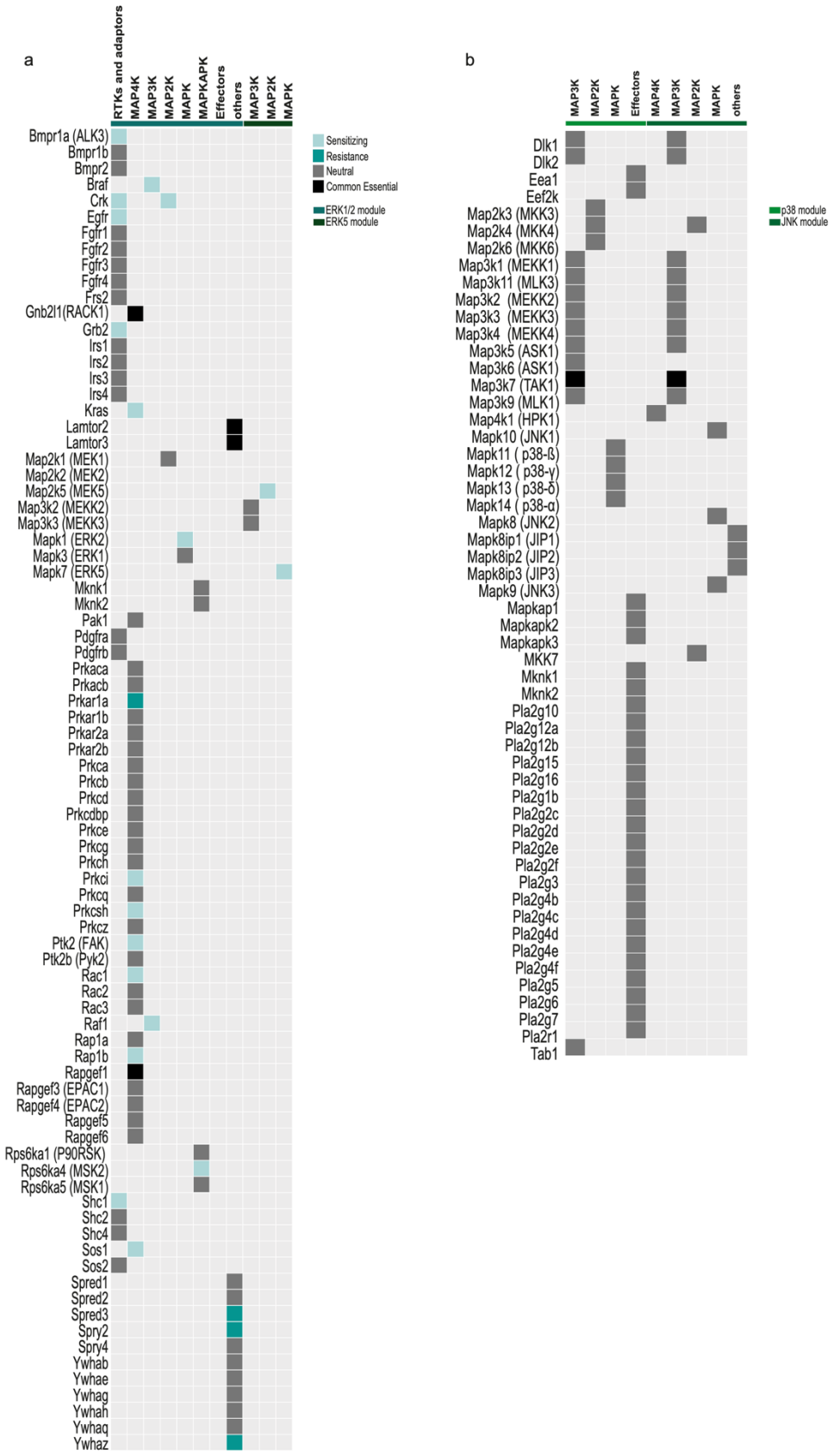

Figure 23: Fingerprint plot of putative genes involved in the MAPK pathway.
The boxes are labeled according to whether knockout of the corresponding gene leads to sensitization (light turquoise), resistance (dark turquoise), no effect (dark grey), or general

essentiality (black). The screens were performed in *Pdk1*$^{\Delta}$ and *Pdk1*^{lox} clones (CV7250 WT clones 1 and 5 and CV7250 Persistent clones 2 and 12) as described in Figure 14c. β-scores and corresponding p-Values for each gene were calculated using the MAGeCKFlute pipeline. The genes were classified as sensitizing, resistance, neutral or common essential based on their β-scores. Common essential are genes that showed a significant negative β-score in both *Pdk1*$^{\Delta}$ and *Pdk1*^{lox} clones. Neutral are genes that shown a β-score around zero with insignificant pValues. Resistance genes are genes with a significant positive β-score in the *Pdk1*$^{\Delta}$ clones. Sensitizing genes are genes with a significant negative β-score in *Pdk1*$^{\Delta}$ clones but not *Pdk1*^{lox} clones. Significance was set based on p-Value <0.05.
a) represents genes in the ERK1/2 and ERK5 modules of MAPK signaling
b) represents genes in the p38 and JNK modules of MAPK signaling

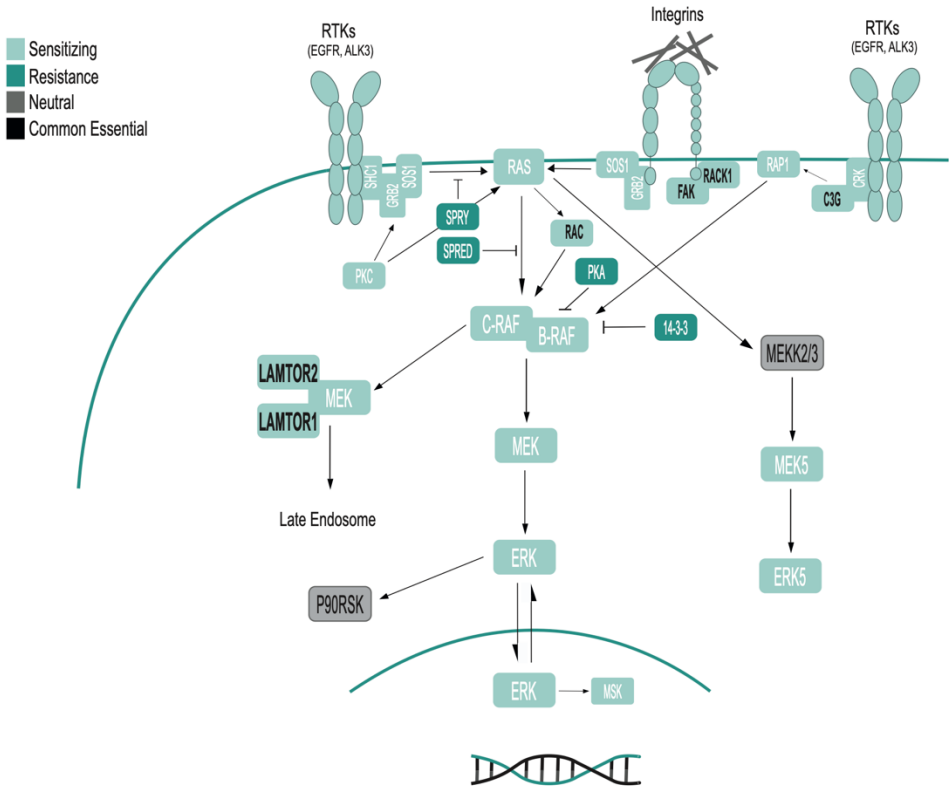

Figure 24: Schematic representation of the genes of the ERK 1/2 module of the MAPK signaling pathway.
The proteins are labeled according to whether knockout of the corresponding gene leads to sensitization (light turquoise), resistance (dark turquoise), no effect (dark grey), or general essentiality (black). The screens were performed in *Pdk1*$^{\Delta}$ and *Pdk1*^{lox} clones (CV7250 WT clone 1 and 5 and CV7250 persistent Clones 2 and 12) as described in Figure 14c. β-scores and corresponding p-Values for each gene were calculated using the MAGeCKFlute pipeline. The genes were classified as sensitizing, resistance, neutral or common essential based on their β-scores. Common essential are genes that showed a significant negative β-score in both *Pdk1*$^{\Delta}$ and *Pdk1*^{lox} clones. Neutral are genes that shown a β-score around zero with insignificant pValues. Resistance genes are genes with a significant positive β-score in the *Pdk1*$^{\Delta}$ clones. Sensitizing genes are genes with a significant negative β-score in *Pdk1*$^{\Delta}$ clones but not *Pdk1*^{lox} clones. Significance was set based p-Value <0.05.

at the gene level (Figure 23). We could clearly identify the importance of both the classical MAPK ERK1/2 and ERK5 modules, known to function downstream of KRAS signaling, in parallel to the PI3K pathway, but not the p38 and JNK modules, that are better known for their role in cellular response to stress. Interestingly, and as expected, negative regulators of the MAPK ERK1/2 classical pathway were enriched in the enrichment map, where their knockout resulted in potentiation of the pathway and most probably increased proliferation of the *Pdk1*$^{\Delta}$ clones, such as *Sprey* and *Spred* (Figure 23 and Figure 24). On the other hand, several genes of the pathway were identified as selectively essential or with increased essentiality degree in the *Pdk1*$^{\Delta}$ clones as compared to the *Pdk1*^{lox} clones (Figure 23 and Figure 24). These included RTKs and their adaptors such as (*Egfr, Bmpr1a, Grb2, Sos1, Shc1*) and genes encoding MAPK kinases such as *Raf1 and Braf*. Interestingly *Raf1* gene had a stronger effect on the survival phenotype compared to *Braf*. *Mapk1* (*Erk2*), but not *Mapk3* (*Erk1*) was shown to have a sensitizing effect. On the other hand, neither *Map2k1* nor *Map2k2* (*Mek1* and *Mek2*) was detected as hits, most likely due to functional redundancy. This is consistent with the findings in literature where *Mek1* and *Mek2* were shown to be redundant for murine embryonic survival as long as a proper protein expression threshold is achieved [378]. On the other hand, *Erk1* and *Erk2* have been shown to exhibit various physiological roles. For instance, *Erk1* knockout mice were viable, fertile, and of normal size [379], whereas *Erk2* knockout resulted in early embryonic lethality suggesting the inability of *Erk1* to compensate for its function [380]. It is noteworthy that this functional redundancy of *Erk1* and *Erk2* remains controversial, and the differential phenotypes have been attributed to differences in expression levels of the two isoforms and In addition, in the ERK5 module of MAPK signaling, we identify *Mapk7* (*Mek5*) and *Map2k5* (*Erk5*) as hits.

To further visualize the hits, the genes were pre-filtered based on their cell-cycle normalized β-scores in the *Pdk1*$^{\Delta}$ clones (β-score <-0.5) to ensure the selection of genes that cause a lethal or sublethal phenotype. Then the β-scores of these genes were compared to those in *Pdk1*^{lox} clones (Figure 25a). Among the genes that show the most differential depletion in *Pdk1*$^{\Delta}$ compared to the *Pdk1*^{lox} clones are genes of the MAPK pathway with *Raf1* being among the strongest hits in this pathway (pinpointed in red in Figure 25a). *Raf1* has a β-score of around -0.9 and 0.06 in the *Pdk1*$^{\Delta}$ and *Pdk1*^{lox} clones respectively showing that it is essential in the context of *Pdk1* deletion but neutral in the *Pdk1*^{lox} clones. We wanted to further validate the combinatorial effect of P*dk1* and *Raf1* deletion on PDAC survival. Towards that end, we used cell lines from the dual recombinase mice (Figure 6a) that contain floxed *Raf1* and *Braf* alleles in addition to *Pdk1*. Similarly, treatment with 4-OHT induces genetic deletion of the three genes by activation of CreERT2. We used the Caspase3/7 activity assay to assess the effect of deleting these three genes on cell survival. Interestingly, and compared to *Pdk1* deletion, the triple knockout of these genes resulted in increased apoptosis as detected by increased induction of caspase 3/7 activity. Bortezomib, a known apoptosis inducer, was used as a positive control (Figure 25b). This shows that *Raf1* and *Braf* deletion, combined with Pdk1 deletion, shifts the phenotype from growth arrest to a cell death phenotype. This prompted

us to further explore the effect of the triple knockout *in vivo* in a syngeneic orthotopic transplantation model of PDAC (Figure 25c). The recipient mice were implanted with *Pdk1*^{lox} cell lines or *Pdk1*^{lox}, *Raf1*^{lox,} and *Braf* ^{lox} cell lines. The tumor-bearing mice were randomized among the treatment arms (Tamoxifen treatment and control groups). Tamoxifen was administered both intravenously and via diet. Both *Pdk1*^{lox} cell lines and *Pdk1*^{lox}, *Raf1*^{lox,} and *Braf* ^{lox} cell lines showed comparable survival in the transplanted control group of 28 days versus 31 days, respectively (Figure 25d). Deletion of Pdk1 led to a reduction in tumor size (data not shown) and a significant increase in mice survival post-transplantation, which was almost doubled. The triple knockout led to impressive ablation of PDAC growth and a normal pancreas macroscopic appearance in the Tamoxifen treated group (Figure 25d). Two out of the six mice in this group were sacrificed at the time of writing this thesis, and the four remaining mice were still alive; hence, the average survival time is yet to be determined. Breedings to generate mouse cell lines with floxed *Raf1* gene alone are ongoing to decipher further the extent of contribution of inhibition of *Braf* and *Raf1* individually and in combination to apoptosis induction and PDAC regression along with *Pdk1* deletion.

We additionally investigated the activation of MAPK signaling in the *Pdk1*$^{\Delta}$ persistent clones. MAPK signaling was detected earlier in the Phospho explorer antibody arrays (Figure 10e). We performed western blot analysis of key effectors in this pathway and compared their phosphorylation status in the *Pdk1*^{lox} and *Pdk1*$^{\Delta}$ clones and the bulk population with acute *Pdk1* deletion (Figure26). cRAF activation, as detected by phosphorylation of the S338 site, was increased after *Pdk1* deletion. This increased activation was also clearly evident in the *Pdk1*$^{\Delta}$ clones compared to the *Pdk1*^{lox} clones. MEK1/2 and ERK1/2, and p90RSK phosphorylation were heterogeneous among the clones, with a tendency to activate the *Pdk1*$^{\Delta}$ clones compared to the *Pdk1*^{lox} clones. This further confirms the overactivation of MAPK signaling after *Pdk1* deletion to compensate for survival in the context of inhibition of the primary oncogenic driver pathway, namely PI3K signaling downstream of KRAS.

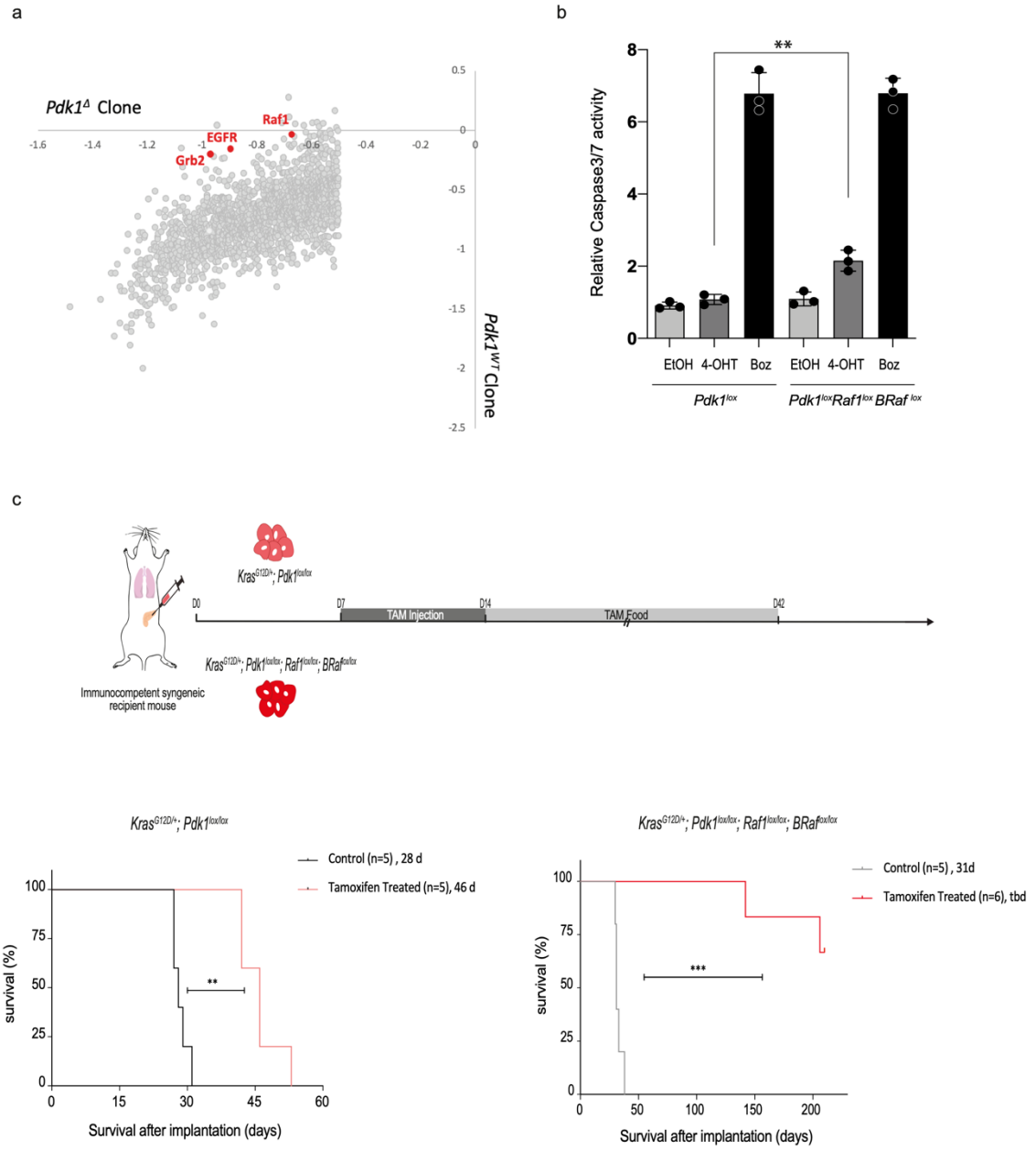

Figure 25: Genetic ablation of *Raf1 and Braf* in combination with *Pdk1* results in complete regression in a syngeneic implantation model of PDAC

a) Comparative analysis of the screens in *Pdk1*$^{\Delta}$ and *Pdk1*^{lox} clones (CV7250 WT clone 1 and 5 and CV7250 persistent Clones 2 and 12). Dots represent genes, and the axis shows depletion β-scores. Red dots represent the most potent hits in the MAPK pathway. The genes were pre-filtered based on their β-scores in the *Pdk1*$^{\Delta}$ clones (<-0.5) to ensure the selection of genes that cause a loss of fitness phenotype.

b) Caspase3/7 activity assay in *Pdk1*^{lox} cell line (CV7250) or *Pdk1*^{lox}, *Raf1*^{lox}, and *Braf* ^{lox} cell line (WM1090) treated with ETOH, 4-OHT, or Bortezomib (Boz) as a positive control. The cells were treated with 600nM 4-OHT or an equivalent volume of EtOH for 7 days. The cells were then seeded at a density of 1000 cells per well in a 96-well plate. After 48 hours, caspase 3/7 activity was determined by measuring luminescence using Caspase-Glo® 3/7assay. The graph represents the induction of caspase 3/7 activity relative to the untreated control. Data are shown as mean ± SD; n =

3 independent replicates. The Caspase assays were done by Mingsong Wang and will be part of his thesis. ***p value* < 0.01, two-tailed student's t test.
c) Schematic representation of the experimental setup to test the combinatorial effect of *Pdk1* versus combined *Pdk1*, *Raf1,* and *Braf* deletion on PDAC progression. TAM (Tamoxifen) injection: 4 mg tamoxifen / 30g body weight intraperitoneally, twice per week, treatment last for one week. TAM food: 400 mg tamoxifen citrate/ kg diet, treatment last for 4 weeks.
d) Kaplan-Meier curve comparing survival in the orthotopic mice model implanted with *Pdk1*^{lox} cell line (CV7250) or *Pdk1*^{lox}, *Raf1*^{lox}, and *Braf* ^{lox} cell line (WM1090) with or without Tamoxifen treatment. The implanted mice were assigned to each treatment group randomly. No statistical method was used to predetermine sample size. No data were excluded from the analyses. The investigators were not blinded to allocation during experiments and outcome assessment The number of mice per condition and the average survival time are indicated. ** indicates p-value of 0.0017 and *** indicates p-value of 0.0007, log-rank test. (NB. 4 out of 6 implanted mice with the *Pdk1*^{lox}, *Raf1*^{lox}, and *Braf* ^{lox} cell line were still alive at the time of preparation of this figure). This experiment was performed by Mingsong Wang with help of KS and will be part of MW´s thesis.

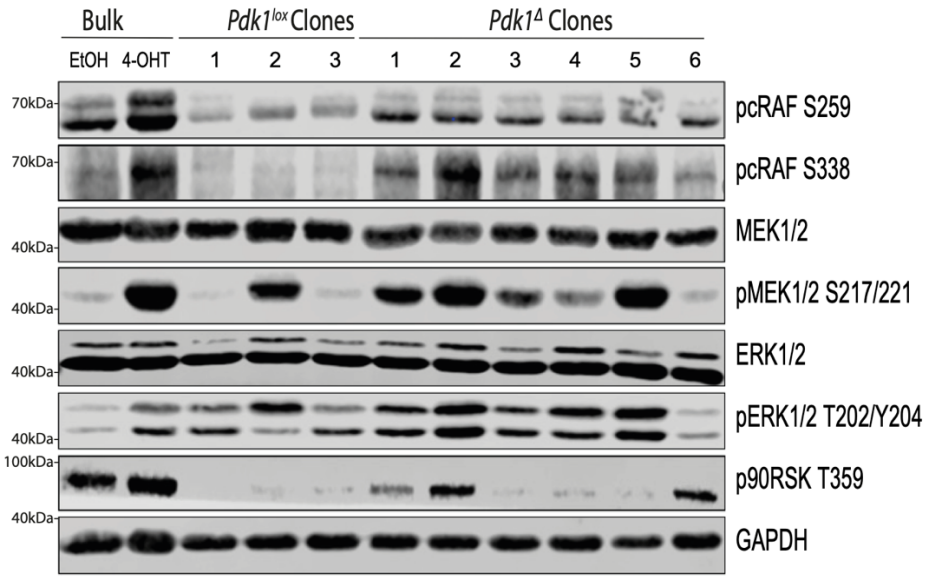

Figure 26: Western blot analysis of key effectors in the MAPK pathway suggests activation of the MAPK pathway in *Pdk1*$^{\Delta}$ and *Pdk1*^{lox} clones.
Pdk1$^{\Delta}$ and *Pdk1*^{lox} clones were isolated as described in Figure 11. Protein lysates were isolated at 70% confluence and analyzed by wester blots. The samples are shown in this order: CV7250 Bulk (EtOH treated), CV7250 Bulk (4-OHT treated), CV7250 WT (*Pdk1*^{lox}) clones 1, 2 and 3 followed by CV7250 persistent (*Pdk1*$^{\Delta}$) clones 1,2,3,4,5, and 6. Michael Otabil and Christian Biedinger participated in this experiment. MO collected the protein samples and CB ran the western blots. KS generated the clones and planned the experiments and trained MO and CB.

5.5.2 Role of other Signaling Pathways in PDAC survival Parallel to PI3K Signaling

Similarly, we mined our data for additional pathways strongly enriched in our network analysis. These included mTOR signaling, Hippo Signaling, and Ral Signaling. Positive and negative mTOR signaling regulators were enriched in both enrichment and depletion networks (Figure 27a and 27b). The negative regulators included components of the TSC-complex (*Tsc1* and *Tsc2*), and members of the Gator complex (*Nlpr2, Nlpr3, and depdc5*). On the other hand, positive regulators and core components of the mTOR signaling that were identified to exhibit stronger essentiality in the context of *Pdk1* deletion included *Mtor* itself in addition to components of the mTOR complexes (mTORC1 and mTORC2) such as *Mlst8*, *Rictor*, and *Rptor*, as well as members of the Ragulator and GATOR2 complexes that positively regulate mTOR signaling including *Mios, Seh1L, Wdr24, Wdr59, RagA,* and *RagC*. *Lamtor1-4* were identified as general essential genes with a more profound effect in the *Pdk1*$^{\Delta}$ clones. Similarly, dissection of the components of the Hippo Signaling pathway identified a crucial role for this pathway in modulating survival in the context of PI3K inhibition (Figure 28a and 28b). *Yap* and its direct regulators such as *Tead1* and *Taz* were identified as sensitizing genes. On the other hand, negative regulators of YAP including direct inhibitors such as *Vgll4* and components of the Hippo Kinase Core such as *Sav1, Lats2,* and *Mob1*, and their upstream regulators such as *Nf2, Amot, Rassf5,* and others were identified as resistance genes.
In addition, components of the Ral pathway were also identified as hits (Figure 29). Although *Rala* and *Ralb* were not among the identified hits, most likely due to redundant function [381], we identify other genes such as *Ralgapa2, Ralgapb,* and *Ralgps2*. This pinpoints the strength of adopting a pathway strategy that we used in contrast to focus on single gene hits. Additionally, we identify genes of NF-kB signaling that are known to be regulated downstream of Ral signaling including *Ikbke, Rel,* and *Relb.*

5.6 Informed Drug screening identifies potential drugs for combinatorial therapies

We sought to evaluate the potential of co-targeting the identified pathways and hits from the CRISPR screens along with *Pdk1* deletion to identify potential combination therapies that could be translated to the clinics. Towards that end, we used the hits identified as sensitizing in the CRISPR screens to prioritize candidates for therapeutic targeting and designed a cherry-picked drug library of 197 compounds that target various pathways and biological processes (Figure 30a and 30b). This targeted drug screening validated many of our results and identify drug candidates with suitable efficacy to pursue for translational purposes. A summary of the pathways and biological targets whose targeting was shown promising in combination with Pdk1 deletion is shown in Figure 30c. We identify the MAPK pathway, mTOR signaling, YAP, Integrin receptors, chromatin regulators, v-ATPases, and VDAC again. It is worth noting that the reproducibility between the acute and chronic *Pdk1* deletion settings is less pronounced than in CRISPR screens, most likely due to high noise in the drug screening with the manual pin tool, and small-scale validation is further required. However, general trends can be firmly

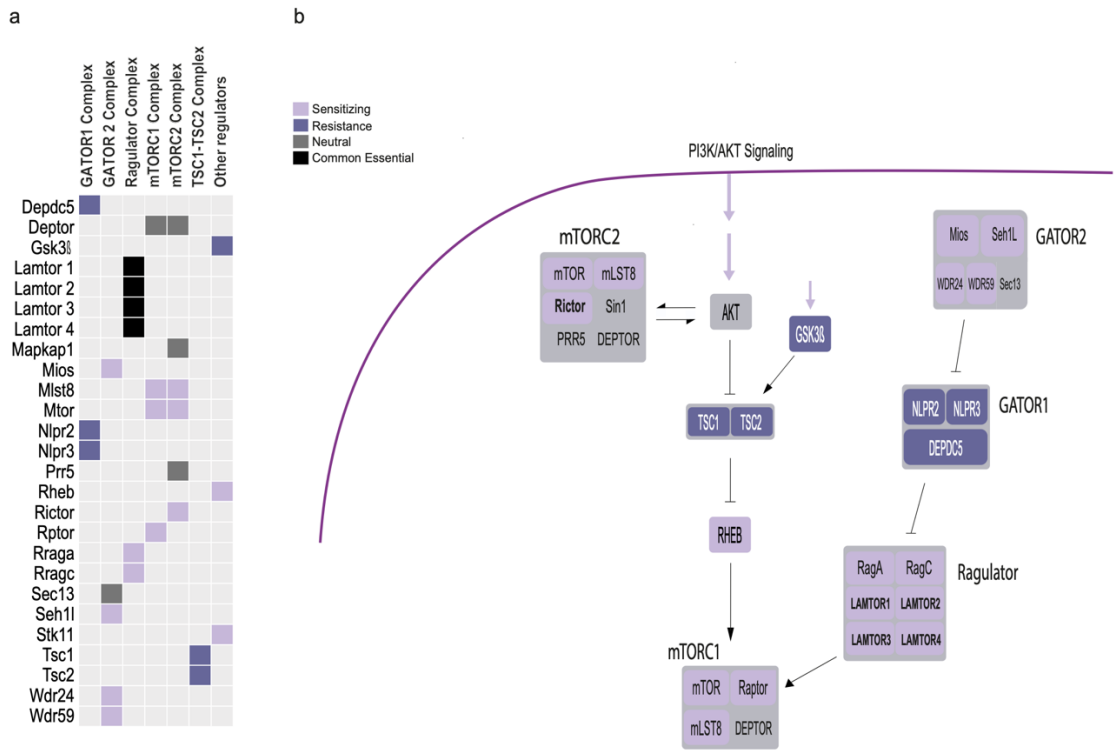

Figure 27: Role of the mTOR Signaling Pathway in PDAC survival along PI3K Signaling
The screens were performed in *Pdk1*$^{\Delta}$ and *Pdk1*^{lox} clones (CV7250 WT clone 1 and 5 and CV7250 persistent Clones 2 and 12) as described in Figure 14c. β-scores and corresponding p-Values for each gene were calculated using the MAGeCKFlute pipeline. The genes were classified as sensitizing, resistance, neutral or common essential based on their β-scores. Common essential are genes that showed a significant negative β-score in both *Pdk1*$^{\Delta}$ and *Pdk1*^{lox} clones. Neutral are genes that shown a β-score around zero with insignificant p-Values. Resistance genes are genes with a significant positive β-score in the *Pdk1*$^{\Delta}$ clones. Sensitizing genes are genes with a significant negative β-score in *Pdk1*$^{\Delta}$ clones but not *Pdk1*^{lox} clones. Significance was set based p-Value <0.05.
a) Fingerprint plot of putative genes involved in the mTOR pathway. The boxes are labeled according to whether knockout of the corresponding gene leads to sensitization (light purple), resistance (dark purple), no effect (dark grey), or general essentiality (black).
b) Schematic representation of the genes of the mTOR signaling pathway. The proteins are labeled according to whether knockout of the corresponding gene leads to sensitization (light purple), resistance (dark purple), no effect (dark grey), or general essentiality (black).

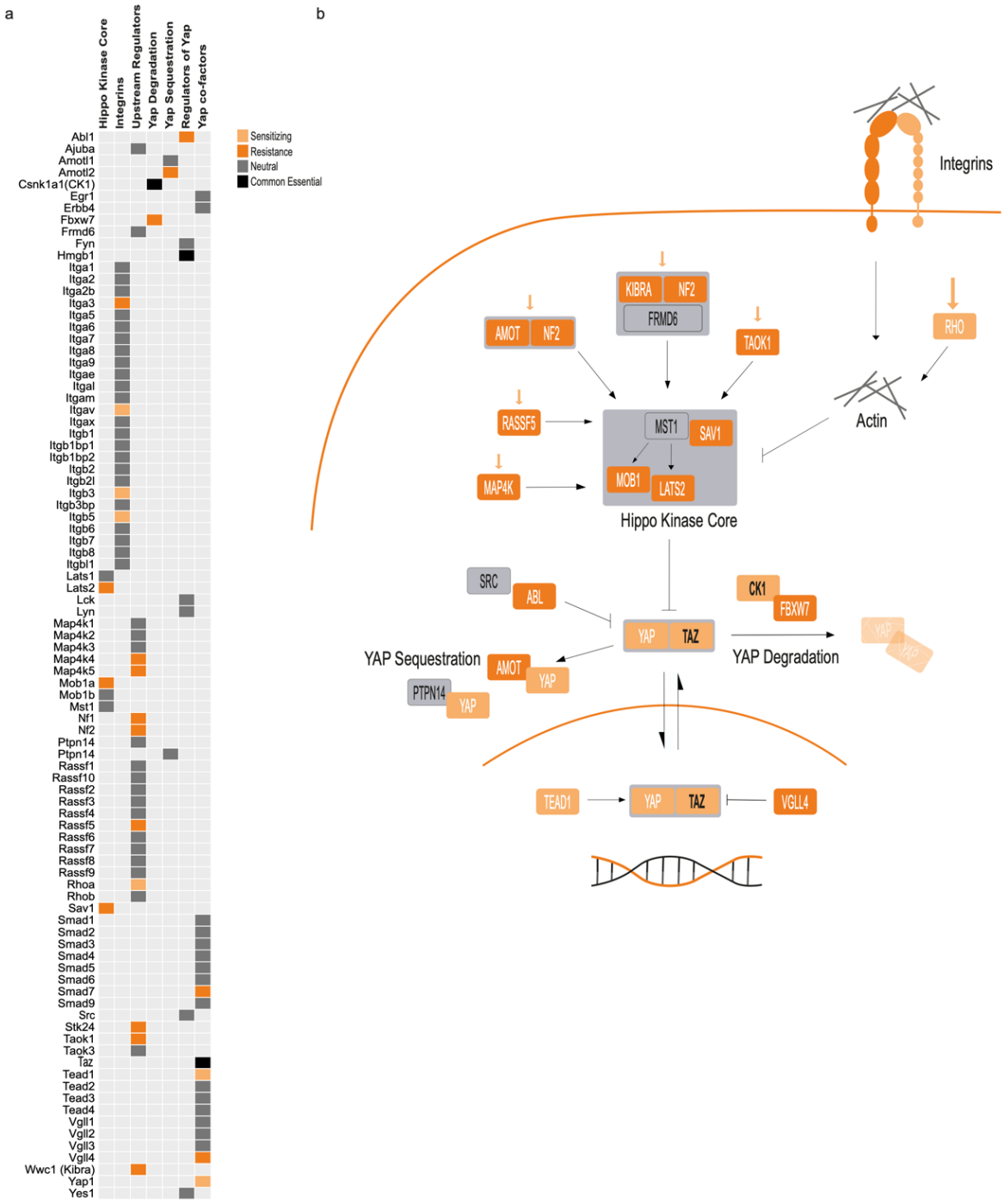

Figure 28: Role of the Hippo Signaling Pathway in PDAC survival along PI3K Signaling
The screens were performed in *Pdk1*$^{\Delta}$ and *Pdk1*^{lox} clones as described in Figure 13c. β-scores and corresponding p-Values for each gene were calculated using the MAGeCKFlute pipeline. The genes were classified as sensitizing, resistance, neutral or common essential based on their β-scores. Common essential are genes that showed a significant negative β-score in both *Pdk1*$^{\Delta}$ and *Pdk1*^{lox} clones. Neutral are genes that shown a β-score around zero with insignificant pValues. Resistance genes are genes with a significant positive β-score in the *Pdk1*$^{\Delta}$ clones. Sensitizing genes are genes

with a significant negative β-score in *Pdk1*$^{\Delta}$ clones but not *Pdk1*^{lox} clones. Significance was set based p-Value <0.05.
a) Fingerprint plot of putative genes involved in the Hippo pathway. The boxes are labeled according to whether knockout of the corresponding gene leads to sensitization (light orange), resistance (dark orange), no effect (dark grey), or general essentiality (black).
b) Schematic representation of the genes of the Hippo signaling pathway. The proteins are labeled according to whether knockout of the corresponding gene leads to sensitization (light orange), resistance (dark orange), no effect (dark grey), or general essentiality (black).

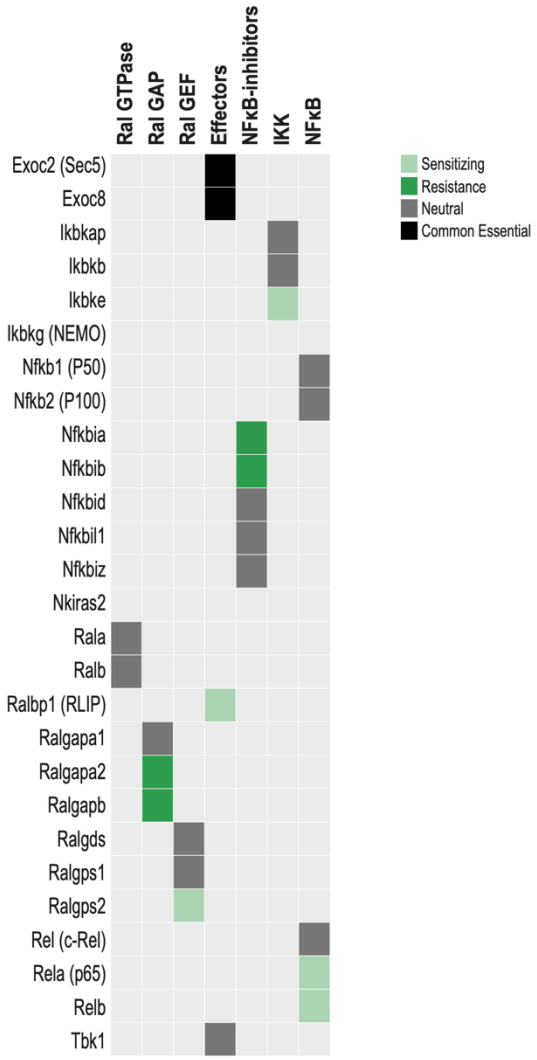

Figure 29: Role of the Ral Signaling Pathway in PDAC survival along PI3K Signaling
Fingerprint plot of putative genes involved in the Ral pathway. The boxes are labeled according to whether knockout of the corresponding gene leads to sensitization (light orange), resistance (dark orange), no effect (dark grey), or general essentiality (black).
The screens were performed in *Pdk1*$^{\Delta}$ and *Pdk1*^{lox} clones as described in Figure 14c. β-scores and corresponding p-Values for each gene were calculated using the MAGeCKFlute pipeline. The genes were classified as sensitizing, resistance, neutral or common essential based on their β-scores.

Common essential are genes that showed a significant negative β-score in both *Pdk1*$^{\Delta}$ and *Pdk1*^{lox} clones. Neutral are genes that shown a β-score around zero with insignificant p-Values. Resistance genes are genes with a significant positive β-score in the *Pdk1*$^{\Delta}$ clones. Sensitizing genes are genes with a significant negative β-score in *Pdk1*$^{\Delta}$ clones but not *Pdk1*^{lox} clones. Significance was set based p-Value <0.05.

concluded from the drug screens. As expected, cell lines with acute and chronic *Pdk1* deletion show resistance to compounds targeting the PI3K pathway (Figure 31a). These mainly include inhibitors of PI3K alpha, but not beta and gamma, in addition to AKT1 and PDK1 inhibitors. Among the tested drugs, the library included several inhibitors targeting the MAPK pathway, from RTKs (EGFR inhibitors), adaptors (inhibitors of SOS1 and SHP2), and MAPK kinases (inhibitors of RAF and ERK), and their downstream targets (FOS inhibitors). Although *Raf1* was among the strongest depletion hits, targeting cRAF using the selective inhibitors, ZM336372and GW5074, pan-RAF inhibitors, TAK-632, and the multi-kinase inhibitor Sorafenib, did not show a solid combinatorial effect on cell growth in combination with *Pdk1* deletion. A mild effect was observed with the bRAF inhibitor SB590885. Interestingly, a robust combinatorial effect was observed with ERK2 specific inhibitors, AZD0364 and VX-11e, with IC50 values of 1.02μM and 0.317μM for VX-11e and 0.157μM 0.027μM for AZD0364 in the ETOH and 4-OHT treated cells respectively. Pan-ERK inhibitors, SCH772984 and Ravoxertinib, also showed a similar effect although to a lesser extent (Figure 31b). This is consistent with the CRISPR dropout screens that showed specific potentiation of *Erk2* essentiality, but not *Erk1*, in the context of *Pdk1* deletion. On the other hand, the library also included various mTOR inhibitors. In accordance with the results of the CRISPR screens, inhibition of mTOR signaling potentiated the defective cell growth phenotype conferred by *Pdk1* deletion (Figure 31c). Interestingly, compounds targeting PI3K and mTOR showed comparable growth inhibition in the *Pdk1* proficient and deficient cells, confirming the combinatorial advantage of simultaneous targeting of PI3K and mTOR signaling. Other exciting targets that were detected in the screen and showed promising results with pharmacological inhibitors are integrins receptors and VDAC (Figure 31d). The CRISPR screens identified several components of the cytoskeleton and its associated signaling. Among these, we detect structural elements such as subunits of the Actin-related protein 2/3 complex (ARPC), including *Actr2*, *Actr3*, *Arpc2*, and *Arpc3*, in addition to integrins receptor subunits such as *Itgav* and *Itgb3,* and cytoskeleton regulating Rho GTPases such as *Rhoa* and *Rac1*. While pharmacological inhibition of ARPC complex and the GTPases RhoA and RAC1 did not show any combinatorial effect with *Pdk1* deletion, inhibition of Integrin receptors showed a promising effect. The αvβ3/5 receptor inhibitor Cilengitide trifluoroacetate showed the most substantial effect (Figure 31d). The αvβ3/5 receptor inhibitor SB273005 and MK-0429 also showed a lower IC50 in the context of *Pdk1* deletion as compared to the control EtOH group (Figure 31c). The ITGAV inhibitor (GLPG0187) showed a strong effect in both conditions with a very low IC50 calculated as -Infinity by the GRmetrics script. The VDAC inhibitor, Erastin, also showed

increased efficacy in the context of *Pdk1* deletion (Figure 31d), purposing it as a promising combination partner with PI3K pathway inhibition.

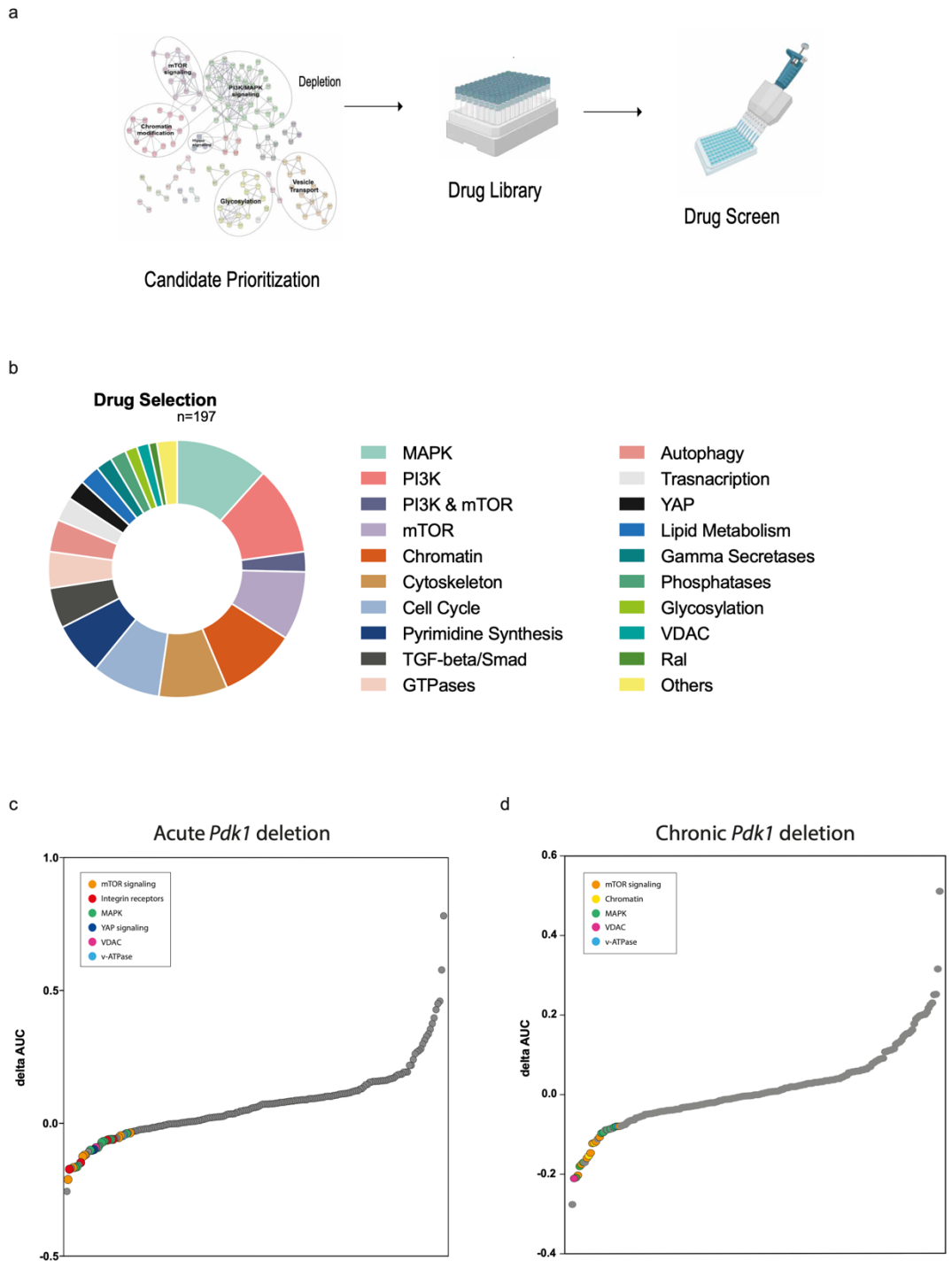

Figure 30: Informed drug screens identify new combination therapies for PDAC

a. Schematic representation of the drug selection process

b. Representation of the drugs selected and the targeted pathways and processes.

c. Rank order plot depicting the differential response of *Pdk1* deficient cells to the screened compounds compared to their *Pdk1* proficient controls (in an acute and chronic deletion setting) as evaluated by differences in the calculated area under the curve (AUC). The dots represent individual

drugs. Drugs showing the most differential sensitivity are color-coded based on their target pathways. CV7250 cells were treated with 600nM of 4-OHT or a corresponding volume of EtOH for 7 days. For the acute *Pdk1* deletion setting, CV7250 cells were treated with ETOH and 4-OHT (600nM) for 7 days and then seeded at a density of 500 and 2000 cells per well respectively in a 96-well plate. After overnight incubation, the cells were treated with 7 concentrations of each of the 200 compounds (3-fold dilutions series) and a solvent control, using a pin tool. 72hrs post-incubation, viability was measured using CellTiter-Glo® Luminescent Assay. The experiment was repeated twice, each with 2 technical replicates. The mean AUC was calculated for the four replicates and the delta AUC was calculated for each compound as follows: $AUC_{(4\text{-}OHT)} - AUC_{(EtOH)}$. Similarly for the chronic *Pdk1* deletion setting, WT (*Pdk1*^{lox} clones) clones 1 and 5 or persistent clones (*Pdk1*$^{\Delta}$ clones) 2 and 12 were seeded at a density of 500 for the WT clones or 1000 cells for the persistent clones per well and screened with the 200 compounds of the library each in two replicates. The mean AUC was calculated for the four replicates of the WT and Persistent clones and the delta AUC was calculated for each compound separately as follows: $AUC_{(persistent)} - AUC_{(WT)}$. The AUC values for each sample are listed in appendix Tables 4 and 5.

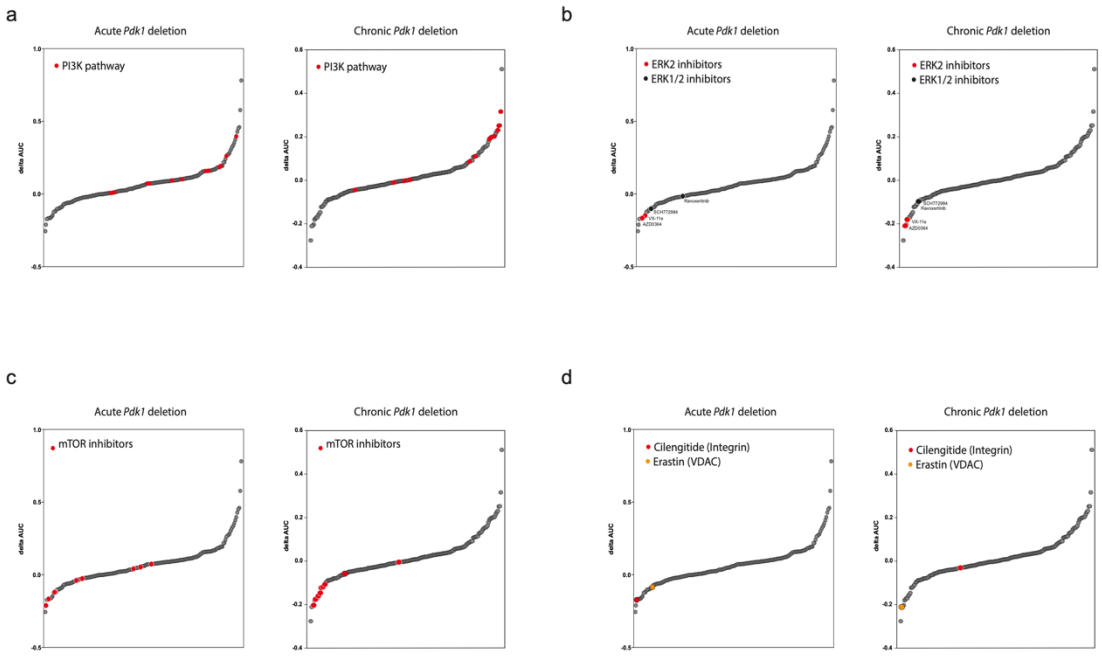

Figure 31: Informed drug screening identifies compounds that show resistance or sensitivity in Pdk1 deficient cells

Rank order plot depicting the differential response of Pdk1 deficient cells response to the screened compounds compared to their *Pdk1* proficient controls (in an acute and chronic deletion setting) as evaluated by differences in the calculated area under the curve (AUC). The dots represent individual drugs. The experimental procedure is the same as described in Figure 26. CV7250 cells were treated with 600nM of 4-OHT or a corresponding volume of EtOH for 7 days. For the acute *Pdk1* deletion setting, CV7250 cells were treated with ETOH and 4-OHT (600nM) for 7 days and then seeded at a density of 500 and 2000 cells per well respectively in a 96-well plate. After overnight incubation, the cells were treated with 7 concentrations of each of the 200 compounds (3-fold dilutions series) and a solvent control, using a pin tool. 72hrs post-incubation, viability was measured using CellTiter-Glo® Luminescent Assay. The experiment was repeated twice, each with 2 technical replicates. The mean AUC was calculated for the four replicates and the delta AUC was calculated for each compound as

follows: $AUC_{(4\text{-}OHT)} - AUC_{(EtOH)}$. Similarly for the chronic *Pdk1* deletion setting, WT (*Pdk1*^{lox} clones) clones 1 and 5 or persistent clones (*Pdk1*$^{\Delta}$ clones) 2 and 12 were seeded at a density of 500 cells for the WT clones or 1000 cells for the persistent clones per well and screened with the 200 compounds of the library each in two replicates. The mean AUC was calculated for the four replicates of the WT and Persistent clones and the delta AUC was calculated for each compound separately as follows: $AUC_{(persistent)} - AUC_{(WT)}$. The AUC values for each sample are listed in appendix Tables 4 and 5.
a) compounds targeting the PI3K pathway are highlighted in red
b) compounds targeting pan-ERK or ERK2 are highlighted in black and red
c) compounds targeting mTOR are highlighted in red
d) compounds targeting Integrin receptors and VDAC are highlighted in red and orange.

5.7 CRISPR screens identify resistance mechanism to the growth arrest induced by *Pdk1* deletion

The CRISPR screens done in both acute and chronic Pdk1 deletion identified various genes that modify the cytostatic effect of Pdk1 deletion and render the cells less sensitive to this growth arrest. To identify these genes, we looked at the top genes that showed a positive enrichment in the context of Pdk1 deletion (positive β-scores) and tried to identify the major pathways and biological processes they are involved in. More specifically, we selected genes with a cell-cycle normalized β-score of > 0.3, and pValue < 0.01 in the clones setting and a cell-cycle normalized β-score of > 0.25, and pValue < 0.05 in the bulk setting. This led to the identification of around 400 genes in both settings (Figure 32a). Using String Database, we built a network with high confidence interaction score of > 0.7 and identified major clusters within this network based on String functional enrichment and manual curation (Figure 32a and 32c). This resulted in the identification of several pathways that contribute to this resistance phenotype including the previously discussed knockout of inhibitors of MAPK, mTOR, and Hippo signaling. In addition, and consistent with the results in the chronic Pdk1 deletion setting (Figure 17a), we identify regulators of the cell cycle in addition to autophagy, various chromatin modifiers, including the SAGA and Mediator complexes, and various genes involved in protein ubiquitylation. In figure 32b, we depict the top resistance genes with their corresponding clusters. A set of these genes was validated in single guide experiments confirming the results. These included *Foxo1*, a known mediator of PI3K inhibition, and that served as a positive for our screens. In addition, we tested *Pten* (the PI3K/AKT pathway), *Tsc2* (mTOR pathway), *Cdkn2b* (cell cycle regulation), *Vgll4,* and N*f2*(Hippo-Yap signaling), *Usp22 and Atxn7l3* (SAGA complex), and *Med16* (Mediator complex). Knockout of these genes showed increased growth in 4-OHT treated cells as compared to control cells expressing non-targeting sgRNAs (Figure 32d and data not shown for *Usp22*, *Atxn7l3* and *Med16*). The efficiency CRISPR cutting for each gene was assessed by Tide analysis and depicted in Figure 32e.

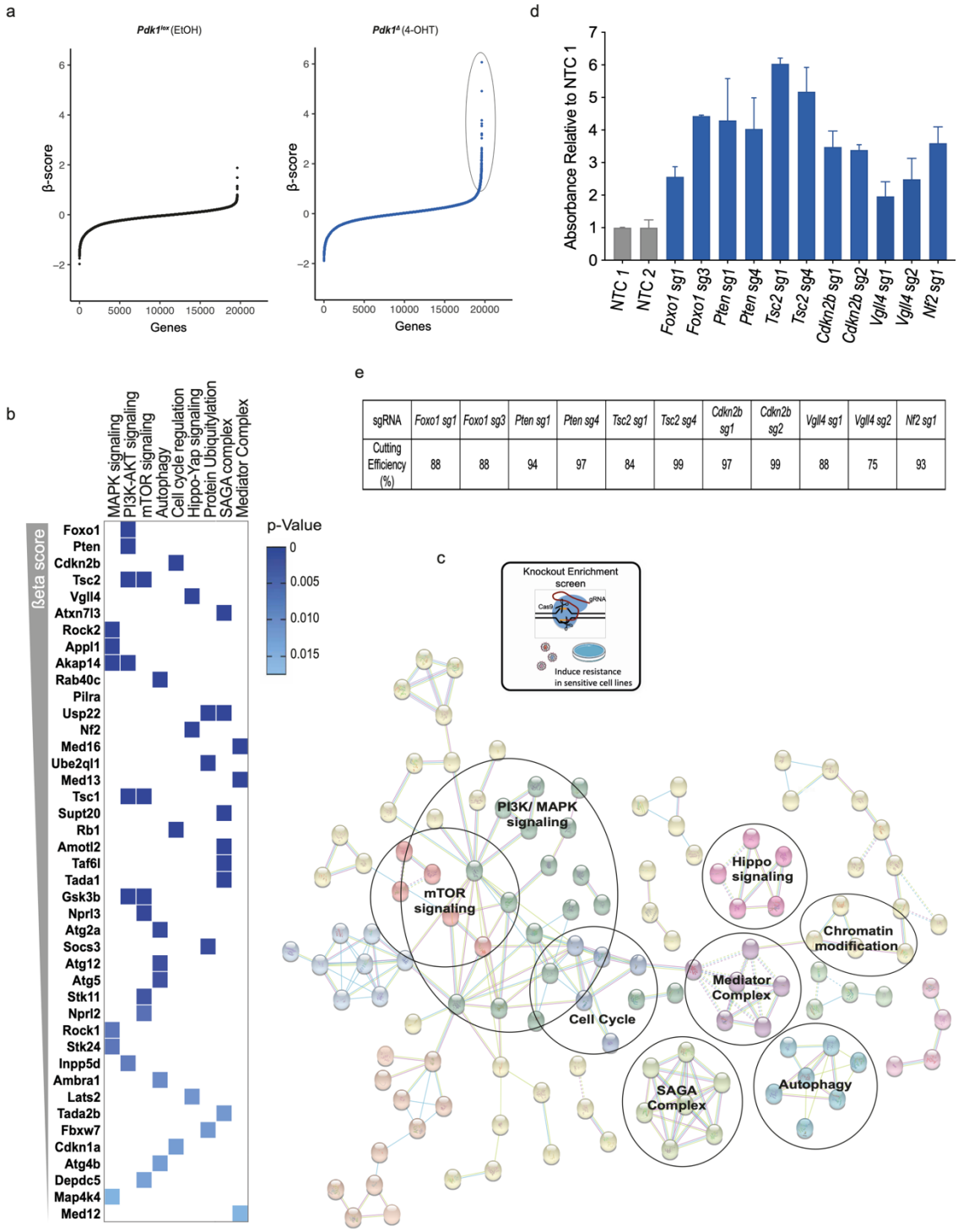

sgRNA	*Foxo1 sg1*	*Foxo1 sg3*	*Pten sg1*	*Pten sg4*	*Tsc2 sg1*	*Tsc2 sg4*	*Cdkn2b sg1*	*Cdkn2b sg2*	*Vgll4 sg1*	*Vgll4 sg2*	*Nf2 sg1*
Cutting Efficiency (%)	88	88	94	97	84	99	97	99	88	75	93

Figure 32: Global view of the resistance mechanisms to *Pdk1* deletion-induced growth arrest identified by CRISPR screens

a) Ranked gene-level β-scores from the genome-wide CRISPR screen with acute *Pdk1* deletion in the ETOH control group and 4-OHT treated group. Genes with specific enrichment in the 4-OHT group are marked. The screens were performed in the bulk CV7250 cell line as described in Figure 14b. The β-scores for each gene were calculated by FW using the MAGeCKFlute pipeline and the genes were ranked based on increasing β-scores.
b) Finger Fingerprint plot of the top genes enriched in the 4-OHT treated group with *Pdk1* deletion and assigned to their functional pathways. The boxes are labeled according to the p-value. The screens were performed in the CV7250 cell line as described in Figure 13b. The β-scores for each gene were calculated by FW using the MAGeCKFlute pipeline and the genes were ranked based on increasing β-scores. The top-ranking genes were selected and assigned to pathways based on string version 11 functional enrichment and manual curation based on literature knowledge.
c) Network of genes enriched in 4-OHT treated group with *Pdk1* deletion and displaying at least one connection with another gene a minimum required interaction score of high confidence (> 0.7) and with PPI enrichment p-value < 1.0e-16. The color of the nodes is based on the clusters. The clusters are assigned based on functional clustering by String version 11 and manual curation (The string analysis was performed in July 2021). The screens were performed in the CV7250 cell line as described in Figure 13b. The β-scores for each gene were calculated by FW using the MAGeCKFlute pipeline and the genes were ranked based on increasing β-scores. Genes with a cell-cycle normalized β-score of > 0.25, and pValue < 0.05 in the 4-OHT setting were selected (around 400 genes) and used for the string analysis. The genes are shown in appendix Table 4.
d) Single guide experiments to validate some of the top genes involved in resistance to *Pdk1* deletion. Cells transduced with sgRNAs targeting the top resistance genes identified in the CRISPR screen were treated with 600nM 4-OHT for 7 days, and their growth was measured relative to 4-0HT treated cells transduced with non-targeting control (NTC) sgRNAs. Growth was assessed by clonogenic assays. The knockout genes include *Foxo1, Pten, Tsc2, Cdkn2b, Vgll4,* and *Nf2.* Data are shown as mean ± SD; n = 3 or more replicates. NTC1 vs NTC2 comparison is ns with pValue= 0.9938. All the other comparisons, target gene vs NTC1, are significant with pValue ranging from 0.0113 to <0.0001 (one-way ANOVA multiple testing).
e) The percentage of Indels in the genomic locus of the indicated genes transduced by the corresponding sgRNA in CV7250. CV7250 cells were transduced by PlentiCRISPRv2 plasmid expressing the indicated sgRNAs and selected with 2.5 μg/ml Puromycin for 7 days. The selected cells were then assessed for the CRISPR/Cas9 cutting efficiency of the corresponding gene. The genomic locus surrounding the expected CRISPR cut site was amplified and sequenced. Tide analysis was used to deconvolute the percentage of insertions and deletions at the site. Kevin Fink participated in these experiments.

5.8 CRISPR screens identify resistance mechanism to the growth arrest induced by *Pdk1* deletion induced by *Pten* loss

Among the identified resistance genes is *Pten*. *Pten* showed a neutral β-score in *Pdk1* proficient cells (ETOH-treated bulk cells and *Pdk1*^{lox} clones) and was specifically enriched in the context of *Pdk1* deletion suggesting that it provides a specific growth advantage upon loss of *Pdk1* (Figure 33a). The effect of *Pten* loss on the 4-OHT treated cells was validated in single guide experiments where PDAC cell lines with floxed *Pdk1* were transduced with non-targeting sgRNA or sgRNAs targeting *Pten* and then treated with ETOH or 4-OHT. As shown

previously, *Pdk1* deletion mediated by 4-OHT induction of Cre led to growth arrest in the cells with the control sgRNAs, on the other hand, cells expressing *Pten* targeting sgRNAs showed a significant increase in proliferation compared to the cells with control sgRNAs specifically in 4-0HT treated cells but not the ETOH treated cells (Figure 33b and 33c). This selective growth advantage conferred by *Pten* loss in context of *Pdk1* deletion was also validated using multicolor competition assays. Cells were transduced with constructs expressing sgRNAS in combination with various fluorescent proteins. Cells expressing control and *Pten* targeting sgRNAs were mixed in equal proportions and treated either with ETOH or 4-OHT and then propagated in culture over a duration of 15 days and the proportion of each population was assessed by flow cytometry. These assays showed selective growth advantage and enrichment of cells expressing a *Pten* targeting sgRNA in the 4-OHT treated setting but not in the ETOH setting (Figure 33d). This phenotype was also confirmed in PTEN KO clones with validated PTEN deletion (Figure 34a-c). As a matter of fact, a clone picked from the bulk population transduced with *Pten*-targeting sgRNAs and showing on in-frame indel mutation in the *Pten* locus (Clone 4), showed sensitivity to *Pdk1* deletion cytostatic effect confirming that efficient *Pten* KO is responsible for the observed phenotype (Figure 34a-c). This resistance phenotype was also confirmed in vivo in a PDAC GEM model. Mice with $Kras^{G12D/+};Pdk1^{lox/lox};Pten^{lox/+}$, and $Kras^{G12D/+};Pdk1^{lox/lox};Pten^{lox/lox}$ genotypes were generated and their survival was compared to $Kras^{G12D/+};Pdk1^{lox/lox}$ mice (Figure 35a). *Pdk1* ablation resulted in an average survival of 736 days in these mice. This average survival was reduced to 234 days and 35 days in mice with heterozygous or homozygous *Pten* deletion respectively (Figure 35b).

In order to understand how Pten loss results in resistance to Pdk1 anti-tumor effects, we performed phospho explorer antibody microarray analysis that allows the simultaneous analysis of multiple signaling pathways using a preprinted array with 1318 antibodies (Figure 36a). The fold change in phosphorylation signal was plotted between cells expressing *Pten* sg1 or NTC after 4-OHT treatment (Figure 36a). Among the most interesting observations was an increase in AKT phosphorylation specifically at the S473 site. We validated this result using western blotting (Figure 36b). Western blot analysis confirmed efficient PTEN knockout and PDK1 loss as expected. In addition, AKT phosphorylation at the T308 site was effectively blocked by *Pdk1* deletion. Interestingly, AKT phosphorylation at the T308 and S473 residues was upregulated upon PTEN loss. However, upon *Pdk1* deletion T308 phosphorylation was blocked again but not of the S473. AKT phosphorylation was increased and sustained upon PTEN deletion even after *Pdk1* deletion. We hypothesized that this sustained AKT phosphorylation might be resulting in partially active AKT that compensates for *Pdk1* deletion and contributes to the resistance phenotype. Western blot analysis supported this hypothesis by showing that Akt-dependent signaling is sustained in cells with PTEN loss following 4-OHT treatment, including the phosphorylation of FoxO1, GSK3β, p38, and EPHA2. This was the result of AKT activation independent of PDK1 as the phosphorylation of direct PDK1 substrate S6 and eIF4B. In order to further confirm the S437 hyperphosphorylated AKT is active and can

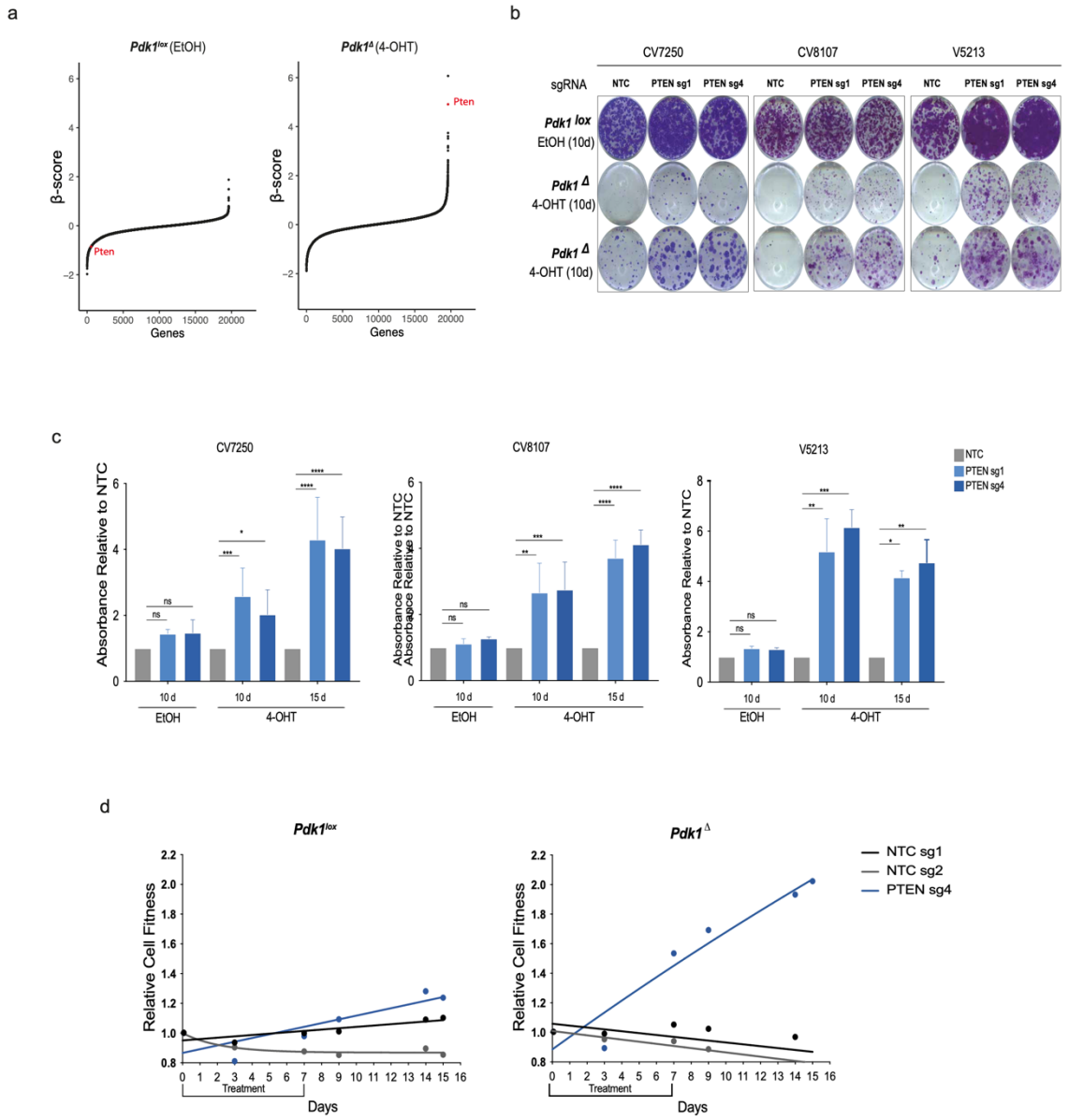

Figure 33: Loss of Pten confers resistance to the growth arrest phenotype induced by *Pdk1* deletion

a) Ranked gene-level β-scores from the genome-wide CRISPR screen with acute *Pdk1* deletion in the ETOH control group and 4-OHT treated group. *Pten* rank is indicated in red. The screens were performed in the CV7250 cell line as described in Figure 13b. The β-scores for each gene were calculated by FW using the MAGeCKFlute pipeline and the genes were ranked based on increasing β-scores.

b) Single guide experiments to validate the effect of *Pten* loss on the growth of *Pdk1* deficient cells. Cell lines (CV7250, CV8107 and V5213) transduced with non-targeting control (NTC) sgRNA or sgRNAs targeting *Pten* were treated with 600nM 4-OHT or EtOH for 7 days, and their growth was assessed by clonogenic assays

c) Quantification of the growth in the clonogenic assays and plotted relative to cells transduced with non-targeting control (NTC) sgRNA. Data are shown as mean ± SD; n = 3 independent experiments from two independent infections ns $p > 0.05$, * $p \leq 0.05$, ** $p \leq 0.01$, *** $p \leq 0.001$, **** $p \leq 0.0001$, Anova multiple comparisons test. Lukas Neudegger performed part of the replicates and this data will be part of his thesis.

d) Multicolor competition assay in PDAC cells showing the increase in cell proliferation upon expression of gRNA targeting *Pten* specifically in the context of *Pdk1* deletion. Cas9 expressing CV7250 cells were transduced with lentiviral vectors expressing sgRNAs targeting *Pten* or control sgRNAs together with RFP or GFP. The GFP and RFP expressing cells were sorted and mixed equal ratios. The mixed cell population was treated with with ETOH or 600nM 4-OHT for seven days and and the relative fraction of each color was assessed by flow cytometry at various time points. For each sgRNA, the percentage of Green/RFP-positive cells was normalized to respective values at Day zero post mixing. The experiment was done in one replicate.

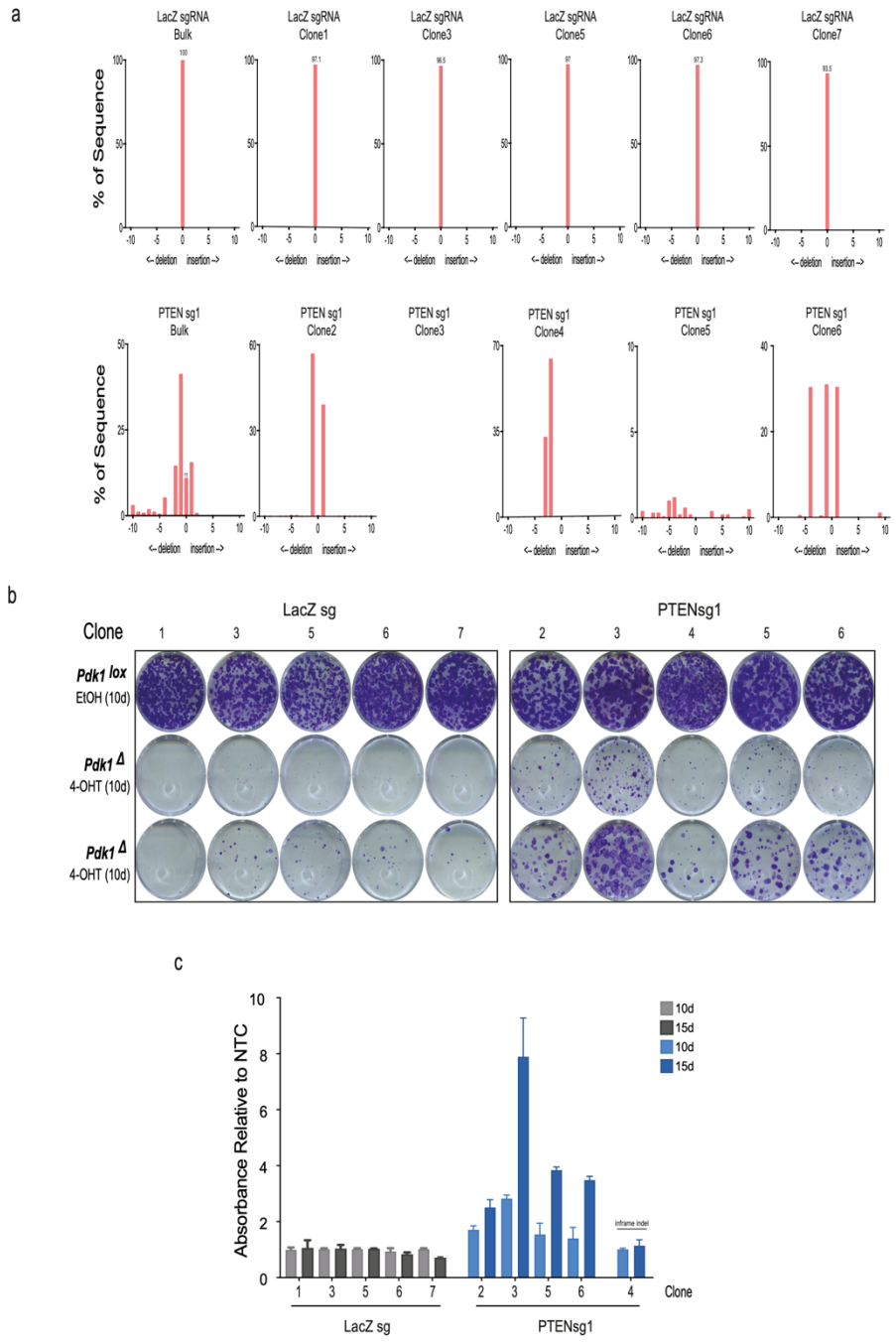

Figure 34: Validation of the Pten KO resistance phenotype in clones.
a) The percentage of Indels in the *Pten* genomic locus of the clones. Single clones were isolated from CV7250 cells transduced with control (LacZ) sgRNAs or sgRNAs targeting *Pten.* The *Pten* genomic locus surrounding the expected CRISPR cut site was amplified and sequenced. Tide analysis was used to deconvolute the percentage of insertions and deletions at the site. NB. Indels could not be detected in Clone 3 expressing Pten-targeting sgRNA1, most likely due to a large-scale deletion induced by CRISPR and inability to amplify the region flanking the expected cut site.
b) Colony formation assay showing the effect of *Pten* on the growth of *Pdk1* deficient clones. The isolated clones were treated with EtOH or 600nM 4-OHT for 7 days and then seeded for colony formation assay.
c) Quantification of the growth of the 4-OHT treated clones in the clonogenic assays and plotted relative to average growth of the clones with non-targeting control (LacZ) sgRNA. Data are shown as mean ± SD; n = 3 replicates. The mean average growth of the Pten KO clones compared that that of the LacZ clones at 15 days is significant with pValue<0.0001 (****, Anova multiple Comparisons)

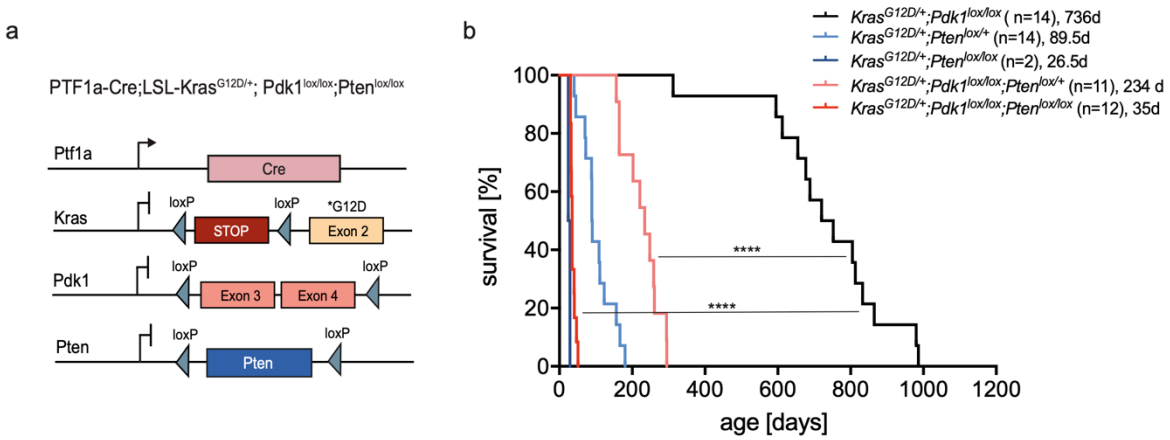

Figure 35: Loss of *Pten* reverses the tumor inititation inhibitory phenotype induced by *Pdk1* deletion *in vivo*
a) Schematic representation of the GEM model that allows deletion of *Pdk1* and *Pten* in *Kras*-induced PDAC model
b) Kaplan-Meier curve comparing survival of mice with *Kras*$^{G12D/+}$;*Pdk1*$^{lox/lox}$, *Kras*$^{G12D/+}$;*Pten*$^{lox/+}$, *Kras*$^{G12D/+}$;*Pten*$^{lox/lox}$, *Kras*$^{G12D/+}$;*Pdk1*$^{lox/lox}$;*Pten*$^{lox/+}$, and *Kras*$^{G12D/+}$;*Pdk1*$^{lox/lox}$;*Pten*$^{lox/lox}$. The number of mice per condition and the average survival time are indicated. **** $p < 0.0001$, log-rank test. Hongkai Yan and Chritian Veltkamp performed part of the breeding and analysis (19 animals were bred and analyzed by KS, 7 animals were bred and analyzed by CV, 7 animals were bred and analyzed by HY and 13 animals were bred and analyzed by former lab members).

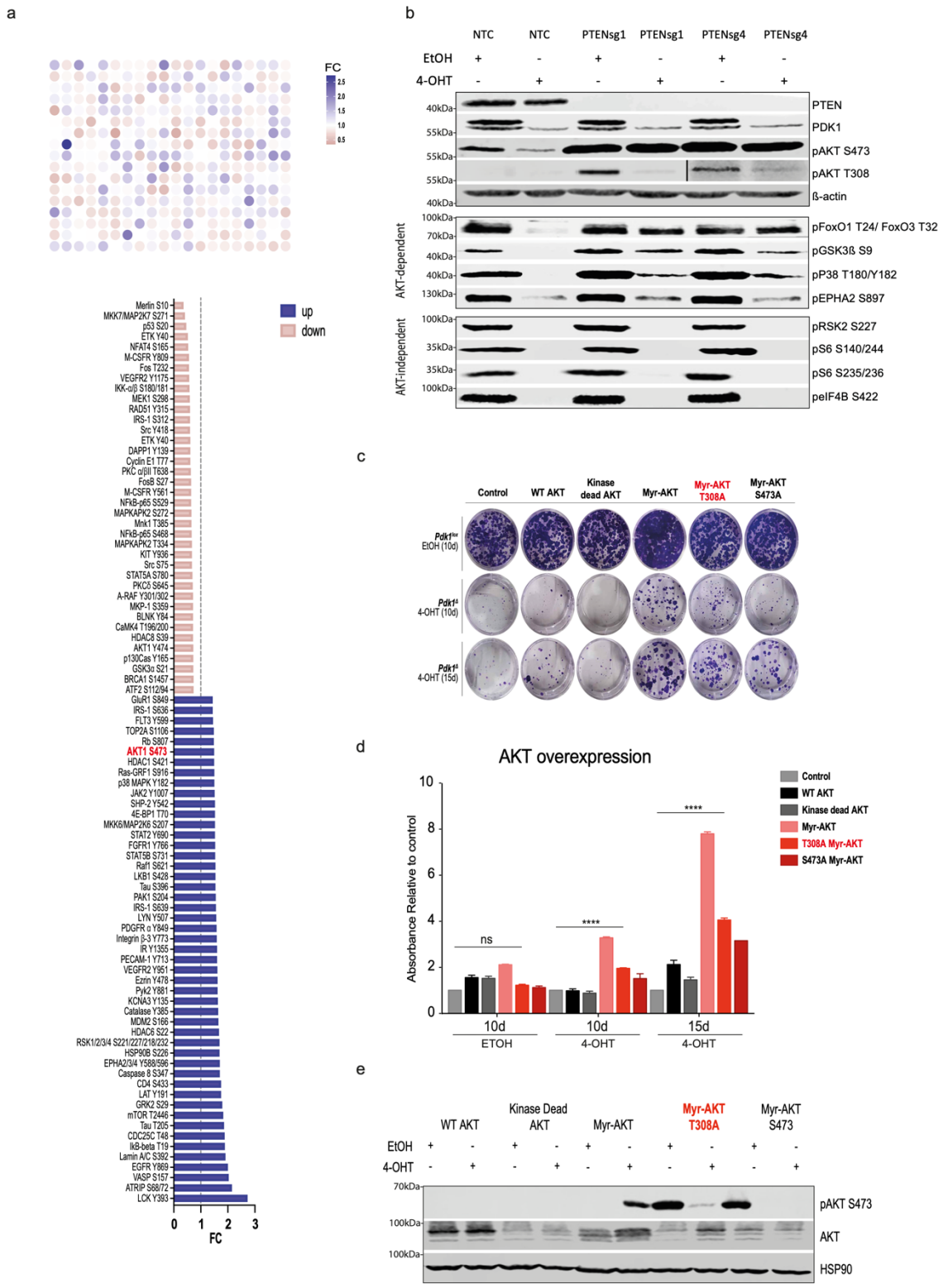

Figure 36: Signaling analysis identifies the resistance mechanism conferred by *Pten* loss

a) Phospho explorer array results of the fold change in phosphorylation levels of proteins in a set of signaling pathways compared between cells expressing *Pten* sg1 or NTC and treated with 4-OHT. CV7250 cells transduced with control sgRNAs or sgRNAs targeting *Pten were* treated with 4-OHT for 7 days. Protein samples were collected and analyzed using the Phospho explorer array. The average

signal for each phospho antibody is then normalized to the average signal of the corresponding non-phospho antibody. Then the ratio of the resistant clone is divided by that of the sensitive clone to calculate the Fold change (FC) for phospho site as shown in appendix Table 5. FC cutoff of 1.4 was used. The array was done once, each antibody had 3 replicate spots.
b) Western blot analysis confirms increased and sustained phosphorylation of AKT S473 residue in *Pten* deficient cells, despite Pdk1 deletion and activation of Akt-dependent targets in the PI3K pathway. CV7250 cells transduced with control sgRNAs or sgRNAs targeting *Pten* were treated with EtOH or 600nM 4-OHT for 7 days and then the protein lysates were collected and analyzed by western blots. Tim Klaubert performed part of the experiment (KS planned the experiment, did the cell culture transduction, treatment, and protein sample collection, and trained TK. TK performed the Western Blots). NB: the pAKT T308 blot was not generated for the CV7250 cells transduced with *Pten* sg4 due to technical problems with the antibody.
c) Validation that overexpression of AKT with sustained S473 phosphorylation (Myr-AKT T308A) can confer resistance to the growth arrest induced by Pdk1 deletion. CV7250 cells were transduced with cDNA expressing the various AKT mutants as indicated. The cells were then treated with EtOH or 600nM 4-OHT for 7 days and seeded for colony formation assay.
d) Quantification of the clonogenic assays. Growth is shown relative to the control. Data are shown as mean ± SD; n = 2 independent infections, each with 3 replicates. ns $p > 0.05$, ****$p \leq 0.0001$, Anova multiple comparisons test
e) Western blot analysis confirming the overexpression of the AKT mutant (Myr-AKT T308A) in CV7250 cell lines

independent of AKT was effectively blocked in the 4-0HT treated PTEN KO cells such as RSK2, rescue the *Pdk1* deletion phenotype, we generated AKT mutants. For that end we used a constitutively active myristoylated AKT (Myr-AKT) construct and mutagenized the T308 residue into T308A, and hence generating an AKT that has blocked T308 phosphorylation and constitutive S473 phosphorylation resembling the status of AKT as detected in PTEN KO cells. Myr-AKT was able to partially rescue the growth arrest phenotype observed after Pdk1 deletion, confirming that this phenotype is at least partially mediated via inhibition of the PI3K/AKT pathway. Interestingly the T308A-Myr AKT mutant was also able to rescue this phenotype confirming that sustained AKT activation by S473 hyperphosphorylation is responsible for the PTEN loss resistance phenotype (Figure 36c-e).
A parallel approach we utilized to understand the resistance mechanism to Pdk1 deletion by PTEN deletion was using genome-wide CRISPR screens. Towards that end, we used clones expressing control or *Pten* targeting sgRNAs (Figure 34) and conducted the screens in an acute Pdk1 deletion setting as described earlier (Figure 37a). The screens confirmed a selective dependency on *Akt* in PTEN knockout cells treated with 4-OHT (Figure 37b). In order to further understand how AKT phosphorylation is mediated in the absence of *Pdk1* and *Pten*, we looked at the putative kinases reported to be involved in AKT phosphorylation and compared their essentiality in 4-OHT treated cells expressing control or *Pten* targeting sgRNAs. Components of the mTORC2 mainly *Mapkap1* that encodes mSIN1 was selectively more essential in cells with PTEN KO, same results were observed with the genes encoding phosphatidylinositol 3-kinase-related kinases (PIKKs), *Atmin* and *Atrip,* that are known to be involved in DNA damage. Consistently, looking at genes involved the DNA damage response (DDR), these tend to show

a more negative β-score in 4-OHT treated cells expressing *Pten* targeting sgRNA (Figure 37c). Drug screening also confirmed the regained sensitivity of 4-OHT treated PTEN KO cells to AKT cells as compared to control 4-OHT treated cells (Figure 37d). In addition, these CRISPR screens identified loss of sensitivity of 4-OHT treated PTEN knockout cells to MAPK inhibition by knockout of various genes in the pathway that was observed in the control 4-OHT treated cells and described above (Figure 38a). This lack of sensitivity to MAPK inhibitors was observed as while pharmacologically in the drug screens (Figure 38b).

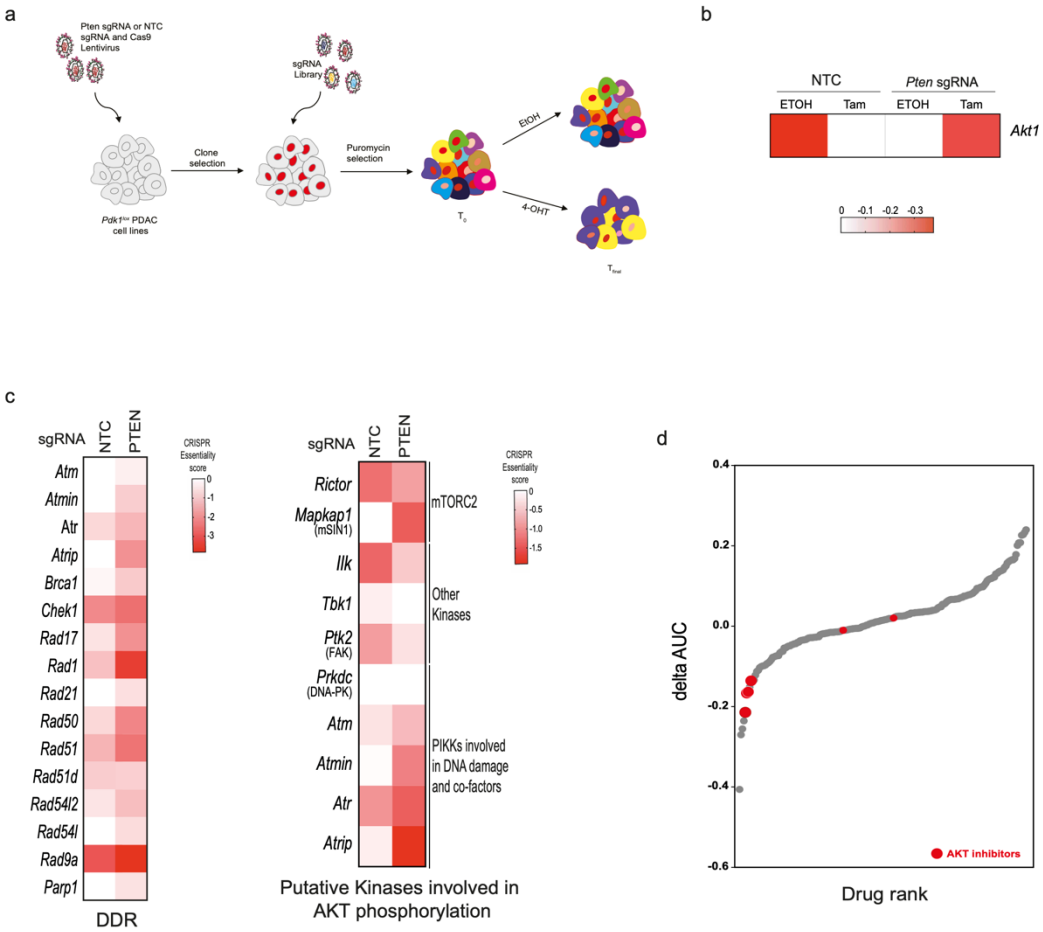

Figure 37: Genome-wide CRISPR screens and drug screens identify vulnerability to AKT1 inhibition in 4-OHT treated cells with Pten knockout

a) Schematic of the CRISPR screens in the context of acute *Pdk1* deletion in CV7250 cells expressing control or *Pten* targeting sgRNA. CV7250 LacZ clone 5 and *Pten* sg1 clone 5 described in Figure 34 were used for the screens. The Screen was performed as described in Figure 14b using CV7250 LacZ clone 5 and *Pten* sg1 clone 5.

b) Heat map showing the essentiality of AKT1 in ETOH and 4-OHT treated cells expressing control or *Pten* targeting sgRNA based on the CRISPR screen results. The β-scores for each gene were calculated by FW using the MAGeCKFlute pipeline.

c) Heat map showing the essentiality of DDR genes and putative kinases involved in AKT phosphorylation in 4-0HT treated cells expressing control or *Pten* targeting sgRNA based on the CRISPR screen results
d) Rank order plot depicting the differential response of Pdk1 deficient cells (4-OHT treated) with Pten loss (*Pten* sgRNA) as compared to control cells with intact *Pten* (NTC sgRNA) to the screened compounds (in an acute Pdk1 deletion setting) as evaluated by differences in the calculated area under the curve (AUC). The dots represent individual drugs. AKT inhibitors are highlighted in red. CV7250 cells transduced with control or *Pten*-targeting sgRNA were treated with 600nM 4-OHT (for 7 days and then seeded at a density of 500 and 1000 cells per well respectively in a 96-well plate. After overnight incubation, the cells were treated with 7 concentrations of each of the 200 compounds (3-fold dilutions series) and a solvent control, using a pin tool. 72hrs post-incubation, viability was measured using CellTiter-Glo® Luminescent Assay. The experiment was done with 2 technical replicates. The mean AUC was calculated for the two replicates and the delta AUC was calculated for each compound as follows: $AUC_{(sgPten)} - AUC_{(NTC)}$.

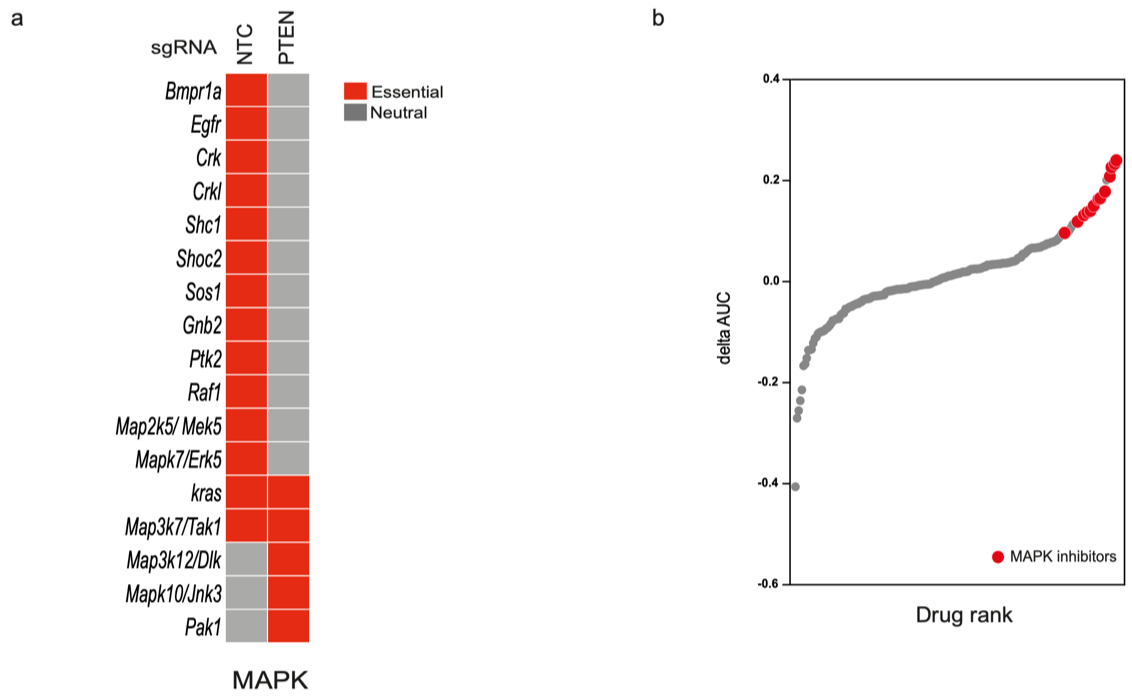

Figure 38: Genome-wide CRISPR screens and drug screens identify resistance to MAPK inhibition in 4-OHT treated cells with Pten knockout
a) Fingerprint plot of MAPK genes in 4-OHT treated cells expressing control or *Pten* targeting sgRNA based on the CRISPR screen results. The boxes are labeled according to whether the gene is essential (red) or neutral (grey). The genes are identified as essential if the corresponding β-score is significantly negative(pValue < 0.05). Same experimental setup as in Figure 37.
b) Rank order plot depicting the differential response of Pdk1 deficient cells (4-OHT treated) with Pten loss (*Pten* sgRNA) as compared to control cells with intact *Pten* (NTC sgRNA) to the screened compounds (in an acute Pdk1 deletion setting) as evaluated by differences in the calculated area under the curve (AUC). The dots represent individual drugs. Inhibitors of various components of the MAPK pathway are highlighted in red. CV7250 cells transduced with control or *Pten*-targeting sgRNA (*Pten* sg1) were treated with 600nM 4-OHT for 7 days and then seeded at a density of 500 cells for

the EtOH treated cells and 1000 cells for the 4-OHT treated cells per well respectively in a 96-well plate. After overnight incubation, the cells were treated with 7 concentrations of each of the 200 compounds (3-fold dilutions series) and a solvent control, using a pin tool. 72hrs post-incubation, viability was measured using CellTiter-Glo® Luminescent Assay. The experiment was done with 2 technical replicates. The mean AUC was calculated for the two replicates and the delta AUC was calculated for each compound as follows: $AUC_{(sg\mathit{Pten})} – AUC_{(NTC)}$.

6. Discussion and Outlook

PDAC remains one of the most devastating diseases to date with a mortality rate higher than 90%. Despite PDAC genetics being relatively well characterized, effective therapies remain missing. A lot of efforts based on targeting KRAS oncogenic signaling in PDAC failed due to primary or secondary resistance. A lot of these resistance mechanisms arise from complex signaling rewiring that renders these targeted therapies ineffective in the long term. As a way to circumvent this resistance, a variety of combination therapies were tested in preclinical models and clinical trials. A major obstacle to the advancement of a number of these combination therapies can be summarized as the increased toxicities associated with the broad inhibition of KRAS effectors. Hence a systematic investigation of possible combination therapies for *KRAS*-driven PDAC and ideal nodes to target efficiently and with minimal toxicity remain to be elucidated.

6.1 The role of PI3K signaling in *Kras*-driven PDAC maintenance

The use of genetically engineered mouse models has allowed the elucidation of a clear role of PI3K signaling in *Kras*-driven PDAC initiation. Major evidence came from two studies, that showed that the genetic inactivation of *Pik3ca,* encoding p110α, and *Pdk1* blocks the development of *Kras*-driven tumors in the pancreas [79, 202]. The development of the dual recombinase mouse model allowed us to investigate the role of *Pdk1* in PDAC maintenance and to explore its potential as a therapeutic target for PDAC [349]. The dual recombinase mouse model allows secondary targeting of *Pdk1* in established tumors, hence mimicking therapeutic intervention. Characterization of this model showed that *Pdk1* deletion resulted in reduced growth of established tumors in endogenous and orthotopic Kras^{G12D}-driven PDAC models. To further characterize *Pdk1* deletion-induced cytostatic effect, we generated cell lines with conditional floxed *Pdk1* and used these for further characterization. In this work, I show that deletion of *Pdk1* results in strong growth inhibition in murine PDAC cells. This growth arrest is mediated by the inhibition of the PI3K signaling cascade and subsequent cell cycle arrest. Isolation of clones post *Pdk1* deletion showed that these clones are able to survive independent of *Pdk1* deletion, despite effective inhibition of PI3K signaling and slowed proliferation. We wanted to further elucidate the mechanisms that allow survival of these *Pdk1*$^{\Delta}$ persistent clones in order to identify therapies that would target these persistent clones that may lead to relapse in a clinical setting.

6.2 Genome-wide genetic and drug screens identify therapeutic vulnerabilities in *Pdk1*-independent clones

Despite the impressive cytostatic effect of Pdk1 deletion on PDAC cells, it fails to eradicate them completely. Analysis of the *Pdk1*$^{\Delta}$ persistent clones shows that they acquire increased

proliferation compared to cells with acute *Pdk1* deletion. This might compromise patient survival in a clinical setting, as these persistent clones might lead to relapse with time. In order to be able to provide better translational solutions for PDAC patients, we rationalized that identifying the mechanisms that maintain the survival of these *Pdk1*$^{\Delta}$ persistent clones, can lead to the prioritization of therapeutic targets that can be targeted along with PDK1, or the PI3K pathway, for complete eradication of PDAC.

Following the advancement of CRISPR/Cas technology and its optimization for genome-wide screening, enormous efforts were aimed at exploiting these functional genomics approaches to identify cancer-specific therapeutic targets. These efforts led by the Broad Institute of MIT and Harvard and the Wellcome Sanger Institute under the Cancer Dependency Map project (DepMap Consortium) and Project Score, aimed at identifying specific cancer vulnerabilities across hundreds of cancer cell lines from multiple cancer entities [343-345]. In addition, these functional screens have been utilized to drive the identification of modifiers of drug response to identify targetable resistance genes and/or synthetic lethalities and candidate drug targets for combinatorial therapies. Similarly, we utilized genome-wide CRISPR screens in order to identify vulnerabilities in *Pdk1*-independent clones. Towards that end, we did the screens both in the context of acute and chronic *Pdk1* deletion. This led to the identification of various pathways and biological processes that collaborate with PI3K signaling to maintain PDAC survival.

Among the identified pathways that alter the *Pdk1* deletion phenotype is the MAPK pathway. MAPK signaling is known to act in parallel to PI3K signaling and various efforts at co-targeting the two pathways have been evaluated in various *Kras*-driven tumors including PDAC [382-384]. Despite their proven anti-tumor efficacy in preclinical models, these combinations showed limited efficacy in clinical trials with toxicity being the main limitation [385-387]. However, most of these studies focused on using MEK inhibitors. and it has been already known that *Mek1* and *Mek2* exhibit redundant functions [378] and their combinatorial ablation in adult mice lead to significant toxicities [74]. This suggests that systematic identification of critical nodes to target within the MAPK pathway that are associated with minimal toxicity is still missing.

Our systematic genetic screening identified *Raf1* among the strongest nodes to drive PDAC cell death in combination with *Pdk1* ablation. *Raf1* knockout showed no effect in *Pdk1*- intact clones consistent with our previous findings where *Raf1* ablation was shown to be dispensable for *Kras*-driven PDAC initiation. However, *Raf1* showed increased essentiality in the context of *Pdk1* deletion, resulting in apoptotic cell death *in vitro*. This anti-tumor effect was validated in orthotopic PDAC models showing impressive response. Systematic elimination of *Raf1* alone or in combination with Braf was shown to be safe in adult mice validating its relevancy as a safe therapeutic target for cancer therapy [74].

In order to translate these findings into the clinic, drug screening with drugs targeting the identified vulnerability genes in *Pdk1*-independent cells was performed. Previous efforts at integrating pharmacological and CRISPR screens showed that around half of the drugs did not have a significant association with their corresponding target gene fitness [388]. One main

explanation can be the lack of on-target effect of the tested compounds. A study by Lin *et al,* 2019 using a genetic target-deconvolution strategy showed that off-target toxicity rather than on-target function is a common mechanism of action of cancer drugs in various stages of clinical testing due to mischaracterization and lack of stringent genetic on-target validation [389]. Numerous compounds have been developed to target the MAPK pathway and failed as monotherapies in *Kras*-driven tumors and combination strategies that co-target the MAPK pathway in combination with the PI3K pathway could be ideal for repurposing these drugs. Despite *Raf1* ablation showing strong genetic essentiality in the context of *Pdk1* deletion, cRAF inhibitors did not show any differential sensitivity between *Pdk1* proficient and deficient clones. Thus the development of highly specific and selective cRAF inhibitors remains urgent. A promising approach to target cRAF is by using PROTACs (Proteolysis Targeting Chimeras) or other molecular degraders [61]. Mutant-selective BRAF PROTACs have been developed and shown superior anti-tumor effect compared to pharmacological BRAF inhibitors, in addition to overcoming acquired resistance [390]. Developing similar PROTACs targeting cRAF holds great promise especially since protein degradation is more likely to recapitulate the therapeutic results observed by CRISPR knockout and genetic ablation in GEM models, compared to pharmacological inhibitors. Pharmacologically, the most promising target in the MAPK pathway was ERK2. *Erk1* and *Erk2* have been suggested to play nonredundant biological functions, although this remains to be better characterized. Interestingly, our genetic screens identified selective essentiality for *Erk2* but not *Erk1* in the context of *Pdk1* deletion. The drug screens also showed increased efficacy of ERK2 inhibitors in *Pdk1*-independent cells, compared to their isogenic *Pdk1* proficient cells. Systematic ablation of *Erk2* showed no significant toxicity [74] and hence can be a suitable target for combination therapies. Further *in vivo* testing of ERK2 inhibitors combined with PI3K inhibition to elucidate the safety of this combination therapy is still required. Interestingly, a new study by Garnett lab using systematic combinatorial drug screening in PDAC and other cancer entities identified the strongest synergies among PI3K and MAPK components in PDAC, more specifically, combinations of the AKT inhibitor MK-2206 with SCH772984, an ERK1/2 inhibitor, and Trametinib, a MEK inhibitor [391]. This is consistent with our findings that co-targeting the PI3K and MAPK pathway results in strong PDAC inhibition.

In addition to the MAPK pathway, other pathways were identified that cooperate with PI3K signaling to maintain PDAC survival, and that can be interesting targets for combination therapies. Among these, we mention the inhibition of mTOR signaling pathway, in addition to VDAC and Integrin receptor inhibitors. Further investigation of these combinations is still ongoing.

6.3 Genome-wide genetic and drug screens identify resistance mechanism to *Pdk1* loss induced growth arrest mediated by *Pten* loss

In addition to investigating possible vulnerabilities in the *Pdk1*-independent clones, our systematic screening approach has allowed the identification of various genes and pathways

that result in resistance to this phenotype. In this work, I generated a comprehensive map of pathways and processes that modify the effect of PI3K pathway inhibition, via *Pdk1* deletion in PDAC. Among these, we identify negative regulators of PI3K-AKT signaling, mTOR signaling, MAPK signaling, and Hippo-Yap Signaling in accordance with the role of these pathways in promoting *Pdk1*-independent survival. For instance, we identify *Foxo1* gene whose knockout results in an enrichment of its targeting sgRNA most likely due to increased proliferation in the context of *Pdk1* deletion. FoxO1 is a known target of the PI3K-AKT pathway that was shown to mediate cell cycle arrest at the G1 phase by various mechanisms that include inhibition of cyclin D/CDK4 [392, 393]. Consistently, negative cell cycle regulators have been identified among the resistance genes. In addition, we identify genes involved in autophagy such as *Atg5, Atg12, Atg2a*, and *Atg4b*. Inhibition of the PI3K pathway has been reported to induce autophagy in various contexts such as peritoneal fibrosis and in malignant blood cells [394, 395]. Indeed, we found that *Pdk1* deletion results in induction of autophagy as detected by LC3 cleavage (data not shown). Hence, autophagy at least partially mediates the effect of PI3K inhibition in PDAC at least partially and blocking autophagy execution, renders PDAC cells resistant to PI3K inhibition. In addition, we identify components of the SAGA complex and Mediator complex. The mediator of RNA polymerase II transcription (Mediator), a large complex with modular organization, that is required for eukaryotic transcription by RNA polymerase II [396]. The SAGA complex is a multi-modular protein complex that consists of a core structural module in addition to a histone acetylation (HAT) module, deubiquitination (DUB) module, a TF-binding (TAF) module, and splicing (SPT) module [397, 398]. SAGA complex has been suggested to play a role in the regulation of cell growth and proliferation [397]. Whether the SAGA complex plays a specific role downstream of PI3K or a general growth function is yet to be determined. Interestingly, CRISPR screens aimed at identifying mTORC1 regulatory networks in Treg cells identified components of the SAGA complex and implicated them in the suppression of mTORC1 activation via limiting the expression of nutrient transporters. The effect of the SAGA complex on mTOR signaling in PDAC warrants further investigation. In light of this, I mention that RNA Seq analysis of the knockout of various components that we detected in our CRISPR screens, showed a modest enrichment of the PI3K-AKT-mTOR and the glycolysis hallmarks in GSEA (data not shown).

6.4 Pten loss confers resistance to *Pdk1* deletion induced growth arrest

One of the most highly enriched resistance genes in the context of *Pdk1* deletion was *Pten*. The identification of Pten as a resistance gene seemed paradoxical at first sight. PTEN acts a negative regulator of PI3K signaling, by counteracting PI3K function and converting PIP_3 back to PIP_2. PDK1 acts further downstream in the PI3K pathway to activate AKT and hence the initial reasoning that PTEN loss would not be expected to confer resistance as the pathway is blocked at a lower node. Extensive validation confirmed the resistance phenotype conferred by *Pten* loss where cells with *Pten* knockout showed increased proliferation as compared to isogenic cells expressing functional *Pten*. This phenotype was validated *in vivo* as well in a

GEM model of PDAC with pancreas-specific ablation of *Pdk1* and *Pten*. Mice with *Pdk1* deletion showed a long survival rate that was massively shortened by the homozygous and heterozygous loss of *Pten*. Unbiased genome-wide screens allowed me to identify the exact mechanism of resistance in *Pten* knockout cells as compared to control cells in the context of *Pdk1* deletion. CRISPR data showed a clear dependence of *Pten* knockout cells on AKT signaling despite *Pdk1* deletion, suggesting that *Pten* loss results in reactivation of the PI3K signaling pathway. Indeed, using proteomics analysis and western blots, I show that AKT is hyperphosphorylated at S473 and that the overexpression Myr-AKT T308A cDNA is able to rescue the growth arrest phenotype conferred by *Pdk1* deletion. In addition, we show that this is due to the reactivation of AKT as it mediates the phosphorylation of its substrates, such as GSK and FoxO1, in *Pten* knockout cells, regardless of Pdk1 status. On the other hand, we show that AKT-independent functions of PDK1 remain blocked. It is a popular belief that AKT activation requires two phosphorylation events at the T308 and S473 residues [106, 399, 400] and that T308 was shown to be the most critical residue for transformation by AKT, whereas the S473 was shown to be dispensable for AKT transformation [401]. However, my data show that hyperphosphorylation of the S473 residue can lead, at least partially, to AKT re-activation. I also tried to better understand, the possible mechanism that lead to this increased phosphorylation of AKT on the S473 site. Our CRISPR data showed increased essentiality of some of the putative kinases involved in AKT phosphorylation. mTORC2 is known to be the kinase that phosphorylates AKT ta the S743 residue [106]. Although Rictor was essential in both cells with control and Pten targeting sgRNAs specifically in the context of Pdk1 deletion, Mapkap1, encoding the mSIN1 subunit of mTORC2, was shown to be specifically essential in Pten knockout cells, but not the control cells. mSIN1 was shown to exhibit a domain that allows mTORC2 to interact with AKT and phosphorylate it [402]. In addition, Phosphatidylinositol 3-kinase-related kinases (PIKKs) have been proposed to promote AKT phosphorylation and activation. ATM, ATR and DNA-PK have been shown to promote full AKT by S473 phosphorylation in response to DNA-damage inducing agents and in various physiological [403-405]. Interestingly, *Atr* and *Atm* and their interacting partners *Atrip* and *Atmin*, in addition of other genes involved in the DDR were shown to have increased essentiality in Pten KO cells. Here we propose a plausible model (Figure 39) where Pten loss induces DNA damage response and activation of PIKKs that result in activation of AKT. In addition, increased PIP3 can lead to increased mTORC2 activation and increased AKT phosphorylation regardless of Pdk1 status. Our data also provide evidence for the induction of a DNA damage response. RNA Seq data comparing PTEN KO cells to control cells with Pdk1 deletion, show enrichment of DNA repair hallmark in GSEA analysis (data not shown). In addition, our phospho data showed a notable increase in ATRIP S68/72 phosphorylation. This ATRIP phosphorylation has been linked to ATR activation [406]. PTEN loss has been linked to increased G2M cell cycle progression and increased DNA damage [407]. Our cell cycle analysis supports an increased number of cells in the G2/M phase in PTEN KO cells independent of Pdk1 status (data not shown). Drug screening confirmed an increased vulnerability of PTEN KO cells on AKT signaling in the context of Pdk1 deletion. Whether targeting the DNA damage

kinases provides a therapeutic option in combination with PI3K inhibition in PTEN deficient cells remains to be tested.

Another interesting finding of our screens is that PTEN KO cells become insensitive to MAPK inhibitors in the context of *Pdk1* deletion as opposed to what we showed earlier with their isogenic cells. This confirms our earlier statement that PI3K/AKT is the dominant effector cascade in PDAC downstream of KRAS and MAPK is a collateral dependency that is essential only in the context of PI3K/AKT inhibition.

These findings have important implications for patient therapy. Although deletion or loss-of-function mutations targeting *PTEN* have not been detected with high frequencies in human PDAC (cBioportal), loss of PTEN expression has been reported to occur in 25% of PDAC patients and to be associated with poor prognosis [408]. In addition, GEM models showed that loss of PTEN function is involved in the progression of pancreatic cancer [122]. This underscores the importance of patient stratification and how a change in their mutational landscape can alter their response to various therapies even within the same pathway. These findings can also be extended beyond PDAC. For instance, in breast cancer patients, loss of PTEN was shown to cause resistance to PI3Kα inhibitors [409]. Our model can also provide a possible explanation for such resistances and drive informed patient therapy

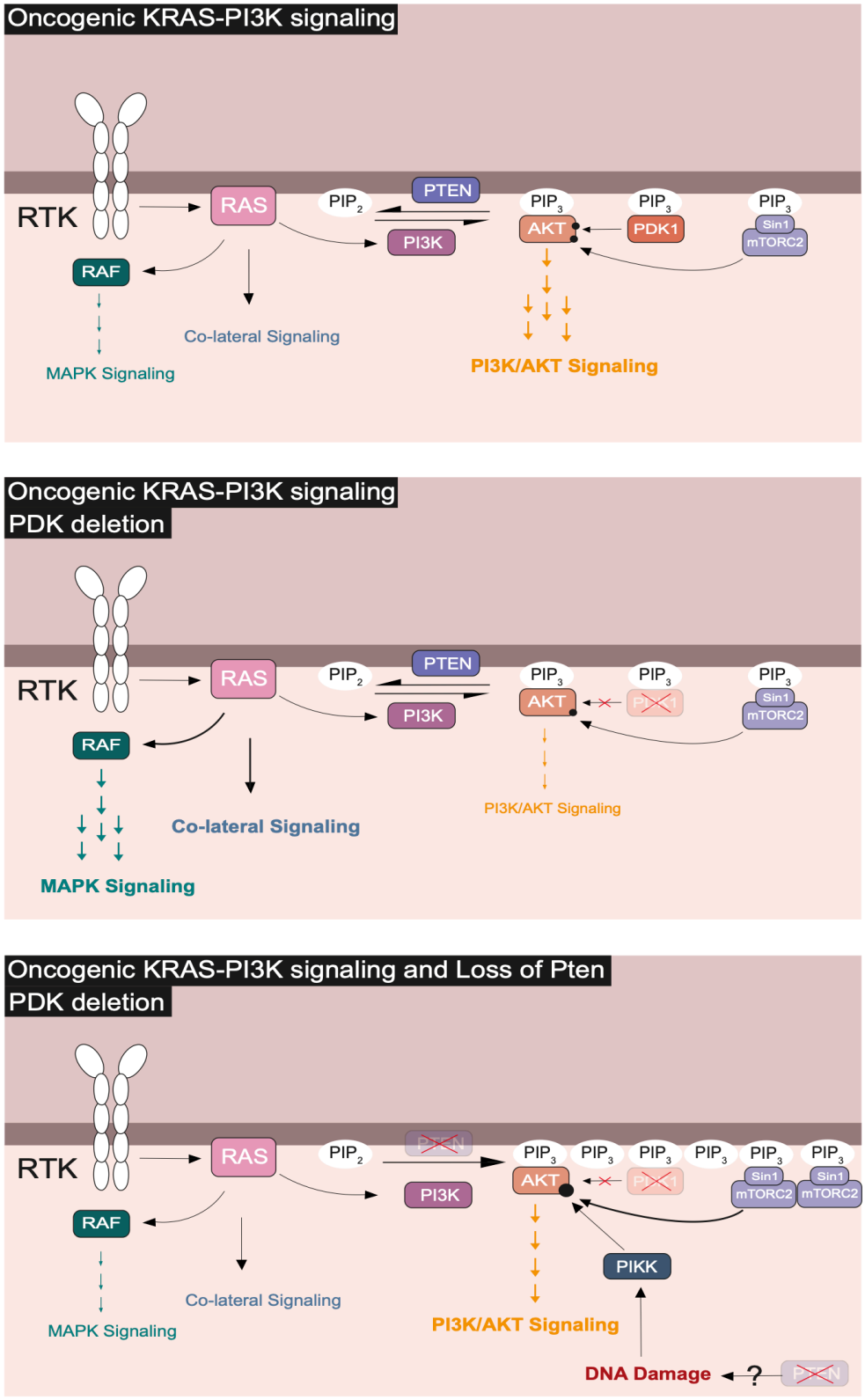

Figure 39: Graphical summary of Signaling downstream of KRAS in PDAC and the variation in vulnerabilities based on the driver oncogene status and the mutational landscape

7. Conclusion

PI3K signaling constitutes the main effector oncogenic signaling cascade in *Kras*-driven PDAC, while MAPK signaling, along other pathways, constitute collateral dependencies with a minor effect on PDAC. Upon, inhibition of the main driver oncogenic signaling pathway, the PI3K pathway, in PDAC, the essentiality of these collateral pathways gets potentiated and hence they constitute therapeutic vulnerabilities in the cells with an oncogenic driver-limited state. Interestingly, targeting different nodes in the PI3K pathway can have differential therapeutic outcomes based on the mutational context. For instance, the loss of *Pten* renders PDAC resistant to *Pdk1* deletion, due to alternative mechanisms that lead to AKT reactivation (summarized in Figure 39). This shows the complexity of the signaling network that can be rewired in unexpected ways and pinpoints the power of unbiased large-scale genetic screens to decipher this signaling complexity.

Acknowledgements

First, I would like to thank Dr Saur for the opportunity to work in his research group and my mentors, Dr Rad and Dr Kaulich for their feedback throughout my PhD studies. I also want to acknowledge the various contribution of the current and previous lab members to this work. Namely, I thank Fengchong Wang for help with the Bioinformatics analysis. I also thank Mingsong Wang for his help with the implantation experiments. In addition, I thank Kevin Fink, Katharina Ondrejkova, Lukas Neudegger, Tim Klaubert, Christian Biedinger, and Michael Otabil that contributed to this work as part of their medical or master's degree training. I also thank Dr Christian Veltkamp, who contributed to analysing the used mouse models and the generation of the cell lines used in this thesis. Similarly, I thank Hongkai Yan for contributing to the PTEN mouse model analysis. In addition, I thank Rupert Öllinger from the group of Dr Rad, for the sequencing services, in addition to the members of the Cell Analysis Core Facility, especially Dr Ritu Mishra, Markus Utzt and Linda Bachmann. I also thank Hannah Jakubowsky for helping preparing the diluted drug libraray. In addition, I thank all the lab members that might not have been directly involved in this project but yet contributed in various ways to lab maintenance and making this work possible.

My deepest gratitude goes to my family, who supported my education from an early time in my life, and Edward, who provided me with his support and love the whole time.

References

1. Rawla, P., T. Sunkara, and V. Gaduputi, *Epidemiology of Pancreatic Cancer: Global Trends, Etiology and Risk Factors.* World J Oncol, 2019. **10**(1): p. 10-27.
2. Grossberg, A.J., et al., *Multidisciplinary standards of care and recent progress in pancreatic ductal adenocarcinoma.* CA Cancer J Clin, 2020. **70**(5): p. 375-403.
3. Von Hoff, D.D., et al., *Increased survival in pancreatic cancer with nab-paclitaxel plus gemcitabine.* N Engl J Med, 2013. **369**(18): p. 1691-703.
4. Cid-Arregui, A. and V. Juarez, *Perspectives in the treatment of pancreatic adenocarcinoma.* World J Gastroenterol, 2015. **21**(31): p. 9297-316.
5. Maitra, A., et al., *Precursors to invasive pancreatic cancer.* Adv Anat Pathol, 2005. **12**(2): p. 81-91.
6. Hruban, R.H., R.E. Wilentz, and S.E. Kern, *Genetic progression in the pancreatic ducts.* Am J Pathol, 2000. **156**(6): p. 1821-5.
7. Morris, J.P.t., S.C. Wang, and M. Hebrok, *KRAS, Hedgehog, Wnt and the twisted developmental biology of pancreatic ductal adenocarcinoma.* Nat Rev Cancer, 2010. **10**(10): p. 683-95.
8. Kanda, M., et al., *Presence of somatic mutations in most early-stage pancreatic intraepithelial neoplasia.* Gastroenterology, 2012. **142**(4): p. 730-733 e9.
9. Hayashi, A., J. Hong, and C.A. Iacobuzio-Donahue, *The pancreatic cancer genome revisited.* Nat Rev Gastroenterol Hepatol, 2021. **18**(7): p. 469-481.
10. Sakamoto, H., et al., *The Evolutionary Origins of Recurrent Pancreatic Cancer.* Cancer Discov, 2020. **10**(6): p. 792-805.
11. Burgess, M.R., et al., *KRAS Allelic Imbalance Enhances Fitness and Modulates MAP Kinase Dependence in Cancer.* Cell, 2017. **168**(5): p. 817-829 e15.
12. Mueller, S., et al., *Evolutionary routes and KRAS dosage define pancreatic cancer phenotypes.* Nature, 2018. **554**(7690): p. 62-68.
13. Schutte, M., et al., *Abrogation of the Rb/p16 tumor-suppressive pathway in virtually all pancreatic carcinomas.* Cancer Res, 1997. **57**(15): p. 3126-30.
14. Esteller, M., et al., *A gene hypermethylation profile of human cancer.* Cancer Res, 2001. **61**(8): p. 3225-9.
15. Waddell, N., et al., *Whole genomes redefine the mutational landscape of pancreatic cancer.* Nature, 2015. **518**(7540): p. 495-501.
16. Cancer Genome Atlas Research Network. Electronic address, a.a.d.h.e. and N. Cancer Genome Atlas Research, *Integrated Genomic Characterization of Pancreatic Ductal Adenocarcinoma.* Cancer Cell, 2017. **32**(2): p. 185-203 e13.
17. Russo, A.A., et al., *Structural basis for inhibition of the cyclin-dependent kinase Cdk6 by the tumour suppressor p16INK4a.* Nature, 1998. **395**(6699): p. 237-43.
18. Sharpless, N.E., *INK4a/ARF: a multifunctional tumor suppressor locus.* Mutat Res, 2005. **576**(1-2): p. 22-38.
19. Itahana, K., et al., *Tumor suppressor ARF degrades B23, a nucleolar protein involved in ribosome biogenesis and cell proliferation.* Mol Cell, 2003. **12**(5): p. 1151-64.
20. Sugimoto, M., et al., *Nucleolar Arf tumor suppressor inhibits ribosomal RNA processing.* Mol Cell, 2003. **11**(2): p. 415-24.
21. Bardeesy, N., et al., *Both p16(Ink4a) and the p19(Arf)-p53 pathway constrain progression of pancreatic adenocarcinoma in the mouse.* Proc Natl Acad Sci U S A, 2006. **103**(15): p. 5947-52.

22. Kim, W.Y. and N.E. Sharpless, *The regulation of INK4/ARF in cancer and aging.* Cell, 2006. **127**(2): p. 265-75.
23. Makohon-Moore, A.P., et al., *Precancerous neoplastic cells can move through the pancreatic ductal system.* Nature, 2018. **561**(7722): p. 201-205.
24. Hosoda, W., et al., *Genetic analyses of isolated high-grade pancreatic intraepithelial neoplasia (HG-PanIN) reveal paucity of alterations in TP53 and SMAD4.* J Pathol, 2017. **242**(1): p. 16-23.
25. Yachida, S., et al., *Clinical significance of the genetic landscape of pancreatic cancer and implications for identification of potential long-term survivors.* Clin Cancer Res, 2012. **18**(22): p. 6339-47.
26. Lane, D.P., *Cancer. p53, guardian of the genome.* Nature, 1992. **358**(6381): p. 15-6.
27. Vogelstein, B., D. Lane, and A.J. Levine, *Surfing the p53 network.* Nature, 2000. **408**(6810): p. 307-10.
28. Bieging, K.T., S.S. Mello, and L.D. Attardi, *Unravelling mechanisms of p53-mediated tumour suppression.* Nat Rev Cancer, 2014. **14**(5): p. 359-70.
29. Hahn, S.A., et al., *DPC4, a candidate tumor suppressor gene at human chromosome 18q21.1.* Science, 1996. **271**(5247): p. 350-3.
30. Massague, J., *TGFbeta signalling in context.* Nat Rev Mol Cell Biol, 2012. **13**(10): p. 616-30.
31. David, C.J. and J. Massague, *Contextual determinants of TGFbeta action in development, immunity and cancer.* Nat Rev Mol Cell Biol, 2018. **19**(7): p. 419-435.
32. Whittle, M.C., et al., *RUNX3 Controls a Metastatic Switch in Pancreatic Ductal Adenocarcinoma.* Cell, 2015. **161**(6): p. 1345-60.
33. Huang, W., et al., *Pattern of Invasion in Human Pancreatic Cancer Organoids Is Associated with Loss of SMAD4 and Clinical Outcome.* Cancer Res, 2020. **80**(13): p. 2804-2817.
34. Su, G.H., et al., *ACVR1B (ALK4, activin receptor type 1B) gene mutations in pancreatic carcinoma.* Proc Natl Acad Sci U S A, 2001. **98**(6): p. 3254-7.
35. Hempen, P.M., et al., *Evidence of selection for clones having genetic inactivation of the activin A type II receptor (ACVR2) gene in gastrointestinal cancers.* Cancer Res, 2003. **63**(5): p. 994-9.
36. Togashi, Y., et al., *Homozygous deletion of the activin A receptor, type IB gene is associated with an aggressive cancer phenotype in pancreatic cancer.* Mol Cancer, 2014. **13**: p. 126.
37. Jones, S., et al., *Core signaling pathways in human pancreatic cancers revealed by global genomic analyses.* Science, 2008. **321**(5897): p. 1801-6.
38. Biankin, A.V., et al., *Pancreatic cancer genomes reveal aberrations in axon guidance pathway genes.* Nature, 2012. **491**(7424): p. 399-405.
39. Witkiewicz, A.K., et al., *Whole-exome sequencing of pancreatic cancer defines genetic diversity and therapeutic targets.* Nat Commun, 2015. **6**: p. 6744.
40. Shain, A.H., et al., *Convergent structural alterations define SWItch/Sucrose NonFermentable (SWI/SNF) chromatin remodeler as a central tumor suppressive complex in pancreatic cancer.* Proc Natl Acad Sci U S A, 2012. **109**(5): p. E252-9.
41. Wang, L. and A. Shilatifard, *UTX Mutations in Human Cancer.* Cancer Cell, 2019. **35**(2): p. 168-176.

42. Andricovich, J., et al., *Loss of KDM6A Activates Super-Enhancers to Induce Gender-Specific Squamous-like Pancreatic Cancer and Confers Sensitivity to BET Inhibitors.* Cancer Cell, 2018. **33**(3): p. 512-526 e8.
43. Roe, J.S., et al., *Enhancer Reprogramming Promotes Pancreatic Cancer Metastasis.* Cell, 2017. **170**(5): p. 875-888 e20.
44. Somerville, T.D., et al., *Squamous trans-differentiation of pancreatic cancer cells promotes stromal inflammation.* Elife, 2020. **9**.
45. Somerville, T.D.D., et al., *TP63-Mediated Enhancer Reprogramming Drives the Squamous Subtype of Pancreatic Ductal Adenocarcinoma.* Cell Rep, 2018. **25**(7): p. 1741-1755 e7.
46. Lowery, M.A., et al., *Prospective Evaluation of Germline Alterations in Patients With Exocrine Pancreatic Neoplasms.* J Natl Cancer Inst, 2018. **110**(10): p. 1067-1074.
47. Mizukami, K., et al., *Genetic characterization of pancreatic cancer patients and prediction of carrier status of germline pathogenic variants in cancer-predisposing genes.* EBioMedicine, 2020. **60**: p. 103033.
48. Roberts, N.J., et al., *Whole Genome Sequencing Defines the Genetic Heterogeneity of Familial Pancreatic Cancer.* Cancer Discov, 2016. **6**(2): p. 166-75.
49. Shindo, K., et al., *Deleterious Germline Mutations in Patients With Apparently Sporadic Pancreatic Adenocarcinoma.* J Clin Oncol, 2017. **35**(30): p. 3382-3390.
50. Patra, K.C., et al., *Mutant GNAS drives pancreatic tumourigenesis by inducing PKA-mediated SIK suppression and reprogramming lipid metabolism.* Nat Cell Biol, 2018. **20**(7): p. 811-822.
51. Pylayeva-Gupta, Y., E. Grabocka, and D. Bar-Sagi, *RAS oncogenes: weaving a tumorigenic web.* Nat Rev Cancer, 2011. **11**(11): p. 761-74.
52. Gimple, R.C. and X. Wang, *RAS: Striking at the Core of the Oncogenic Circuitry.* Front Oncol, 2019. **9**: p. 965.
53. Plowman, S.J. and J.F. Hancock, *Ras signaling from plasma membrane and endomembrane microdomains.* Biochim Biophys Acta, 2005. **1746**(3): p. 274-83.
54. McKay, M.M. and D.K. Morrison, *Integrating signals from RTKs to ERK/MAPK.* Oncogene, 2007. **26**(22): p. 3113-21.
55. Seguin, L., et al., *An integrin beta(3)-KRAS-RalB complex drives tumour stemness and resistance to EGFR inhibition.* Nat Cell Biol, 2014. **16**(5): p. 457-68.
56. Simanshu, D.K., D.V. Nissley, and F. McCormick, *RAS Proteins and Their Regulators in Human Disease.* Cell, 2017. **170**(1): p. 17-33.
57. Scheffzek, K., et al., *The Ras-RasGAP complex: structural basis for GTPase activation and its loss in oncogenic Ras mutants.* Science, 1997. **277**(5324): p. 333-8.
58. Rajalingam, K., et al., *Ras oncogenes and their downstream targets.* Biochim Biophys Acta, 2007. **1773**(8): p. 1177-95.
59. Eser, S., et al., *Oncogenic KRAS signalling in pancreatic cancer.* Br J Cancer, 2014. **111**(5): p. 817-22.
60. Moodie, S.A., et al., *Complexes of Ras.GTP with Raf-1 and mitogen-activated protein kinase kinase.* Science, 1993. **260**(5114): p. 1658-61.
61. Drosten, M. and M. Barbacid, *Targeting the MAPK Pathway in KRAS-Driven Tumors.* Cancer Cell, 2020. **37**(4): p. 543-550.
62. Crews, C.M. and R.L. Erikson, *Extracellular signals and reversible protein phosphorylation: what to Mek of it all.* Cell, 1993. **74**(2): p. 215-7.

63. Marais, R., et al., *Ras recruits Raf-1 to the plasma membrane for activation by tyrosine phosphorylation.* EMBO J, 1995. **14**(13): p. 3136-45.
64. Marais, R., et al., *Requirement of Ras-GTP-Raf complexes for activation of Raf-1 by protein kinase C.* Science, 1998. **280**(5360): p. 109-12.
65. Unal, E.B., F. Uhlitz, and N. Bluthgen, *A compendium of ERK targets.* FEBS Lett, 2017. **591**(17): p. 2607-2615.
66. Hornbeck, P.V., et al., *PhosphoSitePlus: a comprehensive resource for investigating the structure and function of experimentally determined post-translational modifications in man and mouse.* Nucleic Acids Res, 2012. **40**(Database issue): p. D261-70.
67. Yang, L., et al., *Comprehensive Analysis of ERK1/2 Substrates for Potential Combination Immunotherapies.* Trends Pharmacol Sci, 2019. **40**(11): p. 897-910.
68. Schleger, C., et al., *c-MYC activation in primary and metastatic ductal adenocarcinoma of the pancreas: incidence, mechanisms, and clinical significance.* Mod Pathol, 2002. **15**(4): p. 462-9.
69. Hayes, T.K., et al., *Long-Term ERK Inhibition in KRAS-Mutant Pancreatic Cancer Is Associated with MYC Degradation and Senescence-like Growth Suppression.* Cancer Cell, 2016. **29**(1): p. 75-89.
70. Vaseva, A.V., et al., *KRAS Suppression-Induced Degradation of MYC Is Antagonized by a MEK5-ERK5 Compensatory Mechanism.* Cancer Cell, 2018. **34**(5): p. 807-822 e7.
71. Ryan, M.B., et al., *Targeting RAS-mutant cancers: is ERK the key?* Trends Cancer, 2015. **1**(3): p. 183-198.
72. Cargnello, M. and P.P. Roux, *Activation and function of the MAPKs and their substrates, the MAPK-activated protein kinases.* Microbiol Mol Biol Rev, 2011. **75**(1): p. 50-83.
73. Yoon, S. and R. Seger, *The extracellular signal-regulated kinase: multiple substrates regulate diverse cellular functions.* Growth Factors, 2006. **24**(1): p. 21-44.
74. Blasco, R.B., et al., *c-Raf, but not B-Raf, is essential for development of K-Ras oncogene-driven non-small cell lung carcinoma.* Cancer Cell, 2011. **19**(5): p. 652-63.
75. Falcomata, C., et al., *Selective multi-kinase inhibition sensitizes mesenchymal pancreatic cancer to immune checkpoint blockade by remodeling the tumor microenvironment.* Nat Cancer, 2022. **3**(3): p. 318-336.
76. Collisson, E.A., et al., *A central role for RAF-->MEK-->ERK signaling in the genesis of pancreatic ductal adenocarcinoma.* Cancer Discov, 2012. **2**(8): p. 685-93.
77. Ehrenreiter, K., et al., *Raf-1 addiction in Ras-induced skin carcinogenesis.* Cancer Cell, 2009. **16**(2): p. 149-60.
78. Sanclemente, M., et al., *c-RAF Ablation Induces Regression of Advanced Kras/Trp53 Mutant Lung Adenocarcinomas by a Mechanism Independent of MAPK Signaling.* Cancer Cell, 2018. **33**(2): p. 217-228 e4.
79. Eser, S., et al., *Selective requirement of PI3K/PDK1 signaling for Kras oncogene-driven pancreatic cell plasticity and cancer.* Cancer Cell, 2013. **23**(3): p. 406-20.
80. Ardito, C.M., et al., *EGF receptor is required for KRAS-induced pancreatic tumorigenesis.* Cancer Cell, 2012. **22**(3): p. 304-17.
81. Blasco, M.T., et al., *Complete Regression of Advanced Pancreatic Ductal Adenocarcinomas upon Combined Inhibition of EGFR and C-RAF.* Cancer Cell, 2019. **35**(4): p. 573-587 e6.

82. Wang, S., R.N. Ghosh, and S.P. Chellappan, *Raf-1 physically interacts with Rb and regulates its function: a link between mitogenic signaling and cell cycle regulation.* Mol Cell Biol, 1998. **18**(12): p. 7487-98.
83. Kinkade, R., et al., *A small molecule disruptor of Rb/Raf-1 interaction inhibits cell proliferation, angiogenesis, and growth of human tumor xenografts in nude mice.* Cancer Res, 2008. **68**(10): p. 3810-8.
84. Baumann, B., et al., *Raf induces NF-kappaB by membrane shuttle kinase MEKK1, a signaling pathway critical for transformation.* Proc Natl Acad Sci U S A, 2000. **97**(9): p. 4615-20.
85. Wang, H.G., U.R. Rapp, and J.C. Reed, *Bcl-2 targets the protein kinase Raf-1 to mitochondria.* Cell, 1996. **87**(4): p. 629-38.
86. Chen, J., et al., *Raf-1 promotes cell survival by antagonizing apoptosis signal-regulating kinase 1 through a MEK-ERK independent mechanism.* Proc Natl Acad Sci U S A, 2001. **98**(14): p. 7783-8.
87. Ehrenreiter, K., et al., *Raf-1 regulates Rho signaling and cell migration.* J Cell Biol, 2005. **168**(6): p. 955-64.
88. O'Neill, E., et al., *Role of the kinase MST2 in suppression of apoptosis by the proto-oncogene product Raf-1.* Science, 2004. **306**(5705): p. 2267-70.
89. Piazzolla, D., et al., *Raf-1 sets the threshold of Fas sensitivity by modulating Rok-alpha signaling.* J Cell Biol, 2005. **171**(6): p. 1013-22.
90. Mielgo, A., et al., *A MEK-independent role for CRAF in mitosis and tumor progression.* Nat Med, 2011. **17**(12): p. 1641-5.
91. Advani, S.J., et al., *Kinase-independent role for CRAF-driving tumour radioresistance via CHK2.* Nat Commun, 2015. **6**: p. 8154.
92. Morrison, D.K., *MAP kinase pathways.* Cold Spring Harb Perspect Biol, 2012. **4**(11).
93. Zhou, G., Z.Q. Bao, and J.E. Dixon, *Components of a new human protein kinase signal transduction pathway.* J Biol Chem, 1995. **270**(21): p. 12665-9.
94. Wang, Y.N., Y.J. Chen, and W.C. Chang, *Activation of extracellular signal-regulated kinase signaling by epidermal growth factor mediates c-Jun activation and p300 recruitment in keratin 16 gene expression.* Mol Pharmacol, 2006. **69**(1): p. 85-98.
95. Hoang, V.T., et al., *Oncogenic signaling of MEK5-ERK5.* Cancer Lett, 2017. **392**: p. 51-59.
96. Wang, F., et al., *p38gamma MAPK Is Essential for Aerobic Glycolysis and Pancreatic Tumorigenesis.* Cancer Res, 2020. **80**(16): p. 3251-3264.
97. Zhong, Y., et al., *Functional p38 MAPK identified by biomarker profiling of pancreatic cancer restrains growth through JNK inhibition and correlates with improved survival.* Clin Cancer Res, 2014. **20**(23): p. 6200-11.
98. Hoxhaj, G. and B.D. Manning, *The PI3K-AKT network at the interface of oncogenic signalling and cancer metabolism.* Nat Rev Cancer, 2020. **20**(2): p. 74-88.
99. Thorpe, L.M., H. Yuzugullu, and J.J. Zhao, *PI3K in cancer: divergent roles of isoforms, modes of activation and therapeutic targeting.* Nat Rev Cancer, 2015. **15**(1): p. 7-24.
100. Domchek, S.M., et al., *Inhibition of SH2 domain/phosphoprotein association by a nonhydrolyzable phosphonopeptide.* Biochemistry, 1992. **31**(41): p. 9865-70.
101. Ong, S.H., et al., *Stimulation of phosphatidylinositol 3-kinase by fibroblast growth factor receptors is mediated by coordinated recruitment of multiple docking proteins.* Proc Natl Acad Sci U S A, 2001. **98**(11): p. 6074-9.

102. Wang, W., et al., *Essential roles of Gab1 tyrosine phosphorylation in growth factor-mediated signaling and angiogenesis.* Int J Cardiol, 2015. **181**: p. 180-4.
103. Alessi, D.R., et al., *Mechanism of activation of protein kinase B by insulin and IGF-1.* EMBO J, 1996. **15**(23): p. 6541-51.
104. Alessi, D.R., et al., *3-Phosphoinositide-dependent protein kinase-1 (PDK1): structural and functional homology with the Drosophila DSTPK61 kinase.* Curr Biol, 1997. **7**(10): p. 776-89.
105. Currie, R.A., et al., *Role of phosphatidylinositol 3,4,5-trisphosphate in regulating the activity and localization of 3-phosphoinositide-dependent protein kinase-1.* Biochem J, 1999. **337 (Pt 3)**: p. 575-83.
106. Sarbassov, D.D., et al., *Phosphorylation and regulation of Akt/PKB by the rictor-mTOR complex.* Science, 2005. **307**(5712): p. 1098-101.
107. Stronach, E.A., et al., *DNA-PK mediates AKT activation and apoptosis inhibition in clinically acquired platinum resistance.* Neoplasia, 2011. **13**(11): p. 1069-80.
108. Cross, D.A., et al., *Inhibition of glycogen synthase kinase-3 by insulin mediated by protein kinase B.* Nature, 1995. **378**(6559): p. 785-9.
109. Frame, S., P. Cohen, and R.M. Biondi, *A common phosphate binding site explains the unique substrate specificity of GSK3 and its inactivation by phosphorylation.* Mol Cell, 2001. **7**(6): p. 1321-7.
110. Sutherland, C., *What Are the bona fide GSK3 Substrates?* Int J Alzheimers Dis, 2011. **2011**: p. 505607.
111. Brunet, A., et al., *Akt promotes cell survival by phosphorylating and inhibiting a Forkhead transcription factor.* Cell, 1999. **96**(6): p. 857-68.
112. Ho, K.K., S.S. Myatt, and E.W. Lam, *Many forks in the path: cycling with FoxO.* Oncogene, 2008. **27**(16): p. 2300-11.
113. Zhang, X., et al., *Akt, FoxO and regulation of apoptosis.* Biochim Biophys Acta, 2011. **1813**(11): p. 1978-86.
114. Hornsveld, M., et al., *Re-evaluating the role of FOXOs in cancer.* Semin Cancer Biol, 2018. **50**: p. 90-100.
115. Lee, Y.R., M. Chen, and P.P. Pandolfi, *The functions and regulation of the PTEN tumour suppressor: new modes and prospects.* Nat Rev Mol Cell Biol, 2018. **19**(9): p. 547-562.
116. Cerami, E., et al., *The cBio cancer genomics portal: an open platform for exploring multidimensional cancer genomics data.* Cancer Discov, 2012. **2**(5): p. 401-4.
117. Gao, J., et al., *Integrative analysis of complex cancer genomics and clinical profiles using the cBioPortal.* Sci Signal, 2013. **6**(269): p. pl1.
118. Aguirre, A.J., et al., *High-resolution characterization of the pancreatic adenocarcinoma genome.* Proc Natl Acad Sci U S A, 2004. **101**(24): p. 9067-72.
119. Asano, T., et al., *The PI 3-kinase/Akt signaling pathway is activated due to aberrant Pten expression and targets transcription factors NF-kappaB and c-Myc in pancreatic cancer cells.* Oncogene, 2004. **23**(53): p. 8571-80.
120. Schonleben, F., et al., *PIK3CA mutations in intraductal papillary mucinous neoplasm/carcinoma of the pancreas.* Clin Cancer Res, 2006. **12**(12): p. 3851-5.
121. Jaiswal, B.S., et al., *Somatic mutations in p85alpha promote tumorigenesis through class IA PI3K activation.* Cancer Cell, 2009. **16**(6): p. 463-74.

122. Ying, H., et al., *PTEN is a major tumor suppressor in pancreatic ductal adenocarcinoma and regulates an NF-kappaB-cytokine network.* Cancer Discov, 2011. **1**(2): p. 158-69.
123. Payne, S.N., et al., *PIK3CA mutations can initiate pancreatic tumorigenesis and are targetable with PI3K inhibitors.* Oncogenesis, 2015. **4**: p. e169.
124. Cantley, L.C., *The phosphoinositide 3-kinase pathway.* Science, 2002. **296**(5573): p. 1655-7.
125. Heid, I., et al., *Early requirement of Rac1 in a mouse model of pancreatic cancer.* Gastroenterology, 2011. **141**(2): p. 719-30, 730 e1-7.
126. Wu, C.Y., et al., *PI3K regulation of RAC1 is required for KRAS-induced pancreatic tumorigenesis in mice.* Gastroenterology, 2014. **147**(6): p. 1405-16 e7.
127. Bodemann, B.O. and M.A. White, *Ral GTPases and cancer: linchpin support of the tumorigenic platform.* Nat Rev Cancer, 2008. **8**(2): p. 133-40.
128. Neel, N.F., et al., *The RalGEF-Ral Effector Signaling Network: The Road Less Traveled for Anti-Ras Drug Discovery.* Genes Cancer, 2011. **2**(3): p. 275-87.
129. Lim, K.H., et al., *Activation of RalA is critical for Ras-induced tumorigenesis of human cells.* Cancer Cell, 2005. **7**(6): p. 533-45.
130. Lim, K.H., et al., *Divergent roles for RalA and RalB in malignant growth of human pancreatic carcinoma cells.* Curr Biol, 2006. **16**(24): p. 2385-94.
131. Stalnecker, C.A. and C.J. Der, *RAS, wanted dead or alive: Advances in targeting RAS mutant cancers.* Sci Signal, 2020. **13**(624).
132. Ostrem, J.M., et al., *K-Ras(G12C) inhibitors allosterically control GTP affinity and effector interactions.* Nature, 2013. **503**(7477): p. 548-51.
133. Canon, J., et al., *The clinical KRAS(G12C) inhibitor AMG 510 drives anti-tumour immunity.* Nature, 2019. **575**(7781): p. 217-223.
134. Hong, D.S., et al., *KRAS(G12C) Inhibition with Sotorasib in Advanced Solid Tumors.* N Engl J Med, 2020. **383**(13): p. 1207-1217.
135. Lanman, B.A., et al., *Discovery of a Covalent Inhibitor of KRAS(G12C) (AMG 510) for the Treatment of Solid Tumors.* J Med Chem, 2020. **63**(1): p. 52-65.
136. Skoulidis, F., et al., *Sotorasib for Lung Cancers with KRAS p.G12C Mutation.* N Engl J Med, 2021. **384**(25): p. 2371-2381.
137. Hunter, J.C., et al., *Biochemical and Structural Analysis of Common Cancer-Associated KRAS Mutations.* Mol Cancer Res, 2015. **13**(9): p. 1325-35.
138. Welsch, M.E., et al., *Multivalent Small-Molecule Pan-RAS Inhibitors.* Cell, 2017. **168**(5): p. 878-889 e29.
139. Ross, S.J., et al., *Targeting KRAS-dependent tumors with AZD4785, a high-affinity therapeutic antisense oligonucleotide inhibitor of KRAS.* Sci Transl Med, 2017. **9**(394).
140. Ryan, M.B. and R.B. Corcoran, *Therapeutic strategies to target RAS-mutant cancers.* Nat Rev Clin Oncol, 2018. **15**(11): p. 709-720.
141. Collins, M.A., et al., *Oncogenic Kras is required for both the initiation and maintenance of pancreatic cancer in mice.* J Clin Invest, 2012. **122**(2): p. 639-53.
142. Collins, M.A., et al., *Metastatic pancreatic cancer is dependent on oncogenic Kras in mice.* PLoS One, 2012. **7**(12): p. e49707.
143. Kapoor, A., et al., *Yap1 activation enables bypass of oncogenic Kras addiction in pancreatic cancer.* Cell, 2014. **158**(1): p. 185-197.
144. Muzumdar, M.D., et al., *Survival of pancreatic cancer cells lacking KRAS function.* Nat Commun, 2017. **8**(1): p. 1090.

145. Lou, K., et al., *KRAS(G12C) inhibition produces a driver-limited state revealing collateral dependencies.* Sci Signal, 2019. **12**(583).
146. Whyte, D.B., et al., *K- and N-Ras are geranylgeranylated in cells treated with farnesyl protein transferase inhibitors.* J Biol Chem, 1997. **272**(22): p. 14459-64.
147. Basso, A.D., P. Kirschmeier, and W.R. Bishop, *Lipid posttranslational modifications. Farnesyl transferase inhibitors.* J Lipid Res, 2006. **47**(1): p. 15-31.
148. Rowell, C.A., et al., *Direct demonstration of geranylgeranylation and farnesylation of Ki-Ras in vivo.* J Biol Chem, 1997. **272**(22): p. 14093-7.
149. Liu, M., et al., *Targeting the protein prenyltransferases efficiently reduces tumor development in mice with K-RAS-induced lung cancer.* Proc Natl Acad Sci U S A, 2010. **107**(14): p. 6471-6.
150. Papke, B., et al., *Identification of pyrazolopyridazinones as PDEdelta inhibitors.* Nat Commun, 2016. **7**: p. 11360.
151. Hillig, R.C., et al., *Discovery of potent SOS1 inhibitors that block RAS activation via disruption of the RAS-SOS1 interaction.* Proc Natl Acad Sci U S A, 2019. **116**(7): p. 2551-2560.
152. Nijman, S.M., *Synthetic lethality: general principles, utility and detection using genetic screens in human cells.* FEBS Lett, 2011. **585**(1): p. 1-6.
153. Nijman, S.M. and S.H. Friend, *Cancer. Potential of the synthetic lethality principle.* Science, 2013. **342**(6160): p. 809-11.
154. Luo, J., et al., *A genome-wide RNAi screen identifies multiple synthetic lethal interactions with the Ras oncogene.* Cell, 2009. **137**(5): p. 835-48.
155. Scholl, C., et al., *Synthetic lethal interaction between oncogenic KRAS dependency and STK33 suppression in human cancer cells.* Cell, 2009. **137**(5): p. 821-34.
156. Babij, C., et al., *STK33 kinase activity is nonessential in KRAS-dependent cancer cells.* Cancer Res, 2011. **71**(17): p. 5818-26.
157. Frohling, S. and C. Scholl, *STK33 kinase is not essential in KRAS-dependent cells--letter.* Cancer Res, 2011. **71**(24): p. 7716; author reply 7717.
158. Luo, T., et al., *STK33 kinase inhibitor BRD-8899 has no effect on KRAS-dependent cancer cell viability.* Proc Natl Acad Sci U S A, 2012. **109**(8): p. 2860-5.
159. Barbie, D.A., et al., *Systematic RNA interference reveals that oncogenic KRAS-driven cancers require TBK1.* Nature, 2009. **462**(7269): p. 108-12.
160. Muvaffak, A., et al., *Evaluating TBK1 as a therapeutic target in cancers with activated IRF3.* Mol Cancer Res, 2014. **12**(7): p. 1055-66.
161. Aguirre, A.J. and W.C. Hahn, *Synthetic Lethal Vulnerabilities in KRAS-Mutant Cancers.* Cold Spring Harb Perspect Med, 2018. **8**(8).
162. Wang, T., et al., *Gene Essentiality Profiling Reveals Gene Networks and Synthetic Lethal Interactions with Oncogenic Ras.* Cell, 2017. **168**(5): p. 890-903 e15.
163. Yau, E.H., et al., *Genome-Wide CRISPR Screen for Essential Cell Growth Mediators in Mutant KRAS Colorectal Cancers.* Cancer Res, 2017. **77**(22): p. 6330-6339.
164. Wilhelm, S., et al., *Discovery and development of sorafenib: a multikinase inhibitor for treating cancer.* Nat Rev Drug Discov, 2006. **5**(10): p. 835-44.
165. Kim, E.S., et al., *The BATTLE trial: personalizing therapy for lung cancer.* Cancer Discov, 2011. **1**(1): p. 44-53.
166. Hatzivassiliou, G., et al., *RAF inhibitors prime wild-type RAF to activate the MAPK pathway and enhance growth.* Nature, 2010. **464**(7287): p. 431-5.

167. Poulikakos, P.I., et al., *RAF inhibitors transactivate RAF dimers and ERK signalling in cells with wild-type BRAF.* Nature, 2010. **464**(7287): p. 427-30.
168. Callahan, M.K., et al., *Progression of RAS-mutant leukemia during RAF inhibitor treatment.* N Engl J Med, 2012. **367**(24): p. 2316-21.
169. Oberholzer, P.A., et al., *RAS mutations are associated with the development of cutaneous squamous cell tumors in patients treated with RAF inhibitors.* J Clin Oncol, 2012. **30**(3): p. 316-21.
170. Karoulia, Z., E. Gavathiotis, and P.I. Poulikakos, *New perspectives for targeting RAF kinase in human cancer.* Nat Rev Cancer, 2017. **17**(11): p. 676-691.
171. Zhang, C., et al., *RAF inhibitors that evade paradoxical MAPK pathway activation.* Nature, 2015. **526**(7574): p. 583-6.
172. Yao, Z., et al., *RAF inhibitor PLX8394 selectively disrupts BRAF dimers and RAS-independent BRAF-mutant-driven signaling.* Nat Med, 2019. **25**(2): p. 284-291.
173. Peng, S.B., et al., *Inhibition of RAF Isoforms and Active Dimers by LY3009120 Leads to Anti-tumor Activities in RAS or BRAF Mutant Cancers.* Cancer Cell, 2015. **28**(3): p. 384-98.
174. Vakana, E., et al., *LY3009120, a panRAF inhibitor, has significant anti-tumor activity in BRAF and KRAS mutant preclinical models of colorectal cancer.* Oncotarget, 2017. **8**(6): p. 9251-9266.
175. Sullivan, R.J., et al., *A Phase I Study of LY3009120, a Pan-RAF Inhibitor, in Patients with Advanced or Metastatic Cancer.* Mol Cancer Ther, 2020. **19**(2): p. 460-467.
176. Okaniwa, M., et al., *Discovery of a selective kinase inhibitor (TAK-632) targeting pan-RAF inhibition: design, synthesis, and biological evaluation of C-7-substituted 1,3-benzothiazole derivatives.* J Med Chem, 2013. **56**(16): p. 6478-94.
177. Sun, Y., et al., *A brain-penetrant RAF dimer antagonist for the noncanonical BRAF oncoprotein of pediatric low-grade astrocytomas.* Neuro Oncol, 2017. **19**(6): p. 774-785.
178. Nakamura, A., et al., *Antitumor activity of the selective pan-RAF inhibitor TAK-632 in BRAF inhibitor-resistant melanoma.* Cancer Res, 2013. **73**(23): p. 7043-55.
179. Yen, I., et al., *Pharmacological Induction of RAS-GTP Confers RAF Inhibitor Sensitivity in KRAS Mutant Tumors.* Cancer Cell, 2018. **34**(4): p. 611-625 e7.
180. Athuluri-Divakar, S.K., et al., *A Small Molecule RAS-Mimetic Disrupts RAS Association with Effector Proteins to Block Signaling.* Cell, 2016. **165**(3): p. 643-55.
181. Kato-Stankiewicz, J., et al., *Inhibitors of Ras/Raf-1 interaction identified by two-hybrid screening revert Ras-dependent transformation phenotypes in human cancer cells.* Proc Natl Acad Sci U S A, 2002. **99**(22): p. 14398-403.
182. Monaco, K.A., et al., *LXH254, a Potent and Selective ARAF-Sparing Inhibitor of BRAF and CRAF for the Treatment of MAPK-Driven Tumors.* Clin Cancer Res, 2021. **27**(7): p. 2061-2073.
183. Hauschild, A., et al., *Longer Follow-Up Confirms Relapse-Free Survival Benefit With Adjuvant Dabrafenib Plus Trametinib in Patients With Resected BRAF V600-Mutant Stage III Melanoma.* J Clin Oncol, 2018. **36**(35): p. 3441-3449.
184. Rose, A.A.N., *Encorafenib and binimetinib for the treatment of BRAF V600E/K-mutated melanoma.* Drugs Today (Barc), 2019. **55**(4): p. 247-264.
185. Larkin, J., et al., *Combined vemurafenib and cobimetinib in BRAF-mutated melanoma.* N Engl J Med, 2014. **371**(20): p. 1867-76.

186. Bodoky, G., et al., *A phase II open-label randomized study to assess the efficacy and safety of selumetinib (AZD6244 [ARRY-142886]) versus capecitabine in patients with advanced or metastatic pancreatic cancer who have failed first-line gemcitabine therapy.* Invest New Drugs, 2012. **30**(3): p. 1216-23.
187. Infante, J.R., et al., *A randomised, double-blind, placebo-controlled trial of trametinib, an oral MEK inhibitor, in combination with gemcitabine for patients with untreated metastatic adenocarcinoma of the pancreas.* Eur J Cancer, 2014. **50**(12): p. 2072-81.
188. Blumenschein, G.R., Jr., et al., *A randomized phase II study of the MEK1/MEK2 inhibitor trametinib (GSK1120212) compared with docetaxel in KRAS-mutant advanced non-small-cell lung cancer (NSCLC)dagger.* Ann Oncol, 2015. **26**(5): p. 894-901.
189. Janne, P.A., et al., *Selumetinib Plus Docetaxel Compared With Docetaxel Alone and Progression-Free Survival in Patients With KRAS-Mutant Advanced Non-Small Cell Lung Cancer: The SELECT-1 Randomized Clinical Trial.* JAMA, 2017. **317**(18): p. 1844-1853.
190. Wee, S., et al., *PI3K pathway activation mediates resistance to MEK inhibitors in KRAS mutant cancers.* Cancer Res, 2009. **69**(10): p. 4286-93.
191. Lito, P., et al., *Disruption of CRAF-mediated MEK activation is required for effective MEK inhibition in KRAS mutant tumors.* Cancer Cell, 2014. **25**(5): p. 697-710.
192. Bollag, G., et al., *Clinical efficacy of a RAF inhibitor needs broad target blockade in BRAF-mutant melanoma.* Nature, 2010. **467**(7315): p. 596-9.
193. Morris, E.J., et al., *Discovery of a novel ERK inhibitor with activity in models of acquired resistance to BRAF and MEK inhibitors.* Cancer Discov, 2013. **3**(7): p. 742-50.
194. Hatzivassiliou, G., et al., *ERK inhibition overcomes acquired resistance to MEK inhibitors.* Mol Cancer Ther, 2012. **11**(5): p. 1143-54.
195. Tayama, H., et al., *The association between ERK inhibitor sensitivity and molecular characteristics in colorectal cancer.* Biochem Biophys Res Commun, 2021. **560**: p. 59-65.
196. Moschos, S.J., et al., *Development of MK-8353, an orally administered ERK1/2 inhibitor, in patients with advanced solid tumors.* JCI Insight, 2018. **3**(4).
197. Sullivan, R.J., et al., *First-in-Class ERK1/2 Inhibitor Ulixertinib (BVD-523) in Patients with MAPK Mutant Advanced Solid Tumors: Results of a Phase I Dose-Escalation and Expansion Study.* Cancer Discov, 2018. **8**(2): p. 184-195.
198. Goetz, E.M., et al., *ERK mutations confer resistance to mitogen-activated protein kinase pathway inhibitors.* Cancer Res, 2014. **74**(23): p. 7079-89.
199. Jha, S., et al., *Dissecting Therapeutic Resistance to ERK Inhibition.* Mol Cancer Ther, 2016. **15**(4): p. 548-59.
200. Brenan, L., et al., *Phenotypic Characterization of a Comprehensive Set of MAPK1/ERK2 Missense Mutants.* Cell Rep, 2016. **17**(4): p. 1171-1183.
201. Thibault, B., et al., *Pancreatic cancer intrinsic PI3Kalpha activity accelerates metastasis and rewires macrophage component.* EMBO Mol Med, 2021. **13**(7): p. e13502.
202. Baer, R., et al., *Pancreatic cell plasticity and cancer initiation induced by oncogenic Kras is completely dependent on wild-type PI 3-kinase p110alpha.* Genes Dev, 2014. **28**(23): p. 2621-35.
203. Hopkins, B.D., et al., *Suppression of insulin feedback enhances the efficacy of PI3K inhibitors.* Nature, 2018. **560**(7719): p. 499-503.

204. Yap, T.A., et al., *First-in-man clinical trial of the oral pan-AKT inhibitor MK-2206 in patients with advanced solid tumors.* J Clin Oncol, 2011. **29**(35): p. 4688-95.
205. Javle, M.M., et al., *Inhibition of the mammalian target of rapamycin (mTOR) in advanced pancreatic cancer: results of two phase II studies.* BMC Cancer, 2010. **10**: p. 368.
206. Wolpin, B.M., et al., *Oral mTOR inhibitor everolimus in patients with gemcitabine-refractory metastatic pancreatic cancer.* J Clin Oncol, 2009. **27**(2): p. 193-8.
207. Sun, S.Y., et al., *Activation of Akt and eIF4E survival pathways by rapamycin-mediated mammalian target of rapamycin inhibition.* Cancer Res, 2005. **65**(16): p. 7052-8.
208. O'Reilly, K.E., et al., *mTOR inhibition induces upstream receptor tyrosine kinase signaling and activates Akt.* Cancer Res, 2006. **66**(3): p. 1500-8.
209. Conway, J.R., et al., *Combating pancreatic cancer with PI3K pathway inhibitors in the era of personalised medicine.* Gut, 2019. **68**(4): p. 742-758.
210. Rodrik-Outmezguine, V.S., et al., *mTOR kinase inhibition causes feedback-dependent biphasic regulation of AKT signaling.* Cancer Discov, 2011. **1**(3): p. 248-59.
211. Goktuna, S.I., *IKBKE inhibits TSC1 to activate the mTOR/S6K pathway for oncogenic transformation.* Turk J Biol, 2018. **42**(4): p. 268-278.
212. Soares, H.P., et al., *Dual PI3K/mTOR Inhibitors Induce Rapid Overactivation of the MEK/ERK Pathway in Human Pancreatic Cancer Cells through Suppression of mTORC2.* Mol Cancer Ther, 2015. **14**(4): p. 1014-23.
213. Morran, D.C., et al., *Targeting mTOR dependency in pancreatic cancer.* Gut, 2014. **63**(9): p. 1481-9.
214. Kelly, T.J., Jr. and H.O. Smith, *A restriction enzyme from Hemophilus influenzae. II.* J Mol Biol, 1970. **51**(2): p. 393-409.
215. Smith, H.O. and K.W. Wilcox, *A restriction enzyme from Hemophilus influenzae. I. Purification and general properties.* J Mol Biol, 1970. **51**(2): p. 379-91.
216. Danna, K. and D. Nathans, *Specific cleavage of simian virus 40 DNA by restriction endonuclease of Hemophilus influenzae.* Proc Natl Acad Sci U S A, 1971. **68**(12): p. 2913-7.
217. Hsu, P.D., E.S. Lander, and F. Zhang, *Development and applications of CRISPR-Cas9 for genome engineering.* Cell, 2014. **157**(6): p. 1262-1278.
218. Adli, M., *The CRISPR tool kit for genome editing and beyond.* Nat Commun, 2018. **9**(1): p. 1911.
219. Rothstein, R.J., *One-step gene disruption in yeast.* Methods Enzymol, 1983. **101**: p. 202-11.
220. Smithies, O., et al., *Insertion of DNA sequences into the human chromosomal beta-globin locus by homologous recombination.* Nature, 1985. **317**(6034): p. 230-4.
221. Thomas, K.R., K.R. Folger, and M.R. Capecchi, *High frequency targeting of genes to specific sites in the mammalian genome.* Cell, 1986. **44**(3): p. 419-28.
222. Capecchi, M.R., *Altering the genome by homologous recombination.* Science, 1989. **244**(4910): p. 1288-92.
223. Rouet, P., F. Smih, and M. Jasin, *Introduction of double-strand breaks into the genome of mouse cells by expression of a rare-cutting endonuclease.* Mol Cell Biol, 1994. **14**(12): p. 8096-106.
224. Jeggo, P.A., *DNA breakage and repair.* Adv Genet, 1998. **38**: p. 185-218.

225. Bibikova, M., et al., *Targeted chromosomal cleavage and mutagenesis in Drosophila using zinc-finger nucleases.* Genetics, 2002. **161**(3): p. 1169-75.
226. Rosen, L.E., et al., *Homing endonuclease I-CreI derivatives with novel DNA target specificities.* Nucleic Acids Res, 2006. **34**(17): p. 4791-800.
227. Kim, Y.G., J. Cha, and S. Chandrasegaran, *Hybrid restriction enzymes: zinc finger fusions to Fok I cleavage domain.* Proc Natl Acad Sci U S A, 1996. **93**(3): p. 1156-60.
228. Urnov, F.D., et al., *Genome editing with engineered zinc finger nucleases.* Nat Rev Genet, 2010. **11**(9): p. 636-46.
229. Christian, M., et al., *Targeting DNA double-strand breaks with TAL effector nucleases.* Genetics, 2010. **186**(2): p. 757-61.
230. Li, T., et al., *Modularly assembled designer TAL effector nucleases for targeted gene knockout and gene replacement in eukaryotes.* Nucleic Acids Res, 2011. **39**(14): p. 6315-25.
231. Miller, J.C., et al., *A TALE nuclease architecture for efficient genome editing.* Nat Biotechnol, 2011. **29**(2): p. 143-8.
232. Zhang, F., et al., *Efficient construction of sequence-specific TAL effectors for modulating mammalian transcription.* Nat Biotechnol, 2011. **29**(2): p. 149-53.
233. Maeder, M.L., et al., *Rapid "open-source" engineering of customized zinc-finger nucleases for highly efficient gene modification.* Mol Cell, 2008. **31**(2): p. 294-301.
234. Barrangou, R. and P. Horvath, *A decade of discovery: CRISPR functions and applications.* Nat Microbiol, 2017. **2**: p. 17092.
235. Makarova, K.S., et al., *An updated evolutionary classification of CRISPR-Cas systems.* Nat Rev Microbiol, 2015. **13**(11): p. 722-36.
236. van der Oost, J., et al., *Unravelling the structural and mechanistic basis of CRISPR-Cas systems.* Nat Rev Microbiol, 2014. **12**(7): p. 479-92.
237. Wright, A.V., J.K. Nunez, and J.A. Doudna, *Biology and Applications of CRISPR Systems: Harnessing Nature's Toolbox for Genome Engineering.* Cell, 2016. **164**(1-2): p. 29-44.
238. Makarova, K.S., et al., *Evolution and classification of the CRISPR-Cas systems.* Nat Rev Microbiol, 2011. **9**(6): p. 467-77.
239. van der Oost, J., et al., *CRISPR-based adaptive and heritable immunity in prokaryotes.* Trends Biochem Sci, 2009. **34**(8): p. 401-7.
240. Jansen, R., et al., *Identification of genes that are associated with DNA repeats in prokaryotes.* Mol Microbiol, 2002. **43**(6): p. 1565-75.
241. Groenen, P.M., et al., *Nature of DNA polymorphism in the direct repeat cluster of Mycobacterium tuberculosis; application for strain differentiation by a novel typing method.* Mol Microbiol, 1993. **10**(5): p. 1057-65.
242. Hoe, N., et al., *Rapid molecular genetic subtyping of serotype M1 group A Streptococcus strains.* Emerg Infect Dis, 1999. **5**(2): p. 254-63.
243. Ishino, Y., et al., *Nucleotide sequence of the iap gene, responsible for alkaline phosphatase isozyme conversion in Escherichia coli, and identification of the gene product.* J Bacteriol, 1987. **169**(12): p. 5429-33.
244. Masepohl, B., K. Gorlitz, and H. Bohme, *Long tandemly repeated repetitive (LTRR) sequences in the filamentous cyanobacterium Anabaena sp. PCC 7120.* Biochim Biophys Acta, 1996. **1307**(1): p. 26-30.

245. Mojica, F.J., et al., *Long stretches of short tandem repeats are present in the largest replicons of the Archaea Haloferax mediterranei and Haloferax volcanii and could be involved in replicon partitioning.* Mol Microbiol, 1995. **17**(1): p. 85-93.
246. Nakata, A., M. Amemura, and K. Makino, *Unusual nucleotide arrangement with repeated sequences in the Escherichia coli K-12 chromosome.* J Bacteriol, 1989. **171**(6): p. 3553-6.
247. Bolotin, A., et al., *Clustered regularly interspaced short palindrome repeats (CRISPRs) have spacers of extrachromosomal origin.* Microbiology (Reading), 2005. **151**(Pt 8): p. 2551-2561.
248. Mojica, F.J., et al., *Intervening sequences of regularly spaced prokaryotic repeats derive from foreign genetic elements.* J Mol Evol, 2005. **60**(2): p. 174-82.
249. Pourcel, C., G. Salvignol, and G. Vergnaud, *CRISPR elements in Yersinia pestis acquire new repeats by preferential uptake of bacteriophage DNA, and provide additional tools for evolutionary studies.* Microbiology (Reading), 2005. **151**(Pt 3): p. 653-663.
250. Barrangou, R., et al., *CRISPR provides acquired resistance against viruses in prokaryotes.* Science, 2007. **315**(5819): p. 1709-12.
251. Mojica, F.J.M., et al., *Short motif sequences determine the targets of the prokaryotic CRISPR defence system.* Microbiology (Reading), 2009. **155**(Pt 3): p. 733-740.
252. Deveau, H., et al., *Phage response to CRISPR-encoded resistance in Streptococcus thermophilus.* J Bacteriol, 2008. **190**(4): p. 1390-400.
253. Yosef, I., M.G. Goren, and U. Qimron, *Proteins and DNA elements essential for the CRISPR adaptation process in Escherichia coli.* Nucleic Acids Res, 2012. **40**(12): p. 5569-76.
254. Brouns, S.J., et al., *Small CRISPR RNAs guide antiviral defense in prokaryotes.* Science, 2008. **321**(5891): p. 960-4.
255. Carte, J., et al., *Cas6 is an endoribonuclease that generates guide RNAs for invader defense in prokaryotes.* Genes Dev, 2008. **22**(24): p. 3489-96.
256. Garneau, J.E., et al., *The CRISPR/Cas bacterial immune system cleaves bacteriophage and plasmid DNA.* Nature, 2010. **468**(7320): p. 67-71.
257. Deltcheva, E., et al., *CRISPR RNA maturation by trans-encoded small RNA and host factor RNase III.* Nature, 2011. **471**(7340): p. 602-7.
258. Sapranauskas, R., et al., *The Streptococcus thermophilus CRISPR/Cas system provides immunity in Escherichia coli.* Nucleic Acids Res, 2011. **39**(21): p. 9275-82.
259. Gasiunas, G., et al., *Cas9-crRNA ribonucleoprotein complex mediates specific DNA cleavage for adaptive immunity in bacteria.* Proc Natl Acad Sci U S A, 2012. **109**(39): p. E2579-86.
260. Jinek, M., et al., *A programmable dual-RNA-guided DNA endonuclease in adaptive bacterial immunity.* Science, 2012. **337**(6096): p. 816-21.
261. Cong, L., et al., *Multiplex genome engineering using CRISPR/Cas systems.* Science, 2013. **339**(6121): p. 819-23.
262. Jinek, M., et al., *RNA-programmed genome editing in human cells.* Elife, 2013. **2**: p. e00471.
263. Mali, P., et al., *RNA-guided human genome engineering via Cas9.* Science, 2013. **339**(6121): p. 823-6.
264. Li, W., et al., *Genetic modification and screening in rat using haploid embryonic stem cells.* Cell Stem Cell, 2014. **14**(3): p. 404-14.

265. Niu, Y., et al., *Generation of gene-modified cynomolgus monkey via Cas9/RNA-mediated gene targeting in one-cell embryos.* Cell, 2014. **156**(4): p. 836-43.
266. Sander, J.D. and J.K. Joung, *CRISPR-Cas systems for editing, regulating and targeting genomes.* Nat Biotechnol, 2014. **32**(4): p. 347-55.
267. Zhou, J., et al., *One-step generation of different immunodeficient mice with multiple gene modifications by CRISPR/Cas9 mediated genome engineering.* Int J Biochem Cell Biol, 2014. **46**: p. 49-55.
268. Jiang, F. and J.A. Doudna, *CRISPR-Cas9 Structures and Mechanisms.* Annu Rev Biophys, 2017. **46**: p. 505-529.
269. Anders, C., et al., *Structural basis of PAM-dependent target DNA recognition by the Cas9 endonuclease.* Nature, 2014. **513**(7519): p. 569-73.
270. Jinek, M., et al., *Structures of Cas9 endonucleases reveal RNA-mediated conformational activation.* Science, 2014. **343**(6176): p. 1247997.
271. Nishimasu, H., et al., *Crystal structure of Cas9 in complex with guide RNA and target DNA.* Cell, 2014. **156**(5): p. 935-49.
272. Hsu, P.D., et al., *DNA targeting specificity of RNA-guided Cas9 nucleases.* Nat Biotechnol, 2013. **31**(9): p. 827-32.
273. Jackson, R.N., et al., *Structural biology. Crystal structure of the CRISPR RNA-guided surveillance complex from Escherichia coli.* Science, 2014. **345**(6203): p. 1473-9.
274. Kunne, T., D.C. Swarts, and S.J. Brouns, *Planting the seed: target recognition of short guide RNAs.* Trends Microbiol, 2014. **22**(2): p. 74-83.
275. Mulepati, S., A. Heroux, and S. Bailey, *Structural biology. Crystal structure of a CRISPR RNA-guided surveillance complex bound to a ssDNA target.* Science, 2014. **345**(6203): p. 1479-84.
276. Zhao, H., et al., *Crystal structure of the RNA-guided immune surveillance Cascade complex in Escherichia coli.* Nature, 2014. **515**(7525): p. 147-50.
277. Jiang, F., et al., *STRUCTURAL BIOLOGY. A Cas9-guide RNA complex preorganized for target DNA recognition.* Science, 2015. **348**(6242): p. 1477-81.
278. Sternberg, S.H., et al., *DNA interrogation by the CRISPR RNA-guided endonuclease Cas9.* Nature, 2014. **507**(7490): p. 62-7.
279. Knight, S.C., et al., *Dynamics of CRISPR-Cas9 genome interrogation in living cells.* Science, 2015. **350**(6262): p. 823-6.
280. Ma, H., et al., *CRISPR-Cas9 nuclear dynamics and target recognition in living cells.* J Cell Biol, 2016. **214**(5): p. 529-37.
281. Szczelkun, M.D., et al., *Direct observation of R-loop formation by single RNA-guided Cas9 and Cascade effector complexes.* Proc Natl Acad Sci U S A, 2014. **111**(27): p. 9798-803.
282. Ran, F.A., et al., *Genome engineering using the CRISPR-Cas9 system.* Nat Protoc, 2013. **8**(11): p. 2281-2308.
283. Pattanayak, V., et al., *High-throughput profiling of off-target DNA cleavage reveals RNA-programmed Cas9 nuclease specificity.* Nat Biotechnol, 2013. **31**(9): p. 839-43.
284. Fu, Y., et al., *High-frequency off-target mutagenesis induced by CRISPR-Cas nucleases in human cells.* Nat Biotechnol, 2013. **31**(9): p. 822-6.
285. Semenova, E., et al., *Interference by clustered regularly interspaced short palindromic repeat (CRISPR) RNA is governed by a seed sequence.* Proc Natl Acad Sci U S A, 2011. **108**(25): p. 10098-103.

286. Wiedenheft, B., et al., *RNA-guided complex from a bacterial immune system enhances target recognition through seed sequence interactions.* Proc Natl Acad Sci U S A, 2011. **108**(25): p. 10092-7.
287. Kuscu, C., et al., *Genome-wide analysis reveals characteristics of off-target sites bound by the Cas9 endonuclease.* Nat Biotechnol, 2014. **32**(7): p. 677-83.
288. Wu, X., et al., *Genome-wide binding of the CRISPR endonuclease Cas9 in mammalian cells.* Nat Biotechnol, 2014. **32**(7): p. 670-6.
289. Veres, A., et al., *Low incidence of off-target mutations in individual CRISPR-Cas9 and TALEN targeted human stem cell clones detected by whole-genome sequencing.* Cell Stem Cell, 2014. **15**(1): p. 27-30.
290. Smith, C., et al., *Whole-genome sequencing analysis reveals high specificity of CRISPR/Cas9 and TALEN-based genome editing in human iPSCs.* Cell Stem Cell, 2014. **15**(1): p. 12-3.
291. Crosetto, N., et al., *Nucleotide-resolution DNA double-strand break mapping by next-generation sequencing.* Nat Methods, 2013. **10**(4): p. 361-5.
292. Tsai, S.Q., et al., *GUIDE-seq enables genome-wide profiling of off-target cleavage by CRISPR-Cas nucleases.* Nat Biotechnol, 2015. **33**(2): p. 187-197.
293. Kim, D., et al., *Digenome-seq: genome-wide profiling of CRISPR-Cas9 off-target effects in human cells.* Nat Methods, 2015. **12**(3): p. 237-43, 1 p following 243.
294. Cameron, P., et al., *Mapping the genomic landscape of CRISPR-Cas9 cleavage.* Nat Methods, 2017. **14**(6): p. 600-606.
295. Tsai, S.Q., et al., *CIRCLE-seq: a highly sensitive in vitro screen for genome-wide CRISPR-Cas9 nuclease off-targets.* Nat Methods, 2017. **14**(6): p. 607-614.
296. Kang, S.H., et al., *Prediction-based highly sensitive CRISPR off-target validation using target-specific DNA enrichment.* Nat Commun, 2020. **11**(1): p. 3596.
297. Kleinstiver, B.P., et al., *High-fidelity CRISPR-Cas9 nucleases with no detectable genome-wide off-target effects.* Nature, 2016. **529**(7587): p. 490-5.
298. Slaymaker, I.M., et al., *Rationally engineered Cas9 nucleases with improved specificity.* Science, 2016. **351**(6268): p. 84-8.
299. Lee, J.K., et al., *Directed evolution of CRISPR-Cas9 to increase its specificity.* Nat Commun, 2018. **9**(1): p. 3048.
300. Vakulskas, C.A., et al., *A high-fidelity Cas9 mutant delivered as a ribonucleoprotein complex enables efficient gene editing in human hematopoietic stem and progenitor cells.* Nat Med, 2018. **24**(8): p. 1216-1224.
301. Kim, S., et al., *Highly efficient RNA-guided genome editing in human cells via delivery of purified Cas9 ribonucleoproteins.* Genome Res, 2014. **24**(6): p. 1012-9.
302. Lin, S., et al., *Enhanced homology-directed human genome engineering by controlled timing of CRISPR/Cas9 delivery.* Elife, 2014. **3**: p. e04766.
303. Mali, P., et al., *CAS9 transcriptional activators for target specificity screening and paired nickases for cooperative genome engineering.* Nat Biotechnol, 2013. **31**(9): p. 833-8.
304. Guilinger, J.P., D.B. Thompson, and D.R. Liu, *Fusion of catalytically inactive Cas9 to FokI nuclease improves the specificity of genome modification.* Nat Biotechnol, 2014. **32**(6): p. 577-582.
305. Tsai, S.Q., et al., *Dimeric CRISPR RNA-guided FokI nucleases for highly specific genome editing.* Nat Biotechnol, 2014. **32**(6): p. 569-76.

306. Coelho, M.A., et al., *CRISPR GUARD protects off-target sites from Cas9 nuclease activity using short guide RNAs.* Nat Commun, 2020. **11**(1): p. 4132.
307. Kleinstiver, B.P., et al., *Engineered CRISPR-Cas9 nucleases with altered PAM specificities.* Nature, 2015. **523**(7561): p. 481-5.
308. Hu, J.H., et al., *Evolved Cas9 variants with broad PAM compatibility and high DNA specificity.* Nature, 2018. **556**(7699): p. 57-63.
309. Walton, R.T., et al., *Unconstrained genome targeting with near-PAMless engineered CRISPR-Cas9 variants.* Science, 2020. **368**(6488): p. 290-296.
310. Chatterjee, P., N. Jakimo, and J.M. Jacobson, *Minimal PAM specificity of a highly similar SpCas9 ortholog.* Sci Adv, 2018. **4**(10): p. eaau0766.
311. Esvelt, K.M., et al., *Orthogonal Cas9 proteins for RNA-guided gene regulation and editing.* Nat Methods, 2013. **10**(11): p. 1116-21.
312. Zhang, Y., et al., *Processing-independent CRISPR RNAs limit natural transformation in Neisseria meningitidis.* Mol Cell, 2013. **50**(4): p. 488-503.
313. Burstein, D., et al., *New CRISPR-Cas systems from uncultivated microbes.* Nature, 2017. **542**(7640): p. 237-241.
314. Kim, E., et al., *In vivo genome editing with a small Cas9 orthologue derived from Campylobacter jejuni.* Nat Commun, 2017. **8**: p. 14500.
315. Yamada, M., et al., *Crystal Structure of the Minimal Cas9 from Campylobacter jejuni Reveals the Molecular Diversity in the CRISPR-Cas9 Systems.* Mol Cell, 2017. **65**(6): p. 1109-1121 e3.
316. Gaudelli, N.M., et al., *Programmable base editing of A*T to G*C in genomic DNA without DNA cleavage.* Nature, 2017. **551**(7681): p. 464-471.
317. Nishida, K., et al., *Targeted nucleotide editing using hybrid prokaryotic and vertebrate adaptive immune systems.* Science, 2016. **353**(6305).
318. Komor, A.C., et al., *Programmable editing of a target base in genomic DNA without double-stranded DNA cleavage.* Nature, 2016. **533**(7603): p. 420-4.
319. Billon, P., et al., *CRISPR-Mediated Base Editing Enables Efficient Disruption of Eukaryotic Genes through Induction of STOP Codons.* Mol Cell, 2017. **67**(6): p. 1068-1079 e4.
320. Kuscu, C., et al., *CRISPR-STOP: gene silencing through base-editing-induced nonsense mutations.* Nat Methods, 2017. **14**(7): p. 710-712.
321. Komor, A.C., et al., *Improved base excision repair inhibition and bacteriophage Mu Gam protein yields C:G-to-T:A base editors with higher efficiency and product purity.* Sci Adv, 2017. **3**(8): p. eaao4774.
322. Koblan, L.W., et al., *Improving cytidine and adenine base editors by expression optimization and ancestral reconstruction.* Nat Biotechnol, 2018. **36**(9): p. 843-846.
323. Hess, G.T., et al., *Directed evolution using dCas9-targeted somatic hypermutation in mammalian cells.* Nat Methods, 2016. **13**(12): p. 1036-1042.
324. Kuscu, C. and M. Adli, *CRISPR-Cas9-AID base editor is a powerful gain-of-function screening tool.* Nat Methods, 2016. **13**(12): p. 983-984.
325. Ma, Y., et al., *Targeted AID-mediated mutagenesis (TAM) enables efficient genomic diversification in mammalian cells.* Nat Methods, 2016. **13**(12): p. 1029-1035.
326. Qi, L.S., et al., *Repurposing CRISPR as an RNA-guided platform for sequence-specific control of gene expression.* Cell, 2013. **152**(5): p. 1173-83.
327. Pickar-Oliver, A. and C.A. Gersbach, *The next generation of CRISPR-Cas technologies and applications.* Nat Rev Mol Cell Biol, 2019. **20**(8): p. 490-507.

328. Larson, M.H., et al., *CRISPR interference (CRISPRi) for sequence-specific control of gene expression.* Nat Protoc, 2013. **8**(11): p. 2180-96.
329. Gilbert, L.A., et al., *CRISPR-mediated modular RNA-guided regulation of transcription in eukaryotes.* Cell, 2013. **154**(2): p. 442-51.
330. Yeo, N.C., et al., *An enhanced CRISPR repressor for targeted mammalian gene regulation.* Nat Methods, 2018. **15**(8): p. 611-616.
331. Alerasool, N., et al., *An efficient KRAB domain for CRISPRi applications in human cells.* Nat Methods, 2020. **17**(11): p. 1093-1096.
332. Perez-Pinera, P., et al., *RNA-guided gene activation by CRISPR-Cas9-based transcription factors.* Nat Methods, 2013. **10**(10): p. 973-6.
333. Maeder, M.L., et al., *CRISPR RNA-guided activation of endogenous human genes.* Nat Methods, 2013. **10**(10): p. 977-9.
334. Chavez, A., et al., *Highly efficient Cas9-mediated transcriptional programming.* Nat Methods, 2015. **12**(4): p. 326-8.
335. Zalatan, J.G., et al., *Engineering complex synthetic transcriptional programs with CRISPR RNA scaffolds.* Cell, 2015. **160**(1-2): p. 339-50.
336. Konermann, S., et al., *Genome-scale transcriptional activation by an engineered CRISPR-Cas9 complex.* Nature, 2015. **517**(7536): p. 583-8.
337. Tanenbaum, M.E., et al., *A protein-tagging system for signal amplification in gene expression and fluorescence imaging.* Cell, 2014. **159**(3): p. 635-46.
338. Chavez, A., et al., *Comparison of Cas9 activators in multiple species.* Nat Methods, 2016. **13**(7): p. 563-567.
339. Silva, J., et al., *RNA-interference-based functional genomics in mammalian cells: reverse genetics coming of age.* Oncogene, 2004. **23**(51): p. 8401-9.
340. Schuster, A., et al., *RNAi/CRISPR Screens: from a Pool to a Valid Hit.* Trends Biotechnol, 2019. **37**(1): p. 38-55.
341. Wang, T., et al., *Genetic screens in human cells using the CRISPR-Cas9 system.* Science, 2014. **343**(6166): p. 80-4.
342. Shalem, O., et al., *Genome-scale CRISPR-Cas9 knockout screening in human cells.* Science, 2014. **343**(6166): p. 84-87.
343. Behan, F.M., et al., *Prioritization of cancer therapeutic targets using CRISPR-Cas9 screens.* Nature, 2019. **568**(7753): p. 511-516.
344. Meyers, R.M., et al., *Computational correction of copy number effect improves specificity of CRISPR-Cas9 essentiality screens in cancer cells.* Nat Genet, 2017. **49**(12): p. 1779-1784.
345. Tsherniak, A., et al., *Defining a Cancer Dependency Map.* Cell, 2017. **170**(3): p. 564-576 e16.
346. Li, W., et al., *MAGeCK enables robust identification of essential genes from genome-scale CRISPR/Cas9 knockout screens.* Genome Biol, 2014. **15**(12): p. 554.
347. Hart, T. and J. Moffat, *BAGEL: a computational framework for identifying essential genes from pooled library screens.* BMC Bioinformatics, 2016. **17**: p. 164.
348. Wang, B., et al., *Integrative analysis of pooled CRISPR genetic screens using MAGeCKFlute.* Nat Protoc, 2019. **14**(3): p. 756-780.
349. Schonhuber, N., et al., *A next-generation dual-recombinase system for time- and host-specific targeting of pancreatic cancer.* Nat Med, 2014. **20**(11): p. 1340-1347.

350. Nakhai, H., et al., *Ptf1a is essential for the differentiation of GABAergic and glycinergic amacrine cells and horizontal cells in the mouse retina.* Development, 2007. **134**(6): p. 1151-60.
351. Jackson, E.L., et al., *Analysis of lung tumor initiation and progression using conditional expression of oncogenic K-ras.* Genes Dev, 2001. **15**(24): p. 3243-8.
352. Hingorani, S.R., et al., *Preinvasive and invasive ductal pancreatic cancer and its early detection in the mouse.* Cancer Cell, 2003. **4**(6): p. 437-50.
353. Lawlor, M.A., et al., *Essential role of PDK1 in regulating cell size and development in mice.* EMBO J, 2002. **21**(14): p. 3728-38.
354. Lee, C.L., et al., *Generation of primary tumors with Flp recombinase in FRT-flanked p53 mice.* Dis Model Mech, 2012. **5**(3): p. 397-402.
355. Lesche, R., et al., *Cre/loxP-mediated inactivation of the murine Pten tumor suppressor gene.* Genesis, 2002. **32**(2): p. 148-9.
356. Chen, A.P., et al., *Forebrain-specific knockout of B-raf kinase leads to deficits in hippocampal long-term potentiation, learning, and memory.* J Neurosci Res, 2006. **83**(1): p. 28-38.
357. Jesenberger, V., et al., *Protective role of Raf-1 in Salmonella-induced macrophage apoptosis.* J Exp Med, 2001. **193**(3): p. 353-64.
358. Hafner, M., et al., *Growth rate inhibition metrics correct for confounders in measuring sensitivity to cancer drugs.* Nat Methods, 2016. **13**(6): p. 521-7.
359. Clark, N.A., et al., *GRcalculator: an online tool for calculating and mining dose-response data.* BMC Cancer, 2017. **17**(1): p. 698.
360. Love, M.I., W. Huber, and S. Anders, *Moderated estimation of fold change and dispersion for RNA-seq data with DESeq2.* Genome Biol, 2014. **15**(12): p. 550.
361. Raudvere, U., et al., *g:Profiler: a web server for functional enrichment analysis and conversions of gene lists (2019 update).* Nucleic Acids Res, 2019. **47**(W1): p. W191-W198.
362. Subramanian, A., et al., *Gene set enrichment analysis: a knowledge-based approach for interpreting genome-wide expression profiles.* Proc Natl Acad Sci U S A, 2005. **102**(43): p. 15545-50.
363. Liberzon, A., et al., *The Molecular Signatures Database (MSigDB) hallmark gene set collection.* Cell Syst, 2015. **1**(6): p. 417-425.
364. Doench, J.G., et al., *Optimized sgRNA design to maximize activity and minimize off-target effects of CRISPR-Cas9.* Nat Biotechnol, 2016. **34**(2): p. 184-191.
365. Joung, J., et al., *Genome-scale CRISPR-Cas9 knockout and transcriptional activation screening.* Nat Protoc, 2017. **12**(4): p. 828-863.
366. Barthel, A., et al., *Regulation of GLUT1 gene transcription by the serine/threonine kinase Akt1.* J Biol Chem, 1999. **274**(29): p. 20281-6.
367. Muilenburg, D., et al., *Role of autophagy in apoptotic regulation by Akt in pancreatic cancer.* Anticancer Res, 2014. **34**(2): p. 631-7.
368. Dede, M., E. Kim, and T. Hart, *Biases and Blind-Spots in Genome-Wide CRISPR Knockout Screens.* bioRxiv, 2020: p. 2020.01.16.909606.
369. Zhou, Y., et al., *Metascape provides a biologist-oriented resource for the analysis of systems-level datasets.* Nat Commun, 2019. **10**(1): p. 1523.
370. Tzelepis, K., et al., *A CRISPR Dropout Screen Identifies Genetic Vulnerabilities and Therapeutic Targets in Acute Myeloid Leukemia.* Cell Rep, 2016. **17**(4): p. 1193-1205.

371. Zuber, J., et al., *RNAi screen identifies Brd4 as a therapeutic target in acute myeloid leukaemia.* Nature, 2011. **478**(7370): p. 524-8.
372. Snel, B., et al., *STRING: a web-server to retrieve and display the repeatedly occurring neighbourhood of a gene.* Nucleic Acids Res, 2000. **28**(18): p. 3442-4.
373. Szklarczyk, D., et al., *STRING v11: protein-protein association networks with increased coverage, supporting functional discovery in genome-wide experimental datasets.* Nucleic Acids Res, 2019. **47**(D1): p. D607-D613.
374. Szklarczyk, D., et al., *The STRING database in 2021: customizable protein-protein networks, and functional characterization of user-uploaded gene/measurement sets.* Nucleic Acids Res, 2021. **49**(D1): p. D605-D612.
375. Shannon, P., et al., *Cytoscape: a software environment for integrated models of biomolecular interaction networks.* Genome Res, 2003. **13**(11): p. 2498-504.
376. Michlits, G., et al., *Multilayered VBC score predicts sgRNAs that efficiently generate loss-of-function alleles.* Nat Methods, 2020. **17**(7): p. 708-716.
377. Henkel, L., et al., *Genome-scale CRISPR screening at high sensitivity with an empirically designed sgRNA library.* BMC Biol, 2020. **18**(1): p. 174.
378. Aoidi, R., A. Maltais, and J. Charron, *Functional redundancy of the kinases MEK1 and MEK2: Rescue of the Mek1 mutant phenotype by Mek2 knock-in reveals a protein threshold effect.* Sci Signal, 2016. **9**(412): p. ra9.
379. Pages, G., et al., *Defective thymocyte maturation in p44 MAP kinase (Erk 1) knockout mice.* Science, 1999. **286**(5443): p. 1374-7.
380. Saba-El-Leil, M.K., et al., *An essential function of the mitogen-activated protein kinase Erk2 in mouse trophoblast development.* EMBO Rep, 2003. **4**(10): p. 964-8.
381. Peschard, P., et al., *Genetic deletion of RALA and RALB small GTPases reveals redundant functions in development and tumorigenesis.* Curr Biol, 2012. **22**(21): p. 2063-8.
382. Engelman, J.A., et al., *Effective use of PI3K and MEK inhibitors to treat mutant Kras G12D and PIK3CA H1047R murine lung cancers.* Nat Med, 2008. **14**(12): p. 1351-6.
383. She, Q.B., et al., *4E-BP1 is a key effector of the oncogenic activation of the AKT and ERK signaling pathways that integrates their function in tumors.* Cancer Cell, 2010. **18**(1): p. 39-51.
384. Junttila, M.R., et al., *Modeling targeted inhibition of MEK and PI3 kinase in human pancreatic cancer.* Mol Cancer Ther, 2015. **14**(1): p. 40-7.
385. Bedard, P.L., et al., *A phase Ib dose-escalation study of the oral pan-PI3K inhibitor buparlisib (BKM120) in combination with the oral MEK1/2 inhibitor trametinib (GSK1120212) in patients with selected advanced solid tumors.* Clin Cancer Res, 2015. **21**(4): p. 730-8.
386. Tolcher, A.W., et al., *Antitumor activity in RAS-driven tumors by blocking AKT and MEK.* Clin Cancer Res, 2015. **21**(4): p. 739-48.
387. Chung, V., et al., *Effect of Selumetinib and MK-2206 vs Oxaliplatin and Fluorouracil in Patients With Metastatic Pancreatic Cancer After Prior Therapy: SWOG S1115 Study Randomized Clinical Trial.* JAMA Oncol, 2017. **3**(4): p. 516-522.
388. Goncalves, E., et al., *Drug mechanism-of-action discovery through the integration of pharmacological and CRISPR screens.* Mol Syst Biol, 2020. **16**(7): p. e9405.
389. Lin, A., et al., *Off-target toxicity is a common mechanism of action of cancer drugs undergoing clinical trials.* Sci Transl Med, 2019. **11**(509).

390. Alabi, S., et al., *Mutant-selective degradation by BRAF-targeting PROTACs.* Nat Commun, 2021. **12**(1): p. 920.
391. Jaaks, P., et al., *Effective drug combinations in breast, colon and pancreatic cancer cells.* Nature, 2022. **603**(7899): p. 166-173.
392. Medema, R.H., et al., *AFX-like Forkhead transcription factors mediate cell-cycle regulation by Ras and PKB through p27kip1.* Nature, 2000. **404**(6779): p. 782-7.
393. Schmidt, M., et al., *Cell cycle inhibition by FoxO forkhead transcription factors involves downregulation of cyclin D.* Mol Cell Biol, 2002. **22**(22): p. 7842-52.
394. Wang, S., et al., *The Class I PI3K inhibitor S14161 induces autophagy in malignant blood cells by modulating the Beclin 1/Vps34 complex.* J Pharmacol Sci, 2017. **134**(4): p. 197-202.
395. Jia, M., et al., *Inhibition of PI3K/AKT/mTOR Signalling Pathway Activates Autophagy and Suppresses Peritoneal Fibrosis in the Process of Peritoneal Dialysis.* Front Physiol, 2022. **13**: p. 778479.
396. Soutourina, J., *Transcription regulation by the Mediator complex.* Nat Rev Mol Cell Biol, 2018. **19**(4): p. 262-274.
397. Wang, L. and S.Y. Dent, *Functions of SAGA in development and disease.* Epigenomics, 2014. **6**(3): p. 329-39.
398. Helmlinger, D. and L. Tora, *Sharing the SAGA.* Trends Biochem Sci, 2017. **42**(11): p. 850-861.
399. Stokoe, D., et al., *Dual role of phosphatidylinositol-3,4,5-trisphosphate in the activation of protein kinase B.* Science, 1997. **277**(5325): p. 567-70.
400. Bellacosa, A., et al., *Akt activation by growth factors is a multiple-step process: the role of the PH domain.* Oncogene, 1998. **17**(3): p. 313-25.
401. Hart, J.R. and P.K. Vogt, *Phosphorylation of AKT: a mutational analysis.* Oncotarget, 2011. **2**(6): p. 467-76.
402. Yao, C.A., et al., *Association of mSin1 with mTORC2 Ras and Akt reveals a crucial domain on mSin1 involved in Akt phosphorylation.* Oncotarget, 2017. **8**(38): p. 63392-63404.
403. Halaby, M.J., et al., *ATM protein kinase mediates full activation of Akt and regulates glucose transporter 4 translocation by insulin in muscle cells.* Cell Signal, 2008. **20**(8): p. 1555-63.
404. Ma, Y., Y. Vassetzky, and S. Dokudovskaya, *mTORC1 pathway in DNA damage response.* Biochim Biophys Acta Mol Cell Res, 2018. **1865**(9): p. 1293-1311.
405. Liu, L., et al., *DNA-PK promotes activation of the survival kinase AKT in response to DNA damage through an mTORC2-ECT2 pathway.* Sci Signal, 2022. **15**(715): p. eabh2290.
406. Ball, H.L., et al., *Function of a conserved checkpoint recruitment domain in ATRIP proteins.* Mol Cell Biol, 2007. **27**(9): p. 3367-77.
407. Hou, S.Q., et al., *PTEN in the maintenance of genome integrity: From DNA replication to chromosome segregation.* Bioessays, 2017. **39**(10).
408. Foo, W.C., et al., *Loss of phosphatase and tensin homolog expression is associated with recurrence and poor prognosis in patients with pancreatic ductal adenocarcinoma.* Hum Pathol, 2013. **44**(6): p. 1024-30.
409. Costa, C., et al., *PTEN Loss Mediates Clinical Cross-Resistance to CDK4/6 and PI3Kalpha Inhibitors in Breast Cancer.* Cancer Discov, 2020. **10**(1): p. 72-85.

Appendix

Appendix Table 1: Phospho arrays fold changes in Clone 7G9 vs Clone 5E2

ID	Phospho Protein	ID	Non Phospho Protein	Signal Ratio of Phospho Protein to Non-Phospho Protein		Fold Changes in Ratios
				Control Clone 5E2 Tam	Sample Clone 7G9 Tam	Clone 7G9 Tam vs Clone 5E2 Tam
979	14-3-3 beta/zeta (Phospho-Ser184/186)	1119	14-3-3 beta/zeta (Ab-184/186)	0.62	0.49	0.79
891	14-3-3 theta/tau (Phospho-Ser232)	285	14-3-3 theta/tau (Ab-232)	2.26	3.38	1.50
838	14-3-3 zeta (Phospho-Ser58)	702	14-3-3 zeta (Ab-58)		1.26	
892	14-3-3 zeta/delta (Phospho-Thr232)	286	14-3-3 zeta/delta (Ab-232)	0.15	0.13	0.89
1221	4E-BP1 (Phospho-Ser65)	758	4E-BP1 (Ab-65)	0.09	0.19	2.06
176	4E-BP1 (Phospho-Thr36)	61	4E-BP1 (Ab-36)	1.23	1.35	1.10
177	4E-BP1 (Phospho-Thr45)	62	4E-BP1 (Ab-45)	3.50	3.32	0.95
1222	4E-BP1 (Phospho-Thr70)	759	4E-BP1 (Ab-70)	1.27	1.16	0.92
893	6-phosphofructo-2-kinase/fructose-2,6-biphosphatase 2 (PFKFB2) (Phospho-Ser483)	287	6-phosphofructo-2-kinase/fructose-2,6-biphosphatase 2 (PFKFB2) (Ab-483)	0.52	0.66	1.27
1224	Abl1 (Phospho-Tyr204)	760	Abl1 (Ab-204)			
407	Abl1 (Phospho-Thr754/735)	1132	Abl1 (Ab-754/735)	0.55	0.51	0.93
1223	Abl1 (Phospho-Tyr412)					
1225	ACC1 (Phospho-Ser79)	761	ACC1 (Ab-79)	0.63	0.84	1.32
1056	ACC1 (Phospho-Ser80)	594	ACC1 (Ab-80)	0.16	0.22	1.37

116	ACK1 (Phospho-Tyr284)					
894	Actin Pan (a/b/g) (Phospho-Tyr55/53)	288	Actin Pan (a/b/g) (Ab-55/53)	0.71	0.86	1.20
125	ADD1 (Phospho-Ser726)	703	ADD1 (Ab-726)	1.83	2.07	1.13
998	AFX/FOXO4 (Phospho-Ser197)	1038	AFX/FOXO4 (Ab-197)			
1227	AKT1 (Phospho-Ser124)	763	AKT1 (Ab-124)	0.45	0.35	0.77
556	AKT1 (Phospho-Ser246)	1286	AKT1 (Ab-246)	0.76	0.95	1.25
473	AKT1 (Phospho-Thr308)	206	AKT1 (Ab-308)		0.15	
1067	AKT1 (Phospho-Tyr326)	442	AKT1 (Ab-326)			
1226	AKT1 (Phospho-Thr450)	762	AKT1 (Ab-450)	0.94	0.75	0.80
320	AKT1 (Phospho-Ser473)	205	AKT1 (Ab-473)	0.64	0.66	1.03
555	AKT1 (Phospho-Tyr474)	1285	AKT1 (Ab-474)	1.08	1.88	1.74
557	AKT1 (Phospho-Thr72)	1288	AKT1 (Ab-72)			
		1133	AKT1/2/3 (Ab-315)			
87	AKT1S1 (Phospho-Thr246)	931	AKT1S1 (Ab-246)	0.25	0.18	0.73
989	AKT2 (Phospho-Ser474)	1033	AKT2 (Ab-474)	0.76	0.88	1.15
117	ALK (Phospho-Tyr1507)	1141	ALK (Ab-1507)	1.43	2.67	1.87
118	ALK (Phospho-Tyr1604)	1142	ALK (Ab-1604)	0.43	0.56	1.29
1228	AMPK beta1 (Phospho-Ser182)	764	AMPK beta1 (Ab-182)	0.95	0.72	0.76
839	AMPK1/AMPK2 (Phospho-Thr183/172)	704	AMPK1/AMPK2 (Ab-183/172)	0.77	1.67	2.15
1174	AMPK1/AMPK2 (Phospho-Ser485/491)	422	AMPK1/AMPK2 (Ab-485/491)	0.65	0.71	1.10
840	Amyloid beta A4 (Phospho-Thr743/668)	705	Amyloid beta A4 (Ab-743/668)	0.63	0.55	0.87

833	Androgen Receptor (Phospho-Ser213)	692	Androgen Receptor (Ab-213)		1.15	
986	Androgen Receptor (Phospho-Ser650)	693	Androgen Receptor (Ab-650)		0.33	
895	A-RAF (Phospho-Tyr301/302)	289	A-RAF (Ab-301/302)	1.19	2.30	1.94
88	Arrestin-1 (Phospho-Ser412)	932	Arrestin-1 (Ab-412)	0.92	1.39	1.51
35	ASK1 (Phospho-Ser83)	863	ASK1 (Ab-83)	24.86	34.34	1.38
18	ASK1 (Phospho-Ser966)	866	ASK1 (Ab-966)	0.45	0.33	0.73
748	ATF1 (Phospho-Ser63)	469	ATF1 (Ab-63)		0.16	
166	ATF2 (Phospho-Ser112/94)	51	ATF2 (Ab-112/94)	0.49	0.27	0.56
162	ATF2 (Phospho-Ser62/44)	47	ATF2 (Ab-62/44)		0.09	
163	ATF2 (Phospho-Thr69/51)	48	ATF2 (Ab-69/51)	0.88	0.68	0.77
164	ATF2 (Phospho-Thr71/53)	49	ATF2 (Ab-71/53)	1.29	1.45	1.12
165	ATF2 (Phospho-Thr73/55)	50	ATF2 (Ab-73/55)	1.03	1.01	0.99
319	ATF4 (Phospho-Ser245)	204	ATF4 (Ab-245)	0.83	1.52	1.84
		1028	ATM (Ab-1981)			
1086	ATP1A1/Na+K+ ATPase1 (Phospho-Ser23)	801	ATP1A1/Na+K+ ATPase1 (Ab-23)	1.49	1.01	0.68
751	ATPase (Phospho-Ser16)	471	ATPase (Ab-16)	0.82	1.15	1.41
919	ATP-Citrate Lyase (Phospho-Ser454)	634	ATP-Citrate Lyase (Ab-454)	0.81	0.43	0.53
896	ATRIP (Phospho-Ser68/72)	290	ATRIP (Ab-68/72)	0.12	0.07	0.59
1255	AurA (Phospho-Thr288)	967	AurA (Ab-288)	0.53	0.69	1.29
625	AurA (Phospho-Ser342)	969	AurA (Ab-342)	0.87	0.86	0.99
1254	AurB (Phospho-Tyr12)	970	AurB (Ab-12)			
1253	AurB (Phospho-Thr232)	968	AurB (Ab-232)			
		971	AurB/C (Ab-202/175)			

277	AXL (Phospho-Tyr691)					
485	BAD (Phospho-Ser112)	346	BAD (Ab-112)	0.61	0.55	0.91
1069	BAD (Phospho-Ser134)	444	BAD (Ab-134)	1.10	0.97	0.89
486	BAD (Phospho-Ser136)	347	BAD (Ab-136)	1.17	1.16	0.99
487	BAD (Phospho-Ser155)	348	BAD (Ab-155)			
1068	BAD (Phospho-Ser91/128)	443	BAD (Ab-91/128)	0.84	0.50	0.59
212	BAX (Phospho-Thr167)	291	BAX (Ab-167)	0.49	0.30	0.63
482	BCL-2 (Phospho-Thr56)	343	BCL-2 (Ab-56)	0.46	0.44	0.94
897	BCL-2 (Phospho-Thr69)	292	BCL-2 (Ab-69)			
483	BCL-2 (Phospho-Ser70)	344	BCL-2 (Ab-70)	1.64	1.59	0.97
89	BCL-2 (Phospho-Ser87)					
		1306	BCL-6 (Ab-333)			
898	BCL-XL (Phospho-Thr47)	293	BCL-XL (Ab-47)	0.07	0.08	1.17
484	BCL-XL (Phospho-Ser62)	293	BCL-XL (Ab-47)	0.19	0.26	1.35
24	BCR (Phospho-Tyr177)	1206	BCR (Ab-177)	0.49	0.55	1.11
123	BCR (Phospho-Tyr360)	1147	BCR (Ab-360)	1.92	3.35	1.74
90	BID (Phospho-Ser78)	933	BID (Ab-78)	0.38	0.42	1.11
676	BIM (Phospho-Ser69/65)	540	BIM (Ab-69/65)		1.00	
282	BLNK (Phospho-Tyr84)	1143	BLNK (Ab-96)	0.65	0.42	0.64
119	BLNK (Phospho-Tyr96)	1143	BLNK (Ab-96)	0.65	0.86	1.32
408	B-RAF (Phospho-Ser446)	1134	B-RAF (Ab-446)	0.57	0.63	1.11
899	B-RAF (Phospho-Thr598)	294	B-RAF (Ab-598)	0.11	0.08	0.72
900	B-RAF (Phospho-Ser601)	295	B-RAF (Ab-601)	0.50	0.51	1.02
327	BRCA1 (Phospho-Ser1423)					

583	BRCA1 (Phospho-Ser1457)	1307	BRCA1 (Ab-1457)		0.43	
831	BRCA1 (Phospho-Ser1524)	869	BRCA1 (Ab-1524)		0.11	
124	Breast tumor kinase (Phospho-Tyr447)					
1020	BTK (Phospho-Tyr223)	881	BTK (Ab-223)		12.46	
1263	BTK (Phospho-Tyr551)	881	BTK (Ab-223)		0.80	
558	c-Abl (Phospho-Tyr245)	1034	c-Abl (Ab-412)	0.34	0.30	0.88
990	c-Abl (Phospho-Tyr412)	1034	c-Abl (Ab-412)	0.30	0.27	0.91
1070	Calmodulin (Phospho-Thr79/Ser81)	445	Calmodulin (Ab-79/81)		0.10	
111	Calsenilin/KCNIP3 (Phospho-Ser63)	795	Calsenilin/KCNIP3 (Ab-63)	0.30	0.39	1.30
1071	CaMK1-alpha (Phospho-Thr177)	446	CaMK1-alpha (Ab-177)	0.86	0.84	0.97
675	CaMK2A (Phospho-Thr286)	539	CaMK2A (Ab-286)		0.55	
1051	CaMK2 alpha/beta/delta (Phospho-Thr305)					
409	CaMK2-beta/gamma/delta (Phospho-Thr287)	1135	CaMK2-beta/gamma/delta (Ab-287)	0.23	0.26	1.14
1072	CaMK4 (Phospho-Thr196/200)	447	CaMK4 (Ab-196/200)	0.79	1.11	1.41
245	Caspase 1 (Phospho-Ser376)	948	Caspase 1 (Ab-376)	0.45	0.63	1.39
246	Caspase 2 (Phospho-Ser157)	949	Caspase 2 (Ab-157)	1.67	0.94	0.57
1076	Caspase 3 (Phospho-Ser150)	451	Caspase 3 (Ab-150)			
1057	Caspase 6 (Phospho-Ser257)	595	Caspase 6 (Ab-Ser257)	0.53	0.91	1.71
1058	Caspase 8 (Phospho-Ser347)	428	Caspase 8 (Ab-347)	0.73	0.74	1.01
1074	Caspase 9 (Phospho-Ser144)	449	Caspase 9 (Ab-144)			
1075	Caspase 9 (Phospho-Ser196)	450	Caspase 9 (Ab-196)	0.34	0.39	1.14
1059	Caspase 9 (Phospho-Thr125)	596	Caspase 9 (Ab-125)			

1073	Caspase 9 (Phospho-Tyr153)	448	Caspase 9 (Ab-153)	0.47	0.38	0.81
1077	Catalase (Phospho-Tyr385)	452	Catalase (Ab-385)	0.23	0.24	1.04
172	Catenin beta (Phospho-Ser33)	425	Catenin beta (Ab-33)	0.62	0.54	0.87
173	Catenin beta (Phospho-Ser37)	58	Catenin beta (Ab-37)			
830	Catenin beta (Phospho-Thr41/Ser45)	691	Catenin beta (Ab-41/45)		0.73	
398	Catenin beta (Phospho-Tyr489)	1120	Catenin beta (Ab-489)			
1078	Catenin beta (Phospho-Tyr654)	453	Catenin beta (Ab-654)	0.63	0.49	0.79
1245	Catenin delta-1 (Phospho-Tyr228)	617	Catenin delta-1 (Ab-228)	1.67	1.79	1.08
658	Caveolin-1 (Phospho-Tyr14)	700	Caveolin-1 (Ab-14)		0.55	
753	CBL (Phospho-Tyr700)					
752	CBL (Phospho-Tyr774)					
749	CD19 (Phospho-Tyr531)	470	CD19 (Ab-531)		1.13	
1094	CD22/BL-CAM (Phospho-Tyr807)					
1079	CD227/mucin 1 (Phospho-Tyr1243)	606	CD227/mucin 1 (Ab-1243)	1.26	1.28	1.01
1080	CD28 (Phospho-Tyr218)					
		1289	CD32 (FcgammaRIIb) (Ab-292)			
91	CD3Z (Phospho-Tyr142)	934	CD3Z (Ab-142)	0.59	0.87	1.47
1233	CD4 (Phospho-Ser433)	607	CD4 (Ab-433)	0.14	0.17	1.21
1234	CD45 (Phospho-Ser1007)					
126	CD5 (Phospho-Tyr453)	1149	CD5 (Ab-453)	0.42	0.42	1.01
1235	CDC25A (Phospho-Ser124)	608	CDC25A (Ab-124)			
		1121	CDC25A (Ab-178)			
999	CDC25A (Phospho-Ser75)	1039	CDC25A (Ab-75)	0.74	0.37	0.51

1060	CDC25B (Phospho-Ser323)	429	CDC25B (Ab-323)	0.96	0.80	0.83
1236	CDC25B (Phospho-Ser353)	609	CDC25B (Ab-353)			
832	CDC25C (Phospho-Ser216)	1026	CDC25C (Ab-216)	0.06	0.07	1.05
559	CDC25C (Phospho-Thr48)	1026	CDC25C (Ab-216)	0.06	0.06	1.03
92	CDK1/CDC2 (Phospho-Thr14)	935	CDK1/CDC2 (Ab-14)	1.57	3.08	1.96
329	CDK1/CDC2 (Phospho-Tyr15)	214	CDK1/CDC2 (Ab-15)	1.54	1.55	1.01
996	CDK2 (Phospho-Thr160)	699	CDK2 (Ab-160)	0.69	1.12	1.61
275	CDK5 (Phospho-Tyr15)	1314	CDK5 (Ab-15)	0.14	0.12	0.86
1237	CDK7 (Phospho-Thr170)	610	CDK7 (Ab-170)		0.67	
1001	Chk1 (Phospho-Ser280)	853	Chk1 (Ab-280)			
1238	Chk1 (Phospho-Ser286)	611	Chk1 (Ab-286)	0.35	0.37	1.06
560	Chk1 (Phospho-Ser296)					
1239	Chk1 (Phospho-Ser301)					
1002	Chk1 (Phospho-Ser317)	854	Chk1 (Ab-317)	0.65	0.81	1.25
987	Chk1 (Phospho-Ser345)	1027	Chk1 (Ab-345)			
901	Chk2 (Phospho-Thr383)	296	Chk2 (Ab-383)	0.15	0.11	0.70
1229	Chk2 (Phospho-Thr387)	765	Chk2 (Ab-387)	1.08	1.17	1.08
1159	Chk2 (Phospho-Ser516)	857	Chk2 (Ab-516)			
479	Chk2 (Phospho-Thr68)	523	Chk2 (Ab-68)		0.05	
158	c-Jun (Phospho-Ser243)	43	c-Jun (Ab-243)		0.13	
1	c-Jun (Phospho-Ser63)	1178	c-Jun (Ab-63)	0.74	0.79	1.07
3	c-Jun (Phospho-Ser73)					
157	c-Jun (Phospho-Thr239)	42	c-Jun (Ab-239)	1.39	1.40	1.00
154	c-Jun (Phospho-Thr91)	39	c-Jun (Ab-91)			

155	c-Jun (Phospho-Thr93)	40	c-Jun (Ab-93)	1.58	0.65	0.41
156	c-Jun (Phospho-Tyr170)	41	c-Jun (Ab-170)	0.65	0.75	1.16
1089	CK1-A (Phospho-Thr321)	802	CK1-A (Ab-321)	1.03	1.25	1.21
1092	CK1-A/A2 (Phospho-Tyr294)					
924	CK2-b (Phospho-Ser209)	640	CK2-b (Ab-209)	0.81	1.06	1.31
418	Claudin 3 (Phospho-Tyr219)	1317	Claudin 3 (Ab-219)	1.94	2.02	1.04
419	Claudin 6 (Phospho-Tyr219)					
420	Claudin 7 (Phospho-Tyr210)	1318	Claudin 7 (Ab-210)	3.04	4.00	1.32
1241	Coagulation Factor III (Phospho-Ser290)					
1000	Cofilin (Phospho-Ser3)	1040	Cofilin (Ab-3)	0.23	0.17	0.76
494	Connexin 43 (Phospho-Ser367)	359	Connexin 43 (Ab-367)	0.74	1.34	1.81
507	Cortactin (Phospho-Tyr421)	372	Cortactin (Ab-421)	0.91	0.90	0.99
508	Cortactin (Phospho-Tyr466)	373	Cortactin (Ab-466)	0.20	0.09	0.46
677	CPI17 alpha (Phospho-Thr38)	541	CPI17 alpha (Ab-38)		1.20	
1061	c-PLA2 (Phospho-Ser505)	597	c-PLA2 (Ab-505)	1.50	1.18	0.78
226	CREB (Phospho-Ser121)	936	CREB (Ab-121)			
509	CREB (Phospho-Ser129)	374	CREB (Ab-129)		1.49	
318	CREB (Phospho-Ser133)	203	CREB (Ab-133)		39.21	
841	CREB (Phospho-Ser142)	706	CREB (Ab-142)	1.06		
399	CREB (Phospho-Thr100)	1122	CREB (Ab-100)	1.61	1.64	1.02
1022	CrkII (Phospho-Tyr221)	883	CrkII (Ab-221)	0.27	0.27	1.00
1023	CrkL (Phospho-Tyr207)					
1242	CXCR4 (Phospho-Ser339)					

1214	Cyclin B1 (Phospho-Ser126)	430	Cyclin B1 (Ab-126)	0.60	0.53	0.88
562	Cyclin B1 (Phospho-Ser147)	132	Cyclin B1 (Ab-147)		3.13	
584	Cyclin C (Phospho-Ser275)					
1230	Cyclin D1 (Phospho-Thr286)	766	Cyclin D1 (Ab-286)	0.59	0.50	0.84
1230	Cyclin D1 (Phospho-Thr286)	613	Cyclin D1 (Ab-90)	1.42	1.55	1.10
		1308	Cyclin D2 (Ab-280)			
1231	Cyclin D3 (Phospho-Thr283)	767	Cyclin D3 (Ab-283)	0.88	0.97	1.10
1044	Cyclin E1 (Phospho-Thr395)	431	Cyclin E1 (Ab-395)	1.75	2.21	1.26
563	Cyclin E1 (Phospho-Thr77)	133	Cyclin E1 (Ab-77)	0.14	0.13	0.97
147	Cyclin E2 (Phospho-Thr392)	614	Cyclin E2 (Ab-392)	0.86	1.26	1.47
510	DAB1 (Phospho-Tyr220)	375	DAB1 (Ab-220)	0.34	0.34	1.02
495	DAB1 (Phospho-Tyr232)	360	DAB1 (Ab-232)		1.22	
128	DAPP1 (Phospho-Tyr139)	1151	DAPP1 (Ab-139)	1.02	1.37	1.34
663	DARPP-32 (Phospho-Thr34)	376	DARPP-32 (Ab-34)	0.52	0.46	0.89
842	DARPP-32 (Phospho-Thr75)	707	DARPP-32 (Ab-75)	2.12	2.16	1.02
1232	DAXX (Phospho-Ser668)					
129	DDX5/DEAD-box protein 5 (Phospho-Tyr593)	1152	DDX5/DEAD-box protein 5 (Ab-593)	0.50	0.42	0.84
1248	DNA-PK (Phospho-Thr2638)	620	DNA-PK (Ab-2638)	0.69	0.81	1.17
1247	DNA-PK (Phospho-Thr2647)	619	DNA-PK (Ab-2647)		1.21	
		621	DNA-PK (Ab-2056)			
664	Dok-1 (Phospho-Tyr362)	377	Dok-1 (Ab-362)	0.48	0.61	1.26
665	Dok-1 (Phospho-Tyr398)	530	Dok-1 (Ab-398)	0.29	0.19	0.67
666	Dok-2 (Phospho-Tyr299)	531	Dok-2 (Ab-299)	1.05	0.67	0.63

74	DYN1 (Phospho-Ser774)	769	DYN1 (Ab-774)	0.20	0.17	0.85
75	E2F1 (Phospho-Thr433)	770	E2F1 (Ab-433)	0.15	0.22	1.49
1215	EEF2 (Phospho-Thr56)	598	EEF2 (Ab-56)	0.61	0.91	1.48
1176	eEF2K (Phospho-Ser366)	884	eEF2K (Ab-366)	0.37	0.51	1.36
648	EGFR (Phospho-Ser1070)	357	EGFR (Ab-1070)	0.06	0.06	0.94
843	EGFR (Phospho-Thr678)	708	EGFR (Ab-678)	0.96	1.66	1.72
889	EGFR (Phospho-Thr693)	709	EGFR (Ab-693)	0.30	0.18	0.62
227	EGFR (Phospho-Tyr1016)	937	EGFR (Ab-1016)	0.72	1.10	1.54
1249	EGFR (Phospho-Tyr1069)	622	EGFR (Ab-1069)			
649	EGFR (Phospho-Tyr1092)	358	EGFR (Ab-1092)	0.13	0.11	0.86
500	EGFR (Phospho-Tyr1110)	365	EGFR (Ab-1110)	0.71	1.12	1.57
174	EGFR (Phospho-Tyr1172)	59	EGFR (Ab-1172)	0.71		
182	EGFR (Phospho-Tyr1197)	67	EGFR (Ab-1197)	1.09	0.83	0.77
183	EGFR (Phospho-Tyr869)	68	EGFR (Ab-869)	0.10	0.07	0.72
		1123	EGFR (Ab-998)			
667	eIF2A (Phospho-Ser51)	532	eIF2A (Ab-51)	0.50	0.39	0.78
564	eIF4B (Phospho-Ser422)					
187	eIF4E (Phospho-Ser209)	72	eIF4E (Ab-209)	0.89	0.88	0.98
565	eIF4G (Phospho-Ser1108)	134	eIF4G (Ab-1108)	0.57	0.82	1.43
4	Elk1 (Phospho-Ser383)	1181	Elk1 (Ab-383)	0.56	0.69	1.23
303	Elk1 (Phospho-Ser389)	188	Elk1 (Ab-389)			
304	Elk1 (Phospho-Thr417)	189	Elk1 (Ab-417)	0.58	0.47	0.81
1166	eNOS (Phospho-Ser1177)	1197	eNOS (Ab-1177)	0.78	1.06	1.35
256	eNOS (Phospho-Ser615)	960	eNOS (Ab-615)	1.21	1.42	1.17

328	eNOS (Phospho-Thr495)	213	eNOS (Ab-495)	1.44		
		961	eNOS (Ab-1179)			
1097	EPB41 (Phospho-Tyr418/660)	810	EPB41 (Ab-418/660)	0.97	1.29	1.34
925	EPHA2/3/4 (Phospho-Tyr588/596)	641	EPHA2/3/4 (Ab-588/596)	0.40	0.34	0.84
926	EPHB1/2 (Phospho-Tyr594/604)	642	EPHB1/2 (Ab-594/604)			
927	Ephrin B1 (Phospho-Tyr317)	643	Ephrin B1 (Ab-317)	0.68	0.83	1.22
1096	Ephrin B1/B2/B3 (Phospho-Tyr324)					
844	Ephrin B2 (Phospho-Tyr330)	463	Ephrin B2 (Ab-330)		0.24	
928	Epo-R (Phospho-Tyr368)	796	Epo-R (Ab-368)	0.95	0.71	0.74
1250	ERK3 (Phospho-Ser189)	623	ERK3 (Ab-189)			
1251	ERK8 (Phospho-Thr175/Tyr177)					
488	Estrogen Receptor-alpha (Phospho-Ser104)	349	Estrogen Receptor-alpha (Ab-104)	0.08	0.07	0.82
489	Estrogen Receptor-alpha (Phospho-Ser106)	350	Estrogen Receptor-alpha (Ab-106)	0.08	0.04	0.49
490	Estrogen Receptor-alpha (Phospho-Ser118)	351	Estrogen Receptor-alpha (Ab-118)	1.53	3.28	2.15
491	Estrogen Receptor-alpha (Phospho-Ser167)	352	Estrogen Receptor-alpha (Ab-167)			
120	ETK (Phospho-Tyr40)	1144	ETK (Ab-40)	2.20	1.31	0.59
120	ETK (Phospho-Tyr40)	1148	ETK (Ab-566)	2.36	0.91	0.39
27	Ezrin (Phospho-Thr566)	1209	Ezrin (Ab-566)	0.16	0.12	0.76
481	Ezrin (Phospho-Tyr353)	682	Ezrin (Ab-353)	0.78	0.99	1.26
400	Ezrin (Phospho-Tyr478)	1124	Ezrin (Ab-478)	0.64	0.53	0.83
1260	FADD (Phospho-Ser194)					

93	FAK (Phospho-Ser910)	624	FAK (Ab-910)	0.08	0.12	1.50
888	FAK (Phospho-Tyr397)	55	FAK (Ab-397)		0.51	
228	FAK (Phospho-Tyr407)	938	FAK (Ab-407)		1.06	
76	FAK (Phospho-Tyr576)	771	FAK (Ab-576)	0.90	0.89	0.99
477	FAK (Phospho-Tyr861)	512	FAK (Ab-861)	1.13	1.36	1.21
988	FAK (Phospho-Tyr925)	1029	FAK (Ab-925)		0.43	
593	FAS (Phospho-Tyr291)	777	FAS (Ab-291)	0.98	0.53	0.54
278	FER (Phospho-Tyr402)	1316	FER (Ab-402)	1.60	1.74	1.09
324	FGFR1 (Phospho-Tyr154)	209	FGFR1 (Ab-154)	1.24	1.63	1.31
755	FGFR1 (Phospho-Tyr654)					
754	FGFR1 (Phospho-Tyr766)	472	FGFR1 (Ab-766)	0.27	0.44	1.63
1177	Filamin A (Phospho-Ser2152)	885	Filamin A (Ab-2152)	0.31	0.26	0.86
829	FKHR (Phospho-Ser256)	868	FKHR (Ab-256)	0.32	0.49	1.56
997	FKHR (Phospho-Ser319)	1037	FKHR (Ab-319)			
230	FKHR/FOXO1A (Phospho-Ser329)	940	FKHR/FOXO1A (Ab-329)	0.56		
1167	FKHRL1/FOXO3A (Phospho-Ser253)	1198	FKHRL1/FOXO3 A (Ab-253)		0.20	
1180	FLT3 (Phospho-Tyr599)	983	FLT3 (Ab-599)	1.49	0.99	0.66
279	FLT3 (Phospho-Tyr842)	983	FLT3 (Ab-599)	1.22	1.45	1.19
280	FLT3 (Phospho-Tyr969)	983	FLT3 (Ab-599)		1.20	
77	Fos (Phospho-Ser362)					
578	Fos (Phospho-Thr232)	1304	Fos (Ab-232)	0.31	0.42	1.34
		454	Fos (Ab-374)			
94	FosB (Phospho-Ser27)	778	FosB (Ab-27)	1.19	1.24	1.04
229	FOXO1/3/4-pan (Phospho-Thr24/32)	939	FOXO1/3/4-pan (Ab-24/32)	0.34		

231	FOXO1A/3A (Phospho-Ser322/325)					
1095	FRS2 (Phospho-Tyr436)					
750	Fyn (Phospho-Tyr530)					
650	G3BP-1 (Phospho-Ser232)	690	G3BP-1 (Ab-232)	0.28	0.36	1.27
679	Gab1 (Phospho-Tyr627)	543	Gab1 (Ab-627)	0.22	0.52	2.31
902	Gab1 (Phospho-Tyr659)	297	Gab1 (Ab-659)	0.59	0.77	1.31
580	Gab2 (Phospho-Ser159)	1305	Gab2 (Ab-159)	1.39	1.17	0.84
585	Gab2 (Phospho-Tyr643)	455	Gab2 (Ab-623)	1.59	2.59	1.63
845	GABA-RB (Phospho-Ser434)	710	GABA-RB (Ab-434)			
669	GAP43 (Phospho-Ser41)	534	GAP43 (Ab-41)	0.28	0.42	1.47
307	GATA1 (Phospho-Ser142)	192	GATA1 (Ab-142)	0.98	0.97	0.99
308	GATA1 (Phospho-Ser310)	193	GATA1 (Ab-310)		0.61	
497	GluR1 (Phospho-Ser849)	362	GluR1 (Ab-849)	0.02	0.03	1.27
498	GluR1 (Phospho-Ser863)	363	GluR1 (Ab-863)		2.09	
680	GluR2 (Phospho-Ser880)	544	GluR2 (Ab-880)	0.08	0.06	0.79
247	GRB10/Growth factor receptor-bound protein 10 (Phospho-Tyr67)	950	GRB10/Growth factor receptor-bound protein 10 (Ab-67)	1.16	0.93	0.80
78	GRF-1 (Phospho-Tyr1105)					
95	GRK1 (Phospho-Ser21)	779	GRK1 (Ab-21)			
232	GRK2 (Phospho-Ser29)	941	GRK2 (Ab-29)	0.25	0.29	1.16
582	GRK2 (Phospho-Ser685)	941	GRK2 (Ab-29)	0.23	0.10	0.44
7	GSK3 alpha (Phospho-Ser21)	1184	GSK3 alpha (Ab-21)	0.66	0.67	1.02

890	GSK3 alpha/beta (Phospho-Tyr216/279)	427	GSK3 alpha/beta (Ab-216/279)			
2	GSK3 beta (Phospho-Ser9)	1179	GSK3 beta (Ab-9)		1.70	
248	GTPase activating protein (Phospho-Ser387)	951	GTPase activating protein (Ab-387)	0.83	0.82	0.99
130	HCK (Phospho-Tyr410)					
903	HDAC1 (Phospho-Ser421)	298	HDAC1 (Ab-421)	0.06	0.07	1.17
887	HDAC2 (Phospho-Ser394)	1036	HDAC2 (Ab-394)	1.30	2.47	1.90
96	HDAC3 (Phospho-Ser424)	780	HDAC3 (Ab-424)	0.47	0.50	1.06
19	HDAC4 (Phospho-Ser632)	870	HDAC4 (Ab-632)		0.80	
79	HDAC5 (Phospho-Ser259)	772	HDAC5 (Ab-259)		1.28	
20	HDAC5 (Phospho-Ser498)	871	HDAC5 (Ab-498)	0.75	0.83	1.11
97	HDAC6 (Phospho-Ser22)	781	HDAC6 (Ab-22)	0.49	0.47	0.96
21	HDAC8 (Phospho-Ser39)	1024	HDAC8 (Ab-39)	0.59	0.98	1.67
587	HER2 (Phospho-Thr686)	782	HER2 (Ab-686)	1.06	0.64	0.60
646	HER2 (Phospho-Tyr1221/Tyr1222)	355	HER2 (Ab-1221/1222)	0.19	0.17	0.89
647	HER2 (Phospho-Tyr1248)	356	HER2 (Ab-1248)	0.49	0.45	0.90
645	HER2 (Phospho-Tyr877)	354	HER2 (Ab-877)	0.72	0.71	0.98
		1125	HER2 (Ab-1112)			
98	HER3/ErbB3 (Phospho-Tyr1222)	783	HER3/ErbB3 (Ab-1222)	1.00	1.15	1.15
99	HER3/ErbB3 (Phospho-Tyr1289)	784	HER3/ErbB3 (Ab-1289)	1.34	1.15	0.86
100	HER4/ErbB4 (Phospho-Tyr1284)	785	HER4/ErbB4 (Ab-1284)	2.48	2.77	1.12
504	Histone H2A.X (Phospho-Ser139)	369	Histone H2A.X (Ab-139)	0.23	0.26	1.10
34	Histone H3.1 (Phospho-Ser10)	867	Histone H3.1 (Ab-10)			

309	HNF4 alpha (Phospho-Ser313)	194	HNF4 alpha (Ab-313)	1.44	1.31	0.91
267	HRS (Phospho-Tyr334)	1156	HRS (Ab-334)	2.33	1.85	0.79
499	HSF1 (Phospho-Ser303)	364	HSF1 (Ab-303)		0.61	
80	HSL (Phospho-Ser552/563)	773	HSL (Ab-552/563)	0.79	0.80	1.01
1216	HSL (Phospho-Ser554)	599	HSL (Ab-554)	0.94	0.57	0.61
22	HSP27 (Phospho-Ser15)	1025	HSP27 (Ab-15)	2.22	2.05	0.92
332	HSP27 (Phospho-Ser78)	217	HSP27 (Ab-78)			
333	HSP27 (Phospho-Ser82)	218	HSP27 (Ab-82)	0.63	0.37	0.58
249	HSP90 co-chaperone Cdc37 (Phospho-Ser13)	952	HSP90 co-chaperone Cdc37 (Ab-13)	0.57	0.74	1.29
1090	HSP90B (Phospho-Ser226)	803	HSP90B (Ab-226)	3.47	5.42	1.56
846	HSP90B (Phospho-Ser254)	711	HSP90B (Ab-254)			
651	ICAM-1 (Phospho-Tyr512)	694	ICAM-1 (Ab-512)			
281	ICK (Phospho-Tyr159)					
655	IGF1R (Phospho-Tyr1161)	516	IGF1R (Ab-1161)			
656	IGF1R (Phospho-Tyr1165/1166)	517	IGF1R (Ab-1165/1166)			
259	IGF2R (Phospho-Ser2409)	953	IGF2R (Ab-2409)			
		954	IGFBP-3 (Ab-183)			
1164	IkB-alpha (Phospho-Ser32/36)	862	IkB-alpha (Ab-32/36)	8.28	10.97	1.33
250	IkB-alpha (Phospho-Tyr305)					
1172	IkB-alpha (Phospho-Tyr42)	1203	IkB-alpha (Ab-42)	0.41	0.48	1.18
847	IkB-beta (Phospho-Ser23)	774	IkB-beta (Ab-19)			
81	IkB-beta (Phospho-Thr19)	774	IkB-beta (Ab-19)	1.39	1.11	0.80
848	IkB-epsilon (Phospho-Ser22)	712	IkB-epsilon (Ab-22)	0.15	0.11	0.73

992	IKK-alpha (Phospho-Thr23)	1035	IKK-alpha (Ab-23)	0.39	0.39	0.99
82	IKK-alpha/beta (Phospho-Ser180/181)	776	IKK-alpha/beta (Ab-176/177)	0.11	0.22	1.94
82	IKK-alpha/beta (Phospho-Ser180/181)	775	IKK-alpha/beta (Ab-180/181)	0.92	1.38	1.49
83	IKK-beta (Phospho-Tyr188)	929	IKK-beta (Ab-188)	0.34	0.37	1.09
233	IKK-beta (Phospho-Tyr199)	942	IKK-beta (Ab-199)	0.17	0.17	1.03
84	IKK-gamma (Phospho-Ser31)	930	IKK-gamma (Ab-31)	0.09	0.14	1.56
257	IKK-gamma (Phospho-Ser85)	962	IKK-gamma (Ab-85)	0.36	0.35	0.98
268	IL-10R-alpha (Phospho-Tyr496)	1309	IL-10R-alpha (Ab-496)	0.48	0.69	1.43
269	IL-13R/CD213a1 (Phospho-Tyr405)	1310	IL-13R/CD213a1 (Ab-405)	2.08	3.01	1.45
1082	IL-2RA/CD25 (Phospho-Ser268)	798	IL-2RA/CD25 (Ab-268)			
1264	IL3RB (Phospho-Tyr593)	982	IL3RB (Ab-593)	0.44	0.50	1.14
270	IL-4R/CD124 (Phospho-Tyr497)	1311	IL-4R/CD124 (Ab-497)	1.05	0.80	0.76
271	IL7R/CD127 (Phospho-Tyr449)					
1256	Integrin beta-1 (Phospho-Thr788)	972	Integrin beta-1 (Ab-788)	0.33	0.28	0.84
1256	Integrin beta-1 (Phospho-Thr788)	973	Integrin beta-1 (Ab-789)	0.42	0.39	0.94
478	Integrin beta-3 (Phospho-Tyr773)	518	Integrin beta-3 (Ab-773)	0.88	0.83	0.93
670	Integrin beta-3 (Phospho-Tyr785)	535	Integrin beta-3 (Ab-785)			
272	Integrin beta-4 (Phospho-Tyr1510)	1312	Integrin beta-4 (Ab-1510)	1.26	2.33	1.85
768	Interferon-alpha/beta receptor alpha chain (Phospho-Tyr466)	797	Interferon-alpha/beta receptor alpha chain (Ab-466)			
1081	Interferon-gamma receptor alpha chain precursor (Phospho-Tyr457)	975	Interferon-gamma receptor alpha	1.48	1.34	0.91

			chain precursor (Ab-457)			
1265	IR (Phospho-Tyr1355)	984	IR (Ab-1361)	0.48	0.66	1.36
1266	IR (Phospho-Tyr1361)	984	IR (Ab-1361)	0.64	1.10	1.73
85	IRS-1 (Phospho-Ser1101)					
322	IRS-1 (Phospho-Ser307)	207	IRS-1 (Ab-307)	0.49	0.61	1.23
1004	IRS-1 (Phospho-Ser312)	1042	IRS-1 (Ab-312)	0.51	0.34	0.67
234	IRS-1 (Phospho-Ser323)	943	IRS-1 (Ab-323)	0.81	0.26	0.33
86	IRS-1 (Phospho-Ser612)					
184	IRS-1 (Phospho-Ser636)	69	IRS-1 (Ab-636)	0.86	0.61	0.71
185	IRS-1 (Phospho-Ser639)	70	IRS-1 (Ab-639)	0.07	0.04	0.51
566	IRS-1 (Phospho-Ser794)	135	IRS-1 (Ab-794)			
1161	JAK1 (Phospho-Tyr1022)	859	JAK1 (Ab-1022)	0.40	0.41	1.03
1163	JAK2 (Phospho-Tyr1007)	861	JAK2 (Ab-1007)	0.62	0.50	0.80
1162	JAK2 (Phospho-Tyr221)	860	JAK2 (Ab-221)			
235	JNK1/2/3 (Phospho-Thr183/Tyr185)	944	JNK1/2/3 (Ab-183/185)	2.34	1.55	0.66
160	JunB (Phospho-Ser259)	45	JunB (Ab-259)	0.90	0.69	0.76
159	JunB (Phospho-Ser79)	44	JunB (Ab-79)	0.99	0.92	0.93
161	JunD (Phospho-Ser255)	46	JunD (Ab-255)	0.58	0.70	1.22
849	Keratin 18 (Phospho-Ser33)	713	Keratin 18 (Ab-33)			
1243	Keratin 18 (Phospho-Ser52)	615	Keratin 18 (Ab-52)		2.78	
1244	Keratin 8 (Phospho-Ser432)	616	Keratin 8 (Ab-432)	3.16	2.87	0.91
850	Keratin 8 (Phospho-Ser73)	714	Keratin 8 (Ab-73)			
1268	KIT (Phospho-Tyr703)					

325	KIT (Phospho-Tyr721)	210	KIT (Ab-721)	0.40	0.39	0.99
1267	KIT (Phospho-Tyr936)	985	KIT (Ab-936)	2.69	1.90	0.71
1045	KSR (Phospho-Ser392)	432	KSR (Ab-392)		0.84	
273	Kv1.3/KCNA3 (Phospho-Tyr135)	1313	Kv1.3/KCNA3 (Ab-135)	0.64	0.94	1.47
274	Kv2.1/Kcnb1 (Phospho-Tyr128)					
1252	Lamin A (Phospho-Ser22)	814	Lamin A (Ab-22)		2.84	
756	Lamin A/C (Phospho-Ser392)	626	Lamin A/C (Ab-392)	0.04	0.03	0.80
		1301	LAT (Ab-161)			
567	LAT (Phospho-Tyr171)	136	LAT (Ab-171)		0.30	
236	LAT (Phospho-Tyr191)	945	LAT (Ab-191)	0.50	0.42	0.86
577	LCK (Phospho-Ser59)	1303	LCK (Ab-59)	1.08	0.92	0.85
238	LCK (Phospho-Tyr192)	947	LCK (Ab-192)	1.04	1.20	1.15
1157	LCK (Phospho-Tyr393)	1195	LCK (Ab-393)	0.04	0.04	0.88
237	LCK (Phospho-Tyr505)	946	LCK (Ab-505)	4.37	6.15	1.41
991	LIMK1 (Phospho-Thr508)	864	LIMK1 (Ab-508)	0.33	0.34	1.04
991	LIMK1 (Phospho-Thr508)	880	LIMK1/2 (Ab-508/505)	0.11	0.12	1.03
720	LKB1 (Phospho-Ser428)	137	LKB1 (Ab-428)	1.25	1.14	0.91
721	LKB1 (Phospho-Thr189)	138	LKB1 (Ab-189)	0.56	0.66	1.17
		1136	LKB1 (Ab-334)			
744	LYN (Phospho-Tyr507)	467	LYN (Ab-507)	0.11	0.05	0.44
410	MAP3K1/MEKK1 (Phospho-Thr1381)					
255	MAP3K7/TAK1 (Phospho-Thr184)	957	MAP3K7/TAK1 (Ab-184)	0.72	0.79	1.10
255	MAP3K7/TAK1 (Phospho-Thr184)	805	MAP3K7/TAK1 (Ab-187)	1.02	1.04	1.02
255	MAP3K7/TAK1 (Phospho-Thr184)	806	MAP3K7/TAK1 (Ab-439)	0.78	0.65	0.84
1021	MAP3K8/COT (Phospho-Thr290)	882	MAP3K8/COT (Ab-290)			

1021	MAP3K8/COT (Phospho-Thr290)	807	MAP3K8/COT (Ab-400)			
586	MAPKAPK2 (Phospho-Ser272)	456	MAPKAPK2 (Ab-272)	4.05	4.98	1.23
722	MAPKAPK2 (Phospho-Thr222)	456	MAPKAPK2 (Ab-272)		0.36	
1052	MAPKAPK2 (Phospho-Thr334)	456	MAPKAPK2 (Ab-272)	0.43	0.83	1.92
681	MARCKS (Phospho-Ser158)	545	MARCKS (Ab-158)		0.53	
501	MARCKS (Phospho-Ser163)	366	MARCKS (Ab-163)			
127	M-CSF Receptor (Phospho-Tyr561)	1150	M-CSF Receptor (Ab-561)	2.71	4.33	1.60
1269	M-CSF Receptor (Phospho-Tyr809)	1138	M-CSF Receptor (Ab-809)	1.42	1.99	1.40
239	MDM2 (Phospho-Ser166)	1100	MDM2 (Ab-166)	0.06	0.04	0.73
739	MDM4 (Phospho-Ser367)					
851	MEF2A (Phospho-Ser408)	715	MEF2A (Ab-408)	0.27	0.36	1.31
305	MEF2A (Phospho-Thr312)	190	MEF2A (Ab-312)	0.04	0.04	0.97
306	MEF2A (Phospho-Thr319)	191	MEF2A (Ab-319)	0.27	0.25	0.93
740	MEF2C (Phospho-Ser396)	457	MEF2C (Ab-396)	0.71	0.70	0.99
240	MEF2D (Phospho-Ser444)					
30	MEK1 (Phospho-Ser217)	1212	MEK1 (Ab-217)	0.32	0.36	1.10
1171	MEK1 (Phospho-Ser221)	1202	MEK1 (Ab-221)			
723	MEK1 (Phospho-Ser298)	139	MEK1 (Ab-298)	12.39	7.57	0.61
724	MEK1 (Phospho-Thr286)	140	MEK1 (Ab-286)	0.83	0.81	0.97
834	MEK1 (Phospho-Thr291)	546	MEK1 (Ab-291)	0.43	0.42	0.99
8	MEK2 (Phospho-Thr394)	1185	MEK2 (Ab-394)		1.51	
1093	MER/SKY (Phospho-Tyr749/Tyr681)					
1091	Merlin (Phospho-Ser10)	804	Merlin (Ab-10)	0.40	0.55	1.39

502	Merlin (Phospho-Ser518)	367	Merlin (Ab-518)			
1240	Met (Phospho-Tyr1003)	612	Met (Ab-1003)	0.76	0.80	1.06
181	Met (Phospho-Tyr1234)	66	Met (Ab-1234)	2.02	1.70	0.84
323	Met (Phospho-Tyr1349)	208	Met (Ab-1349)		0.55	
1270	Met (Phospho-Tyr1356)					
757	MITF (Phospho-Ser73)	627	MITF (Ab-73)	0.20	0.22	1.10
1158	MKK3/MAP2K3 (Phospho-Ser189)	856	MKK3/MAP2K3 (Ab-189)	0.62		
411	MKK3/MAP2K3 (Phospho-Thr222)	1137	MKK3/MAP2K3 (Ab-222)		0.84	
1085	MKK4/SEK1 (Phospho-Ser257)	800	MKK4/SEK1 (Ab-257)	1.19	0.99	0.83
17	MKK4/SEK1 (Phospho-Ser80)	462	MKK4/SEK1 (Ab-80)	0.12	0.08	0.66
1175	MKK4/SEK1 (Phospho-Thr261)	865	MKK4/SEK1 (Ab-261)			
886	MKK6/MAP2K6 (Phospho-Ser207)	423	MKK6/MAP2K6 (Ab-207)	0.43	0.28	0.66
412	MKK7/MAP2K7 (Phospho-Ser271)	1290	MKK7/MAP2K7 (Ab-271)	0.37	0.28	0.77
413	MKK7/MAP2K7 (Phospho-Thr275)	1290	MKK7/MAP2K7 (Ab-271)	1.13	0.95	0.84
251	MKP-1 (Phospho-Ser359)	955	MKP-1 (Ab-359)	0.42	0.29	0.69
741	MKP-1/2 (Phospho-Ser296/318)	458	MKP-1/2 (Ab-296/318)	0.64	0.65	1.02
1098	Mnk1 (Phospho-Thr385)	811	Mnk1 (Ab-385)	1.19	1.28	1.07
414	MSK1 (Phospho-Ser212)					
725	MSK1 (Phospho-Ser360)	141	MSK1 (Ab-360)	0.16	0.14	0.90
25	MSK1 (Phospho-Ser376)	1207	MSK1 (Ab-376)	0.77	0.75	0.97
726	MSK1 (Phospho-Thr581)	142	MSK1 (Ab-581)	0.42	0.46	1.10
415	MSK2 (Phospho-Thr568)					
920	Mst1/Mst2 (Phospho-Thr183)	635	Mst1/Mst2 (Ab-183)	0.80	1.07	1.34
175	mTOR (Phospho-Ser2448)	60	mTOR (Ab-2448)	0.93	1.03	1.11

727	mTOR (Phospho-Ser2481)	143	mTOR (Ab-2481)	0.73	0.89	1.22
258	mTOR (Phospho-Thr2446)	963	mTOR (Ab-2446)	1.88	0.91	0.48
302	Myc (Phospho-Ser373)	54	Myc (Ab-373)	0.49	0.43	0.88
852	Myc (Phospho-Ser62)	716	Myc (Ab-62)	0.61	0.53	0.88
168	Myc (Phospho-Thr358)	53	Myc (Ab-358)	0.07	0.07	0.93
167	Myc (Phospho-Thr58)	52	Myc (Ab-58)	0.67	0.58	0.87
921	Myosin regulatory light chain 2 (Phospho-Ser18)	636	Myosin regulatory light chain 2 (Ab-18)	1.05	0.81	0.77
910	MYPT1 (Phospho-Thr696)					
911	MYPT1 (Phospho-Thr853)					
		808	MYT1 (Ab-83)			
		459	NFAT3 (Ab-168/170)			
		1101	NFAT3 (Ab-676)			
241	NFAT4 (Phospho-Ser165)	1102	NFAT4 (Ab-165)	1.74	1.47	0.84
15	NFkB-p100/p52 (Phospho-Ser865)	1192	NFkB-p100/p52 (Ab-865)	0.20	0.30	1.54
16	NFkB-p100/p52 (Phospho-Ser869)	1193	NFkB-p100/p52 (Ab-869)		1.07	
252	NFkB-p100/p52 (Phospho-Ser872)					
150	NFkB-p105/p50 (Phospho-Ser337)	1194	NFkB-p105/p50 (Ab-337)	0.48	0.87	1.79
151	NFkB-p105/p50 (Phospho-Ser893)	36	NFkB-p105/p50 (Ab-893)			
152	NFkB-p105/p50 (Phospho-Ser907)	37	NFkB-p105/p50 (Ab-907)	1.73	1.31	0.75
1053	NFkB-p105/p50 (Phospho-Ser927)	588	NFkB-p105/p50 (Ab-927)	0.17	0.12	0.69
336	NFkB-p105/p50 (Phospho-Ser932)	221	NFkB-p105/p50 (Ab-932)	0.80	1.36	1.69
10	NFkB-p65 (Phospho-Thr254)	1187	NFkB-p65 (Ab-254)		0.21	
11	NFkB-p65 (Phospho-Ser276)	1188	NFkB-p65 (Ab-276)	0.81	1.08	1.34
496	NFkB-p65 (Phospho-Ser311)	361	NFkB-p65 (Ab-311)	1.28	1.64	1.29

12	NFkB-p65 (Phospho-Thr435)	1189	NFkB-p65 (Ab-435)	0.97	0.54	0.55
13	NFkB-p65 (Phospho-Ser468)	1190	NFkB-p65 (Ab-468)	1.98	2.43	1.23
345	NFkB-p65 (Phospho-Thr505)	1103	NFkB-p65 (Ab-505)	0.44	0.43	0.97
171	NFkB-p65 (Phospho-Ser529)	57	NFkB-p65 (Ab-529)	10.58	8.76	0.83
14	NFkB-p65 (Phospho-Ser536)	1191	NFkB-p65 (Ab-536)	0.72	0.63	0.87
		1126	NFkB-p65 (Ab-281)			
835	NMDAR1 (Phospho-Ser897)	547	NMDAR1 (Ab-897)		0.81	
264	NMDAR2A/B (Phospho-Tyr1246/1252)					
112	NMDAR2B (Phospho-Tyr1472)	1139	NMDAR2B (Ab-1472)		0.11	
1005	Opioid Receptor (Phospho-Ser375)	717	Opioid Receptor (Ab-375)	2.64	1.50	0.57
922	p130Cas (Phospho-Tyr165)	637	p130Cas (Ab-165)	1.76	1.86	1.06
745	p130Cas (Phospho-Tyr410)	464	p130Cas (Ab-410)	1.72	1.70	0.99
31	p21Cip1 (Phospho-Thr145)	1030	p21Cip1 (Ab-145)	0.78	0.77	0.99
32	p27Kip1 (Phospho-Ser10)	1031	p27Kip1 (Ab-10)			
33	p27Kip1 (Phospho-Thr187)	1032	p27Kip1 (Ab-187)	1.26	1.60	1.27
		1104	p300 (Ab-89)			
337	p38 MAPK (Phospho-Thr180)	424	p38 MAPK (Ab-180)			
338	p38 MAPK (Phospho-Tyr182)	222	p38 MAPK (Ab-182)	0.14	0.21	1.56
904	p38 MAPK (Phospho-Tyr322)	299	p38 MAPK (Ab-322)	1.14	0.58	0.51
330	p44/42 MAPK (Phospho-Thr202)	215	p44/42MAPK (Ab-202)	2.10	1.83	0.87
331	p44/42 MAPK (Phospho-Tyr204)	216	p44/42 MAPK (Ab-204)		1.69	
662	p53 (Phospho-Ser15)	521	p53 (Ab-15)			
815	p53 (Phospho-Thr18)	522	p53 (Ab-18)	0.23	0.23	1.03

242	p53 (Phospho-Ser20)	1105	p53 (Ab-20)	0.29	0.31	1.09
819	p53 (Phospho-Ser315)	527	p53 (Ab-315)	0.23	0.17	0.73
816	p53 (Phospho-Ser33)	524	p53 (Ab-33)			
401	p53 (Phospho-Ser366)					
817	p53 (Phospho-Ser37)	525	p53 (Ab-37)	1.95	1.57	0.81
		1128	p53 (Ab-376)			
402	p53 (Phospho-Ser378)	1129	p53 (Ab-378)			
		1127	p53 (Ab-387)			
243	p53 (Phospho-Ser392)	1106	p53 (Ab-392)	0.98	1.39	1.42
818	p53 (Phospho-Ser46)	526	p53 (Ab-46)	1.11	1.34	1.20
660	p53 (Phospho-Ser6)	519	p53 (Ab-6)			
661	p53 (Phospho-Ser9)	520	p53 (Ab-9)		0.54	
728	p53 (Phospho-Thr81)					
729	p63 (Phospho-Ser455)					
244	P70S6K (Phospho-Thr229)	1107	P70S6K (Ab-229)	0.49	0.44	0.91
378	P70S6K (Phospho-Ser371)	1108	P70S6K (Ab-371)	0.77	0.71	0.93
505	P70S6K (Phospho-Ser411)	370	P70S6K (Ab-411)			
380	P70S6K (Phospho-Ser418)	1109	P70S6K (Ab-418)			
1050	P70S6K (Phospho-Thr421)	426	P70S6K (Ab-421)	1.05	1.10	1.05
672	P70S6K (Phospho-Ser424)	537	P70S6K (Ab-424)	0.98	0.68	0.70
379	P70S6K (Phospho-Thr389)					
		1291	P70S6K (Ab-427)			
568	P70S6K-beta (Phospho-Ser423)	1292	P70S6K-beta (Ab-423)	1.05	1.09	1.04
476	P73 (Phospho-Tyr99)	511	P73 (Ab-99)	0.17	0.15	0.85
382	P90RSK (Phospho-Ser380)	1111	P90RSK (Ab-380)	0.66	0.92	1.41
381	P90RSK (Phospho-Thr359/Ser363)	1110	P90RSK (Ab-359/363)	0.10	0.20	2.00

383	P90RSK (Phospho-Thr573)	1112	P90RSK (Ab-573)	0.49	0.33	0.67
475	P95/NBS1 (Phospho-Ser343)	342	P95/NBS1 (Ab-343)	0.18	0.14	0.77
569	PAK1 (Phospho-Ser204)	1293	PAK1 (Ab-204)	0.63	0.90	1.42
384	PAK1 (Phospho-Thr212)	1113	PAK1 (Ab-212)	1.17	1.26	1.08
253	PAK1/2 (Phospho-Ser199)	956	PAK1/2 (Ab-199)	0.49	0.60	1.23
386	PAK1/2/3 (Phospho-Ser141)	1115	PAK1/2/3 (Ab-141)		0.50	
385	PAK1/2/3 (Phospho-Thr423/402/421)	1114	PAK1/2/3 (Ab-423/402/421)	0.04	0.04	1.20
570	PAK2 (Phospho-Ser192)	1294	PAK2 (Ab-192)	1.69	1.52	0.90
		1295	PAK2 (Ab-197)			
730	PAK2 (Phospho-Ser20)					
571	PAK3 (Phospho-Ser154)	1296	PAK3 (Ab-154)		0.81	
		144	PAK4 (Ab-474)			
657	Paxillin (Phospho-Tyr118)	695	Paxillin (Ab-118)			
26	Paxillin (Phospho-Tyr31)	1208	Paxillin (Ab-31)		0.79	
1259	PDGFR alpha (Phospho-Tyr849)	978	PDGFR alpha (Ab-849)	1.04	2.01	1.92
		974	PDGFR beta (Ab-1009)			
1258	PDGFR beta (Phospho-Tyr1021)	977	PDGFR beta (Ab-1021)	1.33	1.97	1.48
1257	PDGFR beta (Phospho-Tyr740)	976	PDGFR beta (Ab-740)	1.67	2.33	1.39
180	PDGFR beta (Phospho-Tyr751)	65	PDGFR beta (Ab-751)	0.26	0.18	0.70
5	PDK1 (Phospho-Ser241)	1182	PDK1 (Ab-241)	0.14	0.20	1.49
731	PEA-15 (Phospho-Ser104)	1116	PEA-15 (Ab-116)	1.00	1.16	1.16
387	PEA-15 (Phospho-Ser116)	1116	PEA-15 (Ab-116)	0.75	0.77	1.03
113	PECAM-1 (Phospho-Tyr713)	1140	PECAM-1 (Ab-713)	0.10	0.12	1.14
261	PI3-kinase p85-alpha (Phospho-Tyr607)					

260	PI3-kinase p85-subunit alpha/gamma (Phospho-Tyr467/Tyr199)	964	PI3-kinase p85-subunit alpha/gamma (Ab-467/199)	0.57	0.38	0.67
121	Pim-1 (Phospho-Tyr309)	1145	Pim-1 (Ab-309)	1.02	0.67	0.66
1087	PIP5K (Phospho-Ser307)					
388	PKA CAT (Phospho-Thr197)	1117	PKA CAT (Ab-197)	0.60	0.53	0.89
101	PKA-R2B (Phospho-Ser113)					
905	PKC alpha (Phospho-Tyr657)	300	PKC alpha (Ab-657)	1.70	1.81	1.07
732	PKC alpha/beta II (Phospho-Thr638)	145	PKC alpha/beta II (Ab-638)	0.52	0.48	0.93
572	PKC beta/PKCB (Phospho-Ser661)	1297	PKC beta/PKCB (Ab-661)	0.79	0.84	1.06
836	PKC delta (Phospho-Ser645)	548	PKC delta (Ab-645)	0.80		
733	PKC delta (Phospho-Thr505)	146	PKC delta (Ab-505)	0.93	0.84	0.90
734	PKC delta (Phospho-Tyr313)					
906	PKC delta (Phospho-Tyr52)					
573	PKC delta (Phospho-Tyr64)					
907	PKC epsilon (Phospho-Ser729)	301	PKC epsilon (Ab-729)	1.31	1.31	1.00
908	PKC pan activation site (Phospho)	435	PKC pan activation site	1.11	1.01	0.91
837	PKC theta (Phospho-Ser676)	701	PKC theta (Ab-676)	1.03		
735	PKC theta (Phospho-Thr538)	701	PKC theta (Ab-676)		1.68	
1006	PKC zeta (Phospho-Thr410)	718	PKC zeta (Ab-410)		1.06	
909	PKC zeta (Phospho-Thr560)	436	PKC zeta (Ab-560)	1.14	1.10	0.96
1062	PKD1/PKC mu (Phospho-Ser205)	437	PKD1/PKC mu (Ab-205)	0.60	1.00	1.66
736	PKD1/PKC mu (Phospho-Ser910)	149	PKD1/PKC mu (Ab-910)	1.31	1.70	1.29
1063	PKD1/PKC mu (Phospho-Tyr463)	438	PKD1/PKC mu (Ab-463)	0.46	0.46	1.01

		148	PKD1/PKC mu (Ab-744/748)			
1064	PKD2 (Phospho-Ser876)	439	PKD2 (Ab-876)			
668	PKR (Phospho-Thr446)	533	PKR (Ab-446)			
678	PKR (Phospho-Thr451)	542	PKR (Ab-451)	0.39	0.40	1.02
1046	PLC beta3 (Phospho-Ser1105)	433	PLC beta3 (Ab-1105)	0.81	1.52	1.88
737	PLC beta3 (Phospho-Ser537)	283	PLC beta3 (Ab-537)			
912	PLCG1 (Phospho-Tyr1253)					
743	PLCG1 (Phospho-Tyr771)	465	PLCG1 (Ab-771)		0.50	
746	PLCG1 (Phospho-Tyr783)	466	PLCG1 (Ab-783)	1.88	2.34	1.24
913	PLCG2 (Phospho-Tyr1217)	628	PLCG2 (Ab-1217)	1.32	1.39	1.05
747	PLCG2 (Phospho-Tyr753)	468	PLCG2 (Ab-753)	0.56	0.61	1.09
122	PLD1 (Phospho-Ser561)	1146	PLD1 (Ab-561)	0.96	1.40	1.45
421	PLD2 (Phospho-Tyr169)					
1287	PLK1 (Phospho-Thr210)	629	PLK1 (Ab-210)	0.75	0.73	0.97
923	PP1 alpha (Phospho-Thr320)	638	PP1 alpha (Ab-320)	0.78	0.66	0.85
389	PP2A-alpha (Phospho-Tyr307)	1118	PP2A-alpha (Ab-307)	0.10	0.09	0.93
914	PPAR-BP (Phospho-Thr1457)	630	PPAR-BP (Ab-1457)	1.09	0.77	0.71
915	PPAR-gamma (Phospho-Ser112)	631	PPAR-gamma (Ab-112)	0.05	0.05	0.98
644	Progesterone Receptor (Phospho-Ser190)	353	Progesterone Receptor (Ab-190)	0.52	0.59	1.13
480	PTEN (Phospho-Ser370)	341	PTEN (Ab-370)		0.23	
9	PTEN (Phospho-Ser380)	1186	PTEN (Ab-380)			
474	PTEN (Phospho-Ser380/Thr382/Thr383)	340	PTEN (Ab-380/382/383)	0.17	0.10	0.61
114	PTPRA (Phospho-Tyr798)					

170	Pyk2 (Phospho-Tyr402)	56	Pyk2 (Ab-402)	0.81	1.33	1.64
581	Pyk2 (Phospho-Tyr579)					
1047	Pyk2 (Phospho-Tyr580)	601	Pyk2 (Ab-580)	0.36	0.37	1.00
1217	Pyk2 (Phospho-Tyr881)	600	Pyk2 (Ab-881)	0.39	0.36	0.93
28	Rac1/cdc42 (Phospho-Ser71)	1210	Rac1/cdc42 (Ab-71)	0.24	0.17	0.70
1083	RAD51 (Phospho-Tyr315)	812	RAD51 (Ab-309)	0.89	1.06	1.18
1084	RAD52 (Phospho-Tyr104)					
6	Raf1 (Phospho-Ser259)	1183	Raf1 (Ab-259)		0.37	
1153	Raf1 (Phospho-Ser289)	1298	Raf1 (Ab-289)			
561	Raf1 (Phospho-Ser296)	131	Raf1 (Ab-296)	0.36	0.83	2.29
29	Raf1 (Phospho-Ser338)	1211	Raf1 (Ab-338)			
1246	Raf1 (Phospho-Ser43)	618	Raf1 (Ab-43)	0.27	0.20	0.73
391	Raf1 (Phospho-Ser621)	1272	Raf1 (Ab-621)	0.59	0.55	0.93
390	Raf1 (Phospho-Tyr341)	1271	Raf1 (Ab-341)	0.56	0.45	0.82
254	RapGEF1 (Phospho-Tyr504)					
738	Ras-GRF1 (Phospho-Ser916)	284	Ras-GRF1 (Ab-916)	0.30	0.35	1.17
403	Rb (Phospho-Ser608)	1130	Rb (Ab-608)	1.94	1.59	0.82
995	Rb (Phospho-Ser780)	698	Rb (Ab-780)	0.36	0.24	0.66
993	Rb (Phospho-Ser795)	696	Rb (Ab-795)	0.21	0.28	1.29
994	Rb (Phospho-Ser807)	697	Rb (Ab-807)	0.78	0.93	1.20
1065	Rb (Phospho-Ser811)	440	Rb (Ab-811)	0.62	0.89	1.43
1066	Rb (Phospho-Thr821)					
		441	Rb-like-2 (RBL2) (Ab-952)			
153	Rel (Phospho-Ser503)	38	Rel (Ab-503)	1.10		

339	RelB (Phospho-Ser552)	223	RelB (Ab-552)	3.21	3.09	0.96
671	Ret (Phospho-Tyr905)	536	Ret (Ab-905)	0.70	0.68	0.96
262	RGS16 (Phospho-Tyr168)					
263	Rho/Rac guanine nucleotide exchange factor 2 (Phospho-Ser885)	965	Rho/Rac guanine nucleotide exchange factor 2 (Ab-885)	1.10	1.52	1.38
		1273	RhoA (Ab-188)			
574	RSK1/2/3/4 (Phospho-Ser221/227/218/232)	1299	RSK1/2/3/4 (Ab-221/227/218/232)	0.91	1.13	1.25
392	RyR2 (Phospho-Ser2808)	1274	RyR2 (Ab-2808)	0.80		
186	S6 Ribosomal Protein (Phospho-Ser235)	71	S6 Ribosomal Protein (Ab-235)	0.80		
334	SAPK/JNK (Phospho-Thr183)	219	SAPK/JNK (Ab-183)	0.56	0.70	1.25
335	SAPK/JNK (Phospho-Tyr185)	220	SAPK/JNK (Ab-185)	0.76	0.98	1.28
1007	Shc (Phospho-Tyr349)	719	Shc (Ab-349)	0.24	0.44	1.81
1008	Shc (Phospho-Tyr427)	589	Shc (Ab-427)	0.32		
1009	SHP-1 (Phospho-Tyr536)					
1010	SHP-2 (Phospho-Tyr542)	872	SHP-2 (Ab-542)	0.84	0.66	0.79
1011	SHP-2 (Phospho-Tyr580)	873	SHP-2 (Ab-580)		0.62	
576	SLP-76 (Phospho-Tyr128)	1302	SLP-76 (Ab-128)	0.53	0.58	1.10
102	Smad1 (Phospho-Ser187)	786	Smad1 (Ab-187)	0.69	1.27	1.84
1054	Smad1 (Phospho-Ser465)	590	Smad1 (Ab-465)			
103	Smad2 (Phospho-Ser250)	788	Smad2 (Ab-250)	1.00	1.21	1.21
1055	Smad2 (Phospho-Ser467)	591	Smad2 (Ab-467)	0.96	0.79	0.83
104	Smad2 (Phospho-Thr220)	790	Smad2 (Ab-220)	0.50	0.53	1.06

		789	Smad2 (Ab-245)			
		787	Smad2 (Ab-255)			
105	Smad2/3 (Phospho-Thr8)	791	Smad2/3 (Ab-8)	1.73	1.70	0.98
107	Smad3 (Phospho-Ser204)	793	Smad3 (Ab-204)	0.75	0.44	0.59
108	Smad3 (Phospho-Ser208)					
109	Smad3 (Phospho-Ser213)	794	Smad3 (Ab-213)			
1012	Smad3 (Phospho-Ser425)	592	Smad3 (Ab-425)	0.33	0.20	0.60
106	Smad3 (Phospho-Thr179)	792	Smad3 (Ab-179)	0.19	0.10	0.54
23	SMC1 (Phospho-Ser957)	1205	SMC1 (Ab-957)		0.91	
326	SP1 (Phospho-Thr739)	211	SP1 (Ab-739)	0.82	1.47	1.80
575	Src (Phospho-Ser75)	1300	Src (Ab-75)			
579	Src (Phospho-Tyr216)					
659	Src (Phospho-Tyr418)	855	Src (Ab-418)	0.83	0.62	0.75
1165	Src (Phospho-Tyr529)	1196	Src (Ab-529)			
742	SREBP-1 (Phospho-Ser439)	460	SREBP-1 (Ab-439)	0.55	0.46	0.83
404	SRF (Phospho-Ser77)	1131	SRF (Ab-77)	1.04	1.15	1.11
1218	SRF (Phospho-Ser99)	602	SRF (Ab-99)	0.37	0.32	0.87
276	STAM2 (Phospho-Tyr192)	1315	STAM2 (Ab-192)			
1173	STAT1 (Phospho-Ser727)	1204	STAT1 (Ab-727)			
310	STAT1 (Phospho-Tyr701)	195	STAT1 (Ab-701)			
1219	STAT2 (Phospho-Tyr690)	603	STAT2 (Ab-690)	2.45	3.09	1.26
312	STAT3 (Phospho-Ser727)	197	STAT3 (Ab-727)			
311	STAT3 (Phospho-Tyr705)	196	STAT3 (Ab-705)	0.51	0.50	0.99
313	STAT4 (Phospho-Tyr693)	198	STAT4 (Ab-693)	78.31	99.03	1.26

110	STAT5A (Phospho-Ser725)					
315	STAT5A (Phospho-Ser780)	200	STAT5A (Ab-780)	0.08	0.09	1.04
314	STAT5A (Phospho-Tyr694)	199	STAT5A (Ab-694)			
1048	STAT5B (Phospho-Ser731)	434	STAT5B (Ab-731)	0.61	0.81	1.33
317	STAT6 (Phospho-Thr645)	202	STAT6 (Ab-645)	0.15	0.19	1.33
316	STAT6 (Phospho-Tyr641)	201	STAT6 (Ab-641)	1.15	1.46	1.27
321	Stathmin 1 (Phospho-Ser15)	73	Stathmin 1 (Ab-15)	0.46	0.26	0.58
178	Stathmin 1 (Phospho-Ser24)	63	Stathmin 1 (Ab-24)			
179	Stathmin 1 (Phospho-Ser37)	64	Stathmin 1 (Ab-37)		1.28	
1261	Survivin (Phospho-Thr117)	980	Survivin (Ab-117)			
393	SYK (Phospho-Tyr323)					
1049	SYK (Phospho-Tyr348)	604	SYK (Ab-348)	0.80	0.62	0.77
1220	SYK (Phospho-Tyr525)	605	SYK (Ab-525)	0.17		
394	Synapsin (Phospho-Ser62)	1275	Synapsin (Ab-62)		0.43	
503	Synapsin (Phospho-Ser9)	368	Synapsin (Ab-9)	0.50	0.55	1.10
1013	Synaptotagmin (Phospho-Ser309)	874	Synaptotagmin (Ab-309)			
1014	Synaptotagmin (Phospho-Thr202)	875	Synaptotagmin (Ab-202)		0.66	
492	Synuclein alpha (Phospho-Tyr125)	224	Synuclein alpha (Ab-125)	0.51	0.21	0.41
673	Synuclein alpha (Phospho-Tyr133)	538	Synuclein alpha (Ab-133)			
674	Synuclein alpha (Phospho-Tyr136)					
825	Tau (Phospho-Ser214)	686	Tau (Ab-214)	0.48	0.59	1.21
822	Tau (Phospho-Ser235)	683	Tau (Ab-235)	0.09	0.13	1.44
827	Tau (Phospho-Ser262)	688	Tau (Ab-262)			
820	Tau (Phospho-Ser356)	528	Tau (Ab-356)			

821	Tau (Phospho-Ser396)	529	Tau (Ab-396)			
828	Tau (Phospho-Ser404)	689	Tau (Ab-404)	0.88	0.82	0.92
506	Tau (Phospho-Ser422)	371	Tau (Ab-422)		0.51	
823	Tau (Phospho-Thr181)	684	Tau (Ab-181)	0.78	1.43	1.85
824	Tau (Phospho-Thr205)	685	Tau (Ab-205)	0.07	0.07	0.95
493	Tau (Phospho-Thr212)	225	Tau (Ab-212)		0.08	
826	Tau (Phospho-Thr231)	687	Tau (Ab-231)	0.67	0.67	1.00
		958	TGFBR1 (Ab-165)			
		959	TGFBR2 (Ab-250)			
115	TFII-I (Phospho-Tyr248)					
916	TIE2 (Phospho-Tyr1108)					
1099	TIF-IA (Phospho-Ser649)	813	TIF-IA (Ab-649)	1.10	1.39	1.27
		639	TLK1 (Ab-764)			
1262	TOP2A/DNA topoisomerase II (Phospho-Ser1106)	981	TOP2A/DNA topoisomerase II (Ab-1106)	0.28	0.34	1.24
406	Trk A (Phospho-Tyr680/681)	1276	Trk A (Ab-496)	1.28		
405	Trk A (Phospho-Tyr701)	1276	Trk A (Ab-496)	2.35		
1015	Trk A (Phospho-Tyr791)	1276	Trk A (Ab-496)			
1016	Trk B (Phospho-Tyr515)	876	Trk B (Ab-515)	0.39	0.57	1.45
1043	Trk B (Phospho-Tyr705)	876	Trk B (Ab-515)	0.27	0.62	2.28
395	Tuberin/TSC2 (Phospho-Ser939)	1277	Tuberin/TSC2 (Ab-939)	0.13	0.15	1.10
396	Tuberin/TSC2 (Phospho-Thr1462)	1278	Tuberin/TSC2 (Ab-1462)	2.48	3.56	1.44
		461	Tuberin/TSC2 (Ab-981)			
1160	TYK2 (Phospho-Tyr1054)	858	TYK2 (Ab-1054)		0.29	

1017	Tyrosine Hydroxylase (Phospho-Ser19)	877	Tyrosine Hydroxylase (Ab-19)	0.38	0.25	0.66
1018	Tyrosine Hydroxylase (Phospho-Ser31)	878	Tyrosine Hydroxylase (Ab-31)			
1019	Tyrosine Hydroxylase (Phospho-Ser40)	879	Tyrosine Hydroxylase (Ab-40)		0.28	
549	Tyrosine Hydroxylase (Phospho-Ser8)	1279	Tyrosine Hydroxylase (Ab-8)	0.32	0.27	0.86
169	VASP (Phospho-Ser157)	1213	VASP (Ab-157)	0.08	0.04	0.52
1168	VASP (Phospho-Ser238)	1199	VASP (Ab-238)			
1003	VAV1 (Phospho-Tyr174)	1280	VAV1 (Ab-160)	0.44	0.59	1.34
1003	VAV1 (Phospho-Tyr174)	1041	VAV1 (Ab-174)	0.59	0.90	1.52
397	VAV2 (Phospho-Tyr142)	966	VAV2 (Ab-142)		0.98	
416	VE-Cadherin (Phospho-Tyr731)					
550	VEGFR1 (Phospho-Tyr1333)	1281	VEGFR1 (Ab-1333)	0.59	0.56	0.95
265	VEGFR2 (Phospho-Tyr1054)	1154	VEGFR2 (Ab-1054)	0.58	0.53	0.91
551	VEGFR2 (Phospho-Tyr1059)	1282	VEGFR2 (Ab-1059)	0.70	1.26	1.80
652	VEGFR2 (Phospho-Tyr1175)	513	VEGFR2 (Ab-1175)	1.19	0.81	0.68
653	VEGFR2 (Phospho-Tyr1214)	514	VEGFR2 (Ab-1214)		0.05	
654	VEGFR2 (Phospho-Tyr951)	515	VEGFR2 (Ab-951)	0.10	0.09	0.82
266	Vinculin (Phospho-Tyr821)	1155	Vinculin (Ab-821)			
552	WASP (Phospho-Tyr290)	1283	WASP (Ab-290)	0.46	0.85	1.84
917	WAVE1 (Phospho-Tyr125)	632	WAVE1 (Ab-125)		1.57	
799	WEE1 (Phospho-Ser53)	809	WEE1 (Ab-53)			
1088	WEE1 (Phospho-Ser642)	809	WEE1 (Ab-53)	0.99	1.01	1.02
417	WWOX (Phospho-Tyr33)					

918	XIAP (Phospho-Ser87)	633	XIAP (Ab-87)	0.33	0.30	0.90
553	Zap-70 (Phospho-Tyr292)	1284	Zap-70 (Ab-292)	0.48	0.54	1.12
554	Zap-70 (Phospho-Tyr315)					
1169	Zap-70 (Phospho-Tyr319)	1200	Zap-70 (Ab-319)	0.54	0.57	1.06
1170	Zap-70 (Phospho-Tyr493)	1201	Zap-70 (Ab-493)			

Appendix Table 2: Genes specifically depleted in *Pdk1*$^{\Delta}$ clones

Gene	Cell-cycle norm. Beta score in Pdk1^{lox} clones	Cell-cycle norm. Beta score in *Pdk1*$^{\Delta}$ clones	Diff	Rank
Oxsr1	0.19613084	-0.9952903	-1.1914211	1
Fbxo42	0.09851584	-0.990735	-1.0892509	2
Vps29	-0.1995348	-1.1472359	-0.9477011	3
Pkn2	-0.5683157	-1.4451822	-0.8768665	4
Itgb3	-0.3067415	-1.1651482	-0.8584067	5
Myrf	0.16460902	-0.6285284	-0.7931374	6
Arpc4	-0.6865318	-1.4722051	-0.7856733	7
Polr2b	-1.0966551	-1.8755405	-0.7788854	8
Grb2	-0.4017352	-1.1672329	-0.7654976	9
Ctdsp1	0.1612272	-0.600525	-0.7617522	10
Raf1	0.04233995	-0.6898085	-0.7321485	11
Ric8	0.0271572	-0.6763125	-0.7034697	12
Tyms	-1.2331832	-1.931362	-0.6981788	13
Eif2b3	-0.6661818	-1.3625695	-0.6963877	14
Vps26a	-0.0077228	-0.6923178	-0.684595	15
Polr2g	-0.8879126	-1.5651637	-0.6772511	16
Tor1aip2	0.11987004	-0.5462091	-0.6660791	17
Dpm2	-0.1955106	-0.8496757	-0.6541651	18
Cad	-0.1997637	-0.8506794	-0.6509157	19
Rptor	-0.5529942	-1.202517	-0.6495228	20
Rbms1	0.08881341	-0.5544781	-0.6432915	21
Itgav	-0.5758842	-1.2152563	-0.6393721	22
Mat2a	-0.6786975	-1.3038913	-0.6251938	23
Bmpr1a	0.04025105	-0.5799413	-0.6201924	24
Gng5	-0.0232068	-0.6423023	-0.6190955	25
Rhoa	-0.3917891	-1.0097282	-0.6179391	26
Hmgcs1	-1.0021413	-1.6158894	-0.6137481	27
Wdr4	-0.147759	-0.7573965	-0.6096376	28

Etf1	-0.8846637	-1.4852532	-0.6005896	31
Gnb2	0.06215019	-0.5346973	-0.5968475	32
Dhdds	-0.7812154	-1.3714484	-0.590233	34
Pdia3	0.01570332	-0.5727455	-0.5884488	35
Polr2e	-0.9400428	-1.5284898	-0.588447	36
Hspa5	-1.3507347	-1.9346819	-0.5839472	37
Mtor	-0.8617736	-1.4351452	-0.5733715	38
Wwtr1	-0.4484605	-1.0206918	-0.5722313	39
Epc2	0.05125748	-0.5153876	-0.5666451	40
Yars	-1.3496271	-1.9127548	-0.5631277	41
Vps35	-0.1272909	-0.6843113	-0.5570205	42
Alg3	-0.2483571	-0.8044317	-0.5560747	43
Rheb	-0.1094366	-0.6644842	-0.5550476	44
Rps20	-0.8850329	-1.4373842	-0.5523513	45
Rpl39	-0.7457727	-1.2964793	-0.5507066	46
Scaf8	0.01941446	-0.5278799	-0.5472943	48
Shoc2	-0.4307687	-0.9718962	-0.5411276	50
Mettl1	-0.0976888	-0.6385269	-0.540838	51
Polr3a	-1.2528982	-1.7934682	-0.54057	52
Slmap	0.02774127	-0.5093653	-0.5371066	53
Nono	-0.1442369	-0.6774321	-0.5331952	55
Arpc2	-0.7036181	-1.2345584	-0.5309403	56
Dhx15	-0.7863103	-1.3119981	-0.5256879	57
Uxs1	-0.2526693	-0.7778721	-0.5252029	58
Arl4c	-0.0094573	-0.5320954	-0.5226381	59
Arpc3	-0.3278816	-0.8485948	-0.5207132	60
Eif2b4	-0.9163405	-1.4369981	-0.5206576	61
Umps	-0.161685	-0.6820259	-0.5203409	62
Slc33a1	-0.7015802	-1.2143298	-0.5127497	65
Rraga	-0.5036181	-1.0102687	-0.5066506	66
Mios	-0.4248468	-0.9304355	-0.5055887	68
Ppp1cb	-0.6522705	-1.1570414	-0.5047708	69
Snrpa1	-1.2156095	-1.7188851	-0.5032756	70
Etnk1	-0.065467	-0.5676343	-0.5021673	71
U2af1	-1.0036181	-1.5010037	-0.4973856	73
Cwc22	-1.0331537	-1.530034	-0.4968803	74
Wdr24	-0.3926973	-0.8832613	-0.4905639	75
Actr2	-0.7702134	-1.2584157	-0.4882023	76
Cited2	-0.041606	-0.5280883	-0.4864823	77
Wdr46	-0.370782	-0.8535361	-0.4827542	78
Rpl36	-1.3559034	-1.8360871	-0.4801837	79
Vmn1r149	-1.0604002	-1.539685	-0.4792848	81

Rangap1	-0.9998523	-1.4768376	-0.4769852	82
Vcl	-0.1467843	-0.6210547	-0.4742703	83
Egfr	-0.1756184	-0.6486489	-0.4730305	84
Ppp1ca	-0.0737887	-0.5449737	-0.4711851	86
Kras	-0.9127224	-1.3837245	-0.4710021	87
Wdr59	-0.0850698	-0.5539145	-0.4688447	88
Mlst8	-0.2677398	-0.7342495	-0.4665097	93
Wdr48	-0.0767408	-0.5425571	-0.4658164	94
Eif3h	-0.4411356	-0.9026405	-0.4615049	96
Vps25	-1.0562652	-1.513357	-0.4570918	99
Farsa	-0.9026065	-1.3595584	-0.4569519	100
Seh1l	-0.5817027	-1.0385269	-0.4568241	101
Ccdc6	-0.1219818	-0.5784821	-0.4565003	102
Rac1	-0.8596323	-1.3154725	-0.4558402	103
Alg12	-0.1208964	-0.5750695	-0.4541731	104
Polr2c	-0.8170272	-1.2708462	-0.453819	105
Abce1	-0.8788304	-1.3321495	-0.4533191	106
Ash2l	-0.4624898	-0.9086628	-0.4461729	110
Wsb1	-0.0626516	-0.5077826	-0.445131	111
Vps4b	-0.1959093	-0.6407582	-0.4448489	112
Nup54	-0.4982869	-0.9429432	-0.4446562	113
Anln	-0.3660341	-0.8059759	-0.4399418	118
Actr3	-0.5259765	-0.964021	-0.4380445	120
Pigs	-0.0990253	-0.53645	-0.4374246	121
Ruvbl2	-1.3176549	-1.7539376	-0.4362827	122
Chordc1	-0.6614856	-1.0977455	-0.4362599	123
Cdc37	-0.8273647	-1.2574892	-0.4301245	124
Scfd1	-0.895961	-1.3243515	-0.4283904	125
Phb	-1.2265377	-1.6517912	-0.4252535	127
Ctps	-0.3113638	-0.7355466	-0.4241828	128
Junb	-0.5885254	-1.0108863	-0.4223609	129
Pdcl	-0.3636787	-0.7798796	-0.4162009	132
Ppp2r3c	-0.3572916	-0.7727764	-0.4154848	133
Elp5	-0.4508012	-0.8651946	-0.4143934	134
Cct7	-1.2351768	-1.6467727	-0.4115959	136
Atp6v1e1	-0.9246105	-1.3358555	-0.411245	137
Clp1	-0.9437348	-1.3531501	-0.4094153	139
Sin3a	-0.7931034	-1.2023626	-0.4092591	140
Polr2j	-0.8747693	-1.2838944	-0.4091251	141
Rpl5	-1.4093628	-1.8184836	-0.4091209	142
Nckap1	-0.4136454	-0.821958	-0.4083126	143
Rpl14	-1.1065495	-1.514824	-0.4082745	144

Taf13	-0.3014768	-0.7080914	-0.4066146	145
Kif23	-0.5825076	-0.9872607	-0.4047531	148
Aars	-0.8058037	-1.2079216	-0.4021178	151
Gtf2a1	-0.4978291	-0.8986257	-0.4007966	153
Pus3	-0.1321125	-0.5326899	-0.4005774	154

Appendix Table 3: Genes enriched in *Pdk1*$^{\Delta}$ clones (Chronic Setting)

Gene	*Pdk1*^{lox} clones |beta	*Pdk1*^{lox} clones |p-value	*Pdk1*$^{\Delta}$ clones |beta	*Pdk1*$^{\Delta}$ clones |p-value
Tsc2	-1.0219	0	3.3568	0
Tsc1	-1.0704	0	2.793	0
Nf2	-0.069744	0.40137	2.5625	0
Cdkn2b	0.69019	0	2.1346	0
Foxo1	-0.17823	0.019154	2.1143	0
Vgll4	-0.10038	0.19454	1.8177	0
Kctd5	-0.55062	0	1.5428	0
Gsk3b	-0.22005	0.0049337	1.522	0
Pten	-0.13272	0.081407	1.5144	0
Dhx29	-0.71652	0	1.4749	0
Amotl2	0.13804	0.0086098	1.4173	0
3110002H16Rik	-0.084524	0.28693	1.4078	0
Cnot2	-0.88368	0	1.3929	0
Onecut2	0.33256	0	1.2834	0
Ralgapb	-0.51284	0	1.2358	0
Ep300	-0.10035	0.19469	1.1754	0
Inpp5a	-0.19409	0.011464	1.1124	0
Prkar1a	-0.19677	0.010496	1.1035	0
Tada1	0.018404	0.56472	1.0968	0
Nprl3	-0.035357	0.75781	1.0606	0
Cnot3	-1.0603	0	1.0521	0
Depdc5	-0.085872	0.27813	1.0455	0
Ankhd1	0.20614	0.00033859	1.024	0
Rnf146	-0.21625	0.0059495	0.9819	0
Ccz1	-0.4255	0	0.97818	0
Nprl2	-0.18368	0.016349	0.96352	0
Usp22	0.024722	0.49405	0.93888	0
Stk24	-0.10888	0.15638	0.9009	0
Gskip	-0.19866	0.010061	0.88809	0
Atxn7l3	-0.23547	0.0033859	0.88047	0
Usp14	0.18472	0.0009674	0.8722	0
Zc3h12a	-0.3683	4.84E-05	0.86631	0

Taf5l	0.22568	4.84E-05	0.86492	0
Med16	0.22801	4.84E-05	0.85593	0
Rock1	-0.031249	0.80638	0.85081	0
Mospd2	-0.30777	0.00029022	0.84551	0
Hivep1	0.0074387	0.69285	0.8401	0
Ralgapa2	-0.24078	0.0029506	0.83812	0
Stard3	-0.29586	0.00038696	0.83557	0
Lats2	0.049395	0.26831	0.82972	0
Iqgap1	-0.1669	0.029312	0.82553	0
Srf	-0.088847	0.25805	0.82512	0
Grk6	-0.15014	0.048854	0.81377	0
Atg5	-0.088566	0.26013	0.79522	0
Slc39a1	-0.065443	0.43905	0.79509	0
Dgkd	-0.27408	0.00062881	0.77989	0
Thoc6	-0.14987	0.048999	0.77596	0
AW549877	-0.10458	0.17553	0.75727	0
Taok1	-0.038882	0.71578	0.73192	0
Gne	-0.20097	0.0094805	0.72791	0
Dusp4	-0.069127	0.40679	0.72758	0
Supt20	0.26617	0	0.71095	0
Wdr83	-0.61559	0	0.70908	0
Wdr91	-0.28042	0.00058044	0.70358	0
Bcor	-0.14799	0.051949	0.69827	0
Taf6l	0.005118	0.72274	0.68919	0
Rb1	0.26931	0	0.68682	0
Nras	-0.35381	4.84E-05	0.68676	0
Drg1	-0.46099	0	0.6858	0
Brpf1	0.10799	0.032021	0.68533	0
Zmym2	-0.047345	0.62199	0.67872	0
Cmip	-0.23954	0.0029989	0.67483	0
Epb4.1l5	-0.015232	0.98796	0.67225	0
Pdzd8	-0.065555	0.43789	0.66902	0
Fbrs	0.13954	0.0082713	0.66223	0
Fbxw7	-0.19864	0.010061	0.66157	0
Abcd3	-0.16871	0.027281	0.66153	0
Hhex	-0.055667	0.53516	0.66027	0
Epha2	0.06149	0.1868	0.65992	0
Kmt2c	-0.13416	0.078263	0.65964	0
Socs3	-0.25172	0.0017897	0.65954	0
Itga3	0.18102	0.0012576	0.65791	0
Oprd1	-0.074373	0.36558	0.64997	0
Med13	-0.37357	4.84E-05	0.64929	0

Sbk3	0.071153	0.13529	0.6464	0
Cnot8	0.057964	0.20756	0.64469	0
Rbm47	0.14371	0.0066751	0.64326	0
Ccdc130	-0.58838	0	0.64118	0
Aip	0.085147	0.083245	0.6375	0
Ankrd17	-0.39409	0	0.62374	0
Btg1	-0.26809	0.00082229	0.60741	0
Fkbp1a	-0.37745	0	0.60733	0
Cdk17	-0.045787	0.63892	0.60193	0
Kirrel3	-0.11965	0.11875	0.59955	0
Ywhaz	-0.36357	4.84E-05	0.59758	0
Atg12	0.047531	0.28214	0.59676	0
Rasa3	0.10392	0.038212	0.57987	0
Slc16a1	0.26974	0	0.57968	0
Foxp1	0.031609	0.42038	0.56866	0
Kprp	-0.0037802	0.84043	0.55959	0
Rock2	-0.025242	0.87966	0.55554	0
Lin37	0.057687	0.20901	0.55486	0
Gse1	0.040394	0.34125	0.55448	0
Trim28	-0.28488	0.0004837	0.55294	0
Pabpc1	-1.3836	0	0.55251	0
Apopt1	0.051881	0.25027	0.54407	0
Abl1	-0.024682	0.88633	0.54226	0
Mocs1	-0.12711	0.095627	0.54118	0
Dapk3	-0.20421	0.0085131	0.53985	0
Med24	-0.20683	0.0079327	0.53583	0
Pawr	-0.030699	0.813	0.53496	0
Mllt3	-0.048119	0.61285	0.53488	0
Krit1	-0.42639	0	0.53068	0
Nfkbia	0.087787	0.075167	0.52932	0
C1galt1c1	-0.40455	0	0.52861	0
Nfkbib	-0.056176	0.53067	0.52569	0
Paxip1	-0.40895	0	0.52539	0
Stard3nl	-0.13126	0.084551	0.52269	0
Wdr81	-0.1213	0.11261	0.52195	0
Pknox1	-0.1325	0.081987	0.52155	0
Htra1	-0.16909	0.02699	0.52146	0
Atg7	0.014851	0.60757	0.52122	0
Fasn	-0.85103	0	0.52081	0
Pdha1	-0.45889	0	0.52069	0
Rbl1	0.15623	0.0038696	0.51921	0
Glt28d2	0.16208	0.0029022	0.51821	0

Slc22a13	-0.040312	0.69957	0.5164	0
Atg3	-0.033173	0.78369	0.51569	0
Ddx39b	-0.16794	0.028103	0.51499	0
Wwc1	0.077811	0.10598	0.51465	0
Cpeb4	0.1148	0.023363	0.51362	0
Rybp	0.25833	0	0.5124	0
Olfr434	-0.16869	0.027281	0.51223	0
Myl4	-0.0029309	0.8279	0.50762	0
Tada2b	0.34167	0	0.50716	0
Kmt2e	0.047393	0.28345	0.50635	0
Rnf2	0.37353	0	0.50572	0
Gsk3a	-0.12976	0.087937	0.50282	0
Cdkn2a	0.079618	0.10013	0.50064	0
E2f7	0.079391	0.10104	0.50038	0
Kdm3b	-0.070986	0.38972	0.50026	0
Pom121l2	-0.016553	0.99362	0.49967	0
Creb1	-0.41807	0	0.49805	0
Pi4k2a	-0.077026	0.34386	0.49643	0
Ptch2	-0.053857	0.55335	0.49605	0
Kctd9	-0.0009641	0.80284	0.49592	0
Mcoln1	-0.31261	0.00019348	0.49528	0
Cep83	-0.0091892	0.90998	0.49177	0
Ahnak	0.018056	0.56869	0.49032	0
Ranbp9	0.0027996	0.75278	0.48828	0
Cdkn1b	0.15988	0.003531	0.48782	0
Abl2	-0.25986	0.0011125	0.48766	0
Atg16l1	-0.11675	0.12857	0.48654	0
Nbeal2	-0.34313	0.00014511	0.48078	0
Ythdf3	0.053243	0.2405	0.47904	0
Deaf1	0.05267	0.24499	0.47758	0
Plekhg3	0.086692	0.078263	0.47758	0
Cobll1	-0.049547	0.59727	0.47728	0
Adam10	-0.14343	0.060849	0.47643	0
Rpgrip1	-0.059783	0.49308	0.47513	0
Tom1l2	-0.12273	0.10743	0.47478	0
Rbm18	-0.18095	0.017945	0.47352	0
Clk3	-0.06361	0.45473	0.47267	0
Tiparp	-0.10024	0.19498	0.47116	0
Atg10	-0.1144	0.13606	0.46842	0
Zc3h15	-0.098944	0.20175	0.46625	0
Galnt2	0.081911	0.093112	0.46563	0
Ube2k	-0.4623	0	0.46524	0

Cs	-0.52569	0	0.46389	0
Edn1	0.117	0.020799	0.46338	0
Nptn	-0.028164	0.84546	0.4624	0
Sp6	-0.080478	0.31673	0.46145	0
Vwa8	0.031417	0.42241	0.46134	0
St3gal5	-0.058606	0.5073	0.45447	0
Ccm2	-0.34978	9.67E-05	0.45238	0
Itgb1bp1	-0.086207	0.27595	0.4517	0
Dusp5	-0.1459	0.056157	0.45142	0
Trim33	-0.39296	0	0.45109	0
Cdc42se2	-0.19118	0.012576	0.44712	0
Spink10	0.054318	0.23309	0.44692	0
Spin1	0.04893	0.27213	0.4454	0
Suv420h1	0.25311	0	0.44314	0
Lrrc39	-0.098344	0.20504	0.44304	0
Tmem14c	0.052513	0.24591	0.44225	0
Golga7	-0.055379	0.53816	0.4414	0
Med15	-0.18651	0.014656	0.44047	0
Mtmr2	0.019882	0.54827	0.43937	0
Ctsb	-0.077063	0.34357	0.43885	0
Olfr592	-0.023556	0.90128	0.43742	0
Cryl1	-0.0014612	0.80894	0.43536	0
Mon1b	-0.07716	0.34314	0.43323	0
Uchl3	-0.11661	0.129	0.43279	0
Trmt11	-0.11627	0.12987	0.43278	0
Casc3	-0.13373	0.079182	0.43271	0
Snx31	0.057176	0.21249	0.43167	0
Zfp91	-0.038521	0.72033	0.43039	0
Stag2	-0.011963	0.94486	0.43026	0
Gnpat	-0.14911	0.050208	0.42989	0
Ppfia3	0.054877	0.22908	0.42906	0
Birc6	-0.25233	0.0016446	0.42736	0
Eif4g2	-0.37675	4.84E-05	0.42619	0
Pacsin2	0.022441	0.51983	0.42581	0
Maged1	0.098988	0.046774	0.4248	0
Myl6	-0.47828	0	0.42442	0
Ntmt1	0.071768	0.13263	0.42438	0
Rbl2	-0.0005518	0.79694	0.42399	0
Ube2b	0.073231	0.12533	0.42358	0
Tmem177	-0.075683	0.35504	0.42258	0
Slc3a1	-0.12571	0.098578	0.42082	0
Grhpr	-0.026588	0.86471	0.42044	0

Stac2	-0.076214	0.35005	0.42036	0
Fbxo11	-0.09155	0.24253	0.42009	0
Mau2	-0.65403	0	0.41979	0
Tnf	-0.072908	0.37525	0.4193	0
Phlda1	-0.21974	0.0050788	0.41726	0
Emp1	-0.0085675	0.90292	0.41721	0
Mta2	-0.087641	0.26632	0.41712	0
Arhgap21	0.022176	0.52269	0.41691	0
Hdhd2	0.096463	0.052868	0.41629	0
Cc2d1a	0.036161	0.37719	0.41589	0
Errfi1	-0.069598	0.40287	0.4158	0
Tm9sf2	-0.21085	0.0070136	0.41553	0
Usp49	-0.12208	0.11043	0.41546	0
Srgap2	0.077496	0.10695	0.41535	0
Chp1	0.49086	0	0.41512	0
Arhgap5	-0.12013	0.11696	0.415	0
4931414P19Rik	-0.10142	0.19	0.4111	0
Vapa	-0.17138	0.024814	0.41014	0
Picalm	-0.25461	0.0015478	0.40974	0
Ddit4	-0.079324	0.32664	0.40695	0
Tbc1d7	-0.12894	0.09079	0.40687	0
Sav1	0.13363	0.010496	0.40558	0
Otoa	-0.031503	0.80352	0.40421	0
Pramel7	0.058066	0.20654	0.40369	0
Gm94	0.13725	0.0089001	0.40345	0
Fmod	-0.0023437	0.8206	0.40293	0
Aida	-0.12867	0.091468	0.40218	0
Emc9	-0.12803	0.093354	0.40213	0
Sac3d1	-0.082502	0.30217	0.40186	0
Trim8	-0.070623	0.39296	0.40152	0
Nr1h5	-0.10366	0.1796	0.40103	0
Atg4b	-0.080555	0.31619	0.401	0
Mar 05	0.046651	0.28882	0.39908	0
Spryd4	-0.11028	0.15053	0.39899	0
Chodl	-0.079492	0.32509	0.39803	0
Kdm1a	0.074468	0.11943	0.39794	0
Dcbld2	-0.010144	0.92212	0.39738	0
Zzef1	-0.086168	0.2761	0.3973	0
Klhl42	-0.089146	0.25641	0.3972	0
Nkiras2	-0.0098079	0.91796	0.39715	0
St8sia5	-0.042303	0.67713	0.39691	0
Nans	-0.19889	0.010061	0.39683	0

Sertad4	0.19669	0.00053207	0.39678	0
Tmem18	-0.035923	0.75104	0.39288	0
BC048679	0.1184	0.019928	0.39267	0
Ctsl	-0.1321	0.082664	0.39261	0
Mtss1l	-0.0072215	0.8857	0.39261	0
Rras2	0.0014927	0.77053	0.39168	0
Clrn3	0.024418	0.49768	0.38916	0
Arhgap35	-0.16315	0.033182	0.38857	0
Vsig4	0.02358	0.5075	0.38836	0
Smim3	0.11629	0.021525	0.38803	0
Anp32b	-0.34768	9.67E-05	0.38777	0
Tcl1b2	0.05846	0.20402	0.38764	0
2310030G06Rik	-0.046036	0.63568	0.3875	0
Lct	-0.086241	0.27561	0.38704	0
Trim59	-0.11857	0.12233	0.38638	0
Leng1	-0.64827	0	0.38635	0
Cramp1l	0.10063	0.043485	0.38629	0
Il13ra2	0.0099267	0.6648	0.38594	0
Lmo4	0.27286	0	0.38589	0
Mtmr1	0.12711	0.014172	0.38516	0
Sprr2b	0.03918	0.35121	0.3817	0
Hist1h1d	0.006897	0.69938	0.38154	0
Lect1	-0.0085093	0.90234	0.38141	0
Defb14	-0.12454	0.10182	0.38136	0
Med19	-0.31477	0.00019348	0.38077	0
Fscb	0.080936	0.096208	0.38027	0
St3gal2	-0.074002	0.3678	0.38003	0
Tc2n	-0.0028448	0.82655	0.37972	0
Chd9	0.041178	0.3339	0.3795	0
Zfp395	-0.16935	0.0267	0.37946	0
Topors	-0.097402	0.21031	0.37898	0
Hira	-0.10187	0.18806	0.37816	0
Ctla2b	-0.11411	0.13708	0.37709	0
Ubqln1	0.071195	0.13515	0.37545	0
Olfr512	0.041231	0.33356	0.37487	0
Elovl7	0.066698	0.15653	0.37487	0
Etv3	0.0041482	0.73474	0.37421	0
H2-Q2	-0.042784	0.67302	0.37411	0
Cdc42se1	0.066127	0.15904	0.37376	4.84E-05
Supt7l	0.0038326	0.73871	0.37345	4.84E-05
Gpatch2l	-0.071977	0.38227	0.37285	4.84E-05
Cnot6l	-0.15015	0.048854	0.37251	4.84E-05

Otc	0.11441	0.023701	0.3725	4.84E-05
Ccnyl1	0.08795	0.074635	0.37195	4.84E-05
Ube2q1	0.077501	0.10695	0.37169	4.84E-05
Olfr716	-0.024482	0.88894	0.37099	4.84E-05
Foxo3	0.0082779	0.68274	0.37079	4.84E-05
Eda	0.091959	0.063897	0.37001	4.84E-05
Akt1s1	-0.11172	0.14516	0.37	4.84E-05
Il16	-0.079134	0.32819	0.36969	4.84E-05
Spink14	0.1352	0.0099158	0.36935	4.84E-05
Smim12	0.10743	0.032988	0.36893	4.84E-05
D19Bwg1357e	-0.072233	0.38024	0.36871	4.84E-05
Pgd	-0.73063	0	0.36789	4.84E-05
Olfr799	0.04096	0.33593	0.36745	4.84E-05
Nf1	-0.065734	0.43649	0.36727	4.84E-05
Llgl1	-0.023179	0.90621	0.36666	4.84E-05
Rchy1	0.055551	0.22429	0.36559	4.84E-05
Rinl	-0.072104	0.38135	0.36554	4.84E-05
Tmprss5	0.011414	0.64685	0.36546	4.84E-05
Eif4e1b	0.015444	0.60071	0.36416	4.84E-05
Dnajc18	0.058619	0.2032	0.36373	4.84E-05
Slc25a11	0.029921	0.43784	0.36289	4.84E-05
Mesdc1	-0.24	0.0029506	0.36258	4.84E-05
Hspb3	0.074252	0.12034	0.36167	4.84E-05
Zswim6	0.077997	0.10554	0.3611	4.84E-05
4933402D24Rik	-0.064152	0.45003	0.36104	4.84E-05
Cab39	-0.35391	4.84E-05	0.35984	4.84E-05
Ldlrap1	0.094875	0.056254	0.35927	4.84E-05
Rnf216	-0.017857	0.97649	0.35894	4.84E-05
Fbxo31	0.074806	0.11793	0.35799	4.84E-05
Clcn7	0.0018245	0.76618	0.35752	4.84E-05
Adam12	-0.12537	0.099545	0.35719	4.84E-05
Far2	-0.022393	0.91748	0.35656	4.84E-05
Onecut1	-0.0092521	0.9109	0.35648	4.84E-05
Olfr924	0.040963	0.33588	0.35616	4.84E-05
Abcc12	-0.079208	0.32785	0.35561	4.84E-05
Wibg	-0.20991	0.0072071	0.35453	4.84E-05
Slc35f1	0.010881	0.65309	0.35417	4.84E-05
Hras	-0.10458	0.17553	0.35377	4.84E-05
Magi3	-0.16117	0.035262	0.35342	4.84E-05
Olfr138	0.035471	0.38333	0.35307	4.84E-05
Ncoa2	0.093362	0.060559	0.35292	4.84E-05
Tmsb15a	0.089848	0.069895	0.35249	4.84E-05

Mpp4	0.049303	0.26903	0.3523	4.84E-05
Egr3	-0.028368	0.8427	0.35202	4.84E-05
Cxx1b	-0.12117	0.11319	0.35102	4.84E-05
Zfp710	-0.050031	0.59185	0.35091	4.84E-05
Nuggc	0.026245	0.47548	0.35047	4.84E-05
Susd6	-0.1266	0.096305	0.35028	4.84E-05
Prap1	0.12666	0.014366	0.35017	4.84E-05
Nid2	0.060376	0.193	0.34985	4.84E-05
Armc12	-0.081503	0.30971	0.34975	4.84E-05
Nodal	-0.0076131	0.89122	0.34961	9.67E-05
Slain1	0.0036288	0.74132	0.34937	9.67E-05
Hook1	-0.016933	0.98878	0.34918	9.67E-05
Hdac9	0.038325	0.35808	0.34911	9.67E-05
Gprasp1	0.021729	0.52752	0.34881	9.67E-05
Pdlim2	-0.068919	0.4081	0.34824	9.67E-05
Kifc3	-0.0277	0.85044	0.34777	9.67E-05
Oas1f	0.013657	0.62199	0.34725	9.67E-05
Olfr1507	0.058081	0.20649	0.34715	9.67E-05
Pabpc2	0.22607	4.84E-05	0.34669	9.67E-05
Rbm26	-0.21437	0.0063848	0.34609	9.67E-05
Unc5b	-0.091419	0.24311	0.34606	9.67E-05
Tyrp1	-0.075998	0.35208	0.34603	9.67E-05
Hint2	-0.048555	0.60767	0.34537	9.67E-05
Lrrc40	-0.10299	0.18298	0.34524	9.67E-05
Gopc	0.020635	0.5401	0.34477	9.67E-05
Ispd	-0.10197	0.18739	0.34465	9.67E-05
Cd180	0.0737	0.12334	0.34431	9.67E-05
Mbl1	0.081973	0.092967	0.34417	9.67E-05
Tacr2	-0.0065029	0.87603	0.34351	9.67E-05
Tm4sf1	-0.18653	0.014656	0.34348	9.67E-05
Cdca2	-0.058731	0.5059	0.34332	9.67E-05
Cnga3	-0.10546	0.17099	0.34263	9.67E-05
Skil	0.10523	0.036036	0.34241	9.67E-05
Adgrg7	-0.12094	0.11406	0.34219	9.67E-05
Chn2	-0.024023	0.89533	0.34211	9.67E-05
Gng11	-0.033609	0.77827	0.34173	9.67E-05
Zfp521	0.069682	0.14269	0.34168	9.67E-05
Kdm4b	-0.011948	0.94466	0.34113	0.00014511
Pagr1a	-0.40302	0	0.3411	0.00014511
Tnfaip2	0.04686	0.28737	0.34107	0.00014511
Zbtb18	0.028791	0.44974	0.34106	0.00014511
Gm8660	0.30681	0.0080294	0.34093	0.023943

Diap2	0.013533	0.62315	0.34079	0.00014511
Arhgdig	0.015733	0.59698	0.34076	0.00014511
Kcnrg	0.13505	0.0099642	0.34076	0.00014511
Ghdc	-0.055823	0.53328	0.34075	0.00014511
Smim15	0.057537	0.20988	0.34028	0.00014511
Lzic	-0.019638	0.95231	0.34022	0.00014511
2300005B03Rik	-0.13531	0.075892	0.34007	0.00014511
Lysmd3	-0.11254	0.14255	0.33988	0.00014511
Phactr1	0.048301	0.27701	0.33975	0.00014511
Tescl	0.020726	0.53884	0.33896	0.00014511
Fbxl16	0.057597	0.20959	0.33861	0.00014511
Npnt	0.023546	0.50779	0.3379	0.00024185
Olfr165	0.041712	0.32901	0.33697	0.00024185
Itpripl2	-0.1087	0.15696	0.33679	0.00024185
Fgf10	-0.0040573	0.84435	0.33669	0.00024185
Blk	-0.12004	0.11725	0.33622	0.00024185
Mob1a	0.086026	0.080488	0.33622	0.00024185
Fgf5	-0.042881	0.6721	0.33591	0.00024185
Ifi35	-0.17585	0.021428	0.33581	0.00024185
Olfr1512	-0.043327	0.66712	0.33568	0.00024185
Crct1	0.0083725	0.68177	0.33529	0.00029022
1700123O20Rik	0.10802	0.031924	0.33515	0.00029022
Syt16	0.068627	0.14772	0.33513	0.00029022
Slc22a23	0.072153	0.1305	0.3347	0.00029022
Hmgn1	-0.028759	0.83811	0.33446	0.00029022
Gjd4	0.075713	0.11493	0.33417	0.00029022
Idnk	-0.14426	0.059253	0.33412	0.00029022
Ndufs4	0.19617	0.00053207	0.33371	0.00029022
Adam24	-0.059301	0.49869	0.33366	0.00029022
Olfr282	-0.016559	0.99357	0.33352	0.00029022
Lmtk3	0.034978	0.38827	0.33299	0.00033859
Llgl2	-0.13421	0.078069	0.33294	0.00033859

Appendix Table 4: Genes enriched in 4-OHT treated bulk CV7250 cell lines

Gene	ETOH|beta	ETOH|p-value	4_OHT|beta	4_OHT|p-value
Foxo1	-0.43407	0	1.726	0
Pten	-0.30901	0.00029022	1.3968	0
Rbm47	-0.0029506	0.93823	1.0644	0
Cdkn2b	0.51965	0	1.0263	0
Tsc2	-0.44604	0	0.99933	0

Vgll4	-0.098804	0.10965	0.91195	0
Atxn7l3	-0.20887	0.0076424	0.89512	0
Rock2	-0.25137	0.0022734	0.85922	0
Appl1	-0.093256	0.12808	0.74755	0
Akap14	-0.18582	0.013447	0.7449	0
Srebf1	-0.24847	0.002612	0.72553	0
Rab40c	-0.34036	9.67E-05	0.72516	0
Ccdc176	-0.29649	0.00053207	0.69909	0
Ihh	-0.20562	0.0081261	0.6965	0
Sltm	-0.14759	0.032746	0.68735	0
Sgta	-0.15127	0.029893	0.68405	0
Pilra	-0.14279	0.037003	0.66562	0
Prss34	-0.23044	0.0042082	0.66233	0
Usp22	0.015396	0.65594	0.66107	0
Ccdc85c	-0.27671	0.0010641	0.64805	0
Nf2	-0.16161	0.022831	0.64596	0
Med16	-0.046817	0.4466	0.6349	0
Prkar1a	-0.045613	0.45918	0.61634	0
Olfr344	-0.19559	0.010303	0.61408	0
Lyzl4	-0.073736	0.21916	0.6124	0
Synpo	-0.17896	0.015091	0.61063	0
Ifrd1	-0.02624	0.70349	0.60727	0
F13a1	-0.11134	0.07865	0.60131	0
Aip	-0.0034863	0.94631	0.57775	0
Olfr506	-0.18361	0.014172	0.57626	0
Cd209d	-0.1383	0.042469	0.56738	0
Ptms	-0.1556	0.026217	0.55927	0
Ddi1	-0.16705	0.020315	0.55841	0
Camk1	-0.014149	0.88232	0.55562	0
Ube2ql1	-0.13555	0.045516	0.54143	0
Myl6	-0.20545	0.0081261	0.53317	0
Cmtm5	-0.2784	0.0010641	0.52115	0
Med13	-0.23814	0.0035794	0.51464	0
Tsc1	-0.31712	0.00029022	0.51395	0
Dhx29	-0.035342	0.57841	0.50496	0
Supt20	0.040668	0.33457	0.5036	0
G2e3	-0.015662	0.85958	0.49944	0
Ccm2	-0.29188	0.00072555	0.49817	0
Pawr	-0.16011	0.023314	0.49606	0
Rb1	0.14816	0.0009674	0.49461	0
Ifi35	-0.1664	0.020509	0.49201	0
Adam34	-0.10889	0.084502	0.49124	0

Elmsan1	-0.25319	0.002225	0.48834	0
Clp1	-0.31604	0.00029022	0.48628	0
4930430F08Rik	-0.19269	0.011367	0.48429	0
Errfi1	-0.12759	0.053836	0.48405	0
Rasa2	-0.16882	0.019251	0.48382	0
Phc3	-0.15413	0.027571	0.48273	0
Pgf	-0.01466	0.87409	0.48218	0
Pramel7	-0.16242	0.022299	0.48026	4.84E-05
Mt3	-0.094192	0.12508	0.47938	4.84E-05
4930432K21Rik	-0.16114	0.023024	0.47492	9.67E-05
Sgtb	-0.10148	0.10206	0.47424	9.67E-05
Psg28	-0.17953	0.014946	0.47207	9.67E-05
Acpt	-0.090998	0.13703	0.47028	9.67E-05
Tbx22	-0.020968	0.78011	0.46263	0.00014511
Dpf2	-0.27094	0.0012092	0.46212	0.00014511
Tdrd6	-0.1079	0.087356	0.46047	0.00014511
Klra17	-0.072237	0.22758	0.45406	0.00014511
Tuft1	-0.13897	0.041308	0.45227	0.00014511
Kalrn	-0.043259	0.48433	0.45179	0.00014511
Tm2d1	-0.24323	0.0031924	0.45177	0.00014511
Onecut2	-0.016682	0.84449	0.45167	0.00014511
Cml3	-0.16528	0.020993	0.451	0.00014511
Fbxo11	-0.11226	0.076376	0.45071	0.00014511
Fgf16	-0.061155	0.3085	0.45042	0.00014511
Akr1c19	-0.034668	0.58682	0.45025	0.00014511
Emx2	-0.037989	0.54571	0.44661	0.00014511
Bag4	-0.15642	0.025684	0.44633	0.00014511
Slc16a3	-0.015807	0.8575	0.44131	0.00014511
Abo	-0.15977	0.023508	0.44104	0.00014511
Olfr1133	-0.19318	0.011222	0.43933	0.00014511
Mmp14	-0.035781	0.57314	0.4385	0.00014511
Msh3	-0.090434	0.13945	0.43816	0.00014511
Tnfrsf11b	-0.078132	0.19362	0.43377	0.00019348
Ccne2	-0.13802	0.042711	0.43322	0.00019348
Zfp800	-0.16816	0.019687	0.4324	0.00024185
Srm	-0.1463	0.033956	0.43221	0.00024185
Fbxo28	-0.10074	0.10433	0.43184	0.00024185
Pde10a	-0.082667	0.17021	0.43069	0.00029022
Trp73	-0.069595	0.24436	0.4306	0.00029022
Ccdc181	-0.087011	0.15217	0.42989	0.00029022
Kdm1a	-0.28307	0.0010158	0.42793	0.00029022
Tmem51	0.02118	0.57454	0.42789	0.00029022

Angpt4	-0.17027	0.018332	0.42699	0.00029022
Amotl2	-0.086253	0.15483	0.4241	0.00038696
Apobr	-0.083259	0.16741	0.42373	0.00038696
Taf6l	-0.032256	0.61962	0.42118	0.00038696
Ntf3	-0.0278	0.68115	0.4187	0.00038696
Tmem47	-0.087782	0.14956	0.41758	0.00038696
Gm5935	-0.20581	0.0080778	0.41718	0.00038696
Taf5l	0.08868	0.047354	0.41331	0.00038696
Hydin	-0.23727	0.0036277	0.41172	0.00038696
Psmd8	-0.41276	0	0.4112	0.00038696
Myb	-0.09379	0.1261	0.40836	0.00038696
Rabl3	-0.11439	0.072845	0.40793	0.00038696
Elf4	0.009838	0.73459	0.40664	0.00043533
Olfr981	-0.050632	0.40592	0.40606	0.00043533
Tada1	0.043896	0.30086	0.40465	0.00043533
Jtb	-0.276	0.0010641	0.40355	0.00043533
Ap5b1	-0.043629	0.48041	0.40267	0.00043533
Dysf	-0.10157	0.10182	0.40071	0.0004837
Dcpp1	-0.13628	0.044645	0.39961	0.0004837
Zdhhc9	-0.070882	0.23634	0.39939	0.0004837
Gsk3b	0.19079	9.67E-05	0.39637	0.0004837
Gars	-0.18413	0.014076	0.39554	0.0004837
Rfx4	-0.069446	0.24543	0.39409	0.0004837
Gskip	-0.042042	0.49826	0.39385	0.0004837
Katnbl1	-0.07323	0.22216	0.39186	0.0004837
Marf1	-0.069705	0.24364	0.39085	0.0004837
Trim43c	-0.099702	0.1069	0.38822	0.00053207
Scgb2b3	-0.1593	0.02375	0.38819	0.00053207
Gpx1	-0.076305	0.20344	0.38739	0.00062881
Anp32e	-0.12653	0.054948	0.38672	0.00062881
Zfp595	-0.017597	0.83085	0.38648	0.00062881
Fgfr4	-0.14731	0.033037	0.38598	0.00062881
Vmn1r117	-0.21002	0.0073039	0.38249	0.00072555
Dapk3	-0.084654	0.16204	0.38242	0.00072555
Lrba	-0.046054	0.45415	0.38193	0.00072555
Tmem186	0.079426	0.073813	0.38073	0.00077392
Olfr317	-0.10895	0.084406	0.38031	0.00077392
Hivep1	-0.02761	0.68381	0.37746	0.00087066
Mug1	-0.087921	0.14917	0.37643	0.00087066
Slc16a1	-0.071494	0.23256	0.376	0.00087066
Ccnc	-0.25068	0.0023218	0.3757	0.00087066
Abca1	-0.0088432	0.96764	0.3752	0.00087066

Gpx2	-0.15952	0.023653	0.37505	0.00087066
Nprl3	-0.16166	0.022831	0.37499	0.00087066
Il17a	-0.030921	0.63814	0.37485	0.00091903
Ntmt1	-0.1061	0.091274	0.37285	0.0010641
Sf3b1	-0.38308	0	0.37226	0.0010641
Rgs5	-0.15251	0.02907	0.37123	0.0010641
Casc3	-0.059508	0.32195	0.37051	0.0010641
Mum1	-0.14036	0.03947	0.37017	0.0010641
Asb1	-0.11614	0.069411	0.36987	0.0011125
Phox2b	-0.06751	0.25888	0.36936	0.0011125
Trmt44	-0.12851	0.052433	0.36888	0.0011125
Igsf10	-0.22659	0.0049337	0.36842	0.0011125
Olfr160	-0.042797	0.48979	0.36816	0.0011125
Pam	-0.060479	0.31431	0.36679	0.0011609
Tsr3	-0.15008	0.031102	0.36533	0.0012092
Zfp575	-0.11625	0.069121	0.36511	0.0012092
Krit1	-0.17105	0.018139	0.3646	0.0012092
Tm9sf2	-0.27275	0.0011609	0.364	0.0012092
Grasp	-0.13509	0.045855	0.36003	0.0013544
Mospd2	-0.18162	0.014608	0.35969	0.0013544
Naa16	-0.041166	0.50924	0.35944	0.0014027
Rwdd2a	0.010245	0.72869	0.35916	0.0014027
Gm8298	-0.10151	0.10196	0.35865	0.0014511
Paxip1	0.047426	0.26797	0.35845	0.0014511
Cdc42ep1	-0.089281	0.144	0.35839	0.0014511
Zfp82	-0.10936	0.083632	0.35829	0.0014511
Sec24d	-0.10486	0.094031	0.35809	0.0014511
Lgals4	-0.094522	0.12392	0.35809	0.0014511
Dok1	-0.013209	0.89731	0.35747	0.0014995
Ppwd1	-0.32069	0.00029022	0.35744	0.0014995
Pyhin1	-0.14152	0.038261	0.35719	0.0014995
Timm17a	-0.18711	0.012625	0.35574	0.0014995
Il27	-0.037978	0.54576	0.35467	0.0015962
Tas2r131	-0.014847	0.87085	0.35352	0.0016446
Zzz3	-0.28823	0.00082229	0.3525	0.0016929
Iigp1	-0.1203	0.062978	0.35112	0.0017413
Olfr1241	-0.017764	0.82766	0.35059	0.0018381
Acsm1	-0.069432	0.24548	0.35014	0.0018381
Tcp10b	0.0023131	0.85267	0.34929	0.0018381
Mfn1	-0.11006	0.081552	0.34807	0.0020315
Mlph	-0.068396	0.25244	0.34629	0.002225
Vmn2r59	-0.19306	0.01127	0.34573	0.0022734

Herpud1	-0.1127	0.075796	0.34553	0.0022734
Dqx1	-0.020632	0.78437	0.34508	0.0023218
Morc3	-0.1038	0.096498	0.34375	0.0024185
Fam89a	-0.08824	0.14782	0.34319	0.0024669
Car7	-0.07775	0.19566	0.3431	0.0024669
Gm2663	-0.19274	0.011367	0.34281	0.0025152
Tceal5	-0.10947	0.083341	0.34264	0.0025152
Rapgef5	-0.035339	0.57846	0.3423	0.0025636
Zfp91	-0.12139	0.061962	0.34154	0.0026603
Vmn2r5	-0.020394	0.78766	0.34136	0.0026603
Atg2a	-0.16963	0.018719	0.34118	0.0026603
Nabp2	-0.055855	0.35542	0.34053	0.0027087
Slc17a8	-0.12424	0.058286	0.3389	0.0029022
Socs3	-0.041784	0.50155	0.33848	0.0029022
Ovch2	-0.04063	0.51528	0.33846	0.0029022
4930415O20Rik	-0.037741	0.54885	0.33838	0.0029022
2310057N15Rik	-0.14538	0.034391	0.33661	0.0030473
Ddx4	-0.0076296	0.98796	0.3353	0.003144
Vmn1r88	-0.036118	0.56883	0.3351	0.003144
Caskin2	-0.077301	0.19837	0.33492	0.0031924
Rab32	-0.061795	0.30362	0.33491	0.0031924
Rfx1	-0.13732	0.043436	0.33358	0.0032892
Cela3b	-0.0001315	0.8932	0.33336	0.0033375
Pex3	-0.093494	0.12726	0.33146	0.0034826
Slc22a29	-0.1111	0.079182	0.33112	0.003531
Pfpl	-0.20149	0.0091903	0.33096	0.003531
Pgc	-0.071605	0.23193	0.33086	0.003531
Ccdc83	-0.078502	0.19154	0.3308	0.0035794
Rcbtb1	0.0027325	0.84705	0.33016	0.0036277
Eef2kmt	-0.093416	0.12745	0.33015	0.0036277
Pagr1a	-0.063849	0.28558	0.32897	0.0037729
Gmppa	-0.04786	0.43475	0.32895	0.0037729
Vps13c	0.017514	0.62421	0.32811	0.0038212
Gas2	-0.083274	0.16741	0.32796	0.0038212
3110002H16Rik	0.11609	0.010932	0.32795	0.0038212
Atg12	-0.23749	0.0036277	0.32592	0.0042082
Tpm2	-0.030185	0.64719	0.32524	0.0042566
Bhlha15	-0.1457	0.034198	0.32465	0.0043049
Thada	-0.16489	0.021283	0.32384	0.00445
Kazald1	-0.21629	0.0061914	0.32335	0.0044984
M6pr	-0.17954	0.014946	0.32293	0.0045468
Gatsl3	-0.18649	0.01306	0.32275	0.0046435

Atg5	-0.083899	0.16518	0.32243	0.0046435
Dusp5	-0.14352	0.036374	0.32223	0.0047403
Znrf4	-0.065843	0.27111	0.32193	0.0047886
Olfr225	-0.034748	0.58552	0.32169	0.0047886
Arg1	-0.057876	0.33753	0.3213	0.004837
Mpi	-0.1745	0.016204	0.32125	0.004837
Foxi3	-0.15612	0.02583	0.3201	0.0049337
Eppin	-0.061832	0.30304	0.31804	0.0053207
Ablim2	-0.063926	0.28504	0.31803	0.0053207
Inhba	-0.15305	0.028635	0.31761	0.0054174
Mpp5	-0.13908	0.041163	0.31733	0.0054658
Slc20a1	-0.024547	0.72705	0.31724	0.0055625
Stk11	-0.32117	0.00029022	0.31675	0.0055625
Colq	-0.14865	0.031827	0.31659	0.0055625
Pwwp2b	-0.13132	0.049531	0.31606	0.0057077
Gm20854	-0.11021	0.081213	0.31575	0.0058044
Zdhhc23	-0.072207	0.22777	0.31454	0.0059011
Elmod2	-0.039125	0.53333	0.31437	0.0059011
Hnf1a	-0.045224	0.46338	0.31167	0.0060946
Arhgap26	-0.0028204	0.93557	0.31126	0.0062397
Klhl26	-0.083582	0.16625	0.30956	0.0064332
Itga3	0.018453	0.61144	0.30955	0.0064332
BC048562	-0.087318	0.15116	0.30912	0.0064332
Tmem201	-0.15027	0.030957	0.30911	0.0064332
Rab40b	-0.28649	0.00091903	0.30817	0.0064816
Tmem231	0.020893	0.57904	0.3077	0.0064816
Jag2	-0.0075063	0.99018	0.30732	0.0065783
Hcar2	-0.052326	0.38952	0.30711	0.0066267
Epx	-0.077575	0.19677	0.30645	0.0068202
N4bp3	-0.15172	0.029506	0.30641	0.0068202
2210018M11Rik	-0.16764	0.019928	0.30614	0.0068685
Heph	-0.084963	0.16054	0.30556	0.0070136
Ralgapb	-0.19578	0.010158	0.30234	0.0076424
Sntb2	-0.08463	0.16209	0.30198	0.0077392
Nfu1	-0.12212	0.061043	0.30182	0.0077876
Scn9a	-0.15036	0.030957	0.30169	0.0077876
Bmp6	-0.065813	0.27155	0.30133	0.0078359
Pbrm1	-0.12161	0.061768	0.30024	0.0078843
Polr3gl	-0.11722	0.067573	0.30024	0.0078843
Wnt5b	-0.058155	0.33472	0.30009	0.0078843
Myh9	-0.54532	0	0.30002	0.0078843
Med24	-0.2571	0.0020315	0.29809	0.0081261

Akap13	-0.039371	0.53013	0.29752	0.0081745
Ankrd9	-0.13894	0.041405	0.29693	0.0084164
Ibsp	-0.13633	0.044549	0.29688	0.0084164
Atp6ap1l	-0.060491	0.31421	0.29626	0.0085615
Pnpla8	-0.094855	0.12305	0.29601	0.0086098
Sh2d7	-0.05996	0.31832	0.29469	0.0089968
Fam189a2	-0.16224	0.022395	0.29448	0.0089968
Tgif2lx2	-0.093284	0.12789	0.2944	0.0090935
Wdr31	-0.19964	0.0094805	0.29404	0.0092387
Slain2	0.018301	0.61323	0.29393	0.0092387
Txnl4b	-0.25401	0.002225	0.29369	0.009287
Pcgf3	-0.11095	0.07952	0.29339	0.009287
Ephb3	-0.19527	0.010448	0.2933	0.009287
Hmx3	0.040197	0.3398	0.29314	0.009287
Tob1	-0.0057409	0.98167	0.29303	0.009287
Rnf222	-0.17582	0.015962	0.29301	0.009287
Ak3	-0.030088	0.64864	0.29301	0.009287
Utp23	-0.45271	0	0.29238	0.0094805
Ccdc77	-0.17731	0.015575	0.29225	0.0095289
Rps25	-0.38653	0	0.29184	0.009674
Ccdc102a	-0.15266	0.028974	0.29181	0.009674
Nprl2	-0.11492	0.072265	0.29181	0.009674
Evx1	-0.067314	0.26028	0.29175	0.009674
1110032A03Rik	-0.037002	0.55838	0.29128	0.0098675
Cep170	-0.085038	0.1601	0.29076	0.010013
Rasa3	-0.041813	0.50116	0.29057	0.010013
Sec16b	0.010938	0.71849	0.29021	0.010061
Zfp449	-0.10237	0.099739	0.29017	0.010109
Acot5	-0.074464	0.21525	0.29009	0.010158
Tcte1	0.013147	0.68531	0.28999	0.010206
Il18	-0.13763	0.043098	0.28986	0.010206
Myadml2	-0.032987	0.60893	0.28905	0.010496
Rock1	-0.086651	0.15348	0.28897	0.010496
Stk24	-0.073746	0.21912	0.28888	0.010496
Acp6	-0.10974	0.082422	0.28877	0.010496
Zfp628	-0.10234	0.099787	0.28819	0.010545
Uchl4	-0.083453	0.16678	0.28811	0.010545
Arhgap21	-0.090676	0.13853	0.28785	0.01069
Inpp5d	0.007271	0.77334	0.28638	0.011125
Plcd4	-0.05302	0.38328	0.28593	0.01127
Tyro3	-0.12387	0.058818	0.28582	0.011319
Usp1	-0.15323	0.028538	0.28497	0.011464

Scrg1	-0.057399	0.34173	0.28494	0.011464
Calml4	-0.062455	0.29762	0.28434	0.011512
Vmn1r65	-0.017996	0.8233	0.28361	0.011754
Lrrc25	-0.058363	0.33259	0.28324	0.011947
Dusp6	-0.025194	0.71878	0.28282	0.011996
Kdm2b	-0.059882	0.31914	0.28281	0.011996
Kctd5	-0.26433	0.0015478	0.28271	0.011996
S100a14	-0.055141	0.36166	0.28207	0.012238
1700019G17Rik	-0.06573	0.27208	0.2817	0.012286
Wfdc10	-0.13422	0.046484	0.28163	0.012334
Mark1	-0.080841	0.17868	0.28129	0.012479
Sumo3	-0.1094	0.083487	0.28071	0.012625
Omt2a	-0.079288	0.1868	0.28067	0.012625
Ccdc85b	-0.13362	0.046967	0.28061	0.012625
Zcchc3	-0.10746	0.088178	0.28048	0.012625
Zg16	-0.058095	0.3354	0.28022	0.012673
Blm	-0.25784	0.0019832	0.27931	0.01277
Olfr703	-0.0081417	0.97935	0.27872	0.012818
Ambra1	0.090353	0.044258	0.27869	0.012866
Ptges3	-0.020439	0.78693	0.27853	0.012963
1810062G17Rik	-0.096784	0.11556	0.27819	0.01306
Flot2	0.018556	0.6098	0.27799	0.01306
Tmem194	-0.17525	0.01601	0.27764	0.01306
Set	-0.28248	0.0010158	0.27762	0.01306
Igfbp7	-0.11475	0.072555	0.27699	0.01335
Clcn1	-0.10552	0.092435	0.27699	0.01335
Dnajc7	-0.090027	0.141	0.27653	0.013495
Abat	-0.047697	0.43668	0.276	0.01364
Olfr1105	0.014958	0.66189	0.2759	0.013689
Zfp763	-0.05978	0.31987	0.27573	0.013785
Mex3c	-0.076945	0.19996	0.27568	0.013785
Thy1	-0.020613	0.78475	0.27562	0.013785
Lats2	-0.036643	0.56322	0.27544	0.013785
Ccdc43	-0.078827	0.18951	0.27537	0.013785
Klrc2	-0.014434	0.87825	0.27518	0.013931
Olfr1347	-0.14589	0.034101	0.2751	0.013931
Glg1	0.022728	0.55282	0.27508	0.013931
Tada2b	0.13009	0.0043049	0.27482	0.014076
Dlk2	-0.13935	0.040776	0.27425	0.014124
Vmn2r71	0.012918	0.6884	0.27411	0.014124
Fbxw7	0.015909	0.64854	0.27381	0.014172
Olfr530	0.004494	0.81837	0.2736	0.014172

Tbc1d16	-0.13844	0.042275	0.27356	0.014172
Gpd1l	-0.072355	0.22705	0.27349	0.014221
Nudt16	-0.083087	0.16828	0.27337	0.014221
Nudcd2	-0.20321	0.0084164	0.27289	0.014414
Adam2	0.018952	0.60496	0.27284	0.014414
Epb4.1l5	-0.074994	0.21201	0.27271	0.014414
Hmbox1	0.033586	0.41801	0.27174	0.014511
Cdkn1a	-0.12372	0.058963	0.27142	0.014608
Taok1	-0.003158	0.94109	0.27137	0.014656
Atg4b	0.009924	0.73348	0.27101	0.014704
Lsm14a	-0.0059612	0.98447	0.27057	0.014801
Hdgf	-0.023163	0.74833	0.27051	0.014801
Mesdc1	-0.04421	0.47436	0.27009	0.014946
Tmtc3	-0.052529	0.38754	0.26967	0.015043
Otub1	0.045229	0.28746	0.26883	0.015285
Elovl4	-0.029534	0.65667	0.26882	0.015285
Olfr788	0.022671	0.55369	0.26862	0.015333
Depdc5	-0.087555	0.15024	0.26837	0.015382
Bicd2	-0.15163	0.029602	0.26812	0.01543
Ccnjl	-0.10722	0.088372	0.26788	0.01543
Olfr204	0.010412	0.72627	0.26783	0.01543
Lrrc75b	-0.032314	0.61889	0.26782	0.01543
Fam166b	0.045956	0.28151	0.26777	0.01543
Nrn1l	-0.063671	0.28669	0.26765	0.01543
Fancl	-0.18194	0.014511	0.26757	0.01543
Chn2	0.024287	0.53154	0.26725	0.015672
Adgrg6	-0.12826	0.052965	0.26722	0.01572
Hnrnph2	-0.080613	0.17998	0.26716	0.015817
Tcerg1l	-0.047118	0.44321	0.26693	0.015865
Bik	-0.08531	0.1587	0.2669	0.015865
Tmem154	-0.069295	0.24659	0.26449	0.016688
Nudt2	-0.031687	0.6276	0.26426	0.016688
Olfr418	-0.1599	0.023508	0.26284	0.016881
Gna13	-0.097949	0.11202	0.26284	0.016881
Klhl31	-0.02715	0.69	0.26123	0.017123
Gpr34	0.039794	0.34507	0.26109	0.017123
Zfx	-0.15875	0.02404	0.26078	0.017171
Hdx	-0.069102	0.2479	0.2607	0.017171
Nfya	-0.13933	0.040776	0.26065	0.017171
Pvrl4	-0.15719	0.025249	0.26056	0.017171
Map4k4	0.029721	0.46367	0.2604	0.017171
Sox17	0.0059412	0.79365	0.26013	0.01722

Slc4a5	-0.020444	0.78688	0.26	0.017268
Ubap2l	-0.22684	0.0049337	0.25887	0.017413
Clptm1l	-0.063654	0.28683	0.25826	0.017462
Med12	-0.24064	0.0033859	0.25821	0.017462
Samd12	-0.028036	0.67795	0.25803	0.017607
B4galnt1	-0.020614	0.78475	0.25774	0.017703
Rtca	-0.092681	0.13026	0.25738	0.017945
Svs5	-0.10946	0.083341	0.25732	0.017945
Arid3c	-0.040283	0.51944	0.25709	0.017945
Reg3g	-0.11005	0.081552	0.25688	0.01809
Pgls	-0.037942	0.54639	0.25659	0.018139
Psmd5	-0.079558	0.1854	0.25645	0.018139
Myh4	-0.06264	0.29617	0.25488	0.018477
Rcor1	-0.069852	0.24287	0.25474	0.018526
Dlat	-0.081007	0.17786	0.25462	0.018622
Sval2	-0.049702	0.41603	0.25445	0.018864
1700019N19Rik	-0.052135	0.39151	0.25442	0.018864
Slc20a2	-0.045978	0.45502	0.25418	0.018864
Hoxd3	-0.098752	0.1098	0.25416	0.018864
Wdfy2	-0.13221	0.048612	0.25347	0.019203
Otol1	-0.0013319	0.91158	0.25312	0.019396
Camp	-0.054449	0.36824	0.25281	0.019493
Acsl6	-0.11857	0.065445	0.25268	0.019541
Atg10	-0.064421	0.28117	0.25215	0.019687
Tmem129	-0.090844	0.13752	0.25141	0.019928
Kctd21	0.20139	4.84E-05	0.25118	0.020025

Appendix Table 5: Table showing the classic GRmetrics measures of drug sensitivity in the acute *Pdk1* deletion setting in CV7250 cell line

EtOH: EtOH treated CV7250 cell line, Tam: 4-OHT treated CV7250 cells lines, IC50: The half maximal inhibitory concentration, Emax: maximum effect, AUC: area under curve, EC50: Half maximal effective concentration

cell_line	agent	Replicate	fit	IC50	Emax	AUC	EC50
ETOH	EHT1864	1	flat	Inf	0.60027441	0.84056011	0
ETOH	EHT1864	2	flat	Inf	0.55478564	0.80590514	0
ETOH	EHT1864	3	flat	Inf	0.70457528	0.94339285	0
ETOH	EHT1864	4	sigmoid	Inf	0.67585761	0.90556933	1.91129015

ETOH	Fluorouracil	1	sigmoid	2.15945657	0.2124658	0.80371563	1.72336065
ETOH	Fluorouracil	2	sigmoid	1.03397528	0.12143385	0.73958158	0.84027119
ETOH	Fluorouracil	3	sigmoid	2.97032756	0.20417364	0.80054584	2.63847433
ETOH	Fluorouracil	4	sigmoid	1.05849119	0.20848901	0.7289671	0.86083475
ETOH	JQ1	1	sigmoid	0.16528218	0.08981823	0.40394338	0.14939472
ETOH	JQ1	2	sigmoid	0.12166066	0.0882676	0.37332158	0.10436897
ETOH	JQ1	3	sigmoid	0.2035913	0.09985024	0.43977716	0.17230956
ETOH	JQ1	4	sigmoid	0.19107325	0.09540534	0.43067571	0.16478357
ETOH	KU-0063794	1	sigmoid	0.32786682	0.09133398	0.48887955	0.31651155
ETOH	KU-0063794	2	sigmoid	0.27256902	0.10857376	0.48276571	0.22239843
ETOH	KU-0063794	3	sigmoid	0.4295693	0.1537345	0.56909006	0.31654389
ETOH	KU-0063794	4	sigmoid	0.35140959	0.12842863	0.51439727	0.2762295
ETOH	MK-0752	1	flat	Inf	0.88405878	0.92400745	0
ETOH	MK-0752	2	flat	Inf	0.85692557	0.9333794	0
ETOH	MK-0752	3	flat	Inf	0.8328111	0.95568031	0
ETOH	MK-0752	4	flat	Inf	0.96142959	1.02721007	0
ETOH	Pictilisib	1	sigmoid	0.2542211	0.09734549	0.45603224	0.2542211
ETOH	Pictilisib	2	sigmoid	0.22680198	0.09989356	0.45316044	0.18956786
ETOH	Pictilisib	3	sigmoid	0.4917572	0.13699795	0.5334498	0.4917572
ETOH	Pictilisib	4	sigmoid	0.50151902	0.13862309	0.56596901	0.371582
ETOH	Rapamycin	1	flat	#NAME?	0.34448928	0.36521427	0
ETOH	Rapamycin	2	flat	#NAME?	0.27538844	0.33356872	0
ETOH	Rapamycin	3	flat	#NAME?	0.26272192	0.33904572	0
ETOH	Rapamycin	4	flat	#NAME?	0.33455397	0.36553995	0

ETOH	RBC8	1	flat	Inf	0.76616198	1.03392309	0
ETOH	RBC8	2	flat	Inf	0.70006577	0.91430901	0
ETOH	RBC8	3	flat	Inf	1.11768178	1.15453531	0
ETOH	RBC8	4	flat	Inf	0.81613146	0.91135668	0
ETOH	Sapanisertib	1	flat	#NAME?	0.05420422	0.11517014	0
ETOH	Sapanisertib	2	sigmoid	0.00221799	0.04996551	0.1023021	0.00186787
ETOH	Sapanisertib	3	sigmoid	0.00096556	0.08756994	0.16392999	0.00096556
ETOH	Sapanisertib	4	sigmoid	0.00113445	0.09739043	0.18308116	0.00113445
ETOH	TAK-632	1	sigmoid	9.14629861	0.45760143	0.79123666	9.14629861
ETOH	TAK-632	2	sigmoid	5.7942969	0.35693523	0.84606627	5.7942969
ETOH	TAK-632	3	sigmoid	6.67632019	0.38430389	0.77763367	6.67632019
ETOH	TAK-632	4	sigmoid	10.602955	0.50047257	0.86928329	10.602955
ETOH	Verteporfin	1	sigmoid	5.86706479	0.45797429	0.82469312	1.77107563
ETOH	Verteporfin	2	sigmoid	2.91356357	0.24445635	0.75799955	2.74830337
ETOH	Verteporfin	3	sigmoid	5.99379044	0.47538468	0.9713866	2.8172827
ETOH	Verteporfin	4	sigmoid	6.61103595	0.40670753	0.89213364	4.12880123
ETOH	Y15	1	sigmoid	0.58314062	0.00267936	0.61553101	0.57822091
ETOH	Y15	2	sigmoid	0.35811838	0.00133298	0.49872392	0.35578206
ETOH	Y15	3	sigmoid	0.56798301	0.0029834	0.54849818	0.56310123
ETOH	Y15	4	sigmoid	0.68238733	0.00327542	0.5961282	0.67277809
ETOH	BAY 1251152	1	sigmoid	0.03011573	0.03003404	0.16141585	0.02943202
ETOH	BAY 1251152	2	sigmoid	0.03565588	0.02471172	0.17669455	0.0351969
ETOH	BAY 1251152	3	sigmoid	0.03173641	0.02828529	0.16594256	0.03095983
ETOH	BAY 1251152	4	sigmoid	0.03239692	0.03497088	0.16906367	0.03133839

ETOH	BAY1125976	1	sigmoid	1.21736206	0.2931848	0.60382837	1.21736206
ETOH	BAY1125976	2	sigmoid	1.53919802	0.24687649	0.67613426	1.06936085
ETOH	BAY1125976	3	sigmoid	0.62033145	0.1956716	0.55145094	0.62033145
ETOH	BAY1125976	4	sigmoid	1.03961877	0.25892729	0.58721393	1.03961877
ETOH	CK-869	1	sigmoid	3.15950936	0.30011043	0.81566492	2.01099144
ETOH	CK-869	2	sigmoid	3.54522508	0.29628632	0.75668738	3.54522508
ETOH	CK-869	3	sigmoid	3.46537778	0.31315498	0.75930972	3.2366977
ETOH	CK-869	4	sigmoid	4.23847336	0.31228093	0.76670828	4.23847336
ETOH	CM272	1	sigmoid	0.14889998	0.0038244	0.36767864	0.14843821
ETOH	CM272	2	sigmoid	0.14450137	0.00478811	0.3542411	0.14450137
ETOH	CM272	3	sigmoid	0.15581447	0.00744686	0.36660445	0.15581447
ETOH	CM272	4	sigmoid	0.23648195	0.01484677	0.42708008	0.23648195
ETOH	FL-411	1	sigmoid	4.76096819	0.0361691	0.8104848	4.76096819
ETOH	FL-411	2	sigmoid	5.35173343	0.03445663	0.83893124	5.35173343
ETOH	FL-411	3	sigmoid	3.33368207	0.01929481	0.75294034	3.33368207
ETOH	FL-411	4	flat	Inf	0.07088176	0.76050321	0
ETOH	MCP110	1	flat	Inf	0.48430948	0.81147109	0
ETOH	MCP110	2	flat	Inf	0.52597142	0.85061556	0
ETOH	MCP110	3	sigmoid	7.73197683	0.39317076	0.89951219	7.73197683
ETOH	MCP110	4	sigmoid	15.7692403	0.58351953	0.89228942	15.7692403
ETOH	Monastrol	1	flat	Inf	0.7744144	0.89981512	0
ETOH	Monastrol	2	flat	Inf	0.80555061	0.89459996	0
ETOH	Monastrol	3	flat	Inf	0.71451955	0.83031281	0
ETOH	Monastrol	4	flat	Inf	0.90863812	0.93831589	0

ETOH	MYF-01-37	1	sigmoid	11.046795	0.49918498	0.84502582	11.046795
ETOH	MYF-01-37	2	flat	Inf	0.55111144	0.87059446	0
ETOH	MYF-01-37	3	sigmoid	8.39023855	0.43426118	0.87018133	8.39023855
ETOH	MYF-01-37	4	sigmoid	11.5579605	0.53311604	0.99092847	6.81444732
ETOH	Nirogacestat (PF-03084014, PF-3084014)	1	sigmoid	8.38948196	0.43735934	0.83779387	8.38948196
ETOH	Nirogacestat (PF-03084014, PF-3084014)	2	sigmoid	9.27868111	0.43754588	0.78691321	9.27868111
ETOH	Nirogacestat (PF-03084014, PF-3084014)	3	sigmoid	7.27924155	0.3800278	0.84684938	7.27924155
ETOH	Nirogacestat (PF-03084014, PF-3084014)	4	flat	Inf	0.5054169	0.79444445	0
ETOH	Pemetrexed	1	sigmoid	0.73267598	0.27252124	0.63696161	0.35171645
ETOH	Pemetrexed	2	sigmoid	0.73222246	0.23703143	0.6432418	0.42298445
ETOH	Pemetrexed	3	sigmoid	0.49552367	0.29292692	0.59361796	0.25055253
ETOH	Pemetrexed	4	sigmoid	0.77510278	0.26577295	0.62258214	0.40746446
ETOH	TP0427736 HCl	1	sigmoid	Inf	0.49316792	0.60520834	0.02566799
ETOH	TP0427736 HCl	2	sigmoid	Inf	0.6015828	0.67845203	0.04852913
ETOH	TP0427736 HCl	3	sigmoid	9.66620202	0.48797785	0.61269413	0.03736222
ETOH	TP0427736 HCl	4	sigmoid	1.80591114	0.41975666	0.57944784	0.07618649
ETOH	V-9302	1	flat	Inf	0.37650303	0.82234662	0
ETOH	V-9302	2	flat	Inf	0.37370392	0.81693874	0
ETOH	V-9302	3	sigmoid	6.5661837	0.22670595	0.97660251	6.5661837
ETOH	V-9302	4	sigmoid	5.92267515	0.3036023	0.87909495	5.92267515
ETOH	BAY-293	1	sigmoid	1.79492392	0.00283094	0.68087122	1.79492392
ETOH	BAY-293	2	sigmoid	2.09021855	0.00275571	0.74476956	2.09021855

ETOH	BAY-293	3	sigmoid	2.55180527	0.0048961	0.75558798	2.55180527
ETOH	BAY-293	4	sigmoid	2.12214444	0.00269534	0.76651517	2.12214444
ETOH	BI-3406	1	sigmoid	Inf	0.65209393	0.8686721	0.90058378
ETOH	BI-3406	2	sigmoid	12.2551401	0.52049034	0.8727736	12.2551401
ETOH	BI-3406	3	flat	Inf	0.54947082	0.79701139	0
ETOH	BI-3406	4	sigmoid	Inf	0.56353169	0.84074372	1.03385443
ETOH	Dynasore	1	sigmoid	12.552881	0.75664015	1.02751714	12.552881
ETOH	Dynasore	2	sigmoid	12.6925068	0.7668521	0.98387584	12.6925068
ETOH	Dynasore	3	flat	Inf	0.69477943	0.83763359	0
ETOH	Dynasore	4	flat	Inf	0.65998364	0.90400784	0
ETOH	Gallein	1	sigmoid	Inf	0.74535173	0.98845128	3.87713033
ETOH	Gallein	2	sigmoid	Inf	0.75102322	0.96962841	5.10337739
ETOH	Gallein	3	flat	Inf	0.64280301	0.85643791	0
ETOH	Gallein	4	sigmoid	Inf	0.64554679	0.81880356	0.73123633
ETOH	GDC-0077	1	sigmoid	0.83970733	0.34380387	0.5978862	0.2358659
ETOH	GDC-0077	2	sigmoid	1.04415305	0.27626013	0.65248946	0.39764673
ETOH	GDC-0077	3	sigmoid	0.86051613	0.40822395	0.61725705	0.11621972
ETOH	GDC-0077	4	sigmoid	0.7919409	0.26872251	0.66309669	0.23219774
ETOH	GSK2256098	1	sigmoid	Inf	0.81762246	0.95295743	0.79863861
ETOH	GSK2256098	2	flat	Inf	0.70463669	0.84653108	0
ETOH	GSK2256098	3	flat	Inf	0.78505374	1.01570156	0
ETOH	GSK2256098	4	flat	Inf	0.87221091	1.02677768	0
ETOH	IACS-13909	1	sigmoid	10.1293675	0.48029986	0.88336384	10.1293675
ETOH	IACS-13909	2	sigmoid	6.0059972	0.37583334	0.75424401	6.0059972

ETOH	IACS-13909	3	sigmoid	4.76343935	0.27843703	0.79924746	4.76343935
ETOH	IACS-13909	4	sigmoid	2.37278957	0.11429386	0.70418883	2.37278957
ETOH	NSC 23766	1	sigmoid	Inf	0.79174087	1.00216319	4.48835238
ETOH	NSC 23766	2	flat	Inf	0.70568247	0.89881762	0
ETOH	NSC 23766	3	flat	Inf	0.66781324	0.92478346	0
ETOH	NSC 23766	4	sigmoid	14.0576653	0.60376229	0.93515483	14.0576653
ETOH	OSMI-4	1	sigmoid	12.7706237	0.5627049	0.95982198	12.7706237
ETOH	OSMI-4	2	flat	Inf	0.42601035	0.78157867	0
ETOH	OSMI-4	3	sigmoid	7.18833443	0.38599717	0.69786309	7.18833443
ETOH	OSMI-4	4	sigmoid	8.53148258	0.40957389	0.84576358	8.53148258
ETOH	PF-9366	1	sigmoid	7.04299443	0.41241103	0.87572541	5.10434488
ETOH	PF-9366	2	sigmoid	6.75092381	0.3770374	0.82920513	6.75092381
ETOH	PF-9366	3	sigmoid	6.29225641	0.29057288	0.854978	6.29225641
ETOH	PF-9366	4	sigmoid	4.30880136	0.13383407	0.84332115	4.30880136
ETOH	SNDX-5613	1	flat	Inf	0.61292247	0.89300389	0
ETOH	SNDX-5613	2	sigmoid	Inf	0.68953793	0.97196629	4.01839458
ETOH	SNDX-5613	3	sigmoid	9.00435772	0.47154986	0.9785645	5.60339884
ETOH	SNDX-5613	4	sigmoid	32.8013159	0.66750231	0.92320793	32.8013159
ETOH	SR-18292	1	sigmoid	29.4091837	0.64580775	0.87876728	23.73072
ETOH	SR-18292	2	sigmoid	Inf	0.62252769	0.98954338	3.73314155
ETOH	SR-18292	3	sigmoid	Inf	0.71438837	0.98189747	5.5432552
ETOH	SR-18292	4	flat	Inf	0.63910488	1.05187994	0
ETOH	A939572	1	sigmoid	Inf	0.64355849	0.71635636	0.01771584
ETOH	A939572	2	sigmoid	Inf	0.6446969	0.71683388	0.01712281

ETOH	A939572	3	sigmoid	Inf	0.75151911	0.79606084	0.03946279
ETOH	A939572	4	sigmoid	Inf	0.64888381	0.68638053	0.00253666
ETOH	Exo1	1	flat	Inf	0.91681644	0.97967828	0
ETOH	Exo1	2	flat	Inf	0.84101237	0.97727924	0
ETOH	Exo1	3	flat	Inf	0.91257768	1.11951748	0
ETOH	Exo1	4	flat	Inf	0.94532702	0.96941292	0
ETOH	ISRIB	1	flat	Inf	0.99312676	0.98421595	0
ETOH	ISRIB	2	flat	Inf	0.91557769	0.98491105	0
ETOH	ISRIB	3	flat	Inf	1.08875909	1.06669688	0
ETOH	ISRIB	4	flat	Inf	0.92525816	0.92291481	0
ETOH	ITD-1	1	sigmoid	12.1184202	0.47164148	0.83563966	12.1184202
ETOH	ITD-1	2	flat	Inf	0.17584069	0.7144169	0
ETOH	ITD-1	3	sigmoid	6.36610067	0.22747914	0.89214067	6.36610067
ETOH	ITD-1	4	sigmoid	5.14296805	0.18884348	0.80125999	5.14296805
ETOH	LOC14	1	sigmoid	3.94202163	0.17752007	0.79216384	3.94202163
ETOH	LOC14	2	sigmoid	1.80766699	0.03804954	0.6793042	1.80766699
ETOH	LOC14	3	sigmoid	4.73165293	0.04822718	0.81361918	4.73165293
ETOH	LOC14	4	sigmoid	5.07823305	0.09233805	0.90091599	5.07823305
ETOH	NSC15364	1	flat	Inf	1.05313552	1.05883378	0
ETOH	NSC15364	2	flat	Inf	0.86208276	0.91610695	0
ETOH	NSC15364	3	flat	Inf	0.82293258	0.94109426	0
ETOH	NSC15364	4	flat	Inf	0.81593559	0.95125982	0
ETOH	NVP-2	1	flat	#NAME?	0.02233631	0.02532357	0
ETOH	NVP-2	2	flat	#NAME?	0.02814529	0.02962552	0

ETOH	NVP-2	3	flat	#NAME?	0.02556405	0.03132056	0
ETOH	NVP-2	4	flat	#NAME?	0.02614523	0.03195339	0
ETOH	PD153035	1	flat	Inf	0.92594361	0.94255627	0
ETOH	PD153035	2	flat	Inf	0.96573939	1.04096707	0
ETOH	PD153035	3	flat	Inf	0.92543153	0.91603615	0
ETOH	PD153035	4	flat	Inf	0.76696648	0.87074148	0
ETOH	PluriSIn 1 (NSC 14613)	1	sigmoid	13.1284112	0.51554279	0.77533216	13.1284112
ETOH	PluriSIn 1 (NSC 14613)	2	sigmoid	8.28265383	0.47706211	0.81186522	8.28265383
ETOH	PluriSIn 1 (NSC 14613)	3	sigmoid	7.04222601	0.4389572	0.79119429	7.04222601
ETOH	PluriSIn 1 (NSC 14613)	4	sigmoid	11.0167522	0.50152716	0.83843498	11.0167522
ETOH	Raphin1	1	flat	Inf	0.72262866	0.9460228	0
ETOH	Raphin1	2	sigmoid	9.95942492	0.42326936	0.84716226	9.95942492
ETOH	Raphin1	3	sigmoid	Inf	0.6610605	0.93028749	3.76337905
ETOH	Raphin1	4	sigmoid	9.33298986	0.45043231	0.88641522	9.33298986
ETOH	Rhosin hydrochloride	1	flat	Inf	0.73290498	0.84711799	0
ETOH	Rhosin hydrochloride	2	sigmoid	Inf	0.83911928	0.95739697	1.19706807
ETOH	Rhosin hydrochloride	3	flat	Inf	0.68870428	0.84672338	0
ETOH	Rhosin hydrochloride	4	flat	Inf	0.67151826	0.84871357	0
ETOH	TAS-102	1	flat	#NAME?	0.18986201	0.25021602	0
ETOH	TAS-102	2	flat	#NAME?	0.18835998	0.24551709	0
ETOH	TAS-102	3	sigmoid	0.01476496	0.22080582	0.27116194	0.01057529
ETOH	TAS-102	4	sigmoid	0.0004438	0.20180583	0.24443601	0.00019115
ETOH	ASLAN003	1	flat	Inf	0.82188924	1.02023502	0
ETOH	ASLAN003	2	flat	Inf	0.77712854	1.0374338	0

ETOH	ASLAN003	3	flat	Inf	0.78140662	0.92414157	0
ETOH	ASLAN003	4	flat	Inf	0.79184314	0.99689771	0
ETOH	Azaserine	1	flat	Inf	0.92413179	0.92064957	0
ETOH	Azaserine	2	flat	Inf	0.79484239	0.82815224	0
ETOH	Azaserine	3	flat	Inf	0.8926209	1.06057447	0
ETOH	Azaserine	4	flat	Inf	0.92652605	0.93708854	0
ETOH	BAY-299	1	sigmoid	0.77114402	0.12674271	0.6103015	0.674721
ETOH	BAY-299	2	sigmoid	0.49587654	0.13747449	0.57513078	0.37420095
ETOH	BAY-299	3	sigmoid	1.27308109	0.15713508	0.72351681	0.95356965
ETOH	BAY-299	4	sigmoid	0.72143126	0.1318385	0.61168099	0.55779046
ETOH	Dorsomorphin (Compound C)	1	flat	Inf	0.70131404	0.95919248	0
ETOH	Dorsomorphin (Compound C)	2	sigmoid	19.4320687	0.52612148	0.84078714	19.4320687
ETOH	Dorsomorphin (Compound C)	3	flat	Inf	0.53154981	0.82652868	0
ETOH	Dorsomorphin (Compound C)	4	sigmoid	9.20152536	0.45601031	0.94786489	9.20152536
ETOH	Gedatolisib (PF-05212384, PKI-587)	1	sigmoid	0.05045555	0.05021691	0.30609298	0.05045555
ETOH	Gedatolisib (PF-05212384, PKI-587)	2	sigmoid	0.06104732	0.04451585	0.3045394	0.06104732
ETOH	Gedatolisib (PF-05212384, PKI-587)	3	sigmoid	0.06810777	0.05872146	0.33369586	0.06810777
ETOH	Gedatolisib (PF-05212384, PKI-587)	4	sigmoid	0.09402479	0.05864122	0.35555373	0.09402479
ETOH	GSK1059615	1	sigmoid	0.88138771	0.01693905	0.61580558	0.88138771
ETOH	GSK1059615	2	sigmoid	0.38147576	0.019249	0.48145841	0.38147576
ETOH	GSK1059615	3	sigmoid	0.4453148	0.02897789	0.5035719	0.4453148
ETOH	GSK1059615	4	sigmoid	0.5116897	0.03352425	0.57560584	0.49118698
ETOH	LY2109761	1	sigmoid	Inf	0.59567836	0.84116778	0.74198832
ETOH	LY2109761	2	flat	Inf	0.49871277	0.75145744	0

ETOH	LY2109761	3	flat	Inf	0.77419933	1.00883825	0
ETOH	LY2109761	4	sigmoid	Inf	0.64799398	0.88049018	2.42255865
ETOH	MAT2A inhibitor 2	1	flat	Inf	0.93502151	1.06326855	0
ETOH	MAT2A inhibitor 2	2	flat	Inf	0.99179523	1.0168028	0
ETOH	MAT2A inhibitor 2	3	flat	Inf	0.94392413	1.05101268	0
ETOH	MAT2A inhibitor 2	4	flat	Inf	0.96355154	1.04889009	0
ETOH	MGH-CP1	1	sigmoid	10.1998889	0.50667863	0.92656275	10.1998889
ETOH	MGH-CP1	2	sigmoid	7.54078249	0.35478194	0.90387792	7.54078249
ETOH	MGH-CP1	3	sigmoid	10.3682844	0.54461017	0.99181965	10.3682844
ETOH	MGH-CP1	4	sigmoid	10.8228514	0.5964234	1.01177877	10.8228514
ETOH	MK-0429	1	sigmoid	0.05512175	0.21618136	0.36682536	0.02467252
ETOH	MK-0429	2	sigmoid	0.02870391	0.16848465	0.32089075	0.01394069
ETOH	MK-0429	3	sigmoid	0.06198702	0.19731991	0.37840316	0.02940319
ETOH	MK-0429	4	sigmoid	0.06952772	0.23569727	0.40181238	0.02476775
ETOH	Palbociclib	1	sigmoid	11.8602891	0.43452769	0.78994603	11.8602891
ETOH	Palbociclib	2	flat	Inf	0.40618209	0.82123534	0
ETOH	Palbociclib	3	sigmoid	7.32861475	0.36215372	0.72010164	7.32861475
ETOH	Palbociclib	4	sigmoid	9.04946944	0.41240629	0.76278282	9.04946944
ETOH	RMC-4550	1	flat	Inf	0.7387511	0.81653089	0
ETOH	RMC-4550	2	flat	Inf	0.70472717	0.87185196	0
ETOH	RMC-4550	3	flat	Inf	0.60363855	0.78762412	0
ETOH	RMC-4550	4	flat	Inf	0.67713712	0.87971066	0
ETOH	AG-270	1	sigmoid	3.60350185	0.37126694	0.77152208	2.1554566
ETOH	AG-270	2	sigmoid	2.99082844	0.35857175	0.67844128	2.99082844

ETOH	AG-270	3	sigmoid	2.75402558	0.23802367	0.7270168	2.75402558
ETOH	AG-270	4	sigmoid	4.18776217	0.30736605	0.88698104	2.96377601
ETOH	DDO-5936	1	sigmoid	Inf	0.55443379	0.90585591	1.37308227
ETOH	DDO-5936	2	sigmoid	20.676937	0.58520942	0.84691477	20.676937
ETOH	DDO-5936	3	flat	Inf	0.59660817	0.92364529	0
ETOH	DDO-5936	4	sigmoid	21.2362451	0.54668984	0.78934593	21.2362451
ETOH	GLPG0187	1	sigmoid	0.00032405	0.1595151	0.18924379	0.00014
ETOH	GLPG0187	2	flat	#NAME?	0.19460212	0.22304218	0
ETOH	GLPG0187	3	sigmoid	0.00048126	0.19862928	0.24333309	0.00014
ETOH	GLPG0187	4	sigmoid	0.00336643	0.2091285	0.27043576	0.00120647
ETOH	Hydroxy Dynasore	1	sigmoid	6.29294234	0.3821614	0.89131582	4.45252713
ETOH	Hydroxy Dynasore	2	sigmoid	5.44508957	0.33330496	0.77411667	5.44508957
ETOH	Hydroxy Dynasore	3	sigmoid	5.06268012	0.26253522	0.7985956	5.06268012
ETOH	Hydroxy Dynasore	4	sigmoid	5.82056935	0.30131497	0.81549358	5.82056935
ETOH	IGS-1.76	1	flat	Inf	0.58882952	0.8160126	0
ETOH	IGS-1.76	2	flat	Inf	0.85564311	1.06039867	0
ETOH	IGS-1.76	3	flat	Inf	0.65305316	0.86860054	0
ETOH	IGS-1.76	4	flat	Inf	0.84268406	0.94974701	0
ETOH	ILK-IN-2	1	sigmoid	1.10480256	0.00106504	0.63048641	1.10480256
ETOH	ILK-IN-2	2	sigmoid	1.01090152	0.00094297	0.62877677	1.01090152
ETOH	ILK-IN-2	3	sigmoid	1.55628641	0.00114522	0.72231217	1.55628641
ETOH	ILK-IN-2	4	sigmoid	1.32461053	0.00129525	0.70391948	1.32461053
ETOH	NAV-2729	1	sigmoid	2.18884584	0.20954792	0.71092406	2.18884584
ETOH	NAV-2729	2	sigmoid	5.111251	0.44993126	0.83329873	1.15939563

ETOH	NAV-2729	3	sigmoid	1.06063083	0.10584612	0.6348574	1.06063083
ETOH	NAV-2729	4	sigmoid	3.18654308	0.24486361	0.78707512	2.91847896
ETOH	Omipalisib	1	sigmoid	0.01024115	0.01190432	0.12477607	0.00938024
ETOH	Omipalisib	2	sigmoid	0.00938772	0.00571716	0.11283737	0.00865329
ETOH	Omipalisib	3	sigmoid	0.02137618	0.01050147	0.17691261	0.01914067
ETOH	Omipalisib	4	sigmoid	0.01946995	0.01406821	0.16123038	0.0177563
ETOH	PKC-iota inhibitor 1	1	flat	Inf	0.63587144	0.76032535	0
ETOH	PKC-iota inhibitor 1	2	flat	Inf	0.76375261	0.93146195	0
ETOH	PKC-iota inhibitor 1	3	flat	Inf	0.79355739	0.94937896	0
ETOH	PKC-iota inhibitor 1	4	flat	Inf	0.6539693	0.86929392	0
ETOH	SCH772984	1	sigmoid	0.30536591	0.01771065	0.47707551	0.30536591
ETOH	SCH772984	2	sigmoid	0.21468856	0.01964853	0.43550759	0.20727779
ETOH	SCH772984	3	sigmoid	0.25540725	0.0254962	0.47844857	0.23194841
ETOH	SCH772984	4	sigmoid	0.21776485	0.02871315	0.45027873	0.18938533
ETOH	TA-01	1	flat	Inf	0.808014	1.03614583	0
ETOH	TA-01	2	sigmoid	37.9977544	0.66283855	0.87860654	37.9977544
ETOH	TA-01	3	flat	Inf	0.80408926	0.99705369	0
ETOH	TA-01	4	flat	Inf	0.64839339	0.81060779	0
ETOH	Zorifertinib	1	sigmoid	Inf	0.57178964	0.99240333	4.84383554
ETOH	Zorifertinib	2	sigmoid	29.7089608	0.54230848	0.81443465	29.7089608
ETOH	Zorifertinib	3	sigmoid	12.8877947	0.55807273	0.89567538	12.8877947
ETOH	Zorifertinib	4	flat	Inf	0.60018997	0.87908434	0
ETOH	AZD0364	1	sigmoid	0.09431279	0.00441886	0.30181753	0.09330265
ETOH	AZD0364	2	sigmoid	0.19526711	0.00703782	0.40181112	0.19526711

ETOH	AZD0364	3	sigmoid	0.20699462	0.00604683	0.40061001	0.20699462
ETOH	AZD0364	4	sigmoid	0.13136591	0.00532243	0.34807716	0.13136591
ETOH	CAY10566	1	sigmoid	37.710683	0.54561221	0.75392256	37.710683
ETOH	CAY10566	2	sigmoid	54.8872144	0.52957472	0.72461197	54.8872144
ETOH	CAY10566	3	flat	Inf	0.51262982	0.77570482	0
ETOH	CAY10566	4	flat	Inf	0.55299162	0.78568796	0
ETOH	CVT-11127	1	sigmoid	31.519996	0.62492336	0.86174496	22.6805858
ETOH	CVT-11127	2	sigmoid	Inf	0.60196794	0.85351213	0.40894023
ETOH	CVT-11127	3	sigmoid	5.14596993	0.36287429	0.77037443	5.14596993
ETOH	CVT-11127	4	sigmoid	8.49828249	0.46756275	0.85310644	2.83150518
ETOH	Empesertib	1	flat	#NAME?	0.31480494	0.31422386	0
ETOH	Empesertib	2	flat	#NAME?	0.3351211	0.31800981	0
ETOH	Empesertib	3	flat	#NAME?	0.25231789	0.26517725	0
ETOH	Empesertib	4	flat	#NAME?	0.26025281	0.27937628	0
ETOH	LY3295668	1	sigmoid	0.27384837	0.34668957	0.54935803	0.05496129
ETOH	LY3295668	2	sigmoid	0.37800805	0.34191107	0.59169814	0.09463101
ETOH	LY3295668	3	sigmoid	2.09111881	0.37911954	0.66797246	0.22630794
ETOH	LY3295668	4	sigmoid	1.64151898	0.41873463	0.65069719	0.16533099
ETOH	MI-503	1	sigmoid	0.62580682	0.00127372	0.54502039	0.62580682
ETOH	MI-503	2	sigmoid	0.64932052	0.00144051	0.55873925	0.64932052
ETOH	MI-503	3	sigmoid	0.51548541	0.0015274	0.5002409	0.51548541
ETOH	MI-503	4	sigmoid	0.36990101	0.00140119	0.46989218	0.36990101
ETOH	MRT199665	1	sigmoid	0.08546972	0.0074977	0.29978984	0.08546972
ETOH	MRT199665	2	sigmoid	0.07436049	0.00673475	0.28875376	0.07076138

ETOH	MRT199665	3	sigmoid	0.0691918	0.0039714	0.26887953	0.06916239
ETOH	MRT199665	4	sigmoid	0.07929626	0.00554452	0.29138248	0.07728279
ETOH	Pinometostat	1	sigmoid	1.85042489	0.42634071	0.74123368	0.66388976
ETOH	Pinometostat	2	sigmoid	4.57761571	0.36256525	0.86894905	2.35924254
ETOH	Pinometostat	3	sigmoid	2.75179985	0.26408442	0.75725883	2.21507982
ETOH	Pinometostat	4	sigmoid	2.79375556	0.41207329	0.75669621	0.93406857
ETOH	Ravoxertinib	1	sigmoid	8.00612909	0.49143584	0.78474802	8.00612909
ETOH	Ravoxertinib	2	sigmoid	5.42654279	0.39735525	0.77928168	5.42654279
ETOH	Ravoxertinib	3	sigmoid	4.65230936	0.42540613	0.76882403	1.34220031
ETOH	Ravoxertinib	4	sigmoid	5.23967229	0.44564473	0.74783407	5.23967229
ETOH	RO4929097	1	flat	Inf	0.74369172	0.84838291	0
ETOH	RO4929097	2	flat	Inf	0.69013607	0.83875003	0
ETOH	RO4929097	3	flat	Inf	0.65656694	0.85679182	0
ETOH	RO4929097	4	sigmoid	19.1257053	0.78869049	0.97493193	19.1257053
ETOH	SAR405	1	sigmoid	0.4159547	0.07724159	0.5230222	0.38127274
ETOH	SAR405	2	sigmoid	0.46733059	0.07547341	0.52128405	0.46733059
ETOH	SAR405	3	sigmoid	0.320753	0.06779403	0.47624598	0.320753
ETOH	SAR405	4	sigmoid	0.53295147	0.07104879	0.55728243	0.49920098
ETOH	VTP50469	1	flat	Inf	1.03767239	1.02796155	0
ETOH	VTP50469	2	flat	Inf	0.82881371	0.92168463	0
ETOH	VTP50469	3	flat	Inf	0.83136729	0.93515736	0
ETOH	VTP50469	4	flat	Inf	0.686416	0.87746623	0
ETOH	ACBI1	1	sigmoid	Inf	0.55313255	0.80315127	0.5271763
ETOH	ACBI1	2	sigmoid	Inf	0.5118347	0.74845135	0.35635246

ETOH	ACBI1	3	sigmoid	Inf	0.60278644	0.84850097	0.54775906
ETOH	ACBI1	4	sigmoid	3.66551673	0.44560506	0.65571123	3.66551673
ETOH	Bafilomycin A1	1	flat	#NAME?	0.02558276	0.02119246	0
ETOH	Bafilomycin A1	2	flat	#NAME?	0.01754914	0.0205583	0
ETOH	Bafilomycin A1	3	flat	#NAME?	0.0345161	0.02962505	0
ETOH	Bafilomycin A1	4	flat	#NAME?	0.02940216	0.0264786	0
ETOH	Dactolisib	1	sigmoid	0.00265249	0.06932151	0.11236047	0.00218757
ETOH	Dactolisib	2	sigmoid	0.00469027	0.07114642	0.1152964	0.00396723
ETOH	Dactolisib	3	sigmoid	0.00082258	0.10971887	0.17610775	0.00082255
ETOH	Dactolisib	4	flat	#NAME?	0.0882405	0.1355068	0
ETOH	Decoyinine	1	flat	Inf	0.69914474	0.86071601	0
ETOH	Decoyinine	2	flat	Inf	0.80394736	0.91471668	0
ETOH	Decoyinine	3	flat	Inf	0.70169145	0.89398928	0
ETOH	Decoyinine	4	flat	Inf	0.89307028	0.98982038	0
ETOH	GSK467	1	sigmoid	Inf	0.76984276	0.9377199	0.73702525
ETOH	GSK467	2	flat	Inf	0.691858	0.85819197	0
ETOH	GSK467	3	flat	Inf	0.66763669	0.82228235	0
ETOH	GSK467	4	flat	Inf	0.66524197	0.79491977	0
ETOH	LDN-193189	1	sigmoid	1.37023198	0.00340537	0.70491884	1.37023198
ETOH	LDN-193189	2	sigmoid	2.09051819	0.19521611	0.80748576	1.60413131
ETOH	LDN-193189	3	sigmoid	2.2491299	0.35602664	0.72846938	1.02887103
ETOH	LDN-193189	4	sigmoid	2.41585468	0.34256401	0.86143138	1.19137289
ETOH	no_drug	1	sigmoid	16.7183946	0.53025622	0.85068558	16.7183946
ETOH	no_drug	2	sigmoid	18.0293399	0.57802785	0.82971801	18.0293399

ETOH	no_drug	3	flat	Inf	0.84972943	1.05869086	0
ETOH	no_drug	4	sigmoid	14.300483	0.71935152	0.99135487	14.300483
ETOH	no_drug2	1	flat	Inf	0.97472609	1.01397966	0
ETOH	no_drug2	2	sigmoid	Inf	0.87141135	0.98752467	2.98977211
ETOH	no_drug2	3	flat	Inf	0.96671622	0.92851943	0
ETOH	no_drug2	4	flat	Inf	0.90151306	0.94972677	0
ETOH	no_drug3	1	flat	Inf	1.03783776	1.15360622	0
ETOH	no_drug3	2	flat	Inf	1.08845069	1.10920462	0
ETOH	no_drug3	3	flat	Inf	1.13473319	1.17603874	0
ETOH	no_drug3	4	flat	Inf	0.89512825	0.93158178	0
ETOH	PH-064	1	sigmoid	0.7393839	0.02742084	0.59226673	0.7393839
ETOH	PH-064	2	sigmoid	2.63948986	0.05707097	0.74791967	2.63948986
ETOH	PH-064	3	sigmoid	1.26107761	0.06712234	0.62795938	1.26107761
ETOH	PH-064	4	sigmoid	2.49206406	0.06580368	0.75105704	2.49206406
ETOH	T-5224	1	flat	Inf	0.70139383	0.85852599	0
ETOH	T-5224	2	flat	Inf	0.69425534	0.8702182	0
ETOH	T-5224	3	sigmoid	351.918267	0.78807763	0.94056534	26.7694972
ETOH	T-5224	4	flat	Inf	0.63054783	0.7773118	0
ETOH	Trilaciclib	1	flat	Inf	0.64316007	0.74180952	0
ETOH	Trilaciclib	2	flat	Inf	0.62211781	0.79975864	0
ETOH	Trilaciclib	3	sigmoid	Inf	0.60411651	0.78178675	0.33034371
ETOH	Trilaciclib	4	flat	Inf	0.85934802	0.90492024	0
ETOH	6-Diazo-5-oxo-L-norleucine	1	sigmoid	3.53770612	0.31249077	0.79990688	2.30926537
ETOH	6-Diazo-5-oxo-L-norleucine	2	sigmoid	3.65391843	0.30681718	0.76932812	3.65391843

ETOH	6-Diazo-5-oxo-L-norleucine	3	flat	Inf	0.49613635	0.80879056	0
ETOH	6-Diazo-5-oxo-L-norleucine	4	sigmoid	Inf	0.55101178	0.96304664	3.2378736
ETOH	A1874	1	flat	Inf	0.82176573	0.9647126	0
ETOH	A1874	2	flat	Inf	0.92423857	1.00057426	0
ETOH	A1874	3	flat	Inf	0.84682626	0.92945154	0
ETOH	A1874	4	flat	Inf	0.89562446	1.07082632	0
ETOH	Afuresirtib	1	sigmoid	2.29405473	0.11102492	0.74968289	2.29405473
ETOH	Afuresirtib	2	sigmoid	1.9318407	0.17973965	0.68491624	1.9318407
ETOH	Afuresirtib	3	sigmoid	4.22771364	0.35414806	0.7432023	4.22771364
ETOH	Afuresirtib	4	sigmoid	1.98105005	0.26268457	0.68908838	1.98105005
ETOH	Concanamycin	1	flat	#NAME?	0.01030739	0.01214948	0
ETOH	Concanamycin	2	flat	#NAME?	0.00981932	0.01338213	0
ETOH	Concanamycin	3	flat	#NAME?	0.01745189	0.02009749	0
ETOH	Concanamycin	4	flat	#NAME?	0.01548703	0.01951372	0
ETOH	ERK5-IN-1	1	sigmoid	0.82704137	0.00676106	0.60718155	0.82704137
ETOH	ERK5-IN-1	2	sigmoid	0.7080716	0.00758078	0.57442649	0.7080716
ETOH	ERK5-IN-1	3	sigmoid	1.08767669	0.0085513	0.62986159	1.08767669
ETOH	ERK5-IN-1	4	sigmoid	0.99723021	0.00744403	0.6232106	0.99723021
ETOH	LB-100	1	sigmoid	11.4728505	0.59360997	0.9691587	11.4728505
ETOH	LB-100	2	flat	Inf	0.96912197	0.99919342	0
ETOH	LB-100	3	flat	Inf	0.80020443	0.92621508	0
ETOH	LB-100	4	flat	Inf	0.81959835	0.97007892	0
ETOH	Mdivi-1	1	flat	Inf	0.72173111	0.85677992	0
ETOH	Mdivi-1	2	flat	Inf	0.70583323	0.86738137	0

ETOH	Mdivi-1	3	flat	Inf	0.7983481	0.9624765	0
ETOH	Mdivi-1	4	flat	Inf	0.68772421	0.86497808	0
ETOH	Mizoribine	1	sigmoid	3.33077038	0.08359951	0.7584027	3.22969857
ETOH	Mizoribine	2	sigmoid	3.93184312	0.08391225	0.90982966	3.80332623
ETOH	Mizoribine	3	sigmoid	5.05675617	0.1529382	0.93089583	5.05675617
ETOH	Mizoribine	4	sigmoid	4.44716514	0.19245756	0.93011349	4.05843375
ETOH	Perifosine (KRX-0401)	1	sigmoid	5.55835767	0.13903218	0.95556309	5.30845835
ETOH	Perifosine (KRX-0401)	2	sigmoid	2.98839234	0.03121171	0.76544577	2.98839234
ETOH	Perifosine (KRX-0401)	3	flat	Inf	0.75105715	0.97302703	0
ETOH	Perifosine (KRX-0401)	4	flat	Inf	0.74907546	0.96581642	0
ETOH	superTDU	1	flat	Inf	1.14562093	1.10641814	0
ETOH	superTDU	2	flat	Inf	0.95781741	1.01513815	0
ETOH	superTDU	3	flat	Inf	0.93743178	1.05792162	0
ETOH	superTDU	4	flat	Inf	0.6414992	0.7880729	0
ETOH	VBIT-12	1	flat	Inf	0.80170233	0.85344863	0
ETOH	VBIT-12	2	flat	Inf	0.77691487	0.91223428	0
ETOH	VBIT-12	3	flat	Inf	0.69932652	0.81727012	0
ETOH	VBIT-12	4	flat	Inf	0.69437163	0.85751492	0
ETOH	YAP-TEAD inh1	1	sigmoid	Inf	0.53688301	0.88696997	0.62871203
ETOH	YAP-TEAD inh1	2	sigmoid	Inf	0.56880577	0.74820464	0.21986786
ETOH	YAP-TEAD inh1	3	flat	Inf	0.74720113	1.04208702	0
ETOH	YAP-TEAD inh1	4	flat	Inf	0.71026947	0.96974941	0
ETOH	A-674563	1	sigmoid	0.55001816	0.00904988	0.54650901	0.55001816
ETOH	A-674563	2	sigmoid	0.71586879	0.00988217	0.63761694	0.71551969

ETOH	A-674563	3	sigmoid	1.27405819	0.03212536	0.73090837	1.24742372
ETOH	A-674563	4	sigmoid	1.1230015	0.01214423	0.65420014	1.1230015
ETOH	AICAR (Acadesine)	1	sigmoid	0.02315529	0.31012008	0.41314698	0.02315529
ETOH	AICAR (Acadesine)	2	sigmoid	0.51486941	0.34392998	0.54788599	0.07045202
ETOH	AICAR (Acadesine)	3	sigmoid	0.40514336	0.2987116	0.5124444	0.11253678
ETOH	AICAR (Acadesine)	4	sigmoid	0.32780868	0.29964752	0.52787687	0.09311078
ETOH	Alpelisib (BYL719)	1	sigmoid	1.67334033	0.22058885	0.70834348	1.03780375
ETOH	Alpelisib (BYL719)	2	sigmoid	1.83616976	0.27234578	0.72039338	0.97369409
ETOH	Alpelisib (BYL719)	3	sigmoid	5.81132183	0.40028987	0.78761572	5.81132183
ETOH	Alpelisib (BYL719)	4	sigmoid	2.50247948	0.39467507	0.73118741	0.88995315
ETOH	DAPT (GSI-IX)	1	flat	Inf	0.8048433	0.94327105	0
ETOH	DAPT (GSI-IX)	2	flat	Inf	0.87301601	0.93066266	0
ETOH	DAPT (GSI-IX)	3	flat	Inf	1.06810639	1.09048618	0
ETOH	DAPT (GSI-IX)	4	flat	Inf	0.90188672	1.03777156	0
ETOH	GSK1324726A (I-BET726)	1	sigmoid	1.1061446	0.16165089	0.61466439	1.1061446
ETOH	GSK1324726A (I-BET726)	2	sigmoid	1.5396593	0.19486324	0.72468321	1.00052019
ETOH	GSK1324726A (I-BET726)	3	sigmoid	2.9775632	0.32329404	0.78605564	1.28970679
ETOH	GSK1324726A (I-BET726)	4	sigmoid	1.41301461	0.22026854	0.6439574	1.41301461
ETOH	MK-2206 2HCl	1	sigmoid	0.42594723	0.08029869	0.52071488	0.42594723
ETOH	MK-2206 2HCl	2	sigmoid	2.98094944	0.08957367	0.82727107	2.98094944
ETOH	MK-2206 2HCl	3	sigmoid	0.41763074	0.03567612	0.51932705	0.41763074
ETOH	MK-2206 2HCl	4	sigmoid	0.54746411	0.17051359	0.53896241	0.54746411
ETOH	MPI-0479605	1	sigmoid	0.00034113	0.14225421	0.20063984	0.00014
ETOH	MPI-0479605	2	flat	#NAME?	0.1534243	0.22166356	0

ETOH	MPI-0479605	3	sigmoid	0.00604259	0.22532126	0.31070097	0.00146602
ETOH	MPI-0479605	4	sigmoid	0.00055709	0.19487171	0.26376403	0.00014
ETOH	P5091 (P005091)	1	sigmoid	3.31818333	0.00431753	0.80006367	3.31818333
ETOH	P5091 (P005091)	2	sigmoid	3.03406563	0.01286895	0.74384147	3.03406563
ETOH	P5091 (P005091)	3	sigmoid	4.85812606	0.16887217	0.84161543	4.85812606
ETOH	P5091 (P005091)	4	sigmoid	3.65927288	0.13960663	0.80884865	3.65927288
ETOH	PFI-3	1	flat	Inf	0.77632227	0.88173484	0
ETOH	PFI-3	2	sigmoid	382.867937	0.70420232	0.86490375	22.2095094
ETOH	PFI-3	3	flat	Inf	0.67629937	0.81559939	0
ETOH	PFI-3	4	flat	Inf	0.64373846	0.83967415	0
ETOH	Vilazodone	1	sigmoid	5.45098303	0.25798807	0.81580444	5.45098303
ETOH	Vilazodone	2	sigmoid	4.40363028	0.23105171	0.74110065	4.40363028
ETOH	Vilazodone	3	sigmoid	9.9463832	0.49283302	1.0028117	9.9463832
ETOH	Vilazodone	4	sigmoid	5.39265833	0.31786576	0.79854833	5.39265833
ETOH	WAY-600	1	sigmoid	0.35164211	0.03171102	0.49234146	0.35164211
ETOH	WAY-600	2	sigmoid	0.55106593	0.0318567	0.55797594	0.55106593
ETOH	WAY-600	3	sigmoid	0.46838711	0.03988123	0.51898215	0.46838711
ETOH	WAY-600	4	sigmoid	0.37337107	0.03004148	0.49332112	0.37337107
ETOH	WYE-354	1	sigmoid	0.45343333	0.07314141	0.53206325	0.43044684
ETOH	WYE-354	2	sigmoid	0.44057672	0.07566544	0.54025603	0.39908029
ETOH	WYE-354	3	sigmoid	0.66292239	0.13412416	0.57038687	0.65556841
ETOH	WYE-354	4	sigmoid	0.57882257	0.1296423	0.55649689	0.57882257
ETOH	BX-795	1	sigmoid	1.9882118	0.20098174	0.76441359	1.32032689
ETOH	BX-795	2	sigmoid	1.63019869	0.20644349	0.6630132	1.63019869

ETOH	BX-795	3	sigmoid	1.44138015	0.07016672	0.66495457	1.44138015
ETOH	BX-795	4	flat	Inf	0.24078577	0.71119876	0
ETOH	CK-636	1	flat	Inf	0.73448323	0.86894343	0
ETOH	CK-636	2	flat	Inf	0.93225529	0.96592121	0
ETOH	CK-636	3	flat	Inf	0.83063472	0.91098485	0
ETOH	CK-636	4	flat	Inf	0.837866	0.95315028	0
ETOH	D 4476	1	flat	Inf	0.52222137	0.7733249	0
ETOH	D 4476	2	sigmoid	Inf	0.59730459	0.8463882	0.68758924
ETOH	D 4476	3	sigmoid	4.5489722	0.47351545	0.80112895	1.27228112
ETOH	D 4476	4	sigmoid	Inf	0.63781126	0.97526925	2.4654216
ETOH	Everolimus (RAD001)	1	sigmoid	0.00035285	0.19444074	0.32461182	0.00014
ETOH	Everolimus (RAD001)	2	flat	#NAME?	0.18929451	0.30651677	0
ETOH	Everolimus (RAD001)	3	flat	#NAME?	0.18745449	0.34885578	0
ETOH	Everolimus (RAD001)	4	flat	#NAME?	0.23924138	0.39161691	0
ETOH	GW5074	1	flat	Inf	0.77373695	0.84308535	0
ETOH	GW5074	2	flat	Inf	0.89904844	0.92777316	0
ETOH	GW5074	3	flat	Inf	1.02375561	1.01292191	0
ETOH	GW5074	4	flat	Inf	0.99992022	1.0047384	0
ETOH	Mdivi-1&ERK5-IN-1	1	sigmoid	1.08412249	0.02048377	0.62762963	1.08412249
ETOH	Mdivi-1&ERK5-IN-1	2	sigmoid	1.92964717	0.02905656	0.77396041	1.92964717
ETOH	Mdivi-1&ERK5-IN-1	3	sigmoid	1.86107269	0.0114984	0.71228549	1.86107269
ETOH	Mdivi-1&ERK5-IN-1	4	sigmoid	1.53646448	0.01240061	0.70038427	1.53646448
ETOH	MTX-211	1	sigmoid	1.55162803	0.07754641	0.65342631	1.55162803
ETOH	MTX-211	2	sigmoid	2.83721316	0.0835698	0.7687446	2.83721316

ETOH	MTX-211	3	sigmoid	2.35473099	0.08057702	0.70244069	2.35473099
ETOH	MTX-211	4	sigmoid	2.36902823	0.11461814	0.72342245	2.36902823
ETOH	Torin 2	1	sigmoid	0.01051502	0.02861489	0.08271757	0.01021918
ETOH	Torin 2	2	flat	#NAME?	0.02515293	0.07688062	0
ETOH	Torin 2	3	sigmoid	0.00163456	0.01604028	0.12171133	0.00140815
ETOH	Torin 2	4	flat	#NAME?	0.02701322	0.12350724	0
ETOH	Torkinib (PP242)	1	sigmoid	0.22710757	0.07661382	0.43321213	0.22710757
ETOH	Torkinib (PP242)	2	sigmoid	0.31935827	0.08614536	0.47705833	0.30886122
ETOH	Torkinib (PP242)	3	sigmoid	0.30763887	0.10943362	0.51601024	0.25956326
ETOH	Torkinib (PP242)	4	sigmoid	0.51018862	0.13836182	0.57125596	0.39778552
ETOH	TTP 22	1	flat	Inf	0.94839766	1.03256253	0
ETOH	TTP 22	2	flat	Inf	1.02997503	1.00529687	0
ETOH	TTP 22	3	flat	Inf	1.06717185	1.12431953	0
ETOH	TTP 22	4	flat	Inf	1.01324011	0.98672261	0
ETOH	ZM 336372	1	flat	Inf	0.79105981	0.93158551	0
ETOH	ZM 336372	2	sigmoid	31.0453746	0.78977192	0.95984228	31.0453746
ETOH	ZM 336372	3	flat	Inf	0.89262743	1.05308716	0
ETOH	ZM 336372	4	flat	Inf	0.95598723	0.97594468	0
ETOH	AZ191	1	sigmoid	2.25171787	0.02103557	0.74498699	2.25171787
ETOH	AZ191	2	sigmoid	2.41653736	0.04079031	0.76787649	2.41653736
ETOH	AZ191	3	sigmoid	4.12133002	0.05084558	0.94829227	4.12133002
ETOH	AZ191	4	sigmoid	3.6298418	0.02180152	0.88785286	3.6298418
ETOH	Crenolanib (CP-868596)	1	sigmoid	0.82794229	0.00667507	0.65254822	0.74223851
ETOH	Crenolanib (CP-868596)	2	sigmoid	0.69939847	0.006099	0.61610189	0.61225688

ETOH	Crenolanib (CP-868596)	3	sigmoid	1.13364664	0.01260803	0.66568392	1.13364664
ETOH	Crenolanib (CP-868596)	4	sigmoid	1.16115734	0.00828545	0.66797158	1.16115734
ETOH	Duvelisib (IPI-145, INK1197)	1	sigmoid	23.8393625	0.48914116	0.81007645	23.8393625
ETOH	Duvelisib (IPI-145, INK1197)	2	flat	Inf	0.63640712	1.02064915	0
ETOH	Duvelisib (IPI-145, INK1197)	3	flat	Inf	0.76886376	1.04027535	0
ETOH	Duvelisib (IPI-145, INK1197)	4	flat	Inf	0.72168221	0.95106406	0
ETOH	Dyngo-4a	1	sigmoid	0.66648487	0.10519106	0.56811349	0.66648487
ETOH	Dyngo-4a	2	sigmoid	2.32950332	0.1636674	0.81402245	1.96599698
ETOH	Dyngo-4a	3	sigmoid	2.98201414	0.21217415	0.7495238	2.98201414
ETOH	Dyngo-4a	4	sigmoid	2.26342791	0.13431984	0.7757295	2.26342791
ETOH	Ki16425	1	sigmoid	Inf	0.75272736	0.92224507	0.61992038
ETOH	Ki16425	2	sigmoid	Inf	0.68298801	0.80315411	0.12910392
ETOH	Ki16425	3	flat	Inf	0.78454133	0.94576198	0
ETOH	Ki16425	4	flat	Inf	0.62140716	0.79960828	0
ETOH	LY2857785	1	sigmoid	0.07307355	0.01760968	0.25940831	0.07234183
ETOH	LY2857785	2	sigmoid	0.08662261	0.02105751	0.27894792	0.08654041
ETOH	LY2857785	3	sigmoid	0.10548226	0.0200769	0.31730671	0.10330904
ETOH	LY2857785	4	sigmoid	0.14299363	0.02905982	0.35123504	0.14087499
ETOH	PF-562271	1	sigmoid	0.67632941	0.0189311	0.58251684	0.67632941
ETOH	PF-562271	2	sigmoid	0.45862952	0.01777687	0.52577337	0.45862952
ETOH	PF-562271	3	sigmoid	1.19652131	0.02646156	0.66768957	1.19652131
ETOH	PF-562271	4	sigmoid	1.2423169	0.02389339	0.66705485	1.2423169
ETOH	PND-1186 (VS-4718)	1	sigmoid	0.63724818	0.17531957	0.5650107	0.55705367
ETOH	PND-1186 (VS-4718)	2	sigmoid	0.81374822	0.18914367	0.60292994	0.66423752

ETOH	PND-1186 (VS-4718)	3	sigmoid	1.21331234	0.2083109	0.62733979	1.21331234
ETOH	PND-1186 (VS-4718)	4	sigmoid	0.76080258	0.21246398	0.70073482	0.58398296
ETOH	RepSox	1	sigmoid	Inf	0.54824679	0.64520053	0.04041614
ETOH	RepSox	2	sigmoid	Inf	0.54141932	0.60171046	0.02138152
ETOH	RepSox	3	sigmoid	Inf	0.65723854	0.77565244	0.07103713
ETOH	RepSox	4	sigmoid	Inf	0.57923256	0.74565552	0.23386315
ETOH	SB590885	1	flat	#NAME?	0.00700762	0.44168293	0
ETOH	SB590885	2	sigmoid	0.108265	0.01376809	0.42428095	0.108265
ETOH	SB590885	3	sigmoid	0.06603293	0.02468915	0.40522739	0.06603293
ETOH	SB590885	4	sigmoid	0.15011215	0.01135652	0.44747068	0.15011215
ETOH	Sorafenib	1	sigmoid	8.91292979	0.35942712	0.93691369	8.91292979
ETOH	Sorafenib	2	flat	Inf	0.35281293	0.79404088	0
ETOH	Sorafenib	3	flat	Inf	0.70850843	1.1018704	0
ETOH	Sorafenib	4	sigmoid	11.6026514	0.56665763	0.92441946	11.6026514
ETOH	YM155 (Sepantronium Bromide)	1	sigmoid	0.63792202	0.00570633	0.56178492	0.63792202
ETOH	YM155 (Sepantronium Bromide)	2	sigmoid	0.78032584	0.00857145	0.60239906	0.78032584
ETOH	YM155 (Sepantronium Bromide)	3	sigmoid	1.19709332	0.03038843	0.71162837	1.15034727
ETOH	YM155 (Sepantronium Bromide)	4	sigmoid	0.90584493	0.03365337	0.62428458	0.90584493
ETOH	Afuresertib (GSK2110183)	1	sigmoid	1.12647342	0.10225938	0.62927288	1.12647342
ETOH	Afuresertib (GSK2110183)	2	sigmoid	2.18648643	0.20184694	0.71200599	2.18648643
ETOH	Afuresertib (GSK2110183)	3	sigmoid	4.9014018	0.29798235	0.81375785	4.9014018
ETOH	Afuresertib (GSK2110183)	4	sigmoid	5.0743313	0.34586758	0.81080599	5.0743313
ETOH	Alisertib (MLN8237)	1	sigmoid	0.1461292	0.0359773	0.39536419	0.1461292
ETOH	Alisertib (MLN8237)	2	sigmoid	0.27479579	0.36644532	0.57000448	0.06055558

ETOH	Alisertib (MLN8237)	3	sigmoid	Inf	0.57899585	0.68270772	0.08864769
ETOH	Alisertib (MLN8237)	4	sigmoid	2.1626481	0.49708987	0.61637545	0.06361726
ETOH	Brefeldin A	1	sigmoid	0.92026595	0.00244186	0.58251081	0.92026595
ETOH	Brefeldin A	2	sigmoid	0.74159092	0.00272297	0.57097982	0.74159092
ETOH	Brefeldin A	3	sigmoid	0.74118622	0.00420795	0.6019958	0.74118622
ETOH	Brefeldin A	4	sigmoid	0.71801271	0.00387157	0.53527663	0.71801271
ETOH	FTI 277 HCl	1	flat	Inf	0.84874939	1.07475828	0
ETOH	FTI 277 HCl	2	flat	Inf	0.72319841	0.97386458	0
ETOH	FTI 277 HCl	3	flat	Inf	0.72752161	0.85762038	0
ETOH	FTI 277 HCl	4	flat	Inf	0.87138847	1.0128176	0
ETOH	Glycyrrhizin (Glycyrrhizic Acid)	1	flat	Inf	0.59301857	0.81156147	0
ETOH	Glycyrrhizin (Glycyrrhizic Acid)	2	sigmoid	Inf	0.81835686	0.92304059	0.41196763
ETOH	Glycyrrhizin (Glycyrrhizic Acid)	3	flat	Inf	0.76548624	0.85930992	0
ETOH	Glycyrrhizin (Glycyrrhizic Acid)	4	flat	Inf	0.79869367	0.96664451	0
ETOH	Harmine hydrochloride	1	sigmoid	0.91672689	0.33759701	0.56642609	0.69989385
ETOH	Harmine hydrochloride	2	sigmoid	1.40237318	0.31492098	0.61601815	1.37673521
ETOH	Harmine hydrochloride	3	sigmoid	2.53182156	0.40023047	0.70713841	0.58920646
ETOH	Harmine hydrochloride	4	sigmoid	Inf	0.49721894	0.79661837	0.60450968
ETOH	PF-04691502	1	sigmoid	0.04088509	0.01248401	0.22700718	0.03988733
ETOH	PF-04691502	2	sigmoid	0.05708804	0.01384629	0.25851523	0.0557047
ETOH	PF-04691502	3	sigmoid	0.08024005	0.02138789	0.30453365	0.08024005
ETOH	PF-04691502	4	sigmoid	0.07546346	0.02472644	0.30545295	0.07546346
ETOH	SB525334	1	sigmoid	3.14808266	0.45035681	0.6548995	0.18927579
ETOH	SB525334	2	sigmoid	5.10290351	0.44334379	0.70150556	0.25817903

ETOH	SB525334	3	sigmoid	18.4892988	0.54888318	0.8443661	18.4892988
ETOH	SB525334	4	flat	Inf	0.65255577	0.79096178	0
ETOH	SecinH3	1	sigmoid	Inf	0.78313469	0.89387596	0.20537063
ETOH	SecinH3	2	flat	Inf	0.83734101	0.93078874	0
ETOH	SecinH3	3	flat	Inf	0.90300851	0.92112109	0
ETOH	SecinH3	4	flat	Inf	0.95207443	0.96660758	0
ETOH	UNC0642	1	sigmoid	1.56379994	0.00369366	0.67311676	1.56379994
ETOH	UNC0642	2	sigmoid	1.18244724	0.00334791	0.63764793	1.18244724
ETOH	UNC0642	3	sigmoid	1.17109856	0.00580862	0.64804339	1.17109856
ETOH	UNC0642	4	sigmoid	1.39465448	0.00822537	0.66281263	1.39465448
ETOH	VX-11e	1	sigmoid	0.74183632	0.03079665	0.61512338	0.7028226
ETOH	VX-11e	2	sigmoid	1.14174814	0.0891676	0.66506308	1.03796982
ETOH	VX-11e	3	sigmoid	0.9340992	0.14362168	0.69738458	0.70523919
ETOH	VX-11e	4	sigmoid	1.26707996	0.11279986	0.68957074	1.10372613
ETOH	XMD8-92	1	sigmoid	4.30733249	0.29975285	0.80172638	4.30733249
ETOH	XMD8-92	2	sigmoid	3.88537935	0.21770982	0.77493282	3.88537935
ETOH	XMD8-92	3	sigmoid	8.85442629	0.35202508	0.86824759	8.85442629
ETOH	XMD8-92	4	sigmoid	6.22639841	0.40232091	0.97093542	4.59959659
ETOH	AZD8055	1	sigmoid	0.01149603	0.05756981	0.13008226	0.01025243
ETOH	AZD8055	2	sigmoid	0.01222689	0.05862	0.13127139	0.01094971
ETOH	AZD8055	3	sigmoid	0.01791744	0.15025332	0.24486729	0.01253767
ETOH	AZD8055	4	sigmoid	0.00100037	0.11832341	0.18978183	0.00100037
ETOH	BIX 02189	1	flat	Inf	0.95805624	1.05102479	0
ETOH	BIX 02189	2	flat	Inf	0.67685962	0.89972029	0

ETOH	BIX 02189	3	sigmoid	Inf	0.81865745	0.9784256	3.34342449
ETOH	BIX 02189	4	sigmoid	Inf	0.83994176	0.92353791	0.0725329
ETOH	CCG-1423	1	flat	Inf	0.89453444	0.91455132	0
ETOH	CCG-1423	2	flat	Inf	0.95859207	1.11887343	0
ETOH	CCG-1423	3	flat	Inf	1.03830982	1.01175592	0
ETOH	CCG-1423	4	flat	Inf	0.99194908	0.97013916	0
ETOH	Cilengitide?trifluoroacetate	1	sigmoid	1.17507429	0.21279694	0.6273564	1.17507429
ETOH	Cilengitide?trifluoroacetate	2	sigmoid	1.32794564	0.18102849	0.65459954	1.32794564
ETOH	Cilengitide?trifluoroacetate	3	sigmoid	2.22332596	0.22639099	0.67355035	2.22332596
ETOH	Cilengitide?trifluoroacetate	4	sigmoid	2.61431193	0.32648738	0.78839666	1.34191439
ETOH	Erastin	1	sigmoid	0.19015753	0.00411161	0.39321371	0.19015753
ETOH	Erastin	2	sigmoid	0.31203998	0.00555445	0.49696953	0.30641325
ETOH	Erastin	3	sigmoid	0.3830715	0.01187917	0.4992024	0.37972031
ETOH	Erastin	4	sigmoid	0.2709484	0.01558899	0.43755359	0.2709484
ETOH	GGTI 298 TFA salt	1	sigmoid	6.57384336	0.1912051	0.94722945	6.57384336
ETOH	GGTI 298 TFA salt	2	sigmoid	3.87705372	0.10311284	0.77660213	3.87705372
ETOH	GGTI 298 TFA salt	3	sigmoid	4.74271987	0.17121546	0.84026355	4.74271987
ETOH	GGTI 298 TFA salt	4	flat	Inf	0.19899871	0.73592804	0
ETOH	GW788388	1	sigmoid	Inf	0.56520103	0.7979548	0.23448212
ETOH	GW788388	2	sigmoid	Inf	0.64157886	0.86298188	0.39508983
ETOH	GW788388	3	flat	Inf	0.81402566	0.91942379	0
ETOH	GW788388	4	flat	Inf	0.78256376	0.87845666	0
ETOH	MK-8245	1	sigmoid	1.37214241	0.30693903	0.66722585	0.63089001
ETOH	MK-8245	2	sigmoid	1.63044998	0.32533025	0.68082998	0.68982498

ETOH	MK-8245	3	sigmoid	3.95867977	0.39325561	0.72599631	1.15987354
ETOH	MK-8245	4	sigmoid	3.46516355	0.41304922	0.73390605	0.54706543
ETOH	OSI-027	1	sigmoid	1.95479006	0.17813688	0.69826464	1.95479006
ETOH	OSI-027	2	sigmoid	3.29424872	0.20613547	0.80443686	3.29424872
ETOH	OSI-027	3	sigmoid	5.32703972	0.28284413	0.87894985	5.32703972
ETOH	OSI-027	4	sigmoid	2.21455468	0.22183058	0.68844722	2.21455468
ETOH	Rabeprazole	1	flat	Inf	0.97370629	0.97063158	0
ETOH	Rabeprazole	2	flat	Inf	0.85380139	0.94413994	0
ETOH	Rabeprazole	3	flat	Inf	0.67646044	0.84603663	0
ETOH	Rabeprazole	4	flat	Inf	0.79864021	0.86243064	0
ETOH	Raltitrexed	1	sigmoid	0.02209069	0.19734909	0.27838748	0.01566892
ETOH	Raltitrexed	2	sigmoid	0.03614098	0.26426029	0.37783363	0.02578906
ETOH	Raltitrexed	3	sigmoid	0.05997882	0.39201358	0.49862943	0.01979178
ETOH	Raltitrexed	4	sigmoid	0.09058383	0.39035571	0.49640882	0.02780149
ETOH	SB273005	1	sigmoid	0.03284592	0.1400647	0.2867191	0.0227975
ETOH	SB273005	2	sigmoid	0.03413113	0.13579901	0.28825359	0.02303353
ETOH	SB273005	3	sigmoid	0.0477066	0.16570016	0.34173629	0.02705968
ETOH	SB273005	4	sigmoid	0.08807056	0.23239321	0.4100611	0.04787747
ETOH	A-366	1	sigmoid	4.97728972	0.34170009	0.81122476	4.97728972
ETOH	A-366	2	sigmoid	5.67608729	0.31571642	0.76515175	5.67608729
ETOH	A-366	3	sigmoid	5.3951733	0.36430344	0.76935192	5.3951733
ETOH	A-366	4	sigmoid	8.47087378	0.41302348	0.85769281	8.47087378
ETOH	Benproperine phosphate	1	sigmoid	10.9584397	0.52759391	0.98602577	8.17508457
ETOH	Benproperine phosphate	2	sigmoid	9.26293842	0.46261339	0.87228733	9.26293842

ETOH	Benproperine phosphate	3	sigmoid	11.7091426	0.56702649	0.9712646	11.7091426
ETOH	Benproperine phosphate	4	flat	Inf	0.51528353	0.86389814	0
ETOH	CCT128930	1	sigmoid	4.38626432	0.23950409	0.81564179	4.38626432
ETOH	CCT128930	2	sigmoid	3.97041638	0.16152154	0.82647348	3.97041638
ETOH	CCT128930	3	sigmoid	5.43371618	0.28764867	0.84149853	5.43371618
ETOH	CCT128930	4	sigmoid	4.03366869	0.14913429	0.85466506	4.03366869
ETOH	EAD1	1	sigmoid	1.1540305	0.00267711	0.65153967	1.1540305
ETOH	EAD1	2	sigmoid	2.17068099	0.00449865	0.78393353	2.17068099
ETOH	EAD1	3	sigmoid	1.27575064	0.00702503	0.66528556	1.27575064
ETOH	EAD1	4	sigmoid	1.60322116	0.00718121	0.70233812	1.60322116
ETOH	Erlotinib	1	flat	Inf	0.79265887	0.93524796	0
ETOH	Erlotinib	2	sigmoid	1815.14889	0.71448306	0.85417172	20.5591898
ETOH	Erlotinib	3	flat	Inf	0.68666788	0.84667006	0
ETOH	Erlotinib	4	flat	Inf	0.96131331	0.9842484	0
ETOH	Golgicide A	1	sigmoid	7.1108216	0.37870864	0.85855954	7.1108216
ETOH	Golgicide A	2	flat	Inf	0.33610325	0.8277807	0
ETOH	Golgicide A	3	flat	Inf	0.32664224	0.80449909	0
ETOH	Golgicide A	4	flat	Inf	0.3087704	0.81799032	0
ETOH	GSK2334470	1	sigmoid	1.41541387	0.33031879	0.58850222	1.41541387
ETOH	GSK2334470	2	sigmoid	2.40752494	0.34295903	0.69487978	0.92214285
ETOH	GSK2334470	3	sigmoid	3.64246423	0.40337665	0.64664722	3.64246423
ETOH	GSK2334470	4	sigmoid	1.9996066	0.36194289	0.64877073	0.71718188
ETOH	LXS-196	1	sigmoid	6.45424462	0.40136283	0.93060584	4.02645244
ETOH	LXS-196	2	sigmoid	6.26006745	0.32461143	0.92239701	5.84365838

ETOH	LXS-196	3	sigmoid	4.209812	0.29305838	1.01416471	3.5429497
ETOH	LXS-196	4	sigmoid	5.22467196	0.31291662	0.87810632	4.08272398
ETOH	MG149	1	flat	Inf	0.76721054	0.93517392	0
ETOH	MG149	2	flat	Inf	0.71509114	0.86521737	0
ETOH	MG149	3	flat	Inf	0.79258374	0.94326377	0
ETOH	MG149	4	sigmoid	Inf	0.64370749	0.89555703	0.85300307
ETOH	MK-5108 (VX-689)	1	sigmoid	1.87150588	0.34970696	0.63039525	1.87150588
ETOH	MK-5108 (VX-689)	2	sigmoid	Inf	0.40930628	0.81421183	0.36391246
ETOH	MK-5108 (VX-689)	3	sigmoid	Inf	0.56099563	0.83646977	0.77742272
ETOH	MK-5108 (VX-689)	4	sigmoid	Inf	0.53745418	0.80320018	0.53388398
ETOH	PD0166285	1	sigmoid	0.11707533	0.00170427	0.32959094	0.11707533
ETOH	PD0166285	2	sigmoid	0.10531021	0.00165062	0.31988114	0.10531021
ETOH	PD0166285	3	sigmoid	0.1309897	0.00184407	0.34950075	0.1309897
ETOH	PD0166285	4	sigmoid	0.18871725	0.00202293	0.40412407	0.18246323
ETOH	Pluripotin (SC1)	1	sigmoid	0.08718472	0.0103518	0.29502961	0.08718472
ETOH	Pluripotin (SC1)	2	sigmoid	0.07425833	0.01268728	0.27914797	0.07425833
ETOH	Pluripotin (SC1)	3	sigmoid	0.10732971	0.01607011	0.34515373	0.10732971
ETOH	Pluripotin (SC1)	4	sigmoid	0.08781581	0.0164861	0.32421497	0.08781581
ETOH	BAY 2402234	1	sigmoid	0.03838314	0.27235564	0.40287173	0.00606728
ETOH	BAY 2402234	2	sigmoid	0.02169446	0.23312586	0.36295431	0.00495874
ETOH	BAY 2402234	3	sigmoid	0.26780288	0.25458287	0.48560435	0.26780288
ETOH	BAY 2402234	4	sigmoid	0.04327102	0.22489721	0.39424371	0.04327102
ETOH	CeMMEC13	1	flat	Inf	0.642846	0.83128533	0
ETOH	CeMMEC13	2	flat	Inf	0.64398423	0.87412294	0

ETOH	CeMMEC13	3	sigmoid	9.77852505	0.48209217	0.86394638	9.77852505
ETOH	CeMMEC13	4	flat	Inf	0.65521363	0.81419688	0
ETOH	KM91104	1	sigmoid	16.500551	0.60933204	0.90823262	16.500551
ETOH	KM91104	2	sigmoid	27.4216709	0.59898588	0.88217295	27.4216709
ETOH	KM91104	3	sigmoid	6.76071244	0.33019831	0.8672338	6.76071244
ETOH	KM91104	4	flat	Inf	0.75132198	1.12885288	0
ETOH	Metarrestin	1	sigmoid	9.95304667	0.49694086	0.90065157	9.95304667
ETOH	Metarrestin	2	sigmoid	6.49048091	0.35763195	0.857959	6.49048091
ETOH	Metarrestin	3	sigmoid	6.15747268	0.14188176	0.82486886	6.15747268
ETOH	Metarrestin	4	sigmoid	11.7520121	0.6912693	0.99971761	11.7520121
ETOH	Nemiralisib (GSK2269557)	1	sigmoid	2.63846634	0.02864501	0.74332977	2.63846634
ETOH	Nemiralisib (GSK2269557)	2	sigmoid	2.60719188	0.0213441	0.79390427	2.60719188
ETOH	Nemiralisib (GSK2269557)	3	sigmoid	0.89536615	0.00301242	0.60112558	0.89536615
ETOH	Nemiralisib (GSK2269557)	4	sigmoid	2.48419909	0.02262602	0.73492723	2.48419909
ETOH	Oncrasin-1	1	flat	Inf	0.81855747	0.92735552	0
ETOH	Oncrasin-1	2	sigmoid	Inf	0.7440829	0.89412251	4.55621941
ETOH	Oncrasin-1	3	flat	Inf	0.95280136	1.02779904	0
ETOH	Oncrasin-1	4	flat	Inf	0.91216694	1.08537227	0
ETOH	OSMI-1	1	sigmoid	Inf	0.54869736	0.84123958	0.67783299
ETOH	OSMI-1	2	sigmoid	Inf	0.65186988	0.93826935	0.99978878
ETOH	OSMI-1	3	sigmoid	8.93819903	0.46753786	0.83909111	8.93819903
ETOH	OSMI-1	4	sigmoid	17.4141833	0.61731017	0.91053427	17.4141833
ETOH	SEC inhibitor KL-1	1	sigmoid	22.218971	0.61353387	0.96549398	6.23004043
ETOH	SEC inhibitor KL-1	2	sigmoid	20.6956792	0.55886286	0.83812132	20.6956792

ETOH	SEC inhibitor KL-1	3	sigmoid	8.75000384	0.44771861	0.82222845	8.75000384
ETOH	SEC inhibitor KL-1	4	flat	Inf	0.73306712	1.06921295	0
ETOH	Serabelisib (INK-1117,MLN-1117,TAK-117)	1	sigmoid	7.72681545	0.42185082	0.79958249	7.72681545
ETOH	Serabelisib (INK-1117,MLN-1117,TAK-117)	2	sigmoid	3.84749062	0.31024905	0.73556833	3.84749062
ETOH	Serabelisib (INK-1117,MLN-1117,TAK-117)	3	sigmoid	2.40749634	0.20461873	0.70147393	2.40749634
ETOH	Serabelisib (INK-1117,MLN-1117,TAK-117)	4	sigmoid	7.40296758	0.43192081	0.82806154	7.40296758
ETOH	TA-02	1	flat	Inf	0.84985043	0.96313703	0
ETOH	TA-02	2	flat	Inf	0.84776379	1.02922087	0
ETOH	TA-02	3	flat	Inf	0.69685203	0.95134237	0
ETOH	TA-02	4	sigmoid	15327.5683	0.69335363	0.8103712	1000
ETOH	VBIT-4	1	flat	Inf	0.57813774	0.7980556	0
ETOH	VBIT-4	2	flat	Inf	0.62909743	0.84916077	0
ETOH	VBIT-4	3	sigmoid	6.1409986	0.31882929	0.82671178	6.1409986
ETOH	VBIT-4	4	flat	Inf	0.74136331	0.96566025	0
ETOH	YF-2	1	sigmoid	13.3059059	0.51663142	0.88003868	13.3059059
ETOH	YF-2	2	sigmoid	10.0333584	0.50367743	1.0005693	10.0333584
ETOH	YF-2	3	flat	Inf	0.1386087	0.78148308	0
ETOH	YF-2	4	flat	Inf	0.57381434	1.07592208	0
ETOH	Autophinib	1	sigmoid	4.09490892	0.25414	0.89014545	3.30818222
ETOH	Autophinib	2	sigmoid	3.3368812	0.20212382	0.81644355	2.91751995
ETOH	Autophinib	3	sigmoid	4.90736431	0.25879934	0.84282593	4.90736431
ETOH	Autophinib	4	sigmoid	5.68337876	0.25166828	0.90542222	5.68337876

ETOH	AZD3759	1	flat	Inf	0.81463062	1.11558395	0
ETOH	AZD3759	2	flat	Inf	0.79373487	0.98273434	0
ETOH	AZD3759	3	flat	Inf	0.7419086	0.96358515	0
ETOH	AZD3759	4	sigmoid	35.8298739	0.73969855	0.93999342	35.8298739
ETOH	EN6	1	sigmoid	Inf	0.60237264	0.83181693	0.92023679
ETOH	EN6	2	sigmoid	17.5771156	0.53510982	0.9019945	2.94054772
ETOH	EN6	3	sigmoid	Inf	0.62620584	0.87964	0.96691865
ETOH	EN6	4	flat	Inf	0.64769873	1.05642926	0
ETOH	Folinic acid	1	sigmoid	Inf	0.81770301	0.94645276	0.7550474
ETOH	Folinic acid	2	flat	Inf	0.98363503	1.04586033	0
ETOH	Folinic acid	3	flat	Inf	0.86297373	0.98837536	0
ETOH	Folinic acid	4	flat	Inf	0.899903	0.95745732	0
ETOH	GSK2636771	1	flat	Inf	0.99517172	0.98560618	0
ETOH	GSK2636771	2	flat	Inf	0.89863667	0.96208723	0
ETOH	GSK2636771	3	flat	Inf	0.95087331	0.97635163	0
ETOH	GSK2636771	4	flat	Inf	1.03531659	0.999642	0
ETOH	H3B-120	1	sigmoid	28.6988295	0.60514041	0.84262472	28.6988295
ETOH	H3B-120	2	sigmoid	31.5614231	0.63738733	0.86496416	23.6009515
ETOH	H3B-120	3	flat	Inf	0.71886992	0.99773813	0
ETOH	H3B-120	4	flat	Inf	0.66658594	0.82973683	0
ETOH	IPI-549	1	sigmoid	11.0835103	0.48101095	0.83859561	11.0835103
ETOH	IPI-549	2	sigmoid	9.33382568	0.48324351	0.85261583	9.33382568
ETOH	IPI-549	3	sigmoid	Inf	0.44999485	0.87158763	0.90538617
ETOH	IPI-549	4	sigmoid	9.3782299	0.43705267	0.86515268	9.3782299

ETOH	JX06	1	sigmoid	0.08902684	0.00211934	0.26430391	0.08885835
ETOH	JX06	2	sigmoid	0.06953166	0.00198323	0.23295962	0.06948843
ETOH	JX06	3	sigmoid	0.11369802	0.00219853	0.30081239	0.11369802
ETOH	JX06	4	sigmoid	0.08196554	0.00236303	0.25294044	0.08180494
ETOH	P110	1	flat	Inf	0.93459839	0.90861169	0
ETOH	P110	2	flat	Inf	0.90105719	0.95191339	0
ETOH	P110	3	flat	Inf	0.946378	0.97502172	0
ETOH	P110	4	flat	Inf	0.93727148	0.95655439	0
ETOH	Sephin-1	1	flat	Inf	1.12726217	1.14838634	0
ETOH	Sephin-1	2	flat	Inf	1.01587876	0.99712808	0
ETOH	Sephin-1	3	flat	Inf	0.89937835	0.9156899	0
ETOH	Sephin-1	4	flat	Inf	0.99200051	1.04366443	0
ETOH	SGC2085	1	flat	Inf	0.71930643	0.88799862	0
ETOH	SGC2085	2	flat	Inf	0.71215192	1.01220641	0
ETOH	SGC2085	3	flat	Inf	0.60627921	0.89855662	0
ETOH	SGC2085	4	flat	Inf	0.64048484	0.84984956	0
ETOH	SHP099	1	sigmoid	38.0945312	0.75187257	0.94880905	38.0945312
ETOH	SHP099	2	sigmoid	Inf	0.76267157	0.93845319	1.58820873
ETOH	SHP099	3	flat	Inf	0.69048086	0.87139376	0
ETOH	SHP099	4	sigmoid	235.346278	0.72050362	0.87876777	22.2301133
Tam	EHT1864	1	sigmoid	11.6413394	0.68109416	0.96899766	11.6413394
Tam	EHT1864	2	sigmoid	11.5819517	0.67511654	1.01836867	11.5819517
Tam	EHT1864	3	sigmoid	1.87287138	0.28101051	0.77668005	1.42713501
Tam	EHT1864	4	flat	Inf	1.04737426	0.98804284	0

Tam	Fluorouracil	1	sigmoid	3.71604479	0.2814545	0.82378119	2.81852163
Tam	Fluorouracil	2	sigmoid	2.89844458	0.28924623	0.71954917	2.89844458
Tam	Fluorouracil	3	sigmoid	4.17877071	0.40501925	0.79411561	1.59519226
Tam	Fluorouracil	4	sigmoid	6.58296454	0.42828915	0.89628636	3.17610746
Tam	JQ1	1	sigmoid	0.05530764	0.12806334	0.30787614	0.04386028
Tam	JQ1	2	sigmoid	0.07238409	0.15324191	0.35629718	0.05031147
Tam	JQ1	3	sigmoid	0.08636444	0.17735873	0.37156533	0.05952967
Tam	JQ1	4	sigmoid	0.13488619	0.18279531	0.45803576	0.08893069
Tam	KU-0063794	1	sigmoid	0.03693264	0.11487116	0.2796926	0.02693425
Tam	KU-0063794	2	sigmoid	0.10365917	0.16470588	0.40474535	0.07534182
Tam	KU-0063794	3	sigmoid	0.08713348	0.20648678	0.41010596	0.0550973
Tam	KU-0063794	4	sigmoid	0.06891488	0.17379046	0.38118897	0.03386094
Tam	MK-0752	1	flat	Inf	0.86577498	0.96854278	0
Tam	MK-0752	2	flat	Inf	0.81924256	0.89464553	0
Tam	MK-0752	3	flat	Inf	0.90286397	0.99970983	0
Tam	MK-0752	4	flat	Inf	0.77416198	0.963127	0
Tam	Pictilisib	1	sigmoid	0.32265721	0.23384517	0.50919279	0.1600149
Tam	Pictilisib	2	sigmoid	0.50638759	0.24885713	0.53997694	0.28269835
Tam	Pictilisib	3	sigmoid	0.67291518	0.2655439	0.55183825	0.67291518
Tam	Pictilisib	4	sigmoid	0.84154479	0.34909637	0.5974918	0.18336206
Tam	Rapamycin	1	flat	#NAME?	0.27747994	0.27709844	0
Tam	Rapamycin	2	flat	#NAME?	0.25194987	0.24493523	0
Tam	Rapamycin	3	flat	#NAME?	0.38357638	0.34586589	0
Tam	Rapamycin	4	flat	#NAME?	0.32129617	0.33479007	0

Tam	RBC8	1	sigmoid	Inf	0.76648288	0.92413494	2.43206082
Tam	RBC8	2	flat	Inf	0.55016015	0.88052803	0
Tam	RBC8	3	flat	Inf	1.02133881	1.05765491	0
Tam	RBC8	4	flat	Inf	1.07099687	1.04550464	0
Tam	Sapanisertib	1	sigmoid	0.00955585	0.12098352	0.1480642	0.00894468
Tam	Sapanisertib	2	sigmoid	0.00923388	0.10849565	0.13574096	0.00870221
Tam	Sapanisertib	3	sigmoid	0.0003252	0.15085977	0.18721877	0.00014
Tam	Sapanisertib	4	sigmoid	0.00014	0.18543846	0.22220462	0.00014
Tam	TAK-632	1	sigmoid	1.60945391	0.15818542	0.67069679	1.60945391
Tam	TAK-632	2	sigmoid	1.73679754	0.1741155	0.74674736	1.31343781
Tam	TAK-632	3	sigmoid	3.22387801	0.18551807	0.76950941	3.22387801
Tam	TAK-632	4	sigmoid	2.27118734	0.19570603	0.70846586	2.27118734
Tam	Verteporfin	1	sigmoid	0.71874337	0.09382457	0.57885321	0.71874337
Tam	Verteporfin	2	sigmoid	5.23666085	0.3276149	0.79895321	5.23666085
Tam	Verteporfin	3	sigmoid	10.8592513	0.4673284	0.76616298	10.8592513
Tam	Verteporfin	4	sigmoid	12.7264275	0.49432091	0.83772036	1.3091405
Tam	Y15	1	sigmoid	1.36943515	0.01241659	0.67648022	1.36943515
Tam	Y15	2	sigmoid	1.10644967	0.01416855	0.62209429	1.10644967
Tam	Y15	3	sigmoid	1.47749194	0.01655699	0.69376698	1.46414189
Tam	Y15	4	sigmoid	2.30828735	0.02630675	0.81166759	2.30529679
Tam	BAY 1251152	1	sigmoid	0.03405636	0.04778759	0.20403066	0.03213544
Tam	BAY 1251152	2	sigmoid	0.05283758	0.05990225	0.25783678	0.04886344
Tam	BAY 1251152	3	sigmoid	0.05177962	0.07391873	0.25416933	0.04747322
Tam	BAY 1251152	4	sigmoid	0.04675643	0.0693084	0.24394297	0.04228743

Tam	BAY1125976	1	flat	Inf	0.47898057	0.8327074	0
Tam	BAY1125976	2	flat	Inf	0.45312826	0.78398017	0
Tam	BAY1125976	3	sigmoid	5.42545777	0.38634777	0.7167082	5.42545777
Tam	BAY1125976	4	flat	Inf	0.33727386	0.7264343	0
Tam	CK-869	1	sigmoid	8.59983017	0.46910604	0.88934393	4.46476381
Tam	CK-869	2	sigmoid	14.8595405	0.54914003	0.87714437	3.93603962
Tam	CK-869	3	sigmoid	8.87893247	0.498948	0.9222366	3.14507891
Tam	CK-869	4	sigmoid	Inf	0.56719926	0.98645822	4.37687455
Tam	CM272	1	sigmoid	1.56275166	0.01028345	0.72453384	1.56275166
Tam	CM272	2	sigmoid	1.28203766	0.00876952	0.64969735	1.28203766
Tam	CM272	3	sigmoid	1.40471757	0.01552	0.66265982	1.40471757
Tam	CM272	4	sigmoid	1.31802715	0.01400943	0.68655969	1.31802715
Tam	FL-411	1	sigmoid	4.83962393	0.05096799	0.81130592	4.83962393
Tam	FL-411	2	sigmoid	6.22594987	0.06952406	0.91364621	6.22594987
Tam	FL-411	3	sigmoid	6.1907425	0.03474747	0.95094507	6.1907425
Tam	FL-411	4	sigmoid	6.27286613	0.15434818	0.90983571	6.27286613
Tam	MCP110	1	sigmoid	Inf	0.82388913	0.98376243	1.53269364
Tam	MCP110	2	flat	Inf	0.96144578	0.9960138	0
Tam	MCP110	3	flat	Inf	0.93566469	1.04233378	0
Tam	MCP110	4	flat	Inf	0.91290377	0.98098505	0
Tam	Monastrol	1	flat	Inf	0.82569964	0.87503232	0
Tam	Monastrol	2	flat	Inf	0.98214217	0.93994767	0
Tam	Monastrol	3	flat	Inf	0.9332769	0.9327434	0
Tam	Monastrol	4	flat	Inf	1.02158207	1.06099569	0

Tam	MYF-01-37	1	sigmoid	15.0841177	0.55422734	0.90340734	4.61383597
Tam	MYF-01-37	2	sigmoid	11.5647312	0.51590791	0.89697232	3.63747471
Tam	MYF-01-37	3	sigmoid	Inf	0.50660028	0.81115432	0.71183324
Tam	MYF-01-37	4	sigmoid	Inf	0.62608499	0.92231854	1.68145288
Tam	Nirogacestat (PF-03084014, PF-3084014)	1	flat	Inf	0.71597004	0.91276812	0
Tam	Nirogacestat (PF-03084014, PF-3084014)	2	sigmoid	47.1767407	0.75381913	0.93448635	29.3704688
Tam	Nirogacestat (PF-03084014, PF-3084014)	3	flat	Inf	0.76198657	1.03239294	0
Tam	Nirogacestat (PF-03084014, PF-3084014)	4	sigmoid	Inf	0.58258703	0.9726606	5.17594
Tam	Pemetrexed	1	flat	Inf	1.20059311	1.0371394	0
Tam	Pemetrexed	2	flat	Inf	1.0310728	0.96970052	0
Tam	Pemetrexed	3	flat	Inf	1.19820465	1.18214164	0
Tam	Pemetrexed	4	flat	Inf	0.84316617	0.91943836	0
Tam	TP0427736 HCl	1	flat	Inf	0.87392171	0.90677417	0
Tam	TP0427736 HCl	2	flat	Inf	0.95911996	1.02068745	0
Tam	TP0427736 HCl	3	flat	Inf	0.92048205	0.99199284	0
Tam	TP0427736 HCl	4	flat	Inf	0.81809426	0.87296364	0
Tam	V-9302	1	flat	Inf	0.72743106	1.03393668	0
Tam	V-9302	2	flat	Inf	0.46018921	0.85129848	0
Tam	V-9302	3	flat	Inf	0.53039755	0.88851601	0
Tam	V-9302	4	sigmoid	12.372071	0.53815643	0.9525562	5.76487129
Tam	BAY-293	1	sigmoid	1.50348973	0.00381622	0.68346156	1.50348973
Tam	BAY-293	2	sigmoid	1.33644081	0.00439077	0.66140336	1.33644081

Tam	BAY-293	3	sigmoid	3.22423764	0.00464037	0.85098758	3.22423764
Tam	BAY-293	4	sigmoid	2.31790957	0.00386415	0.73809221	2.31790957
Tam	BI-3406	1	sigmoid	Inf	0.58607559	0.76357808	0.4015427
Tam	BI-3406	2	sigmoid	69.5234789	0.57871007	0.72377076	69.5234789
Tam	BI-3406	3	flat	Inf	0.54120451	0.74074995	0
Tam	BI-3406	4	sigmoid	147.129818	0.61174404	0.79790255	147.129818
Tam	Dynasore	1	sigmoid	4.32472633	0.26327535	0.83897685	3.9342838
Tam	Dynasore	2	flat	Inf	0.92664414	0.9853237	0
Tam	Dynasore	3	sigmoid	Inf	0.59433933	0.95000984	3.63298671
Tam	Dynasore	4	flat	Inf	0.89419311	0.92242346	0
Tam	Gallein	1	sigmoid	Inf	0.66558157	0.90092523	1.84380552
Tam	Gallein	2	sigmoid	29.1611208	0.676831	0.88828492	27.0693902
Tam	Gallein	3	sigmoid	Inf	0.64403505	0.90100589	1.34392106
Tam	Gallein	4	sigmoid	Inf	0.6787652	0.93577967	4.29546389
Tam	GDC-0077	1	sigmoid	51.7019249	0.58736817	0.81004931	18.3202392
Tam	GDC-0077	2	sigmoid	Inf	0.59147297	0.73280474	0.06891522
Tam	GDC-0077	3	sigmoid	Inf	0.65881903	0.83012908	0.29294991
Tam	GDC-0077	4	sigmoid	Inf	0.51542057	0.69012133	0.08825455
Tam	GSK2256098	1	flat	Inf	0.85982478	0.87122402	0
Tam	GSK2256098	2	flat	Inf	0.76814062	0.8403908	0
Tam	GSK2256098	3	flat	Inf	1.15013462	1.1202598	0
Tam	GSK2256098	4	flat	Inf	0.81524722	0.92263746	0
Tam	IACS-13909	1	sigmoid	1.29468359	0.26547063	0.62297006	1.25253093
Tam	IACS-13909	2	sigmoid	2.59834681	0.24413965	0.68974695	2.59834681

Tam	IACS-13909	3	sigmoid	3.1774349	0.25090343	0.73335898	3.1774349
Tam	IACS-13909	4	sigmoid	3.13325884	0.2151927	0.72401201	3.13325884
Tam	NSC 23766	1	flat	Inf	0.96816531	1.05084382	0
Tam	NSC 23766	2	flat	Inf	1.04332744	1.12479025	0
Tam	NSC 23766	3	flat	Inf	0.81149107	1.02713716	0
Tam	NSC 23766	4	flat	Inf	1.044234	1.1294373	0
Tam	OSMI-4	1	flat	Inf	0.63657831	0.93372085	0
Tam	OSMI-4	2	flat	Inf	0.66492694	0.8640841	0
Tam	OSMI-4	3	flat	Inf	0.7567616	1.09335432	0
Tam	OSMI-4	4	flat	Inf	0.77940843	0.93760652	0
Tam	PF-9366	1	sigmoid	13.8096441	0.55868336	0.91851577	13.8096441
Tam	PF-9366	2	sigmoid	14.5537176	0.53683125	0.86488742	14.5537176
Tam	PF-9366	3	sigmoid	Inf	0.58129563	0.95668605	4.0150174
Tam	PF-9366	4	sigmoid	10.3138556	0.49914052	0.88516045	10.3138556
Tam	SNDX-5613	1	sigmoid	5.00623801	0.14955789	0.83399113	5.00623801
Tam	SNDX-5613	2	sigmoid	17.8391895	0.57759737	0.87539426	17.8391895
Tam	SNDX-5613	3	sigmoid	8.64759126	0.37266972	1.01515921	7.9277576
Tam	SNDX-5613	4	flat	Inf	0.74241837	0.93330957	0
Tam	SR-18292	1	sigmoid	Inf	0.72057524	0.93446555	2.0305662
Tam	SR-18292	2	flat	Inf	0.76860733	1.01763965	0
Tam	SR-18292	3	sigmoid	28.6966369	0.61624394	0.89246359	28.6966369
Tam	SR-18292	4	flat	Inf	0.76131449	0.98387074	0
Tam	A939572	1	flat	Inf	0.85551875	0.8595118	0
Tam	A939572	2	flat	Inf	0.88406178	0.82742312	0

Tam	A939572	3	flat	Inf	0.8903303	0.93007524	0
Tam	A939572	4	flat	Inf	0.71729363	0.83084182	0
Tam	Exo1	1	flat	Inf	0.79742138	0.95861582	0
Tam	Exo1	2	flat	Inf	0.82198757	0.93649167	0
Tam	Exo1	3	flat	Inf	0.82756808	0.88111747	0
Tam	Exo1	4	flat	Inf	0.91627233	1.02618073	0
Tam	ISRIB	1	flat	Inf	1.02389952	1.10842409	0
Tam	ISRIB	2	flat	Inf	0.94173709	0.93240406	0
Tam	ISRIB	3	flat	Inf	0.79518043	0.91674507	0
Tam	ISRIB	4	flat	Inf	0.97283014	1.00835321	0
Tam	ITD-1	1	flat	Inf	0.74465107	0.92066023	0
Tam	ITD-1	2	flat	Inf	0.70231113	0.92456695	0
Tam	ITD-1	3	flat	Inf	0.56762498	0.84444613	0
Tam	ITD-1	4	flat	Inf	0.50349564	0.82594061	0
Tam	LOC14	1	sigmoid	4.85497161	0.05427937	1.02112525	4.85497161
Tam	LOC14	2	sigmoid	3.41042492	0.07419877	0.77455735	3.41042492
Tam	LOC14	3	sigmoid	4.51353117	0.19252994	0.8698254	4.51353117
Tam	LOC14	4	sigmoid	4.44625246	0.12323581	0.82573176	4.44625246
Tam	NSC15364	1	flat	Inf	0.94026337	0.93339752	0
Tam	NSC15364	2	flat	Inf	0.97542379	0.98820536	0
Tam	NSC15364	3	flat	Inf	0.85761267	0.90967247	0
Tam	NSC15364	4	flat	Inf	0.92014567	0.89821439	0
Tam	NVP-2	1	sigmoid	0.01147258	0.04754568	0.07328516	0.01119785
Tam	NVP-2	2	sigmoid	0.01137703	0.04864092	0.07560443	0.01109236

Tam	NVP-2	3	sigmoid	0.01174301	0.04348704	0.07774864	0.01145854
Tam	NVP-2	4	sigmoid	0.00736083	0.05331208	0.08150331	0.00685389
Tam	PD153035	1	flat	Inf	0.78091374	0.84690164	0
Tam	PD153035	2	flat	Inf	0.8203411	0.84729881	0
Tam	PD153035	3	flat	Inf	0.73828317	0.74951156	0
Tam	PD153035	4	flat	Inf	0.89350605	0.9972615	0
Tam	PluriSIn 1 (NSC 14613)	1	sigmoid	16.2103143	0.53048112	0.82204464	16.2103143
Tam	PluriSIn 1 (NSC 14613)	2	flat	Inf	0.67381432	0.83119788	0
Tam	PluriSIn 1 (NSC 14613)	3	sigmoid	44.5435508	0.5904282	0.8914307	3.2483696
Tam	PluriSIn 1 (NSC 14613)	4	sigmoid	127.157077	0.59926342	0.80799268	127.157077
Tam	Raphin1	1	sigmoid	11.9661788	0.61270672	0.9390587	11.9661788
Tam	Raphin1	2	flat	Inf	0.89579881	1.00999484	0
Tam	Raphin1	3	sigmoid	16.224411	0.64260365	0.95081011	16.224411
Tam	Raphin1	4	sigmoid	23.4564705	0.67070375	0.92478049	23.4564705
Tam	Rhosin hydrochloride	1	flat	Inf	0.80132313	1.02499705	0
Tam	Rhosin hydrochloride	2	flat	Inf	0.79558217	0.89818878	0
Tam	Rhosin hydrochloride	3	flat	Inf	0.8368895	0.97567259	0
Tam	Rhosin hydrochloride	4	flat	Inf	0.9013975	0.96429407	0
Tam	TAS-102	1	sigmoid	14.8815467	0.50646515	0.82418657	14.8815467
Tam	TAS-102	2	flat	Inf	0.71862083	0.90149538	0
Tam	TAS-102	3	sigmoid	Inf	0.64441079	0.74802907	0.03182766
Tam	TAS-102	4	flat	Inf	0.62469334	0.74807807	0
Tam	ASLAN003	1	flat	Inf	0.83013916	0.91966661	0
Tam	ASLAN003	2	flat	Inf	0.80225388	0.92692343	0

Tam	ASLAN003	3	flat	Inf	0.86965891	0.90546622	0
Tam	ASLAN003	4	flat	Inf	0.89927647	1.03836989	0
Tam	Azaserine	1	flat	Inf	0.87235442	1.03611254	0
Tam	Azaserine	2	flat	Inf	0.84125616	1.04186199	0
Tam	Azaserine	3	sigmoid	Inf	0.87258105	0.93462568	0.10798337
Tam	Azaserine	4	flat	Inf	0.84164312	0.92546567	0
Tam	BAY-299	1	sigmoid	5.26164462	0.43257157	0.79039231	1.8738693
Tam	BAY-299	2	sigmoid	9.05486117	0.49005563	0.92258314	2.9008278
Tam	BAY-299	3	sigmoid	5.75164369	0.37647361	0.80855876	5.75164369
Tam	BAY-299	4	sigmoid	7.36548687	0.40588634	0.77255456	7.36548687
Tam	Dorsomorphin (Compound C)	1	sigmoid	5848.98991	0.75130957	0.8526431	20.8846394
Tam	Dorsomorphin (Compound C)	2	flat	Inf	0.81549235	1.0333126	0
Tam	Dorsomorphin (Compound C)	3	flat	Inf	0.83025054	0.94130664	0
Tam	Dorsomorphin (Compound C)	4	flat	Inf	0.72465364	1.00189032	0
Tam	Gedatolisib (PF-05212384, PKI-587)	1	sigmoid	0.82138927	0.19097158	0.62156918	0.57799469
Tam	Gedatolisib (PF-05212384, PKI-587)	2	sigmoid	0.47541876	0.16140939	0.52812761	0.47541876
Tam	Gedatolisib (PF-05212384, PKI-587)	3	sigmoid	0.89393877	0.19382899	0.59935323	0.89393877
Tam	Gedatolisib (PF-05212384, PKI-587)	4	sigmoid	0.58248322	0.21446984	0.54592378	0.51366921
Tam	GSK1059615	1	sigmoid	0.19469438	0.0356648	0.40138029	0.1946261
Tam	GSK1059615	2	sigmoid	0.51483544	0.04507055	0.53694471	0.51483544
Tam	GSK1059615	3	sigmoid	0.25901316	0.051349	0.45445279	0.24297632
Tam	GSK1059615	4	sigmoid	0.59274941	0.06678469	0.55685029	0.59274941
Tam	LY2109761	1	flat	Inf	0.79237327	0.88293694	0
Tam	LY2109761	2	flat	Inf	1.05208025	1.05535352	0

Tam	LY2109761	3	flat	Inf	0.87662461	0.94521696	0
Tam	LY2109761	4	flat	Inf	0.76535146	0.89234424	0
Tam	MAT2A inhibitor 2	1	flat	Inf	0.93344699	0.95147185	0
Tam	MAT2A inhibitor 2	2	flat	Inf	1.07455382	1.08491575	0
Tam	MAT2A inhibitor 2	3	flat	Inf	0.99023902	1.00531984	0
Tam	MAT2A inhibitor 2	4	flat	Inf	1.0637485	1.03393879	0
Tam	MGH-CP1	1	sigmoid	Inf	0.61335937	0.91612945	3.03110947
Tam	MGH-CP1	2	sigmoid	Inf	0.6413534	0.99881687	5.10166318
Tam	MGH-CP1	3	flat	Inf	0.89027835	0.96818792	0
Tam	MGH-CP1	4	sigmoid	8.56750726	0.42896579	0.89605108	8.56750726
Tam	MK-0429	1	sigmoid	0.00395554	0.21144233	0.2709379	0.00208139
Tam	MK-0429	2	sigmoid	0.01094601	0.22899199	0.28176075	0.00510196
Tam	MK-0429	3	sigmoid	0.01327477	0.22498736	0.31203644	0.00471622
Tam	MK-0429	4	sigmoid	0.01161051	0.23464407	0.31581935	0.00359831
Tam	Palbociclib	1	flat	Inf	0.71515816	0.86609511	0
Tam	Palbociclib	2	flat	Inf	0.66745025	0.80800917	0
Tam	Palbociclib	3	flat	Inf	0.6803188	0.88911258	0
Tam	Palbociclib	4	flat	Inf	0.70018294	0.8811969	0
Tam	RMC-4550	1	sigmoid	Inf	0.63312318	0.79005478	0.17702504
Tam	RMC-4550	2	sigmoid	Inf	0.54922842	0.7234529	0.09049243
Tam	RMC-4550	3	sigmoid	20.2630927	0.51109226	0.76521169	20.2630927
Tam	RMC-4550	4	sigmoid	11.2087795	0.44456629	0.76115653	11.2087795
Tam	AG-270	1	sigmoid	27.4999918	0.59521266	0.7922016	18.6784015
Tam	AG-270	2	sigmoid	Inf	0.62385034	0.88405215	1.50150018

Tam	AG-270	3	sigmoid	29.0873022	0.55797495	0.81976133	29.0873022
Tam	AG-270	4	sigmoid	Inf	0.69823954	0.94432119	2.37015056
Tam	DDO-5936	1	sigmoid	14.7639269	0.55663388	0.84002036	8.20091286
Tam	DDO-5936	2	sigmoid	17.0227089	0.53295459	0.78865537	17.0227089
Tam	DDO-5936	3	sigmoid	12.438026	0.52262486	0.84783045	12.438026
Tam	DDO-5936	4	sigmoid	15.1800539	0.55137771	0.84823947	15.1800539
Tam	GLPG0187	1	flat	#NAME?	0.21538133	0.23439016	0
Tam	GLPG0187	2	flat	#NAME?	0.19244683	0.20816758	0
Tam	GLPG0187	3	flat	#NAME?	0.21939694	0.23673288	0
Tam	GLPG0187	4	flat	#NAME?	0.23313688	0.23905001	0
Tam	Hydroxy Dynasore	1	sigmoid	38.9439155	0.66963684	0.88161596	26.9892173
Tam	Hydroxy Dynasore	2	sigmoid	Inf	0.60162288	0.91423737	3.45128854
Tam	Hydroxy Dynasore	3	sigmoid	12.291826	0.61084097	0.98590001	12.291826
Tam	Hydroxy Dynasore	4	flat	Inf	0.53970859	0.84387953	0
Tam	IGS-1.76	1	flat	Inf	0.74389601	0.95990758	0
Tam	IGS-1.76	2	sigmoid	Inf	0.71890065	0.80264546	0.03630689
Tam	IGS-1.76	3	sigmoid	215.378386	0.66558741	0.80436108	215.378386
Tam	IGS-1.76	4	flat	Inf	0.70545398	0.86555428	0
Tam	ILK-IN-2	1	sigmoid	1.38968234	0.00130565	0.67940618	1.38968234
Tam	ILK-IN-2	2	sigmoid	1.07467694	0.00132087	0.63331837	1.07467694
Tam	ILK-IN-2	3	sigmoid	1.81802194	0.00148113	0.7272893	1.81802194
Tam	ILK-IN-2	4	sigmoid	1.5192678	0.00137514	0.7413861	1.5192678
Tam	NAV-2729	1	sigmoid	18.8454135	0.51071569	0.8858181	2.20716322
Tam	NAV-2729	2	sigmoid	Inf	0.55638533	0.93988596	2.32936427

Tam	NAV-2729	3	sigmoid	4.51854382	0.36786725	0.73997734	4.51854382
Tam	NAV-2729	4	sigmoid	5.35224262	0.29222471	0.8179841	5.35224262
Tam	Omipalisib	1	sigmoid	0.01542013	0.02544427	0.22117511	0.01260279
Tam	Omipalisib	2	sigmoid	0.01277942	0.03382628	0.24420176	0.01277942
Tam	Omipalisib	3	sigmoid	0.06330944	0.04617647	0.34190427	0.04371232
Tam	Omipalisib	4	sigmoid	0.03331053	0.02890173	0.29085558	0.02369455
Tam	PKC-iota inhibitor 1	1	sigmoid	5.29261337	0.35808332	0.8444225	3.85006815
Tam	PKC-iota inhibitor 1	2	flat	Inf	0.56802177	0.82528211	0
Tam	PKC-iota inhibitor 1	3	sigmoid	24.047056	0.44381425	0.79892785	0.63476395
Tam	PKC-iota inhibitor 1	4	sigmoid	5.7537672	0.34909122	0.72020394	5.7537672
Tam	SCH772984	1	sigmoid	0.10925292	0.01054704	0.3388552	0.10678079
Tam	SCH772984	2	sigmoid	0.0580275	0.01279462	0.2671721	0.0580275
Tam	SCH772984	3	sigmoid	0.12406566	0.00998279	0.35651856	0.12406566
Tam	SCH772984	4	sigmoid	0.13269156	0.04905271	0.374367	0.12076882
Tam	TA-01	1	flat	Inf	1.21928184	1.04743103	0
Tam	TA-01	2	flat	Inf	1.12948277	0.96923787	0
Tam	TA-01	3	flat	Inf	0.9964187	0.93807554	0
Tam	TA-01	4	flat	Inf	1.27032918	1.1605608	0
Tam	Zorifertinib	1	sigmoid	8.12911913	0.45031077	0.75493667	8.12911913
Tam	Zorifertinib	2	sigmoid	11.5314719	0.52695265	0.79897779	3.49886787
Tam	Zorifertinib	3	flat	Inf	0.61500816	1.03619974	0
Tam	Zorifertinib	4	sigmoid	16.5433719	0.52609069	0.77504498	16.5433719
Tam	AZD0364	1	sigmoid	0.01577948	0.0037636	0.12289209	0.01577948
Tam	AZD0364	2	sigmoid	0.034196	0.00494346	0.19197148	0.034196

Tam	AZD0364	3	sigmoid	0.012792	0.00349686	0.14301812	0.012792
Tam	AZD0364	4	sigmoid	0.04498087	0.00565976	0.23230759	0.04498087
Tam	CAY10566	1	sigmoid	15.2770384	0.59349411	0.95095241	6.98250508
Tam	CAY10566	2	flat	Inf	0.75174335	0.86713395	0
Tam	CAY10566	3	sigmoid	94.6500542	0.6911315	0.86072659	94.6500542
Tam	CAY10566	4	flat	Inf	0.85478407	0.97470713	0
Tam	CVT-11127	1	flat	Inf	0.65626721	0.81903438	0
Tam	CVT-11127	2	flat	Inf	0.8238816	0.81742373	0
Tam	CVT-11127	3	sigmoid	Inf	0.85803967	0.89046343	0.0841006
Tam	CVT-11127	4	sigmoid	Inf	0.56806306	0.68647951	0.05883328
Tam	Empesertib	1	flat	Inf	0.66746391	0.62114554	0
Tam	Empesertib	2	flat	Inf	0.60566103	0.55701463	0
Tam	Empesertib	3	flat	Inf	0.6874849	0.71226275	0
Tam	Empesertib	4	flat	Inf	0.67256592	0.68629219	0
Tam	LY3295668	1	sigmoid	Inf	0.59274792	0.80642543	0.52675297
Tam	LY3295668	2	flat	Inf	0.80941049	0.83873053	0
Tam	LY3295668	3	sigmoid	Inf	0.69793671	0.84668941	0.38819904
Tam	LY3295668	4	sigmoid	65.9848129	0.66703168	0.82826783	21.5601918
Tam	MI-503	1	sigmoid	1.08597924	0.00233754	0.63113551	1.08597924
Tam	MI-503	2	sigmoid	1.20091424	0.00294094	0.63089393	1.20091424
Tam	MI-503	3	sigmoid	1.04382172	0.0056517	0.6369075	1.04382172
Tam	MI-503	4	sigmoid	0.92822633	0.00320483	0.62391967	0.92822633
Tam	MRT199665	1	sigmoid	0.11080903	0.05101026	0.35984172	0.0976297
Tam	MRT199665	2	sigmoid	0.10222689	0.05162633	0.3443315	0.09214481

Tam	MRT199665	3	sigmoid	0.10781141	0.02985615	0.3383649	0.1020725
Tam	MRT199665	4	sigmoid	0.13766789	0.05195314	0.37979392	0.1252189
Tam	Pinometostat	1	sigmoid	13.0560313	0.54655356	0.8856363	6.47974507
Tam	Pinometostat	2	sigmoid	Inf	0.66616987	0.91224262	3.27898331
Tam	Pinometostat	3	sigmoid	10.2330173	0.52470529	0.79999889	10.2330173
Tam	Pinometostat	4	sigmoid	14.0169438	0.50359456	0.8454636	1.88082765
Tam	Ravoxertinib	1	sigmoid	3.77733265	0.41431216	0.74063744	0.63466195
Tam	Ravoxertinib	2	sigmoid	3.03191137	0.45240734	0.65927867	0.19712306
Tam	Ravoxertinib	3	sigmoid	3.30456964	0.39694327	0.76969671	1.02497833
Tam	Ravoxertinib	4	sigmoid	7.14181612	0.44516595	0.74173109	7.14181612
Tam	RO4929097	1	sigmoid	4.28250919	0.34287007	0.74090905	4.28250919
Tam	RO4929097	2	flat	Inf	0.8004386	0.92868548	0
Tam	RO4929097	3	sigmoid	8.88533125	0.48209857	0.80898353	8.88533125
Tam	RO4929097	4	sigmoid	Inf	0.7107703	0.89619014	0.83440076
Tam	SAR405	1	sigmoid	1.55202727	0.26966845	0.63791116	1.55202727
Tam	SAR405	2	sigmoid	2.13514798	0.34034976	0.72491068	0.84423775
Tam	SAR405	3	sigmoid	2.63972272	0.31823061	0.7724237	1.22156206
Tam	SAR405	4	sigmoid	1.3928634	0.30346044	0.71739795	0.53416637
Tam	VTP50469	1	sigmoid	129.554028	0.69346487	0.89790267	22.5457203
Tam	VTP50469	2	flat	Inf	0.72876302	0.91184867	0
Tam	VTP50469	3	flat	Inf	0.76858192	0.9294544	0
Tam	VTP50469	4	flat	Inf	0.83961547	0.94355598	0
Tam	ACBI1	1	sigmoid	Inf	0.55814494	0.70837354	0.09973858
Tam	ACBI1	2	sigmoid	Inf	0.7021902	0.75853022	0.03724262

Tam	ACBI1	3	sigmoid	Inf	0.58985907	0.77080645	0.38708573
Tam	ACBI1	4	sigmoid	Inf	0.570354	0.71383638	0.14639521
Tam	Bafilomycin A1	1	sigmoid	0.01097856	0.05317949	0.06462182	0.0107552
Tam	Bafilomycin A1	2	sigmoid	0.01158455	0.06185694	0.07449686	0.01131474
Tam	Bafilomycin A1	3	sigmoid	0.01100118	0.06338428	0.0657823	0.01076829
Tam	Bafilomycin A1	4	sigmoid	0.01124669	0.0529988	0.07231232	0.01098174
Tam	Dactolisib	1	sigmoid	0.00017366	0.08871318	0.14849435	0.00014
Tam	Dactolisib	2	sigmoid	0.00054492	0.1120129	0.15830785	0.00054491
Tam	Dactolisib	3	sigmoid	0.00088149	0.14836147	0.21122456	0.00088149
Tam	Dactolisib	4	sigmoid	0.00018298	0.15383186	0.22656486	0.00017979
Tam	Decoyinine	1	flat	Inf	0.8358092	0.91041322	0
Tam	Decoyinine	2	flat	Inf	0.97439933	1.03043746	0
Tam	Decoyinine	3	flat	Inf	0.78995487	0.93707488	0
Tam	Decoyinine	4	flat	Inf	0.80065347	0.92182654	0
Tam	GSK467	1	flat	Inf	0.78835464	0.87939313	0
Tam	GSK467	2	flat	Inf	0.85412352	0.88183987	0
Tam	GSK467	3	flat	Inf	0.81213566	0.94885481	0
Tam	GSK467	4	flat	Inf	0.85105689	0.91923873	0
Tam	LDN-193189	1	sigmoid	0.70628273	0.18140856	0.56151919	0.70628273
Tam	LDN-193189	2	sigmoid	0.55570123	0.26175419	0.53229357	0.55570123
Tam	LDN-193189	3	sigmoid	0.72217341	0.17471291	0.56274929	0.72217341
Tam	LDN-193189	4	sigmoid	3.96975156	0.3701151	0.7208571	3.96975156
Tam	no_drug	1	sigmoid	1.08673584	0.11909934	0.67187144	0.94014669
Tam	no_drug	2	sigmoid	4.24579605	0.36820223	0.76687009	4.24579605

Tam	no_drug	3	sigmoid	1.96938557	0.104793	0.71670847	1.96938557
Tam	no_drug	4	sigmoid	10.5773222	0.42539753	0.82390742	10.5773222
Tam	no_drug2	1	sigmoid	Inf	0.81073296	0.95510453	2.11001264
Tam	no_drug2	2	flat	Inf	0.96800438	0.99990014	0
Tam	no_drug2	3	flat	Inf	0.73520233	0.80715362	0
Tam	no_drug2	4	flat	Inf	0.94139855	1.05904048	0
Tam	no_drug3	1	sigmoid	Inf	0.78794225	0.9037764	0.25109469
Tam	no_drug3	2	sigmoid	Inf	0.84735562	0.97718183	0.96492885
Tam	no_drug3	3	flat	Inf	0.87294242	0.93920966	0
Tam	no_drug3	4	flat	Inf	0.83553656	0.92587992	0
Tam	PH-064	1	flat	Inf	0.10896123	0.7150898	0
Tam	PH-064	2	sigmoid	5.254549	0.15018598	0.86642013	5.254549
Tam	PH-064	3	sigmoid	5.40729528	0.31951959	0.75946818	5.40729528
Tam	PH-064	4	sigmoid	6.53174203	0.32159943	0.89582986	6.53174203
Tam	T-5224	1	sigmoid	18.0715358	0.59269861	0.88776752	18.0715358
Tam	T-5224	2	sigmoid	10.9995656	0.55275251	0.94102146	10.9995656
Tam	T-5224	3	sigmoid	Inf	0.62372012	0.92240125	3.3587274
Tam	T-5224	4	flat	Inf	0.70555581	0.97849042	0
Tam	Trilaciclib	1	flat	Inf	0.81303079	0.85778501	0
Tam	Trilaciclib	2	flat	Inf	0.80154033	0.8235963	0
Tam	Trilaciclib	3	flat	Inf	0.68599111	0.79910565	0
Tam	Trilaciclib	4	flat	Inf	0.84883832	1.02719286	0
Tam	6-Diazo-5-oxo-L-norleucine	1	sigmoid	33.6582849	0.63973821	0.87211995	33.6582849
Tam	6-Diazo-5-oxo-L-norleucine	2	sigmoid	Inf	0.6864267	0.93068109	2.8272532

Tam	6-Diazo-5-oxo-L-norleucine	3	sigmoid	Inf	0.70756567	0.93584902	2.6038625
Tam	6-Diazo-5-oxo-L-norleucine	4	flat	Inf	0.74499315	0.91007103	0
Tam	A1874	1	flat	Inf	0.7964183	0.86802145	0
Tam	A1874	2	flat	Inf	0.79828415	0.96356219	0
Tam	A1874	3	flat	Inf	0.86604789	1.02706053	0
Tam	A1874	4	flat	Inf	0.7251244	0.91616878	0
Tam	Afuresirtib	1	sigmoid	11.7359255	0.5136701	0.88149388	11.7359255
Tam	Afuresirtib	2	sigmoid	Inf	0.59868834	0.967562	5.43660294
Tam	Afuresirtib	3	sigmoid	5.44828586	0.082435	0.93396463	5.44828586
Tam	Afuresirtib	4	flat	Inf	0.35407104	0.75478977	0
Tam	Concanamycin	1	flat	#NAME?	0.06340244	0.06102736	0
Tam	Concanamycin	2	flat	#NAME?	0.0555978	0.054118	0
Tam	Concanamycin	3	flat	#NAME?	0.05654137	0.053457	0
Tam	Concanamycin	4	flat	#NAME?	0.05236296	0.04402625	0
Tam	ERK5-IN-1	1	sigmoid	0.41202913	0.02501132	0.50128209	0.41202913
Tam	ERK5-IN-1	2	sigmoid	0.89525551	0.03695585	0.61363822	0.89525551
Tam	ERK5-IN-1	3	sigmoid	0.6460361	0.03348963	0.57697601	0.6460361
Tam	ERK5-IN-1	4	sigmoid	0.65955549	0.02961884	0.56338069	0.65955549
Tam	LB-100	1	flat	Inf	0.86099239	0.95725885	0
Tam	LB-100	2	flat	Inf	0.98564701	1.1477149	0
Tam	LB-100	3	sigmoid	Inf	0.55547531	0.85536337	0.91747295
Tam	LB-100	4	flat	Inf	0.77654255	0.93843874	0
Tam	Mdivi-1	1	flat	Inf	0.8231726	0.88017025	0
Tam	Mdivi-1	2	flat	Inf	0.90347669	0.95389083	0

Tam	Mdivi-1	3	flat	Inf	0.95221991	1.04584266	0
Tam	Mdivi-1	4	flat	Inf	0.88218337	0.92391852	0
Tam	Mizoribine	1	sigmoid	3.87400122	0.22885077	1.02442964	3.43912164
Tam	Mizoribine	2	sigmoid	3.60109119	0.22859909	0.95905614	3.19588908
Tam	Mizoribine	3	sigmoid	1.66199357	0.04266114	0.78164585	1.61696721
Tam	Mizoribine	4	sigmoid	3.07603858	0.12993002	0.76176082	3.07603858
Tam	Perifosine (KRX-0401)	1	sigmoid	5.8763017	0.33800884	0.8593359	5.45547035
Tam	Perifosine (KRX-0401)	2	sigmoid	5.47752077	0.3556705	0.80163079	5.47752077
Tam	Perifosine (KRX-0401)	3	sigmoid	5.2373603	0.44667396	0.88092854	2.48664525
Tam	Perifosine (KRX-0401)	4	sigmoid	20.8173791	0.57147943	0.99472421	5.47689554
Tam	superTDU	1	flat	Inf	0.93258451	0.95206752	0
Tam	superTDU	2	flat	Inf	0.85461415	0.90131088	0
Tam	superTDU	3	flat	Inf	0.86512067	1.000258	0
Tam	superTDU	4	flat	Inf	0.89359054	1.0156173	0
Tam	VBIT-12	1	flat	Inf	0.9468049	0.97604469	0
Tam	VBIT-12	2	flat	Inf	0.97036581	1.06860927	0
Tam	VBIT-12	3	flat	Inf	0.81633372	0.89506855	0
Tam	VBIT-12	4	flat	Inf	0.80776957	0.98801956	0
Tam	YAP-TEAD inh1	1	sigmoid	Inf	0.52686844	0.75831201	0.3896502
Tam	YAP-TEAD inh1	2	sigmoid	0.9123026	0.41260986	0.74726041	0.45849426
Tam	YAP-TEAD inh1	3	sigmoid	Inf	0.53778957	0.86031247	1.12064636
Tam	YAP-TEAD inh1	4	sigmoid	Inf	0.49810377	0.8146739	0.8201938
Tam	A-674563	1	sigmoid	0.44643458	0.01197244	0.53162198	0.44643458
Tam	A-674563	2	sigmoid	0.57333255	0.01049636	0.54927115	0.57333255

Tam	A-674563	3	sigmoid	1.65975641	0.02217701	0.72811696	1.6333189
Tam	A-674563	4	sigmoid	2.04541415	0.0227395	0.80590528	2.04541415
Tam	AICAR (Acadesine)	1	flat	#NAME?	0.27240537	0.32555243	0
Tam	AICAR (Acadesine)	2	sigmoid	0.00626743	0.3068621	0.36473319	0.00100569
Tam	AICAR (Acadesine)	3	flat	#NAME?	0.3663274	0.38957097	0
Tam	AICAR (Acadesine)	4	sigmoid	0.03048994	0.34341298	0.4282134	0.00161643
Tam	Alpelisib (BYL719)	1	sigmoid	Inf	0.44202794	0.76496072	0.28962563
Tam	Alpelisib (BYL719)	2	sigmoid	Inf	0.51868996	0.79353343	0.17151109
Tam	Alpelisib (BYL719)	3	sigmoid	19.6450455	0.55126579	0.80941261	17.7995934
Tam	Alpelisib (BYL719)	4	sigmoid	14.5278566	0.54442283	0.88721418	14.5278566
Tam	DAPT (GSI-IX)	1	sigmoid	13.5956314	0.55659149	0.87854212	13.5956314
Tam	DAPT (GSI-IX)	2	flat	Inf	0.62487166	0.87046657	0
Tam	DAPT (GSI-IX)	3	sigmoid	47.5061862	0.65370438	0.899928	47.5061862
Tam	DAPT (GSI-IX)	4	flat	Inf	0.83530689	1.00961917	0
Tam	GSK1324726A (I-BET726)	1	sigmoid	0.74370672	0.20818403	0.59871927	0.49727208
Tam	GSK1324726A (I-BET726)	2	sigmoid	0.74404698	0.2277161	0.63059329	0.43895217
Tam	GSK1324726A (I-BET726)	3	sigmoid	1.61454337	0.26339422	0.7069834	0.93666296
Tam	GSK1324726A (I-BET726)	4	sigmoid	1.1690696	0.28308237	0.6391202	0.60418319
Tam	MK-2206 2HCl	1	flat	Inf	0.13931372	0.6675095	0
Tam	MK-2206 2HCl	2	sigmoid	3.53813941	0.06003803	0.76411558	3.53813941
Tam	MK-2206 2HCl	3	sigmoid	8.84758406	0.3693532	0.76947	8.84758406
Tam	MK-2206 2HCl	4	flat	Inf	0.3043008	0.74524196	0
Tam	MPI-0479605	1	sigmoid	0.16787365	0.23761901	0.45400149	0.07643936
Tam	MPI-0479605	2	sigmoid	0.79688634	0.33624665	0.54081623	0.79688634

Tam	MPI-0479605	3	sigmoid	0.64337534	0.28053721	0.53607782	0.64337534
Tam	MPI-0479605	4	sigmoid	1.23513387	0.4360374	0.55869608	0.01808663
Tam	P5091 (P005091)	1	sigmoid	0.6181257	0.00823317	0.56816545	0.6181257
Tam	P5091 (P005091)	2	sigmoid	1.91286638	0.00471968	0.69972237	1.91286638
Tam	P5091 (P005091)	3	sigmoid	0.25783258	0.07680244	0.46596566	0.25783258
Tam	P5091 (P005091)	4	sigmoid	4.66870383	0.15558017	0.85928891	4.66870383
Tam	PFI-3	1	flat	Inf	0.80518281	0.97511435	0
Tam	PFI-3	2	sigmoid	Inf	0.86977129	0.98551873	2.58424471
Tam	PFI-3	3	flat	Inf	0.86691338	0.9890885	0
Tam	PFI-3	4	flat	Inf	0.9060217	1.0130163	0
Tam	Vilazodone	1	sigmoid	6.81632098	0.35655771	0.84819612	6.81632098
Tam	Vilazodone	2	flat	Inf	0.34328088	0.80378958	0
Tam	Vilazodone	3	sigmoid	9.51125439	0.43687272	0.9353438	9.51125439
Tam	Vilazodone	4	sigmoid	9.92602716	0.48982595	1.0198438	9.92602716
Tam	WAY-600	1	sigmoid	0.14186152	0.09116445	0.40466804	0.11028537
Tam	WAY-600	2	sigmoid	0.12829007	0.08816899	0.40304622	0.09480139
Tam	WAY-600	3	sigmoid	0.33576663	0.11496171	0.4901902	0.33576663
Tam	WAY-600	4	sigmoid	0.37488132	0.09326933	0.50921326	0.34162927
Tam	WYE-354	1	sigmoid	0.05151355	0.08575556	0.28829765	0.04170889
Tam	WYE-354	2	sigmoid	0.06425319	0.08389209	0.31177723	0.05306479
Tam	WYE-354	3	sigmoid	0.15791697	0.14760274	0.44674081	0.10812664
Tam	WYE-354	4	sigmoid	0.09574456	0.14493193	0.38517949	0.06283032
Tam	BX-795	1	sigmoid	6.23028932	0.33963983	0.87109179	6.23028932
Tam	BX-795	2	sigmoid	10.1916668	0.51097977	1.00715618	10.1916668

Tam	BX-795	3	sigmoid	10.9471992	0.44670843	0.82121391	10.9471992
Tam	BX-795	4	flat	Inf	0.55201441	1.04942593	0
Tam	CK-636	1	flat	Inf	0.88690129	0.93842259	0
Tam	CK-636	2	flat	Inf	0.79732934	0.82164557	0
Tam	CK-636	3	flat	Inf	0.85788753	0.95071946	0
Tam	CK-636	4	flat	Inf	1.03472658	1.07327027	0
Tam	D 4476	1	flat	Inf	0.83363888	1.0092083	0
Tam	D 4476	2	flat	Inf	0.7668984	0.99218677	0
Tam	D 4476	3	flat	Inf	0.88744824	1.04692966	0
Tam	D 4476	4	flat	Inf	0.90804732	1.0196235	0
Tam	Everolimus (RAD001)	1	flat	#NAME?	0.26389343	0.27173534	0
Tam	Everolimus (RAD001)	2	flat	#NAME?	0.2271439	0.35149799	0
Tam	Everolimus (RAD001)	3	flat	#NAME?	0.35190067	0.37420495	0
Tam	Everolimus (RAD001)	4	flat	#NAME?	0.35059207	0.39209614	0
Tam	GW5074	1	flat	Inf	0.87231013	1.00634088	0
Tam	GW5074	2	flat	Inf	1.0362488	1.04304233	0
Tam	GW5074	3	flat	Inf	1.00913024	1.03596659	0
Tam	GW5074	4	flat	Inf	1.02859097	1.05117081	0
Tam	Mdivi-1&ERK5-IN-1	1	sigmoid	0.39182635	0.04738158	0.50571699	0.39182635
Tam	Mdivi-1&ERK5-IN-1	2	sigmoid	0.72203336	0.07111721	0.58596499	0.72203336
Tam	Mdivi-1&ERK5-IN-1	3	sigmoid	0.90734135	0.06150427	0.6124437	0.90734135
Tam	Mdivi-1&ERK5-IN-1	4	sigmoid	0.78793366	0.03511311	0.60434953	0.78793366
Tam	MTX-211	1	sigmoid	2.26664146	0.24319551	0.70319775	2.26664146
Tam	MTX-211	2	sigmoid	2.94873569	0.28350516	0.75066093	2.91841641

Tam	MTX-211	3	sigmoid	4.58369658	0.32840567	0.81503414	4.58369658
Tam	MTX-211	4	sigmoid	4.60628213	0.32049321	0.81518256	4.60628213
Tam	Torin 2	1	flat	#NAME?	0.06216516	0.11981474	0
Tam	Torin 2	2	sigmoid	0.00019725	0.05960851	0.12319927	0.00014
Tam	Torin 2	3	sigmoid	0.00057135	0.08265598	0.18689116	0.00057135
Tam	Torin 2	4	sigmoid	0.00069332	0.05942971	0.17028157	0.00069331
Tam	Torkinib (PP242)	1	sigmoid	0.04154809	0.16131948	0.29709796	0.02887571
Tam	Torkinib (PP242)	2	sigmoid	0.04410362	0.16939612	0.30147901	0.03176637
Tam	Torkinib (PP242)	3	sigmoid	0.08403144	0.23182092	0.39715641	0.04893658
Tam	Torkinib (PP242)	4	sigmoid	0.08778787	0.24997836	0.42497337	0.05661402
Tam	TTP 22	1	flat	Inf	0.69955116	1.06558072	0
Tam	TTP 22	2	flat	Inf	0.87014581	1.05542272	0
Tam	TTP 22	3	flat	Inf	0.87694148	0.9949574	0
Tam	TTP 22	4	flat	Inf	0.83234903	0.96780539	0
Tam	ZM 336372	1	sigmoid	4.64448196	0.39366435	0.77412759	2.06506085
Tam	ZM 336372	2	flat	Inf	0.7420311	0.91026266	0
Tam	ZM 336372	3	sigmoid	Inf	0.57655172	0.90410172	0.96473745
Tam	ZM 336372	4	flat	Inf	0.87505394	0.99040202	0
Tam	AZ191	1	sigmoid	3.84884053	0.09355471	0.91868709	3.70409863
Tam	AZ191	2	sigmoid	4.87871164	0.16300167	0.84493335	4.87871164
Tam	AZ191	3	sigmoid	3.45799164	0.10998085	0.87860655	3.29628653
Tam	AZ191	4	sigmoid	3.97176945	0.20008398	0.9010361	3.59756348
Tam	Crenolanib (CP-868596)	1	sigmoid	3.47116784	0.07139936	0.86731705	3.47116784
Tam	Crenolanib (CP-868596)	2	sigmoid	4.12182963	0.13709141	0.91849464	3.84877193

Tam	Crenolanib (CP-868596)	3	sigmoid	4.2938375	0.10332439	0.93874838	4.12878489
Tam	Crenolanib (CP-868596)	4	sigmoid	4.2003319	0.15600997	0.89840736	3.90505848
Tam	Duvelisib (IPI-145, INK1197)	1	sigmoid	12.8012167	0.55267737	0.90222609	12.8012167
Tam	Duvelisib (IPI-145, INK1197)	2	sigmoid	21.9173775	0.55606708	0.86119987	21.9173775
Tam	Duvelisib (IPI-145, INK1197)	3	sigmoid	Inf	0.89444964	0.96091144	0.62592144
Tam	Duvelisib (IPI-145, INK1197)	4	sigmoid	252.656701	0.73358975	0.88261528	252.656701
Tam	Dyngo-4a	1	sigmoid	0.02168625	0.14692964	0.26720001	0.01395007
Tam	Dyngo-4a	2	sigmoid	0.17844129	0.18110136	0.46552469	0.11284638
Tam	Dyngo-4a	3	sigmoid	0.08045796	0.19729703	0.38301342	0.04703725
Tam	Dyngo-4a	4	sigmoid	0.51766604	0.29180712	0.66673097	0.35974963
Tam	Ki16425	1	sigmoid	279.35866	0.70166184	0.87674091	23.2110409
Tam	Ki16425	2	flat	Inf	0.58781425	0.89139583	0
Tam	Ki16425	3	sigmoid	11.4715293	0.51890267	0.88896511	11.4715293
Tam	Ki16425	4	flat	Inf	0.81703409	1.01173005	0
Tam	LY2857785	1	sigmoid	0.13129253	0.07280839	0.3884063	0.12724051
Tam	LY2857785	2	sigmoid	0.15679474	0.0541326	0.38956625	0.15154834
Tam	LY2857785	3	sigmoid	0.15110832	0.08487361	0.37468743	0.14144345
Tam	LY2857785	4	sigmoid	0.17768142	0.06844011	0.41348846	0.16784584
Tam	PF-562271	1	sigmoid	1.51358705	0.06702521	0.6623262	1.51358705
Tam	PF-562271	2	sigmoid	3.89191461	0.1124706	0.77777618	3.89191461
Tam	PF-562271	3	sigmoid	4.78446447	0.2830874	0.82231111	4.78446447
Tam	PF-562271	4	sigmoid	8.29653982	0.45249358	0.81321012	8.29653982
Tam	PND-1186 (VS-4718)	1	sigmoid	2.67397478	0.42596382	0.63216339	1.78232717
Tam	PND-1186 (VS-4718)	2	sigmoid	5.03216682	0.47015707	0.6923597	0.2159485

Tam	PND-1186 (VS-4718)	3	sigmoid	2.82226914	0.39359859	0.67251357	1.8394259
Tam	PND-1186 (VS-4718)	4	sigmoid	9.67287007	0.50338011	0.74384098	9.67287007
Tam	RepSox	1	sigmoid	34507.4213	0.74051176	0.88742329	22.5943833
Tam	RepSox	2	sigmoid	269.574628	0.76332251	0.92171354	26.2504654
Tam	RepSox	3	flat	Inf	0.90092299	0.99092829	0
Tam	RepSox	4	sigmoid	Inf	0.761495	0.94325338	1.19053163
Tam	SB590885	1	flat	#NAME?	0.03406242	0.3624636	0
Tam	SB590885	2	flat	#NAME?	0.04554732	0.38577125	0
Tam	SB590885	3	flat	#NAME?	0.07927907	0.4178136	0
Tam	SB590885	4	sigmoid	0.11342093	0.06617214	0.44034715	0.11342093
Tam	Sorafenib	1	sigmoid	Inf	0.7360138	0.91604736	1.00505062
Tam	Sorafenib	2	flat	Inf	0.80530895	1.07284521	0
Tam	Sorafenib	3	sigmoid	Inf	0.73587089	0.99962948	3.48075041
Tam	Sorafenib	4	flat	Inf	0.90364487	1.00566404	0
Tam	YM155 (Sepantronium Bromide)	1	sigmoid	9.9103653	0.49424867	0.89775532	9.9103653
Tam	YM155 (Sepantronium Bromide)	2	sigmoid	11.5264928	0.67044948	1.01352751	11.5264928
Tam	YM155 (Sepantronium Bromide)	3	sigmoid	13.4607231	0.58006342	0.9353674	13.4607231
Tam	YM155 (Sepantronium Bromide)	4	sigmoid	9.9781031	0.49947634	0.89980788	5.4744166
Tam	Afuresertib (GSK2110183)	1	sigmoid	7.07647704	0.48462805	0.76504656	1.11725773
Tam	Afuresertib (GSK2110183)	2	sigmoid	6.68372124	0.43828954	0.83181963	3.63162477
Tam	Afuresertib (GSK2110183)	3	sigmoid	4.1444718	0.34887265	0.84735291	2.43429772
Tam	Afuresertib (GSK2110183)	4	sigmoid	10.189536	0.51461823	0.79327417	3.50741289
Tam	Alisertib (MLN8237)	1	sigmoid	10.9873478	0.44011934	0.7113605	0.20848838
Tam	Alisertib (MLN8237)	2	sigmoid	Inf	0.52023636	0.71420382	0.14804673

Tam	Alisertib (MLN8237)	3	sigmoid	2.62857758	0.39649117	0.69579059	0.31032652
Tam	Alisertib (MLN8237)	4	sigmoid	Inf	0.52371568	0.67898	0.10839543
Tam	Brefeldin A	1	sigmoid	0.42187626	0.02228684	0.56249602	0.40865239
Tam	Brefeldin A	2	sigmoid	0.60432948	0.02206374	0.62092297	0.59194504
Tam	Brefeldin A	3	sigmoid	0.46202384	0.02262755	0.53561175	0.45006539
Tam	Brefeldin A	4	sigmoid	0.5302678	0.02783137	0.53264381	0.5302678
Tam	FTI 277 HCl	1	sigmoid	64.7460354	0.82042004	0.97521144	29.1889756
Tam	FTI 277 HCl	2	flat	Inf	0.8697943	1.06020257	0
Tam	FTI 277 HCl	3	flat	Inf	0.95757284	0.99323815	0
Tam	FTI 277 HCl	4	flat	Inf	0.83453013	0.93106982	0
Tam	Glycyrrhizin (Glycyrrhizic Acid)	1	flat	Inf	0.91744655	0.99069829	0
Tam	Glycyrrhizin (Glycyrrhizic Acid)	2	flat	Inf	0.90435915	1.00439475	0
Tam	Glycyrrhizin (Glycyrrhizic Acid)	3	flat	Inf	0.87004204	0.92484328	0
Tam	Glycyrrhizin (Glycyrrhizic Acid)	4	flat	Inf	0.88527091	0.93136893	0
Tam	Harmine hydrochloride	1	sigmoid	1.9915621	0.33214572	0.63612671	1.9915621
Tam	Harmine hydrochloride	2	sigmoid	0.89262375	0.35988701	0.64293011	0.27334158
Tam	Harmine hydrochloride	3	sigmoid	1.10005124	0.42593225	0.61651443	0.14270024
Tam	Harmine hydrochloride	4	sigmoid	1.82465158	0.36638004	0.63049167	0.9771553
Tam	PF-04691502	1	sigmoid	0.05235838	0.05002759	0.29740112	0.04394484
Tam	PF-04691502	2	sigmoid	0.046216	0.04994869	0.28780091	0.03637999
Tam	PF-04691502	3	sigmoid	0.10023537	0.0754982	0.36709701	0.08584809
Tam	PF-04691502	4	sigmoid	0.08866482	0.08184128	0.36137969	0.07924454
Tam	SB525334	1	flat	Inf	1.10634367	1.10643823	0
Tam	SB525334	2	flat	Inf	0.938564	0.97484472	0

Tam	SB525334	3	flat	Inf	0.94945104	1.03281201	0
Tam	SB525334	4	flat	Inf	0.91196132	1.02785068	0
Tam	SecinH3	1	flat	Inf	0.75445819	0.88516143	0
Tam	SecinH3	2	sigmoid	72.7240566	0.73623338	0.92495505	72.7240566
Tam	SecinH3	3	flat	Inf	0.84729788	0.96066987	0
Tam	SecinH3	4	sigmoid	56.1831335	0.71059296	0.91393182	56.1831335
Tam	UNC0642	1	sigmoid	1.7410937	0.00477825	0.69400465	1.7410937
Tam	UNC0642	2	sigmoid	1.18855417	0.00721311	0.62536761	1.18855417
Tam	UNC0642	3	sigmoid	1.66798361	0.00808461	0.71386601	1.66798361
Tam	UNC0642	4	sigmoid	1.6235131	0.00902669	0.68642431	1.6235131
Tam	VX-11e	1	sigmoid	0.35083897	0.07333255	0.51641365	0.31589405
Tam	VX-11e	2	sigmoid	0.33377225	0.07920232	0.50182817	0.29736866
Tam	VX-11e	3	sigmoid	0.29395576	0.06909158	0.48090429	0.26617937
Tam	VX-11e	4	sigmoid	0.28974266	0.06302071	0.47727653	0.26258109
Tam	XMD8-92	1	sigmoid	5.23697569	0.28615994	0.84928327	5.23697569
Tam	XMD8-92	2	sigmoid	4.47516411	0.28543498	0.8056457	4.47516411
Tam	XMD8-92	3	sigmoid	7.21138971	0.38847173	0.88154069	7.21138971
Tam	XMD8-92	4	sigmoid	6.60329559	0.45883889	0.96216245	4.1264515
Tam	AZD8055	1	sigmoid	0.00028868	0.13046222	0.17157519	0.00014
Tam	AZD8055	2	sigmoid	0.00029256	0.14289611	0.1713445	0.00014
Tam	AZD8055	3	sigmoid	0.00020499	0.11430089	0.20620984	0.00018666
Tam	AZD8055	4	sigmoid	0.00040827	0.18499639	0.21347485	0.00014
Tam	BIX 02189	1	flat	Inf	0.88830676	1.05499345	0
Tam	BIX 02189	2	sigmoid	Inf	0.70929072	0.95783198	3.03797436

Tam	BIX 02189	3	flat	Inf	0.78520205	1.03870266	0
Tam	BIX 02189	4	flat	Inf	0.91048078	1.05642282	0
Tam	CCG-1423	1	flat	Inf	0.84268941	1.00537412	0
Tam	CCG-1423	2	flat	Inf	0.80631416	0.88861082	0
Tam	CCG-1423	3	flat	Inf	0.93684461	0.98642689	0
Tam	CCG-1423	4	flat	Inf	1.02981945	1.04902131	0
Tam	Cilengitide?trifluoroacetate	1	sigmoid	0.16305644	0.10825948	0.42136111	0.12663086
Tam	Cilengitide?trifluoroacetate	2	sigmoid	0.10614746	0.14655124	0.39153418	0.07703446
Tam	Cilengitide?trifluoroacetate	3	sigmoid	0.50475605	0.19822354	0.61989865	0.3158945
Tam	Cilengitide?trifluoroacetate	4	sigmoid	0.36459819	0.2283815	0.52013317	0.18992975
Tam	Erastin	1	sigmoid	0.12125336	0.00962565	0.33597098	0.12125336
Tam	Erastin	2	sigmoid	0.08994454	0.00771998	0.29901215	0.08994454
Tam	Erastin	3	sigmoid	0.16677594	0.01688876	0.38331564	0.16341493
Tam	Erastin	4	sigmoid	0.15265385	0.01421831	0.3698882	0.15265385
Tam	GGTI 298 TFA salt	1	flat	Inf	0.5523994	0.84184366	0
Tam	GGTI 298 TFA salt	2	sigmoid	8.31910814	0.36004725	0.88753274	8.31910814
Tam	GGTI 298 TFA salt	3	sigmoid	10.7186826	0.56674469	0.95014685	10.7186826
Tam	GGTI 298 TFA salt	4	sigmoid	10.1206098	0.51463233	0.94637645	10.1206098
Tam	GW788388	1	flat	Inf	0.98160218	0.92426106	0
Tam	GW788388	2	flat	Inf	0.93001635	0.99660016	0
Tam	GW788388	3	flat	Inf	1.04518999	1.03209914	0
Tam	GW788388	4	flat	Inf	1.0554011	1.03896343	0
Tam	MK-8245	1	sigmoid	0.39451114	0.2465892	0.51446645	0.26545894
Tam	MK-8245	2	sigmoid	0.47854465	0.25250242	0.53740498	0.24657196

Tam	MK-8245	3	sigmoid	0.94601771	0.33672298	0.57607078	0.35289996
Tam	MK-8245	4	sigmoid	1.50950501	0.34487098	0.65424749	0.39840065
Tam	OSI-027	1	sigmoid	0.29441637	0.14654548	0.49315675	0.22700878
Tam	OSI-027	2	sigmoid	0.35210699	0.14251506	0.54236836	0.27237011
Tam	OSI-027	3	sigmoid	0.4573405	0.19026093	0.54504771	0.28037222
Tam	OSI-027	4	sigmoid	0.4892233	0.1959624	0.54323165	0.34646047
Tam	Rabeprazole	1	flat	Inf	1.04817661	1.1017625	0
Tam	Rabeprazole	2	flat	Inf	0.97810249	1.08275867	0
Tam	Rabeprazole	3	flat	Inf	1.11315205	1.07694206	0
Tam	Rabeprazole	4	flat	Inf	1.09914066	1.03625846	0
Tam	Raltitrexed	1	flat	Inf	0.77732323	0.8424483	0
Tam	Raltitrexed	2	sigmoid	95.5830322	0.74545428	0.92030662	25.2704818
Tam	Raltitrexed	3	sigmoid	Inf	0.69839849	0.80438107	0.14059189
Tam	Raltitrexed	4	sigmoid	Inf	0.7550786	0.82392704	0.03775901
Tam	SB273005	1	sigmoid	0.00038335	0.15766511	0.25029428	0.00014
Tam	SB273005	2	sigmoid	0.00046239	0.19168193	0.25035144	0.00014
Tam	SB273005	3	sigmoid	0.0023425	0.1383052	0.22282754	0.00234239
Tam	SB273005	4	sigmoid	0.01694332	0.18663036	0.26131232	0.01211577
Tam	A-366	1	sigmoid	4.34644157	0.26658569	0.75730145	4.34644157
Tam	A-366	2	sigmoid	9.82285149	0.44265691	0.75383394	9.82285149
Tam	A-366	3	sigmoid	15.30666	0.52510236	0.83859244	15.30666
Tam	A-366	4	sigmoid	10.1447056	0.42824709	0.67320383	10.1447056
Tam	Benproperine phosphate	1	sigmoid	Inf	0.57990227	0.91184417	2.59986537
Tam	Benproperine phosphate	2	flat	Inf	0.61456636	0.88371439	0

Tam	Benproperine phosphate	3	sigmoid	11.0598471	0.55615848	0.98975919	11.0598471
Tam	Benproperine phosphate	4	flat	Inf	0.41856124	0.81599333	0
Tam	CCT128930	1	sigmoid	6.07585123	0.38542378	0.86763683	4.52697976
Tam	CCT128930	2	sigmoid	7.19520064	0.38504525	0.80095435	7.19520064
Tam	CCT128930	3	sigmoid	7.22095332	0.32775371	0.85829177	7.22095332
Tam	CCT128930	4	sigmoid	3.36504268	0.32272109	0.74331812	2.28564308
Tam	EAD1	1	sigmoid	3.59193702	0.00997363	0.83365313	3.59193702
Tam	EAD1	2	sigmoid	3.78115429	0.00661218	0.86760736	3.78115429
Tam	EAD1	3	sigmoid	1.75011867	0.00435934	0.72509109	1.75011867
Tam	EAD1	4	sigmoid	1.44881195	0.003826	0.64705368	1.44881195
Tam	Erlotinib	1	sigmoid	1.30291317	0.19759706	0.63706818	1.30291317
Tam	Erlotinib	2	sigmoid	106.239003	0.52849729	0.6928539	0.13928126
Tam	Erlotinib	3	sigmoid	11.4033316	0.49765025	0.70487577	0.40209257
Tam	Erlotinib	4	sigmoid	43.1074784	0.56859434	0.83155755	21.1197915
Tam	Golgicide A	1	sigmoid	8.46274768	0.29864525	1.02499296	8.46274768
Tam	Golgicide A	2	sigmoid	5.69082328	0.19021061	0.81171028	5.69082328
Tam	Golgicide A	3	sigmoid	6.81026142	0.15123938	0.87431468	6.81026142
Tam	Golgicide A	4	sigmoid	6.4803987	0.13905469	0.93498763	6.4803987
Tam	GSK2334470	1	flat	Inf	1.08385819	1.00521538	0
Tam	GSK2334470	2	flat	Inf	1.07876384	1.01284135	0
Tam	GSK2334470	3	flat	Inf	1.03882845	1.02357352	0
Tam	GSK2334470	4	flat	Inf	0.94711937	1.02433075	0
Tam	LXS-196	1	sigmoid	0.1622806	0.17683642	0.43789487	0.09614306
Tam	LXS-196	2	sigmoid	3.61155748	0.25914879	0.8141138	3.03354359

Tam	LXS-196	3	sigmoid	3.02495361	0.3057507	0.76503492	2.03519486
Tam	LXS-196	4	sigmoid	5.47640154	0.36945195	0.95165657	3.68063944
Tam	MG149	1	sigmoid	7.28161614	0.46794974	0.80095337	1.5468792
Tam	MG149	2	flat	Inf	0.65055714	0.88893749	0
Tam	MG149	3	flat	Inf	0.62553382	1.01622178	0
Tam	MG149	4	sigmoid	Inf	0.63135348	0.93411302	3.92250251
Tam	MK-5108 (VX-689)	1	sigmoid	55.6774783	0.62810685	0.84300978	55.6774783
Tam	MK-5108 (VX-689)	2	sigmoid	Inf	0.63124831	0.86134305	0.54612442
Tam	MK-5108 (VX-689)	3	sigmoid	87.8461411	0.60970009	0.83868324	87.8461411
Tam	MK-5108 (VX-689)	4	sigmoid	Inf	0.68733123	0.88300778	0.15682694
Tam	PD0166285	1	sigmoid	0.37942517	0.00165055	0.5335332	0.35671831
Tam	PD0166285	2	sigmoid	0.22244336	0.00178687	0.42305575	0.22244336
Tam	PD0166285	3	sigmoid	0.3623469	0.0020082	0.50700001	0.35361836
Tam	PD0166285	4	sigmoid	0.39938535	0.00227772	0.57592681	0.37872118
Tam	Pluripotin (SC1)	1	sigmoid	0.07300924	0.03580323	0.28926859	0.07038903
Tam	Pluripotin (SC1)	2	sigmoid	0.07730205	0.03559984	0.2905143	0.07442009
Tam	Pluripotin (SC1)	3	sigmoid	0.08979155	0.04178239	0.31561888	0.08387922
Tam	Pluripotin (SC1)	4	sigmoid	0.06487455	0.02927139	0.27665029	0.06277654
Tam	BAY 2402234	1	sigmoid	43.6420592	0.61697048	0.8393494	43.6420592
Tam	BAY 2402234	2	flat	Inf	0.63067474	0.86404653	0
Tam	BAY 2402234	3	sigmoid	52.9449418	0.57315634	0.80074518	17.3156576
Tam	BAY 2402234	4	sigmoid	35.6641508	0.59588342	0.84321074	20.3969465
Tam	CeMMEC13	1	flat	Inf	0.59667373	0.94671004	0
Tam	CeMMEC13	2	sigmoid	10.4798967	0.47443182	0.89481779	10.4798967

Tam	CeMMEC13	3	flat	Inf	0.82022413	1.02469819	0
Tam	CeMMEC13	4	sigmoid	Inf	0.61565575	0.90871743	0.6554117
Tam	KM91104	1	sigmoid	11.1435231	0.49050479	0.79964921	11.1435231
Tam	KM91104	2	sigmoid	11.1169687	0.52083226	0.9044246	11.1169687
Tam	KM91104	3	sigmoid	10.0839054	0.50220921	0.86783864	10.0839054
Tam	KM91104	4	sigmoid	Inf	0.67773135	0.97149984	5.12583806
Tam	Metarrestin	1	flat	Inf	0.56206336	0.89197229	0
Tam	Metarrestin	2	sigmoid	10.1280844	0.51217314	0.93999255	10.1280844
Tam	Metarrestin	3	flat	Inf	0.88669723	0.95487471	0
Tam	Metarrestin	4	flat	Inf	0.87531475	1.10371748	0
Tam	Nemiralisib (GSK2269557)	1	sigmoid	1.28072059	0.04849641	0.64867289	1.28072059
Tam	Nemiralisib (GSK2269557)	2	sigmoid	1.2848908	0.0327665	0.64727968	1.2848908
Tam	Nemiralisib (GSK2269557)	3	sigmoid	3.12368928	0.17170106	0.77850857	3.12368928
Tam	Nemiralisib (GSK2269557)	4	sigmoid	2.98280771	0.0647644	0.79780532	2.98280771
Tam	Oncrasin-1	1	flat	Inf	0.85632797	0.89100716	0
Tam	Oncrasin-1	2	flat	Inf	0.83693146	0.95591032	0
Tam	Oncrasin-1	3	flat	Inf	0.77065988	0.8607491	0
Tam	Oncrasin-1	4	flat	Inf	0.90734907	0.94174792	0
Tam	OSMI-1	1	flat	Inf	0.61618714	0.86827002	0
Tam	OSMI-1	2	sigmoid	25.6309363	0.6141565	0.86844496	25.6309363
Tam	OSMI-1	3	flat	Inf	0.82781411	1.00650847	0
Tam	OSMI-1	4	flat	Inf	0.71293744	0.89884253	0
Tam	SEC inhibitor KL-1	1	flat	Inf	0.69352216	1.03711756	0
Tam	SEC inhibitor KL-1	2	sigmoid	Inf	0.6024253	0.88328177	1.63016176

Tam	SEC inhibitor KL-1	3	flat	Inf	0.79506551	0.93864347	0
Tam	SEC inhibitor KL-1	4	sigmoid	Inf	0.81000182	0.93693642	1.4380495
Tam	Serabelisib (INK-1117,MLN-1117,TAK-117)	1	sigmoid	3.35453023	0.30700518	0.75962428	3.11583673
Tam	Serabelisib (INK-1117,MLN-1117,TAK-117)	2	sigmoid	2.77045159	0.3054926	0.69801244	2.77045159
Tam	Serabelisib (INK-1117,MLN-1117,TAK-117)	3	sigmoid	2.13038237	0.32370046	0.72068269	1.05950872
Tam	Serabelisib (INK-1117,MLN-1117,TAK-117)	4	sigmoid	5.6368793	0.3817872	0.77912209	5.6368793
Tam	TA-02	1	flat	Inf	0.9579283	1.04306393	0
Tam	TA-02	2	flat	Inf	0.78589267	0.84163329	0
Tam	TA-02	3	flat	Inf	0.70143836	0.96155556	0
Tam	TA-02	4	flat	Inf	0.79281909	0.9510502	0
Tam	VBIT-4	1	flat	Inf	0.68610353	0.89515011	0
Tam	VBIT-4	2	flat	Inf	0.7077721	0.9349384	0
Tam	VBIT-4	3	flat	Inf	0.82939834	1.02646139	0
Tam	VBIT-4	4	flat	Inf	0.69470119	1.06406508	0
Tam	YF-2	1	sigmoid	8.26801085	0.27604922	1.00396336	8.26801085
Tam	YF-2	2	flat	Inf	0.5534897	1.07841376	0
Tam	YF-2	3	sigmoid	10.9482035	0.51884601	0.9892634	6.49313098
Tam	YF-2	4	sigmoid	14.6902545	0.70194573	0.9881436	14.6902545
Tam	Autophinib	1	flat	Inf	0.67874353	1.65408429	0
Tam	Autophinib	2	flat	Inf	0.68084134	1.61534615	0
Tam	Autophinib	3	flat	Inf	0.86346034	1.61556307	0
Tam	Autophinib	4	flat	Inf	0.89444535	1.59395963	0

Tam	AZD3759	1	flat	Inf	0.78395225	1.06680782	0
Tam	AZD3759	2	sigmoid	Inf	0.61400491	0.85741582	1.23849171
Tam	AZD3759	3	sigmoid	33560.7952	0.71329576	0.85425432	20.6149301
Tam	AZD3759	4	sigmoid	12004.8305	0.70070642	0.85672354	19.9448749
Tam	EN6	1	sigmoid	13.2136726	0.50208539	0.81401497	13.2136726
Tam	EN6	2	sigmoid	7.92150585	0.46600366	0.85226881	3.43083352
Tam	EN6	3	sigmoid	Inf	0.5538365	0.93180836	3.58909284
Tam	EN6	4	sigmoid	14.1426193	0.57629755	0.89066576	14.1426193
Tam	Folinic acid	1	flat	Inf	0.83107026	0.90108312	0
Tam	Folinic acid	2	flat	Inf	0.84508036	0.97522007	0
Tam	Folinic acid	3	flat	Inf	0.96982973	1.07453796	0
Tam	Folinic acid	4	flat	Inf	0.95207173	0.91375018	0
Tam	GSK2636771	1	flat	Inf	1.12559219	1.04529782	0
Tam	GSK2636771	2	flat	Inf	1.00541873	1.01891032	0
Tam	GSK2636771	3	flat	Inf	0.96142692	0.89389911	0
Tam	GSK2636771	4	flat	Inf	1.0279679	1.00762885	0
Tam	H3B-120	1	sigmoid	Inf	0.63103896	0.91252241	2.88645
Tam	H3B-120	2	sigmoid	Inf	0.57286588	0.97648387	4.51447186
Tam	H3B-120	3	sigmoid	Inf	0.70716132	0.95701289	3.12690628
Tam	H3B-120	4	sigmoid	55.7254354	0.73111606	0.91751619	55.7254354
Tam	IPI-549	1	sigmoid	188.711442	0.62357144	0.76768432	188.711442
Tam	IPI-549	2	sigmoid	59.1843312	0.59833082	0.77778038	59.1843312
Tam	IPI-549	3	sigmoid	Inf	0.75889903	0.85455268	0.18733873
Tam	IPI-549	4	flat	Inf	0.84014755	1.00866848	0

Tam	JX06	1	sigmoid	0.09132724	0.00250167	0.28234577	0.090831
Tam	JX06	2	sigmoid	0.0972474	0.00246054	0.3098411	0.09659754
Tam	JX06	3	sigmoid	0.11480092	0.00298891	0.33456065	0.11390426
Tam	JX06	4	sigmoid	0.09918479	0.00349149	0.31549234	0.09770954
Tam	P110	1	flat	Inf	1.029948	1.05383867	0
Tam	P110	2	sigmoid	204.52795	0.81627447	0.93698191	204.52795
Tam	P110	3	sigmoid	400.402546	0.75790642	0.91143611	400.402546
Tam	P110	4	flat	Inf	1.07116756	1.09345056	0
Tam	Sephin-1	1	flat	Inf	1.02706408	0.9941358	0
Tam	Sephin-1	2	flat	Inf	1.04699698	1.03280618	0
Tam	Sephin-1	3	flat	Inf	1.0833496	1.1463584	0
Tam	Sephin-1	4	flat	Inf	1.04595029	0.99709907	0
Tam	SGC2085	1	flat	Inf	0.85994982	0.96702605	0
Tam	SGC2085	2	sigmoid	Inf	0.78410544	0.9425828	2.59070496
Tam	SGC2085	3	flat	Inf	0.82038415	1.04822904	0
Tam	SGC2085	4	flat	Inf	0.85631191	1.07514978	0
Tam	SHP099	1	sigmoid	5.59440558	0.43725617	0.740271	5.59440558
Tam	SHP099	2	sigmoid	9.43701727	0.48090523	0.80742104	9.43701727
Tam	SHP099	3	sigmoid	11.5804587	0.51843419	0.91984997	11.5804587
Tam	SHP099	4	sigmoid	Inf	0.61838376	1.00889748	5.18780742

Appendix Table 6: Table showing the classic GRmetrics measures of drug sensitivity in the chronic *Pdk1* deletion setting in CV7250 cell line

Res 12: persistent clone 12, Res 2: persistent clone 2 , WT1: WT clone 1, WT5: WT clone 5, IC50: The half maximal inhibitory concentration, Emax: maximum effect, AUC: area under curve, EC50: Half maximal effective concentration

cell_line	treatment	replicate	fit	IC50	AUC	Emax	EC50
Res12	6.Diazo.5.oxo.L.norleucine	1	flat	Inf	3.11312596	0.79144359	0
Res12	6.Diazo.5.oxo.L.norleucine	2	curve	5.88604296	3.02720308	0.38794009	4.1673739
Res12	A.366	1	curve	6.27249968	2.53304857	0.3792839	6.27249968
Res12	A.366	2	curve	22.8774417	3.1712145	0.71587816	22.8774417
Res12	A.674563	1	curve	1.14114207	2.40124589	0.00425943	1.14114207
Res12	A.674563	2	curve	1.44901566	2.61279487	0.00548551	1.44901566
Res12	A1874	1	flat	Inf	3.25456672	0.93592104	0
Res12	A1874	2	flat	Inf	3.39925406	0.93907695	0
Res12	A939572	1	curve	78.148968	2.7569135	0.63532262	78.148968
Res12	A939572	2	curve	195.022774	2.92052314	0.70702574	53.1346936
Res12	ACBI1	1	curve	0.78870611	2.35934868	0.44766117	0.17729314
Res12	ACBI1	2	curve	0.66119924	2.27630127	0.44896677	0.12969636
Res12	AG.270	1	curve	11.553859	2.88145225	0.51168288	6.35765583
Res12	AG.270	2	curve	14.3002501	2.7884051	0.54493723	14.3002501
Res12	AICAR	1	curve	1.18290785	2.16631083	0.42398803	0.13649479
Res12	AICAR	2	curve	2.14731608	2.28245391	0.4676755	0.1037842
Res12	ASLAN003	1	flat	Inf	3.38006778	0.92352932	0
Res12	ASLAN003	2	flat	Inf	3.37451635	0.9805788	0
Res12	AZ191	1	curve	2.97466597	2.77055717	0.00825853	2.97466597
Res12	AZ191	2	curve	2.74075637	2.65057251	0.02543067	2.74075637
Res12	AZD0364	1	curve	0.03403476	0.87698868	0.00182045	0.03403476
Res12	AZD0364	2	curve	0.08941529	1.23038249	0.00181371	0.08941529
Res12	AZD3759	1	curve	Inf	3.1665784	0.83632761	1.01249446

Res12	AZD3759	2	flat	Inf	2.92890394	0.66986911	0
Res12	AZD8055	1	curve	0.01204378	0.69240051	0.09833004	0.01143248
Res12	Afuresertib	1	flat	Inf	3.48459884	0.74127621	0
Res12	Afuresertib	2	curve	11.3765575	3.26083404	0.59424139	11.3765575
Res12	Afuresirtib	1	curve	7.26944266	3.10267259	0.22131859	7.26944266
Res12	Afuresirtib	2	curve	9.62260225	3.1254998	0.47778171	9.62260225
Res12	Alisertib	1	curve	Inf	2.40889975	0.57338077	0.06925457
Res12	Alisertib	2	curve	Inf	2.42436713	0.57044033	0.07005143
Res12	Alpelisib	1	curve	23.2484264	2.96208664	0.60384851	23.2484264
Res12	Alpelisib	2	curve	Inf	3.13592393	0.74214069	5.20977429
Res12	Autophinib	1	flat	Inf	4.55976037	0.549191	0
Res12	Autophinib	2	flat	Inf	4.30585995	0.35691264	0
Res12	Azaserine	1	flat	Inf	3.22281235	0.84990243	0
Res12	Azaserine	2	flat	Inf	3.16211519	0.81111844	0
Res12	BAY.1251152	1	curve	0.06663946	1.18931706	0.04872348	0.06385713
Res12	BAY.1251152	2	curve	0.04325327	1.03692703	0.05021465	0.0409408
Res12	BAY.2402234	1	curve	0.08884783	1.92986623	0.41846751	0.02087921
Res12	BAY.2402234	2	curve	0.07172135	1.88305744	0.39654211	0.01872619
Res12	BAY.293	1	curve	3.56776591	2.66788367	0.00308278	3.56776591
Res12	BAY.293	2	curve	1.96068436	2.39673927	0.00270497	1.96068436
Res12	BAY.299	1	curve	1.93892069	2.54510042	0.0982176	1.93892069
Res12	BAY.299	2	curve	1.45666844	2.33412252	0.17815621	1.45666844
Res12	BAY1125976	1	curve	11.1202567	3.23841145	0.61908106	10.6577721
Res12	BAY1125976	2	curve	8.58473604	3.09932985	0.49371774	4.06561989

Res12	BI.3406	1	curve	65.5230454	2.95048558	0.65983445	65.5230454
Res12	BI.3406	2	flat	Inf	2.84914129	0.63083774	0
Res12	BIX.02189	1	curve	35.2091654	3.08343027	0.68437084	35.2091654
Res12	BX.795	1	curve	4.13373399	2.75871937	0.25814879	4.13373399
Res12	BX.795	2	curve	2.8178099	2.58703599	0.19757888	2.8178099
Res12	Bafilomycin.A1	1	curve	0.00881209	0.37330886	0.02655668	0.00873021
Res12	Bafilomycin.A1	2	curve	0.00831577	0.3452594	0.02006778	0.00825335
Res12	Benproperine.phosphate	1	flat	Inf	2.92736832	0.53466631	0
Res12	Benproperine.phosphate	2	flat	Inf	3.07871049	0.72037956	0
Res12	Brefeldin.A	1	curve	0.56912682	2.04432076	0.0068082	0.56912682
Res12	Brefeldin.A	2	curve	0.44712635	1.86645735	0.0070533	0.44712635
Res12	CAY10566	1	curve	9.69643619	2.94052863	0.4701958	9.69643619
Res12	CAY10566	2	curve	33.4361319	3.01574871	0.64405372	33.4361319
Res12	CCG.1423	1	flat	Inf	3.31116615	0.98226331	0
Res12	CCT128930	1	curve	6.49242202	3.10817598	0.230177	6.49242202
Res12	CCT128930	2	curve	10.7437594	2.90976713	0.48041692	10.7437594
Res12	CK.636	1	flat	Inf	3.40273561	1.09594826	0
Res12	CK.636	2	curve	894.175269	3.11524704	0.82248555	894.175269
Res12	CK.869	1	curve	6.9871778	3.00702989	0.3455227	6.9871778
Res12	CK.869	2	curve	2.63932529	2.7921061	0.33077031	1.75062281
Res12	CM272	1	curve	2.71346992	2.74511409	0.00430841	2.71346992
Res12	CM272	2	curve	1.41714563	2.34822162	0.00481782	1.41714563
Res12	CVT.11127	1	curve	33.484224	2.81481047	0.62166722	33.484224
Res12	CVT.11127	2	flat	Inf	2.79213888	0.68309074	0

Res12	CeMMEC13	1	flat	Inf	3.00497191	0.80440078	0
Res12	CeMMEC13	2	curve	345.106851	3.13271182	0.82268929	143.962293
Res12	Cilengitide.trifluoroacetate	1	curve	1.73718409	2.41837782	0.26070084	1.22085026
Res12	Concanamycin	1	curve	7.99E-04	0.28864982	0.01923696	7.96E-04
Res12	Concanamycin	2	curve	7.99E-04	0.28373986	0.01367106	7.96E-04
Res12	Crenolanib	1	curve	1.70376844	2.75223894	0.00529916	1.64342392
Res12	Crenolanib	2	curve	1.13798373	2.64759369	0.01331437	1.05575717
Res12	D.4476	1	curve	18.9116827	2.91227537	0.55133707	18.9116827
Res12	D.4476	2	curve	110.900311	3.03471163	0.7467843	48.9363713
Res12	DAPT	1	flat	Inf	3.23157079	0.86820441	0
Res12	DAPT	2	flat	Inf	3.25454608	0.90136218	0
Res12	DDO.5936	1	curve	53.2510947	2.94281052	0.59549789	2.82849583
Res12	DDO.5936	2	curve	Inf	3.08375088	0.66494323	1.06320005
Res12	Dactolisib	1	curve	0.01006023	0.78066417	0.09394383	0.00930337
Res12	Dactolisib	2	curve	0.0103662	0.78062359	0.08515006	0.00946043
Res12	Decoyinine	1	flat	Inf	3.26081105	0.98503267	0
Res12	Decoyinine	2	flat	Inf	3.11281546	0.9117043	0
Res12	Dorsomorphin..Compound.C	1	flat	Inf	3.31889913	0.87472092	0
Res12	Dorsomorphin..Compound.C	2	flat	Inf	3.19767958	0.69881105	0
Res12	Duvelisib	1	curve	29.4414262	3.25961258	0.77164304	21.3062044
Res12	Duvelisib	2	flat	Inf	3.01131043	0.74017003	0
Res12	Dynasore	1	flat	Inf	3.35596218	0.82819522	0
Res12	Dynasore	2	curve	Inf	3.24928312	0.78892789	3.99970296
Res12	Dyngo.4a	1	curve	0.15859877	1.64113557	0.12132824	0.11962942

Res12	Dyngo.4a	2	curve	4.0241677	2.67428233	0.47823415	0.89200353
Res12	EAD1	1	curve	2.74812745	2.69383519	0.00163303	2.74812745
Res12	EAD1	2	curve	2.39940266	2.50365981	0.00435966	2.39940266
Res12	EHT1864	1	curve	20.0870812	3.27061151	0.71896587	20.0870812
Res12	EHT1864	2	flat	Inf	3.36178031	0.9003926	0
Res12	EN6	1	curve	Inf	3.17095751	0.81460811	2.26702432
Res12	EN6	2	curve	15.2944543	3.11838848	0.60983464	15.2944543
Res12	ERK5.IN.1	1	curve	0.98674496	2.2393264	0.01027885	0.98674496
Res12	ERK5.IN.1	2	curve	1.23565943	2.29724832	0.0185368	1.23565943
Res12	Empesertib	1	curve	0.01137709	1.49018267	0.39106058	0.0082667
Res12	Empesertib	2	curve	0.01076377	1.43034745	0.38314916	0.00806972
Res12	Erastin	1	curve	0.11184983	1.34742575	0.00183469	0.11184983
Res12	Erlotinib	1	curve	3.14888217	2.57081866	0.11970383	3.14888217
Res12	Erlotinib	2	curve	Inf	3.09492464	0.80927421	1.05039134
Res12	Everolimus	1	curve	0.01388452	1.67207555	0.36946056	0.00874307
Res12	Everolimus	2	curve	0.01538826	1.70194236	0.39708427	0.00926182
Res12	Exo1	1	flat	Inf	3.2939304	0.88618642	0
Res12	Exo1	2	flat	Inf	3.05514017	0.85622287	0
Res12	FL.411	1	curve	4.55113241	2.79358556	0.00888872	4.55113241
Res12	FL.411	2	curve	3.97914337	2.90890401	0.00292183	3.97914337
Res12	FTI.277.HCl	1	curve	14.1488796	3.30269716	0.8271287	13.1139269
Res12	FTI.277.HCl	2	flat	Inf	3.28430521	0.86918629	0
Res12	Fluorouracil	1	curve	1.93164008	2.86851755	0.15032306	1.66628385
Res12	Fluorouracil	2	curve	2.13464517	2.75553945	0.11562152	1.94572605

Res12	Folinic.acid	1	flat	Inf	3.35979124	0.9323409	0
Res12	Folinic.acid	2	flat	Inf	3.20972082	0.80826191	0
Res12	GDC.0077	1	curve	Inf	3.00907781	0.80980017	0.38593785
Res12	GDC.0077	2	curve	2265.28094	2.85625822	0.76760418	191.574123
Res12	GGTI.298.TFA.salt	1	curve	8.2419758	3.2123335	0.27511029	8.2419758
Res12	GLPG0187	1	curve	0.0101225	0.79856992	0.14329055	0.00934323
Res12	GLPG0187	2	curve	0.01023469	0.75885744	0.12012897	0.00953144
Res12	GSK1059615	1	curve	1.024108	2.8472796	0.27432652	1.024108
Res12	GSK1059615	2	curve	0.35281072	2.61976849	0.04016966	0.35281072
Res12	GSK1324726A	1	curve	1.82390166	2.42275832	0.21706341	1.82390166
Res12	GSK1324726A	2	curve	2.6337533	2.49342876	0.25635304	2.6337533
Res12	GSK2256098	1	flat	Inf	2.99934486	0.78218914	0
Res12	GSK2256098	2	flat	Inf	3.02833989	0.81086464	0
Res12	GSK2334470	1	flat	Inf	3.14214124	0.8020235	0
Res12	GSK2334470	2	flat	Inf	3.13594617	0.92073576	0
Res12	GSK2636771	1	flat	Inf	3.89913189	1.21956148	0
Res12	GSK2636771	2	flat	Inf	3.22945761	0.93139395	0
Res12	GSK467	1	flat	Inf	3.02547811	0.85200343	0
Res12	GSK467	2	flat	Inf	3.11608405	0.87507457	0
Res12	GW5074	1	flat	Inf	3.23279232	0.94234898	0
Res12	GW5074	2	flat	Inf	3.35098518	1.01021754	0
Res12	GW788388	1	flat	Inf	2.95467669	0.85440707	0
Res12	Gallein	1	curve	Inf	3.16123865	0.67763381	3.66088372
Res12	Gallein	2	curve	Inf	3.12031151	0.66415829	4.08994854

Res12	Gedatolisib	1	curve	0.1992951	2.18344638	0.15575739	0.1992951
Res12	Gedatolisib	2	curve	0.12861766	2.06680311	0.09962001	0.12861766
Res12	Glycyrrhizin	1	flat	Inf	3.21204858	0.90606278	0
Res12	Glycyrrhizin	2	flat	Inf	3.2316305	0.97159959	0
Res12	Golgicide.A	1	curve	6.03519363	2.96073389	0.06028217	6.03519363
Res12	Golgicide.A	2	curve	7.62533198	3.18827089	0.19890326	7.62533198
Res12	H3B.120	1	curve	Inf	2.9942049	0.62150692	1.43731409
Res12	H3B.120	2	curve	Inf	3.00279578	0.63362033	1.20297816
Res12	Harmine.hydrochloride	1	curve	23.384676	2.78722793	0.57238424	9.53501974
Res12	Harmine.hydrochloride	2	curve	Inf	2.90198254	0.54077274	1.31237982
Res12	Hydroxy.Dynasore	1	curve	18.5674037	2.99177705	0.60273352	18.5674037
Res12	Hydroxy.Dynasore	2	curve	Inf	3.13418658	0.6556465	3.66770329
Res12	IACS.13909	1	flat	Inf	2.71530651	0.36138853	0
Res12	IACS.13909	2	curve	5.79049903	2.77431888	0.30740161	5.79049903
Res12	IGS.1.76	1	curve	21.1808481	2.81381793	0.581402	21.1808481
Res12	IGS.1.76	2	curve	28.2986865	2.87540873	0.63704969	13.290335
Res12	ILK.IN.2	1	curve	2.2210022	2.67543986	0.00140048	2.2210022
Res12	ILK.IN.2	2	curve	1.95200713	2.51170134	0.00138751	1.95200713
Res12	IPI.549	1	flat	Inf	3.20777795	0.79771215	0
Res12	IPI.549	2	curve	24.6321108	3.03974315	0.64010459	14.9741283
Res12	ISRIB	1	flat	Inf	3.17360747	0.89120914	0
Res12	ISRIB	2	flat	Inf	3.26671085	0.92673306	0
Res12	ITD.1	1	curve	6.35698555	2.83655622	0.27967729	6.35698555
Res12	ITD.1	2	curve	10.5870505	2.96152777	0.50063215	10.5870505

Res12	JQ1	1	curve	0.0609075	1.35143832	0.11195365	0.04487547
Res12	JQ1	2	curve	0.06549426	1.40632459	0.12438771	0.04816906
Res12	JX06	1	curve	0.0829847	1.25573976	0.00259196	0.08225099
Res12	JX06	2	curve	0.0786714	1.20545614	0.00238622	0.07814237
Res12	KM91104	1	curve	8.86642955	3.10325371	0.4167721	8.86642955
Res12	KM91104	2	curve	9.27846666	2.98650316	0.46139441	9.27846666
Res12	KU.0063794	1	curve	0.13360138	1.56368962	0.0807782	0.11711658
Res12	KU.0063794	2	curve	0.10821725	1.41334613	0.06656935	0.0981056
Res12	Ki16425	1	curve	12.1418849	3.1193015	0.54943119	12.1418849
Res12	Ki16425	2	curve	55.1317487	2.74658358	0.61973692	55.1317487
Res12	LB.100	1	flat	Inf	3.31569016	0.93924871	0
Res12	LB.100	2	flat	Inf	3.21592001	0.79591579	0
Res12	LDN.193189	1	curve	1.64585971	2.79662452	0.29459998	0.88902434
Res12	LDN.193189	2	curve	2.21481573	2.70635257	0.01190142	2.21481573
Res12	LOC14	1	curve	4.17298011	2.97206293	0.045574	4.17298011
Res12	LOC14	2	curve	5.29424293	2.96257343	0.21905181	5.29424293
Res12	LXS.196	1	curve	0.57862418	2.12644354	0.16863194	0.3923822
Res12	LXS.196	2	curve	7.78160583	2.85983217	0.44660925	7.78160583
Res12	LY2109761	1	curve	17.3934496	2.94131217	0.70528728	7.62389664
Res12	LY2109761	2	curve	Inf	3.00349399	0.75088497	0.10111686
Res12	LY2857785	1	curve	0.0889356	1.30187439	0.01679478	0.08821172
Res12	LY2857785	2	curve	0.10786293	1.3424902	0.01543007	0.10751746
Res12	LY3295668	1	curve	Inf	2.47980206	0.53459128	0.14177467
Res12	LY3295668	2	curve	Inf	2.57890611	0.50392912	0.27540151

Res12	MAT2A.inhibitor.2	1	flat	Inf	3.31784879	0.96565502	0
Res12	MAT2A.inhibitor.2	2	flat	Inf	3.1164852	0.84930443	0
Res12	MCP110	1	curve	13.5623646	3.22567754	0.65753995	13.5623646
Res12	MCP110	2	flat	Inf	3.14236424	0.57535268	0
Res12	MG149	1	flat	Inf	3.06786269	0.78907025	0
Res12	MG149	2	flat	Inf	3.09822963	0.72872146	0
Res12	MGH.CP1	1	curve	12.9542013	3.31580125	0.50800453	4.68385665
Res12	MGH.CP1	2	curve	6.76784312	3.33054436	0.42892549	4.746467
Res12	MI.503	1	curve	1.0268982	2.18983824	0.00172293	1.0268982
Res12	MI.503	2	curve	1.49364866	2.31250737	0.00194929	1.49364866
Res12	MK.0429	1	curve	0.03069884	1.27930536	0.16162202	0.01927629
Res12	MK.0429	2	curve	0.02106689	1.16076365	0.15809967	0.01506927
Res12	MK.0752	1	curve	76.981707	3.07585478	0.73136713	36.8404935
Res12	MK.0752	2	flat	Inf	3.12167179	0.81701375	0
Res12	MK.2206.2HCl	1	curve	5.87564247	2.97288931	0.06699394	5.87564247
Res12	MK.2206.2HCl	2	flat	Inf	3.05759661	0.63333682	0
Res12	MK.5108	1	curve	Inf	2.99524105	0.65652468	0.82317408
Res12	MK.5108	2	curve	Inf	2.79976725	0.61995671	1.21264213
Res12	MK.8245	1	flat	Inf	3.0588561	0.73407873	0
Res12	MPI.0479605	1	curve	0.01020802	1.32461623	0.33636243	0.00807353
Res12	MPI.0479605	2	curve	0.01308541	1.4101994	0.37710228	0.01007454
Res12	MRT199665	1	curve	0.14671572	1.59789838	0.01076713	0.13387736
Res12	MRT199665	2	curve	0.1351193	1.55807272	0.01704593	0.1201491
Res12	MTX.211	1	curve	5.46990993	2.90324453	0.26287221	5.46990993

Res12	MTX.211	2	curve	5.85247453	2.94292512	0.27502891	5.85247453
Res12	MYF.01.37	1	curve	10.6556507	2.99495126	0.50990019	10.6556507
Res12	MYF.01.37	2	curve	8.32754494	2.94798277	0.46246045	5.7839002
Res12	Mdivi.1	1	flat	Inf	3.26202116	0.89896037	0
Res12	Mdivi.1	2	flat	Inf	3.35803128	0.89911379	0
Res12	Mdivi.1.ERK5.IN.1	1	curve	0.97289708	2.2985939	0.04159641	0.97289708
Res12	Mdivi.1.ERK5.IN.1	2	curve	0.72915899	2.1436082	0.03602973	0.72915899
Res12	Mdivi.1.ERK5.IN.1	3	curve	1.43718594	2.51877197	0.0433431	1.43718594
Res12	Mdivi.1.ERK5.IN.1	4	curve	1.02012655	2.30096043	0.04567047	1.02012655
Res12	Metarrestin	1	curve	7.38317145	3.00649953	0.38265237	7.38317145
Res12	Metarrestin	2	curve	8.50521977	3.07923169	0.44380857	7.78668183
Res12	Mizoribine	1	curve	13.2677485	3.22038128	0.64919338	11.3901898
Res12	Mizoribine	2	curve	5.17460181	2.88816557	0.19018892	5.17460181
Res12	Monastrol	1	flat	Inf	3.09133793	0.85845743	0
Res12	Monastrol	2	flat	Inf	3.05957098	0.88008086	0
Res12	NAV.2729	1	flat	Inf	2.91781869	0.68434358	0
Res12	NAV.2729	2	curve	45.3413972	2.80957026	0.52167318	1.53010416
Res12	NSC.23766	1	flat	Inf	3.33452265	0.910657	0
Res12	NSC.23766	2	flat	Inf	3.14056246	0.83512301	0
Res12	NSC15364	1	flat	Inf	3.14021594	0.92009824	0
Res12	NSC15364	2	flat	Inf	3.36976041	0.94113394	0
Res12	NVP.2	1	curve	0.01252365	0.50188864	0.01543655	0.01234407
Res12	NVP.2	2	curve	0.01267696	0.50642471	0.01408235	0.01249763
Res12	Nemiralisib	1	curve	2.75033503	2.62976217	0.01587492	2.75033503

Res12	Nemiralisib	2	curve	4.3061698	2.77349502	0.02942594	4.3061698
Res12	Nirogacestat	1	flat	Inf	3.02051418	0.65937971	0
Res12	Nirogacestat	2	flat	Inf	3.01409776	0.65908673	0
Res12	OSI.027	1	curve	0.6055593	2.07477293	0.04896844	0.6055593
Res12	OSMI.1	1	curve	8.48749997	2.78381819	0.43618301	8.48749997
Res12	OSMI.1	2	curve	12.4864487	3.04119497	0.53952201	12.4864487
Res12	OSMI.4	1	curve	12.0927243	3.02133173	0.54585642	12.0927243
Res12	OSMI.4	2	curve	10.582666	3.04334588	0.5142191	10.582666
Res12	Omipalisib	1	curve	0.04501199	1.20503324	0.08842186	0.03660501
Res12	Omipalisib	2	curve	0.053648	1.26978927	0.10563438	0.0443151
Res12	Oncrasin.1	1	flat	Inf	3.68795284	0.98036156	0
Res12	Oncrasin.1	2	flat	Inf	3.61810297	0.98204333	0
Res12	P110	1	flat	Inf	3.17998936	0.8830865	0
Res12	P110	2	flat	Inf	3.20619596	0.88165892	0
Res12	P5091	1	curve	5.35422102	3.07668093	0.00389957	5.35422102
Res12	P5091	2	curve	6.31420147	3.10578529	0.10310024	6.31420147
Res12	PD0166285	1	curve	0.22609191	1.70450801	0.00146857	0.21917582
Res12	PD0166285	2	curve	0.25568702	1.69207388	0.00206554	0.24702833
Res12	PD153035	1	flat	Inf	3.26644679	0.77828849	0
Res12	PD153035	2	curve	44.3879261	3.16883334	0.76320728	44.3879261
Res12	PF.04691502	1	curve	0.15189318	1.52246091	0.01381751	0.15189318
Res12	PF.04691502	2	curve	0.12144072	1.42811797	0.03190561	0.12144072
Res12	PF.562271	1	curve	1.72783194	2.48419403	0.02095633	1.72783194
Res12	PF.562271	2	curve	1.5628314	2.43476941	0.04380432	1.5628314

Res12	PF.9366	1	curve	Inf	3.22950124	0.55296291	4.33556007
Res12	PF.9366	2	curve	12.5496591	3.20744232	0.56851849	9.41376197
Res12	PFI.3	1	curve	102.616158	3.26738648	0.8516367	63.1273993
Res12	PFI.3	2	flat	Inf	2.97512553	0.83153504	0
Res12	PH.064	1	curve	5.36316146	2.96067876	0.15281763	5.36316146
Res12	PH.064	2	curve	4.1590217	2.68632246	0.22896126	4.1590217
Res12	PKC.iota.inhibitor.1	1	curve	32.4379196	2.92887509	0.59679899	32.4379196
Res12	PKC.iota.inhibitor.1	2	curve	12.2745173	2.91050201	0.51751572	12.2745173
Res12	PND.1186	1	curve	0.88202336	2.18114112	0.26956961	0.51302017
Res12	PND.1186	2	curve	0.96081628	2.13529339	0.3091902	0.53616018
Res12	Palbociclib	1	curve	1.9339966	2.9143427	0.45209072	1.9339966
Res12	Palbociclib	2	curve	1.69781474	2.87389443	0.41859973	1.69781474
Res12	Pemetrexed	1	curve	3.86697003	2.81818411	0.27725479	3.12011275
Res12	Pemetrexed	2	curve	2.63899311	2.59747021	0.25862858	1.93804862
Res12	Perifosine	1	curve	5.8423104	3.08602002	0.38432397	4.43655797
Res12	Perifosine	2	curve	7.60172653	3.10676403	0.35841796	7.60172653
Res12	Pictilisib	1	flat	Inf	2.64099825	0.18469395	0
Res12	Pictilisib	2	curve	2.16025654	2.43438048	0.23184356	2.16025654
Res12	Pinometostat	1	curve	Inf	3.00288315	0.70828151	2.11373897
Res12	Pinometostat	2	curve	22.2981226	3.13203409	0.68108005	22.2981226
Res12	PluriSIn.1..NSC.14613.	1	curve	Inf	2.93883195	0.58770383	0.82189832
Res12	PluriSIn.1..NSC.14613.	2	curve	Inf	3.08491026	0.63722876	3.78695191
Res12	Pluripotin.SC1	1	curve	0.05895296	1.1552535	0.00844637	0.05667749
Res12	Pluripotin.SC1	2	curve	0.09419461	1.32893316	0.01822159	0.0912028

Res12	RBC8	1	flat	Inf	3.22555584	0.93835564	0
Res12	RBC8	2	flat	Inf	3.20163481	0.86196888	0
Res12	RMC.4550	1	curve	263.59501	3.04067812	0.77737208	99.5538916
Res12	RMC.4550	2	flat	Inf	2.66328043	0.73142428	0
Res12	RO4929097	1	curve	4.79107848	2.79205014	0.2730276	4.79107848
Res12	RO4929097	2	curve	523.511528	2.85940651	0.72204448	84.5651898
Res12	Rabeprazole	1	flat	Inf	3.22307117	0.98644916	0
Res12	Raltitrexed	1	curve	0.05515363	1.47750967	0.19038814	0.04325695
Res12	Rapamycin	1	curve	0.01023691	1.30885483	0.34359128	0.00814229
Res12	Rapamycin	2	curve	0.01090511	1.40148801	0.34330648	0.00835732
Res12	Raphin1	1	curve	19.1271443	3.23775338	0.72629426	19.1271443
Res12	Raphin1	2	flat	Inf	3.45039489	0.88015917	0
Res12	Ravoxertinib	1	curve	5.70909483	2.62803307	0.42023097	3.20035555
Res12	Ravoxertinib	2	curve	11.0326565	2.78383389	0.49445512	1.75680091
Res12	RepSox	1	curve	Inf	2.60352296	0.71471712	0.01423484
Res12	RepSox	2	curve	Inf	2.50608466	0.66996777	0.01618098
Res12	Rhosin.hydrochloride	1	flat	Inf	3.17932028	0.86331456	0
Res12	Rhosin.hydrochloride	2	flat	Inf	3.11801722	0.87791541	0
Res12	SAR405	1	curve	0.69963266	2.33408629	0.21305649	0.49479965
Res12	SAR405	2	curve	0.84347878	2.3280917	0.22222826	0.58122957
Res12	SB273005	1	curve	0.02747528	1.15640499	0.12404702	0.02111672
Res12	SB525334	1	curve	Inf	2.67737498	0.77453483	0.01576559
Res12	SB525334	2	curve	Inf	2.71844881	0.76174386	0.03608358
Res12	SB590885	1	flat	Inf	1.72367368	0.00879611	0

Res12	SB590885	2	flat	Inf	2.05218066	0.0267143	0
Res12	SCH772984	1	curve	0.18576049	1.55819454	0.00299198	0.18576049
Res12	SCH772984	2	curve	0.14531093	1.46026914	0.0025773	0.14531093
Res12	SEC.inhibitor.KL.1	1	flat	Inf	3.21951911	0.77563192	0
Res12	SEC.inhibitor.KL.1	2	flat	Inf	3.24023456	0.81831059	0
Res12	SGC2085	1	flat	Inf	3.33447579	0.95604178	0
Res12	SGC2085	2	curve	Inf	3.3215226	0.81873123	3.23825562
Res12	SHP099	1	curve	Inf	3.13636717	0.64165274	2.2156335
Res12	SHP099	2	curve	5.81774855	2.95681086	0.35386055	4.77535959
Res12	SNDX.5613	1	flat	Inf	2.86051551	0.58302242	0
Res12	SNDX.5613	2	flat	Inf	3.04156175	0.82741882	0
Res12	SR.18292	1	curve	50.077055	3.0103352	0.67068002	50.077055
Res12	SR.18292	2	curve	34.1584601	3.22185863	0.75835234	23.6826666
Res12	Sapanisertib	1	curve	0.01050933	0.55862504	0.07094996	0.01015061
Res12	Sapanisertib	2	curve	0.01087802	0.57106176	0.07360529	0.01050224
Res12	SecinH3	1	flat	Inf	2.80331597	0.76129103	0
Res12	SecinH3	2	flat	Inf	3.1172562	0.85635953	0
Res12	Sephin.1	1	flat	Inf	3.33526202	1.00386595	0
Res12	Sephin.1	2	curve	13.0362432	3.29347642	0.76572295	12.1260607
Res12	Serabelisib	1	curve	7.33892663	2.78899122	0.39133365	7.33892663
Res12	Serabelisib	2	curve	5.96596	2.89475044	0.31088663	5.96596
Res12	Sorafenib	1	curve	7.89246219	3.06055157	0.33907786	7.89246219
Res12	Sorafenib	2	curve	12.1665532	3.03399635	0.54606715	12.1665532
Res12	T.5224	1	curve	11.0786208	3.21664101	0.58942638	10.3231739

Res12	T.5224	2	flat	Inf	3.36400797	0.76106526	0
Res12	TA.01	1	flat	Inf	3.05662767	0.87290555	0
Res12	TA.01	2	flat	Inf	3.42768922	1.04134675	0
Res12	TA.02	1	flat	Inf	3.48130606	0.84816266	0
Res12	TA.02	2	flat	Inf	3.23748997	0.92725692	0
Res12	TAK.632	1	curve	2.94953798	2.67510637	0.10026356	2.94953798
Res12	TAK.632	2	curve	2.51166655	2.53307421	0.16043846	2.51166655
Res12	TAS.102	1	curve	0.02430674	1.36899303	0.27224356	0.01691622
Res12	TAS.102	2	curve	0.02895637	1.38705371	0.28100408	0.01951562
Res12	TP0427736.HCl	1	flat	Inf	2.85567174	0.86935793	0
Res12	TP0427736.HCl	2	flat	Inf	2.8722516	0.8256991	0
Res12	TTP.22	1	flat	Inf	3.34071155	0.96729972	0
Res12	TTP.22	2	flat	Inf	3.26848988	0.98471744	0
Res12	Torin.2	1	curve	0.01005694	0.52698141	0.0438339	0.00975109
Res12	Torin.2	2	curve	0.00963644	0.50629326	0.04597173	0.00935634
Res12	Torkinib	1	curve	0.13314426	1.52778629	0.12277824	0.11229008
Res12	Torkinib	2	curve	0.10760295	1.45566123	0.10829256	0.09055763
Res12	Trilaciclib	1	flat	Inf	3.0324923	0.84738159	0
Res12	Trilaciclib	2	flat	Inf	2.96290156	0.81226418	0
Res12	UNC0642	1	curve	2.91638806	2.68723209	0.00245394	2.91638806
Res12	UNC0642	2	curve	1.37246064	2.39601092	0.00256322	1.37246064
Res12	V.9302	1	curve	10.8006694	3.17410361	0.55448835	10.8006694
Res12	V.9302	2	curve	9.28208985	3.09689964	0.44993665	8.3971953
Res12	VBIT.12	1	flat	Inf	3.07759949	0.84590023	0

Res12	VBIT.12	2	flat	Inf	3.22700508	0.90193797	0
Res12	VBIT.4	1	curve	10.8673286	3.12214679	0.53808937	10.8673286
Res12	VBIT.4	2	flat	Inf	3.3243157	0.77586571	0
Res12	VTP50469	1	flat	Inf	3.0664605	0.75400127	0
Res12	VTP50469	2	flat	Inf	3.00992663	0.82321292	0
Res12	VX.11e	1	curve	0.38306093	1.90743509	0.02345888	0.38306093
Res12	VX.11e	2	curve	0.19185503	1.63459557	0.01674895	0.18878761
Res12	Verteporfin	1	curve	13.8715165	3.17419717	0.55484792	5.39526344
Res12	Verteporfin	2	curve	14.8593975	3.07225663	0.60737627	14.8593975
Res12	Vilazodone	1	curve	7.36316008	3.02803776	0.32780548	7.36316008
Res12	Vilazodone	2	curve	9.96653694	2.97862031	0.48650007	9.96653694
Res12	WAY.600	1	curve	0.40464117	1.93267642	0.08123291	0.37935822
Res12	WAY.600	2	curve	0.68042251	2.19290529	0.1007282	0.61423678
Res12	WYE.354	1	curve	0.2609049	1.70291974	0.02916546	0.2609049
Res12	WYE.354	2	curve	0.31056964	1.80324389	0.02752521	0.31056964
Res12	XMD8.92	1	curve	6.92230328	3.04023308	0.25301976	6.92230328
Res12	XMD8.92	2	curve	4.51383555	2.85744115	0.23264351	4.51383555
Res12	Y15	1	curve	0.9852036	2.33544813	0.00308261	0.96841967
Res12	Y15	2	curve	0.91519535	2.17623454	0.0034085	0.91519535
Res12	YAP.TEAD.inh1	1	curve	0.93329141	2.17543684	0.29361273	0.4107573
Res12	YAP.TEAD.inh1	2	curve	Inf	2.76550963	0.58662792	0.74192317
Res12	YF.2	1	curve	Inf	3.28525671	0.64165301	3.66871964
Res12	YF.2	2	curve	7.26608729	3.35428623	0.14216535	7.26608729
Res12	YM155	1	flat	Inf	3.44155193	1.07605585	0

Res12	YM155	2	flat	Inf	3.15781945	0.93562131	0
Res12	ZM.336372	1	flat	Inf	3.13273101	0.89865912	0
Res12	ZM.336372	2	flat	Inf	3.00223503	0.78673635	0
Res12	Zorifertinib	1	curve	18.9291096	3.18341736	0.68590932	14.3925922
Res12	Zorifertinib	2	curve	Inf	3.17228136	0.67251082	3.54411174
Res12	superTDU	1	flat	Inf	3.12530235	0.8641888	0
Res12	superTDU	2	flat	Inf	3.53095939	1.01126376	0
Res2	6.Diazo.5.oxo.L.norleucine	1	flat	Inf	3.06877557	0.81618271	0
Res2	6.Diazo.5.oxo.L.norleucine	2	curve	Inf	3.13852375	0.78366082	2.1947947
Res2	A.366	1	curve	8.98083209	2.62296441	0.41220096	8.98083209
Res2	A.366	2	flat	Inf	2.75140342	0.51054676	0
Res2	A.674563	1	curve	1.34618486	2.45199938	0.02275552	1.34618486
Res2	A.674563	2	curve	0.89260194	2.27580758	0.01766417	0.89260194
Res2	A1874	1	flat	Inf	3.37241522	0.79434765	0
Res2	A1874	2	flat	Inf	3.53446604	0.85867955	0
Res2	A939572	1	flat	Inf	3.29472422	0.92253917	0
Res2	A939572	2	flat	Inf	2.97088843	0.81747108	0
Res2	ACBI1	1	curve	11.2565226	2.62488812	0.52542114	1.79360848
Res2	ACBI1	2	flat	Inf	2.77738671	0.64207632	0
Res2	AG.270	1	curve	7.58889064	3.01984971	0.43369751	5.69336853
Res2	AG.270	2	curve	9.34149029	3.06669788	0.49195279	2.96283601
Res2	AICAR	1	curve	0.44730401	2.09018385	0.20006994	0.24939169
Res2	AICAR	2	curve	0.43181453	2.04520637	0.19195149	0.24790584
Res2	ASLAN003	1	flat	Inf	3.10327861	0.83965205	0

Res2	ASLAN003	2	flat	Inf	3.18616865	0.9118813	0
Res2	AZ191	1	curve	3.9114206	3.02724335	0.0983228	3.75076539
Res2	AZ191	2	curve	3.46703207	2.96893528	0.06630014	3.37619778
Res2	AZD0364	1	curve	0.01649296	0.64532068	0.0019705	0.01604842
Res2	AZD0364	2	curve	0.02794121	0.79721311	0.0016418	0.02794121
Res2	AZD3759	1	curve	Inf	3.1536023	0.81031559	1.2499649
Res2	AZD3759	2	curve	19.0967291	3.15014714	0.65697145	19.0967291
Res2	AZD8055	1	curve	0.01130944	0.77455191	0.12964058	0.01054919
Res2	AZD8055	2	curve	0.0112816	0.83275337	0.15073279	0.01039086
Res2	Afuresertib	1	flat	Inf	3.15515035	0.87645119	0
Res2	Afuresertib	2	curve	Inf	3.23014685	0.81712982	3.38062529
Res2	Afuresirtib	1	flat	Inf	3.29185032	0.4601532	0
Res2	Afuresirtib	2	curve	6.0894706	2.91056796	0.17454717	6.0894706
Res2	Alisertib	1	curve	1.65087567	2.2679829	0.48942189	0.08039108
Res2	Alisertib	2	curve	0.27180949	2.01131887	0.42045212	0.04287431
Res2	Alpelisib	1	curve	Inf	3.22513528	0.75562562	5.98070408
Res2	Alpelisib	2	curve	22.1003597	3.15033716	0.68569036	22.1003597
Res2	Autophinib	1	flat	Inf	4.11759904	0.64734413	0
Res2	Autophinib	2	flat	Inf	4.5674841	0.74256491	0
Res2	Azaserine	1	curve	Inf	3.16036534	0.86107043	0.46278312
Res2	Azaserine	2	flat	Inf	3.24200147	0.90729921	0
Res2	BAY.1251152	1	curve	0.03853927	1.02817741	0.04835495	0.03542179
Res2	BAY.1251152	2	curve	0.03598667	1.07153721	0.06835515	0.03262854
Res2	BAY.2402234	1	curve	0.19502187	1.99972645	0.36755283	0.02222384

Res2	BAY.2402234	2	curve	0.96736349	2.08026774	0.38089683	0.02893996
Res2	BAY.293	1	curve	3.87905277	2.81602344	0.00297602	3.87905277
Res2	BAY.293	2	curve	3.76327191	2.84216303	0.00296196	3.76327191
Res2	BAY.299	1	curve	2.13420964	2.5769288	0.13335389	2.13420964
Res2	BAY.299	2	curve	1.89053084	2.52811055	0.08737502	1.89053084
Res2	BAY1125976	1	flat	Inf	2.8951286	0.56390436	0
Res2	BAY1125976	2	curve	39.0591582	2.81750958	0.63900726	39.0591582
Res2	BI.3406	1	curve	12.0058677	2.57476848	0.51223768	12.0058677
Res2	BI.3406	2	curve	15.0878726	2.83563465	0.50708244	15.0878726
Res2	BIX.02189	1	flat	Inf	2.99207781	0.52383833	0
Res2	BIX.02189	2	flat	Inf	2.96506328	0.55309464	0
Res2	BX.795	1	flat	Inf	2.64367627	0.21664488	0
Res2	BX.795	2	flat	Inf	2.52466669	0.20249422	0
Res2	Bafilomycin.A1	1	curve	0.00962746	0.43349762	0.02976472	0.00950086
Res2	Bafilomycin.A1	2	curve	0.00949411	0.43005682	0.0273726	0.00936707
Res2	Benproperine.phosphate	1	flat	Inf	2.88884329	0.470354	0
Res2	Benproperine.phosphate	2	curve	13.1627752	3.13790331	0.62081711	13.1627752
Res2	Brefeldin.A	1	curve	1.01810143	2.22403074	0.00643042	1.01810143
Res2	Brefeldin.A	2	curve	0.87614941	2.07698323	0.00525829	0.87614941
Res2	CAY10566	1	curve	10.7169231	2.78760941	0.50152666	10.7169231
Res2	CAY10566	2	flat	Inf	3.02052407	0.64367625	0
Res2	CCG.1423	1	flat	Inf	3.42277048	0.95291553	0
Res2	CCG.1423	2	flat	Inf	3.23893198	0.85504031	0
Res2	CCT128930	1	curve	2.20333612	2.59090334	0.1946164	2.07517622

Res2	CCT128930	2	curve	2.4691286	2.49535636	0.19432127	2.4691286
Res2	CK.636	1	flat	Inf	3.02051752	0.8914485	0
Res2	CK.636	2	flat	Inf	2.98383308	0.8381753	0
Res2	CK.869	1	curve	6.244507	2.97846955	0.31950705	6.244507
Res2	CK.869	2	curve	4.24047836	2.8584656	0.31870999	2.97934334
Res2	CM272	1	curve	1.23019272	2.28947581	0.012182	1.23019272
Res2	CM272	2	curve	0.93180113	2.11372571	0.00989032	0.93180113
Res2	CVT.11127	1	curve	4.96633683	2.5518097	0.40013283	4.96633683
Res2	CVT.11127	2	curve	41.6760129	2.74669234	0.58985908	41.6760129
Res2	CeMMEC13	1	flat	Inf	3.17032586	0.78787489	0
Res2	CeMMEC13	2	flat	Inf	2.84963726	0.66797243	0
Res2	Cilengitide.trifluoroacetate	1	curve	0.54524609	2.09376863	0.11774946	0.40385991
Res2	Cilengitide.trifluoroacetate	2	curve	0.35788422	1.84999131	0.12291923	0.32116435
Res2	Concanamycin	1	curve	8.03E-04	0.33728701	0.03202847	7.95E-04
Res2	Concanamycin	2	curve	8.04E-04	0.35424711	0.03867804	7.94E-04
Res2	Crenolanib	1	curve	2.56510654	2.65878956	0.11503443	2.38777927
Res2	Crenolanib	2	curve	2.79678491	2.83057025	0.08939218	2.66527614
Res2	D.4476	1	flat	Inf	3.03304619	0.59882513	0
Res2	D.4476	2	flat	Inf	2.8505894	0.49604571	0
Res2	DAPT	1	flat	Inf	3.19684761	0.79720305	0
Res2	DAPT	2	flat	Inf	3.10312008	0.81448423	0
Res2	DDO.5936	1	curve	Inf	2.91368088	0.55924171	1.95594975
Res2	DDO.5936	2	curve	Inf	3.05464018	0.62698275	2.20804378
Res2	Dactolisib	1	curve	0.00915801	0.68536039	0.07275604	0.00872216

Res2	Dactolisib	2	curve	0.00948908	0.73544335	0.07897412	0.00894344
Res2	Decoyinine	1	flat	Inf	3.27204662	0.86944672	0
Res2	Decoyinine	2	flat	Inf	3.13228316	0.82821819	0
Res2	Dorsomorphin..Compound.C	1	flat	Inf	3.21994966	0.96753868	0
Res2	Dorsomorphin..Compound.C	2	flat	Inf	2.98691038	0.84685126	0
Res2	Duvelisib	1	flat	Inf	3.3470521	0.9004925	0
Res2	Duvelisib	2	flat	Inf	3.16173831	0.78918805	0
Res2	Dynasore	1	curve	1.40877951	2.34663143	0.06187451	1.40877951
Res2	Dynasore	2	flat	Inf	3.5227565	0.71332129	0
Res2	Dyngo.4a	1	flat	Inf	3.68921388	0.99755112	0
Res2	Dyngo.4a	2	curve	Inf	3.2106452	0.78108267	1.42956979
Res2	EAD1	1	curve	0.79353602	2.13294672	0.00175454	0.79353602
Res2	EAD1	2	curve	0.59501866	2.06514347	0.00149313	0.59501866
Res2	EHT1864	1	flat	Inf	3.15476651	0.86942374	0
Res2	EHT1864	2	flat	Inf	3.12276697	0.75497116	0
Res2	EN6	1	flat	Inf	2.79589004	0.58673064	0
Res2	EN6	2	flat	Inf	3.1232377	0.72549343	0
Res2	ERK5.IN.1	1	curve	0.40404576	1.86182049	0.02402823	0.40404576
Res2	ERK5.IN.1	2	curve	0.4782628	1.96089828	0.01994207	0.4782628
Res2	Empesertib	1	curve	0.01096862	1.50456734	0.42380434	0.00783098
Res2	Empesertib	2	curve	0.01255932	1.57180643	0.43513106	0.00848483
Res2	Erastin	1	curve	0.1082895	1.4000107	0.00235979	0.10671805
Res2	Erastin	2	curve	0.13795645	1.38314746	0.00189608	0.13795645
Res2	Erlotinib	1	curve	2.16760295	2.53252198	0.11416166	2.16760295

Res2	Erlotinib	2	curve	18.9369834	2.95174277	0.53609643	18.9369834
Res2	Everolimus	1	curve	0.00952375	1.10647415	0.25148192	0.0081317
Res2	Everolimus	2	curve	0.00936626	1.11903261	0.23918974	0.00795978
Res2	Exo1	1	flat	Inf	3.51623271	0.97636818	0
Res2	Exo1	2	flat	Inf	3.21398508	0.93344026	0
Res2	FL.411	1	curve	5.08212862	2.8992717	0.12111292	5.08212862
Res2	FL.411	2	curve	5.25324515	3.05633869	0.1031819	5.25324515
Res2	FTI.277.HCl	1	flat	Inf	3.14371526	0.84766396	0
Res2	FTI.277.HCl	2	flat	Inf	3.20254988	0.87152623	0
Res2	Fluorouracil	1	curve	2.61230045	2.63484266	0.2616351	1.93951317
Res2	Fluorouracil	2	curve	1.92232978	2.60888363	0.2398295	1.26403642
Res2	Folinic.acid	1	curve	20.7015348	3.01543776	0.62170804	20.7015348
Res2	Folinic.acid	2	flat	Inf	2.97644212	0.75714216	0
Res2	GDC.0077	1	flat	Inf	2.99677539	0.81361371	0
Res2	GDC.0077	2	flat	Inf	3.07450845	0.77942542	0
Res2	GGTI.298.TFA.salt	1	curve	7.19067907	2.87669619	0.35175859	7.19067907
Res2	GGTI.298.TFA.salt	2	curve	6.32115662	2.88358632	0.26748253	6.32115662
Res2	GLPG0187	1	curve	0.00894568	0.62457089	0.10686852	0.00849176
Res2	GLPG0187	2	curve	0.00911766	0.65619445	0.11115948	0.00861318
Res2	GSK1059615	1	curve	0.02069994	1.42883924	0.03411062	0.01932268
Res2	GSK1059615	2	curve	0.07849603	1.85666412	0.0351647	0.07849603
Res2	GSK1324726A	1	curve	0.41280647	1.9270735	0.13084071	0.34652861
Res2	GSK1324726A	2	curve	0.45054588	2.0604557	0.13514364	0.33185429
Res2	GSK2256098	1	flat	Inf	3.43517641	0.87081303	0

Res2	GSK2256098	2	curve	Inf	3.23523584	0.84511024	1.74631996
Res2	GSK2334470	1	flat	Inf	2.99682789	0.64808295	0
Res2	GSK2334470	2	curve	13.213825	3.29589877	0.77576944	12.252507
Res2	GSK2636771	1	flat	Inf	3.40172154	1.03472275	0
Res2	GSK2636771	2	flat	Inf	3.29118464	1.02705244	0
Res2	GSK467	1	flat	Inf	2.84861114	0.68079993	0
Res2	GSK467	2	flat	Inf	3.10853953	0.76732704	0
Res2	GW5074	1	flat	Inf	3.31591613	0.95874585	0
Res2	GW5074	2	flat	Inf	3.15613136	0.93713715	0
Res2	GW788388	1	flat	Inf	3.0616024	0.85080972	0
Res2	GW788388	2	flat	Inf	3.17026912	0.87774971	0
Res2	Gallein	1	flat	Inf	3.44974888	0.70809908	0
Res2	Gallein	2	curve	Inf	3.26896543	0.75499014	8.05717699
Res2	Gedatolisib	1	curve	0.12208923	2.144222	0.17895292	0.09045519
Res2	Gedatolisib	2	curve	0.11595577	2.12600094	0.15477768	0.08850867
Res2	Glycyrrhizin	1	flat	Inf	3.06312469	0.81288337	0
Res2	Glycyrrhizin	2	flat	Inf	3.05615626	0.87796581	0
Res2	Golgicide.A	1	flat	Inf	2.94319996	0.78990033	0
Res2	Golgicide.A	2	curve	9.42033163	3.06170778	0.43654537	8.94690324
Res2	H3B.120	1	flat	Inf	2.87917315	0.74408017	0
Res2	H3B.120	2	flat	Inf	2.9240465	0.55024396	0
Res2	Harmine.hydrochloride	1	curve	9.24739489	2.8386928	0.46389305	9.24739489
Res2	Harmine.hydrochloride	2	flat	Inf	2.66274358	0.46242619	0
Res2	Hydroxy.Dynasore	1	flat	Inf	2.90343883	0.67160272	0

Res2	Hydroxy.Dynasore	2	flat	Inf	3.37110941	0.73987078	0
Res2	IACS.13909	1	curve	10.0858171	2.88160877	0.46321271	10.0858171
Res2	IACS.13909	2	curve	4.36459015	2.69176436	0.16011592	4.36459015
Res2	IGS.1.76	1	flat	Inf	2.74261709	0.58699891	0
Res2	IGS.1.76	2	flat	Inf	2.93806941	0.73583088	0
Res2	ILK.IN.2	1	curve	2.49458494	2.70665789	0.00128912	2.49458494
Res2	ILK.IN.2	2	curve	3.03752823	2.85954015	0.00139685	3.03752823
Res2	IPI.549	1	flat	Inf	3.03225119	0.69248554	0
Res2	IPI.549	2	curve	32.1980272	3.20689163	0.74921439	32.1980272
Res2	ISRIB	1	flat	Inf	3.45315011	1.05935244	0
Res2	ISRIB	2	flat	Inf	3.3966342	1.00637389	0
Res2	ITD.1	1	curve	10.4129779	3.14894768	0.52396148	10.4129779
Res2	ITD.1	2	curve	10.3521432	3.10098774	0.52226535	10.3521432
Res2	JQ1	1	curve	0.06024635	1.24318592	0.067938	0.0518816
Res2	JQ1	2	curve	0.04977969	1.20432939	0.0709695	0.042758
Res2	JX06	1	curve	0.09090325	1.21891002	0.00232186	0.09090325
Res2	JX06	2	curve	0.11820282	1.39556572	0.00248333	0.11748399
Res2	KM91104	1	curve	5.61446731	2.87776774	0.3400472	5.61446731
Res2	KM91104	2	curve	7.27651652	2.93493874	0.40310564	7.27651652
Res2	KU.0063794	1	curve	0.11816876	1.61297632	0.11841348	0.08901044
Res2	KU.0063794	2	curve	0.1062435	1.55171261	0.11327481	0.07809935
Res2	Ki16425	1	flat	Inf	2.80283755	0.72523103	0
Res2	Ki16425	2	flat	Inf	2.66041935	0.63341977	0
Res2	LB.100	1	curve	622.394252	2.97870641	0.77254747	146.730534

Res2	LB.100	2	flat	Inf	3.06573826	0.84788262	0
Res2	LDN.193189	1	curve	0.85294997	2.41880621	0.17223359	0.64433497
Res2	LDN.193189	2	curve	1.67844479	2.52940716	0.00314923	1.67844479
Res2	LOC14	1	curve	9.02932203	3.17759984	0.39556247	8.5485484
Res2	LOC14	2	curve	8.4592516	3.11036199	0.35959523	8.4592516
Res2	LXS.196	1	curve	0.12439172	1.64178889	0.16692631	0.07532993
Res2	LXS.196	2	curve	6.20885069	2.8761587	0.29105174	6.20885069
Res2	LY2109761	1	flat	Inf	3.3858947	0.99774975	0
Res2	LY2109761	2	flat	Inf	3.13128092	0.86402193	0
Res2	LY2857785	1	curve	0.17458733	1.66679413	0.03649203	0.17117321
Res2	LY2857785	2	curve	0.14622137	1.6091449	0.04389774	0.14343315
Res2	LY3295668	1	curve	Inf	2.47246887	0.44369772	0.1177804
Res2	LY3295668	2	curve	1.29423255	2.29951048	0.41090582	0.19604839
Res2	MAT2A.inhibitor.2	1	flat	Inf	3.37876176	1.0846427	0
Res2	MAT2A.inhibitor.2	2	flat	Inf	3.36074401	1.02152766	0
Res2	MCP110	1	flat	Inf	3.16770459	0.88982619	0
Res2	MCP110	2	flat	Inf	3.13647837	0.85149417	0
Res2	MG149	1	curve	10.2514832	2.92495758	0.50079685	7.56883963
Res2	MG149	2	flat	Inf	3.26822905	0.8305343	0
Res2	MGH.CP1	1	curve	10.8923747	3.2579977	0.60467411	10.8923747
Res2	MGH.CP1	2	flat	Inf	3.00712103	0.66583108	0
Res2	MI.503	1	curve	1.01247845	2.1146544	0.00169081	1.01247845
Res2	MI.503	2	curve	0.96007633	2.1089797	0.00596205	0.96007633
Res2	MK.0429	1	curve	0.01661566	1.08770797	0.13559812	0.0132782

Res2	MK.0429	2	curve	0.01998653	1.08286798	0.12847914	0.01559641
Res2	MK.0752	1	flat	Inf	3.03848862	0.7789794	0
Res2	MK.0752	2	flat	Inf	3.38904639	0.86093421	0
Res2	MK.2206.2HCl	1	flat	Inf	2.60126603	0.41466161	0
Res2	MK.2206.2HCl	2	curve	6.49528465	2.87631648	0.26432665	6.49528465
Res2	MK.5108	1	curve	10.3598068	3.14862173	0.50951638	10.3598068
Res2	MK.5108	2	curve	26.2412093	2.748844	0.53844647	1.78899229
Res2	MK.8245	1	curve	0.01406706	1.29815669	0.2793454	0.01157884
Res2	MK.8245	2	curve	0.14822003	1.88451964	0.32448679	0.04672579
Res2	MPI.0479605	1	curve	0.01121377	1.20290205	0.27135312	0.00934858
Res2	MPI.0479605	2	curve	0.01121213	1.27845373	0.30830196	0.00905625
Res2	MRT199665	1	curve	0.07375891	1.32555347	0.04535288	0.06312665
Res2	MRT199665	2	curve	0.12248455	1.53741231	0.044199	0.10402745
Res2	MTX.211	1	curve	6.21980646	2.9108493	0.35065549	6.21980646
Res2	MTX.211	2	curve	5.10055146	2.74887793	0.37893637	4.52090712
Res2	MYF.01.37	1	curve	Inf	2.98722489	0.52378108	2.60137715
Res2	MYF.01.37	2	curve	10.5681152	2.96132263	0.45456346	10.5681152
Res2	Mdivi.1	1	flat	Inf	2.86083288	0.76022714	0
Res2	Mdivi.1	2	flat	Inf	3.28425169	0.9119124	0
Res2	Mdivi.1.ERK5.IN.1	1	curve	0.80476234	2.1503825	0.06947886	0.80476234
Res2	Mdivi.1.ERK5.IN.1	2	curve	0.89932017	2.29040513	0.06888381	0.81408646
Res2	Mdivi.1.ERK5.IN.1	3	curve	1.07791367	2.29405283	0.06608175	1.07791367
Res2	Mdivi.1.ERK5.IN.1	4	curve	0.60583311	2.04065699	0.0726219	0.60583311
Res2	Metarrestin	1	flat	Inf	3.30537005	0.81125298	0

Res2	Metarrestin	2	flat	Inf	3.38670337	0.8221069	0
Res2	Mizoribine	1	curve	1.72905941	2.48550797	0.02489757	1.7103094
Res2	Mizoribine	2	curve	8.34703618	2.99949651	0.44154078	8.34703618
Res2	Monastrol	1	flat	Inf	3.31089022	0.91914082	0
Res2	Monastrol	2	flat	Inf	3.0781062	0.84636832	0
Res2	NAV.2729	1	curve	4.2995662	2.82694181	0.27097041	3.56320969
Res2	NAV.2729	2	curve	13.7083083	2.929349	0.55550816	13.7083083
Res2	NSC.23766	1	flat	Inf	3.22728955	0.86088221	0
Res2	NSC.23766	2	flat	Inf	3.20956592	0.82517928	0
Res2	NSC15364	1	flat	Inf	3.24417825	0.98929873	0
Res2	NSC15364	2	flat	Inf	3.19195559	0.91494908	0
Res2	NVP.2	1	curve	0.01066143	0.46293862	0.04134116	0.01045668
Res2	NVP.2	2	curve	0.01026905	0.44111109	0.04378486	0.01008752
Res2	Nemiralisib	1	flat	Inf	2.47286256	0.03567458	0
Res2	Nemiralisib	2	curve	2.5066247	2.53149422	0.04116498	2.5066247
Res2	Nirogacestat	1	flat	Inf	2.80506201	0.61890797	0
Res2	Nirogacestat	2	curve	Inf	3.07705984	0.71491837	0.88145707
Res2	OSI.027	1	curve	0.97680385	2.37565833	0.14758091	0.68200642
Res2	OSI.027	2	curve	0.71458455	2.12978087	0.13476727	0.63953106
Res2	OSMI.1	1	flat	Inf	3.05609263	0.68854506	0
Res2	OSMI.1	2	flat	Inf	2.92090335	0.62945581	0
Res2	OSMI.4	1	flat	Inf	3.21527392	0.68968388	0
Res2	OSMI.4	2	curve	15.5459599	2.97567038	0.55017146	15.5459599
Res2	Omipalisib	1	curve	0.03531876	1.10309433	0.03698981	0.02963096

Res2	Omipalisib	2	curve	0.04559599	1.21146017	0.07230502	0.03668402
Res2	Oncrasin.1	1	flat	Inf	3.2784366	0.7480839	0
Res2	Oncrasin.1	2	flat	Inf	3.32715866	0.77355084	0
Res2	P110	1	flat	Inf	3.43006175	1.03402814	0
Res2	P110	2	flat	Inf	3.45142015	0.97631731	0
Res2	P5091	1	curve	6.5629815	2.97659256	0.25879225	6.5629815
Res2	P5091	2	curve	4.67112408	2.71701593	0.17339246	4.67112408
Res2	PD0166285	1	curve	0.17134585	1.65240227	0.00117802	0.15978849
Res2	PD0166285	2	curve	0.17634803	1.56843713	0.00200481	0.16960937
Res2	PD153035	1	curve	Inf	3.17845142	0.87139441	0.52984439
Res2	PD153035	2	curve	Inf	3.00907339	0.84311402	0.18819523
Res2	PF.04691502	1	curve	0.0856709	1.37261371	0.05027462	0.07381229
Res2	PF.04691502	2	curve	0.08363455	1.35684656	0.04588377	0.07262204
Res2	PF.562271	1	curve	Inf	2.64627153	0.48755291	0.52685198
Res2	PF.562271	2	curve	1.98929948	2.58672957	0.48166234	0.5369379
Res2	PF.9366	1	curve	13.2427775	3.09015486	0.56853708	13.2427775
Res2	PF.9366	2	curve	11.3655152	2.89590181	0.48894644	11.3655152
Res2	PFI.3	1	flat	Inf	2.94911448	0.75344662	0
Res2	PFI.3	2	flat	Inf	3.3034805	0.65083713	0
Res2	PH.064	1	curve	0.35148799	1.95136938	0.13801987	0.20919983
Res2	PH.064	2	curve	2.15021185	2.4958214	0.17045411	2.15021185
Res2	PKC.iota.inhibitor.1	1	curve	4.96957697	2.77723156	0.25185621	4.96957697
Res2	PKC.iota.inhibitor.1	2	curve	28.1722709	3.05343277	0.66701983	28.1722709
Res2	PND.1186	1	curve	3.78378777	2.62124827	0.34808438	3.14107855

Res2	PND.1186	2	curve	2.20427294	2.44359643	0.33101543	1.56104847
Res2	Palbociclib	1	flat	Inf	2.86772205	0.62236898	0
Res2	Palbociclib	2	flat	Inf	3.00324392	0.57445121	0
Res2	Pemetrexed	1	flat	Inf	2.92552517	0.55658497	0
Res2	Pemetrexed	2	curve	17.49568	2.93641262	0.57811457	17.49568
Res2	Perifosine	1	flat	Inf	3.34962161	0.62568512	0
Res2	Perifosine	2	curve	7.16544218	3.20420566	0.44190983	4.88474475
Res2	Pictilisib	1	curve	3.67665288	2.5793527	0.31191265	3.67665288
Res2	Pictilisib	2	curve	2.82597164	2.51011377	0.26474004	2.82597164
Res2	Pinometostat	1	flat	Inf	3.24473012	0.60066015	0
Res2	Pinometostat	2	curve	13.1941595	3.13892018	0.58927174	13.1941595
Res2	PluriSIn.1..NSC.14613.	1	flat	Inf	2.82829212	0.62611066	0
Res2	PluriSIn.1..NSC.14613.	2	curve	Inf	3.07468314	0.68080626	1.45656699
Res2	Pluripotin.SC1	1	curve	0.09211678	1.29234213	0.00761967	0.09211678
Res2	Pluripotin.SC1	2	curve	0.07992907	1.22329615	0.00626081	0.07992907
Res2	RBC8	1	flat	Inf	3.18015285	0.86810805	0
Res2	RBC8	2	flat	Inf	3.14410727	0.86340653	0
Res2	RMC.4550	1	curve	20.6451816	2.60062112	0.51672409	20.6451816
Res2	RMC.4550	2	curve	24.4265887	2.74536586	0.55616398	24.4265887
Res2	RO4929097	1	curve	2.32726134	2.59248262	0.30583164	1.60576228
Res2	RO4929097	2	curve	797.817296	3.15929586	0.84526275	301.605644
Res2	Rabeprazole	1	flat	Inf	2.95649846	0.71576748	0
Res2	Rabeprazole	2	flat	Inf	3.14985966	0.96360522	0
Res2	Raltitrexed	1	curve	0.18053377	1.98725263	0.35403668	0.06535215

Res2	Raltitrexed	2	curve	0.1727403	2.0190352	0.35589912	0.0683699
Res2	Rapamycin	1	curve	0.00939988	1.2121857	0.31888928	0.00773245
Res2	Rapamycin	2	curve	0.01012555	1.18711825	0.28896392	0.00841238
Res2	Raphin1	1	flat	Inf	3.99778373	0.99512014	0
Res2	Raphin1	2	flat	Inf	3.28136325	0.949528	0
Res2	Ravoxertinib	1	curve	1.24123471	2.39242175	0.30845858	0.70896906
Res2	Ravoxertinib	2	curve	2.52560212	2.48620199	0.33652421	1.79004714
Res2	RepSox	1	curve	90.234808	2.73917894	0.59817647	2.02322702
Res2	RepSox	2	curve	30.8237146	2.65214749	0.54639194	0.80962433
Res2	Rhosin.hydrochloride	1	flat	Inf	3.06105889	0.852143	0
Res2	Rhosin.hydrochloride	2	flat	Inf	2.97598024	0.83327884	0
Res2	SAR405	1	curve	0.46373216	1.91999803	0.13118617	0.46373216
Res2	SAR405	2	curve	0.46495463	1.94625357	0.16305914	0.38879203
Res2	SB273005	1	curve	0.01489735	0.89692903	0.0972033	0.01325513
Res2	SB273005	2	curve	0.0137376	0.87492022	0.10743788	0.01238508
Res2	SB525334	1	curve	Inf	2.9767432	0.6846267	1.68643659
Res2	SB525334	2	flat	Inf	2.70892078	0.61138506	0
Res2	SB590885	1	curve	1.44657845	2.27202503	0.04413941	1.44657845
Res2	SB590885	2	curve	0.88572145	2.10748972	0.01767304	0.88572145
Res2	SCH772984	1	curve	0.07684244	1.24137591	0.01087247	0.07684244
Res2	SCH772984	2	curve	0.10666742	1.3866147	0.00256543	0.10595151
Res2	SEC.inhibitor.KL.1	1	curve	Inf	3.04970807	0.77020383	6.89518926
Res2	SEC.inhibitor.KL.1	2	flat	Inf	2.95282147	0.63728092	0
Res2	SGC2085	1	flat	Inf	3.20255578	0.84105068	0

Res2	SGC2085	2	flat	Inf	3.11189682	0.82536039	0
Res2	SHP099	1	curve	9.35776121	2.95863222	0.47753692	9.35776121
Res2	SHP099	2	curve	12.5069361	3.21346736	0.515995	3.32434476
Res2	SNDX.5613	1	curve	5.26312697	2.96842562	0.1057285	5.26312697
Res2	SNDX.5613	2	curve	15.4787727	2.88662327	0.51078331	15.4787727
Res2	SR.18292	1	curve	Inf	3.15662393	0.52388173	4.19768612
Res2	SR.18292	2	curve	12.2858723	3.37494642	0.710469	11.3710968
Res2	Sapanisertib	1	curve	0.01065414	0.66650269	0.09963735	0.01010783
Res2	Sapanisertib	2	curve	0.01039935	0.62721639	0.10031975	0.00992048
Res2	SecinH3	1	flat	Inf	3.38574328	0.98379496	0
Res2	SecinH3	2	flat	Inf	3.25410245	0.83982436	0
Res2	Sephin.1	1	flat	Inf	3.27378681	0.99630007	0
Res2	Sephin.1	2	flat	Inf	3.49101276	1.01968653	0
Res2	Serabelisib	1	flat	Inf	2.75432915	0.2492354	0
Res2	Serabelisib	2	curve	6.90952935	2.75783439	0.40589895	6.90952935
Res2	Sorafenib	1	flat	Inf	3.14894679	0.76554002	0
Res2	Sorafenib	2	curve	Inf	3.08875032	0.73753638	1.92717718
Res2	T.5224	1	flat	Inf	2.88060033	0.66797015	0
Res2	T.5224	2	flat	Inf	2.87827004	0.71101051	0
Res2	TA.01	1	flat	Inf	2.96916791	0.89504349	0
Res2	TA.01	2	flat	Inf	3.3709867	0.95683336	0
Res2	TA.02	1	flat	Inf	3.13156003	0.87794605	0
Res2	TA.02	2	flat	Inf	3.13502145	0.69104199	0
Res2	TAK.632	1	curve	2.28578263	2.67303845	0.11820908	2.28578263

Res2	TAK.632	2	curve	1.16784654	2.25253543	0.09795226	1.16784654
Res2	TAS.102	1	curve	0.02031931	1.50610341	0.33460163	0.01306315
Res2	TAS.102	2	curve	0.02284785	1.52526202	0.36384793	0.01354942
Res2	TP0427736.HCl	1	flat	Inf	3.02125278	0.80650674	0
Res2	TP0427736.HCl	2	flat	Inf	3.36444053	0.96736235	0
Res2	TTP.22	1	flat	Inf	3.09809387	0.90560039	0
Res2	TTP.22	2	flat	Inf	3.3351269	0.99042211	0
Res2	Torin.2	1	curve	0.01052739	0.63647665	0.03019211	0.01005998
Res2	Torin.2	2	curve	0.01052232	0.62896605	0.03648211	0.01006492
Res2	Torkinib	1	curve	0.0974879	1.54351663	0.16582634	0.07270722
Res2	Torkinib	2	curve	0.08684895	1.45881296	0.1341668	0.06655166
Res2	Trilaciclib	1	flat	Inf	3.01110819	0.78927863	0
Res2	Trilaciclib	2	flat	Inf	2.90706787	0.75138252	0
Res2	UNC0642	1	curve	2.69568052	2.68991725	0.00398828	2.69568052
Res2	UNC0642	2	curve	2.18081659	2.49072332	0.00357614	2.18081659
Res2	V.9302	1	flat	Inf	3.12235441	0.69043536	0
Res2	V.9302	2	flat	Inf	3.01474903	0.6550343	0
Res2	VBIT.12	1	flat	Inf	3.19849728	0.80873829	0
Res2	VBIT.12	2	flat	Inf	3.16030855	0.86122516	0
Res2	VBIT.4	1	curve	155.848903	3.07689811	0.76052131	66.3643049
Res2	VBIT.4	2	curve	13.7653526	3.18697559	0.67969138	11.9092239
Res2	VTP50469	1	curve	Inf	3.18051128	0.84152082	1.67330753
Res2	VTP50469	2	flat	Inf	3.50014329	1.02220396	0
Res2	VX.11e	1	curve	0.28259788	1.82356679	0.02405026	0.27739689

Res2	VX.11e	2	curve	0.39851713	1.90152688	0.02288888	0.39851713
Res2	Verteporfin	1	curve	12.375106	3.041476	0.53659124	12.375106
Res2	Verteporfin	2	curve	9.96086942	3.21372276	0.49628284	9.96086942
Res2	Vilazodone	1	curve	7.3458343	2.97269923	0.36536321	7.3458343
Res2	Vilazodone	2	curve	10.7595135	3.16449008	0.52438971	10.7595135
Res2	WAY.600	1	curve	0.64254358	2.14984824	0.12378501	0.51387714
Res2	WAY.600	2	curve	0.38857933	1.92037461	0.1165935	0.3341427
Res2	WYE.354	1	curve	0.13985737	1.54754725	0.07396659	0.1210966
Res2	WYE.354	2	curve	0.16690729	1.6439911	0.0829466	0.14200305
Res2	XMD8.92	1	curve	4.27223914	2.8352769	0.2372123	4.27223914
Res2	XMD8.92	2	curve	4.27506306	2.77823724	0.20289885	4.27506306
Res2	Y15	1	curve	0.95656685	2.24070031	0.00395688	0.94626428
Res2	Y15	2	curve	0.85693967	2.25048893	0.00280762	0.84719137
Res2	YAP.TEAD.inh1	1	curve	4.35697975	2.64674523	0.2921128	4.35697975
Res2	YAP.TEAD.inh1	2	curve	1.30770457	2.59361681	0.28437912	0.81291291
Res2	YF.2	1	curve	5.65663417	3.11091757	0.17151861	5.65663417
Res2	YF.2	2	curve	Inf	3.22810065	0.67281053	4.59266785
Res2	YM155	1	curve	6.01286225	2.88490199	0.2918874	6.01286225
Res2	YM155	2	curve	5.35208252	2.73199693	0.27792984	5.35208252
Res2	ZM.336372	1	flat	Inf	3.23253544	0.90197867	0
Res2	ZM.336372	2	flat	Inf	2.99274427	0.82654601	0
Res2	Zorifertinib	1	curve	16.4140059	2.8396496	0.55155359	16.4140059
Res2	Zorifertinib	2	flat	Inf	2.94473559	0.60767209	0
Res2	superTDU	1	flat	Inf	3.30312795	0.9792088	0

Res2	superTDU	2	flat	Inf	3.39544923	1.0022491	0
WT1	6.Diazo.5.oxo.L.norleucine	1	curve	4.80053372	2.77753649	0.22017839	4.80053372
WT1	6.Diazo.5.oxo.L.norleucine	2	curve	5.54048354	2.92711187	0.23995509	5.54048354
WT1	A.366	1	curve	16.9178368	2.85492369	0.55270842	16.9178368
WT1	A.366	2	curve	16.0072083	2.95133474	0.55864027	16.0072083
WT1	A.674563	1	curve	0.46601616	2.09400458	0.0095623	0.45974325
WT1	A.674563	2	curve	0.95428263	2.26866409	0.01975484	0.95428263
WT1	A1874	1	flat	Inf	3.35920356	0.84556314	0
WT1	A1874	2	flat	Inf	3.2499141	0.80925983	0
WT1	A939572	1	curve	Inf	2.50447057	0.63655073	0.05213664
WT1	A939572	2	curve	Inf	2.44049844	0.61179329	0.02514993
WT1	ACBI1	1	curve	Inf	2.66398501	0.51897681	0.50555133
WT1	ACBI1	2	curve	55.7947957	2.68518996	0.53430546	0.83568318
WT1	AG.270	1	curve	3.37678273	2.6060421	0.29613525	3.37678273
WT1	AG.270	2	curve	3.49932044	2.62990228	0.30380972	3.49932044
WT1	AICAR	1	curve	Inf	2.16863591	0.543918	0.01030172
WT1	AICAR	2	flat	Inf	2.31629403	0.46357948	0
WT1	ASLAN003	1	curve	16.7872853	3.14032524	0.67047943	16.7872853
WT1	ASLAN003	2	curve	17.4979868	3.11241118	0.64601992	12.91207
WT1	AZ191	1	curve	1.49286863	2.35930653	0.01560054	1.49286863
WT1	AZ191	2	curve	1.77600829	2.41983159	0.08002214	1.77600829
WT1	AZD0364	1	curve	0.09365581	1.2870815	0.0046772	0.09286941
WT1	AZD0364	2	curve	0.18296809	1.5570888	0.00788309	0.18296809
WT1	AZD3759	1	curve	Inf	2.96605417	0.60837632	1.01108672

WT1	AZD3759	2	curve	117.15008	3.16347346	0.63533175	4.87379937
WT1	AZD8055	1	curve	0.01850594	1.1040257	0.15171481	0.01417023
WT1	AZD8055	2	curve	0.01543826	1.03908694	0.13149531	0.01238163
WT1	Afuresertib	1	curve	3.93274133	2.74477235	0.26277521	3.93274133
WT1	Afuresertib	2	curve	2.65058684	2.5242526	0.16728505	2.65058684
WT1	Afuresirtib	1	curve	2.99046236	2.56338662	0.01196011	2.99046236
WT1	Afuresirtib	2	curve	4.67665281	2.88253368	0.14910832	4.67665281
WT1	Alisertib	1	curve	0.56645512	1.98298164	0.04492762	0.56645512
WT1	Alisertib	2	curve	1.03485174	2.29180353	0.3181064	0.20255374
WT1	Alpelisib	1	curve	6.0510864	2.62410521	0.42272091	2.70378997
WT1	Alpelisib	2	curve	5.07797426	2.66298128	0.43335636	1.66900018
WT1	Autophinib	1	curve	2.25355888	2.65563441	0.20076908	1.80809207
WT1	Autophinib	2	curve	3.45947696	2.73313956	0.26899231	2.63884069
WT1	Azaserine	1	flat	Inf	3.16800992	0.83243598	0
WT1	Azaserine	2	flat	Inf	3.14884839	0.83285017	0
WT1	BAY.1251152	1	curve	0.02832943	0.87938142	0.03878152	0.02713888
WT1	BAY.1251152	2	curve	0.03447234	0.95089657	0.04825674	0.03282611
WT1	BAY.2402234	1	curve	0.01408598	1.33701925	0.27822171	0.01112635
WT1	BAY.2402234	2	curve	0.01565277	1.33585515	0.27080595	0.01174876
WT1	BAY.293	1	curve	3.24298844	2.65138283	0.00317038	3.24298844
WT1	BAY.293	2	curve	3.34815878	2.66116266	0.00301605	3.34815878
WT1	BAY.299	1	curve	0.49679921	2.16740165	0.16934638	0.32752462
WT1	BAY.299	2	curve	0.42634374	1.99986386	0.13510713	0.29303385
WT1	BAY1125976	1	curve	2.34052595	2.39201557	0.29443201	2.34052595

WT1	BAY1125976	2	curve	2.28023287	2.52979844	0.31952518	1.19535857
WT1	BI.3406	1	curve	25.2745188	2.86239591	0.607601	25.2745188
WT1	BI.3406	2	curve	18.9162007	3.00941426	0.62150199	18.9162007
WT1	BIX.02189	1	curve	Inf	3.18389399	0.54163674	4.61680575
WT1	BIX.02189	2	curve	14.4453694	3.12110072	0.59735572	14.4453694
WT1	BX.795	1	curve	2.30801928	2.59910311	0.00994914	2.30801928
WT1	BX.795	2	curve	2.33367041	2.61743049	0.04111862	2.33367041
WT1	Bafilomycin.A1	1	curve	0.01000892	0.42802196	0.01260524	0.00990583
WT1	Bafilomycin.A1	2	curve	0.00939095	0.40174531	0.01415124	0.00929628
WT1	Benproperine.phosphate	1	curve	12.0744762	2.96948043	0.53499412	12.0744762
WT1	Benproperine.phosphate	2	flat	Inf	3.16331832	0.64830404	0
WT1	Brefeldin.A	1	curve	0.60410499	2.08247542	0.00247438	0.60410499
WT1	Brefeldin.A	2	curve	0.73053137	2.19111943	0.00296553	0.73053137
WT1	CAY10566	1	curve	6.09852701	2.41480788	0.40670411	6.09852701
WT1	CAY10566	2	curve	7.93895631	2.48264226	0.44494762	7.93895631
WT1	CCG.1423	1	flat	Inf	3.29897374	0.9387244	0
WT1	CCG.1423	2	flat	Inf	3.26406408	0.91080439	0
WT1	CCT128930	1	curve	7.16643265	3.14559757	0.31010206	7.16643265
WT1	CCT128930	2	curve	5.93810943	2.98736754	0.28256655	5.93810943
WT1	CK.636	1	flat	Inf	3.25664033	0.83683331	0
WT1	CK.636	2	flat	Inf	3.06766492	0.7711882	0
WT1	CK.869	1	curve	3.90023458	2.98840316	0.37990321	2.40137601
WT1	CK.869	2	curve	4.01165072	3.03336564	0.39935414	2.91980541
WT1	CM272	1	curve	0.43157904	1.85855521	0.0073939	0.43157904

WT1	CM272	2	curve	0.43171001	1.84819542	0.01149213	0.43171001
WT1	CVT.11127	1	curve	8.07737039	2.53229278	0.47209015	3.01857586
WT1	CVT.11127	2	curve	Inf	2.658926	0.61092639	0.31175013
WT1	CeMMEC13	1	flat	Inf	3.2467347	0.86571303	0
WT1	CeMMEC13	2	flat	Inf	3.25999305	0.86763682	0
WT1	Cilengitide.trifluoroacetate	1	curve	2.22673102	2.41050786	0.285635	2.22673102
WT1	Cilengitide.trifluoroacetate	2	curve	3.9728925	2.60754196	0.35100142	3.9728925
WT1	Concanamycin	1	curve	8.02E-04	0.29798407	0.01300333	7.98E-04
WT1	Concanamycin	2	curve	8.00E-04	0.29632814	0.01548537	7.97E-04
WT1	Crenolanib	1	curve	1.74520479	2.52730593	0.0142664	1.74520479
WT1	Crenolanib	2	curve	1.73380882	2.58088029	0.02002899	1.73380882
WT1	D.4476	1	flat	Inf	3.3289554	0.729021	0
WT1	D.4476	2	curve	Inf	3.08010862	0.73423337	1.64132074
WT1	DAPT	1	curve	528.508875	3.12525459	0.82140941	167.153482
WT1	DAPT	2	flat	Inf	3.03379223	0.8618107	0
WT1	DDO.5936	1	curve	Inf	2.9897362	0.66234584	1.48016222
WT1	DDO.5936	2	curve	22.3364551	2.95975478	0.6228292	22.3364551
WT1	Dactolisib	1	curve	0.01516122	1.00835671	0.1205084	0.01171633
WT1	Dactolisib	2	curve	0.01090509	0.96012135	0.10742282	0.00928551
WT1	Decoyinine	1	curve	Inf	3.04611803	0.78347965	0.74204009
WT1	Decoyinine	2	flat	Inf	3.01283791	0.78619758	0
WT1	Dorsomorphin..Compound.C	1	curve	3.38440137	3.07009983	0.58477011	1.18319621
WT1	Dorsomorphin..Compound.C	2	curve	1.51629823	2.96672671	0.39340604	1.51629823
WT1	Duvelisib	1	curve	Inf	3.06239747	0.5629842	2.12700446

WT1	Duvelisib	2	curve	21.0827352	2.94891793	0.5960484	21.0827352
WT1	Dynasore	1	curve	20.0381517	3.29272858	0.7195947	15.563947
WT1	Dynasore	2	curve	Inf	3.18973581	0.78848228	2.72093094
WT1	Dyngo.4a	1	curve	7.53188955	3.14496047	0.48463575	3.97827209
WT1	Dyngo.4a	2	curve	10.1108875	3.01934344	0.49775426	10.1108875
WT1	EAD1	1	curve	2.36283508	2.50070435	0.00421272	2.36283508
WT1	EAD1	2	curve	2.72006327	2.67957161	0.00414522	2.72006327
WT1	EHT1864	1	flat	Inf	3.19456577	0.73123351	0
WT1	EHT1864	2	curve	66.7841236	3.04467869	0.72007037	33.713494
WT1	EN6	1	curve	13.4599531	2.90483497	0.5347922	13.4599531
WT1	EN6	2	curve	Inf	3.14866761	0.59441412	3.77791039
WT1	ERK5.IN.1	1	curve	0.8397323	2.09471379	0.00562871	0.8397323
WT1	ERK5.IN.1	2	curve	0.98499757	2.1986766	0.00524624	0.98499757
WT1	Empesertib	1	curve	0.01044827	1.21819381	0.27458281	0.00863185
WT1	Empesertib	2	curve	0.01159322	1.28534451	0.31170068	0.00939467
WT1	Erastin	1	curve	0.39566964	1.84024317	0.0115386	0.39566964
WT1	Erastin	2	curve	0.51546087	2.06612979	0.01600844	0.50625578
WT1	Erlotinib	1	curve	22.4083121	2.86852031	0.60210865	22.4083121
WT1	Erlotinib	2	curve	Inf	2.93571838	0.69660255	1.1724869
WT1	Everolimus	1	curve	0.0528349	1.37829083	0.20622548	0.02585376
WT1	Everolimus	2	flat	Inf	1.66103229	0.24242313	0
WT1	Exo1	1	curve	Inf	3.02037115	0.72376849	0.91564025
WT1	Exo1	2	curve	85.3231118	3.10465532	0.75687225	85.3231118
WT1	FL.411	1	curve	4.02106078	2.9020751	0.11826018	3.82065008

WT1	FL.411	2	curve	4.16610231	2.84419716	0.05654504	4.16610231
WT1	FTI.277.HCl	1	flat	Inf	3.14455677	0.81774268	0
WT1	FTI.277.HCl	2	flat	Inf	3.35926225	0.93368528	0
WT1	Fluorouracil	1	curve	1.89434624	2.56001159	0.22631505	1.40641318
WT1	Fluorouracil	2	curve	2.13846942	2.72616596	0.26804261	1.34481649
WT1	Folinic.acid	1	curve	162.501008	2.9650534	0.71835112	162.501008
WT1	Folinic.acid	2	flat	Inf	3.29123178	0.84935943	0
WT1	GDC.0077	1	curve	0.94064293	2.11339359	0.42079999	0.07170957
WT1	GDC.0077	2	curve	3.87705036	2.32505025	0.48232786	0.13285493
WT1	GGTI.298.TFA.salt	1	curve	5.84782306	2.96204798	0.15700621	5.84782306
WT1	GGTI.298.TFA.salt	2	curve	5.33336855	3.09398723	0.13623942	5.08276606
WT1	GLPG0187	1	curve	0.01018739	0.84392521	0.13424292	0.0093148
WT1	GLPG0187	2	curve	0.01023348	0.87502856	0.15381403	0.00930428
WT1	GSK1059615	1	curve	0.029487	1.53979989	0.03321298	0.0280049
WT1	GSK1059615	2	curve	0.0119251	1.14054397	0.02540283	0.0119251
WT1	GSK1324726A	1	curve	1.89475371	2.53092944	0.15895811	1.89475371
WT1	GSK1324726A	2	curve	3.03402889	2.7399672	0.27420724	2.16169957
WT1	GSK2256098	1	flat	Inf	3.01519363	0.80851899	0
WT1	GSK2256098	2	flat	Inf	3.10546827	0.85027025	0
WT1	GSK2334470	1	curve	4.30686453	2.69118581	0.35218327	3.74757837
WT1	GSK2334470	2	curve	4.41302384	2.58647282	0.34870034	4.41302384
WT1	GSK2636771	1	flat	Inf	3.56620486	0.96601012	0
WT1	GSK2636771	2	flat	Inf	3.57999837	1.02325888	0
WT1	GSK467	1	curve	Inf	3.24560832	0.7453545	3.2696189

WT1	GSK467	2	flat	Inf	3.08671189	0.80767556	0
WT1	GW5074	1	flat	Inf	3.32696878	0.92582854	0
WT1	GW5074	2	flat	Inf	3.26312732	0.98139416	0
WT1	GW788388	1	flat	Inf	2.9117526	0.76387744	0
WT1	GW788388	2	curve	Inf	3.1325075	0.73086438	1.75486232
WT1	Gallein	1	curve	27.3484183	3.02498902	0.65313656	16.13172999
WT1	Gallein	2	curve	Inf	3.10230166	0.69050872	4.87396166
WT1	Gedatolisib	1	curve	0.08883805	1.94594653	0.10950783	0.08669796
WT1	Gedatolisib	2	curve	0.06002838	1.78817403	0.09260681	0.06002838
WT1	Glycyrrhizin	1	curve	Inf	3.24255614	0.85350685	2.25491158
WT1	Glycyrrhizin	2	flat	Inf	3.14797562	0.8771938	0
WT1	Golgicide.A	1	curve	7.79036918	3.01332872	0.38236662	7.79036918
WT1	Golgicide.A	2	curve	7.81908039	3.05104391	0.36328772	7.81908039
WT1	H3B.120	1	curve	17.2558043	3.1168522	0.57956613	5.56147034
WT1	H3B.120	2	curve	24.0783062	2.97233634	0.60077773	24.0783062
WT1	Harmine.hydrochloride	1	curve	3.12360707	2.64453862	0.30570877	1.824582
WT1	Harmine.hydrochloride	2	curve	4.00025063	2.78545457	0.22845121	4.00025063
WT1	Hydroxy.Dynasore	1	curve	12.3636987	2.87944591	0.5259655	12.3636987
WT1	Hydroxy.Dynasore	2	curve	17.673882	3.1285629	0.60082435	6.6987766
WT1	IACS.13909	1	curve	8.78631051	2.97243173	0.46986991	5.90875228
WT1	IACS.13909	2	curve	12.5883336	2.81613861	0.4835089	12.5883336
WT1	IGS.1.76	1	curve	Inf	3.03536793	0.75331657	1.1694048
WT1	IGS.1.76	2	curve	Inf	2.97790646	0.72081203	1.05995325
WT1	ILK.IN.2	1	curve	2.68371906	2.66230218	0.00132096	2.68371906

WT1	ILK.IN.2	2	curve	2.9978291	2.67119106	0.00128285	2.9978291
WT1	IPI.549	1	curve	7.44284961	2.8014793	0.45340512	4.99853064
WT1	IPI.549	2	curve	15.7527614	2.94208958	0.57195961	15.7527614
WT1	ISRIB	1	flat	Inf	3.32010607	0.90968489	0
WT1	ISRIB	2	flat	Inf	3.67873989	1.03675094	0
WT1	ITD.1	1	curve	7.16326257	3.14219404	0.39136136	5.33353041
WT1	ITD.1	2	flat	Inf	2.9022403	0.42961267	0
WT1	JQ1	1	curve	0.11384495	1.47092098	0.07142328	0.09969294
WT1	JQ1	2	curve	0.12765768	1.49514657	0.0767524	0.11319694
WT1	JX06	1	curve	0.06008286	1.08896863	0.00228295	0.05995909
WT1	JX06	2	curve	0.08413801	1.22417125	0.00253385	0.08385097
WT1	KM91104	1	curve	Inf	3.22283133	0.59453025	3.93329493
WT1	KM91104	2	curve	11.6874405	3.26483419	0.59454768	10.21383
WT1	KU.0063794	1	curve	0.54144535	2.15064953	0.17921847	0.37674083
WT1	KU.0063794	2	curve	0.36412021	1.99763587	0.16200203	0.24594763
WT1	Ki16425	1	curve	219.11322	3.20990102	0.85573869	118.900675
WT1	Ki16425	2	flat	Inf	3.30584934	0.86799893	0
WT1	LB.100	1	flat	Inf	3.14064164	0.8222939	0
WT1	LB.100	2	flat	Inf	3.24573793	0.85329411	0
WT1	LDN.193189	1	curve	1.13456516	2.29029607	8.38E-04	1.13456516
WT1	LDN.193189	2	curve	2.21460883	2.57661437	0.00178924	2.21460883
WT1	LOC14	1	curve	4.27306698	2.71778873	0.17134392	4.27306698
WT1	LOC14	2	curve	6.29312857	2.84831873	0.30297748	6.29312857
WT1	LXS.196	1	curve	5.53689448	3.33966852	0.43235999	3.75730569

WT1	LXS.196	2	curve	6.45835279	3.0838173	0.42018635	3.87627323
WT1	LY2109761	1	curve	3.23057108	2.86127231	0.56716815	3.23057108
WT1	LY2109761	2	curve	1.30436497	2.71789194	0.44967736	1.30436497
WT1	LY2857785	1	curve	0.06293835	1.15747956	0.02500916	0.06166084
WT1	LY2857785	2	curve	0.06594439	1.19766972	0.03232058	0.06435863
WT1	LY3295668	1	curve	0.83626722	2.15233933	0.33709384	0.17866661
WT1	LY3295668	2	curve	8.73370001	2.63420528	0.45177457	0.318298
WT1	MAT2A.inhibitor.2	1	flat	Inf	3.18979252	0.90707773	0
WT1	MAT2A.inhibitor.2	2	flat	Inf	3.11388543	0.8394407	0
WT1	MCP110	1	curve	26.9462834	3.170247	0.71115366	26.9462834
WT1	MCP110	2	curve	20.3159061	3.10590696	0.67061415	20.3159061
WT1	MG149	1	flat	Inf	3.13997133	0.83638588	0
WT1	MG149	2	flat	Inf	3.18493445	0.85222022	0
WT1	MGH.CP1	1	curve	9.50949752	3.27999396	0.49808485	4.24538161
WT1	MGH.CP1	2	curve	7.81196449	3.00421352	0.40386881	7.81196449
WT1	MI.503	1	curve	1.0673053	2.26595154	0.00157357	1.05398729
WT1	MI.503	2	curve	1.63506257	2.47083069	0.0024717	1.63506257
WT1	MK.0429	1	curve	0.04359778	1.35452827	0.17593987	0.02674625
WT1	MK.0429	2	curve	0.03955312	1.39796994	0.19616876	0.02174544
WT1	MK.0752	1	flat	Inf	3.21715441	0.80954172	0
WT1	MK.0752	2	flat	Inf	2.90430181	0.76920214	0
WT1	MK.2206.2HCl	1	curve	1.68949144	2.4191417	0.02624703	1.68949144
WT1	MK.2206.2HCl	2	curve	2.68725327	2.40814837	0.26316017	2.68725327
WT1	MK.5108	1	curve	Inf	2.94688396	0.51816759	1.16825073

WT1	MK.5108	2	curve	6.46583823	2.74592098	0.47816723	1.17044062
WT1	MK.8245	1	curve	26.4645605	3.08613206	0.68134491	26.4645605
WT1	MK.8245	2	curve	44.9567098	3.25014493	0.78476066	30.2009783
WT1	MPI.0479605	1	curve	0.01122851	1.18891293	0.18370975	0.00947341
WT1	MPI.0479605	2	curve	0.01070202	1.31414063	0.29345727	0.0085263
WT1	MRT199665	1	curve	0.14627037	1.52781869	0.01357303	0.14005274
WT1	MRT199665	2	curve	0.219299	1.67838902	0.01974631	0.219299
WT1	MTX.211	1	curve	1.77096339	2.4899274	0.05618185	1.77096339
WT1	MTX.211	2	curve	2.0698887	2.52296805	0.11276775	2.0698887
WT1	MYF.01.37	1	curve	8.36129361	2.98560585	0.47401785	3.4265231
WT1	MYF.01.37	2	curve	Inf	3.04929441	0.57584794	2.76124742
WT1	Mdivi.1	1	flat	Inf	3.10381235	0.81547831	0
WT1	Mdivi.1	2	flat	Inf	3.30424062	0.87161125	0
WT1	Mdivi.1.ERK5.IN.1	1	curve	0.49788853	1.96201364	0.0049486	0.49788853
WT1	Mdivi.1.ERK5.IN.1	2	curve	0.80218626	2.19750655	0.00631801	0.80218626
WT1	Mdivi.1.ERK5.IN.1	3	curve	1.14396322	2.38105809	0.00703918	1.14396322
WT1	Mdivi.1.ERK5.IN.1	4	curve	1.07624753	2.24974404	0.00740725	1.07624753
WT1	Metarrestin	1	flat	Inf	3.04012262	0.83224133	0
WT1	Metarrestin	2	flat	Inf	3.37485462	0.87485782	0
WT1	Mizoribine	1	curve	4.47702875	2.91010173	0.16559352	4.13936705
WT1	Mizoribine	2	curve	4.73557074	3.14573074	0.22250646	4.24139033
WT1	Monastrol	1	curve	7.24452044	2.91048459	0.35221356	7.24452044
WT1	Monastrol	2	flat	Inf	3.3013039	0.90496008	0
WT1	NAV.2729	1	curve	33.8611663	3.01941755	0.66125929	33.8611663

WT1	NAV.2729	2	curve	8.67760274	2.8124875	0.48081939	6.3942416
WT1	NSC.23766	1	flat	Inf	3.07157544	0.81149731	0
WT1	NSC.23766	2	curve	Inf	3.18506546	0.79518606	1.11019295
WT1	NSC15364	1	flat	Inf	3.1021305	0.87592336	0
WT1	NSC15364	2	flat	Inf	3.21313875	0.83496217	0
WT1	NVP.2	1	curve	0.00849932	0.3761704	0.03127681	0.00837564
WT1	NVP.2	2	curve	0.00861753	0.38466727	0.03522722	0.0084852
WT1	Nemiralisib	1	flat	Inf	2.31270016	0.0267477	0
WT1	Nemiralisib	2	curve	3.66633666	2.791798	0.10447523	3.66633666
WT1	Nirogacestat	1	curve	120.777035	2.88124853	0.66533794	120.777035
WT1	Nirogacestat	2	flat	Inf	2.95127396	0.73199038	0
WT1	OSI.027	1	curve	2.74754112	2.64906477	0.27880931	1.82436258
WT1	OSI.027	2	curve	4.89004381	2.80755381	0.34233514	4.89004381
WT1	OSMI.1	1	flat	Inf	3.27647606	0.73299324	0
WT1	OSMI.1	2	flat	Inf	3.0020953	0.7341012	0
WT1	OSMI.4	1	curve	8.74511386	2.9280387	0.45654767	8.74511386
WT1	OSMI.4	2	curve	11.4855109	2.93491019	0.52943873	11.4855109
WT1	Omipalisib	1	curve	0.02327042	0.95527044	0.01579097	0.01979289
WT1	Omipalisib	2	curve	0.02411161	0.95713649	0.01893984	0.02063067
WT1	Oncrasin.1	1	flat	Inf	3.2520439	0.90709694	0
WT1	Oncrasin.1	2	flat	Inf	3.42628304	0.92583684	0
WT1	P110	1	flat	Inf	3.24985705	0.8936227	0
WT1	P110	2	flat	Inf	3.39073905	0.90923821	0
WT1	P5091	1	curve	3.4706259	2.73716209	0.02517953	3.4706259

WT1	P5091	2	curve	5.02985585	3.18043124	0.22004418	4.52542241
WT1	PD0166285	1	curve	0.14690124	1.49929821	0.00174008	0.14606235
WT1	PD0166285	2	curve	0.1608992	1.52346783	0.00183452	0.15891937
WT1	PD153035	1	curve	Inf	3.14345445	0.74960433	1.57209708
WT1	PD153035	2	curve	Inf	2.98638796	0.69770727	0.91196718
WT1	PF.04691502	1	curve	0.07497497	1.31102229	0.03254417	0.06692188
WT1	PF.04691502	2	curve	0.07472144	1.28428536	0.02833933	0.06898472
WT1	PF.562271	1	curve	0.98293876	2.31836728	0.02731478	0.98293876
WT1	PF.562271	2	curve	0.9205857	2.21018952	0.03004177	0.9205857
WT1	PF.9366	1	curve	9.15988299	3.03722431	0.47768871	5.7260309
WT1	PF.9366	2	curve	6.76828249	2.84727954	0.37105268	6.76828249
WT1	PFI.3	1	curve	Inf	3.1753486	0.8037277	2.91878535
WT1	PFI.3	2	flat	Inf	3.42197003	0.86291282	0
WT1	PH.064	1	curve	0.19708931	1.73488894	0.05237766	0.14146665
WT1	PH.064	2	curve	2.89245855	2.65075304	0.10515192	2.89245855
WT1	PKC.iota.inhibitor.1	1	flat	Inf	3.21987441	0.84483247	0
WT1	PKC.iota.inhibitor.1	2	curve	43.3962522	3.09338145	0.71574221	43.3962522
WT1	PND.1186	1	curve	0.67055825	2.13384681	0.1830926	0.49200771
WT1	PND.1186	2	curve	0.79819613	2.23498683	0.19424095	0.5876566
WT1	Palbociclib	1	curve	1.1230672	3.0036452	0.37982863	0.69170071
WT1	Palbociclib	2	curve	1.39258573	2.97969194	0.38381217	1.39258573
WT1	Pemetrexed	1	curve	1.55852464	2.65159851	0.23368581	1.07232312
WT1	Pemetrexed	2	curve	1.85075585	2.48159949	0.28499161	1.11559558
WT1	Perifosine	1	curve	9.30191604	3.09809499	0.47083102	7.8060349

WT1	Perifosine	2	curve	Inf	3.34555848	0.64445423	4.84673044
WT1	Pictilisib	1	flat	Inf	2.04041455	0.13076946	0
WT1	Pictilisib	2	flat	Inf	2.34538164	0.15197395	0
WT1	Pinometostat	1	curve	Inf	2.85764483	0.63330984	0.53898904
WT1	Pinometostat	2	curve	Inf	3.22202026	0.71465447	2.39465602
WT1	PluriSIn.1..NSC.14613.	1	curve	4.98679728	2.86620842	0.44093093	2.15424672
WT1	PluriSIn.1..NSC.14613.	2	curve	7.00476769	3.01280859	0.45153869	3.15845305
WT1	Pluripotin.SC1	1	curve	0.08297316	1.2733067	0.01441603	0.08230511
WT1	Pluripotin.SC1	2	curve	0.20781077	1.87576958	0.02329244	0.19720745
WT1	RBC8	1	flat	Inf	2.96106896	0.78125059	0
WT1	RBC8	2	flat	Inf	3.24815454	0.89205854	0
WT1	RMC.4550	1	curve	145.594491	2.94683539	0.7166233	48.2837477
WT1	RMC.4550	2	curve	123.132793	2.69466974	0.62667065	20.0085011
WT1	RO4929097	1	curve	57.2688999	2.96558173	0.67653611	57.2688999
WT1	RO4929097	2	curve	187.622254	3.00970547	0.75140019	65.8131189
WT1	Rabeprazole	1	flat	Inf	3.23324661	0.8346496	0
WT1	Rabeprazole	2	flat	Inf	3.03997766	0.74217289	0
WT1	Raltitrexed	1	curve	0.03013948	1.39784525	0.25374252	0.02007816
WT1	Raltitrexed	2	curve	0.03591617	1.50318558	0.25864619	0.02500474
WT1	Rapamycin	1	curve	0.01434323	1.66162028	0.33733772	0.00930302
WT1	Rapamycin	2	curve	Inf	1.98973101	0.41091904	0.00867425
WT1	Raphin1	1	curve	7.79926687	2.89420286	0.42682482	7.79926687
WT1	Raphin1	2	curve	Inf	3.15586204	0.61305039	3.38288805
WT1	Ravoxertinib	1	curve	3.93347704	2.69895303	0.35408062	2.57701524

WT1	Ravoxertinib	2	curve	5.55309492	2.82822235	0.44273283	1.9502218
WT1	RepSox	1	curve	Inf	2.49200016	0.58751735	0.1064531
WT1	RepSox	2	curve	Inf	2.52472937	0.60683052	0.04056106
WT1	Rhosin.hydrochloride	1	flat	Inf	2.96767318	0.67421249	0
WT1	Rhosin.hydrochloride	2	flat	Inf	3.09192335	0.72006725	0
WT1	SAR405	1	curve	0.34758441	1.97185221	0.09658319	0.26781028
WT1	SAR405	2	curve	0.48573056	2.08876332	0.12156005	0.36212462
WT1	SB273005	1	curve	0.05738253	1.4145733	0.17005787	0.03563671
WT1	SB273005	2	curve	0.05717682	1.46720468	0.17364374	0.03525326
WT1	SB525334	1	curve	9.30883058	2.75500308	0.41931923	9.30883058
WT1	SB525334	2	curve	7.93313494	2.57484376	0.37999243	7.93313494
WT1	SB590885	1	curve	2.24942201	2.54006485	0.00984639	2.24942201
WT1	SB590885	2	curve	1.24427487	2.20387879	0.01182802	1.24427487
WT1	SCH772984	1	curve	0.17266115	1.59279037	0.03273069	0.16819623
WT1	SCH772984	2	curve	0.1917204	1.62642105	0.02925018	0.1917204
WT1	SEC.inhibitor.KL.1	1	curve	Inf	3.15082862	0.62574282	3.96773912
WT1	SEC.inhibitor.KL.1	2	flat	Inf	3.22739707	0.68744204	0
WT1	SGC2085	1	curve	Inf	3.16862331	0.64438493	3.75839354
WT1	SGC2085	2	curve	Inf	3.29242608	0.80251307	3.20296351
WT1	SHP099	1	curve	Inf	3.17597287	0.54261752	2.93850625
WT1	SHP099	2	curve	Inf	3.19758328	0.6505047	2.68254701
WT1	SNDX.5613	1	curve	4.56876917	2.92954354	0.02718271	4.56876917
WT1	SNDX.5613	2	flat	Inf	2.87071159	0.72571387	0
WT1	SR.18292	1	curve	Inf	3.18383695	0.67497958	4.73051911

WT1	SR.18292	2	curve	29.0278703	3.1148424	0.69602294	18.9510284
WT1	Sapanisertib	1	curve	0.0132476	1.10414753	0.15405395	0.01111793
WT1	Sapanisertib	2	curve	0.02009484	1.1418187	0.13047677	0.01450373
WT1	SecinH3	1	flat	Inf	3.11570486	0.86043205	0
WT1	SecinH3	2	flat	Inf	3.21835621	0.80334657	0
WT1	Sephin.1	1	flat	Inf	3.21917603	0.88589193	0
WT1	Sephin.1	2	flat	Inf	3.24922488	0.91133562	0
WT1	Serabelisib	1	flat	Inf	2.87318866	0.44250722	0
WT1	Serabelisib	2	curve	Inf	3.14878921	0.51702043	3.48996593
WT1	Sorafenib	1	curve	8.76644072	3.1080308	0.42019775	8.76644072
WT1	Sorafenib	2	curve	6.97286688	3.16054613	0.36721086	5.60497547
WT1	T.5224	1	flat	Inf	2.85363174	0.65186658	0
WT1	T.5224	2	flat	Inf	3.23252281	0.70581155	0
WT1	TA.01	1	curve	55.7738334	3.03718737	0.72381287	55.7738334
WT1	TA.01	2	flat	Inf	3.09055059	0.71262508	0
WT1	TA.02	1	flat	Inf	3.52646286	0.95167694	0
WT1	TA.02	2	flat	Inf	3.26033364	0.97264535	0
WT1	TAK.632	1	curve	3.06469447	2.51427465	0.25494824	3.06469447
WT1	TAK.632	2	curve	3.81726944	2.5451503	0.29645734	3.81726944
WT1	TAS.102	1	curve	0.01350927	1.04048527	0.21516019	0.01201623
WT1	TAS.102	2	curve	0.01395406	1.0458864	0.21532709	0.01227068
WT1	TP0427736.HCl	1	curve	Inf	2.55736805	0.612204	0.13630257
WT1	TP0427736.HCl	2	curve	53.2583811	2.71902168	0.60074602	53.2583811
WT1	TTP.22	1	curve	Inf	3.28434958	0.70048927	5.07853487

WT1	TTP.22	2	flat	Inf	3.37994274	1.00340367	0
WT1	Torin.2	1	curve	0.01165909	0.68546215	0.00829107	0.01112317
WT1	Torin.2	2	curve	0.01180165	0.69773321	0.01324729	0.0112355
WT1	Torkinib	1	curve	0.18674433	1.75140099	0.12873418	0.15349917
WT1	Torkinib	2	curve	0.2321123	1.77794353	0.11940144	0.1855732
WT1	Trilaciclib	1	curve	Inf	2.77005211	0.64229114	0.34498423
WT1	Trilaciclib	2	curve	96.0917288	2.78722912	0.66287867	24.6300587
WT1	UNC0642	1	curve	1.79157196	2.44589692	0.00548865	1.79157196
WT1	UNC0642	2	curve	1.70240089	2.40809808	0.00590823	1.70240089
WT1	V.9302	1	curve	7.14038155	3.10138672	0.25924673	7.14038155
WT1	V.9302	2	curve	8.89210373	3.10252704	0.43337703	8.89210373
WT1	VBIT.12	1	flat	Inf	3.21094819	0.82772366	0
WT1	VBIT.12	2	flat	Inf	3.13007924	0.86463764	0
WT1	VBIT.4	1	flat	Inf	3.0399654	0.66785573	0
WT1	VBIT.4	2	flat	Inf	3.20924203	0.83715788	0
WT1	VTP50469	1	flat	Inf	3.30631034	0.83162416	0
WT1	VTP50469	2	flat	Inf	3.32530879	0.81379603	0
WT1	VX.11e	1	curve	0.59855788	2.09746763	0.02542131	0.59855788
WT1	VX.11e	2	curve	0.41448607	1.94449219	0.00954778	0.41448607
WT1	Verteporfin	1	curve	11.8131122	3.06920855	0.54123426	11.0856363
WT1	Verteporfin	2	flat	Inf	3.28679804	0.56045949	0
WT1	Vilazodone	1	curve	6.82594253	3.03749555	0.29092057	6.82594253
WT1	Vilazodone	2	curve	7.6416467	2.88654733	0.39372385	7.6416467
WT1	WAY.600	1	flat	Inf	3.06226226	0.11525716	0

WT1	WAY.600	2	curve	0.94688712	2.16542952	0.07881278	0.94688712
WT1	WYE.354	1	curve	0.70357333	2.20814436	0.15030826	0.56066509
WT1	WYE.354	2	curve	1.19436434	2.31836809	0.20316559	0.97600301
WT1	XMD8.92	1	curve	4.84585907	2.78805199	0.09886878	4.84585907
WT1	XMD8.92	2	curve	3.59141941	2.74952974	0.09902706	3.59141941
WT1	Y15	1	curve	0.54137513	1.99503162	0.00148055	0.53983923
WT1	Y15	2	curve	0.52100901	2.08189731	0.00183136	0.51433
WT1	YAP.TEAD.inh1	1	flat	Inf	2.57694221	0.64929856	0
WT1	YAP.TEAD.inh1	2	curve	8.36031576	2.80078187	0.49726482	2.50266212
WT1	YF.2	1	flat	Inf	3.07962002	0.61611173	0
WT1	YF.2	2	curve	12.8039951	3.3457702	0.68818942	11.4424056
WT1	YM155	1	curve	1.86234348	2.42809227	0.07867551	1.86234348
WT1	YM155	2	curve	2.10218047	2.53702006	0.10514668	2.10218047
WT1	ZM.336372	1	flat	Inf	3.37423627	0.88505674	0
WT1	ZM.336372	2	flat	Inf	3.23222406	0.88456846	0
WT1	Zorifertinib	1	curve	9.11410067	2.95006799	0.47922503	5.42810394
WT1	Zorifertinib	2	curve	13.514452	3.01357975	0.55607546	12.4327297
WT1	superTDU	1	flat	Inf	3.24022924	0.82673657	0
WT1	superTDU	2	flat	Inf	3.46484297	0.8618191	0
WT5	6.Diazo.5.oxo.L.norleucine	1	curve	7.07582821	2.84243304	0.38109684	7.07582821
WT5	6.Diazo.5.oxo.L.norleucine	2	curve	4.74560006	3.12708376	0.36726053	3.66268127
WT5	A.366	1	curve	Inf	2.93540267	0.75949542	0.25304647
WT5	A.366	2	flat	Inf	3.24270346	0.79560053	0
WT5	A.674563	1	curve	0.72854529	2.20901998	0.00234839	0.72854529

WT5	A.674563	2	curve	0.63671243	2.134526	0.00198651	0.63671243
WT5	A1874	1	flat	Inf	3.29066358	0.8137617	0
WT5	A1874	2	curve	Inf	3.22661925	0.75311265	2.01684839
WT5	A939572	1	curve	Inf	2.77986286	0.68573949	0.06187281
WT5	A939572	2	curve	Inf	2.4745034	0.49674188	0.03984815
WT5	ACBI1	1	curve	Inf	2.53067691	0.4988952	0.16111116
WT5	ACBI1	2	curve	42.6255463	2.55694421	0.52246303	0.31180152
WT5	AG.270	1	curve	2.45370847	2.54019665	0.19413185	2.45370847
WT5	AG.270	2	curve	2.45586965	2.70006175	0.27654142	1.67217812
WT5	AICAR	1	curve	1.40683789	2.45934184	0.19293454	1.00112575
WT5	AICAR	2	curve	0.47433588	2.00292136	0.10625281	0.40438564
WT5	ASLAN003	1	curve	11.6705731	3.11930286	0.55228352	9.31129244
WT5	ASLAN003	2	curve	11.5243255	2.93639946	0.47603064	11.5243255
WT5	AZ191	1	curve	2.31089619	2.52082775	0.03129919	2.31089619
WT5	AZ191	2	curve	1.83758406	2.45700833	0.01395374	1.83758406
WT5	AZD0364	1	curve	0.19335629	1.60368969	0.00418485	0.19335629
WT5	AZD0364	2	curve	0.2684208	1.76377861	0.0055865	0.26812744
WT5	AZD3759	1	curve	19.4119256	2.85675677	0.57996455	19.4119256
WT5	AZD3759	2	curve	Inf	2.97851912	0.66936242	1.50189931
WT5	AZD8055	1	curve	0.01842322	0.80821616	0.05469242	0.01683999
WT5	AZD8055	2	curve	0.0222468	0.89186384	0.06535485	0.01952494
WT5	Afuresertib	1	curve	10.26012	2.87893955	0.51188156	3.06389528
WT5	Afuresertib	2	curve	5.61125747	2.66048204	0.37240629	5.61125747
WT5	Afuresirtib	1	curve	4.5824898	2.8313222	0.09140196	4.5824898

WT5	Afuresirtib	2	curve	6.16804836	2.88305525	0.36522697	6.16804836
WT5	Alisertib	1	curve	0.54437852	2.28196118	0.27421671	0.23488705
WT5	Alisertib	2	curve	0.3562929	2.20629221	0.30145925	0.15343222
WT5	Alpelisib	1	curve	1.39554352	2.49044472	0.3576816	0.42671227
WT5	Alpelisib	2	curve	1.75509198	2.41079753	0.27446714	1.09429075
WT5	Autophinib	1	curve	4.78837455	3.12985932	0.26155896	4.16075453
WT5	Autophinib	2	curve	5.35901947	3.23525125	0.35185329	4.25169796
WT5	Azaserine	1	flat	Inf	3.48486478	0.86278445	0
WT5	Azaserine	2	flat	Inf	3.211068	0.86286584	0
WT5	BAY.1251152	1	curve	0.08376093	1.22485774	0.00449984	0.08376093
WT5	BAY.1251152	2	curve	0.05547068	1.07280026	0.00412607	0.05547068
WT5	BAY.2402234	1	curve	0.01163057	0.98153557	0.15840356	0.01039958
WT5	BAY.2402234	2	curve	0.01232174	1.01747597	0.16294154	0.01096676
WT5	BAY.293	1	curve	3.15145162	2.89920282	0.00325713	3.15145162
WT5	BAY.293	2	curve	3.53646831	2.83661074	0.003176	3.53646831
WT5	BAY.299	1	curve	0.67576896	2.1080792	0.06592954	0.67576896
WT5	BAY.299	2	curve	0.4575307	1.97333023	0.05335405	0.43601617
WT5	BAY1125976	1	curve	1.09565647	2.1217387	0.25648424	1.09565647
WT5	BAY1125976	2	curve	0.95959979	2.09540537	0.28177198	0.59803937
WT5	BI.3406	1	curve	19.0916058	3.17294363	0.73076471	19.0916058
WT5	BI.3406	2	curve	71.7273299	3.13220418	0.73513554	71.7273299
WT5	BIX.02189	1	curve	31.2810088	2.99771246	0.63376335	31.2810088
WT5	BIX.02189	2	curve	12.6694469	3.34226328	0.60395653	10.3139033
WT5	BX.795	1	curve	2.37405486	2.64739557	0.12563486	2.37405486

WT5	BX.795	2	curve	2.73757667	2.76899243	0.09623639	2.73757667
WT5	Bafilomycin.A1	1	curve	0.00860644	0.33420982	0.01140981	0.00857084
WT5	Bafilomycin.A1	2	curve	0.00809863	0.31348077	0.00787568	0.00807023
WT5	Benproperine.phosphate	1	curve	8.85569324	2.93448287	0.44521523	8.85569324
WT5	Benproperine.phosphate	2	curve	9.69107873	2.95543476	0.47920687	9.69107873
WT5	Brefeldin.A	1	curve	1.49120576	2.58340226	0.00309258	1.4906838
WT5	Brefeldin.A	2	curve	1.24848791	2.31448582	0.00256307	1.24848791
WT5	CAY10566	1	curve	Inf	2.24553608	0.45366948	0.04492833
WT5	CAY10566	2	curve	8.18035173	2.53383825	0.45411705	8.18035173
WT5	CCG.1423	1	curve	27.3846052	3.24418005	0.84595177	21.6802861
WT5	CCG.1423	2	curve	Inf	3.10943175	0.83406875	0.77250146
WT5	CCT128930	1	curve	3.97036635	2.78039333	0.26593778	3.97036635
WT5	CCT128930	2	curve	4.20187203	2.83088867	0.24465655	4.20187203
WT5	CK.636	1	flat	Inf	3.30723092	0.87393603	0
WT5	CK.636	2	flat	Inf	3.09686107	0.82040712	0
WT5	CK.869	1	curve	4.91032079	3.10416967	0.20421328	4.46223991
WT5	CK.869	2	curve	4.42654125	2.89198689	0.25106408	3.68637184
WT5	CM272	1	curve	0.36194853	1.78426541	0.00149385	0.36194853
WT5	CM272	2	curve	0.212113	1.5857286	0.00138632	0.212113
WT5	CVT.11127	1	curve	4.48676257	2.65653177	0.34811899	4.48676257
WT5	CVT.11127	2	curve	7.44896771	2.80375439	0.44916282	7.44896771
WT5	CeMMEC13	1	flat	Inf	3.30631637	0.93352028	0
WT5	CeMMEC13	2	curve	96.439062	3.21922062	0.84212305	59.941369
WT5	Cilengitide.trifluoroacetate	1	curve	0.49079769	1.99248659	0.12845568	0.43633895

WT5	Cilengitide.trifluoroacetate	2	curve	0.57794154	2.16354378	0.13263485	0.4519395
WT5	Concanamycin	1	curve	7.98E-04	0.27058916	0.00823725	7.98E-04
WT5	Concanamycin	2	curve	7.99E-04	0.27104873	0.00763641	7.99E-04
WT5	Crenolanib	1	curve	1.37455285	2.46339895	0.00251514	1.37455285
WT5	Crenolanib	2	curve	1.24266849	2.51509158	0.00232817	1.14158106
WT5	D.4476	1	flat	Inf	2.82745203	0.59080134	0
WT5	D.4476	2	curve	37.7080762	3.01264007	0.66557168	37.7080762
WT5	DAPT	1	flat	Inf	3.08962359	0.7830704	0
WT5	DAPT	2	flat	Inf	3.29698044	0.80063298	0
WT5	DDO.5936	1	flat	Inf	3.34185122	0.83296972	0
WT5	DDO.5936	2	flat	Inf	3.12186994	0.8616758	0
WT5	Dactolisib	1	curve	0.01069869	0.66949035	0.03716397	0.01008842
WT5	Dactolisib	2	curve	0.00981227	0.63920697	0.04089185	0.00935811
WT5	Decoyinine	1	flat	Inf	3.56178469	0.9822896	0
WT5	Decoyinine	2	flat	Inf	2.83061048	0.78529839	0
WT5	Dorsomorphin..Compound.C	1	flat	Inf	3.26507412	0.76319345	0
WT5	Dorsomorphin..Compound.C	2	curve	2.93039617	3.08358302	0.61968517	2.93039617
WT5	Duvelisib	1	curve	11.9962622	2.98277529	0.51737188	11.9962622
WT5	Duvelisib	2	curve	8.19748639	2.80098243	0.4277672	8.19748639
WT5	Dynasore	1	curve	Inf	3.2268511	0.61479132	3.49620517
WT5	Dynasore	2	flat	Inf	3.16176079	0.79369007	0
WT5	Dyngo.4a	1	curve	71.4107437	2.89196309	0.67894479	71.4107437
WT5	Dyngo.4a	2	curve	8.21702108	3.13139999	0.4498391	5.22849038
WT5	EAD1	1	curve	2.00489699	2.53718762	0.00212884	2.00489699

WT5	EAD1	2	curve	1.98508632	2.56522014	0.00274361	1.98508632
WT5	EHT1864	1	curve	6.10945438	3.01842047	0.38299997	4.20186483
WT5	EHT1864	2	curve	7.01816888	3.00178744	0.38942068	7.01816888
WT5	EN6	1	flat	Inf	3.11568378	0.69613302	0
WT5	EN6	2	flat	Inf	3.11755246	0.84139493	0
WT5	ERK5.IN.1	1	curve	1.78369673	2.47555646	0.041877	1.78369673
WT5	ERK5.IN.1	2	curve	1.5627529	2.35779644	0.04438775	1.5627529
WT5	Empesertib	1	curve	0.00931325	0.78766737	0.13796928	0.00859271
WT5	Empesertib	2	curve	0.0100127	0.95223546	0.18220458	0.00893478
WT5	Erastin	1	curve	0.62907355	2.0436791	0.00362377	0.62907355
WT5	Erastin	2	curve	0.4889973	1.95540162	0.00205582	0.4889973
WT5	Erlotinib	1	curve	Inf	3.15944074	0.74080713	1.96298899
WT5	Erlotinib	2	curve	20.1988494	2.91704594	0.5868034	20.1988494
WT5	Everolimus	1	curve	0.0198236	1.79469296	0.36897593	0.01031169
WT5	Everolimus	2	curve	0.0152011	1.66406666	0.39187292	0.00977459
WT5	Exo1	1	flat	Inf	3.09632137	0.80567389	0
WT5	Exo1	2	flat	Inf	3.61492503	1.02599179	0
WT5	FL.411	1	curve	6.38458657	3.33767557	0.30124979	5.48202152
WT5	FL.411	2	curve	8.33562387	3.26271598	0.34245021	7.81935575
WT5	FTI.277.HCl	1	flat	Inf	3.40950873	0.84410385	0
WT5	FTI.277.HCl	2	flat	Inf	3.64555772	1.01377616	0
WT5	Fluorouracil	1	curve	3.52354406	2.76028197	0.27722665	2.57374551
WT5	Fluorouracil	2	curve	3.24921782	2.76677852	0.2814234	2.4634563
WT5	Folinic.acid	1	curve	Inf	2.56529106	0.66295896	0.01032864

WT5	Folinic.acid	2	flat	Inf	3.088791 12	0.844783 53	0
WT5	GDC.0077	1	curv e	0.130489 34	1.890745 46	0.199100 57	0.062008 92
WT5	GDC.0077	2	curv e	0.262066 12	1.940923 24	0.259793 25	0.104953 49
WT5	GGTI.298.TFA.salt	1	curv e	4.703648 05	3.020479 04	0.102006 07	4.703648 05
WT5	GGTI.298.TFA.salt	2	curv e	4.963647 53	2.944076 74	0.100514 84	4.963647 53
WT5	GLPG0187	1	curv e	0.009158	0.550044 21	0.073274 26	0.008811 79
WT5	GLPG0187	2	curv e	0.009044 39	0.510648 9	0.062526 61	0.008754 08
WT5	GSK1059615	1	curv e	0.426328 2	2.513253 75	0.006119 75	0.426328 2
WT5	GSK1059615	2	curv e	0.163349 55	2.216713 11	0.005232 69	0.163349 55
WT5	GSK1324726A	1	curv e	4.845903 4	2.867697 73	0.312282 61	4.845903 4
WT5	GSK1324726A	2	curv e	3.541048 73	2.632265 63	0.229618 67	3.541048 73
WT5	GSK2256098	1	flat	Inf	3.357084 77	0.929859 27	0
WT5	GSK2256098	2	flat	Inf	3.117512 93	0.852128 86	0
WT5	GSK2334470	1	curv e	3.394646 32	2.507333	0.384084 82	0.801956 07
WT5	GSK2334470	2	curv e	3.148305 29	2.621388 86	0.334894 23	1.457391 93
WT5	GSK2636771	1	flat	Inf	3.541311 91	1.030746 18	0
WT5	GSK2636771	2	flat	Inf	3.562806 81	1.090173 87	0
WT5	GSK467	1	curv e	Inf	2.831643 3	0.856034 66	0.007609 62
WT5	GSK467	2	flat	Inf	3.155364 13	0.874402 64	0
WT5	GW5074	1	flat	Inf	3.161846 21	0.833470 73	0
WT5	GW5074	2	flat	Inf	3.209790 64	0.839249 5	0
WT5	GW788388	1	curv e	Inf	2.893571 72	0.677166 46	0.309309 31
WT5	GW788388	2	curv e	8.482508 58	2.514552 76	0.450326 32	8.482508 58
WT5	Gallein	1	flat	Inf	3.429058 33	0.672761 46	0

WT5	Gallein	2	flat	Inf	3.4371342	0.74477079	0
WT5	Gedatolisib	1	curve	0.02949118	1.54880192	0.05475656	0.02740655
WT5	Gedatolisib	2	curve	0.02055711	1.41054307	0.0449778	0.01896967
WT5	Glycyrrhizin	1	flat	Inf	3.3756399	1.00185351	0
WT5	Glycyrrhizin	2	flat	Inf	3.34669707	0.90636728	0
WT5	Golgicide.A	1	curve	10.052731	3.09748564	0.50301804	10.052731
WT5	Golgicide.A	2	curve	Inf	3.06391724	0.5880732	3.62415347
WT5	H3B.120	1	flat	Inf	3.03607071	0.79556237	0
WT5	H3B.120	2	curve	79.902543	3.17699813	0.77746962	43.7060708
WT5	Harmine.hydrochloride	1	curve	Inf	3.10742686	0.68102193	2.97285498
WT5	Harmine.hydrochloride	2	curve	Inf	2.99817466	0.71200362	1.1831426
WT5	Hydroxy.Dynasore	1	curve	34.1716034	3.07794956	0.6845545	34.1716034
WT5	Hydroxy.Dynasore	2	curve	314.210608	3.124033	0.80910377	314.210608
WT5	IACS.13909	1	curve	8.4897558	3.09006355	0.39722636	8.4897558
WT5	IACS.13909	2	curve	9.66447157	3.251254	0.47776942	9.66447157
WT5	IGS.1.76	1	curve	Inf	3.15143823	0.73435962	2.86107337
WT5	IGS.1.76	2	flat	Inf	3.22474079	0.84859379	0
WT5	ILK.IN.2	1	curve	1.19344903	2.3345478	0.00103749	1.19344903
WT5	ILK.IN.2	2	curve	1.7348312	2.42101726	0.00112866	1.7348312
WT5	IPI.549	1	curve	4.46666421	2.75750686	0.24983008	4.46666421
WT5	IPI.549	2	curve	5.18402721	2.69510569	0.37231832	5.18402721
WT5	ISRIB	1	flat	Inf	3.28898188	0.93908334	0
WT5	ISRIB	2	curve	Inf	3.22744904	0.87406987	1.15020009
WT5	ITD.1	1	flat	Inf	2.76211781	0.39447966	0

WT5	ITD.1	2	curve	7.62205333	3.12343565	0.20246623	7.62205333
WT5	JQ1	1	curve	0.30866349	1.94699883	0.09380538	0.24045446
WT5	JQ1	2	curve	0.22914534	1.79770726	0.07662467	0.17950461
WT5	JX06	1	curve	0.11994413	1.31397986	0.00260225	0.11984755
WT5	JX06	2	curve	0.13051895	1.46848614	0.00275663	0.13021477
WT5	KM91104	1	curve	11.5982099	3.29370811	0.61054002	10.4347678
WT5	KM91104	2	curve	9.96044263	2.98151179	0.4956551	9.96044263
WT5	KU.0063794	1	curve	0.56245666	1.99442814	0.07217997	0.56245666
WT5	KU.0063794	2	curve	0.63739229	2.08589093	0.08045134	0.63739229
WT5	Ki16425	1	flat	Inf	3.25595442	0.92313363	0
WT5	Ki16425	2	curve	115.995861	2.9389298	0.68911176	115.995861
WT5	LB.100	1	flat	Inf	3.19574293	0.92439716	0
WT5	LB.100	2	flat	Inf	3.32556986	0.91448225	0
WT5	LDN.193189	1	curve	0.75901277	2.11063206	8.67E-04	0.75901277
WT5	LDN.193189	2	curve	1.03483246	2.2734063	0.18605826	0.86005587
WT5	LOC14	1	curve	3.42793437	2.71155347	0.10367952	3.42793437
WT5	LOC14	2	curve	2.68168023	2.53674318	0.07527051	2.68168023
WT5	LXS.196	1	curve	5.68747031	3.24376622	0.41237588	3.69119988
WT5	LXS.196	2	curve	6.46611833	3.07352694	0.39422289	4.27026191
WT5	LY2109761	1	flat	Inf	3.22574698	0.72018182	0
WT5	LY2109761	2	flat	Inf	2.94005542	0.67790782	0
WT5	LY2857785	1	curve	0.13203863	1.38371692	0.00270362	0.13203863
WT5	LY2857785	2	curve	0.109671	1.33310519	0.00281425	0.109671
WT5	LY3295668	1	curve	0.26957214	2.14084822	0.27308071	0.18517221

WT5	LY3295668	2	curve	2.46560156	2.700454	0.44069235	0.35128462
WT5	MAT2A.inhibitor.2	1	flat	Inf	3.51311032	1.02932257	0
WT5	MAT2A.inhibitor.2	2	flat	Inf	3.47856979	1.09245132	0
WT5	MCP110	1	curve	8.88083128	3.1620401	0.4316335	8.88083128
WT5	MCP110	2	curve	7.18377156	2.98078727	0.37247485	7.18377156
WT5	MG149	1	flat	Inf	3.34973261	0.90312388	0
WT5	MG149	2	flat	Inf	3.26110184	0.92891783	0
WT5	MGH.CP1	1	curve	9.33827087	3.4598089	0.41035646	9.33827087
WT5	MGH.CP1	2	curve	6.47464041	2.87926964	0.31789375	6.47464041
WT5	MI.503	1	curve	1.038783	2.4427394	0.00150344	1.038783
WT5	MI.503	2	curve	0.86398232	2.25150104	0.00157844	0.86398232
WT5	MK.0429	1	curve	0.03554228	1.16517631	0.08016612	0.02859154
WT5	MK.0429	2	curve	0.02996838	1.08362653	0.07828043	0.02418425
WT5	MK.0752	1	flat	Inf	3.16451198	0.86572452	0
WT5	MK.0752	2	flat	Inf	3.04815601	0.85936003	0
WT5	MK.2206.2HCl	1	curve	1.49900182	2.32581053	0.18907722	1.49900182
WT5	MK.2206.2HCl	2	curve	1.02462553	2.27214968	0.001943	1.02462553
WT5	MK.5108	1	curve	2.17511457	2.67883876	0.39673389	0.94243792
WT5	MK.5108	2	curve	2.77542071	2.98114836	0.43496786	1.1707393
WT5	MK.8245	1	curve	1.81530775	2.61518938	0.4231781	0.42059871
WT5	MK.8245	2	curve	2.62492662	2.4371323	0.4465157	0.19855931
WT5	MPI.0479605	1	curve	0.01137557	0.99293086	0.17931001	0.01011902
WT5	MPI.0479605	2	curve	0.01035274	0.96606114	0.18354997	0.00922063
WT5	MRT199665	1	curve	0.11470709	1.46581099	0.00270864	0.1083442

WT5	MRT199665	2	curve	0.11013031	1.41532664	0.00240829	0.10658341
WT5	MTX.211	1	curve	2.40387906	2.66791552	0.1098799	2.40387906
WT5	MTX.211	2	curve	2.20656155	2.62879762	0.08955242	2.20656155
WT5	MYF.01.37	1	curve	Inf	2.9325833	0.58428873	1.52633102
WT5	MYF.01.37	2	curve	Inf	3.05591922	0.69350297	1.91980057
WT5	Mdivi.1	1	flat	Inf	3.24048534	0.86813297	0
WT5	Mdivi.1	2	flat	Inf	3.10817449	0.83734742	0
WT5	Mdivi.1.ERK5.IN.1	1	curve	1.86704526	2.47581931	0.08178849	1.86704526
WT5	Mdivi.1.ERK5.IN.1	2	curve	1.59727295	2.46973628	0.07458179	1.59727295
WT5	Mdivi.1.ERK5.IN.1	3	curve	2.92464359	2.72150153	0.13498013	2.92464359
WT5	Mdivi.1.ERK5.IN.1	4	curve	3.33116429	2.82054853	0.12194005	3.33116429
WT5	Metarrestin	1	curve	8.77653768	2.98941727	0.44964937	8.77653768
WT5	Metarrestin	2	curve	5.7577722	2.8542847	0.4236778	2.45685995
WT5	Mizoribine	1	curve	5.16406232	3.15340841	0.11826794	4.95866808
WT5	Mizoribine	2	curve	4.61399225	2.80479673	0.1224419	4.61399225
WT5	Monastrol	1	flat	Inf	3.50156548	1.05636051	0
WT5	Monastrol	2	flat	Inf	3.47035428	1.03193226	0
WT5	NAV.2729	1	curve	1.0467662	2.40558011	0.34414779	0.49709816
WT5	NAV.2729	2	curve	Inf	3.14920911	0.53188181	3.44237783
WT5	NSC.23766	1	flat	Inf	3.40967939	0.94822889	0
WT5	NSC.23766	2	flat	Inf	3.37852133	0.89548167	0
WT5	NSC15364	1	flat	Inf	3.56091895	1.07224064	0
WT5	NSC15364	2	flat	Inf	3.17820058	1.0202434	0
WT5	NVP.2	1	curve	0.00874801	0.29490477	0.00674578	0.00872735

WT5	NVP.2	2	curve	0.01022555	0.34089027	0.0066039	0.01019422
WT5	Nemiralisib	1	curve	4.50381862	2.88919792	0.04429606	4.50381862
WT5	Nemiralisib	2	curve	3.87899231	2.66403866	0.02687325	3.87899231
WT5	Nirogacestat	1	flat	Inf	2.76762932	0.55307634	0
WT5	Nirogacestat	2	flat	Inf	2.59657608	0.45739428	0
WT5	OSI.027	1	curve	3.2506626	2.73169935	0.2069458	3.2506626
WT5	OSI.027	2	curve	3.08507393	2.79485654	0.16968428	3.08507393
WT5	OSMI.1	1	flat	Inf	3.04377126	0.76203205	0
WT5	OSMI.1	2	curve	39.069705	3.18858508	0.76497179	25.379136
WT5	OSMI.4	1	curve	7.75715892	2.85630808	0.43091945	7.75715892
WT5	OSMI.4	2	curve	11.1995418	3.28674021	0.57004959	11.1995418
WT5	Omipalisib	1	curve	0.01187476	0.52667948	0.00302025	0.0116256
WT5	Omipalisib	2	curve	0.01491397	0.65918363	0.00879364	0.01424212
WT5	Oncrasin.1	1	curve	43.076112	3.20918514	0.7883633	43.076112
WT5	Oncrasin.1	2	flat	Inf	3.29539679	0.78700191	0
WT5	P110	1	flat	Inf	3.61939894	1.07832353	0
WT5	P110	2	flat	Inf	3.31412445	0.88475575	0
WT5	P5091	1	curve	6.39297574	3.1741974	0.08297013	6.39297574
WT5	P5091	2	curve	5.07444759	2.94470022	0.00685304	5.07444759
WT5	PD0166285	1	curve	0.05137684	1.05891434	0.0016528	0.05137684
WT5	PD0166285	2	curve	0.03445279	0.90327532	0.00148447	0.0341195
WT5	PD153035	1	flat	Inf	3.16252928	0.68943596	0
WT5	PD153035	2	curve	Inf	3.01445923	0.61942996	2.08749605
WT5	PF.04691502	1	curve	0.05211211	1.12440496	0.00811227	0.0498677

WT5	PF.04691502	2	curve	0.04517278	1.08693583	0.00901568	0.04282837
WT5	PF.562271	1	curve	0.96170751	2.33200246	0.0037656	0.89587214
WT5	PF.562271	2	curve	0.68056138	2.26861263	0.00216802	0.5900236
WT5	PF.9366	1	curve	8.30029888	3.01509736	0.40404885	8.30029888
WT5	PF.9366	2	flat	Inf	2.94358598	0.44192184	0
WT5	PFI.3	1	flat	Inf	3.29083501	0.90684373	0
WT5	PFI.3	2	curve	43.4234471	3.20677273	0.79083205	43.4234471
WT5	PH.064	1	flat	Inf	2.45846482	0.01646227	0
WT5	PH.064	2	curve	4.98282423	2.80128782	0.07287141	4.98282423
WT5	PKC.iota.inhibitor.1	1	flat	Inf	2.98671265	0.70172977	0
WT5	PKC.iota.inhibitor.1	2	flat	Inf	3.39500367	0.79041885	0
WT5	PND.1186	1	curve	2.34201156	2.61704096	0.17279638	2.33168593
WT5	PND.1186	2	curve	1.02625127	2.47091304	0.18666014	0.89089209
WT5	Palbociclib	1	flat	Inf	3.16021505	0.45975016	0
WT5	Palbociclib	2	curve	1.66878708	3.09189509	0.38522884	1.66878708
WT5	Pemetrexed	1	curve	0.55473293	2.18030279	0.08574861	0.49819668
WT5	Pemetrexed	2	curve	0.49781338	2.18511688	0.08646508	0.44761749
WT5	Perifosine	1	curve	4.27857889	3.08216977	0.24163153	3.76591334
WT5	Perifosine	2	curve	6.69496912	3.33060087	0.41797352	4.8256663
WT5	Pictilisib	1	curve	0.09066627	1.36361866	0.06621902	0.08090274
WT5	Pictilisib	2	curve	0.19435304	1.67959647	0.07938976	0.17041143
WT5	Pinometostat	1	curve	Inf	3.17376533	0.76203752	2.36751421
WT5	Pinometostat	2	flat	Inf	2.82353443	0.65436847	0
WT5	PluriSIn.1	1	curve	23.6676342	3.09241291	0.6361629	23.6676342

WT5	PluriSIn.1	2	flat	Inf	3.4895929	0.73631549	0
WT5	Pluripotin.SC1	1	curve	0.05663276	1.10184579	0.00520781	0.05663276
WT5	Pluripotin.SC1	2	curve	0.06419896	1.15035236	0.00570047	0.06383202
WT5	RBC8	1	flat	Inf	3.27540612	0.89973986	0
WT5	RBC8	2	flat	Inf	3.27101577	0.92506695	0
WT5	RMC.4550	1	flat	Inf	3.15307126	0.76642092	0
WT5	RMC.4550	2	flat	Inf	3.32297448	0.80260015	0
WT5	RO4929097	1	flat	Inf	3.12820875	0.87357272	0
WT5	RO4929097	2	curve	Inf	2.72012767	0.71776953	0.01271365
WT5	Rabeprazole	1	flat	Inf	3.16568755	0.92127388	0
WT5	Rabeprazole	2	flat	Inf	3.49496622	0.80894428	0
WT5	Raltitrexed	1	curve	0.01531498	0.72634115	0.06157706	0.01453245
WT5	Raltitrexed	2	curve	0.01767363	0.77487817	0.0664358	0.01666947
WT5	Rapamycin	1	curve	0.01415952	1.64519763	0.3102421	0.00941228
WT5	Rapamycin	2	flat	Inf	1.6861058	0.20257601	0
WT5	Raphin1	1	flat	Inf	3.00121422	0.76901907	0
WT5	Raphin1	2	curve	11.1679311	3.04853858	0.5182901	11.1679311
WT5	Ravoxertinib	1	curve	12.1622417	2.9652251	0.49604322	1.80637471
WT5	Ravoxertinib	2	curve	Inf	2.9315412	0.69532645	0.95489876
WT5	RepSox	1	curve	Inf	1.91581173	0.49845574	0.01124573
WT5	RepSox	2	curve	Inf	1.99138989	0.47417943	0.01751634
WT5	Rhosin.hydrochloride	1	flat	Inf	3.44672128	1.04365051	0
WT5	Rhosin.hydrochloride	2	flat	Inf	3.46074685	1.01781698	0
WT5	SAR405	1	curve	1.12587356	2.34192919	0.07209226	1.12587356

WT5	SAR405	2	curve	1.05267742	2.33834605	0.09069003	0.96850753
WT5	SB273005	1	curve	0.02381054	0.95427361	0.07999704	0.02123031
WT5	SB273005	2	curve	0.02996798	1.0613048	0.07527627	0.02709928
WT5	SB525334	1	curve	2.75231715	2.39448012	0.29850371	2.75231715
WT5	SB525334	2	curve	2.56939583	2.47473381	0.23797114	2.56939583
WT5	SB590885	1	curve	4.88751163	2.85538857	0.07940833	4.88751163
WT5	SB590885	2	curve	3.08991357	2.69384497	0.0062029	3.08991357
WT5	SCH772984	1	curve	0.19156903	1.70297586	0.0414596	0.16739854
WT5	SCH772984	2	curve	0.28255716	1.88714272	0.06161945	0.22401852
WT5	SEC.inhibitor.KL.1	1	flat	Inf	3.19548852	0.78858002	0
WT5	SEC.inhibitor.KL.1	2	flat	Inf	3.41492218	0.73200769	0
WT5	SGC2085	1	curve	Inf	3.12604379	0.73738528	3.23054744
WT5	SGC2085	2	curve	Inf	3.21549267	0.80010199	2.2062158
WT5	SHP099	1	curve	Inf	2.91066199	0.60388207	1.58532705
WT5	SHP099	2	curve	Inf	2.9727591	0.66608873	1.33327409
WT5	SNDX.5613	1	flat	Inf	2.96665729	0.64022473	0
WT5	SNDX.5613	2	curve	Inf	3.1311996	0.89273583	0.06861148
WT5	SR.18292	1	flat	Inf	3.38887537	0.69849469	0
WT5	SR.18292	2	curve	20.7951589	3.17086894	0.64593243	20.7951589
WT5	Sapanisertib	1	curve	0.01839514	0.85642657	0.05947352	0.01636573
WT5	Sapanisertib	2	curve	0.01616453	0.79283143	0.05626028	0.01455894
WT5	SecinH3	1	flat	Inf	3.44810901	0.98136455	0
WT5	SecinH3	2	curve	Inf	3.24080671	0.76852468	3.64485067
WT5	Sephin.1	1	flat	Inf	3.35337221	0.89623131	0

WT5	Sephin.1	2	flat	Inf	3.20685559	0.86023739	0
WT5	Serabelisib	1	curve	5.08768479	2.6729048	0.31064065	5.08768479
WT5	Serabelisib	2	curve	7.43631119	3.04376928	0.38963593	7.43631119
WT5	Sorafenib	1	curve	4.03174631	3.0629265	0.22843211	3.58029922
WT5	Sorafenib	2	curve	4.81155043	2.96162077	0.22403904	4.81155043
WT5	T.5224	1	flat	Inf	3.32609148	0.93977416	0
WT5	T.5224	2	flat	Inf	3.33957606	0.95459422	0
WT5	TA.01	1	curve	28.8247936	3.08567794	0.67064863	28.8247936
WT5	TA.01	2	curve	17.359861	3.18878566	0.71331841	17.359861
WT5	TA.02	1	flat	Inf	3.02372765	0.79208107	0
WT5	TA.02	2	curve	18.3979085	3.21989012	0.63142325	8.9856388
WT5	TAK.632	1	curve	7.76761226	2.83283514	0.40339147	7.76761226
WT5	TAK.632	2	curve	5.64397844	3.18855707	0.39215134	4.21333439
WT5	TAS.102	1	curve	0.0088408	0.41698789	0.04733736	0.00867108
WT5	TAS.102	2	curve	0.00929029	0.42859789	0.0507787	0.00910547
WT5	TP0427736.HCl	1	curve	Inf	2.18030593	0.47380886	0.03693591
WT5	TP0427736.HCl	2	curve	Inf	2.29299168	0.50949089	0.04215177
WT5	TTP.22	1	flat	Inf	3.13934793	0.85790798	0
WT5	TTP.22	2	flat	Inf	3.47729179	0.95805551	0
WT5	Torin.2	1	curve	0.01119332	0.50193051	0.01073575	0.01096159
WT5	Torin.2	2	curve	0.01207178	0.56503784	0.01231836	0.01174068
WT5	Torkinib	1	curve	0.37570279	1.91900662	0.06148165	0.3502239
WT5	Torkinib	2	curve	0.3582089	1.99856883	0.07729132	0.3225394
WT5	Trilaciclib	1	curve	59.5572181	3.05978242	0.73174765	59.5572181

WT5	Trilaciclib	2	flat	Inf	3.213089 03	0.865255 15	0
WT5	UNC0642	1	curve	1.890038 83	2.491097 63	0.002676 11	1.890038 83
WT5	UNC0642	2	curve	1.520106 83	2.377141 78	0.002777 61	1.520106 83
WT5	V.9302	1	curve	6.477722 24	2.876444 52	0.301244 33	6.477722 24
WT5	V.9302	2	curve	4.721538 53	3.016186 53	0.255184 9	4.000686 81
WT5	VBIT.12	1	flat	Inf	3.402675 21	1.006581 51	0
WT5	VBIT.12	2	flat	Inf	3.398875 03	1.015352 21	0
WT5	VBIT.4	1	curve	8.364286 54	3.154350 64	0.425495 59	8.364286 54
WT5	VBIT.4	2	curve	7.700096 95	2.984886 18	0.365531 36	7.700096 95
WT5	VTP50469	1	curve	Inf	3.221431 41	0.616688 88	3.947077 6
WT5	VTP50469	2	curve	112.4835 58	3.107390 72	0.765080 19	53.51316 45
WT5	VX.11e	1	curve	2.266781 46	2.736342 63	0.281530 51	1.527665 83
WT5	VX.11e	2	curve	1.704669 19	2.539987 87	0.209033 33	1.260679 79
WT5	Verteporfin	1	flat	Inf	3.418218 32	0.632731 17	0
WT5	Verteporfin	2	curve	9.027005 72	2.916108 78	0.465090 67	9.027005 72
WT5	Vilazodone	1	curve	6.885895 39	3.080147 82	0.320714 97	6.885895 39
WT5	Vilazodone	2	curve	5.478407 85	2.939927 3	0.256369 01	5.478407 85
WT5	WAY.600	1	curve	1.000688 29	2.252494 74	0.023567 45	1.000688 29
WT5	WAY.600	2	curve	0.853560 08	2.168540 92	0.021009 7	0.853560 08
WT5	WYE.354	1	curve	0.450051 66	1.914494 54	0.048336 05	0.450051 66
WT5	WYE.354	2	curve	0.574203 5	2.118490 63	0.051264 9	0.539986 56
WT5	XMD8.92	1	curve	6.948345 53	2.850022 77	0.352750 98	6.948345 53
WT5	XMD8.92	2	curve	8.017290 15	2.871055 75	0.410559 3	8.017290 15
WT5	Y15	1	curve	0.822298 83	2.252947 97	0.001825 9	0.818509 17

WT5	Y15	2	curve	0.88100106	2.22251102	0.00155936	0.88100106
WT5	YAP.TEAD.inh1	1	curve	2.94633431	2.41805231	0.2824234	2.94633431
WT5	YAP.TEAD.inh1	2	curve	8.15276899	2.68483774	0.3515122	8.15276899
WT5	YF.2	1	flat	Inf	2.95107632	0.66148345	0
WT5	YF.2	2	curve	16.843195	3.03589451	0.61031488	16.843195
WT5	YM155	1	curve	0.94934572	2.41720501	0.01222461	0.9145048
WT5	YM155	2	curve	0.70145362	2.30495265	0.00257003	0.68272038
WT5	ZM.336372	1	flat	Inf	3.22134392	0.868083	0
WT5	ZM.336372	2	flat	Inf	3.35403517	0.90167822	0
WT5	Zorifertinib	1	curve	8.59137826	2.77365652	0.40366954	8.59137826
WT5	Zorifertinib	2	curve	12.1321619	2.60911297	0.45619612	12.1321619
WT5	superTDU	1	flat	Inf	3.01920358	0.78175064	0
WT5	superTDU	2	flat	Inf	3.23528565	0.87384876	0

Appendix Table 7: Phospho arrays fold changes in 4-OHT treated CV7250 cells transduced with *Pten* sgRNA 1 relative to a non-targeting sgRNA

ID	Phospho Protein	ID	Non Phospho Protein	Signal Ratio of Phospho Protein to Non-Phospho Protein		Fold Changes in Ratios
				LacZ sgRNA/ 4-OHT	PTEN sgRNA/ 4-OHT	PTEN sgRNA/4-OHT vs LacZ sgRNA/4-OHT
979	14-3-3 beta/zeta (Phospho-Ser184/186)	1119	14-3-3 beta/zeta (Ab-184/186)		0.56	
891	14-3-3 theta/tau (Phospho-Ser232)	285	14-3-3 theta/tau (Ab-232)	1.53	1.97	1.29

838	14-3-3 zeta (Phospho-Ser58)	702	14-3-3 zeta (Ab-58)			
892	14-3-3 zeta/delta (Phospho-Thr232)	286	14-3-3 zeta/delta (Ab-232)	0.12	0.16	1.36
1221	4E-BP1 (Phospho-Ser65)	758	4E-BP1 (Ab-65)	0.18	0.23	1.27
176	4E-BP1 (Phospho-Thr36)	61	4E-BP1 (Ab-36)		1.52	
177	4E-BP1 (Phospho-Thr45)	62	4E-BP1 (Ab-45)	6.23	6.94	1.11
1222	4E-BP1 (Phospho-Thr70)	759	4E-BP1 (Ab-70)	0.58	0.87	1.50
893	6-phosphofructo-2-kinase/fructose-2,6-biphosphatase 2 (PFKFB2) (Phospho-Ser483)	287	6-phosphofructo-2-kinase/fructose-2,6-biphosphatase 2 (PFKFB2) (Ab-483)		0.89	
1224	Abl1 (Phospho-Tyr204)	760	Abl1 (Ab-204)		0.15	
407	Abl1 (Phospho-Thr754/735)	1132	Abl1 (Ab-754/735)		0.54	
1223	Abl1 (Phospho-Tyr412)					
1225	ACC1 (Phospho-Ser79)	761	ACC1 (Ab-79)		0.89	
1056	ACC1 (Phospho-Ser80)	594	ACC1 (Ab-80)	0.35	0.35	0.99
116	ACK1 (Phospho-Tyr284)					

894	Actin Pan (a/b/g) (Phospho-Tyr55/53)	288	Actin Pan (a/b/g) (Ab-55/53)	0.54	0.61	1.14
125	ADD1 (Phospho-Ser726)	703	ADD1 (Ab-726)	1.96	1.62	0.83
998	AFX/FOXO4 (Phospho-Ser197)	1038	AFX/FOXO 4 (Ab-197)			
1227	AKT1 (Phospho-Ser124)	763	AKT1 (Ab-124)	0.63	0.69	1.09
556	AKT1 (Phospho-Ser246)	1286	AKT1 (Ab-246)	0.73	0.59	0.81
473	AKT1 (Phospho-Thr308)	206	AKT1 (Ab-308)	0.67	0.71	1.06
1067	AKT1 (Phospho-Tyr326)	442	AKT1 (Ab-326)	0.91		
1226	AKT1 (Phospho-Thr450)	762	AKT1 (Ab-450)		0.58	
320	AKT1 (Phospho-Ser473)	205	AKT1 (Ab-473)	0.82	1.20	1.47
555	AKT1 (Phospho-Tyr474)	1285	AKT1 (Ab-474)	1.58	1.10	0.70
557	AKT1 (Phospho-Thr72)	1288	AKT1 (Ab-72)			
		1133	AKT1/2/3 (Ab-315)			
87	AKT1S1 (Phospho-Thr246)	931	AKT1S1 (Ab-246)	0.30	0.27	0.89
989	AKT2 (Phospho-Ser474)	1033	AKT2 (Ab-474)	0.88	0.75	0.86
117	ALK (Phospho-Tyr1507)	1141	ALK (Ab-1507)	1.42	1.23	0.87

118	ALK (Phospho-Tyr1604)	1142	ALK (Ab-1604)		0.95	
1228	AMPK beta1 (Phospho-Ser182)	764	AMPK beta1 (Ab-182)	0.94	0.72	0.76
839	AMPK1 (Phospho-Thr172)	704	AMPK1 (Ab-172)		0.72	
1174	AMPK1/AMPK2 (Phospho-Ser485/491)	422	AMPK1/AMPK2 (Ab-485/491)	1.09	0.86	0.79
840	Amyloid beta A4 (Phospho-Thr743/668)	705	Amyloid beta A4 (Ab-743/668)	0.67		
833	Androgen Receptor (Phospho-Ser213)	692	Androgen Receptor (Ab-213)		0.90	
986	Androgen Receptor (Phospho-Ser650)	693	Androgen Receptor (Ab-650)			
895	A-RAF (Phospho-Tyr301/302)	289	A-RAF (Ab-301/302)	1.53	1.05	0.69
88	Arrestin-1 (Phospho-Ser412)	932	Arrestin-1 (Ab-412)	1.24	1.00	0.80
35	ASK1 (Phospho-Ser83)	863	ASK1 (Ab-83)		3.28	
18	ASK1 (Phospho-Ser966)	866	ASK1 (Ab-966)		0.67	
748	ATF1 (Phospho-Ser63)	469	ATF1 (Ab-63)		0.51	
166	ATF2 (Phospho-Ser112/94)	51	ATF2 (Ab-112/94)	0.94	0.67	0.71
162	ATF2 (Phospho-Ser62/44)	47	ATF2 (Ab-62/44)			

163	ATF2 (Phospho-Thr69/51)	48	ATF2 (Ab-69/51)	0.99		
164	ATF2 (Phospho-Thr71/53)	49	ATF2 (Ab-71/53)	1.29	1.42	1.10
165	ATF2 (Phospho-Thr73/55)	50	ATF2 (Ab-73/55)	1.14	1.14	1.00
319	ATF4 (Phospho-Ser245)	204	ATF4 (Ab-245)	1.39	1.36	0.98
		1028	ATM (Ab-1981)			
1086	ATP1A1/Na+K+ ATPase1 (Phospho-Ser23)	801	ATP1A1/Na+K+ ATPase1 (Ab-23)	1.51	1.21	0.80
751	ATPase (Phospho-Ser16)	471	ATPase (Ab-16)	0.92		
919	ATP-Citrate Lyase (Phospho-Ser454)	634	ATP-Citrate Lyase (Ab-454)	0.96	0.75	0.78
896	ATRIP (Phospho-Ser68/72)	290	ATRIP (Ab-68/72)	0.12	0.26	2.13
1255	AurA (Phospho-Thr288)	967	AurA (Ab-288)		0.62	
625	AurA (Phospho-Ser342)	969	AurA (Ab-342)	1.16	1.16	1.00
1254	AurB (Phospho-Tyr12)	970	AurB (Ab-12)		1.19	
1253	AurB (Phospho-Thr232)	968	AurB (Ab-232)		0.94	
		971	AurB/C (Ab-202/175)			
277	AXL (Phospho-Tyr691)					
485	BAD (Phospho-Ser112)	346	BAD (Ab-112)			

1069	BAD (Phospho-Ser134)	444	BAD (Ab-134)	1.07	1.14	1.06
486	BAD (Phospho-Ser136)	347	BAD (Ab-136)	1.07		
487	BAD (Phospho-Ser155)	348	BAD (Ab-155)			
1068	BAD (Phospho-Ser91/128)	443	BAD (Ab-91/128)	0.99		
212	BAX (Phospho-Thr167)	291	BAX (Ab-167)	0.76	0.67	0.89
482	BCL-2 (Phospho-Thr56)	343	BCL-2 (Ab-56)		1.37	
897	BCL-2 (Phospho-Thr69)	292	BCL-2 (Ab-69)			
483	BCL-2 (Phospho-Ser70)	344	BCL-2 (Ab-70)		1.36	
89	BCL-2 (Phospho-Ser87)					
		1306	BCL-6 (Ab-333)			
898	BCL-XL (Phospho-Thr47)	293	BCL-XL (Ab-47)	0.14	0.19	1.38
484	BCL-XL (Phospho-Ser62)	293	BCL-XL (Ab-47)	0.35	0.31	0.88
24	BCR (Phospho-Tyr177)	1206	BCR (Ab-177)			
123	BCR (Phospho-Tyr360)	1147	BCR (Ab-360)	1.43	1.47	1.03
90	BID (Phospho-Ser78)	933	BID (Ab-78)	0.82	0.65	0.79
676	BIM (Phospho-Ser69/65)	540	BIM (Ab-69/65)		0.65	
282	BLNK (Phospho-Tyr84)	1143	BLNK (Ab-96)	0.64	0.45	0.69
119	BLNK (Phospho-Tyr96)	1143	BLNK (Ab-96)	0.69	0.57	0.82

408	B-RAF (Phospho-Ser446)	1134	B-RAF (Ab-446)	1.00	0.94	0.94
899	B-RAF (Phospho-Thr598)	294	B-RAF (Ab-598)	0.10	0.12	1.18
900	B-RAF (Phospho-Ser601)	295	B-RAF (Ab-601)	1.30	1.30	1.01
327	BRCA1 (Phospho-Ser1423)					
583	BRCA1 (Phospho-Ser1457)	1307	BRCA1 (Ab-1457)	0.60	0.42	0.71
831	BRCA1 (Phospho-Ser1524)	869	BRCA1 (Ab-1524)			
124	Breast tumor kinase (Phospho-Tyr447)					
1020	BTK (Phospho-Tyr223)	881	BTK (Ab-223)	6.38	5.03	0.79
1263	BTK (Phospho-Tyr551)	881	BTK (Ab-223)		1.05	
558	c-Abl (Phospho-Tyr245)	1034	c-Abl (Ab-412)	0.50	0.58	1.14
990	c-Abl (Phospho-Tyr412)	1034	c-Abl (Ab-412)	0.43	0.40	0.93
1070	Calmodulin (Phospho-Thr79/Ser81)	445	Calmodulin (Ab-79/81)	0.85		
111	Calsenilin/KCNIP3 (Phospho-Ser63)	795	Calsenilin/KCNIP3 (Ab-63)	0.39	0.33	0.85
1071	CaMK1-alpha (Phospho-Thr177)	446	CaMK1-alpha (Ab-177)		1.33	
675	CaMK2A (Phospho-Thr286)	539	CaMK2A (Ab-286)			

1051	CaMK2 alpha/beta/delta (Phospho-Thr305)					
409	CaMK2-beta/gamma/delta (Phospho-Thr287)	1135	CaMK2-beta/gamma/delta (Ab-287)	0.37	0.33	0.89
1072	CaMK4 (Phospho-Thr196/200)	447	CaMK4 (Ab-196/200)	0.98	0.68	0.69
245	Caspase 1 (Phospho-Ser376)	948	Caspase 1 (Ab-376)	0.91	0.84	0.92
246	Caspase 2 (Phospho-Ser157)	949	Caspase 2 (Ab-157)	1.05		
1076	Caspase 3 (Phospho-Ser150)	451	Caspase 3 (Ab-150)			
1057	Caspase 6 (Phospho-Ser257)	595	Caspase 6 (Ab-Ser257)			
1058	Caspase 8 (Phospho-Ser347)	428	Caspase 8 (Ab-347)	0.57	0.95	1.68
1074	Caspase 9 (Phospho-Ser144)	449	Caspase 9 (Ab-144)	1.40	1.22	0.87
1075	Caspase 9 (Phospho-Ser196)	450	Caspase 9 (Ab-196)	0.48	0.49	1.03
1059	Caspase 9 (Phospho-Thr125)	596	Caspase 9 (Ab-125)	1.04		
1073	Caspase 9 (Phospho-Tyr153)	448	Caspase 9 (Ab-153)	0.31	0.25	0.80
1077	Catalase (Phospho-Tyr385)	452	Catalase (Ab-385)	0.32	0.52	1.62
172	Catenin beta (Phospho-Ser33)	425	Catenin beta (Ab-33)	1.31	1.29	0.99

173	Catenin beta (Phospho-Ser37)	58	Catenin beta (Ab-37)			
830	Catenin beta (Phospho-Thr41/Ser45)	691	Catenin beta (Ab-41/45)	0.99		
398	Catenin beta (Phospho-Tyr489)	1120	Catenin beta (Ab-489)			
1078	Catenin beta (Phospho-Tyr654)	453	Catenin beta (Ab-654)	0.78	0.66	0.85
1245	Catenin delta-1 (Phospho-Tyr228)	617	Catenin delta-1 (Ab-228)	1.58	1.47	0.93
658	Caveolin-1 (Phospho-Tyr14)	700	Caveolin-1 (Ab-14)			
753	CBL (Phospho-Tyr700)					
752	CBL (Phospho-Tyr774)					
749	CD19 (Phospho-Tyr531)	470	CD19 (Ab-531)			
1094	CD22/BL-CAM (Phospho-Tyr807)					
1079	CD227/mucin 1 (Phospho-Tyr1243)	606	CD227/mucin 1 (Ab-1243)			
1080	CD28 (Phospho-Tyr218)					
		1289	CD32 (Fcgamma RIIb) (Ab-292)			
91	CD3Z (Phospho-Tyr142)	934	CD3Z (Ab-142)	1.85	1.63	0.88
1233	CD4 (Phospho-Ser433)	607	CD4 (Ab-433)	0.21	0.36	1.73

1234	CD45 (Phospho-Ser1007)					
126	CD5 (Phospho-Tyr453)	1149	CD5 (Ab-453)	0.46	0.41	0.88
1235	CDC25A (Phospho-Ser124)	608	CDC25A (Ab-124)			
		1121	CDC25A (Ab-178)			
999	CDC25A (Phospho-Ser75)	1039	CDC25A (Ab-75)			
1060	CDC25B (Phospho-Ser323)	429	CDC25B (Ab-323)	1.25	1.23	0.98
1236	CDC25B (Phospho-Ser353)	609	CDC25B (Ab-353)			
832	CDC25C (Phospho-Ser216)	1026	CDC25C (Ab-216)	0.09	0.10	1.09
559	CDC25C (Phospho-Thr48)	1026	CDC25C (Ab-216)	0.07	0.14	1.86
92	CDK1/CDC2 (Phospho-Thr14)	935	CDK1/CDC2 (Ab-14)			
329	CDK1/CDC2 (Phospho-Tyr15)	214	CDK1/CDC2 (Ab-15)			
996	CDK2 (Phospho-Thr160)	699	CDK2 (Ab-160)	1.09		
275	CDK5 (Phospho-Tyr15)	1314	CDK5 (Ab-15)	0.19	0.25	1.34
1237	CDK7 (Phospho-Thr170)	610	CDK7 (Ab-170)			
1001	Chk1 (Phospho-Ser280)	853	Chk1 (Ab-280)		1.80	

1238	Chk1 (Phospho-Ser286)	611	Chk1 (Ab-286)	0.68	0.67	0.98
560	Chk1 (Phospho-Ser296)					
1239	Chk1 (Phospho-Ser301)					
1002	Chk1 (Phospho-Ser317)	854	Chk1 (Ab-317)	1.70	1.28	0.75
987	Chk1 (Phospho-Ser345)	1027	Chk1 (Ab-345)			
901	Chk2 (Phospho-Thr383)	296	Chk2 (Ab-383)		0.63	
1229	Chk2 (Phospho-Thr387)	765	Chk2 (Ab-387)	1.66	1.22	0.74
1159	Chk2 (Phospho-Ser516)	857	Chk2 (Ab-516)			
479	Chk2 (Phospho-Thr68)	523	Chk2 (Ab-68)			
158	c-Jun (Phospho-Ser243)	43	c-Jun (Ab-243)		0.55	
1	c-Jun (Phospho-Ser63)	1178	c-Jun (Ab-63)		0.76	
3	c-Jun (Phospho-Ser73)					
157	c-Jun (Phospho-Thr239)	42	c-Jun (Ab-239)	1.11	0.84	0.76
154	c-Jun (Phospho-Thr91)	39	c-Jun (Ab-91)			
155	c-Jun (Phospho-Thr93)	40	c-Jun (Ab-93)	1.30	1.58	1.22

156	c-Jun (Phospho-Tyr170)	41	c-Jun (Ab-170)		1.17	
1089	CK1-A (Phospho-Thr321)	802	CK1-A (Ab-321)	1.20	1.24	1.04
1092	CK1-A/A2 (Phospho-Tyr294)					
924	CK2-b (Phospho-Ser209)	640	CK2-b (Ab-209)	0.89	1.09	1.23
418	Claudin 3 (Phospho-Tyr219)	1317	Claudin 3 (Ab-219)		1.40	
419	Claudin 6 (Phospho-Tyr219)					
420	Claudin 7 (Phospho-Tyr210)	1318	Claudin 7 (Ab-210)	1.76	1.55	0.88
1241	Coagulation Factor III (Phospho-Ser290)					
1000	Cofilin (Phospho-Ser3)	1040	Cofilin (Ab-3)			
494	Connexin 43 (Phospho-Ser367)	359	Connexin 43 (Ab-367)	1.06	0.88	0.84
507	Cortactin (Phospho-Tyr421)	372	Cortactin (Ab-421)	1.39	1.73	1.25
508	Cortactin (Phospho-Tyr466)	373	Cortactin (Ab-466)	0.58	0.47	0.81
677	CPI17 alpha (Phospho-Thr38)	541	CPI17 alpha (Ab-38)			
1061	c-PLA2 (Phospho-Ser505)	597	c-PLA2 (Ab-505)	1.54	1.78	1.16

226	CREB (Phospho-Ser121)	936	CREB (Ab-121)		1.52	
509	CREB (Phospho-Ser129)	374	CREB (Ab-129)			
318	CREB (Phospho-Ser133)	203	CREB (Ab-133)		10.42	
841	CREB (Phospho-Ser142)	706	CREB (Ab-142)			
399	CREB (Phospho-Thr100)	1122	CREB (Ab-100)	1.10		
1022	CrkII (Phospho-Tyr221)	883	CrkII (Ab-221)	0.47	0.39	0.84
1023	CrkL (Phospho-Tyr207)					
1242	CXCR4 (Phospho-Ser339)					
1214	Cyclin B1 (Phospho-Ser126)	430	Cyclin B1 (Ab-126)		0.91	
562	Cyclin B1 (Phospho-Ser147)	132	Cyclin B1 (Ab-147)			
584	Cyclin C (Phospho-Ser275)					
1230	Cyclin D1 (Phospho-Thr286)	766	Cyclin D1 (Ab-286)	0.53	0.66	1.25
1230	Cyclin D1 (Phospho-Thr286)	613	Cyclin D1 (Ab-90)	1.45	1.62	1.12
		1308	Cyclin D2 (Ab-280)			
1231	Cyclin D3 (Phospho-Thr283)	767	Cyclin D3 (Ab-283)	0.77	0.99	1.29
1044	Cyclin E1 (Phospho-Thr395)	431	Cyclin E1 (Ab-395)	1.57	1.96	1.25

563	Cyclin E1 (Phospho-Thr77)	133	Cyclin E1 (Ab-77)	0.23	0.13	0.59
147	Cyclin E2 (Phospho-Thr392)	614	Cyclin E2 (Ab-392)	1.53	1.19	0.78
510	DAB1 (Phospho-Tyr220)	375	DAB1 (Ab-220)	0.79	0.61	0.78
495	DAB1 (Phospho-Tyr232)	360	DAB1 (Ab-232)			
128	DAPP1 (Phospho-Tyr139)	1151	DAPP1 (Ab-139)	1.68	1.00	0.59
663	DARPP-32 (Phospho-Thr34)	376	DARPP-32 (Ab-34)	0.52	0.45	0.86
842	DARPP-32 (Phospho-Thr75)	707	DARPP-32 (Ab-75)	1.03	1.43	1.39
1232	DAXX (Phospho-Ser668)					
129	DDX5/DEAD-box protein 5 (Phospho-Tyr593)	1152	DDX5/DEAD-box protein 5 (Ab-593)	1.23	0.96	0.78
1248	DNA-PK (Phospho-Thr2638)	620	DNA-PK (Ab-2638)	1.15	1.28	1.11
1247	DNA-PK (Phospho-Thr2647)	619	DNA-PK (Ab-2647)			
		621	DNA-PK (Ab-2056)			
664	Dok-1 (Phospho-Tyr362)	377	Dok-1 (Ab-362)		0.61	
665	Dok-1 (Phospho-Tyr398)	530	Dok-1 (Ab-398)		0.40	
666	Dok-2 (Phospho-Tyr299)	531	Dok-2 (Ab-299)			

74	DYN1 (Phospho-Ser774)	769	DYN1 (Ab-774)	0.30	0.41	1.37
75	E2F1 (Phospho-Thr433)	770	E2F1 (Ab-433)	0.21	0.19	0.88
1215	EEF2 (Phospho-Thr56)	598	EEF2 (Ab-56)	1.08	1.34	1.24
1176	eEF2K (Phospho-Ser366)	884	eEF2K (Ab-366)	0.49	0.46	0.94
648	EGFR (Phospho-Ser1070)	357	EGFR (Ab-1070)	0.11		
843	EGFR (Phospho-Thr678)	708	EGFR (Ab-678)	1.03	1.29	1.25
889	EGFR (Phospho-Thr693)	709	EGFR (Ab-693)	0.84	0.75	0.88
227	EGFR (Phospho-Tyr1016)	937	EGFR (Ab-1016)	1.39	1.29	0.92
1249	EGFR (Phospho-Tyr1069)	622	EGFR (Ab-1069)	2.59		
649	EGFR (Phospho-Tyr1092)	358	EGFR (Ab-1092)	0.45	0.47	1.05
500	EGFR (Phospho-Tyr1110)	365	EGFR (Ab-1110)	1.47	1.60	1.09
174	EGFR (Phospho-Tyr1172)	59	EGFR (Ab-1172)			
182	EGFR (Phospho-Tyr1197)	67	EGFR (Ab-1197)	1.40		
183	EGFR (Phospho-Tyr869)	68	EGFR (Ab-869)	0.16	0.33	1.98
		1123	EGFR (Ab-998)			

667	eIF2A (Phospho-Ser51)	532	eIF2A (Ab-51)	0.55	0.63	1.15
564	eIF4B (Phospho-Ser422)					
187	eIF4E (Phospho-Ser209)	72	eIF4E (Ab-209)	0.79	0.68	0.86
565	eIF4G (Phospho-Ser1108)	134	eIF4G (Ab-1108)	0.78	0.88	1.13
4	Elk1 (Phospho-Ser383)	1181	Elk1 (Ab-383)	1.51	1.14	0.76
303	Elk1 (Phospho-Ser389)	188	Elk1 (Ab-389)			
304	Elk1 (Phospho-Thr417)	189	Elk1 (Ab-417)	0.86	0.83	0.97
1166	eNOS (Phospho-Ser1177)	1197	eNOS (Ab-1177)		0.94	
256	eNOS (Phospho-Ser615)	960	eNOS (Ab-615)	1.23	1.09	0.88
328	eNOS (Phospho-Thr495)	213	eNOS (Ab-495)		0.97	
		961	eNOS (Ab-1179)			
1097	EPB41 (Phospho-Tyr418/660)	810	EPB41 (Ab-418/660)	0.96	0.81	0.85
925	EPHA2/3/4 (Phospho-Tyr588/596)	641	EPHA2/3/4 (Ab-588/596)	0.81	1.36	1.68
926	EPHB1/2 (Phospho-Tyr594/604)	642	EPHB1/2 (Ab-594/604)			
927	Ephrin B1 (Phospho-Tyr317)	643	Ephrin B1 (Ab-317)	0.87	0.92	1.06
1096	Ephrin B1/B2/B3 (Phospho-Tyr324)					

844	Ephrin B2 (Phospho-Tyr330)	463	Ephrin B2 (Ab-330)	0.55		
928	Epo-R (Phospho-Tyr368)	796	Epo-R (Ab-368)	0.77	0.74	0.96
1250	ERK3 (Phospho-Ser189)	623	ERK3 (Ab-189)	1.58		
1251	ERK8 (Phospho-Thr175/Tyr177)					
488	Estrogen Receptor-alpha (Phospho-Ser104)	349	Estrogen Receptor-alpha (Ab-104)			
489	Estrogen Receptor-alpha (Phospho-Ser106)	350	Estrogen Receptor-alpha (Ab-106)	0.11		
490	Estrogen Receptor-alpha (Phospho-Ser118)	351	Estrogen Receptor-alpha (Ab-118)		1.19	
491	Estrogen Receptor-alpha (Phospho-Ser167)	352	Estrogen Receptor-alpha (Ab-167)	0.37	0.45	1.23
120	ETK (Phospho-Tyr40)	1144	ETK (Ab-40)	1.69	0.99	0.59
120	ETK (Phospho-Tyr40)	1148	ETK (Ab-566)	1.90	0.95	0.50
27	Ezrin (Phospho-Thr566)	1209	Ezrin (Ab-566)	0.28	0.29	1.06
481	Ezrin (Phospho-Tyr353)	682	Ezrin (Ab-353)		1.42	
400	Ezrin (Phospho-Tyr478)	1124	Ezrin (Ab-478)	0.75	1.20	1.60

1260	FADD (Phospho-Ser194)					
93	FAK (Phospho-Ser910)	624	FAK (Ab-910)	0.20	0.24	1.20
888	FAK (Phospho-Tyr397)	55	FAK (Ab-397)		0.66	
228	FAK (Phospho-Tyr407)	938	FAK (Ab-407)		1.55	
76	FAK (Phospho-Tyr576)	771	FAK (Ab-576)	1.11	1.41	1.27
477	FAK (Phospho-Tyr861)	512	FAK (Ab-861)			
988	FAK (Phospho-Tyr925)	1029	FAK (Ab-925)			
593	FAS (Phospho-Tyr291)	777	FAS (Ab-291)	0.64	0.79	1.24
278	FER (Phospho-Tyr402)	1316	FER (Ab-402)	1.81	1.89	1.04
324	FGFR1 (Phospho-Tyr154)	209	FGFR1 (Ab-154)		1.02	
755	FGFR1 (Phospho-Tyr654)					
754	FGFR1 (Phospho-Tyr766)	472	FGFR1 (Ab-766)	0.39	0.59	1.51
1177	Filamin A (Phospho-Ser2152)	885	Filamin A (Ab-2152)			
829	FKHR (Phospho-Ser256)	868	FKHR (Ab-256)	0.99	1.29	1.31
997	FKHR (Phospho-Ser319)	1037	FKHR (Ab-319)			
230	FKHR/FOXO1A (Phospho-Ser329)	940	FKHR/FOXO1A (Ab-329)			
1167	FKHRL1/FOXO3A (Phospho-Ser253)	1198	FKHRL1/FOXO3A (Ab-253)			
1180	FLT3 (Phospho-Tyr599)	983	FLT3 (Ab-599)	0.94	1.34	1.43

279	FLT3 (Phospho-Tyr842)	983	FLT3 (Ab-599)	1.03	1.09	1.06
280	FLT3 (Phospho-Tyr969)	983	FLT3 (Ab-599)	0.88		
77	Fos (Phospho-Ser362)					
578	Fos (Phospho-Thr232)	1304	Fos (Ab-232)	0.60	0.33	0.54
		454	Fos (Ab-374)			
94	FosB (Phospho-Ser27)	778	FosB (Ab-27)	1.94	1.20	0.62
229	FOXO1/3/4-pan (Phospho-Thr24/32)	939	FOXO1/3/4-pan (Ab-24/32)			
231	FOXO1A/3A (Phospho-Ser322/325)					
1095	FRS2 (Phospho-Tyr436)					
750	Fyn (Phospho-Tyr530)					
650	G3BP-1 (Phospho-Ser232)	690	G3BP-1 (Ab-232)			
679	Gab1 (Phospho-Tyr627)	543	Gab1 (Ab-627)	0.79	0.96	1.20
902	Gab1 (Phospho-Tyr659)	297	Gab1 (Ab-659)	0.85	0.70	0.82
580	Gab2 (Phospho-Ser159)	1305	Gab2 (Ab-159)	0.97	0.98	1.01
585	Gab2 (Phospho-Tyr643)	455	Gab2 (Ab-623)	2.70	2.10	0.78
845	GABA-RB (Phospho-Ser434)	710	GABA-RB (Ab-434)		1.64	
669	GAP43 (Phospho-Ser41)	534	GAP43 (Ab-41)		1.04	

307	GATA1 (Phospho-Ser142)	192	GATA1 (Ab-142)		1.12	
308	GATA1 (Phospho-Ser310)	193	GATA1 (Ab-310)			
497	GluR1 (Phospho-Ser849)	362	GluR1 (Ab-849)	0.06	0.09	1.42
498	GluR1 (Phospho-Ser863)	363	GluR1 (Ab-863)		1.42	
680	GluR2 (Phospho-Ser880)	544	GluR2 (Ab-880)	0.18	0.19	1.06
247	GRB10/Growth factor receptor-bound protein 10 (Phospho-Tyr67)	950	GRB10/Growth factor receptor-bound protein 10 (Ab-67)		1.04	
78	GRF-1 (Phospho-Tyr1105)					
95	GRK1 (Phospho-Ser21)	779	GRK1 (Ab-21)			
232	GRK2 (Phospho-Ser29)	941	GRK2 (Ab-29)	0.34	0.60	1.77
582	GRK2 (Phospho-Ser685)	941	GRK2 (Ab-29)	0.27		
7	GSK3 alpha (Phospho-Ser21)	1184	GSK3 alpha (Ab-21)	0.71	0.50	0.70
890	GSK3 alpha/beta (Phospho-Tyr216/279)	427	GSK3 alpha/beta (Ab-216/279)		1.34	
2	GSK3 beta (Phospho-Ser9)	1179	GSK3 beta (Ab-9)			

248	GTPase activating protein (Phospho-Ser387)	951	GTPase activating protein (Ab-387)	1.68	1.44	0.86
130	HCK (Phospho-Tyr410)					
903	HDAC1 (Phospho-Ser421)	298	HDAC1 (Ab-421)	0.16	0.24	1.47
887	HDAC2 (Phospho-Ser394)	1036	HDAC2 (Ab-394)	1.54	1.59	1.03
96	HDAC3 (Phospho-Ser424)	780	HDAC3 (Ab-424)	0.72		
19	HDAC4 (Phospho-Ser632)	870	HDAC4 (Ab-632)	0.99	1.20	1.21
79	HDAC5 (Phospho-Ser259)	772	HDAC5 (Ab-259)			
20	HDAC5 (Phospho-Ser498)	871	HDAC5 (Ab-498)		0.98	
97	HDAC6 (Phospho-Ser22)	781	HDAC6 (Ab-22)	0.51	0.83	1.65
21	HDAC8 (Phospho-Ser39)	1024	HDAC8 (Ab-39)	1.11	0.77	0.69
587	HER2 (Phospho-Thr686)	782	HER2 (Ab-686)	1.29	1.50	1.17
646	HER2 (Phospho-Tyr1221/Tyr1222)	355	HER2 (Ab-1221/1222)		0.36	
647	HER2 (Phospho-Tyr1248)	356	HER2 (Ab-1248)	0.69	0.70	1.02
645	HER2 (Phospho-Tyr877)	354	HER2 (Ab-877)	0.88		

		1125	HER2 (Ab-1112)			
98	HER3/ErbB3 (Phospho-Tyr1222)	783	HER3/ErbB3 (Ab-1222)	1.26	1.31	1.04
99	HER3/ErbB3 (Phospho-Tyr1289)	784	HER3/ErbB3 (Ab-1289)	0.95	0.89	0.94
100	HER4/ErbB4 (Phospho-Tyr1284)	785	HER4/ErbB4 (Ab-1284)	1.71	1.41	0.82
504	Histone H2A.X (Phospho-Ser139)	369	Histone H2A.X (Ab-139)	0.53	0.57	1.07
34	Histone H3.1 (Phospho-Ser10)	867	Histone H3.1 (Ab-10)	0.72		
309	HNF4 alpha (Phospho-Ser313)	194	HNF4 alpha (Ab-313)			
267	HRS (Phospho-Tyr334)	1156	HRS (Ab-334)	1.49	1.33	0.89
499	HSF1 (Phospho-Ser303)	364	HSF1 (Ab-303)			
80	HSL (Phospho-Ser552/563)	773	HSL (Ab-552/563)		0.63	
1216	HSL (Phospho-Ser554)	599	HSL (Ab-554)	0.97	0.93	0.95
22	HSP27 (Phospho-Ser15)	1025	HSP27 (Ab-15)			
332	HSP27 (Phospho-Ser78)	217	HSP27 (Ab-78)			
333	HSP27 (Phospho-Ser82)	218	HSP27 (Ab-82)	0.62	0.68	1.10
249	HSP90 co-chaperone Cdc37 (Phospho-Ser13)	952	HSP90 co-chaperone Cdc37 (Ab-13)	1.14	1.18	1.03

1090	HSP90B (Phospho-Ser226)	803	HSP90B (Ab-226)	1.11	1.86	1.67
846	HSP90B (Phospho-Ser254)	711	HSP90B (Ab-254)			
651	ICAM-1 (Phospho-Tyr512)	694	ICAM-1 (Ab-512)			
281	ICK (Phospho-Tyr159)					
655	IGF1R (Phospho-Tyr1161)	516	IGF1R (Ab-1161)			
656	IGF1R (Phospho-Tyr1165/1166)	517	IGF1R (Ab-1165/1166)		1.31	
259	IGF2R (Phospho-Ser2409)	953	IGF2R (Ab-2409)			
		954	IGFBP-3 (Ab-183)			
1164	IkB-alpha (Phospho-Ser32/36)	862	IkB-alpha (Ab-32/36)	3.88	4.11	1.06
250	IkB-alpha (Phospho-Tyr305)					
1172	IkB-alpha (Phospho-Tyr42)	1203	IkB-alpha (Ab-42)	0.61	0.45	0.74
847	IkB-beta (Phospho-Ser23)	774	IkB-beta (Ab-19)			
81	IkB-beta (Phospho-Thr19)	774	IkB-beta (Ab-19)	0.90	1.69	1.87
848	IkB-epsilon (Phospho-Ser22)	712	IkB-epsilon (Ab-22)			
992	IKK-alpha (Phospho-Thr23)	1035	IKK-alpha (Ab-23)			

82	IKK-alpha/beta (Phospho-Ser180/181)	776	IKK-alpha/beta (Ab-176/177)	0.33	0.18	0.56
82	IKK-alpha/beta (Phospho-Ser180/181)	775	IKK-alpha/beta (Ab-180/181)	0.90	0.68	0.76
83	IKK-beta (Phospho-Tyr188)	929	IKK-beta (Ab-188)	0.59	0.51	0.86
233	IKK-beta (Phospho-Tyr199)	942	IKK-beta (Ab-199)	0.25	0.31	1.24
84	IKK-gamma (Phospho-Ser31)	930	IKK-gamma (Ab-31)	0.16		
257	IKK-gamma (Phospho-Ser85)	962	IKK-gamma (Ab-85)	0.65	0.54	0.83
268	IL-10R-alpha (Phospho-Tyr496)	1309	IL-10R-alpha (Ab-496)	0.59	0.51	0.87
269	IL-13R/CD213a1 (Phospho-Tyr405)	1310	IL-13R/CD213a1 (Ab-405)	2.20	1.87	0.85
1082	IL-2RA/CD25 (Phospho-Ser268)	798	IL-2RA/CD25 (Ab-268)		1.19	
1264	IL3RB (Phospho-Tyr593)	982	IL3RB (Ab-593)	0.65	0.55	0.85
270	IL-4R/CD124 (Phospho-Tyr497)	1311	IL-4R/CD124 (Ab-497)	0.92	1.10	1.20
271	IL7R/CD127 (Phospho-Tyr449)					
1256	Integrin beta-1 (Phospho-Thr788)	972	Integrin beta-1 (Ab-788)	0.75	0.62	0.83
1256	Integrin beta-1 (Phospho-Thr788)	973	Integrin beta-1 (Ab-789)	0.46	0.50	1.09

478	Integrin beta-3 (Phospho-Tyr773)	518	Integrin beta-3 (Ab-773)	0.91	1.43	1.57
670	Integrin beta-3 (Phospho-Tyr785)	535	Integrin beta-3 (Ab-785)	1.21	1.24	1.03
272	Integrin beta-4 (Phospho-Tyr1510)	1312	Integrin beta-4 (Ab-1510)	1.01	1.03	1.02
768	Interferon-alpha/beta receptor alpha chain (Phospho-Tyr466)	797	Interferon-alpha/beta receptor alpha chain (Ab-466)			
1081	Interferon-gamma receptor alpha chain precursor (Phospho-Tyr457)	975	Interferon-gamma receptor alpha chain precursor (Ab-457)	1.18	1.11	0.94
1265	IR (Phospho-Tyr1355)	984	IR (Ab-1361)	0.92	1.45	1.58
1266	IR (Phospho-Tyr1361)	984	IR (Ab-1361)	1.02	1.40	1.37
85	IRS-1 (Phospho-Ser1101)					
322	IRS-1 (Phospho-Ser307)	207	IRS-1 (Ab-307)			
1004	IRS-1 (Phospho-Ser312)	1042	IRS-1 (Ab-312)	0.68	0.40	0.58
234	IRS-1 (Phospho-Ser323)	943	IRS-1 (Ab-323)			
86	IRS-1 (Phospho-Ser612)					
184	IRS-1 (Phospho-Ser636)	69	IRS-1 (Ab-636)	1.16	1.65	1.42

185	IRS-1 (Phospho-Ser639)	70	IRS-1 (Ab-639)	0.19	0.29	1.54
566	IRS-1 (Phospho-Ser794)	135	IRS-1 (Ab-794)		1.34	
1161	JAK1 (Phospho-Tyr1022)	859	JAK1 (Ab-1022)			
1163	JAK2 (Phospho-Tyr1007)	861	JAK2 (Ab-1007)	0.63	0.94	1.49
1162	JAK2 (Phospho-Tyr221)	860	JAK2 (Ab-221)			
235	JNK1/2/3 (Phospho-Thr183/Tyr185)	944	JNK1/2/3 (Ab-183/185)	1.07	1.17	1.09
160	JunB (Phospho-Ser259)	45	JunB (Ab-259)	0.85	0.85	1.01
159	JunB (Phospho-Ser79)	44	JunB (Ab-79)	0.62	0.60	0.97
161	JunD (Phospho-Ser255)	46	JunD (Ab-255)		0.85	
849	Keratin 18 (Phospho-Ser33)	713	Keratin 18 (Ab-33)			
1243	Keratin 18 (Phospho-Ser52)	615	Keratin 18 (Ab-52)		1.03	
1244	Keratin 8 (Phospho-Ser432)	616	Keratin 8 (Ab-432)	1.95	2.55	1.31
850	Keratin 8 (Phospho-Ser73)	714	Keratin 8 (Ab-73)			
1268	KIT (Phospho-Tyr703)					
325	KIT (Phospho-Tyr721)	210	KIT (Ab-721)			
1267	KIT (Phospho-Tyr936)	985	KIT (Ab-936)	1.33	0.86	0.65
1045	KSR (Phospho-Ser392)	432	KSR (Ab-392)	1.14		
273	Kv1.3/KCNA3 (Phospho-Tyr135)	1313	Kv1.3/KCNA3 (Ab-135)	0.51	0.82	1.61

274	Kv2.1/Kcnb1 (Phospho-Tyr128)					
1252	Lamin A (Phospho-Ser22)	814	Lamin A (Ab-22)	1.18	1.49	1.27
756	Lamin A/C (Phospho-Ser392)	626	Lamin A/C (Ab-392)	0.07	0.13	1.89
		1301	LAT (Ab-161)			
567	LAT (Phospho-Tyr171)	136	LAT (Ab-171)			
236	LAT (Phospho-Tyr191)	945	LAT (Ab-191)	0.84	1.46	1.73
577	LCK (Phospho-Ser59)	1303	LCK (Ab-59)	0.98	1.03	1.05
238	LCK (Phospho-Tyr192)	947	LCK (Ab-192)		1.04	
1157	LCK (Phospho-Tyr393)	1195	LCK (Ab-393)	0.08	0.22	2.71
237	LCK (Phospho-Tyr505)	946	LCK (Ab-505)	2.16	2.04	0.94
991	LIMK1 (Phospho-Thr508)	864	LIMK1 (Ab-508)	0.57	0.54	0.95
991	LIMK1 (Phospho-Thr508)	880	LIMK1/2 (Ab-508/505)	0.38	0.38	1.01
720	LKB1 (Phospho-Ser428)	137	LKB1 (Ab-428)	1.03	1.57	1.52
721	LKB1 (Phospho-Thr189)	138	LKB1 (Ab-189)	1.03	1.07	1.04
		1136	LKB1 (Ab-334)			
744	LYN (Phospho-Tyr507)	467	LYN (Ab-507)	0.13	0.20	1.55
410	MAP3K1/MEKK1 (Phospho-Thr1381)					
255	MAP3K7/TAK1 (Phospho-Thr184)	957	MAP3K7/TAK1 (Ab-184)	0.96	1.05	1.09

255	MAP3K7/TAK1 (Phospho-Thr184)	805	MAP3K7/TAK1 (Ab-187)	1.27	1.21	0.95
255	MAP3K7/TAK1 (Phospho-Thr184)	806	MAP3K7/TAK1 (Ab-439)	0.97	0.76	0.78
1021	MAP3K8/COT (Phospho-Thr290)	882	MAP3K8/COT (Ab-290)			
1021	MAP3K8/COT (Phospho-Thr290)	807	MAP3K8/COT (Ab-400)			
586	MAPKAPK2 (Phospho-Ser272)	456	MAPKAPK2 (Ab-272)	1.78	1.11	0.63
722	MAPKAPK2 (Phospho-Thr222)	456	MAPKAPK2 (Ab-272)	0.67	0.69	1.02
1052	MAPKAPK2 (Phospho-Thr334)	456	MAPKAPK2 (Ab-272)	0.87	0.56	0.65
681	MARCKS (Phospho-Ser158)	545	MARCKS (Ab-158)	0.73	0.94	1.29
501	MARCKS (Phospho-Ser163)	366	MARCKS (Ab-163)			
127	M-CSF Receptor (Phospho-Tyr561)	1150	M-CSF Receptor (Ab-561)	1.83	1.13	0.62
1269	M-CSF Receptor (Phospho-Tyr809)	1138	M-CSF Receptor (Ab-809)	1.56	0.85	0.54
239	MDM2 (Phospho-Ser166)	1100	MDM2 (Ab-166)	0.10	0.16	1.63
739	MDM4 (Phospho-Ser367)					
851	MEF2A (Phospho-Ser408)	715	MEF2A (Ab-408)	0.37	0.35	0.94

305	MEF2A (Phospho-Thr312)	190	MEF2A (Ab-312)	0.07	0.08	1.04
306	MEF2A (Phospho-Thr319)	191	MEF2A (Ab-319)	0.49	0.49	1.00
740	MEF2C (Phospho-Ser396)	457	MEF2C (Ab-396)	1.11	1.17	1.06
240	MEF2D (Phospho-Ser444)					
30	MEK1 (Phospho-Ser217)	1212	MEK1 (Ab-217)	0.63		
1171	MEK1 (Phospho-Ser221)	1202	MEK1 (Ab-221)		2.24	
723	MEK1 (Phospho-Ser298)	139	MEK1 (Ab-298)	3.51	2.01	0.57
724	MEK1 (Phospho-Thr286)	140	MEK1 (Ab-286)	0.88	0.75	0.85
834	MEK1 (Phospho-Thr291)	546	MEK1 (Ab-291)	0.65	0.76	1.17
8	MEK2 (Phospho-Thr394)	1185	MEK2 (Ab-394)			
1093	MER/SKY (Phospho-Tyr749/Tyr681)					
1091	Merlin (Phospho-Ser10)	804	Merlin (Ab-10)	1.52	0.52	0.34
502	Merlin (Phospho-Ser518)	367	Merlin (Ab-518)		1.19	
1240	Met (Phospho-Tyr1003)	612	Met (Ab-1003)			
181	Met (Phospho-Tyr1234)	66	Met (Ab-1234)	1.54	1.61	1.04

323	Met (Phospho-Tyr1349)	208	Met (Ab-1349)			
1270	Met (Phospho-Tyr1356)					
757	MITF (Phospho-Ser73)	627	MITF (Ab-73)	0.43	0.47	1.10
1158	MKK3/MAP2K3 (Phospho-Ser189)	856	MKK3/MAP2K3 (Ab-189)			
411	MKK3/MAP2K3 (Phospho-Thr222)	1137	MKK3/MAP2K3 (Ab-222)	0.78		
1085	MKK4/SEK1 (Phospho-Ser257)	800	MKK4/SEK1 (Ab-257)		1.33	
17	MKK4/SEK1 (Phospho-Ser80)	462	MKK4/SEK1 (Ab-80)		0.23	
1175	MKK4/SEK1 (Phospho-Thr261)	865	MKK4/SEK1 (Ab-261)	0.20	0.17	0.86
886	MKK6/MAP2K6 (Phospho-Ser207)	423	MKK6/MAP2K6 (Ab-207)	0.29	0.44	1.50
412	MKK7/MAP2K7 (Phospho-Ser271)	1290	MKK7/MAP2K7 (Ab-271)	1.06	0.41	0.39
413	MKK7/MAP2K7 (Phospho-Thr275)	1290	MKK7/MAP2K7 (Ab-271)	0.81	0.73	0.89
251	MKP-1 (Phospho-Ser359)	955	MKP-1 (Ab-359)	1.14	0.79	0.69
741	MKP-1/2 (Phospho-Ser296/318)	458	MKP-1/2 (Ab-296/318)	0.91	0.79	0.87
1098	Mnk1 (Phospho-Thr385)	811	Mnk1 (Ab-385)	1.12	0.71	0.63
414	MSK1 (Phospho-Ser212)					

725	MSK1 (Phospho-Ser360)	141	MSK1 (Ab-360)	0.18	0.25	1.33
25	MSK1 (Phospho-Ser376)	1207	MSK1 (Ab-376)	0.92	1.12	1.21
726	MSK1 (Phospho-Thr581)	142	MSK1 (Ab-581)	0.66		
415	MSK2 (Phospho-Thr568)					
920	Mst1/Mst2 (Phospho-Thr183)	635	Mst1/Mst 2 (Ab-183)			
175	mTOR (Phospho-Ser2448)	60	mTOR (Ab-2448)		1.44	
727	mTOR (Phospho-Ser2481)	143	mTOR (Ab-2481)	1.30	1.22	0.93
258	mTOR (Phospho-Thr2446)	963	mTOR (Ab-2446)	0.89	1.62	1.81
302	Myc (Phospho-Ser373)	54	Myc (Ab-373)	0.42	0.59	1.40
852	Myc (Phospho-Ser62)	716	Myc (Ab-62)	1.03	1.01	0.98
168	Myc (Phospho-Thr358)	53	Myc (Ab-358)	0.13	0.12	0.90
167	Myc (Phospho-Thr58)	52	Myc (Ab-58)	0.62		
921	Myosin regulatory light chain 2 (Phospho-Ser18)	636	Myosin regulatory light chain 2 (Ab-18)	0.86	0.73	0.86
910	MYPT1 (Phospho-Thr696)					
911	MYPT1 (Phospho-Thr853)					
		808	MYT1 (Ab-83)			

		459	NFAT3 (Ab-168/170)			
		1101	NFAT3 (Ab-676)			
241	NFAT4 (Phospho-Ser165)	1102	NFAT4 (Ab-165)	2.10	1.06	0.51
15	NFkB-p100/p52 (Phospho-Ser865)	1192	NFkB-p100/p52 (Ab-865)	0.44	0.44	1.00
16	NFkB-p100/p52 (Phospho-Ser869)	1193	NFkB-p100/p52 (Ab-869)	1.09		
252	NFkB-p100/p52 (Phospho-Ser872)					
150	NFkB-p105/p50 (Phospho-Ser337)	1194	NFkB-p105/p50 (Ab-337)	1.08	0.81	0.75
151	NFkB-p105/p50 (Phospho-Ser893)	36	NFkB-p105/p50 (Ab-893)			
152	NFkB-p105/p50 (Phospho-Ser907)	37	NFkB-p105/p50 (Ab-907)	0.98		
1053	NFkB-p105/p50 (Phospho-Ser927)	588	NFkB-p105/p50 (Ab-927)	0.70	0.55	0.79
336	NFkB-p105/p50 (Phospho-Ser932)	221	NFkB-p105/p50 (Ab-932)			
10	NFkB-p65 (Phospho-Thr254)	1187	NFkB-p65 (Ab-254)	0.93		

11	NFkB-p65 (Phospho-Ser276)	1188	NFkB-p65 (Ab-276)	0.97	1.12	1.16
496	NFkB-p65 (Phospho-Ser311)	361	NFkB-p65 (Ab-311)	1.39	1.36	0.98
12	NFkB-p65 (Phospho-Thr435)	1189	NFkB-p65 (Ab-435)	1.36	1.28	0.95
13	NFkB-p65 (Phospho-Ser468)	1190	NFkB-p65 (Ab-468)	1.80	1.15	0.64
345	NFkB-p65 (Phospho-Thr505)	1103	NFkB-p65 (Ab-505)	0.62	0.71	1.14
171	NFkB-p65 (Phospho-Ser529)	57	NFkB-p65 (Ab-529)	5.93	3.66	0.62
14	NFkB-p65 (Phospho-Ser536)	1191	NFkB-p65 (Ab-536)	1.02	1.01	0.99
		1126	NFkB-p65 (Ab-281)			
835	NMDAR1 (Phospho-Ser897)	547	NMDAR1 (Ab-897)		0.98	
264	NMDAR2A/B (Phospho-Tyr1246/1252)					
112	NMDAR2B (Phospho-Tyr1472)	1139	NMDAR2B (Ab-1472)		0.30	
1005	Opioid Receptor (Phospho-Ser375)	717	Opioid Receptor (Ab-375)	1.67	1.22	0.73
922	p130Cas (Phospho-Tyr165)	637	p130Cas (Ab-165)	1.35	0.95	0.70
745	p130Cas (Phospho-Tyr410)	464	p130Cas (Ab-410)		1.11	

31	p21Cip1 (Phospho-Thr145)	1030	p21Cip1 (Ab-145)	1.55	1.45	0.93
32	p27Kip1 (Phospho-Ser10)	1031	p27Kip1 (Ab-10)			
33	p27Kip1 (Phospho-Thr187)	1032	p27Kip1 (Ab-187)	1.41	1.34	0.96
		1104	p300 (Ab-89)			
337	p38 MAPK (Phospho-Thr180)	424	p38 MAPK (Ab-180)		1.28	
338	p38 MAPK (Phospho-Tyr182)	222	p38 MAPK (Ab-182)	0.15	0.22	1.48
904	p38 MAPK (Phospho-Tyr322)	299	p38 MAPK (Ab-322)		1.23	
330	p44/42 MAPK (Phospho-Thr202)	215	p44/42MAPK (Ab-202)	1.11	1.41	1.27
331	p44/42 MAPK (Phospho-Tyr204)	216	p44/42 MAPK (Ab-204)		1.57	
662	p53 (Phospho-Ser15)	521	p53 (Ab-15)			
815	p53 (Phospho-Thr18)	522	p53 (Ab-18)			
242	p53 (Phospho-Ser20)	1105	p53 (Ab-20)	0.91	0.40	0.44
819	p53 (Phospho-Ser315)	527	p53 (Ab-315)	0.29	0.39	1.33
816	p53 (Phospho-Ser33)	524	p53 (Ab-33)			
401	p53 (Phospho-Ser366)					
817	p53 (Phospho-Ser37)	525	p53 (Ab-37)	1.00	1.06	1.05
		1128	p53 (Ab-376)			
402	p53 (Phospho-Ser378)	1129	p53 (Ab-378)			

		1127	p53 (Ab-387)			
243	p53 (Phospho-Ser392)	1106	p53 (Ab-392)	1.55		
818	p53 (Phospho-Ser46)	526	p53 (Ab-46)	0.90	0.79	0.87
660	p53 (Phospho-Ser6)	519	p53 (Ab-6)			
661	p53 (Phospho-Ser9)	520	p53 (Ab-9)			
728	p53 (Phospho-Thr81)					
729	p63 (Phospho-Ser455)					
244	P70S6K (Phospho-Thr229)	1107	P70S6K (Ab-229)	0.62	0.81	1.32
378	P70S6K (Phospho-Ser371)	1108	P70S6K (Ab-371)	0.73	0.99	1.35
505	P70S6K (Phospho-Ser411)	370	P70S6K (Ab-411)			
380	P70S6K (Phospho-Ser418)	1109	P70S6K (Ab-418)	1.00	1.23	1.23
1050	P70S6K (Phospho-Thr421)	426	P70S6K (Ab-421)	1.59	1.45	0.91
672	P70S6K (Phospho-Ser424)	537	P70S6K (Ab-424)		1.61	
379	P70S6K (Phospho-Thr389)					
		1291	P70S6K (Ab-427)			
568	P70S6K-beta (Phospho-Ser423)	1292	P70S6K-beta (Ab-423)	1.09	1.17	1.07
476	P73 (Phospho-Tyr99)	511	P73 (Ab-99)	0.50	0.56	1.12
382	P90RSK (Phospho-Ser380)	1111	P90RSK (Ab-380)	1.13	0.94	0.84

381	P90RSK (Phospho-Thr359/Ser363)	1110	P90RSK (Ab-359/363)	0.19	0.20	1.07
383	P90RSK (Phospho-Thr573)	1112	P90RSK (Ab-573)	0.44	0.51	1.16
475	P95/NBS1 (Phospho-Ser343)	342	P95/NBS1 (Ab-343)			
569	PAK1 (Phospho-Ser204)	1293	PAK1 (Ab-204)	0.78	1.19	1.53
384	PAK1 (Phospho-Thr212)	1113	PAK1 (Ab-212)	0.88	1.07	1.21
253	PAK1/2 (Phospho-Ser199)	956	PAK1/2 (Ab-199)	0.74	0.94	1.27
386	PAK1/2/3 (Phospho-Ser141)	1115	PAK1/2/3 (Ab-141)			
385	PAK1/2/3 (Phospho-Thr423/402/421)	1114	PAK1/2/3 (Ab-423/402/421)	0.09	0.08	0.84
570	PAK2 (Phospho-Ser192)	1294	PAK2 (Ab-192)		0.92	
		1295	PAK2 (Ab-197)			
730	PAK2 (Phospho-Ser20)					
571	PAK3 (Phospho-Ser154)	1296	PAK3 (Ab-154)	0.92	0.81	0.89
		144	PAK4 (Ab-474)			
657	Paxillin (Phospho-Tyr118)	695	Paxillin (Ab-118)		1.38	
26	Paxillin (Phospho-Tyr31)	1208	Paxillin (Ab-31)		1.35	

1259	PDGFR alpha (Phospho-Tyr849)	978	PDGFR alpha (Ab-849)	1.09	1.69	1.56
		974	PDGFR beta (Ab-1009)			
1258	PDGFR beta (Phospho-Tyr1021)	977	PDGFR beta (Ab-1021)	1.54	1.40	0.91
1257	PDGFR beta (Phospho-Tyr740)	976	PDGFR beta (Ab-740)		1.05	
180	PDGFR beta (Phospho-Tyr751)	65	PDGFR beta (Ab-751)	0.47	0.54	1.15
5	PDK1 (Phospho-Ser241)	1182	PDK1 (Ab-241)	0.34	0.37	1.09
731	PEA-15 (Phospho-Ser104)	1116	PEA-15 (Ab-116)	0.95	0.87	0.91
387	PEA-15 (Phospho-Ser116)	1116	PEA-15 (Ab-116)	0.91	0.73	0.80
113	PECAM-1 (Phospho-Tyr713)	1140	PECAM-1 (Ab-713)	0.15	0.24	1.58
261	PI3-kinase p85-alpha (Phospho-Tyr607)					
260	PI3-kinase p85-subunit alpha/gamma (Phospho-Tyr467/Tyr199)	964	PI3-kinase p85-subunit alpha/gamma (Ab-467/199)			
121	Pim-1 (Phospho-Tyr309)	1145	Pim-1 (Ab-309)	1.02	0.78	0.77
1087	PIP5K (Phospho-Ser307)					

388	PKA CAT (Phospho-Thr197)	1117	PKA CAT (Ab-197)	0.80	1.01	1.26
101	PKA-R2B (Phospho-Ser113)					
905	PKC alpha (Phospho-Tyr657)	300	PKC alpha (Ab-657)	1.75		
732	PKC alpha/beta II (Phospho-Thr638)	145	PKC alpha/beta II (Ab-638)	1.29	0.79	0.61
572	PKC beta/PKCB (Phospho-Ser661)	1297	PKC beta/PKCB (Ab-661)	0.99	0.99	1.00
836	PKC delta (Phospho-Ser645)	548	PKC delta (Ab-645)	1.00	0.68	0.68
733	PKC delta (Phospho-Thr505)	146	PKC delta (Ab-505)		0.88	
734	PKC delta (Phospho-Tyr313)					
906	PKC delta (Phospho-Tyr52)					
573	PKC delta (Phospho-Tyr64)					
907	PKC epsilon (Phospho-Ser729)	301	PKC epsilon (Ab-729)	0.84	0.94	1.12
908	PKC pan activation site (Phospho)	435	PKC pan activation site		1.24	
837	PKC theta (Phospho-Ser676)	701	PKC theta (Ab-676)		0.99	
735	PKC theta (Phospho-Thr538)	701	PKC theta (Ab-676)			

1006	PKC zeta (Phospho-Thr410)	718	PKC zeta (Ab-410)		1.31	
909	PKC zeta (Phospho-Thr560)	436	PKC zeta (Ab-560)	1.51	1.50	0.99
1062	PKD1/PKC mu (Phospho-Ser205)	437	PKD1/PKC mu (Ab-205)	0.79	0.95	1.20
736	PKD1/PKC mu (Phospho-Ser910)	149	PKD1/PKC mu (Ab-910)	0.88	1.11	1.26
1063	PKD1/PKC mu (Phospho-Tyr463)	438	PKD1/PKC mu (Ab-463)	0.68	0.82	1.21
		148	PKD1/PKC mu (Ab-744/748)			
1064	PKD2 (Phospho-Ser876)	439	PKD2 (Ab-876)			
668	PKR (Phospho-Thr446)	533	PKR (Ab-446)			
678	PKR (Phospho-Thr451)	542	PKR (Ab-451)		0.89	
1046	PLC beta3 (Phospho-Ser1105)	433	PLC beta3 (Ab-1105)		0.95	
737	PLC beta3 (Phospho-Ser537)	283	PLC beta3 (Ab-537)		1.29	
912	PLCG1 (Phospho-Tyr1253)					
743	PLCG1 (Phospho-Tyr771)	465	PLCG1 (Ab-771)		1.81	
746	PLCG1 (Phospho-Tyr783)	466	PLCG1 (Ab-783)	1.11	0.88	0.80
913	PLCG2 (Phospho-Tyr1217)	628	PLCG2 (Ab-1217)	1.39		

747	PLCG2 (Phospho-Tyr753)	468	PLCG2 (Ab-753)	0.85	0.83	0.98
122	PLD1 (Phospho-Ser561)	1146	PLD1 (Ab-561)	0.68	0.76	1.11
421	PLD2 (Phospho-Tyr169)					
1287	PLK1 (Phospho-Thr210)	629	PLK1 (Ab-210)	0.59	0.68	1.16
923	PP1 alpha (Phospho-Thr320)	638	PP1 alpha (Ab-320)	0.88		
389	PP2A-alpha (Phospho-Tyr307)	1118	PP2A-alpha (Ab-307)	0.24	0.21	0.85
914	PPAR-BP (Phospho-Thr1457)	630	PPAR-BP (Ab-1457)	0.77	0.81	1.05
915	PPAR-gamma (Phospho-Ser112)	631	PPAR-gamma (Ab-112)	0.10	0.11	1.13
644	Progesterone Receptor (Phospho-Ser190)	353	Progesterone Receptor (Ab-190)			
480	PTEN (Phospho-Ser370)	341	PTEN (Ab-370)			
9	PTEN (Phospho-Ser380)	1186	PTEN (Ab-380)			
474	PTEN (Phospho-Ser380/Thr382/Thr383)	340	PTEN (Ab-380/382/383)			
114	PTPRA (Phospho-Tyr798)					
170	Pyk2 (Phospho-Tyr402)	56	Pyk2 (Ab-402)	1.03	0.94	0.91

581	Pyk2 (Phospho-Tyr579)					
1047	Pyk2 (Phospho-Tyr580)	601	Pyk2 (Ab-580)	0.45	0.46	1.04
1217	Pyk2 (Phospho-Tyr881)	600	Pyk2 (Ab-881)	0.50	0.80	1.60
28	Rac1/cdc42 (Phospho-Ser71)	1210	Rac1/cdc42 (Ab-71)			
1083	RAD51 (Phospho-Tyr315)	812	RAD51 (Ab-309)	1.18	0.68	0.58
1084	RAD52 (Phospho-Tyr104)					
6	Raf1 (Phospho-Ser259)	1183	Raf1 (Ab-259)		0.58	
1153	Raf1 (Phospho-Ser289)	1298	Raf1 (Ab-289)		0.52	
561	Raf1 (Phospho-Ser296)	131	Raf1 (Ab-296)	1.01	0.90	0.89
29	Raf1 (Phospho-Ser338)	1211	Raf1 (Ab-338)			
1246	Raf1 (Phospho-Ser43)	618	Raf1 (Ab-43)	0.37	0.32	0.87
391	Raf1 (Phospho-Ser621)	1272	Raf1 (Ab-621)	0.71	1.08	1.52
390	Raf1 (Phospho-Tyr341)	1271	Raf1 (Ab-341)	0.87	1.21	1.39
254	RapGEF1 (Phospho-Tyr504)					
738	Ras-GRF1 (Phospho-Ser916)	284	Ras-GRF1 (Ab-916)	0.68	1.00	1.48
403	Rb (Phospho-Ser608)	1130	Rb (Ab-608)		1.83	
995	Rb (Phospho-Ser780)	698	Rb (Ab-780)			
993	Rb (Phospho-Ser795)	696	Rb (Ab-795)	0.81	0.64	0.80

994	Rb (Phospho-Ser807)	697	Rb (Ab-807)	0.87	1.27	1.46
1065	Rb (Phospho-Ser811)	440	Rb (Ab-811)	1.02	1.11	1.08
1066	Rb (Phospho-Thr821)					
		441	Rb-like-2 (RBL2) (Ab-952)			
153	Rel (Phospho-Ser503)	38	Rel (Ab-503)			
339	RelB (Phospho-Ser552)	223	RelB (Ab-552)	2.03	1.94	0.96
671	Ret (Phospho-Tyr905)	536	Ret (Ab-905)			
262	RGS16 (Phospho-Tyr168)					
263	Rho/Rac guanine nucleotide exchange factor 2 (Phospho-Ser885)	965	Rho/Rac guanine nucleotide exchange factor 2 (Ab-885)	1.05	1.14	1.09
		1273	RhoA (Ab-188)			
574	RSK1/2/3/4 (Phospho-Ser221/227/218/232)	1299	RSK1/2/3/4 (Ab-221/227/218/232)	0.63	1.05	1.67
392	RyR2 (Phospho-Ser2808)	1274	RyR2 (Ab-2808)		1.04	
186	S6 Ribosomal Protein (Phospho-Ser235)	71	S6 Ribosomal Protein (Ab-235)	1.13		
334	SAPK/JNK (Phospho-Thr183)	219	SAPK/JNK (Ab-183)	1.00	0.79	0.79
335	SAPK/JNK (Phospho-Tyr185)	220	SAPK/JNK (Ab-185)	1.02	0.92	0.90

1007	Shc (Phospho-Tyr349)	719	Shc (Ab-349)			
1008	Shc (Phospho-Tyr427)	589	Shc (Ab-427)	0.52		
1009	SHP-1 (Phospho-Tyr536)					
1010	SHP-2 (Phospho-Tyr542)	872	SHP-2 (Ab-542)	0.74	1.11	1.50
1011	SHP-2 (Phospho-Tyr580)	873	SHP-2 (Ab-580)	1.03		
576	SLP-76 (Phospho-Tyr128)	1302	SLP-76 (Ab-128)	1.19	0.86	0.72
102	Smad1 (Phospho-Ser187)	786	Smad1 (Ab-187)		1.04	
1054	Smad1 (Phospho-Ser465)	590	Smad1 (Ab-465)			
103	Smad2 (Phospho-Ser250)	788	Smad2 (Ab-250)	1.04	0.97	0.93
1055	Smad2 (Phospho-Ser467)	591	Smad2 (Ab-467)	1.32	1.01	0.76
104	Smad2 (Phospho-Thr220)	790	Smad2 (Ab-220)	0.81	1.02	1.26
		789	Smad2 (Ab-245)			
		787	Smad2 (Ab-255)			
105	Smad2/3 (Phospho-Thr8)	791	Smad2/3 (Ab-8)	1.38	1.22	0.88
107	Smad3 (Phospho-Ser204)	793	Smad3 (Ab-204)	0.68	0.66	0.97
108	Smad3 (Phospho-Ser208)					

109	Smad3 (Phospho-Ser213)	794	Smad3 (Ab-213)			
1012	Smad3 (Phospho-Ser425)	592	Smad3 (Ab-425)	1.21	1.37	1.13
106	Smad3 (Phospho-Thr179)	792	Smad3 (Ab-179)	0.55	0.52	0.94
23	SMC1 (Phospho-Ser957)	1205	SMC1 (Ab-957)	0.84		
326	SP1 (Phospho-Thr739)	211	SP1 (Ab-739)			
575	Src (Phospho-Ser75)	1300	Src (Ab-75)	1.01	0.66	0.65
579	Src (Phospho-Tyr216)					
659	Src (Phospho-Tyr418)	855	Src (Ab-418)	0.57	0.33	0.58
1165	Src (Phospho-Tyr529)	1196	Src (Ab-529)	0.58		
742	SREBP-1 (Phospho-Ser439)	460	SREBP-1 (Ab-439)		0.64	
404	SRF (Phospho-Ser77)	1131	SRF (Ab-77)			
1218	SRF (Phospho-Ser99)	602	SRF (Ab-99)	0.51	0.57	1.12
276	STAM2 (Phospho-Tyr192)	1315	STAM2 (Ab-192)	1.73		
1173	STAT1 (Phospho-Ser727)	1204	STAT1 (Ab-727)	0.94		
310	STAT1 (Phospho-Tyr701)	195	STAT1 (Ab-701)			
1219	STAT2 (Phospho-Tyr690)	603	STAT2 (Ab-690)	1.30	1.95	1.50
312	STAT3 (Phospho-Ser727)	197	STAT3 (Ab-727)			

311	STAT3 (Phospho-Tyr705)	196	STAT3 (Ab-705)	0.71	0.73	1.02
313	STAT4 (Phospho-Tyr693)	198	STAT4 (Ab-693)		24.98	
110	STAT5A (Phospho-Ser725)					
315	STAT5A (Phospho-Ser780)	200	STAT5A (Ab-780)	0.19	0.13	0.67
314	STAT5A (Phospho-Tyr694)	199	STAT5A (Ab-694)			
1048	STAT5B (Phospho-Ser731)	434	STAT5B (Ab-731)	0.63	0.96	1.51
317	STAT6 (Phospho-Thr645)	202	STAT6 (Ab-645)	0.31	0.37	1.19
316	STAT6 (Phospho-Tyr641)	201	STAT6 (Ab-641)		0.98	
321	Stathmin 1 (Phospho-Ser15)	73	Stathmin 1 (Ab-15)			
178	Stathmin 1 (Phospho-Ser24)	63	Stathmin 1 (Ab-24)			
179	Stathmin 1 (Phospho-Ser37)	64	Stathmin 1 (Ab-37)			
1261	Survivin (Phospho-Thr117)	980	Survivin (Ab-117)			
393	SYK (Phospho-Tyr323)					
1049	SYK (Phospho-Tyr348)	604	SYK (Ab-348)	0.67	0.69	1.03
1220	SYK (Phospho-Tyr525)	605	SYK (Ab-525)	0.81	0.62	0.76
394	Synapsin (Phospho-Ser62)	1275	Synapsin (Ab-62)			

503	Synapsin (Phospho-Ser9)	368	Synapsin (Ab-9)	1.17	0.95	0.81
1013	Synaptotagmin (Phospho-Ser309)	874	Synaptotagmin (Ab-309)			
1014	Synaptotagmin (Phospho-Thr202)	875	Synaptotagmin (Ab-202)			
492	Synuclein alpha (Phospho-Tyr125)	224	Synuclein alpha (Ab-125)	0.75		
673	Synuclein alpha (Phospho-Tyr133)	538	Synuclein alpha (Ab-133)		0.68	
674	Synuclein alpha (Phospho-Tyr136)					
825	Tau (Phospho-Ser214)	686	Tau (Ab-214)	0.92		
822	Tau (Phospho-Ser235)	683	Tau (Ab-235)	0.07	0.07	0.93
827	Tau (Phospho-Ser262)	688	Tau (Ab-262)			
820	Tau (Phospho-Ser356)	528	Tau (Ab-356)			
821	Tau (Phospho-Ser396)	529	Tau (Ab-396)	0.42	0.65	1.52
828	Tau (Phospho-Ser404)	689	Tau (Ab-404)	1.07	0.85	0.80
506	Tau (Phospho-Ser422)	371	Tau (Ab-422)	1.02		
823	Tau (Phospho-Thr181)	684	Tau (Ab-181)		1.11	
824	Tau (Phospho-Thr205)	685	Tau (Ab-205)	0.37	0.67	1.84
493	Tau (Phospho-Thr212)	225	Tau (Ab-212)		0.28	
826	Tau (Phospho-Thr231)	687	Tau (Ab-231)		0.72	
		958	TGFBR1 (Ab-165)			

		959	TGFBR2 (Ab-250)			
115	TFII-I (Phospho-Tyr248)					
916	TIE2 (Phospho-Tyr1108)					
1099	TIF-IA (Phospho-Ser649)	813	TIF-IA (Ab-649)	1.13	1.15	1.02
		639	TLK1 (Ab-764)			
1262	TOP2A/DNA topoisomerase II (Phospho-Ser1106)	981	TOP2A/DNA topoisomerase II (Ab-1106)	0.45	0.66	1.46
406	Trk A (Phospho-Tyr680/681)	1276	Trk A (Ab-496)		1.36	
405	Trk A (Phospho-Tyr701)	1276	Trk A (Ab-496)		1.08	
1015	Trk A (Phospho-Tyr791)	1276	Trk A (Ab-496)			
1016	Trk B (Phospho-Tyr515)	876	Trk B (Ab-515)	0.81	0.68	0.85
1043	Trk B (Phospho-Tyr705)	876	Trk B (Ab-515)	0.69	0.65	0.95
395	Tuberin/TSC2 (Phospho-Ser939)	1277	Tuberin/TSC2 (Ab-939)	0.35	0.33	0.95
396	Tuberin/TSC2 (Phospho-Thr1462)	1278	Tuberin/TSC2 (Ab-1462)	1.86	1.64	0.88
		461	Tuberin/TSC2 (Ab-981)			
1160	TYK2 (Phospho-Tyr1054)	858	TYK2 (Ab-1054)			

1017	Tyrosine Hydroxylase (Phospho-Ser19)	877	Tyrosine Hydroxylase (Ab-19)			
1018	Tyrosine Hydroxylase (Phospho-Ser31)	878	Tyrosine Hydroxylase (Ab-31)			
1019	Tyrosine Hydroxylase (Phospho-Ser40)	879	Tyrosine Hydroxylase (Ab-40)			
549	Tyrosine Hydroxylase (Phospho-Ser8)	1279	Tyrosine Hydroxylase (Ab-8)		0.71	
169	VASP (Phospho-Ser157)	1213	VASP (Ab-157)	0.18	0.37	2.01
1168	VASP (Phospho-Ser238)	1199	VASP (Ab-238)		1.01	
1003	VAV1 (Phospho-Tyr174)	1280	VAV1 (Ab-160)	1.00	0.76	0.76
1003	VAV1 (Phospho-Tyr174)	1041	VAV1 (Ab-174)	1.28	0.94	0.73
397	VAV2 (Phospho-Tyr142)	966	VAV2 (Ab-142)	1.28	1.76	1.37
416	VE-Cadherin (Phospho-Tyr731)					
550	VEGFR1 (Phospho-Tyr1333)	1281	VEGFR1 (Ab-1333)			
265	VEGFR2 (Phospho-Tyr1054)	1154	VEGFR2 (Ab-1054)	0.53	0.51	0.96
551	VEGFR2 (Phospho-Tyr1059)	1282	VEGFR2 (Ab-1059)		0.77	

652	VEGFR2 (Phospho-Tyr1175)	513	VEGFR2 (Ab-1175)	1.36	0.75	0.55
653	VEGFR2 (Phospho-Tyr1214)	514	VEGFR2 (Ab-1214)		0.14	
654	VEGFR2 (Phospho-Tyr951)	515	VEGFR2 (Ab-951)	0.11	0.17	1.59
266	Vinculin (Phospho-Tyr821)	1155	Vinculin (Ab-821)	1.85	1.61	0.87
552	WASP (Phospho-Tyr290)	1283	WASP (Ab-290)			
917	WAVE1 (Phospho-Tyr125)	632	WAVE1 (Ab-125)			
799	WEE1 (Phospho-Ser53)	809	WEE1 (Ab-53)			
1088	WEE1 (Phospho-Ser642)	809	WEE1 (Ab-53)	1.21	1.45	1.20
417	WWOX (Phospho-Tyr33)					
918	XIAP (Phospho-Ser87)	633	XIAP (Ab-87)			
553	Zap-70 (Phospho-Tyr292)	1284	Zap-70 (Ab-292)	0.96	1.18	1.24
554	Zap-70 (Phospho-Tyr315)					
1169	Zap-70 (Phospho-Tyr319)	1200	Zap-70 (Ab-319)	0.56	0.52	0.93
1170	Zap-70 (Phospho-Tyr493)	1201	Zap-70 (Ab-493)			

iThenticate Report

thesis2

ORIGINALITY REPORT

25%
SIMILARITY INDEX

PRIMARY SOURCES

1	d-nb.info Internet	1652 words — 5%
2	www.nature.com Internet	920 words — 3%
3	www.ncbi.nlm.nih.gov Internet	698 words — 2%
4	mediatum.ub.tum.de Internet	467 words — 1%
5	www.cell.com Internet	220 words — 1%
6	Matthias Drosten, Mariano Barbacid. "Targeting the MAPK Pathway in KRAS-Driven Tumors", Cancer Cell, 2020 Crossref	206 words — 1%
7	v3r.esp.org Internet	177 words — < 1%
8	dspace.mit.edu Internet	158 words — < 1%
9	www.annualreviews.org Internet	142 words — < 1%

10	www.rj-robbins.com Internet	96 words — < 1%
11	Sahraoui, Yasmina Marielle Elizabeth. "Systems-Wide Analysis of Isoform Specific RAL Biology", The University of Liverpool (United Kingdom), 2022 ProQuest	92 words — < 1%
12	"Encyclopedia of Signaling Molecules", Springer Nature, 2012 Crossref	89 words — < 1%
13	Michele Olivieri, Tiffany Cho, Alejandro Álvarez-Quilón, Kejiao Li et al. "A Genetic Map of the Response to DNA Damage in Human Cells", Cell, 2020 Crossref	78 words — < 1%
14	Marco Ranzani, Kristel Kemper, Magali Michaut, Oscar Krijgsman et al. " A screen for combination therapies in wild type melanoma identifies nilotinib plus MEK inhibitor as a synergistic combination ", Cold Spring Harbor Laboratory, 2017 Crossref Posted Content	63 words — < 1%
15	perspectivesinmedicine.cshlp.org Internet	63 words — < 1%
16	Weiwei Guo, Xue You, Xiao Wang, Lin Wang, Yan Chen. "A synthetic peptide hijacks the catalytic subunit of class I PI3K to suppress the growth of cancer cells", Cancer Letters, 2017 Crossref	62 words — < 1%
17	www.mdpi.com Internet	57 words — < 1%

18	Kevin Lou, Veronica Steri, Alex Y. Ge, Y. Christina Hwang et al. " KRAS inhibition produces a driver-limited state revealing collateral dependencies ", Science Signaling, 2019 Crossref	56 words — < 1%
19	www.frontiersin.org Internet	56 words — < 1%
20	theses.gla.ac.uk Internet	49 words — < 1%
21	Meagan B. Ryan, Ryan B. Corcoran. "Therapeutic strategies to target RAS-mutant cancers", Nature Reviews Clinical Oncology, 2018 Crossref	48 words — < 1%
22	Anne Schuster, Hélène Erasimus, Sabrina Fritah, Petr V. Nazarov, Eric van Dyck, Simone P. Niclou, Anna Golebiewska. "RNAi/CRISPR Screens: from a Pool to a Valid Hit", Trends in Biotechnology, 2018 Crossref	47 words — < 1%
23	Manavalan, T.T.. "Differential expression of microRNA expression in tamoxifen-sensitive MCF-7 versus tamoxifen-resistant LY2 human breast cancer cells", Cancer Letters, 20111226 Crossref	47 words — < 1%
24	ddbj.nig.ac.jp Internet	45 words — < 1%
25	cyberleninka.org Internet	43 words — < 1%
26	Adrian Pickar-Oliver, Charles A. Gersbach. "The next generation of CRISPR–Cas technologies and	42 words — < 1%

applications", Nature Reviews Molecular Cell Biology, 2019
Crossref

27	digitalcommons.library.tmc.edu Internet	41 words — < 1%
28	eprints.gla.ac.uk Internet	41 words — < 1%
29	journals.sagepub.com Internet	39 words — < 1%
30	mdpi-res.com Internet	39 words — < 1%
31	www.science.gov Internet	39 words — < 1%
32	Bhatt, Akshita B.. "Targeting the MEK5, MEK1/2, and/or Pi3k Pathways Reverses Epithelial to Mesenchymal Transition and Enhances Chemotherapeutic Sensitivity in Breast and Brain Cancers with a Mesenchymal Phenotype", Duquesne University, 2021 ProQuest	38 words — < 1%
33	edoc.ub.uni-muenchen.de Internet	38 words — < 1%
34	Warren, Hannah Rose. "Identification of Drug Resistance Mechanisms Induced in Response to KRAS Therapeutics", The University of Liverpool (United Kingdom), 2022 ProQuest	37 words — < 1%
35	pharmaceuticalintelligence.com Internet	37 words — < 1%

36 Krishnaraj Rajalingam, Ralf Schreck, Ulf R. Rapp, Štefan Albert. "Ras oncogenes and their downstream targets", Biochimica et Biophysica Acta (BBA) - Molecular Cell Research, 2007
Crossref
35 words — < 1%

37 cdr.lib.unc.edu
Internet
35 words — < 1%

38 Pawel Sledzinski, Magdalena Dabrowska, Mateusz Nowaczyk, Marta Olejniczak. "Paving the way towards precise and safe CRISPR genome editing", Biotechnology Advances, 2021
Crossref
34 words — < 1%

39 Molecular Genetics of Pancreatic Cancer, 2013.
Crossref
33 words — < 1%

40 Wassermann Dozorets, Rina. "C/EBPb Lip-Mediated Augmentation of ER Stress-Triggered Cell Death: Mechanisms of Action.", The Weizmann Institute of Science (Israel), 2021
ProQuest
33 words — < 1%

41 Recinto, Sherilyn Junelle. "Insight into the Physiology of Human Rhomboid Protease RHBDL4: Proteolytic Mechanism and Cellular Role", McGill University (Canada), 2021
ProQuest
32 words — < 1%

42 www.zora.uzh.ch
Internet
32 words — < 1%

43 Bailee H. Sliker, Paul M. Campbell. "Ras and Ras Signaling as a Therapeutic Target in Cancer", Elsevier BV, 2021
Crossref
31 words — < 1%

44	dx.doi.org Internet	31 words — < 1%
45	insight.jci.org Internet	31 words — < 1%
46	Wallace, Taylor Renee Rutherford. "Sempahorin-7A Promotes Features of Tumor Initiation and Progression during Normal Postpartum Mammary Gland Involution", University of Colorado Denver, Anschutz Medical Campus, 2022 ProQuest	30 words — < 1%
47	Zaver, Shivam A.. "New Insights into Cyclic GMP-AMP Signaling in Innate Immunity", University of Washington, 2021 ProQuest	29 words — < 1%
48	journals.plos.org Internet	28 words — < 1%
49	doras.dcu.ie Internet	26 words — < 1%
50	www.biorxiv.org Internet	26 words — < 1%
51	www.science.org Internet	26 words — < 1%
52	Julia Joung, Silvana Konermann, Jonathan S Gootenberg, Omar O Abudayyeh et al. "Genome-scale CRISPR-Cas9 knockout and transcriptional activation screening", Nature Protocols, 2017 Crossref	25 words — < 1%

53 Kristen Foster. "Dependence on PI3K/Akt signaling for malignant rhabdoid tumor cell survival", Cancer Chemotherapy and Pharmacology, 04/2009
Crossref
25 words — < 1%

54 ijcrr.info
Internet
25 words — < 1%

55 openprairie.sdstate.edu
Internet
25 words — < 1%

56 Becker, Andrew E.. "The Mutual Regulation Between ERK1/2 and DHPS Involving Non-Kinase and Non-Hypusinating Functions", The Medical College of Wisconsin, 2022
ProQuest
24 words — < 1%

57 C. Braet. "Glycosylated Rat Prolactin: Isolation and Structural Characterization", Archives of Physiology and Biochemistry, 4/1/2001
Crossref
24 words — < 1%

58 Chiara Falcomatà, Stefanie Bärthel, Sebastian A. Widholz, Christian Schneeweis et al. "Selective multi-kinase inhibition sensitizes mesenchymal pancreatic cancer to immune checkpoint blockade by remodeling the tumor microenvironment", Nature Cancer, 2022
Crossref
24 words — < 1%

59 Hirsch, E.. "Taming the PI3K team to hold inflammation and cancer at bay", Pharmacology and Therapeutics, 200805
Crossref
24 words — < 1%

60 Iuri Viotti Perisse, Zhiqiang Fan, Galina N. Singina, Kenneth L. White, Irina A. Polejaeva.
24 words — < 1%

"Improvements in Gene Editing Technology Boost Its Applications in Livestock", Frontiers in Genetics, 2021
Crossref

61	dmr.amegroups.com Internet	24 words — < 1%
62	Matthew E. Welsch, Anna Kaplan, Jennifer M. Chambers, Michael E. Stokes et al. "Multivalent Small-Molecule Pan-RAS Inhibitors", Cell, 2017 Crossref	23 words — < 1%
63	mcr.aacrjournals.org Internet	23 words — < 1%
64	Alexandros K. Kanellopoulos, Vittoria Mariano, Marco Spinazzi, Young Jae Woo et al. "Aralar Sequesters GABA into Hyperactive Mitochondria, Causing Social Behavior Deficits", Cell, 2020 Crossref	22 words — < 1%
65	Copley, James. "Pikk-Dependent Activation of the DNA Damage Response by Long Wavelength Ultraviolet Radiation", Lancaster University (United Kingdom), 2020 ProQuest	22 words — < 1%
66	Yoshitaka Fujihara, Masahito Ikawa. "CRISPR/Cas9-Based Genome Editing in Mice by Single Plasmid Injection", Elsevier BV, 2014 Crossref	22 words — < 1%
67	www.researchgate.net Internet	22 words — < 1%
68	Nicolas Dumaz, Céleste Lebbé. "New perspectives on targeting RAF, MEK and ERK in melanoma", Current Opinion in Oncology, 2021	21 words — < 1%

Crossref

69	"Abstracts", Molecular Therapy, 2014. Crossref	20 words — < 1%
70	AddisonV. Wright, JamesK. Nuñez, JenniferA. Doudna. "Biology and Applications of CRISPR Systems: Harnessing Nature's Toolbox for Genome Engineering", Cell, 2016 Crossref	20 words — < 1%
71	Fuguo Jiang, Jennifer A. Doudna. "CRISPR–Cas9 Structures and Mechanisms", Annual Review of Biophysics, 2017 Crossref	20 words — < 1%
72	PatrickD. Hsu, EricS. Lander, Feng Zhang. "Development and Applications of CRISPR-Cas9 for Genome Engineering", Cell, 2014 Crossref	20 words — < 1%
73	theses.ncl.ac.uk Internet	20 words — < 1%
74	Aird, Eric J.. "Novel Precise Genome Editing Technologies", University of Minnesota, 2021 ProQuest	19 words — < 1%
75	Methods in Molecular Biology, 2016. Crossref	19 words — < 1%
76	www.repository.cam.ac.uk Internet	19 words — < 1%
77	"Molecular Diagnostics for Melanoma", Springer Science and Business Media LLC, 2014 Crossref	18 words — < 1%

78 Adele P. Chen. "Forebrain-specific knockout of B-raf kinase leads to deficits in hippocampal long-term potentiation, learning, and memory", Journal of Neuroscience Research, 01/2006
Crossref
18 words — < 1%

79 Ann Lin, Christopher J. Giuliano, Ann Palladino, Kristen M. John et al. "Off-target toxicity is a common mechanism of action of cancer drugs undergoing clinical trials", Science Translational Medicine, 2019
Crossref
18 words — < 1%

80 S Yonehara. "Novel cell death by downregulation of eEF1A1 expression in tetraploids", Cell Death and Differentiation, 09/26/2008
Crossref
18 words — < 1%

81 hdl.handle.net
Internet
18 words — < 1%

82 pure.unamur.be
Internet
18 words — < 1%

83 researcharchive.vuw.ac.nz
Internet
18 words — < 1%

84 www.bostonscienceandengineeringlectures.com
Internet
18 words — < 1%

85 "Abstracts of 52nd EASD Annual Meeting", Diabetologia, 2016
Crossref
17 words — < 1%

86 Ahmad A. Cluntun, Rachit Badolia, Sandra Lettlova, K. Mark Parnell et al. "The pyruvate-lactate axis modulates cardiac hypertrophy and heart failure", Cell Metabolism, 2020
17 words — < 1%

Crossref

87 Alberto Bavelloni, Enrico Focaccia, Manuela Piazzi, Arianna Orsini et al. "Therapeutic potential of nvp - bkm120 in human osteosarcomas cells", Journal of Cellular Physiology, 2018
Crossref
17 words — < 1%

88 Martin Kampmann. "CRISPRi and CRISPRa Screens in Mammalian Cells for Precision Biology and Medicine", ACS Chemical Biology, 2017
Crossref
17 words — < 1%

89 Mehul Salaria, Jennifer Frazee, Rishabh Nautiyal, Saurabh Sudha Dhiman, Jitender Sharma. "Role of the CRISPR Technique in Decoding the Principles of Quorum Sensing", American Chemical Society (ACS), 2020
Crossref
17 words — < 1%

90 Samuel J. Tingle, George R. Severs, John A.G. Moir, Steven A. White. "Calcium channel blockers in pancreatic cancer: increased overall survival in a retrospective cohort study", Anti-Cancer Drugs, 2020
Crossref
17 words — < 1%

91 www.escholar.manchester.ac.uk
Internet
17 words — < 1%

92 www.pnas.org
Internet
17 words — < 1%

93 Dejun Yang, Yuan Tang, Hongbing Fu, Jiapeng Xu, Zunqi Hu, Yu Zhang, Qingping Cai. "Integrin β1 promotes gemcitabine resistance in pancreatic cancer through Cdc42 activation of PI3K p110β signaling", Biochemical and Biophysical Research Communications, 2018
Crossref
16 words — < 1%

94 Dingar, D.. "Characterization of the expression and regulation of MK5 in the murine ventricular myocardium", Cellular Signalling, 201007
Crossref
16 words — < 1%

95 Sugi, Takuma. "Genome Editing in C. elegans and Other Nematode Species", International Journal of Molecular Sciences, 2016.
Crossref
16 words — < 1%

96 Tim Wang, Haiyan Yu, Nicholas W. Hughes, Bingxu Liu et al. "Gene Essentiality Profiling Reveals Gene Networks and Synthetic Lethal Interactions with Oncogenic Ras", Cell, 2017
Crossref
16 words — < 1%

97 kuscholarworks.ku.edu
Internet
16 words — < 1%

98 www.bioseek.eu
Internet
16 words — < 1%

99 www.sigmaaldrich.com
Internet
16 words — < 1%

100 Barbara Kenner, Suresh T. Chari, David Kelsen, David S. Klimstra et al. "Artificial Intelligence and Early Detection of Pancreatic Cancer", Pancreas, 2021
Crossref
15 words — < 1%

101 Fiona M. Behan, Francesco Iorio, Gabriele Picco, Emanuel Gonçalves et al. "Prioritization of cancer therapeutic targets using CRISPR–Cas9 screens", Nature, 2019
Crossref
15 words — < 1%

102 Massague, J.. "A Very Private TGF-@b Receptor Embrace", Molecular Cell, 20080201
Crossref
15 words — < 1%

103 Yuji Nakata, Susan Shetzline, Chizuko Sakashita, Anna Kalota et al. " c-Myb Contributes to G /M Cell Cycle Transition in Human Hematopoietic Cells by Direct Regulation of Cyclin B1 Expression ", Molecular and Cellular Biology, 2007
Crossref
15 words — < 1%

104 tuprints.ulb.tu-darmstadt.de
Internet
15 words — < 1%

105 Ebi, Hiromichi, Anthony C. Faber, Jeffrey A. Engelman, and Seiji Yano. "Not just gRASping at flaws: Finding vulnerabilities to develop novel therapies for treating KRAS mutant cancers", Cancer Science, 2014.
Crossref
14 words — < 1%

106 Meagan B. Ryan, Channing J. Der, Andrea Wang-Gillam, Adrienne D. Cox. "Targeting RAS -mutant Cancers: Is ERK the Key?", Trends in Cancer, 2015
Crossref
14 words — < 1%

107 Michael Bauer, Justin W. Flatt, Daria Seiler, Bettina Cardel et al. "The E3Ubiquitin Ligase Mind Bomb 1 Controls Adenovirus Genome Release at the Nuclear Pore Complex", Cell Reports, 2019
Crossref
14 words — < 1%

108 Plowman, S.J.. "Ras signaling from plasma membrane and endomembrane microdomains", BBA - Molecular Cell Research, 20051230
Crossref
14 words — < 1%

109 Stein, Marcello Francesco. "Characterization of the CD83 Promoter/Enhancer Complex.", Friedrich-Alexander-Universitaet Erlangen-Nuernberg (Germany), 2021
ProQuest
14 words — < 1%

110	academic.oup.com Internet	14 words — < 1%
111	bonndoc.ulb.uni-bonn.de Internet	14 words — < 1%
112	d-scholarship.pitt.edu Internet	14 words — < 1%
113	docksci.com Internet	14 words — < 1%
114	jvi.asm.org Internet	14 words — < 1%
115	rupress.org Internet	14 words — < 1%
116	"HDAC/HAT Function Assessment and Inhibitor Development", Springer Science and Business Media LLC, 2017 Crossref	13 words — < 1%
117	"Ras Superfamily Small G Proteins: Biology and Mechanisms 1", Springer Nature, 2014 Crossref	13 words — < 1%
118	"Tuberous Sclerosis Complex", Wiley, 2010 Crossref	13 words — < 1%
119	Christopher D. Graham, Niroop Kaza, Barbara J. Klocke, G. Yancey Gillespie, Lalita A. Shevde, Steven L. Carroll, Kevin A. Roth. "Tamoxifen Induces Cytotoxic Autophagy in Glioblastoma", Journal of Neuropathology & Experimental Neurology, 2016 Crossref	13 words — < 1%

120 Cory M. Dungan, David L. Williamson. "Regulation of skeletal muscle insulin-stimulated signaling through the MEK-REDD1-mTOR axis", Biochemical and Biophysical Research Communications, 2017 — 13 words — < 1%
Crossref

121 Devashish Desai, Pushti Khandwala, Meghana Parsi, Rashmika Potdar. "PARP inhibitors: shifting the paradigm in thetreatment of pancreatic cancer", Medical Oncology, 2021 — 13 words — < 1%
Crossref

122 Fiona C. Lewis, Beverley J. Cottle, Victoria Shone, Giovanna Marazzi et al. "Transplantation of Allogeneic PW1 pos /Pax7 neg Interstitial Cells EnhanceEndogenous Repair of InjuredPorcine Skeletal Muscle", JACC: Basic to Translational Science, 2017 — 13 words — < 1%
Crossref

123 Irina Heid, Clara Lubeseder–Martellato, Bence Sipos, Pawel K. Mazur, Marina Lesina, Roland M. Schmid, Jens T. Siveke. "Early Requirement of Rac1 in a Mouse Model of Pancreatic Cancer", Gastroenterology, 2011 — 13 words — < 1%
Crossref

124 Lander, Noelia, Miguel A. Chiurillo, and Roberto Docampo. "Genome Editing by CRISPR/Cas9: a Game Change in the Genetic Manipulation of Protists", Journal of Eukaryotic Microbiology, 2016. — 13 words — < 1%
Crossref

125 Murugan, Karthik. "Characterizing the Specificity and Nicking Activity of CRISPR Endonucleases, Cas9 and Cas12a.", Iowa State University, 2020 — 13 words — < 1%
ProQuest

126 doc.rero.ch

Internet

13 words — < 1%

127 ebin.pub
Internet

13 words — < 1%

128 pure.eur.nl
Internet

13 words — < 1%

129 www.derma.ch
Internet

13 words — < 1%

130 Daesik Kim, Kevin Luk, Scot A. Wolfe, Jin-Soo Kim. "Evaluating and Enhancing Target Specificity of Gene-Editing Nucleases and Deaminases", Annual Review of Biochemistry, 2019
Crossref

12 words — < 1%

131 Fei Sun, Fa-Xi Wang, He Zhu, Tian-Tian Yue et al. "SUMOylation of PDPK1 Is required to maintain glycolysis-dependent CD4 T-cell homeostasis", Cell Death & Disease, 2022
Crossref

12 words — < 1%

132 Laia Richart, Enrique Carrillo-de Santa Pau, Ana Río-Machín, Mónica P. de Andrés et al. "BPTF is required for c-MYC transcriptional activity and in vivo tumorigenesis", Nature Communications, 2016
Crossref

12 words — < 1%

133 Sara Monteiro Lopes, Luís Pereira de Almeida. "Gene editing and central nervous system regeneration", Elsevier BV, 2020
Crossref

12 words — < 1%

134 William Pao, A John Iafrate, Zengliu Su. "Genetically informed lung cancer medicine", The

12 words — < 1%

Journal of Pathology, 2011
Crossref

135 patents.google.com
Internet
12 words — < 1%

136 "Genome Editing in Drug Discovery", Wiley, 2022
Crossref
11 words — < 1%

137 2021.igem.org
Internet
11 words — < 1%

138 Anna Meiliana, Nurrani Mustika Dewi, Andi Wijaya. "Genome Editing with Crispr-Cas9 Systems: Basic Research and Clinical Applications", The Indonesian Biomedical Journal, 2017
Crossref
11 words — < 1%

139 Michele Olivieri, Tiffany Cho, Alejandro Álvarez-Quilón, Kejiao Li et al. "A genetic map of the response to DNA damage in human cells", Cold Spring Harbor Laboratory, 2019
Crossref Posted Content
11 words — < 1%

140 S.J. Plowman, J.F. Hancock. "Ras signaling from plasma membrane and endomembrane microdomains", Biochimica et Biophysica Acta (BBA) - Molecular Cell Research, 2005
Crossref
11 words — < 1%

141 Schweitzer, Amie R.. "Apoptotic and Bioenergetic Changes in Pancreatic Cells After Exposure to Individual Toxicants and Their Mixtures", Oklahoma State University, 2021
ProQuest
11 words — < 1%

142 moam.info
Internet
11 words — < 1%

143 oro.open.ac.uk
Internet
11 words — < 1%

144 www.dtic.mil
Internet
11 words — < 1%

145 www.irnase.csic.es
Internet
11 words — < 1%

146 www.researchsquare.com
Internet
11 words — < 1%

147 "CRISPR", Springer Science and Business Media LLC, 2022
Crossref
10 words — < 1%

148 Abed, Firas Mohammed. "Genetics of Canine Pheochromocytoma", University of Florida, 2021
ProQuest
10 words — < 1%

149 Ahmad A. Cluntun, Rachit Badolia, Sandra Lettlova, K. Mark Parnell et al. "The pyruvate-lactate axis modulates cardiac hypertrophy and heart failure", Cell Metabolism, 2021
Crossref
10 words — < 1%

150 Arvind Dasari, Alexandria Phan, Sanjay Gupta, Asif Rashid et al. "Phase I study of the anti-IGF1R antibody cixutumumab with everolimus and octreotide in advanced well-differentiated neuroendocrine tumors", Endocrine-Related Cancer, 2015
Crossref
10 words — < 1%

151 B Verret, J Cortes, T Bachelot, F Andre, M Arnedos. "Efficacy of PI3K inhibitors in advanced breast cancer", Annals of Oncology, 2019
Crossref
10 words — < 1%

152 Chia, Chester. "Protecting Sub-types of Primary Auditory Neurons from Acoustic Trauma.", Harvard University, 2020
ProQuest
10 words — < 1%

153 Daniel P. S. Osborn, Rosa Maria Roccasecca, Fiona McMurray, Victor Hernandez-Hernandez et al. "Loss of FTO Antagonises Wnt Signaling and Leads to Developmental Defects Associated with Ciliopathies", PLoS ONE, 2014
Crossref
10 words — < 1%

154 Degoutin, Joffrey L., Claire C. Milton, Eefang Yu, Marla Tipping, Floris Bosveld, Liu Yang, Yohanns Bellaiche, Alexey Veraksa, and Kieran F. Harvey. "Riquiqui and Minibrain are regulators of the Hippo pathway downstream of Dachsous", Nature Cell Biology, 2013.
Crossref
10 words — < 1%

155 McGrath, Brian T.. "Histone H2A Mono-Ubiquitination in Neurodevelopmental Disorders: Molecular Insights from Rare Genetic Variants", University of Michigan, 2021
ProQuest
10 words — < 1%

156 Schönhuber, Nina, Barbara Seidler, Kathleen Schuck, Christian Veltkamp, Christina Schachtler, Magdalena Zukowska, Stefan Eser, Thorsten B Feyerabend, Mariel C Paul, Philipp Eser, Sabine Klein, Andrew M Lowy, Ruby Banerjee, Fangtang Yang, Chang-Lung Lee, Everett J Moding, David G Kirsch, Angelika Scheideler, Dario R Alessi, Ignacio Varela, Allan Bradley, Alexander Kind, Angelika E Schnieke, Hans-Reimer Rodewald, Roland Rad, Roland M Schmid, Günter Schneider, and Dieter Saur. "A next-generation dual-recombinase system for time- and host-specific targeting of pancreatic cancer", Nature Medicine, 2014.
Crossref
10 words — < 1%

157 Wang, Jingrui. "A Method for the Directed Evolution and Protein Engineering of Synthetic CRISPR-Cas9 Inhibitors", University of Toronto (Canada), 2020
ProQuest
10 words — < 1%

158 Wenshan Liu, Xiaohong Zhu, Mingguang Lei, Qingyou Xia, Jose Ramon Botella, Jian-Kang Zhu, Yanfei Mao. "A detailed procedure for CRISPR/Cas9-mediated gene editing in Arabidopsis thaliana", Science Bulletin, 2015
Crossref
10 words — < 1%

159 Yang Xi, Jiansheng Liu, Haiwei Wang, Shang Li, Yanghua Yi, Yanzhi Du. "New small‐molecule compound Hu‐17 inhibits estrogen biosynthesis by aromatase in human ovarian granulosa cancer cells", Cancer Medicine, 2020
Crossref
10 words — < 1%

160 bmcbiol.biomedcentral.com
Internet
10 words — < 1%

161 veterina.com.hr
Internet
10 words — < 1%

162 www.yumpu.com
Internet
10 words — < 1%

163 "Current and Emerging Therapies in Pancreatic Cancer", Springer Science and Business Media LLC, 2018
Crossref
9 words — < 1%

164 "Epigenome Editing", Springer Science and Business Media LLC, 2018
Crossref
9 words — < 1%

165 De Ascensao, Ana Rute da Cruz Ferreira. "Biochemical Aspects of Cell Wall Strengthening in Banana Roots in Response to Elicitors from Fusarium oxysporum", University of Johannesburg (South Africa), 2021
ProQuest
9 words — < 1%

166 Eva J Schaefer, Wang C Wang, Clifford A Meyer, Paloma Cejas et al. " and mutations disrupt PRC1.1 repressive function in leukemia by unlinking the RING-PCGF1 enzymatic core from target genes ", Cold Spring Harbor Laboratory, 2021
Crossref Posted Content
9 words — < 1%

167 Hu, Shuiqing. "Intracellular Regulatory Mechanisms of the Activation of Human Eosinophils by TSLP, IL-27 and Ligands of NOD-like Receptors in Allergic Inflammation", Proquest, 20111003
ProQuest
9 words — < 1%

168 Janice S. Chen, Jennifer A. Doudna. "The chemistry of Cas9 and its CRISPR colleagues", Nature Reviews Chemistry, 2017
Crossref
9 words — < 1%

169 Klepikova, Anna V., Maria D. Logacheva, Sergey E. Dmitriev, and Aleksey A. Penin. "RNA-seq analysis of an apical meristem time series reveals a critical point in Arabidopsis thaliana flower initiation", BMC Genomics, 2015.
Crossref
9 words — < 1%

170 Liang, Q.. "Noninvasive of adenovirus tumor retargeting in living subjects by a soluble adenovirus receptor-epidermal growth factor (sCAR-EGF) fusion protein", Molecular Imaging and Biology, 200411/12
Crossref
9 words — < 1%

171 Mohammad, Dara Khorshed. "Role of AKT/ PKB and 14-3-3 in the Regulation of B Cell Receptor Signaling and Signalosome Assembly", Karolinska Institutet (Sweden), 2021
ProQuest
9 words — < 1%

172 Monish Ram Makena, Myungjun Ko, Allatah X. Mekile, Nanami Senoo et al. "Secretory pathway Ca2+-ATPase SPCA2 regulates mitochondrial respiration and DNA damage response through store-independent calcium entry", Redox Biology, 2022
Crossref
9 words — < 1%

173 Myungjin Jo, Shinrye Lee, Kiyoung Kim, Seongsoo Lee, Sang Ryong Kim, Hyung-Jun Kim. "Inhibition of MEK5 suppresses TDP-43 toxicity via the mTOR-independent activation of the autophagy-lysosome pathway", Biochemical and Biophysical Research Communications, 2019
Crossref
9 words — < 1%

174 Pablo Lopez-Bergami. "The role of mitogen- and stress-activated protein kinase pathways in melanoma : The role of MAPK pathways in melanoma", Pigment Cell & Melanoma Research, 10/2011
Crossref
9 words — < 1%

175 Sheikh, Adnan Ahmed. "The Role of S100A8 and S100A8 Proteins in the Pancreatic and Colorectal Cancer Microenvironment.", The University of Liverpool (United Kingdom), 2020
ProQuest
9 words — < 1%

176 V Stoll. "Dominant negative inhibitors of signalling through the phosphoinositol 3-kinase pathway for gene therapy of pancreatic cancer", Gut, 2005
Crossref
9 words — < 1%

177	Weigelt, Britta, and Julian Downward. "Genomic Determinants of PI3K Pathway Inhibitor Response in Cancer", Frontiers in Oncology, 2012. Crossref	9 words — < 1%
178	Yichang Jia. "A molecular brake that modulates spliceosome pausing at detained introns contributes to neurodegeneration", Cold Spring Harbor Laboratory, 2022 Crossref Posted Content	9 words — < 1%
179	bio-protocol.org Internet	9 words — < 1%
180	ir.vanderbilt.edu Internet	9 words — < 1%
181	nbn-resolving.de Internet	9 words — < 1%
182	spiral.imperial.ac.uk Internet	9 words — < 1%
183	www.39kf.com Internet	9 words — < 1%
184	www120.secure.griffith.edu.au Internet	9 words — < 1%
185	"Apoptosis", Springer Science and Business Media LLC, 2009 Crossref	8 words — < 1%
186	"Phosphoinositide 3-Kinase: Diverse Roles in Immune Cell Activation", Annual Review of Immunology, 04/23/2004 Crossref	8 words — < 1%

187 Alnefaie, Ghaliah Obaid F. "Epigenetic Sensitisation of Chemotherapeutic Compounds in Non- Small Cell Lung Cancer", The University of Liverpool (United Kingdom), 2020
ProQuest
8 words — < 1%

188 Bainbridge, Callum S. "Investigating the Expression of Topoisomerase Ii Beta in Aged Neurons: Development of a Murine Cell Line and Drosophila Model.", University of Northumbria at Newcastle (United Kingdom), 2021
ProQuest
8 words — < 1%

189 Leal, Joseph M., IV. "Crosstalk between Innate and Adaptive Immune Cells within Lymph Node Microenvironments Shapes Immunity to Vaccines", University of Washington
ProQuest
8 words — < 1%

190 Lu Liu, Xixi Huang, Chunfang Xu, Chunqin Chen, Weijie Zhao, Dajin Li, Liping Li, Li Wang, Meirong Du. "Decidual CD8+T cells exhibit both residency and tolerance signatures modulated by decidual stromal cells", Journal of Translational Medicine, 2020
Crossref
8 words — < 1%

191 Macsphere.mcmaster.ca
Internet
8 words — < 1%

192 Matthew A. Coelho, Etienne De Braekeleer, Mike Firth, Michal Bista et al. "CRISPR GUARD protects off-target sites from Cas9 nuclease activity using short guide RNAs", Nature Communications, 2020
Crossref
8 words — < 1%

193 Montes, Marta, Morten M. Nielsen, Giulia Maglieri, Anders Jacobsen, Jonas Højfeldt, Shuchi Agrawal-Singh, Klaus Hansen, Kristian Helin, Harmen J. G. van de
8 words — < 1%

Werken, Jakob S. Pedersen, and Anders H. Lund. "The lncRNA MIR31HG regulates p16INK4A expression to modulate senescence", Nature Communications, 2015.
Crossref

194 Munshi Azad Hossain. "CRISPR-Cas9: A fascinating journey from bacterial immune system to human gene editing", Elsevier BV, 2021 — 8 words — < 1%
Crossref

195 Rao, Trisha. "Investigating the Phosphatidylinositol 3' Kinase Signalling Pathway in Transgenic Mouse Models of Breast Cancer.", McGill University (Canada), 2021 — 8 words — < 1%
ProQuest

196 Rodrigo Pinheiro Araldi, Charbel Khalil, Pedro Henrique Grignet, Michelli Ramires Teixeira et al. "Medical Applications of Clustered Regularly Interspaced Short Palindromic Repeats (CRISPR/Cas) Tool: A Comprehensive Overview", Gene, 2020 — 8 words — < 1%
Crossref

197 Rui Niu, Ying Liu, Ying Zhang, Yuan Zhang, Hui Wang, Yongbin Wang, Wei Wang, Xiaohui Li. "iTRAQ-Based Proteomics Reveals Novel Biomarkers for Idiopathic Pulmonary Fibrosis", PLOS ONE, 2017 — 8 words — < 1%
Crossref

198 Wenyan Jiang, Luciano A. Marraffini. "CRISPR-Cas: New Tools for Genetic Manipulations from Bacterial Immunity Systems", Annual Review of Microbiology, 2015 — 8 words — < 1%
Crossref

199 Yang, Zhenjie. "TUBB4B Was Identified as Novel Therapeutic Target of Nonalcoholic Fatty Liver Disease Associated-Hepatocellular Carcinoma", The Chinese University of Hong Kong (Hong Kong) — 8 words — < 1%

ProQuest

200 Yoshishige Kimura, Koji Tsutsumi, Alu Konno, Koji Ikegami et al. "Environmental responsiveness of tubulin glutamylation in sensory cilia is regulated by the p38 MAPK pathway", Scientific Reports, 2018 — 8 words — < 1%
Crossref

201 Zagore, Leah Louise. "The Molecular Function of the RNA Binding Protein DAZL in Male Germ Cell Survival.", Case Western Reserve University, 2020 — 8 words — < 1%
ProQuest

202 Zhang, Hualin. "Investigating the Role of CD109 in Skin Immune Homeostasis and Disease", McGill University (Canada) — 8 words — < 1%
ProQuest

203 Zhao, Yulei. "Exploring the Regulation of YAP and TAZ in Antitubulin Drug Response and Mammary Tumorigenesis", Queen's University (Canada), 2021 — 8 words — < 1%
ProQuest

204 core.ac.uk — 8 words — < 1%
Internet

205 digital.library.adelaide.edu.au — 8 words — < 1%
Internet

206 edoc.hu-berlin.de — 8 words — < 1%
Internet

207 encyclopedia.pub — 8 words — < 1%
Internet

208 epdf.pub — 8 words — < 1%
Internet

209	epub.uni-regensburg.de Internet	8 words — < 1%
210	europepmc.org Internet	8 words — < 1%
211	insights.ovid.com Internet	8 words — < 1%
212	kups.ub.uni-koeln.de Internet	8 words — < 1%
213	livrepository.liverpool.ac.uk Internet	8 words — < 1%
214	mobt3ath.com Internet	8 words — < 1%
215	molecularneurodegeneration.biomedcentral.com Internet	8 words — < 1%
216	pearl.plymouth.ac.uk Internet	8 words — < 1%
217	www.fedoa.unina.it Internet	8 words — < 1%
218	www.spandidos-publications.com Internet	8 words — < 1%
219	"Therapeutic Kinase Inhibitors", Springer Science and Business Media LLC, 2012 Crossref	7 words — < 1%
220	Baohui Chen, Juan Guan, Bo Huang. "Imaging Specific Genomic DNA in Living Cells", Annual Review of Biophysics, 2016	7 words — < 1%

Crossref

221 Baty, Roua Sami. "Modulation of Breast Cancer Stem Cell Plasticity and Tumourigenesis: Evidence for Regulatory Roles of Heparan Sulphates.", The University of Liverpool (United Kingdom), 2021 — 7 words — < 1%
ProQuest

222 D. Alfano, G. Votta, A. Schulze, J. Downward, M. Caputi, M. P. Stoppelli, I. Iaccarino. "Modulation of Cellular Migration and Survival by c-Myc through the Downregulation of Urokinase (uPA) and uPA Receptor", Molecular and Cellular Biology, 2010 — 7 words — < 1%
Crossref

223 Gerta Hoxhaj, Brendan D. Manning. "The PI3K–AKT network at the interface of oncogenic signalling and cancer metabolism", Nature Reviews Cancer, 2019 — 7 words — < 1%
Crossref

224 Haizhen Wang, Zhenghua Tang, Ting Li, Menglu Liu, Yong Li, Baoling Xing. "CRISPR/Cas9-Mediated Gene Knockout of ARID1A Promotes Primary Progesterone Resistance by Downregulating Progesterone Receptor B in Endometrial Cancer Cells", Oncology Research Featuring Preclinical and Clinical Cancer Therapeutics, 2019 — 7 words — < 1%
Crossref

225 Rodrigo Romero, Francisco J. Sánchez-Rivera, Peter M. K. Westcott, Kim L. Mercer et al. "Keap1 mutation renders lung adenocarcinomas dependent on Slc33a1", Nature Cancer, 2020 — 7 words — < 1%
Crossref

226 Sekhejane, Palesa Rose. "Effect of Low Level Laser Irradiation on Expression of Cytokines and Growth — 7 words — < 1%

Factors Involved in Wound Healing", University of Johannesburg (South Africa), 2021
ProQuest

227 Uma Lakshmipathy, Brad Love, Christopher Adams, Bhaskar Thyagarajan, Jonathan D. Chesnut. "Chapter 8 Micro RNA Profiling", Springer Science and Business Media LLC, 2007
Crossref
7 words — < 1%

228 Yuliya Pylayeva-Gupta. "RAS oncogenes: weaving a tumorigenic web", Nature Reviews Cancer, 10/13/2011
Crossref
7 words — < 1%

229 Akimasa Hayashi, Jungeui Hong, Christine A. Iacobuzio-Donahue. "The pancreatic cancer genome revisited", Nature Reviews Gastroenterology & Hepatology, 2021
Crossref
6 words — < 1%

230 Andrew J. Aguirre, William C. Hahn. " Synthetic Lethal Vulnerabilities in -Mutant Cancers ", Cold Spring Harbor Perspectives in Medicine, 2018
Crossref
6 words — < 1%

231 Arango Tamayo, Daniel A.. "The Immune-Modulatory and Anti-Carcinogenic Mechanisms of the Flavonoid Apigenin", The Ohio State University, 2021
ProQuest
6 words — < 1%

232 Carefoot, Esther I.. "The Src/Stat3 Axis in Met Signaling in Human Invasive Breast Cancer: A Potential Predictive Marker", Queen's University (Canada), 2021
ProQuest
6 words — < 1%

233 Douglas E. Biancur, Kevin S. Kapner, Keisuke Yamamoto, Robert S. Banh et al. "Functional
6 words — < 1%

Genomics Identifies Metabolic Vulnerabilities in Pancreatic Cancer", Cell Metabolism, 2021
Crossref

234 L. Gremer. "Duplication of Glu37 in the switch I region of HRAS impairs effector/GAP binding and underlies Costello syndrome by promoting enhanced growth factor-dependent MAPK and AKT activation", Human Molecular Genetics, 12/08/2009
Crossref
6 words — < 1%

235 Molecular Pathogenesis of Colorectal Cancer, 2013.
Crossref
6 words — < 1%

236 Philip M. Nussenzweig, Luciano A. Marraffini. "Molecular Mechanisms of CRISPR-Cas Immunity in Bacteria", Annual Review of Genetics, 2020
Crossref
6 words — < 1%

237 Ryan C. Gimple, Xiuxing Wang. "RAS: Striking at the Core of the Oncogenic Circuitry", Frontiers in Oncology, 2019
Crossref
6 words — < 1%

238 Sanne E. Klompe, Samuel H. Sternberg. "Harnessing “A Billion Years of Experimentation”: The Ongoing Exploration and Exploitation of CRISPR–Cas Immune Systems", The CRISPR Journal, 2018
Crossref
6 words — < 1%

239 Wilson, Gary M.. "Application and Development of Mass Spectrometry Technologies to Enable Biological Investigations", The University of Wisconsin - Madison, 2021
ProQuest
6 words — < 1%

240 Withey, Sarah. "Differentiation of Hepatocyte-Like Cells from Human Pluripotent Stem Cells", The University of Manchester (United Kingdom), 2021
ProQuest

6 words — < 1%

EXCLUDE QUOTES	OFF	EXCLUDE SOURCES	OFF
EXCLUDE BIBLIOGRAPHY	ON	EXCLUDE MATCHES	OFF